RELIABILITY ANALYSIS OF FABRIC STRUCTURES

A Thesis submitted to the degree of Doctor of Philosophy in the School of Civil Engineering and Geosciences at Newcastle University

by

ZHANG LEI

Supervisor: Prof. P. D. Gosling

Newcastle upon Tyne, 2010

Abstract

This PhD thesis demonstrates a reliability analysis methodology to solve the safety issues existing in the current structural design of fabric structures: The safety coefficients proposed by different countries and academic institutes are not consistent, and the leading structural safeties are obscure and require a justification. A reliability tool specific for fabric structures is developed to estimate the structural safety and justify the safety coefficients for structural design based on the variations of the design variables like loads, material strength.

The research work includes three main parts: the first one aims at a finite element formulation proposed for a highly accurate and efficient deterministic analysis. Four element types have been compared and discussed, and the linear strain triangle coupled with Dynamic Relaxation algorithm are shown to be most efficient with the satisfactory accuracy,

The second part is focus on a probabilistic methodology to identify and analyze the material uncertainties based on the experiment data. The probabilistic models to qualify the variation in the fabric strength and Young's modulus under uniaxial tension are demonstrated, and a practical algorithm to determine best data-fit distributions is also presented.

The third part is the reliability formulation which consists of first order reliability method(FORM) and the finite element method based on the six node linear strain triangles. The analytical method with the principle of chain rule is applied in deriving the gradients of the limit state functions. The sensitivities of the structural safety corresponding to different uncertainties are compared and analyzed through numerical examples. Finally a case study based a realistic design example is undertaken, and safety factors for loads, materials, and other design elements are justified and discussed.

This thesis demonstrates that the safety coefficients currently used in the fabric structure design may not be either economic or safe. Based on the uncertainty information of the design elements, the appropriate safety factors required for the structural safety standards can be evaluated using the reliability tool, and then an optimized design decision in consideration of safety and cost can be subsequently determined.

Acknowledgement

I would like to acknowledge my supervisor Professor P.D Gosling for his great guidance and supports. I would like thank Mr. Bill Cragie for his technical supports for the experiments. I also thank all the other technician and staffs the civil Engineering and Geo-sciences, especially Mr. Fred Beadle and Mr. Stuart Patterson for their technical helps and advices. I would like to thank Dr. Ben Bridgens, Dr. Sean Wilkinson and Dr. Colin Davie for their academic supports.

I acknowledge my industry sponsors: Architen-Landrell, ARUP, FERRARI and TENSYS for their financial and academic supports. Especially thanks to Mr. Lance Rowell, Mr. Alex Heslop, Dr. Ben Bridgens, Mr. Matthew Birchall, Dr. Farid Sahnoune and Dr. David Wakefield for all the valuable advices.

I would like to thank my colleagues Dr. Peng Jing Rui, Dr. Arthit Petchsasithon and Mr Faimun Faimun for their helps and advices for this research.

I would like to thank my parents Mr. Zhang Yuan Ji and Mrs,Huang You Ju for encouraging me to pursue this degree, and my uncle Mr.Zhang Yuan Huan for his sponsorship for my study in UK. Special thanks to my wife Mrs. Gao Yixin for her supporting and encouraging to finish this research.

I also thank my friends Mr. Liu Shih Yun, Mr. He Wei, Mr. Qiu Fan, and Miss Li Jing for their supports in life and spirit during my PhD study.

Contents

List of Figures

List of Tables

Notation

a_1, a_2	The gradient vectors responding to different random variables for the index calculation
a^t	The transpose of the gradient vector for the index calculation
a, b	The parameters of the candidate distribution for the data-fitting test.
A	A surface element of area
A_i	The combination of reduction safety factors depending on load case
a_x, a_y, a_z	The sub-terms in the function of the transformation between the global nodal coordinate system
α	The significance levels
α^c	An iteration coefficient for deriving B matrix of meso CST element.
α_w	The angle of wrinkling direction and local X axis
b	The constant terms in the limit state function.
b_x, b_y, b_z	The sub-terms in the function of the transformation between the global nodal coordinate system
B	Shape Function Matrix
B_L	Linear part of Shape Function Matrix
B_{NL}	Nonlinear part of Shape Function Matrix
$[B^{tr}]$	Shape Function Matrix of triangular element
β_s	The strength reduction factor depending on loading(ASCE)
β	Safety index
c_x, c_y, c_z	The sub-terms in the function of the transformation between the global nodal coordinate system

COV	The ratio of standard deviation and mean value of a statistical variable
D	Uniaxial specimen width
D_n^{α}	Critical values in K-S test with significance levels α
D_{al}	The deformation allowance
D_{max}	The maximum deformation.
δ_i	Displacement vector of presedo cable
$\delta_1, \delta_2, \delta_3$	Extension of triangular element sides
Δ	A function of all the higher order terms in the small strain CST element.
δ_{pq}	The nodal displacement of p^{th} node in the q^{th} direction.
ΔZ_s	the change in structural responses Z_s corresponding to the small change of random variable
E_X,E_Y	Young's Modulus along orthogonal axes
$[E_{mod}]$	A modified elastic stiffness matrix for wrinkling
EI, EII, and EIII	Young's modulus in predefined Zone I, II, and III
F	Applied load vectors
f_d	The allowable stresses (German Design Code)
F_c	Deterministic value of design loads
f_{tk}	The tensile strength defined as 5% -fractile of at least 5 strips 10cm wide, tested at 23° C(codes: DIN 53 354, ISO 1421).
$f_X(x)$	A joint probability density function
F_f	Failure loads of test samples
F_{pre}	Pre-defined designed prestress
F_1	Loading point at 12-15% of the ultimate tension strength(UTS)
F_2	Loading point at 25% of UTS
$G(\ ) = 0$	A given limit state function
$G_i(X_s)$	Limit state functioned of the random variable X_s

G_{XY}	The shear modulus across X and Y
γ_f	The safety factor applied on the design load.
γ_M	The material safety coefficient for all approved materials
γ_t	Safety factor proposed in the Japan Design Guide
γ_{XY}	The local shear stress across local axis X and Y Displacement along X axis
γ_s	The third central moment of the variable X_s
J	Jacobian Matrix of finite element formulations
K	Stiffness matrix
k	The number of intervals for Chi-square test
K_q	The factor for membrane quality (French Design Guide)
K_e	A scale factor which takes into account the increased risk of a critical defect as the surface area increases (French Design Guide)
$K_{\overline{X}}$	Curvature in $\overline{X}$ axis
$K_{\overline{Y}}$	Curvature in $\overline{Y}$ axis
$K_{\overline{XY}}$	Torsion in $\overline{X}$ and $\overline{Y}$ plane $\overline{Y}$ axis
$[K_t^e]$	Stiffness Matrix
$[K_E^e]$	Elastic Stiffness Matrix
$[K_\sigma^e]$	Nonelastic Stiffness Matrix
$[K_E^{tr}]$	The elastic stiffness matrix of the triangular element
$[K_\delta^{pc}]$	The geometric stiffness matrix
$\underline{K_{pq}}$	The p^{th} nodal stiffness selected from the terms of the element stiffness matrix of node
$l_1, l_2, l_3, \cdots l_7$	Safety factors applied in fabric strengths (IASS Recommendation)
L_t	The safety factor corresponding to life cycle (ASCE)
l	A cable element of current length
l_i, m_i, n_i	The direction cosines between global coordinate and local flat coordinate axis.

$\lambda_1, \lambda_2, \lambda_3$	Sub-terms in the function of transformation between local and global coordinate system
M_{pq}	The fictitious nodal mass of p^{th} node in the q^{th} direction
$[M_p]$	A matrix for deriving transformation function between local and global coordinate systems
$\mu_X, Var(X), \sigma_X$	Mean value, Variance and standard deviation of a statistical variable
μ_{Xs}, σ_{Xs}	Mean and standard deviation of a random variable X_s
μ	Mean value of a statistical variable
$[N]$	Element shape functions
n	The number of samples
ν_{YX}	Possion's ratio in Y direction etc.
ν_{wf}	Poison's ratio between the warp and fill
ω	Modification coefficient on the stiffness matrix due to wrinkling
Ω_s	A function of safe zone
Ω_f	A function of failure zone
ω_A	The whole volume of the element
P	The penalization parameter applied the modification of element stiffness in case of wrinkling
p_f	Probability of failure
P_N	Axis Force in linear element
P_A, P_B	Force vectors at the geometry configuration A and B
$\underline{P_{pq}}$	The external load vector of p^{th} node in the q^{th} direction.
$\Phi(y)$	Standard normal density of the independent statistical variables involved in the structure system
$[R]$	The transformation matrix applied in wrinkling procedure
R^m	Membrane element reaction force vectors
R^c	Cable element reaction force vectors

$\underline{R_{pq}}$	The out-of-balance nodal force (or residual) of p^{th} node in the q^{th} direction
S_f	The security factor depending on level of pollution/environment degradation (French Design Guide)
$S_n(X_s), F(X_s)$	Judgement functions for K-S test
σ	A surface element of isotropic stress
σ_I	Maximum element principal stress
σ_{II}	Minimum element principal stress
σ_X	Element Stress along X axis
σ_Y	Element Stress along Y axis
σ_i	Element strains in presedo cable
σ_n	The normal stress
σ_I, σ_{11}	The max element principal stress
σ_{II}, σ_{22}	The minimum element principal stress
σ_{ult}	Ultimate uniaxial stress of a test sample
σ_0	Stress vectors from the pretension
σ_E	Stress vectors from the elastic deformation
σ^f_{per}	Permissible stress in the fill direction
σ^w_{per}	Permissible stress in the warp direction
σ^f_{max}	Maximum stress in the fill direction
σ^w_{max}	Maximum stress in the warp direction
σ^f_{ult}	Ultimate fill strength
σ^w_{ult}	Ultimate warp strength
σ^p_{min}	Minimum principal membrane stress
σ^p_{per}	A predefined lower limit of membrane stresses
σ_s	Standard derivation of a statistical variable
T	Cable element tension

$[T]$	Transformation Matrix
T_p	The permissible stress of a coated woven fabric (French Design Guide)
T_{sm}	The specified minimum breaking strength (French Design Guide)
T_{sw}	Minimum breaking strengths in warp.
T_{sf}	Minimum breaking strengths in weft.
T_1, T_2, T_3	The element side force
T_{c1}, T_{c2}, T_{c3}	The pseudo cable element forces
$[T_1]$	The transformation matrix between the global and local flat coordinate systems
$[T_2]$	The transformation matrix between the local flat and local curved coordinate spaces
T_N	Axis tension force in presedo cable
t, t^*	Nearest point coordinate vector of the limit state surface in the standard normal space.
t_{load}	The ratio of applied load F and deterministic load F_c
$\{T_c\}$	The linear element force vector
T^c	Transformation vector for cable elements
τ_{XY}	Element Shear Stress between X and Y axis
θ_p	The angle between wrinkle direction and local X axis
θ_{Xs}	The skewness coefficient of the variable X_s
U_d	The nodal displacements in local coordinate system
u_d	The nodal displacements in global coordinate system
u , v , w	Displacements separately along x , y , z axis in global coordinate system
U , V , W	Displacements along X , Y , Z axis in Local curved coordinate system
$\overline{U}$, $\overline{V}$, $\overline{W}$	Displacements along $\overline{X}$, $\overline{Y}$, $\overline{Z}$ axis in Local Plane coordinate system

u_A, u_B	Displacements at the geometry configuration A and B
ε_X	Stress along local axis X
ε_Y	Stress along local axis Y
$\varepsilon_I, \varepsilon_{11}$	The max element principal strain
$\varepsilon_{II}, \varepsilon_{22}$	The minimum element principal strain
$Var(X_s)$	The variance of the random variable X_s
X_s	Statistical variables
$X_{s1}, X_{s2}, X_{s3}, \cdots, X_{s7}$	Defined random variables for a reliability analysis
$x\ , y\ , z$	Coordinate in Global coordinate system
$X\ , Y\ , Z$	Coordinate in Local curved coordinate system
$\overline{X}\ , \overline{Y}\ , \overline{Z}$	Coordinate in Local plane coordinate system
x_i, y_i, z_i	The global nodal coordinates of ith node.
x_p, y_p, z_p	The global coordinates of a single point p along the local Y axis
$\overrightarrow{X}, \overrightarrow{Y}, \overrightarrow{Z}$	The vectors representing the local flat coordinate axes
X_s	Statistical random variables
x_s^*	The minimum distance point on the limit state surface in the original coordinate system
$x_s'^*$	The minimum distance point on the limit state surface in the reduced coordinate system.
$\xi_1\ , \xi_2\ , \xi_3$	Coordinates in the Local Area coordinated system
Z_s	The structural response variables

Chapter 1

Introduction

1.1 Background

Ancient fabric structures in the form of tents(fig.1.1) have existed for thousands of years. Most structures of this types were designed and constructed for temporary use. Ancient fabric structures may have been constructed and erected from a variety of basic materials such as cloth, animal skins forming the membrane, ropes and tree branches, for example forming the other structural components. The reliability of such structures was comparatively low when subject to environmental loading.

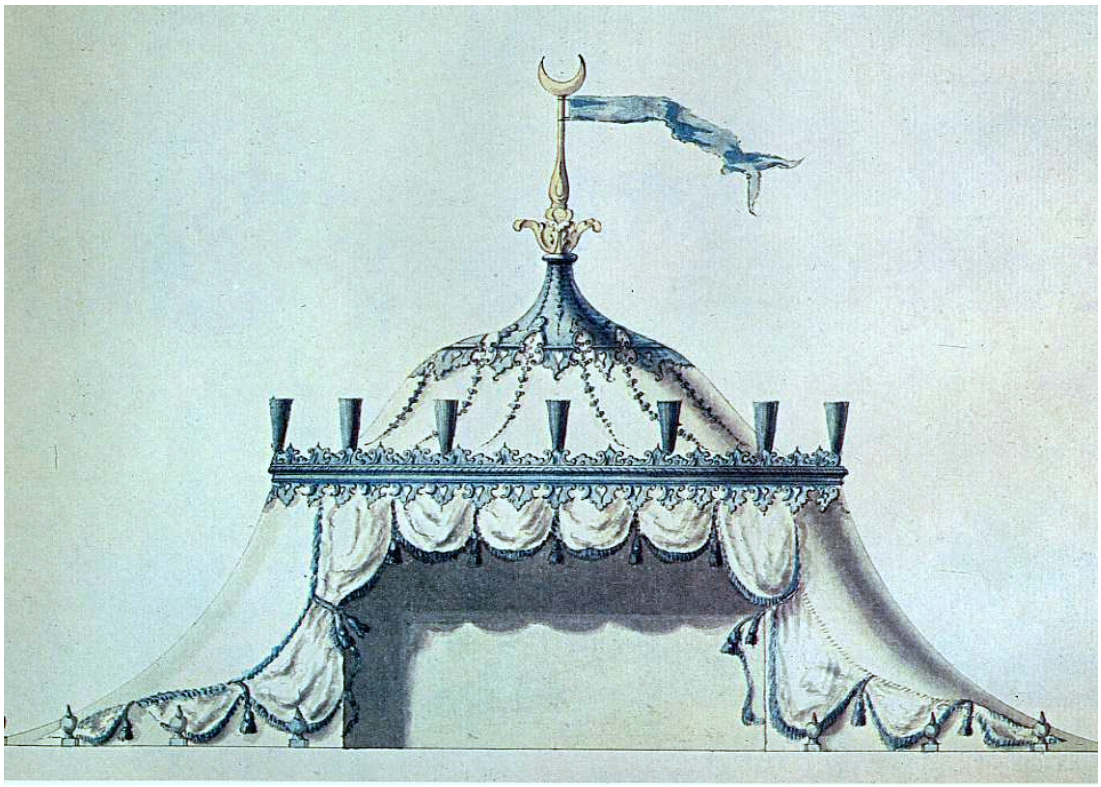

Figure 1.1: Henry Keene's design for a Turkish Kent (c1755), as used for the re-construction at Painshill

Modern fabric structures(fig.1.2-1.4) designed for permanent purposes have been developed with increasing popularity since the 1950s. Compared with ancient fabric forms, higher requirements in both aesthetics and structural stability must be satisfied in modern fabric structures. The key mechanism to achieve the increased performance is correct generation of tensile forces to induce smooth geometries. In this way, the modern fabric structures are also called tensile structures.

Fabric materials have little compression or bending stiffness. They are, therefore, prone to fold and wrinkle under external forces when not adequately tensioned by pretension. The applied pretension stresses can largely improve the stability and stiffness of the fabric surface, and the negative strain produced by loads can be compensated by the initial positive strain due to pretensions.

Figure 1.2: Student Center (University of La Verne) La Verne, California, USA, 1973

Figure 1.3: Price Waterhouse - Cooper building, Brussels,2003

Figure 1.4: II Grande Bigo, Genova, Italy, 1992

Generally, tensioned fabric structures are designed to three basic shapes – conic, saddle, and arches, or their combinations as figure.1.5, and the surface geometries with the doubly curved shapes, are complicated by the supporting boundary. To achieve the stress balance within the surface, the two main curvatures at any point of the surface are opposite. For a uniformly stressed membrane surface, zero mean curvatures(two same large main curvatures but opposite) are found at any point of the surface.

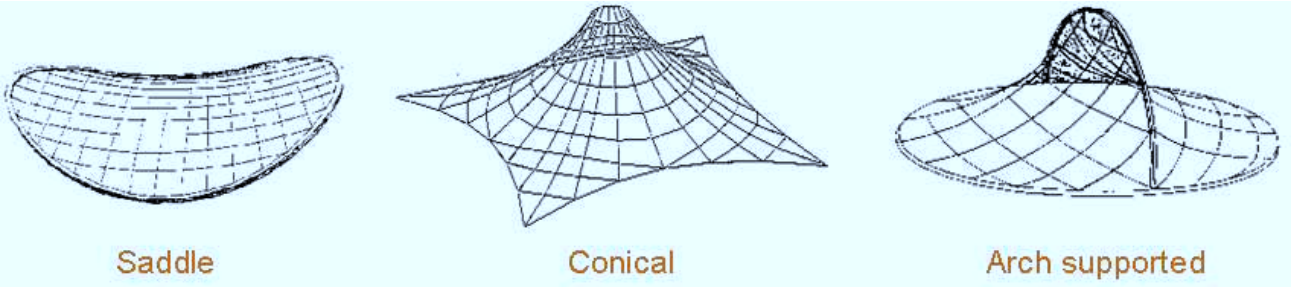

Figure 1.5: Three basic shapes of modern fabric structures

1.1.1 Design and construction

Fabric structural design has three main stages – form-finding, pattern cutting and loading analysis. The tensioned fabric may form a double curved surface satisfying the stress equilibrium of the surface and the boundary constraints. The detailed geometry of the fabric, which is necessary for the structural design and construction, must be obtained through a "Form-finding" procedure using physical or numerical models(fig.1.6 and 1.7).

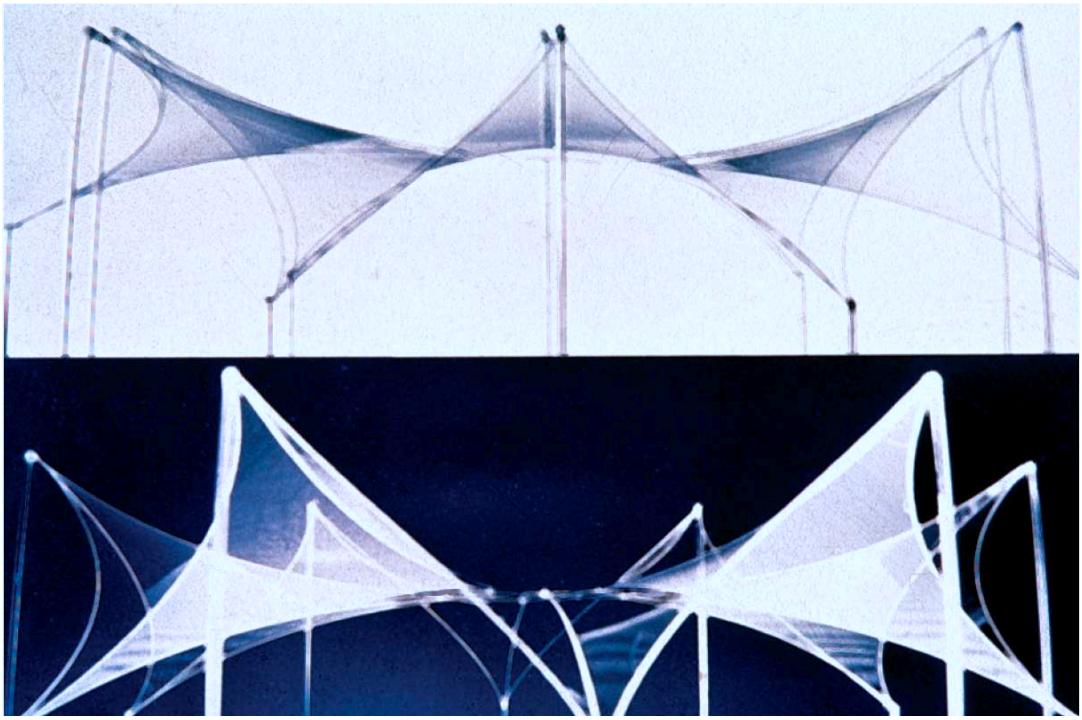

Figure 1.6: Soap film model of a Starwave tent. Studies for the fountain tent, Cologne [3]

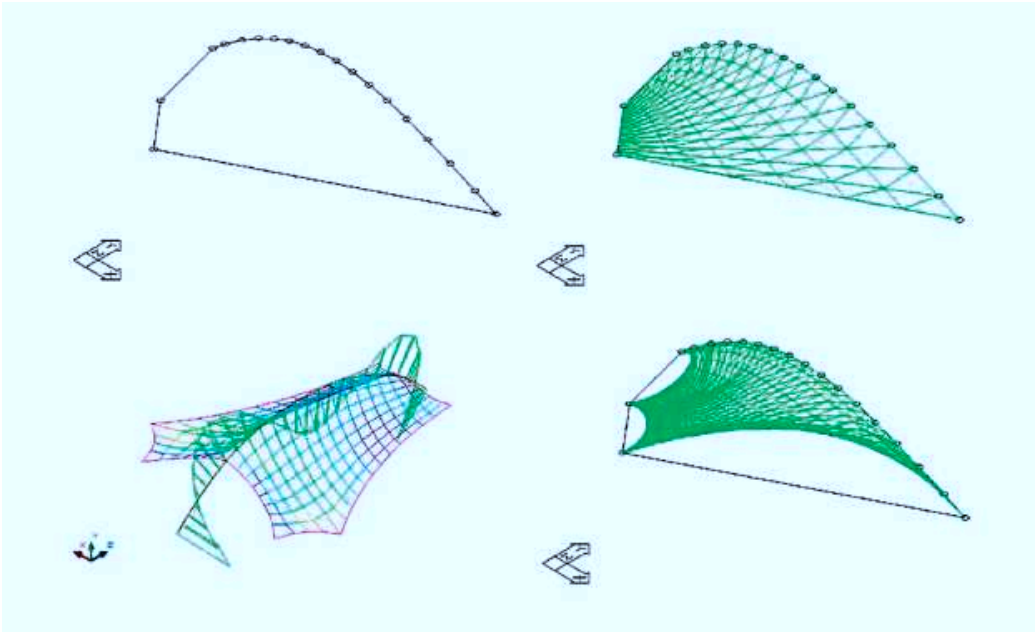

Figure 1.7: Digital Form finding process with PAM Lisa: Architekturburo Rasch + Bradatsch 2003 [3]

After the initial shape of fabric structures is obtained by assuming the initial in-plane tension force, which is an ideal form presented by the designer at the first stage of design, these shapes have to be achieved by practical construction approaches – patterning and sewing of fabrics. Also, the fabric has limitations for width and length due to its material characteristic from manufacture. Therefore, the 3-D initial shapes have to be divided into several 2-D plane strips for construction of the so-called cutting pattern.

Pattern cutting is an additional design procedure requiring the membrane shape found in the form-finding procedure to be developed into a 2-D plane via a series of fabric panels consistent with the proposed fabric for construction (e.g. roll width and compensation values) (e.g. Figure 1.8), which can be cut from the fabric sheet manufactured. The fabric structure is assembled from patterns, which must fulfill the requirements in both physical and architectural aspects.

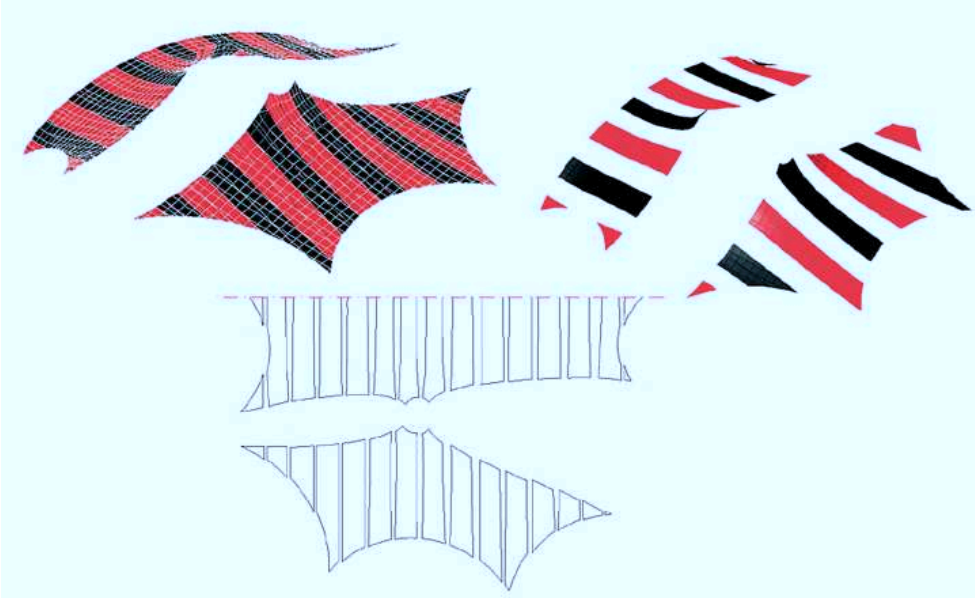

Figure 1.8: Digital Cutting patterns layout, stripes and cutting patterns: Tent for Mercedes Benz Magdeburg, SL Rasch, Germany, 1994 [3]

Loading analysis for the pretensioned membrane defined in the form-finding procedure is required to consider both material and geometric stiffness in defining equilibrium. Normally, selfweight, wind load, and snow load are considered as the primary loads. Wind load is normally the critical load for fabric structures, and is calculated as static load defined by a dynamical pressure C_p which may be calculated using standard national codes unless the structure shape and form lead to a sensitive or large deflection. In such cases, wind tunnel tests (fig. 1.9) may be undertaken to estimate the C_p value. Snow loads may be also taken into account and especially when the structure length is over 50m [3]. Extra attention may be paid on the relevant environmental impacts such as rain, falling leaves, sands.

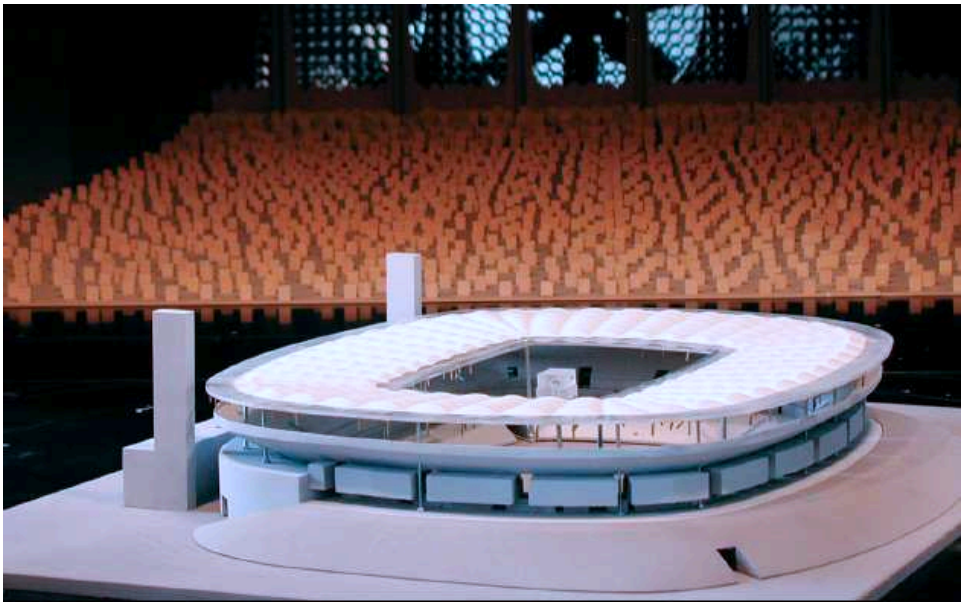

Figure 1.9: Wind tunnel stadium, Wacker Ingenleure

1.1.2 Structural safety

Driven by architectural demands, fabric structures are required to achieve increasing levels of performance, with corresponding more accurate analysis tools and advanced construction technologies. In the present fabric structure design, it is recommended that large safety coefficients and conservative failure criteria should be used especially for any fabric structure with a complicated geometry or new fabric materials [3]. Large safety margins are necessary to account for the significant uncertainties in the structural design, material properties and construction technologies in addition to structural requirements such as tear propagation. These uncertainties are being reduced by the development in fabric industry, but they are still regarded as most important factors affecting fabric structural analysis and design. Using large safety factors could reduce the probability of fabric structure failure, but in so many cases, good material mechanical properties are wasted due to low application ratio, and aesthetic functions may be limited in architectural designs.

The implementation of a reliability analysis tool is extremely useful for the fabric structural design. Appropriate safety factors according to different structural elements and environmental situations can be evaluated based on the reliability analysis result for the different confidence of the structural safety. The high safety factors allowing for the potential effects of the randomness can be well justified, and the utilization ratio of fabric strengths may be largely improved. The extra cost for excessive safety margin owing to large safety factors can be reduced and more economic design decision can be made.

1.2 Aim and objectives

The aim of this research is to produce an analysis system that couples a high fidelity computational tool with material structure uncertainty in an integrated system for design. The structural reliability work can be divided into three parts. The first part is to develop an efficient structural analysis tool for fabric structures as a computational engine for the reliability calculation. This part is extremely important for the reliability frame work, because a reliability calculation may include a large quantity of structural analysis. The efficiency of the reliability work may be largely dependent on the structural analysis formulation.

The second part aims at the applicable methodology of the measurement and analysis of the uncertainties in fabric material properties relevant to the structural design and analysis. Innumerate design variables (e.g. loading, construction quality) may be involved in a full reliability analysis. The investigation of the randomness in fabric materials is urgently demanded and primary for fabric structures. The statistical information of other random variables general for common structures may have been investigated and possibly available from the published data.

The third is the reliability estimation corresponding the uncertainty information. This part focuses on developing an efficient reliability tool allowing for characteristics of fabric structures.

Specific objectives are to:

- formulate an efficient finite element for fabric structure analysis.
- develop a Fortran 95 finite element program for fabric structure analysis.
- establish a probabilistic measurement and analysis methodology for fabric material properties
- implement a reliability-based analysis theory combining material uncertainty and a quadratic finite element approximation
- develop a Fortran 95 program to estimate the reliability of the fabric structures.
- propose a procedure to examine the current used safety factors and to provide appropriate safety indices.

1.3 Scope

This first part of this research focus on finite-element based deterministic modelling and analysis including form-finding, loading analysis.

The second part is concerned with the development of a probabilistic analysis methodology for fabric material uncertainties based on experimental data. An existing analysis theory is adopted and implemented.
Other uncertainty types like loading, pollution, and other material tests are not within the scope of this research.

The reliability formulation combines the first order reliability method and the finite element formulation recommended by the first part of this research, with a limited number of uncertainty input like loads, strength and Young's modulus. The high order reliability formulations and other uncertainties(e.g. loading, pollution, construction quality, work skills) are not within the scope of this research.

1.4 Thesis structure

Chapter 2 – **Literature Review**. States the fabric design principle currently used, and demonstrates the importance of developing a reliability tool for the safety estimation. The approaches on fabric structural modelling, probabilistic material properties, reliability methodologies are reviewed.

Chapter 3 – **Finite Element Formulation For Fabric Structures**. To develop a high efficiency structural analysis tool, four types of different finite element formulations coupled with different solution algorithms have been introduced and compared. An appropriate finite element formulation is concluded for the reliability analysis.

Chapter 4 – **Probabilistic Properties of Structural Fabric**. A probabilistic analysis methodology including data-based uncertainty collection and mathematical presentation of the mechanical property of fabrics is proposed.

Chapter 5 – **Reliability Analysis of Fabric Structures**. A reliability formulation combining the finite element method proposed in Chapter 3 and one classical reliability formulation, is developed. Using this formulation, the safety of a given fabric structure can be evaluated, and appropriate safety factors can be estimated.

Chapter 6 – **Conclusion** Summary of the conclusions of each chapter, and recommendations are made for further work.

Bibliography – The latex bibliography system is used for all the reference papers and books.

Appendix – All test data, basic knowledge of statistical distributions, part derivatives of reliability formulations, and a guide to Fortran programs developed within the research.

Chapter 2

Literature Review

2.1 A probabilistic approach to the analysis of fabric structures

Currently the design of fabric structures varies at international level, typically through the application of safety factors. In this section, the potential of a reliability analysis tool to estimate safety factors is demonstrated, based on the principles of the structural safety given in Eurocode 0.

For a designer, safety factors are decided based on two aspects: (1) uncertainties of the human actions, material properties and the corresponding environment impacts. (2) Limited knowledge of the designer to predict the physical behavior of all the relevant quantities. "With development in science and technology, the element of ignorance can be largely eliminated, while the uncertainties, being changed in the form and magnitude, can never be removed" [29]. Especially in the case of advanced material developments and new structured forms, the problem of uncertainties are considered using the statistical investigation and stochastic analysis for safe and economic design.

Engineering groups in different countries have adopted a variety of safety coefficients which are derived using a nember of approaches. Most of these approaches are based on the permissible stress method instead of the limit state method used in the current traditional structures like steel and concrete, due to the highly nonlinear-geometrical behaviour of fabric structures. A series of uncertainties potentially exist in fabric structure design and construction, and are taken into account via a range of safety factors. However these safety coefficients contain difference and uncertainties.

The European Design Guide for Tensile Structures [3] summarizes the design methods and safety calculation approaches currently used as outlined below,

IASS Recommendation [5] :

IASS working group 7 recommendations propose a safety estimation approach for air-supported

membranes. The material quality, load uncertainty, accuracy of the calculation, and environmental impact are taken into account in the safety factor calculation. The general safety factor value is a product of a series of safety factors estimated using different aspects:

$$L = 2 \cdot l_1 \cdot l_2 \cdot l_3 \cdots l_7 \tag{2.1}$$

In which, l_1 represents unevenness of fabric surface: l_1=1.25 for warp and 1.43 for fill. l_2 represents calculation accuracy: l_2=1.0 when confirmed by experiment, otherwise 1.3. l_3, l_4, l_6 represents loading uncertainty, application and execution respectively (normally 1.0). l_5 represents material reliability / reliability of test results, in the range 1.1-1.3, and for other or unforeseen aspects (min 1.2). l_7 represents environmental impact such as ultra-violet radiation, cyclic loading, high temperature, creep and humidity, in the range 2.0-2.4.

In IASS Recommendation, the unevenness of the fabric is highlighted out of the material quality, and large safety factor is normally applied in the membrane degradation due to environmental impacts instead of loading. However the details of these environmental impacts may be not obtained accurately (e.g cyclic loading, creep), and the total integrated effect may not be easy to estimate.

French Design Guide [6] :

The permissible stress T_p has been given in French Design Guide for Permanent Fabrics,

$$T_p = (K_q \cdot K_e \cdot T_{sm})/S_f \tag{2.2}$$

Where T_{sm} is the specified minimum breaking strength, K_q is the factor for membrane quality, 1.0 for tested or certified seams and fabric, 0.8 for otherwise. K_e is a scale factor which takes into account the increased risk of a critical defect as the surface area increases (this should perhaps relate to the area of any surface region bounded by cables or other support elements), 1.0 for surface area $< 50\ m^2$, and 0.8 for surface area $> 1000\ m^2$ (typically). S_f is the security factor depending on level of pollution/environment degradation, 4.0 for soft pollution, 4.5 for strong pollution.

In the French design guide, the structure scale is taken into account in the safety factor estimation, and the fabric structure with a large area is assumed to have higher variance in the uncertainties rather than the small scale structure type. As in the IASS recommendations, pollution/environment impact is the most significant uncertainty, with a corresponding large of safety factor will be applied for it.

German Design Code [7] :

In German Design Code (DIN 4134 - Tragluftbauten), the allowable stresses f_d are given as,

$$f_d = \frac{f_{tk}}{\gamma_f \cdot \gamma_M \cdot A_i} = f_{tk}/A_{res} \tag{2.3}$$

Where f_{tk} is the tensile strength defined as 5% -fractile of at least 5 strips 10cm wide, tested at 23° C(codes: DIN 53 354, ISO 1421). (Alternatively, from Minte, 0.868 × mean tensile strength for the fabric or 0.802 × mean strength for/near the seams. γ_f is the load factor. γ_M is the material safety coefficient for all approved materials: $\gamma_M = 1.4$ within the fabric surface, or 1.5 for connections. A_i is the combination of reduction factors depending on load case.

The safety factor of fabric structures in German Design Code combines the traditional load factor γ_f and the other coefficient allowing for the specific uncertainties for membrane. That means the total safety coefficient varies with different load combinations. In this code, the connection detail is specified as an important aspect with a relevant high partial safety coefficients.

Italian Design Code [8] :

"The safety factors applied in the fabric structures in Italian Design Code are similar to the German Code [3]", but more detail is provided related to the connections. Generally, three classes of connections are defined;

- "1st class - connections designed and fabricated by licensed personnel using methodologies defined (that characterise all the parameters and work conditions) by the coated fabric manufacturer or from the membrane fabricator and tested by the membrane fabricator."
- "2nd class - connections analysed by licensed personnel using methodologies defined (that characterise all the parameters and work conditions) by the coated fabric manufacturer or from the membrane fabricator and not tested by the membrane fabricator."
- "3rd class - connections, however designed and fabricated, permitted exclusively for the realisation of secondary elements or sealing."

Different connection classes are allowed in different structures. For example, 1st and 2nd connectors can be used in tents having a primary load bearing textile structure connection, while only 1st can be used in membranes. As such this regulation can guarantee the connection quality of the membrane, and enhance the reliability of the membrane. When the similar safety coefficients are applied with the qualified connections, Italian Design Code can achieve better structural safety compared with German Design Guide.

Japan Design Guide [1] :

In Japanese design guide , the safety factors are calculated based on the load types and the structure types, while other aspects like material reliability, environment impact are not specified. The permissible stress is

$$f_s = T_{sm}/\gamma_t \tag{2.4}$$

Load Case	General	Cladding on primary space or framed structure
Sustain load	γ_t=8.0	γ_t=6.0
Temporary load	γ_t=4.0	γ_t=3.0

Where

Safety factor proposed in the Japan Design Guide are high, and leave large margins for possible uncertainty sources which are not specified. However the material quality and reliability are not reflected by this formula, meaning that the mechanical resistance of fabric structures made of different quality materials are assumed to be similar. The advantage of the accurate calculation and characteristics of loads are also not taken into account in this formula.

ASCE Standard [9] :

The effect of load combination and cyclic loading on fabric structures is highlighted in the ASCE Standard. It is proposed that the material strength should be further reduced when the structure carries biaxial load.

$$T_p = \beta_s \cdot L_t \cdot T_{sm} \text{ - applied to warp or weft diection} \tag{2.5}$$

Where β_s is the strength reduction factor depending on loading systems / combinations. $\beta_s = 0.27$ for most loading combinations. L_t is the life cycle factor, and $L_t = 0.75$ for fabric and webbing materials which are certified to retain at least 75% of initial strength over their intended life. For structures subject to repeated loading, $L_t = 0.6$.

For structures subject to bi-axial loading, in addition to the coefficient given in Eqn.2.5, it is proposed that the sum of the stresses in warp and weft should be less than $0.8\beta \cdot (T_{sw} + T_{sf})$, where $(T_{sw} + T_{sf})$ is the sum of the specified minimum breaking strengths in warp and weft.

The safety coefficients proposed by different countries and academic institutes are summarized in Table.2.1, considering a series of uncertainties including material conditions, loading situation, working statement and so on. From one perspective, these high safety coefficients are applied because in the fabric structure design unfactored loads are used due to the highly nonlinear-geometrical behavior of fabric structures such that the load increment will significantly alter the geometry and stress of the distribution of the fabric, and hence make the analysis diverge from the true response.

The safety factors obtained empirically and from experience seem very large but reflect a conservative design requirement. However, they may not be as economical as possible because of the low utilization of the material strength. These factors may result in the structure achieving an unnecessarily high reliability, and limit the further use of the fabric material. A reliability approach may assist a designer to judge these safety factors in achieving an optimized design.

A further issue is the importance of the uncertainty source. For example, as shown in Table. 2.1, the ASCE standard gives safety factors of 3.3-4.2 allowing for the variation of loading,

Design Guide or regulation	Safety coefficient	Corresponding consideration
IASS recommendation	4.2 - 6.0 for warp 5.0 - 7.0 for fill	Fabric waveness & reliability Calculation accuracy Loading uncertainty Environmental degradation Unforeseen aspects
French Design Guide	5.0 - 7.0	Fabric quality Structure scale Pollution level (Environmental degradation)
German Practice & Italian Code	4.9 - 6.4 Permanent 2.9 - 3.2 Wind storm 4.4 - 5.1 Maximum snow	Loading type Surface information Connection conditions
Japan guide	8/6 for sustained loads 4/3 for temporary loads	Function type
ASCE Standard	3.3 - 4.2	Strength reduction depending on loading combinations Life cycle

Table 2.1: A review of safety coefficient on fabric strength by European Design Guide [4]

while in German and Italian practice, much higher values of safety factors are applied. For a given design case, a fabric structure is affected by a series of uncertainty sources which have different influences on it, and the corresponding safety factors should be decided when the consequence of the importance of these uncertainties are fully taken into account. However, without a special reliability tool, the effects from the uncertainties are very hard to be quantified so that a correct judgment is difficult to achieve.

Clearly, the safety coefficients proposed by different countries and academic institutes vary, and their effects on structural safety are also implicit even though so many uncertainties are considered. There are still some important uncertainties not included in these safety factor calculations. For example, the tear strength is not involved explicitly in these methods.

However since the purpose of the existing sets of safety coefficients is to ensure sufficient structural safety / reliability, these different approaches can be uniformly judged by considering if the minimum structural safety / reliability are achieved, and the safety margin is reasonable when using these safety coefficients. Inadequate structural safety / reliability may lead to structural collapse, and an excessive safety margin may make the structure uneconomic.

Eurocode 0 [253] regulates the basic reliability requirement for structure types of different importance.

As shown in Table.2.2, a general building category is given according to the consequence of the structural failure is defined. Fabric structures may be also classified to different category based on its structural application. For example, as the cladding system of a office building, fabric structures can be generally in category RC2, with a target safety index ($\beta = 4.7$ for 1 year and $\beta = 3.8$ for 50 years referring the Eurocode 0). Of course, Table.2.2 only

Building Category	Use age	Target p_f(safety index)
RC3: High consequence for loss of human life, or economic, social or environmental consequences very great	1 year	10^{-5}%(β=5.2)
	50 years	1.5×10^{-4} %(β=4.3)
RC2: Medium consequence for loss of human life, economic, or environmental consequences considerable	1 year	0.13×10^{-3}%(β=4.7)
	50 years	0.73×10^{-2}%(β=3.8)
RC1: Low consequence for loss of human life, and economic, social or environmental consequences small or negligible	1 year	0.13×10^{-2}%(β=4.2)
	50 years	4.83×10^{-2}%(β=3.3)

Table 2.2: Target Reliabilities for different building categories given by Euro code 0 [253]

gives a general reliability requirement, and the exact safety index specific for a given fabric structure may be calculated on a case-to-case basis, and may vary from one to another. As a basis of structural design, the principle of structural reliability must be followed through the whole fabric structural design process. However in many cases the reliability estimation is complicated, especially for fabric structures due to high variability of the materials and nonlinearity of the structural performance. The fabric structural reliability estimation may require a considerable amount of material uncertainty information, and more importantly, a reliable and efficient reliability estimation approach which can reasonably combine the material information and the characteristics of the fabric structural performance.
The reliability requirement of a structure may be also related to different limit states as listed in Table. 2.3. Here the reliability requirement of a fabric structure for different limit states may be distinctive. As a relatively new and developing structure type, fabric structures may exhibit characteristic structural failure modes(e.g. tear failure) and serviceability failure (e.g. ponding). These characteristics should be taken into account when determining a reliability estimate. The reliability approach used for traditional structural forms may not be directly used for fabric structures, and a specific reliability method is desired to enable fabric structures to be designed within a consistent uncertainty or probabilistic framework.

Limit state	Maximum p_f(Minimum Safety index)	
	1 year	50 year
Ultimate	0.13×10^{-3}%(β=4.7)	0.723×10^{-2}%(β=3.8)
Fatigue		6.78% - 0.723×10^{-2}% (β= 1.5 to 3.8)
Serviceability	0.187%(β=2.9)	0.678%(β=1.5)

Table 2.3: Target Reliability of RC2 building type in different limit states given by Euro code [253]

Based on the reliability requirement given by Eurocode, a consistent fabric structural design approach may be achieved using a specific reliability tool with capability to estimate the safety factors based on the relevant uncertainty information and reliability requirement. This reliability tool must have three functions:

- Structural analysis function - in addition to an essential capability for structural design and analysis, this function must be accurate and efficient and capture the characteristics

of fabric structures - strong geometric nonlinearity. The accuracy of calculation is a very important aspect in fabric structure design. For example, calculation accuracy is highlighted in the IASS recommendation. However, one reliability analysis will normally require many structural analysis iterations, meaning that a highly efficient analysis is necessary for the reliability analysis.

- Material probability analysis function - to investigate the uncertainty existing in the given fabric material based on the material test data. In the case that the probabilistic property of the given fabric material is unknown, the specific material test must be undertaken using a suitable methodology. For the reliability analysis all the probabilistic characteristics obtained either from published data or material tests must be represented mathematically as statistical functions.

- Reliability estimation function - to calculate the probability of the structural failure for a given structure based on the uncertainty or probabilistic information. Then appropriate design decision like safety factors can be determined to achieve the optimization of safety and cost.

2.1.1 Conclusion

The importance and necessity of developing a reliability approach specified for fabric structures arises from the current development status of fabric structural analysis and design. The design approaches proposed by different countries and academic institutes are united, and different uncertainty aspects are highlighted in the calculations of the safety coefficients. The safety / reliability of the fabric structures to be designed using these safety factors is implicit, and may be verified using a reliability tool. The reliability requirements given by Eurocode provide a good base to judge these safety coefficients when the structural safety margin can be estimated explicitly based on the uncertainty information of the structure and the relevant environments. An objective combined recommendation of safety factors may then be given to achieve a suitable structural reliability.

2.2 Modelling of fabric structures

In this section, fabric structure modelling is reviewed ranging from physical models through to computational methods. The main point of the literature review in this section is to demonstrate that a good numerical tool is required and that the best approach is through the development of the finite element - based simulation tool for structural mechanics.

2.2.1 Physical model of fabric structures

The most famous physical model for tensioned fabric structures is the soap film model(as fig.2.1) proposed, and initially applied in tensioned fabric structures by Frei Otto [14] for the design of the Munich Olympic Stadium. A soap film has a minimum surface which has zero mean curvature. It can be easily formed by dipping a frame (either flexible or rigid) into a soap solution as shown as figure2.3. A soap film model can display the basic geometry of a tensioned membrane with a given boundary shape illustrated as figure 2.2, provided that a minimal surface can be generated by the boundary conditions.

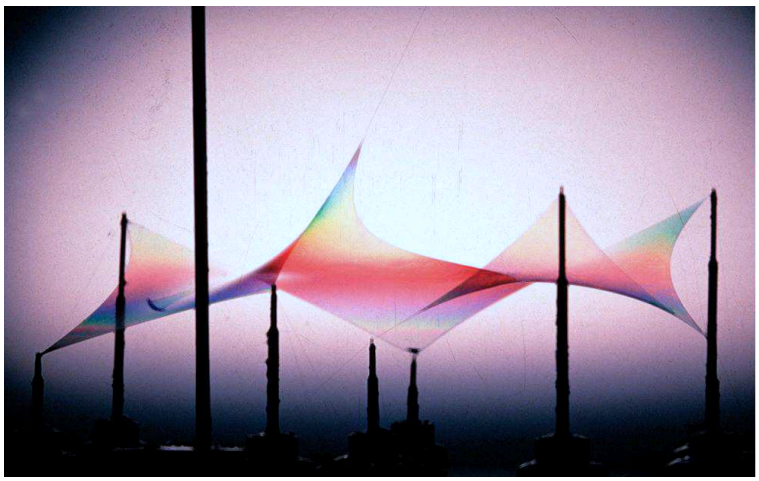

Figure 2.1: Soap film model applied by Frei Otto

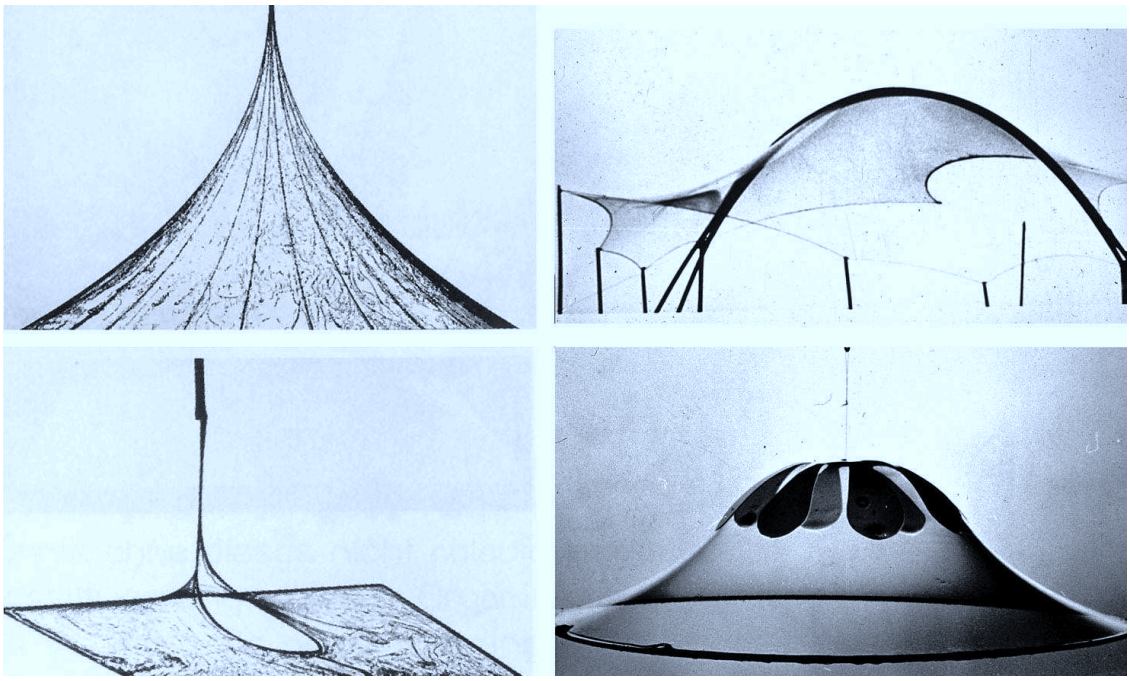

Figure 2.2: Exploring potential membrane geometries with different boundaries using soap film

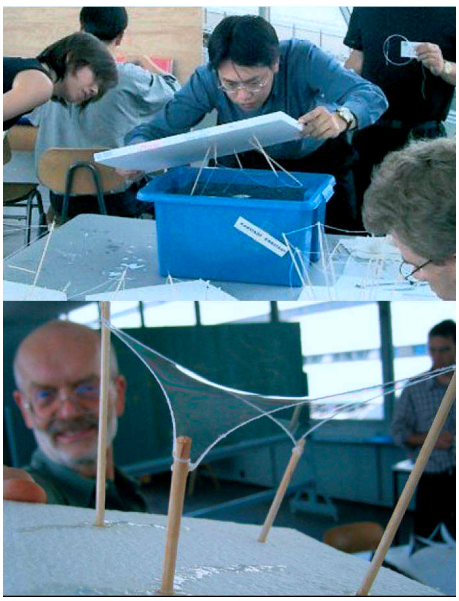

Figure 2.3: Soap film model making [3]

Physical models may also be used in the development of cutting patterns. Making a small scale physical model of a fabric structure can help designers to understand how the variety of curved membrane surfaces are to be created from cutting and joining flat fabric panels. In current fabric structure design, physical models may be still used. However their use is only limited normally to the concept design stage [11]. Detailed structural analysis are carried via numerical models.

2.2.2 Surface representation and structural mechanics

Same as soap films, the uniform stressed membrane will also form minimal surfaces. To obtain the initial geometry of the stressed membrane, the research on minimal surfaces was undertaken by Grundig [213]. Because on the minimal surface, two principal curvatures are equal but opposite sign at any point, the characteristics of the minimal surface can be expressed using a mathematical formulation. The surface can be arbitrarily discretized into many small elements (e.g. triangles or quadrangles), then the nodal coordinates will be checked if the node positions are satisfied the requirement of minimal surfaces, and then updated until the sum of the element areas is minimized.

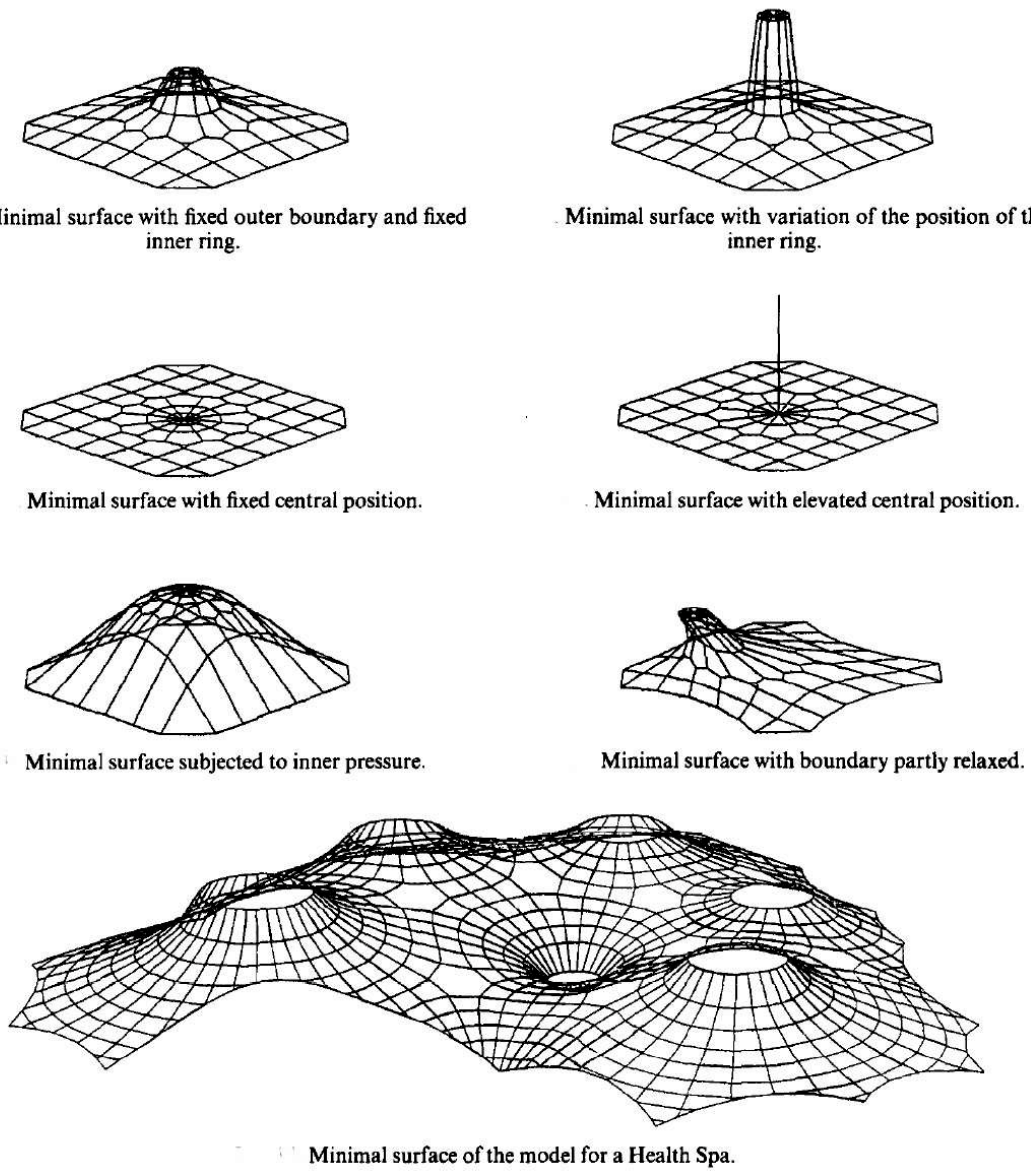

Figure 2.4: Form-finding using minimal surfaces(Grundig [213])

Nowadays, finite element methods (F.E.M) are popularly applied in engineering, since computer technology is highly developed enough to calculate complicated structures with fine mesh, and fabric structures may be carried out based on the geometry of the finite element mesh. Therefore numerical models of fabric structure using F.E.M are widely used in fabric structural design and analysis, even though physical models are still often built and tested for a general conception design.

Generally the thickness of fabric membranes is very small, and the stress and strain are assumed to be uniform across the thickness. Therefore fabric structures are often presented by planar elements like triangle or quadrilateral. Since the bending and compression stiffness of fabric materials are often ignored, then nodal rotations are often excluded in the element formulation.

Constant strain & linear strain triangular element – general principles

The application of finite elements to the fabric structure analysis started with the simplest element type, three node constant strain triangle(CST) with upgrading configuration by the geometrical nonlinear effects [98–102]. This element type, initially presented by Zienkiewicz [113], was proposed to solve 2-D plane structural analysis, and its capability and efficiency had often been discussed and compared with high order elements developed subsequently.

Felippa [103] researched the application of a 6-node triangular element in the analysis of linear and nonlinear plane problems, and compared this element with a classic triangular element, both in elastic and elastoplastic analysis. He found the classic constant strain triangle provided in general a reasonable displacement, but the interpretation of element stresses was often difficult, especially in regions of high gradients as shown in Figure 2.5,and 2.6.. Different averaging procedures to obtain nodal point stresses have been proposed [104, 105], but the results are usually poor near boundaries, where extrapolation (not averaging) is required.

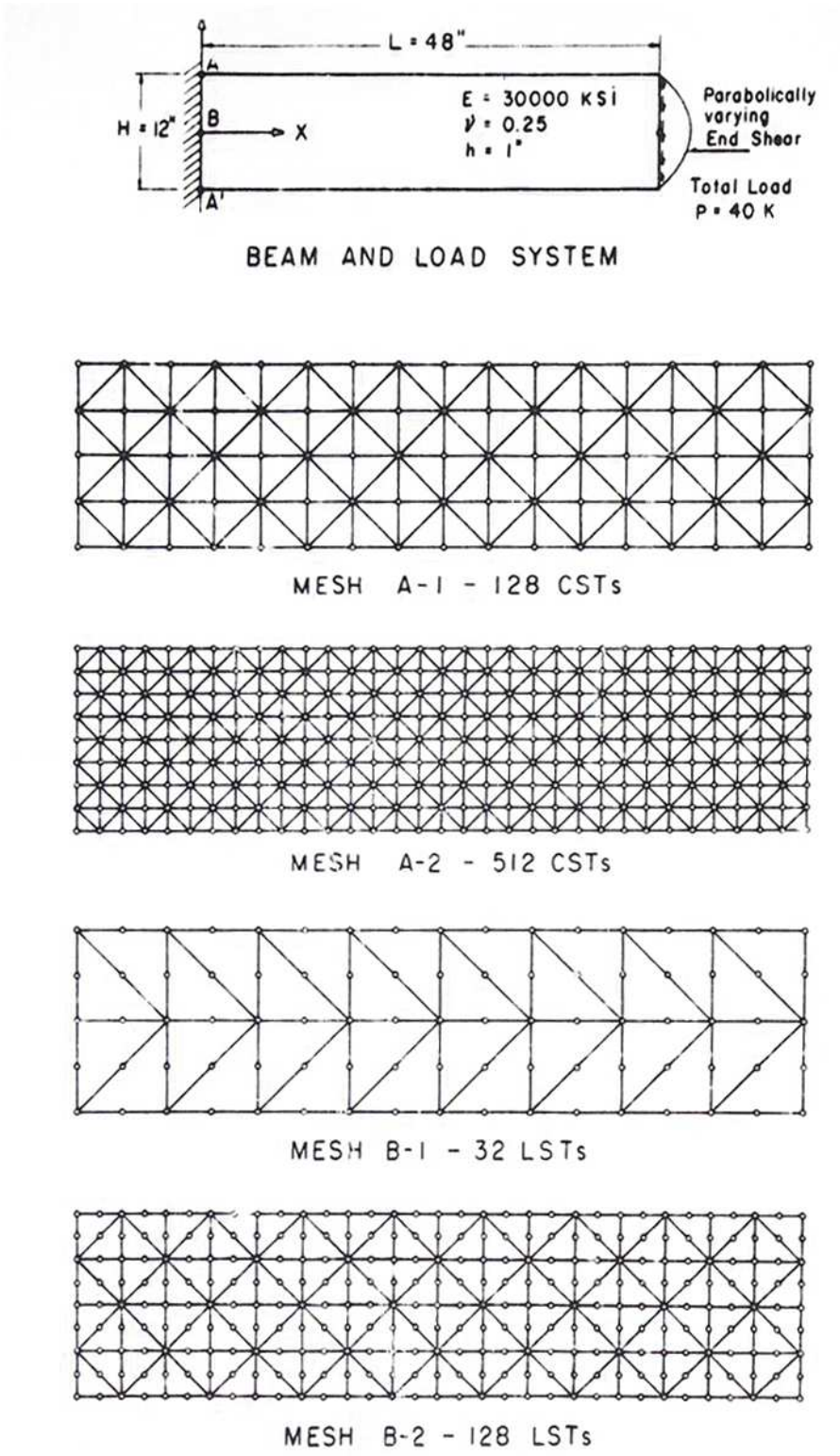

Figure 2.5: Cantilever Beam And Finite Element Mesh [103]

DEFLECTION AND NORMAL STRESS			
Element	Mesh	Tip Deflection $\delta = v_C$	Stress σ_x at X = 9", Y = 6"
CST	A-1 A-2	0.30556 0.34188	51.225 57.342
LST	B-1 B-2	0.35506 0.35569	59.145 60.024
Beam Theory (upper bound for v_C)		0.35583	60.000

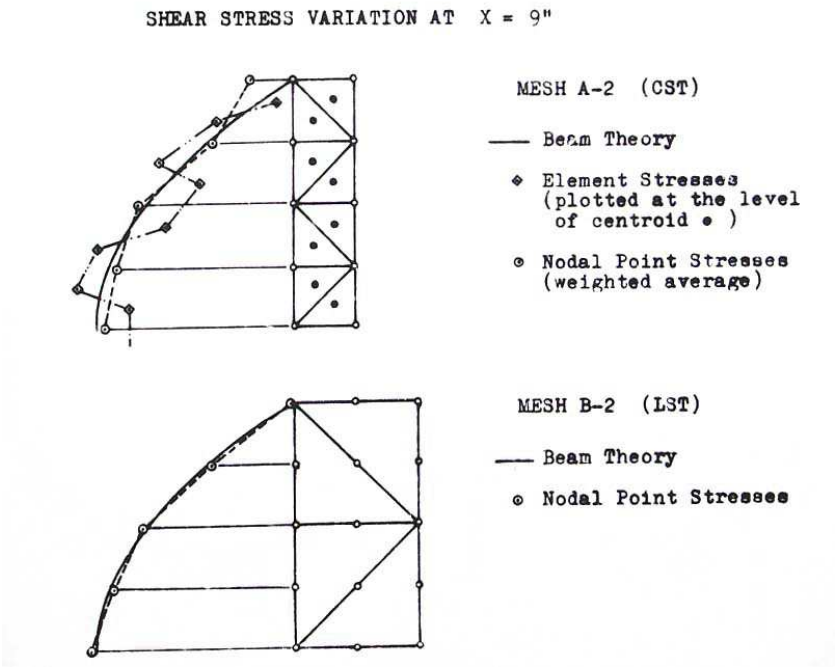

Figure 2.6: Cantilever Beam :Comparison between LST and CST [103]

This linear strain triangle has been extensively tried by De Veubeke [106] and found to represent a significant improvement over CST meshed having similar or larger numbers of degree of freedom. In particular, interface strain "jumps" are greatly reduced; nodal stresses obtained by simple averaging are extremely consistent and maybe used with confidence.

To overcome the disadvantage of the constant strain triangle element, Subramanian [107] advised that where using this element, a reasonable refined mesh can increase the accuracy of the result and reduce the computing time. For example it may be simple to use small-sized elements near areas of large stress gradients and large-sized elements in areas of small stress gradients. However the research of Dario [108] presented that for a same element mesh, the linear strain triangle may achieve a better solution than the constant strain triangle, even though the latter involve many more elements.

Hopefully any of linear strain triangle, constant triangle or other finite element can provide an adequate solution to virtually any plane problem if enough elements are used in the idealiza-

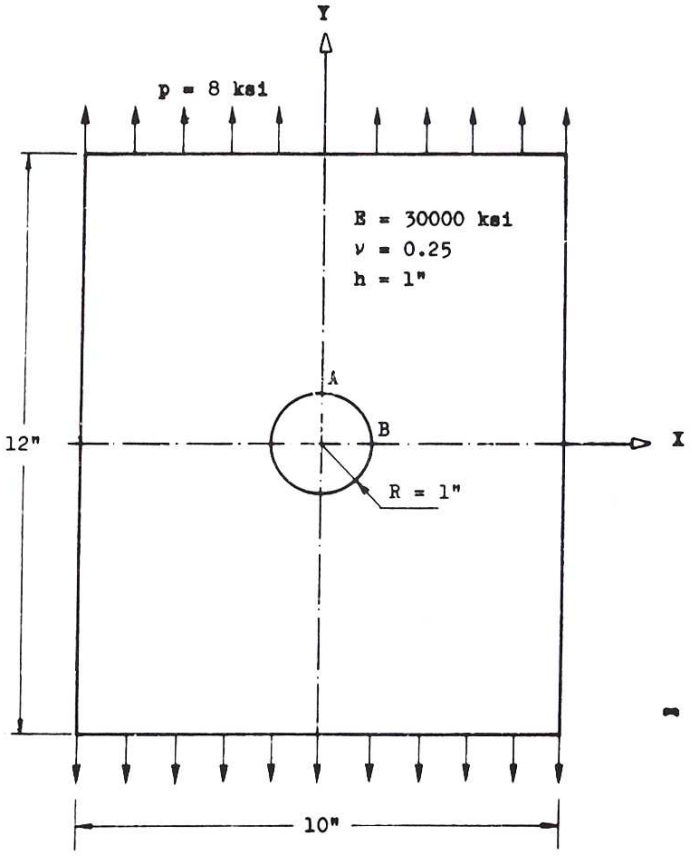

Figure 2.7: Plate with a Circular Hole under Uniaxial Tension [110]

tion. However, Lawrence [109] stated "the relative cost of obtaining acceptable solutions using the various element alternatives is normally the primary criterion for choosing one element type over another." He found the CST seems to be most economical element for problems where both flexure and high stress gradients are absent. While in cases where flexure or high stress gradients occur, the linear strain element appears to be the most economical.

To compare constant strain and linear strain triangle element using the same number of D.O.F, a specific case of a plate with a circular hole had been analyzed by D.Radaj [110] in figure 2.7, 2.8. He found both element type can achieve the analysis result(e.g. stress) with similar accuracy, when a large number of D.O.F are used. A very remarkable difference was found when using a relatively small number of D.O.F. LST gives remarkably better results. As the number of unknowns is restricted in practical problems, as far as possible, LST should be preferred to CST in practical problems.

D.G.Harrison [111] compared between low-order and high-order triangular element in solving field problem (e.g plate stress due to thermal affects), and his paper showed that consistently better results were obtained using high-order elements with same the number of elements, and roughly the accuracy level was related to the D.O.F involved in the element. He pointed out that computing time using two element types may be different, and the high order element

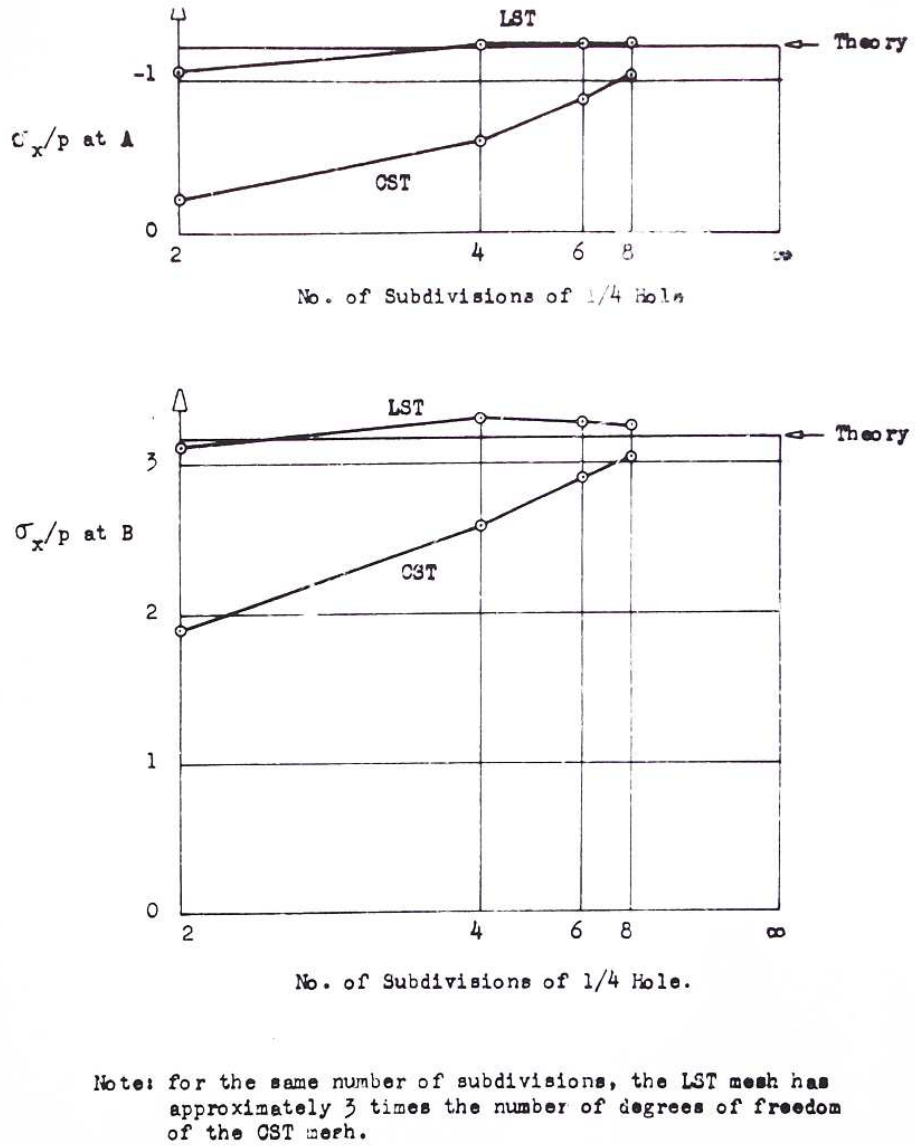

Figure 2.8: Plate with Circular Hole:Comparison of LST and CST Stress Concentration Factors [110]

can yield a more satisfactory result when more details like stress derivatives are required.

More high-order polynomial triangular finite elements have been compared by P.Silvester [112] when calculating the free vibration modes of an isosceles right triangular flexible membrane. The linear strain triangular element shows its better performance only for the first vibration mode (N=1), while the constant strain triangle had better efficiency with approximately the same accuracy in other vibration modes. His researches demonstrated that the LST was not found to be superior of CST in all cases, while their efficiency are still dependent on the cases.

For high order elements, the quality of elements may be significantly reduced when the relative displacement between middle nodes and vertex may produce a distorted element shape that will reduce the accuracy of the finite element formulation. In cases where the Jacobian of the finite element formulation vanishes (i.e $|J| \leq 0$), the element is considered to be collapsed because the finite element formulation will otherwise produce erroneous results. Many researchers [19–21] judge the element quality simply on the nonvanishing of the Jacobian, and more accurate mesh quality metric for the surface elements are developed [18].
In the form-finding procedure, the element distortion should be minimized to facilitate the subsequent loading analysis and pattern cutting, therefore element quality must be controlled in the form-finding procedure. Gosling [82] suggested the element distortion can be judged and controlled by evaluating and adjusting the ratios of nodal movement of the element.

Literature comparing the performance of the constant strain and linear strain triangular elements does not give a general conclusion about if which type of element is better under all the conditions. Generally, constant strain triangle may be sufficiently effective for a structure with a smooth geometry or stress distribution, and linear strain triangle may be better in the efficiency in case of structures with complicated shapes or high stress concentrations, and may provide more detailed information(e.g. linear stress contour) within the element. It is notable that in this section, the comparison of CST and LST is taken in the area of plane structures. When these elements are applied into fabric structural analysis, they may have different performance. Therefore Therefore either CST or LST cannot be verified to be advanced over the other from the literature review, and both element types may be worth trying for fabric structural analysis, and further comparison will be taken in Chapter 3.

2.2.3 Finite element formulation for membrane structures

The main problem of applying F.E.M in fabric structural analysis is the geometric nonlinearity. Because of the slenderness of geometry nonlinear structures such as fabric or fabric structures, the structural responses are nonlinear even if the strains are within the elastic range. For this reason, the nonlinear relationships between strains and displacements should be considered. To determine the responses of this type of structures, geometric nonlinearity has to be considered.

In the early work of finite element analysis for fabric structure [90], flat constant strain triangles

were implemented and the isotropic elastic material was assummed. The traditional Newton-Raphson solution procedure was adopted for form-finding and loading analysis. However this approach seemed to be only efficient when the form-finding started from a good initial trial geometry configuration, which may be not known before a initial analysis. To enhance the rate of convergence, a first analysis using a comparatively coarse mesh was advised, following a more refined mesh.

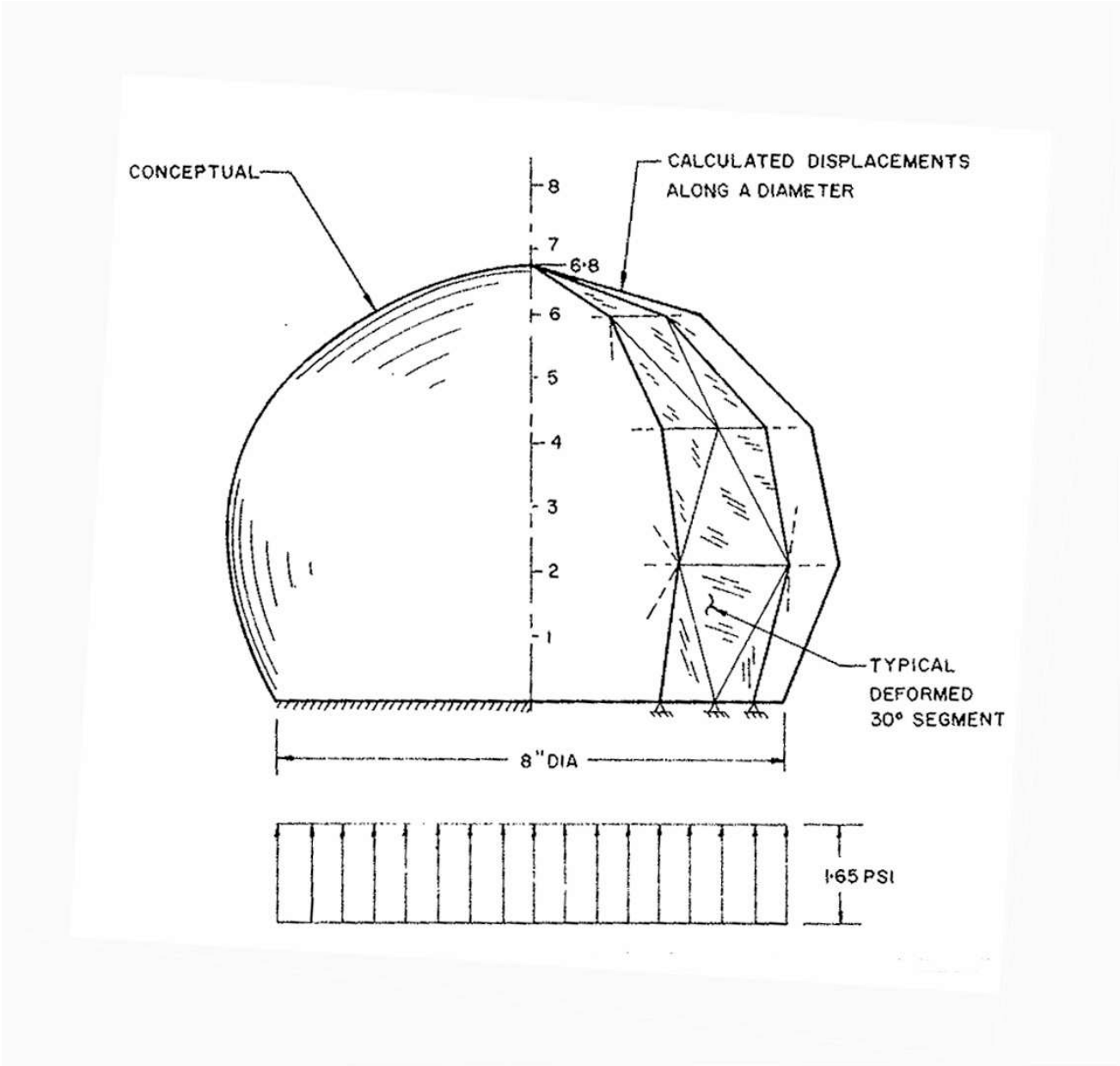

Figure 2.9: F.E analysis of an initially flat synthetic rubber membrane due to uniform pressure (Oden [90])

Tabarrok and Qin [85] developed a nonlinear triangular element formulation for the form-finding, loading analysis and pattern cutting of the membrane structures. The second order

derivatives of nodal displacements are involved in the element strain. In the form-finding and loading analysis, boundary cables and space frames are also taken into account as straight beam elements. To satisfy all the architectural and structural requirement of different types tension structures, three option types of form-finding algorithms, minimum surface, nonuniform stress surface and nonlinear displacement analysis approaches have been demonstrated. The wrinkling criterion based on the element principal stresses are also taken into account.

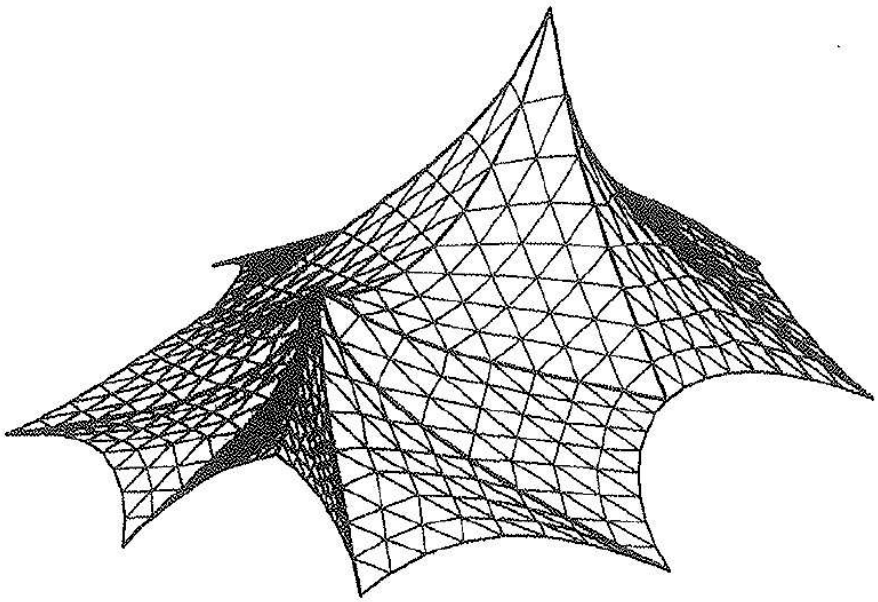

Figure 2.10: Form-finding using F.E method(Tabarrok & Qin [85])

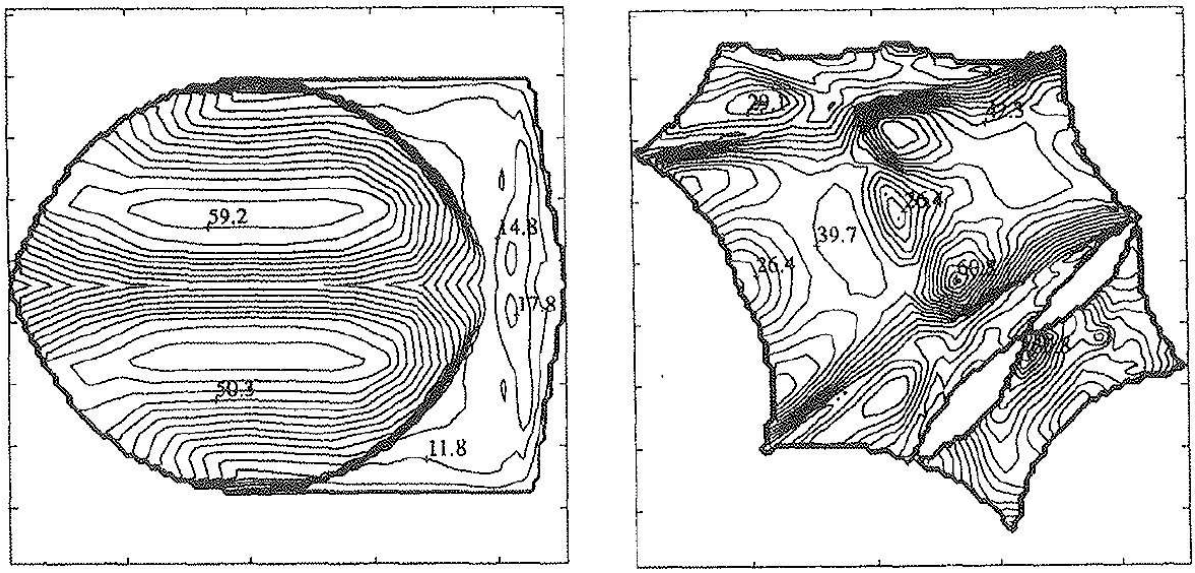

Figure 2.11: Stress contour obtained using F.E method(Tabarrok & Qin [85])

Besides triangle elements, quadrilateral elements were also applied to represent the fabric surface in the form-finding procedure by Gosling [212]. Coupled with a Dynamic Relaxation algorithm, this finite element formulation achieved high accuracy and computational efficiency

using only the diagonal terms of the element stiffness matrix. However the element curvatures and the relevant effects on the membrane stresses are not involved in the analysis.

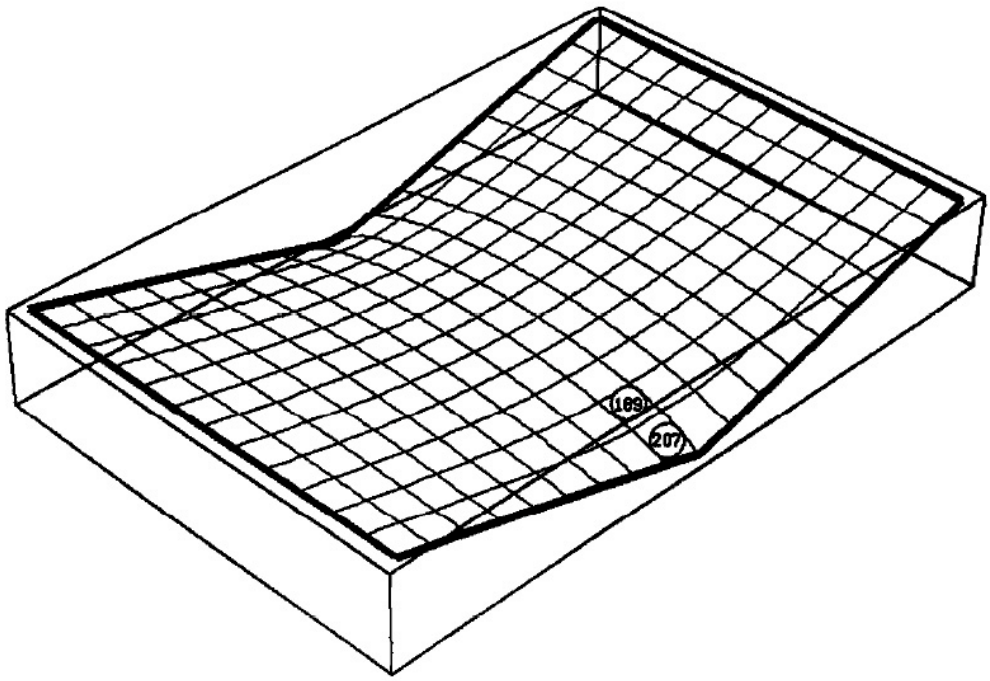

Figure 2.12: Form finding using quadrilateral element (Gosling [212])

Yexiao bing [217] has also suggested the relation between strains and curvatures in thin shell theory could be applied in fabric structural analysis. He succeeded in applying curvatures to the fabric structural analysis using LST elements without adding D.O.F. The curvatures can be spontaneously decided by the element geometry and updated during the calculation iteration.

According to the European Design Guide of Tensile Surface Structures [3], surface curvature is one of key things to decide the stiffness of fabric structures . In the CST finite element method, fabric surface is discretized by flat elements, then the curvatures are only implicit in the finite element formulation, but in higher order element method [217], curvatures of elements become most important factors to decide the membrane stiffness component normal to the element surface, and the curvature changing in membrane surface could be represented mathematically using different curvature terms in the local coordinate system.

2.2.4 Numerical method for solving the state equations

For membrane nonlinear model with both the material and geometry nonlinearities, the nonlinear equations derived from finite element formulation are often too large and complicated to solve directly, and a solution algorithm or approximation must be applied to ensure the

results are convergent and stable. Two basic approaches to solve the problems in form-finding and load analysis have been developed and applied in practice: matrix and vector methods.

The matrix methods are typically an application of more standard non-linear structural analysis such as the Newton-Raphson method [206]. In this method, the structure overall tangent stiffness is updated incrementally until convergence is obtained. Special controls limiting the maximum incremental deflections and nodal residual forces may be required. The stress-strain relations for the individual elements are coupled with the equilibrium and compatibility requirements for the whole structure.

A classic solution method with effective convergence rate, the Newton-Raphson method was applied in the form-finding [22] by Caner. However due to difficulties in producing the first derivative of the structural stiffness for the equation solving, computing costs are always high in cases with fine meshes.

In vector methods the conditions of equilibrium and compatibility are decoupled until convergence to an equilibrium solution. The most common approaches are Dynamic Relaxation (DR) [37, 38] and the Scaled Conjugate Gradient Method [39]. The former has been widely accepted for the analysis of tension structures because of its clear physical analogy and ease of implementation of the necessary controls and constraints. Nodal stiffness is used to calculate the displacements rather than stiffness matrix of complete structure, which is only to estimate the residual force based on the incremental nodal displacements from the last iteration.

A further method has been applied specifically to the form-finding of fabric or cable structures. This is the Force Density method, described originally by Scheck [16]. Force Density is defined as the ratio of forces to lengths, and the higher force density ratio means the shorter element for a given force. It is observed that a minimal surface is generated when the force densities for a node are equal and evenly distributed around the node. Once the equilibrium shape is determined, the unstressed cable length could be calculated from strain-stress relationship.

Although the Force Density method was initially applied in cable-net structures, recent research has extend the concept to triangular surface element with the name of the Surface Stress Density Method [40], in which the stress density is defined as the ratio of isotropic stresses to element areas.

The advantage of the density method is that it transforms the nonlinear equations to equivalent linear equations. The controlling element variable is that of force/stress density(for example T/l for a cable element of current tension T and length l, and σ/A for a surface element of isotropic stress and area).

As noted in [40], the main drawback of density methods is that because the geometric stiffness is difficult to be evaluated, "the shape developed is not easily foreseeable and stress distribution difficult to evaluate." This could be overcome by an "iterative smoothing" procedure with updated force densities by using a nonlinear solution procedure(e.g. Jacobi or Gauss-Siedal

method), but this would seem to make the equations still nonlinear and negate the advantage of a linearized solution.

The Force Density method is able to reduce the computing time to obtain approximate solutions, but these solutions may be inaccurate and mesh-dependent. The error analysis in the approximate finite element solutions has been taken by Bognar [68].

Another issue for these finite element methods and relevant solution procedures is their applicability for the cutting pattern generation, which is an important stage in the fabric structure design and construction. A suitable finite element should be consistently applicable during the main procedures of fabric structure design.

Phelan and Harber [51] suggests the analysis tool should be integrated with the design procedure, which follows three steps (a) reference configuration as determined by the initial equilibrium; (b) equilibrium analysis of loaded structures; and (c) determination of cutting pattern geometry.

Ishii [52] developed cutting pattern generation by using the geodesic line concept. To apply this concept to a curved membrane surface, he approximated the surface as a polyhedron consisting of triangular elements. For the geodesic line technique, Ataka and Kozuka [53] introduced a variation of the method, where the geodesic lines are approximated as linear elements.

Tabarrok and Qin [59] presented a cutting method for fabric tension structures by the finite element method. They used a weighted least-squares minimization flattening approach to minimize the change in general link lengths and to generate plane cloth coordinates. However, these works did not consider the material's extension after construction. Some discrepancies could occur between actual stress and designed stress because material properties are not considered. Due to this problem, fabric structures may encounter unexpected structural problems such as wrinkling and excessive stress after completed construction. Therefore, it is most important that the deviation between actual stress at the construction stage and design stress given by the designer is diminished as much as possible. Such a cutting pattern procedure is defined as optimum cutting patterning.

Tsubota [60–62] firstly introduced an optimization procedure which forms a membrane stress distribution in the actual assembled equilibrium state as close as possible to the uniform stress distribution specified in the design stage. In Tsubota's procedure, the boundary nodal points in the 2-D coordinate system are selected as control variables to determine the optimum cutting patterns. By this method, the actual assembled state is brought close to the uniform stress distribution specified by successively is considered as somewhat inconvenient for two reasons: (1) Separating elements into inner and exterior, and (2) the line fitting procedure on exterior points at each iteration. Yagi and Ohmori [63, 64] presented a new approach for cutting pattern analysis of membrane structures. The equilibrium state after deformation is

simultaneously considered together with the configuration of the cutting pattern as the state of pre-deformation.

Even though the pattern cutting procedure is not directly involved in this PhD thesis, it is a very important procedure in the fabric structure design and construction. The reviews on the applicaton of FEM on patterning demonstrates that a efficient pattern cutting can be achieved by based on a form-finding result using F.E.M, and from another aspect, reveals the potential of the finite element on the fabric structural analysis.

Wrinkling is another important issue of the fabric structural analysis. Because most fabric materials have little resistance in compression, when the tension stress reduces to zero along any direction, the membrane surface will start to buckle along that direction, and wrinkling will subsequently appear with the further compressive strain. Wrinkling will cause the bad appearance of fabric structure, and negative effects in architecture, and most important, may cause membrane surface distortion and stress concentration and probably result in the structural failure due to the stress concentration at local areas. Therefore wrinkling is always to be avoided in the fabric structural design and analysis as one type of structural failure.

Wrinkling can be considered in a good analysis tool for fabric structures. The first issue is to detect the wrinkling existing during an analysis. Initially Frei Otto [87] proposed a wrinkling judgement criteria based on the element principal stresses as table.2.4. The constitutive equations (for an isotropic material) are evaluated for given strains. Any influence of the wrinkle remains unconsidered, and the stress-strain relationship may change in the wrinkle area. The maximum principal stress σ_I may be overestimated by using the stress-strain formulation without wrinkling effects.

Stress state	Wrinkling	Membrane
$\sigma_{II} > 0$	No	Taut
$\sigma_I > 0$ and $\sigma_{II} < 0$	Uniaxial	Wrinkled
$\sigma_I \leq 0$	Biaxial	Slack

Table 2.4: Wrinkling criteria based on principal stresses

Miller [88] proposed another wrinkling criteria based on element principal strain as table 2.5, however this method is only limited to isotropic material.

Stress state	Wrinkling	Membrane
$\varepsilon_I \geq 0$ and $\varepsilon_{II} \geq \upsilon\varepsilon_I$	No	Taut
$\varepsilon_I \geq 0$ and $\varepsilon_{II} \leq -\upsilon\varepsilon_I$	Uniaxial	Wrinkled
$\varepsilon_I \leq 0$	Biaxial	Slack

Table 2.5: Wrinkling criteria based on principal strains

To overcome the disadvantages of both criteria either based on the principal stresses or the principal strains, Roddeman [89] used a wrinkling judgement criteria combining principal strain and stress as shown in Table 2.6. That method is applicable for both isotropic and

anisotropic materials. If the minimum principal stress is greater than zero, the membrane is taut. When the maximum strain is less than zero, the membrane is slack. In other cases, the membrane is wrinkled.

Stress state	Wrinkling	Membrane
$\sigma_{II} > 0$	No	Taut
$\varepsilon_I \geq 0$ and $\sigma_{II} \leq 0$	Uniaxial	Wrinkled
$\varepsilon_I \leq 0$	Biaxial	Slack

Table 2.6: Wrinkling criteria based on principal strains and stresses

If wrinkling is detected in the membrane, the procedure of the element enrichment must be taken immediately. When partial wrinkling happens, near the wrinkle area, the membrane only has stiffness and stress vectors along the wrinkle directions, so modification of the stiffness is necessary. During the calculation, if stiffness normal to the wrinkle direction is set to zero, then any force vector could cause infinite displacement, which is obviously unreasonable for membrane analysis, and the loss of ability to carry load due to wrinkling may be temporary , and disappear with further displacements. In the iterative process of calculation, the elastic stiffness matrix is modified only due to large deformation of the structure, and the geometric stiffness matrix takes into account a wrinkling effect using modified actual stresses. When wrinkling is detected in any element, the nodal reaction force of the element will also be modified according the wrinkle condition, so that when any force vector is applied in the wrinkled area, out-of-balance forces of the wrinkling elements will remain or partially remain until the wrinkle disappears.

Reviewing the research of the element enrichment, there are two different approaches developed: one, proposed by Roddeman [89] is to define an effective deformation gradient, which is a function of the normal displacement and a term connected with wrinkling formation. The other approach is to modify the relationship between strain and stress (material properties). The former is more rigorous than the latter, but it is commonly recognized that the convergent result is not always smooth.

The main advantage of the second approach is that the implementation for the element enrichment is independent from the element used, so the simple wrinkling procedure can be settled easily to the material model. Unfortunately, the solution convergence tends to be very difficult, and the stabilization is necessary.

Rossi [237] proposed an algorithm for the stabilization of the material manipulation. Using his method, if the membrane is in a "wrinkled state", a modified elastic stiffness has a small but non-zero value across the wrinkling direction, then a stable convergent solution can be achieved since there is no zero stiffness matrix. Even though that will result in some compression force left in the first iteration, however the compression force can be eliminated by reducing stiffness in the following iteration.

In this PhD thesis, the wrinkling analysis aims at wrinkle detection and element stress mod-

ification during the fabric analysis. The wrinkle details like wrinkle patterns and depths are out of the scope of this PhD research and not involved in this thesis.

2.2.5 Conclusion

With the development of computers, detailed fabric structural analysis has been made using numerical models, and physical models like soap films are limited to the conceptual stage. With an efficient solution strategy, a minimal surface approach based on minimal area calculation can give a good representation of the membrane surface. However it is mainly limited to the form-finding stage.

The fabric surfaces can be also possibly represented using finite element methods. Constant strain and linear strain triangle elements have been compared and discussed for their efficiency and accuracy. However it seems that either type of element may have better performance over the other one in different cases, and it is hard to justify which type is better to be applied in the reliability analysis of fabric structure from the literature. It is recommended that both types of elements may be tested as trials, and further judgement can be made based on more detailed comparison in accuracy and computation efficiency which are given in Chapter. 3.

Both flat and curved element types have been applied to form-finding and analysis of fabric structures. Currently, the constant strain triangular element has been widely applied in fabric structural design and analysis, because it is the first and simplest application of the finite element form on the fabric, and its neat formulation is very helpful for achieving a smooth convergent solution. While curved elements with linear strains may have a better simulation in the geometry of the fabric surfaces which normally have double curved shape, and the membrane stresses and surface geometry can be explicitly related by element curvatures.

To solve the difficulty in the form-finding and loading analysis owing to the high geometrical nonlinearity, different numerical methods for solving the state equations are reviewed and compared. The matrix methods like the Newton-Raphson method may have difficulties to produce an highly efficient solution procedure, and the computation costs of obtaining the derivatives of the stiffness matrix may be too high. Both the force density method and Dynamic Relaxation algorithm can provide very efficient solution processes, by avoiding the complicated matrix operation, however the accuracy of the density method may be insufficient and mesh-dependent.

For the wrinkling issue, the wrinkle appearance in a fabric can be judged by element principal strains and stresses. A wrinkling criterion combining principal strains and stresses is recommended by the literature to avoid the wrinkling effect in the stress-strain calculation. To achieve a smooth solution procedure with wrinkling, the element stiffness across the wrinkling directions are assumed to be low ratios of the original stiffness values to avoid ill-condition in the stiff matrix.

2.3 Probabilistic testing of fabric materials

Researches on the basic characteristics and test methods of fabric materials are reviewed initially in this section. Several existing deterministic modelling approaches of fabric materials are then discussed, and their potential uses for probabilistic analysis are also reviewed. Finally the discussion concentrated on the current research on probabilistic properties of fabric materials, and their contributions to the probabilistic testing and analysis of this thesis.

2.3.1 Nature of coated woven fabric

Fibres, yarns, coating & weaving

The coated woven fabric is the composite of woven yarns and coating materials as illustrated as fig.2.13.

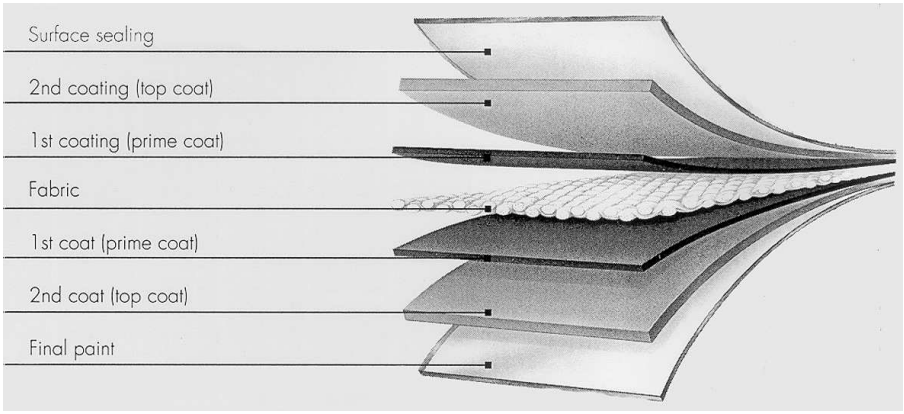

Figure 2.13: The components of coated woven fabric [12]

The basic elements of composite fabric are fibres, and most of them exhibit nonlinear stress-strain relations, creep under loads, and viscoelastic mechanic properties. That inevitably determines their assembles - fabric owning inelastic and nonlinear mechanism. There are variety of fabric fibre and yarns used in structural fabrics. Polyester and glass fibre are the most common fibres used for architectural fabrics, and other yarns include Aramid(aromatic polyamide) and LCP(liquid crystal polymer based on aromatic polyester).

Both Polyester and glass fibre exhibit non-linear and inelastic tensile behaviour [117, 118]. Their strength and elastic modulus vary in some range instead of a single value [119], but glass fibres and polyester fibres are fundamentally different in terms of micro-structure and hence stress-strain response: Glass fibres have an approximately linear stress-strain response as fig.2.15, whereas polyester fibres are distinctly non-linear as fig.2.14.

The mechanical properties of different common fibres are viewed by Buckley [117]. He demonstrated some fibres are very prone to be affected by environmental factors like temperature, humidity, and the "aging", which may significantly reduce the fibre stiffness. The geometries of the fibres are also important to their mechanical behavior, for example, twisting and bending may complicate the stress-strain relations of the fibres.

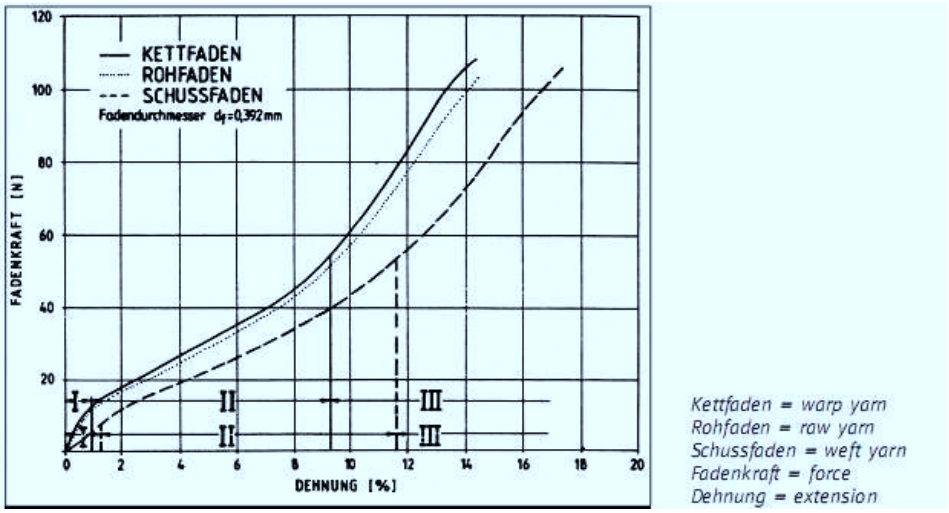

Figure 2.14: Stress-strain relation of polyester yarns [12]

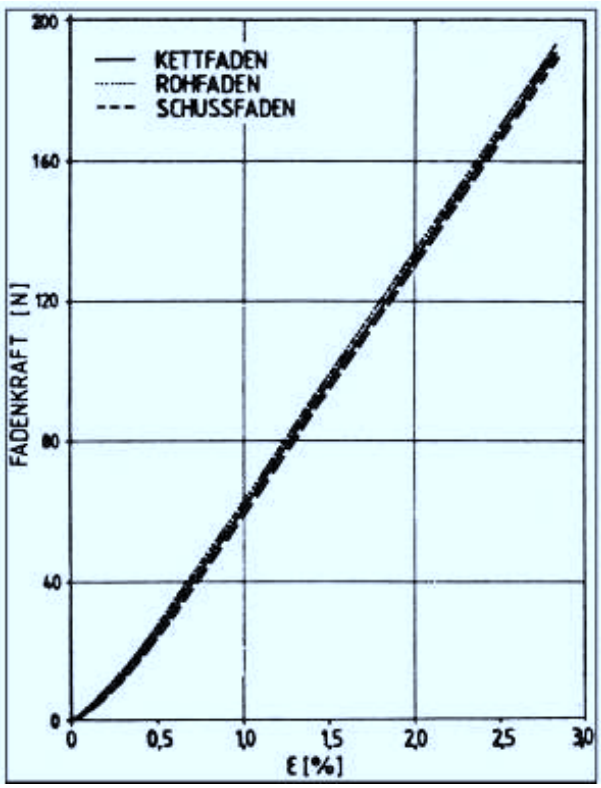

Figure 2.15: Stress-strain relation of glassfiber1 yarns [12]

The mechanical behavior of the yarns in a fabric is normally complicated, and the load-deformation relation is hard to express using the traditional analysis method, Jong [41] developed an energy optimization method to investigate the recoverable mechanisms of fabric deformation, based on the principle of minimum strain energy.

As a protection of yarns, coating materials provide a lot of good chemical resistance like fire retardance and fungal resistance. The coating improves the properties of woven fabric in both shear and tension strength, because the coating will restrain the yarn movements and interactions, adding a visco-elastic effect to any deformation mechanism [123]. Coatings can penetrate between the yarn fibres and modify the yarn properties. If friction between yarns is ignored, an uncoated fabric offers no resistance to yarn rotation and therefore has no shear stiffness, so the resistance to shear deformations arises almost entirely from the coating [124]. The coatings are normally made of PVC or PTFE materials [12].

Coated woven fabric

A woven fabric is composed of two sets of yarns that pass over and under one another in a specific pattern. The warp yarns run along the length of the fabric and the fill yarns across the width. These two sets of yarns are at right angles to each other in the plane of the fabric as shown in fig.2.16. Because of the weaving, the yarns assume a waviness, called crimp [125],in a plane perpendicular to that of the fabric. When tension is applied in the plane of the fabric, say in the warp direction, the effect is to reduce the warp crimp and increase the fill crimp. This is called crimp interchange because the warp and the fill crimps always remain complementary.

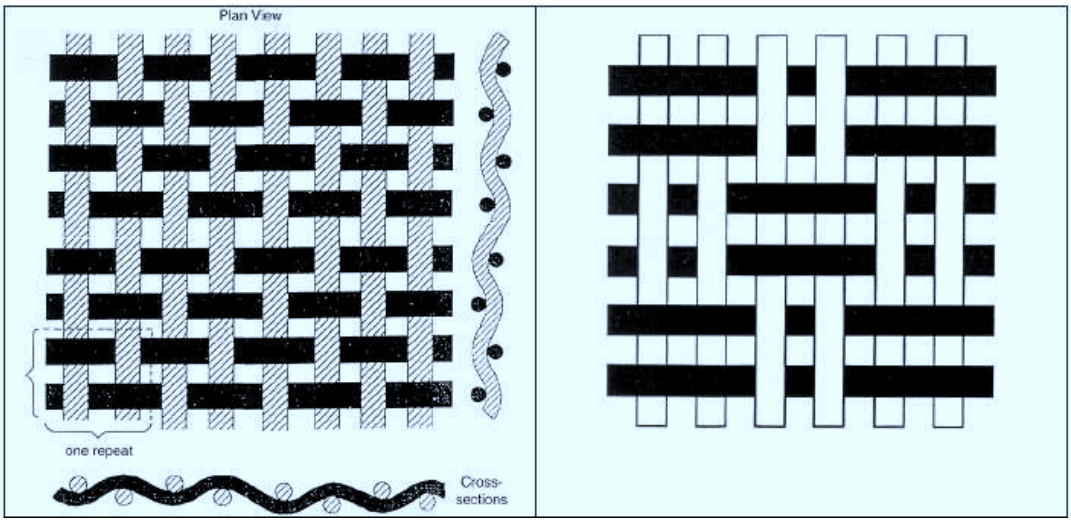

Figure 2.16: Plain weave pattern and basket weave pattern [12]

As a woven composite material, fabric exhibits highly nonlinear mechanical behavior owing to the viscoplastic nature of its fibre elements. The crimp interchange also complicates the load-deformation relations especially when carrying various loads in biaxial directions. The

material failure mode and ultimate strength of the fabric are shown to be related to the micro-structure form of the matrix [24].

The manufacture and properties of the fabric material had been reviewed by Hearle [42], and he emphasized that compared with traditional structural material, fabric material has more uncertain and sophisticated mechanical properties owing to the uncertainties during its manufacture process. For example, the elemental fibers have a variety of cross-section, and also numerous weaving patterns. All these variations lead to the instability of the fabric material in mechanic properties.

The analysis of the tensile behavior of plain woven fabric was taken by Leaf [45] with one small strain and two large strain approaches. He pointed out that assuming circular yarn cross-section in the fabric analysis is not realistic, because the compression from the transverse yarns will impose on them and change the geometry.

From the research [28, 36, 43, 124] into the fabric behaviour under tension, the stress-strain relation of the material largely depends on the ratio of stresses applied to the membrane, because the meso-structure form of the crimp changes under various loads that is deemed to affect the strain exchange ratios of the warp/fill yarns. The simulation of the meso-structure of the crimp is very important in predicting the mechanical behaviors of the fabric under different loads, and a lot of researchers [126, 144, 163] proposed their models, amongst which, the truss model [163] based on the lattice formation of the fabric is found to be effective and accurate for both uniaxial and biaxial tensioned fabric membranes. The membrane cell which composes double yarns in both fill and warp directions, is simulated by a set of bar elements, and the stress-strain relation is derived based on the mechanical response of the simulated truss system.

YI Honglei [28] believed that the uniaxial and biaxial elastic models of the fabric material are not independent, and the uniaxial loading states can be considered as one special type of unaxial state with zero stress along one direction. The stress strain relation under the biaxial loads with different loading ratios can be approximately estimated based on the unaxial deformation properties obtained from uniaxial tension tests, however the accuracy of this estimation is not hard to be justified because of the highly nonlinear mechanical performance of woven fabrics.

The review of the nature of coated woven fabrics demonstrates that high mechanical nonlinearity, variability and complexity are the basic characteristics for the fabric as a composite made of woven yarns and coatings. Large variability already exists in the fibres and yarns, and their composites could have much higher probabilistic properties. Crimp-interchange with visco-elastic yarns leads to a complicated structural performance (e.g stress-strain relations) when dealing with loads. Therefore the probabilistic investigation and analysis of coated woven fabric must allow for its highly nonlinear and inelastic mechanical behaviour with the environment aspects (e.g. thermal effect)

2.3.2 Determination of fabric material properties(structural analysis & probabilistic analysis

Material test method

There are a series of tests given by the European Design Guide for Tensile Surface Structures [13] as fig.2.17 to measure the mechanical properties of fabric materials. However not every test method and procedure has been given in national codes and standards, and further research and development is still desired for most of these test methods. The uniaxial tensile test is the simplest of these tests, and most countries have similar test procedures regulated in their national codes. Of course, in the real case, the fabric is tensioned in biaixial directions. Therefore the realistic fabric mechanical strengths may be more related to the ultimate stresses obtained from biaixial tests. However because the biaxial tension strength is very difficult to obtain directly [13], currently the uniaxial test is still the most important test to measure the fabric material strength.

Mechanical characteristics of the coated fabric	Unit	EN standard	ISO standard	National standards	Alternative Proposal
· Tensile strength (warp, weft)	daN/5cm		EN ISO 1421	NF G 37103 ; BS 3424 part 4 Method 6 ; DIN 53354 ASTM D 4851	
· Tear strength (warp, weft) - trapezoïdal test	N		EN ISO 4674-2	NF G 37130 ; BS 7304 part 44; ASTM D 4851; DIN 53363	LBV 1111
· Elongation at break (tensile test)	%		EN ISO 1421	NF G 37103	
· Coating adhesion			EN ISO 2411 ISO 5978	NF G 37107 ; BS 3424 part 7 ; DIN 53357	
· Biaxial behaviour ratios 1/1, 2/1, 1/2,5/1,	daN/5cm				LBV 1106 /(LBV 1107)
· Elastic modulus					LBV 1501
· Poisson´s ratios					
· Creep, relaxation		EN ISO 899-1			
· Fatigue behaviour					
· Shear modulus shear angle					LBV 1110 LBV 1112 (uniaxial)

Figure 2.17: Commonly used standards for fabric tests [12]

Uniaxial fabric testing

Uniaxial strip tests for coated woven fabrics are defined by BS EN ISO 1421:1998. The most common way is to measure the ultimate strength of 50mm width fabric strips, cut along yarn directions. Nowadays this test is the most important test to determine fabric ultimate tensile strength, because the test procedure is very simple to operate with, while the biaxial strength is hard to measure [13], even though fabrics are normally tensioned biaxially. Therefore, in most cases the realistic structural fabric strengths are more relative to the biaxial strengths which is generally less than the uniaixial strength, because of extra strains produced by the yarns in the other direction due to the crimp interchange [13].

Biaxial fabric tensile testing

Currently, there are no British or European standards for the biaxial testing of coated woven fabrics. The biaxial test method using a cruciform fabric specimen has been developed by a

number of researchers [147–149, 152]. The main purpose of this test is to observe the stress-strain relations when the fabrics are tensioned in both fill and warp directions. The typical cruciform biaxial test is illustrated as fig. 2.18.

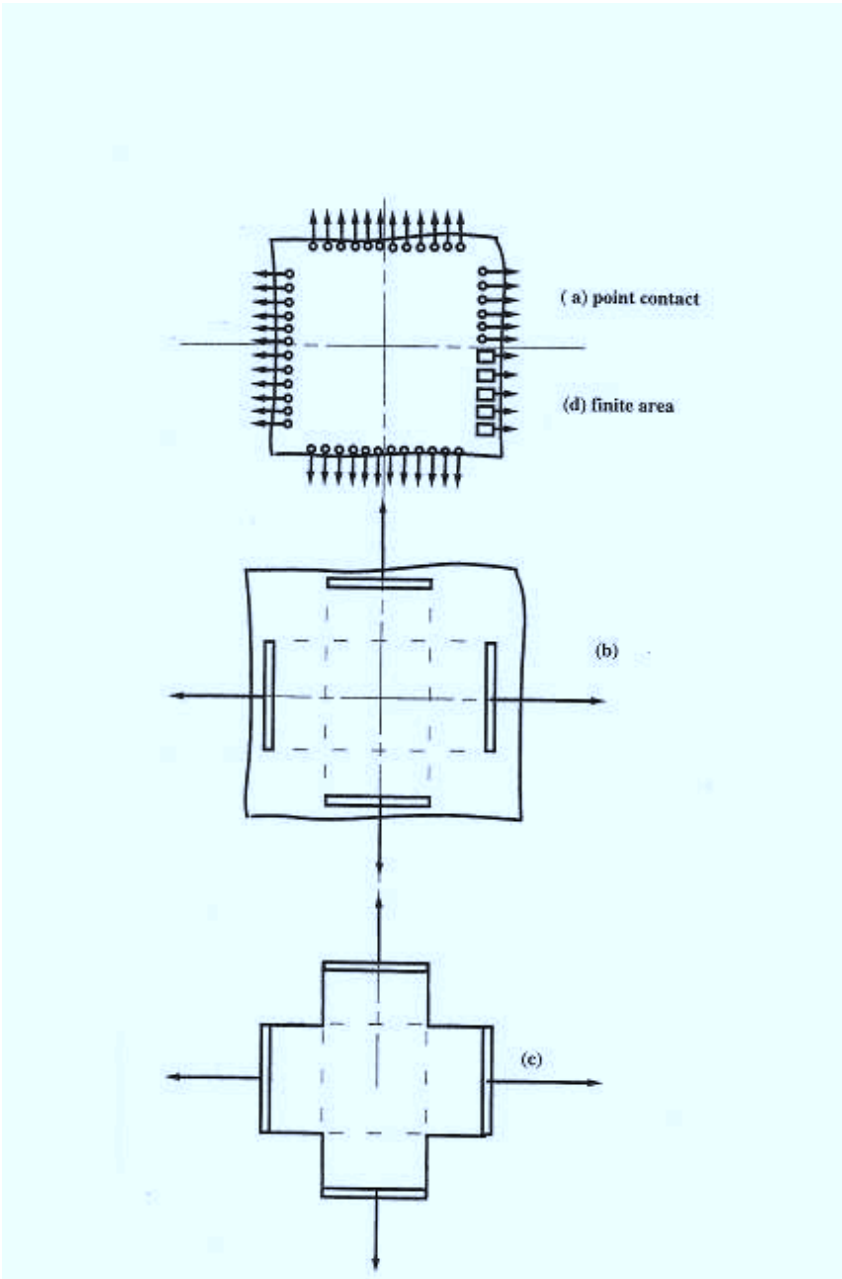

Figure 2.18: Biaxial test of a Cruciform fabric specimen [152]

This cruciform test sample can make it easy to test the stress-strain relation under different stress ratios between fill and warp yarns. However this test will be much more time-consuming and difficult to handle, because the crimp will not be immediately adjusted with the applied biaxial loading, while be slowly deformed until a balanced crimp configuration, due to the viscoelastic property of the yarns.

Shear fabric test

The shear modulus of a coated woven fabric can be obtained through either biaxial(fig.2.19)or uniaxial test(fig.2.20). The major difficulty of the shear test is the buckling of the fabric, which may be resulted by shear strains. Because once buckling happens, the load observed will be contributed by not only by shear forces, but also biaxial forces from fills and warps. Therefore the shear angle have to be limited to ensure non-negative stresses in test samples.

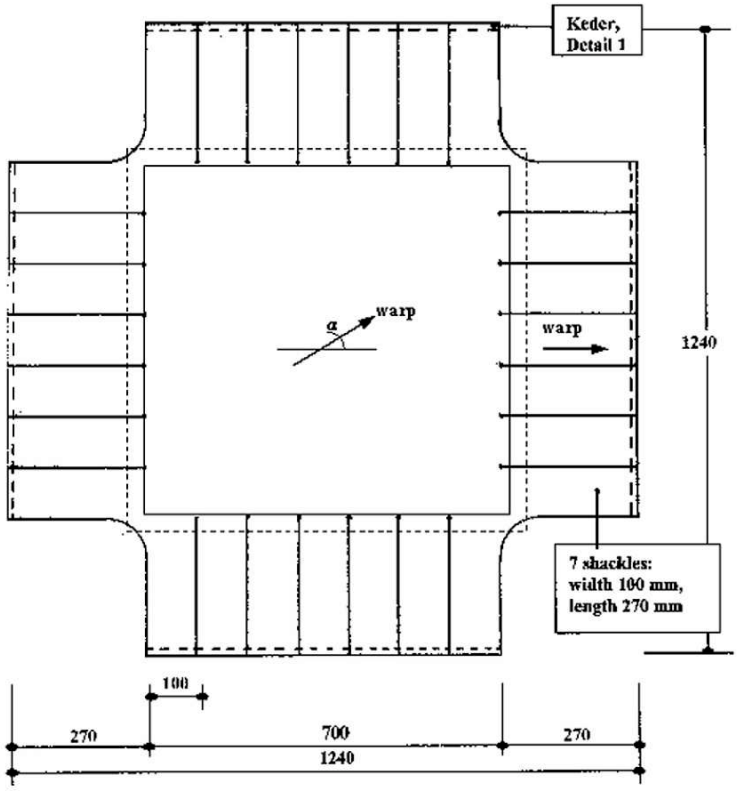

Figure 2.19: Biaxial test for shear modulus [13]

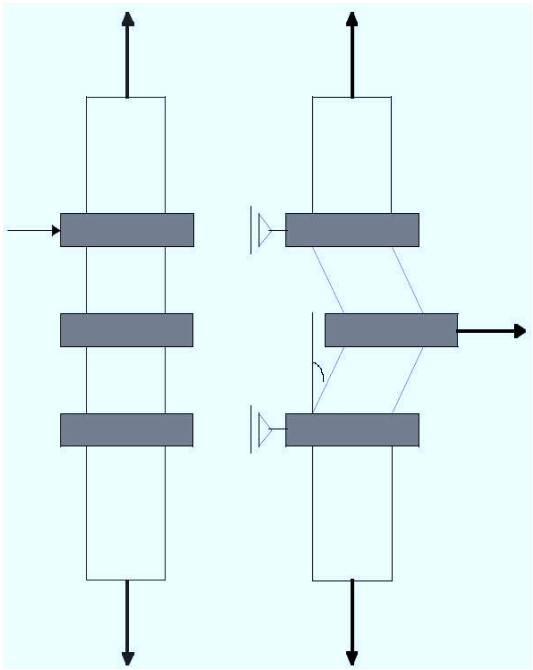

Figure 2.20: Uniaxial test for shear modulus [13]

Potential of numerical/analytical material models as physical continuum

A lot of numerical and analytical models had been proposed to represent the mechanical behaviour of the meso-structure of the woven fabric as fig. 2.21-2.24, however most of them do not account for the interaction between yarns like crimp interchange, locking and relative yarn rotation, and the implementation of these meso-structural models is shown to be difficult for more general load cases. King [25] developed a new continuum constitutive model which simulates the woven fabric as a anisotorpic continuum, and takes the meso-structure behaviour into account. His macro-structural model is shown to be accurate and efficient to predict the fabric behaviours under uniaxial loads, however was not verified by biaxial tension experiments.

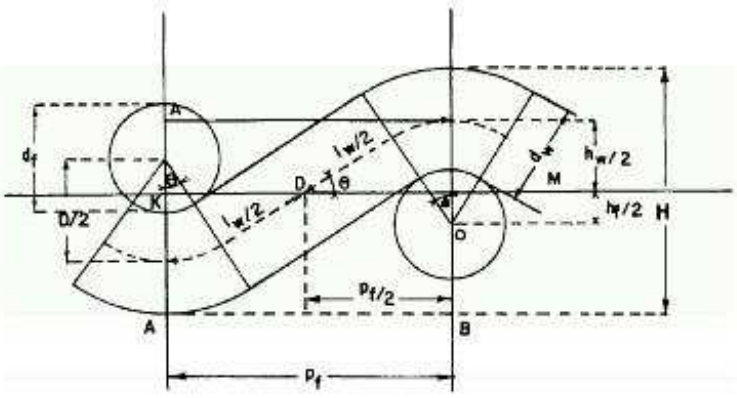

Figure 2.21: Geometry proposed by Peirce(1937) [50]

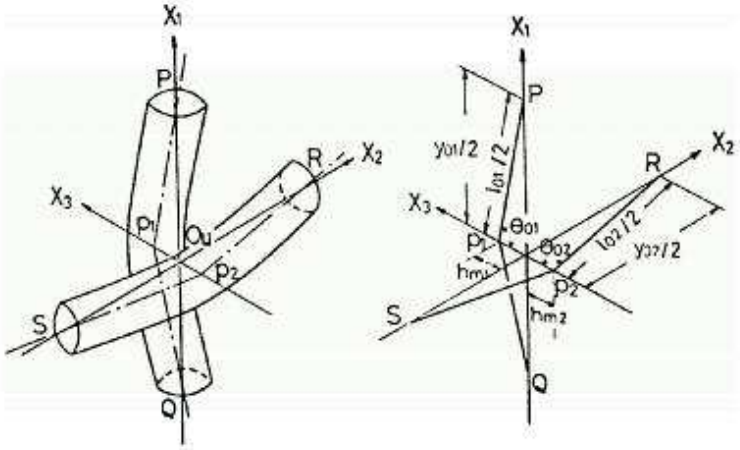

Figure 2.22: Geometry proposed by Kawabata et. al. (1973) [144]

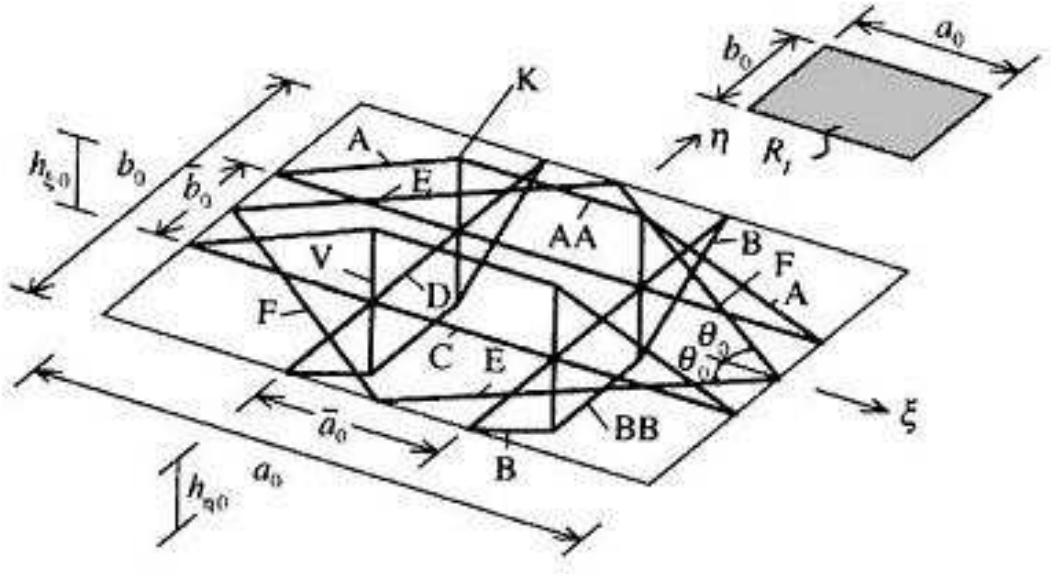

Figure 2.23: Fabric lattice geometry propsed by Kato et. al. (1999) [163]

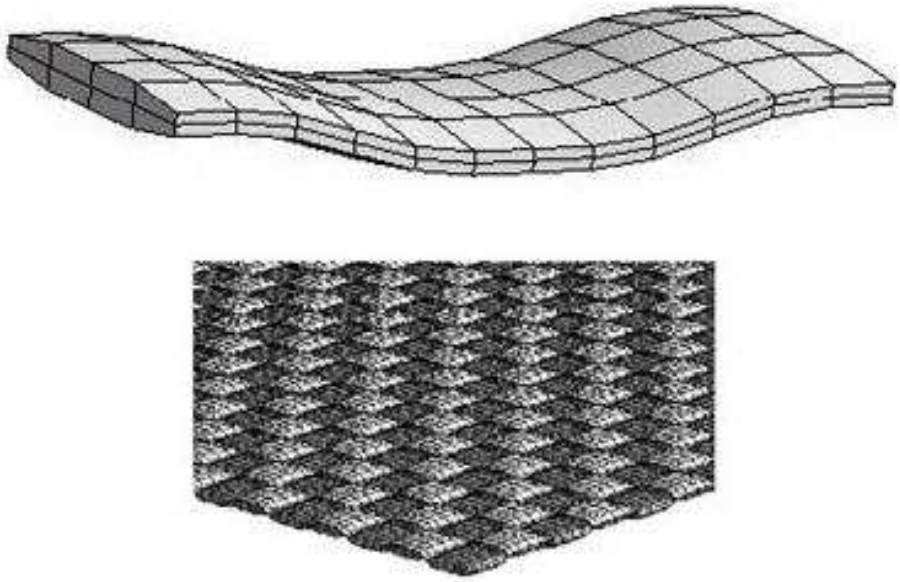

Figure 2.24: Shockey's detailed FE model of a plain weave reinforcing fabric (Shockey et al.,1999 [164]

In many cases, fabric is assumed to be an orthogonal material, that warp and fill yarns are woven at right angles, however owing to the variation in manufacturing, the yarns in two directions may be invalid for orthogonal material assumption. Yu [26] developed a non-orthogonal constitutive model for fabric reinforced thermoplastic such that the micro-structure information (i.e. the fibre angle) was incorporated into the constitutive stiffness matrix. His model is shown to be capable of predicting angle change of the composite under the loading draping.

Potluri [27] had simulated the meso-structure of the fabric crimp under uniaxial and biaxial tensions using a finite element model that indicates the uniaxial tension will increase the modulus along the tension direction while reduce the stiffness in the transverse. In contrast, biaxial tension will increase the stiffness in both directions as the results of crimp reduction.

Tremendous amount of work dedicated to the modelling of woven composites intends to predict the elastic properties of the materials and only few of them consider the failure behaviour. The reason for this is the complex phenomena affecting the progressive failure behaviour of woven fabric composites. These phenomena are the material non-linearity of the matrix material combined with the geometrical non-linearity of the fibre reorientation and the damage accumulation with stress concentration in the interacting constitutes.

The material failure mode and ultimate strength of the fabric are shown to be related to the micro-structure form of the matrix, which is often simulated by a finite element or other numerical model [24]. Many constitutive models of the composite materials are developed,

accounting for all the major behavioural characteristics. However, the accuracy of these numerical models need to be quantified by a large number of experimental tests, that are normally expensive and impracticable.

Modelling coated woven fabrics as a continuum is very useful for the structural analysis especially in large-scale and meso-scale, because estimated stiffness fully accounting for the crimp behaviors can be easily coordinated with the existing finite element formulation. The application of these formulations can be achieved by only adjusting the constitutive stiffness matrix according to different material type and loading conditions.

Potential of numerical/analytical material models as physical analogues

The unit cell approach is employed in the analysis of most material models of woven composite structures. The composite structure is divided into repeated cells, representing the properties and the behaviour of the whole lamina. The classical 1-D models of Ishikawa and Chou [131, 132, 134, 135] were extended to 2-D elastic models by Naik et al. [136, 137]. Naik and Ganesh [137] considered the failure in the fill yarn direction of loading only. Naik and Ganesh [137] divided the sub-cells of their representative volume cell (RVC) into many slices. They used different failure criteria for the different constituents: Tsai-Wu failure criterion for the fill strand, maximum strain criterion for the warp strand and maximum stress criterion for the pure matrix material. After the matrix material failure in the "gap" region, the fill strand is modelled as a curved cantilever slender beam.

Naik [139] developed 3-D micro-mechanical material models of woven and braided fabric composite materials with failure. The failure criteria and the stiffness degradation scheme are presented by Blackketter et al. [140]. Blackketter et al. applied shear material non-linearity and stiffness degradation to a finite element model of the woven fabric composite RVC and successfully simulated the damage propagation in tension and pure shear loadings in the yarn direction. The micro-mechanical material model of Naik is incorporated in a computer code called TEXCAD, which is used for failure analysis of fabric composite materials.

Tabiei et al. [141] suggested a micro-mechanical material model of woven fabric composite materials to simulate the progressive failure. The quarter sub-cell of the RVC is divided in many blocks. Micro-mechanical failure criteria for each constituent material in the block and corresponding stiffness degradation are adopted there. The material shear non-linearity described by Hahn and Tsai is included in the model.

The material models of woven fabric composites described above are suitable for non-linear finite element failure analysis of composite structures, but because of the high degree of RVC discretization, they are computationally inefficient to be applied in explicit finite element codes. The non-linear finite element codes with explicit time integration are very powerful for large-scale simulations but because of the inherent small time step for stable solution they require high computational efficiency of the material models. This characteristic is an

obstacle for complicated micro-mechanical models to be implemented in the explicit codes. Ala Tabiei [142] developed a computationally efficient and simplified micro-mechanical model of woven fabric composite materials to predict their elastic properties. The advantage of the model is the lack of RVC discretization and good elastic property prediction. The choice of the RVC is intended to account for geometrical non-linearity and simple and efficient technique for fibre reorientation was incorporated in the model [143].

These cell approaches applied the fabrics can help to understand the mechanical behaviour in small-scale especially for the material failure. A lot of phenomena and information observed during material testing can be potentially analyzed using these methods. The structural failure process of fabrics (e.g. material rupture and propagation) can be possibly well explained by the analysis using one of these formulations.

Current research on probabilistic material properties of coated woven fabric

Normal distribution is most widely applied statistical distribution in the engineering industry. During the fabric manufacture, variations of fabric strengths may be affected by the uncertainties(e.g. measurement errors) following normal distribution, and a lot of researchers found the ultimate strength of the yarns as the assembles of fibres follows Weibull distributions [158], which is often used for extreme values of a set of observations.

The statistical properties of the yarns, cables, ropes are deemed to be related with the uncertainties of the fibres. Considering these materials as bundles of fibres, Phoenix [46] developed a statistical model to predict the stochastic behaviour of these materials, assuming that the fibre strengths follow Weibull distribution. In his model, more attention was paid in how the fibre length affected the stochastic property of fibre assembly.

As a composite of yarns and coating materials, fabric materials were initially modelled as bundles of yarns, and their probabilistic properties are often estimated based on the assumption of yarn distribution [133]. However it was found that the mechanical performance of single yarns is significantly different from that in coated woven fabrics, because of yarn-to-yarn frictions especially for biaxial loading. The simulation of realistic yarns structural behaivour can be estimated using reduced yarn lengths which vary with different fabric types. However this simulation lacks the theoretical support.

To solve this problem, Ning Pan [43] proposed a prediction model of uniaxial and biaxial fabric strength, based on the assumption of the Weibull distributed yarn strength, fully taking into account the yarn-yarn interaction at the interlacing point. He separated the yarn-yarn interaction into two components: adhesive and frictional ones, and the latter is shown to have much more effect on the fabric tensile strength. In his model, a fabric is assumed to be made of many sub-bundles of yarns, with the critical lengths of which are shorter than the realistic length of yarns, and derived based on the crimp conditions. With the simulation of the yarn-yarn interaction, the prediction accuracy of the fabric strength including mean

and standard deviation is significantly improved compared with the pure yarn-assembly model, however higher accuracy and stochastic details are still further desired for a qualified reliability analysis.

Currently, the research on the stochastic property of coated woven fabrics is mainly focused on the numerical modelling of the fabric inner structures, while the probabilistic investigation and analysis mainly based on the large quantity of material experiments are absent. With the lack of investigation on the realistic behaviour of coated fabric, the probabilistic estimation models are difficult to be verified. Therefore to achieve the accurate probabilistic information of the coated woven fabric, the investigation based on a quantity of material test may be taken.

2.3.3 Manipulation /transformation of material property data into a statistical form and available statistical forms

To facilitate the reliability analysis, all the uncertainties must be investigated and represented mathematically. Especially for the non-cognitive or aleatory uncertainty sources, a statistical investigation and analysis must be taken to obtain the stochastic information of the variables(e.g. wind speed, material strength) in the engineering system of interest with the mathematical description. Based on a certain quantity of past records and test data, the variations and distributions of the loads and resistance are determined through the statistical measurements. The common way to determine the statistical distribution for a variable of interest is to select closest distribution among a set of optional distributions which are usually applied in engineering through a data-fitting test(e.g. χ^2 test).

Except than normal and log-normal distribution, other distributions like extreme value distributions have been often utilized as well since the fact that the maximum and minimum values of statistical variables often take very important roles in the reliability analysis, for example, the maximum wind load and minimum load resistance. In a lot of composite materials, the material strength may depend on the failure stress or strain of the weakest fibre if the failure propagation across the fibres is immediate.

There are three types of extreme value distribution commonly applied in the structural reliability analysis: Gumbel, Frechet, and Weibull distributions. Their parameters can be estimated based on the moment method and likelihood method traditionally, however the accuracy and the stability of these methods are case-dependent, and in some case (e.g three parameters Weibull distribution), the parameter estimation using traditional approaches is troublesome. This problem is solved by using the method of order statistics which was developed by Lieblein [248]. In this method, initially the test data will be separated in to several groups with approximately the same sizes, and in each group, the data are rearranged with an increasing order. Then the parameters will be evaluated through the order statistical formulation, based on the principle of the moment method. The advantage of the order statistics

method is simple and efficient by avoiding solving nonlinear equations as in the traditional approaches.

Weibull distribution [158] is known to fit the failure strength of a lot of materials. The application of Weibull distribution in composite structures was demonstrated by Barbero [47], a new parameter estimation method was proposed for two parameter Weibull distribution based on the data size.

An appropriate distribution may be determined not only based on the data-fitting test, but also on statistical analysis of the material behaviour according to the relevant physical arguments. Based on limit test data, Zhao [246] had developed an approach to determine the proper distribution for the steel fatigue life, fulling taking into account the mechanical process of the steel fatigue. He pointed out a reasonable distribution should fit both the test data and physical argument, and analyzing the mechanism of the material behaviours(like structural failure) can verify the corresponding uncertainty sources and decide the possible suitable distribution for further selection.

Except the traditional data-fitting test, χ^2 test, a series of goodness fit tests for distributions are developed, Stephens [247] reviewed several common data fitting tests like the EDF test, K-S test, Anderson-Darling test, and so on, and these tests are based on the difference between the CDF of the estimated distribution and sample accumulative frequency. Compared to the χ^2 test, these goodness tests seem more effective and accurate, however there is no evidence to show one statistical test more superior than the others in all the cases.

Normally in common engineering problems, the statistical variables of interest are not independent, and are related to each other. In that case, the reliability work need to cope with these stochastic variables as multivariates characterized by the joint distribution, and Bayesian network [244] is believed to be an effective and efficient method to deal with these types of statistical quantities.

Guan [245] developed a load space formulation to increase the efficiency of the reliability calculation by replacing a small number of statistical variables of the large quantity of statistical variables discretized from the structure system. These new statistical variables represent the stochastic relation between random field and the structural response, and the implementation of the new variables are shown to reduce the computational cost dramatically.

Considering the expense of statistical experiments, Harth [48] proposed a constitutive model to generate artificial data with the same stochastic behavior as the experimental data using a stochastic simulation. This method combines the test data and artificially generated data, to identify the material parameters using a nonlinear mathematical model, and enables a stochastic analysis based on limited test data, and the result accuracy can be checked at the end of the analysis. The limitation of this approach is that those artificial test data are produced based on the experimental data, and do not add any new stochastic information. The accuracy of the stochastic simulation is dependent on the quality of the test data, meaning

that this approach requires that the uncertainty information can be adequately represented by the limited experiment data.

The accurate probability of structural failure will be only obtained when all types of uncertainty sources are taken into account comprehensively, however that will be a huge work, which is beyond a three-year PhD research, therefore in this thesis, the uncertainty investigation is limited to fabric material properties(Chapter.4), and only the variances in load and material properties are taken into account in the reliability analysis(Chapter.5).

2.3.4 Conclusion

The high variability exists in the elemental components of coated woven fabrics, like fibres, yarns, and coated materials, and their mechanical performance differs based on different environment(e.g. temperature) and loading conditions. As inelastic composite material, coated woven fabrics have complicated nonlinear mechanical behaviours owing to the crimps interchange with visco-elastic yarns. The stress-strain relations will vary depending on the ratio of stresses applied to the fill and warp. All these highly nonlinear and inelastic mechanical behaviours have to be taken into account in the probabilistic analysis.

Different material test have been proposed to measure full types of mechanical properties of fabric, however not all types of test has been detailed in national code and standards(e.g. axial test), and different countries and associates may have slightly different test approaches and for the measurement of similar types of properties. The uniaxial tension test is currently the most common and simplest test to measure the fabric strength, and similar test procedures have been used in most countries. When a large quantity of experimental data are required for a probabilistic analysis approach and the published data are not sufficient, unaxial testing is a feasible way to start with to collect the probabilistic information.

The numerical/analytical material models of the woven fabric as physical continuum and analogues have been reviewed. These approaches may not be directly applied in the probabilistic analysis formulation, however they are extremely helpful in understanding the mechanical behaviours of the woven fabric, especially during the material tests.

Currently, the probabilistic investigations of the fabric materials are still limited to the yarns and their assemblies, because the accurate statistical analysis requires a large quantity of statistical tests. Some efforts on predicting the probabilistic properties of coated woven fabric are based on the assumption that fabrics are regarded as assemblies of yarns, whose strength are normally assumed to follow Weibull distributions. However the results estimated by these models are still not satisfactory. The probabilistic approach combining a fabric test and statistical analysis are still highly encouraged.

The statistical approach and models are reviewed for transforming material property data to statistical forms. Several commonly used distributions like Normal, Log-normal and extreme value distributions may be applied to represent the statistical variables like loads and material

failure strength. From the review of the data-fitting tests, the test methods based on the CDF of the estimated distribution were shown to be more effective and accurate than the Chi-square test.

In Chapter 3, a probabilistic fabric test philosophy has been proposed based on a large number of material test results, which may be still limited compared with innumerous fabric material, but is enough to demonstrate a test and analysis as a methodology guide.

2.4 The reliability approach

In this section, the traditional uncertainties dealt for the general structural safety are summarized, and those particularly important for fabric structures are discussed. Then the general reliability methods to deal with these uncertainties are reviewed and discussed, and the reliability methods specific to the structural safety are highlighted and their possible application on the fabric structures are also discussed. This section will demonstrate that FORM(at least initially) coupled with a good finite element method is the preferred option.

2.4.1 General uncertainties involved in a structural reliability analysis

For traditional structural form, the causal relationship between designs and consequential results can be derived using the classical mechanical principles and referring to the past experience. However for new material and new structural form like fabric structures, the past experience may be inadequate and unreliable to represent the original statistical behavior of the structure type. In such cases, a general type of uncertainties which possibly affect the structural behaviour need to be taken into account in a structural reliability analysis. As listed in Table.2.7, Freudenthal [29] separated the general uncertainties in the structural analysis into three categories: "strain", which represents the loads and the relevant effects, "resistance", and their intermediate - computation. These uncertainties may have different importance to the structural reliability of a given building, however most of them affects the structural safety more or less, and cooperate together. Of course, for a given case, their sensitivities to the structural safety may not be the same, and the safety factors may be evaluated mainly based on one or more uncertainties rather than the others.

These uncertainties given in Table.2.7 should also be considered for a reliability analysis of fabric structures, and more attention may be paid especially in the aspects of "Resistance" and "modelling" since fabric structures generally have a higher variation in the material properties, which may be complicated by their most important characteristic - high geometrical-nonlinearity. A lot of existing data and information on the probabilities of "strain" including loads, environmental impact and soil properties generally for structural design are published, while comparatively in the "resistance" aspect, further efforts and extensive surveys specific for fabric structures are desired to obtain the detailed descriptions of the randomness like the variation of fabric strengths and Young's moduli.

Based on the point that different type of uncertainty may require a different approach for data collection and use in reliability evaluation, Halder [180] classified the uncertainty sources in engineering systems into two main types: Non-cognitive(quantitative) and cognitive(qualitative) Sources as Table.2.8. The non-cognitive sources include the inherent randomness, statistical uncertainty and modelling uncertainty, and the cognitive sources relate to the vagueness of the problem arising from intellectual abstractions of reality. The former type of uncertainty

Group A	Cause of Fluctuation in "Strain"
	I. Uncertainty and variability of loading conditions ∗ Dead Load. ∗ Live load(including dynamic effects) II. Uncertainty and variability of external conditions that are independent of the load. ∗ Change of temperature. ∗ Wind force. ∗ Uncertainty of behavior of the subsoil.
Inter-Group	Causes of Uncertainty of "Strain" Computation.
	III. Variation of rigidity. IV. Imperfection of methods and shortcoming of assumptions. ∗ Accuracy of method and tolerances of numerical computation. ∗ Inadequacy of assumptions concerning initial and boundary conditions, stress concentration, and secondary strain.
Group B	Causes of Fluctuation of Resistance.
	V. Uncertainty and inaccuracy of the assumed mechanism of resistance. ∗ Inaccuracy or inadequacy of conceived mechanism. ∗ Variability of resistance limits of materials. VI. Variation of structural dimensions.

Table 2.7: Structural Uncertainty Source reviewed by Freudenthal [29]

are normally addressed by collecting a large number of observations and past experience, and the latter is originally difficult to be represented mathematically and usually dealt with using fuzzy set theory.

This classification is helpful when a conceptual approach is being made to do the uncertainty assessment, and gives a basic guide for a wide uncertainty investigation in different structure types. In this research, the uncertainty analysis is concentrated in the mechanical properties of fabric materials, therefore a statistical approach will be applied for the uncertainty assessment.

Non-cognitive Sources	1.Inherent uncertainty - Repeated measurements of the same physical quantity do not yield the same value due to numerous fluctuations int the environment, test procedure, instruments, observer, and so on 2. Statistical uncertainty - No precise information about the variability of the physical quantity of interest due to limited data. 3. Modeling uncertainty - System analysis models are only approximate representations of system behavior.
Cognitive Sources	1. The definitions of certain parameters, such as structural performance (failure or survival), quality, deterioration, skill and experience of construction workers and engineering, environmental impact of projects, and conditions of existing structures. 2. Other human factors 3. Definitions of the interrelationships among the parameters of the problem, especially for complex system.

Table 2.8: Uncertainty Resource in engineering system reviewed by Haldar (2000)

Another classification of the uncertainty sources was given by Igusa [249], who divided the uncertainty within the structural engineering context into aleatory and epistemic. Aleatory uncertainty represents the inherent physical randomness of a system, as compared with epistemic uncertainty, which is knowledge based, and these two uncertainty sources can be integrated by Bayesian techniques [250].

For cognitive or epistemic uncertainty sources, considerable research [249, 251, 252] has been undertaken to incorporate these uncertainties into the reliability or probability analysis of the engineering system, however, these uncertainty source types are very complicated to have accurate mathematical representations, because the validation of the corresponding mathematical model is often difficult to be justified. From a practice prospect, the investigation of the non-cognitive or aleatory uncertainties like material properties and loads are more concerned through the statistical analysis based on the test data and records.

The reviews of the common uncertainties, which are generally involved in the engineering industry may be very helpful in identifying the randomness during the reliability analysis of fabric structures. The relevant recommendations provide good guides for dealing with these uncertainties. The literature demonstrates that a structural reliability analysis can be a complicated framework coupled with a large quantity of uncertainties, which may be identified and analyzed using different approaches. For the practical reason, the reliability analysis may be started with a limited number of uncertainty types with most significant importance, and be further expanded with consideration of additional uncertainty types.

2.4.2 A review of general reliability theories and methods

The structural reliability of a given structure is often explained as the probability of that during a certain time the structural performance is satisfied by the structural requirements which are normally expressed as limit states. In a structural reliability analysis, a series of random variables (e.g material properties, loads) will be included as a vector denoted as X, described by a joint probability density function $f_X(x)$. For a given limit state function G(x)=0, the safe and failure zone can be defined as $\Omega_s = \{x|G(x) > 0\}$ and domain $\Omega_f = \{x|G(x) < 0\}$ separately, and the failure probability is

$$P_f = \int_{\Omega} f_X(x)dx \tag{2.6}$$

In many cases, this integral cannot be directly evaluated, especially when more random variables and several limit states are included. To solve this problem, a variety of approximated approaches have been developed. In this subsection, three typical reliability methods: Monte-Carlo method, Directional method, and Moment method (FORM/SORM) will be reviewed.

The Monte Carlo method [73] is a powerful tool used to simulate random variables. It is simple and intuitive to apply in most structure types, and able to simulate the random variables that are suitable for any distribution. However,it demands a large amount of calculation if a relatively precise solution is needed, meaning that the Monte Carlo method may not be practical for a realistic and complicated engineering structure. Owing to the limitation of the computational efficiency, a lot of researches [74–76, 181, 197] are undertaken in in tackling the problem described about sampling.

Jin guoliang [181] combined the Monte Carlo method with a finite element formulation, and the research work was conducted repeatedly, over and over again,and the Monte Carlo finite element method of reliability analysis for any complicated engineering structures was finally put forward.

There are so many efforts [74–76] to enhance the Monte Carlo method by using Importance Sampling methods, however compared with moment methods like FORM/SORM, Monte Carlo method is still much less efficient especially when the failure probability is low [31]

Directional simulation and importance directional simulation have been studied by Ditlevsen et al. [197]. and Melchers et al. [198], among others. The directional simulation method involves generating uniformly distributed direction vectors and performing a one-dimensional integration along each direction. The importance directional simulation method uses the importance sampling technique to concentrate the direction vectors in the regions of interest. Although directional simulation methods are relatively efficient compared to other Monte Carlo simulation approaches, these methods may diminish in accuracy when the limit state $G(u)$ is highly nonlinear unless the number of sampling directions is large. Moreover, for a system reliability analysis that is supported by finite element modelling, the number of

directions required to limit the error in P_f must be held to a minimum for the analysis to be performed efficiently.

Same as the Monte-Carlo method, the accuracy of the directional method depends on how the design points are choosen, and often need to use a variety of enhancing approaches like importance sampling technology [31] to enhance its performance. Jiesuo Nie [32] pointed out that even with enhanced formulation, the directional method is still only efficient to low demensional spaces.

First order reliability (FORM) is often used based on replacing the limit state surface by a first order surface fitted to the design points in the standard normal space. The first order estimate of the failure probability is given as:

$$p_f = \int_{\omega} \Phi(y)dy = \Phi(-\beta) \tag{2.7}$$

where $\Phi(y)$ denotes standard normal density of the independent statistical variables involved in the structure system. β is called the safety index which is approximated as the shortest distance from the origin to the limit state surface in the standard normal space,

$$\beta = \sqrt{t^*, t} \tag{2.8}$$

where, t and t^* denote the nearest point coordinate vector of the limit state surface in the standard normal space. Rackwitz and Fiessler [242] developed a very efficient FORM algorithm which is found to work well for most structural systems when the gradients of statistical variables within the structures can be accurately estimated.

In FORM, all the non-normal distributed variables are required to be transformed to the the equivalent normal distribution based on the same CDF at the design points. A common approach is first to transform the random vector $X_s = [X_1, X_2, ..., X_d]^T$ to an independent standard normal random vector $U = [U_1, U_2, ..., U_d]^T$ by the Rosenblatt transformation $U = T(X)$. The transformation has to be repeated at every iteration in seeking the most probable point (MPP) of the safety criteria surface.

Hong [30] developed a normal polynomial function to approximate many common distributions. Different from the traditional data fitting methods, it used fractile constraints instead of statistical moment fitting. With the Rosenblatt transformation, the limit state function in the space of independent standard normal variables may become a highly nonlinear function.

As an analytical tool for the reliability approximation, FORM is one of the most reliable methods [191]. Over the past three decades, numerous studies on FORM and its application on different types of reliability problems have been taken, and now FORM has become a basic method for structural reliability. The weakness of this method is that when the performance function is highly nonlinear, the linear approximation using FORM will lead to low accuracy. To sort this problem, the second-order reliability method(SORM) was established to improve

the accuracy of the FORM using second-order approximation of the limit state functions [185]. Once FORM cannot achieve adequate accuracy, the SORM can be used instead, however the judgment about when FORM fail to satisfy the accuracy requirement is very difficult, because the result of the reliability analysis is seldom validated by the feedback of reliability accidents [193], while the most practical way is to control the error in the approximation calculation.

YanGang [192] proposed an moment method to enhance the FORM accuracy and efficiency using the high order moments to approximate the distribution of random variables. Based on FORM, second order and third order moments method can be developed to reduce the error from the linear approximation of the limit state functions.

FORM/SORM accuracy and efficiency can be also enhanced by modifying the limit state surface. Armen [194] developed a "bulge" method to reduce the errors during the searching of multiple design points. The deformed surface was determined and updated with a "bulge" function specified based on the design points obtained from last iteration. His method demonstrates that a satisfied accuracy and successively finding of the multiple design points without large errors can be achieved by using FORM with the enhanced formulation.

To enhance the efficiency of FORM, Grandhi and Wang [97] developed a reliability algorithm using two-point adaptive nonlinear approximation. In this method, both first order and second order approximations of the performance function were used. The design point derived based on linear approximation is assigned as the previous point X_k in the current iteration, and the design point from nonlinear approximation is the current one X_k. The updated design points are produced by both linear and nonlinear formulation alternatively. With this design point search technology, the computational costs in safety index calculation and optimization are significantly reduced.

Eurocode 0 [253] states different types of reliability method used for the calibration of safety factors under limit states as fig.2.25, and the current safety coefficients in the Euro code are estimated based on the deterministic method. It points out that full probabilistic reliability can provide "in principle correct answers" to the reliability analysis, but it is seldom used for the calibration of safety factors in the design code because the relevant statistical data are not sufficient. While FORM can be well used for the further development for most structural types, and the sufficient accuracy of this method can be achieved when the approximations are properly made.

The general view on the reliability approaches demonstrates that the Monte-Carlo method may be the simplest reliability method to be applied without deriving a specific reliability formulation, however its accuracy and efficiency are often not satisfactory especially for a complicated structural system. FORM/SORM are proved to be very reliable and efficient methods for many reliability problems. Compared with SORM, FORM may achieve better efficiency in computing cost with a satisfactory accuracy. Actually the literature presents that even for those with highly nonlinear limit state function, FORM can be still a good base for the

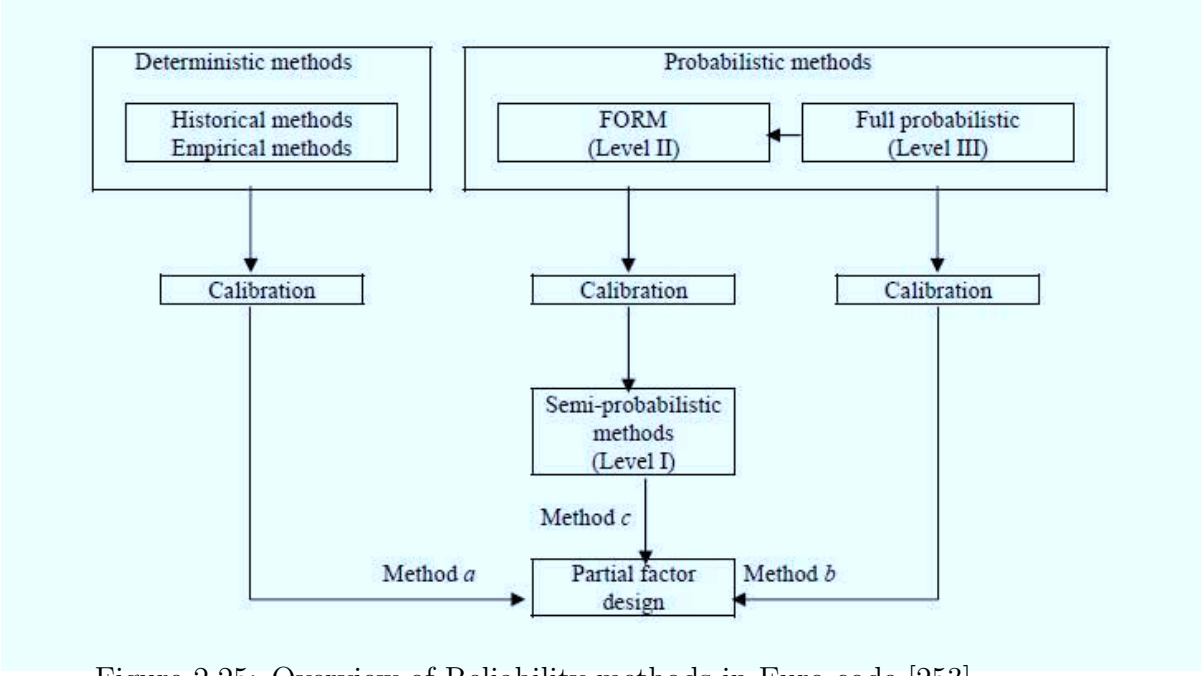

Figure 2.25: Overview of Reliability methods in Euro code [253]

further enhanced approaches with higher accuracy and efficiency. Therefore, FORM is very valuable for the reliability estimation of different structure types, and is an ideal reliability approach to be started with for the fabric structural reliability analysis.

2.4.3 Finite element probability approach

One of the important tasks of structural reliability analysis is to find the structural load response(stress). For complicated structural systems, analytical methods may not be feasible, and numerical methods may be necessary to be applied to calculate their load response. The finite element method has become an effective numerical method along with the rapid development of the technique of the electronic computer.

The traditional finite element method is built upon the basis of determinacy of the structural system which considers that the structural geometrical size and the load it is subjected to are definite values. But, in fact, the geometrical size of the structure, the load, the material resistance,etc., are usually random variables. Structural reliability analysis is used to synthesize the indeterminacy of each variable to assess the bearing capacity of the structure. With some appropriate improvement in finite element methods, the reliability estimation may be enhanced significantly in computational efficiency.

If the structural response can be described analytically, the reliability can be evaluated without the aid of the finite element method. For most structural systems, it is necessary to use the finite element methods to evaluate the structural response. The classical reliability approaches like FORM are often combined with finite element formulation in deriving the safety of a structural system. The early work on finite element reliability were undertaken by Liu and Der Kiureghian [69, 83] for geometrically and /or material nonlinear structures. Their finite element reliability analysis includes two main efforts. One is implementation of a first-order

or a second-order reliability method, by improving the failure surface in the standard normal space. The other is to apply the finite element in computing the gradients of structural responses like load, material properties, and geometry variables.

The combined use of finite element formulation and reliability methods is very popular in comtemparory reliability assessment, and is often called the "stochastic finite element reliability method" [180], in which, the sensitivities of the finite element formulation with respect to the basic statistical variables are evaluated at the design points in the iteration process of seeking the safety index.

Finite difference method [239] has been applied to calculate the gradients of the limit state function with respect to the basic statistical variables, however this method is shown to be time-consuming and only efficient in a system with a small mount of variables. The analytical method applying the chain rule of differentiation is shown to "enjoy the same advantage" [243] as the finite difference method (also called perturbation method) and have better accuracy and efficiency in the computing cost, when applied to the traditional structural system like reinforced concrete [77].

The implementation of the finite element formulation in the FORM and SORM is introduced by Liu [83] for the reliability analysis of geometrically nonlinear uncertain structures. He pointed out that the key thing in seeking the design point using the finite element reliability method is to compute the vector gradients, and he also compared the computational efficiency of FORM and SORM coupled with analytical and finite difference method, and found that FORM exhibited a good estimation of the reliability even for the high-nonlinear structure type with non-normal distributed uncertainties, and when coupled with analytical method, the computational efficiency is much higher than SORM method with point-fitting method.

Teigen [71] applied the finite element reliability method in nonlinear concrete structures, considering the nonlinearities in material and geometry, and randomness in loading, material and geometry. The perturbation method is applied to calculate the structural response gradients using first and second order terms of the Taylor series expansion of the limit state equation. His approach succeeded in avoiding the requirement of explicit limit state function and the time-consuming computation, and the numerical test results are encouraging, and demonstrate that more effort is desired to develop the finite element method.

Frangopol [35] applied the finite element reliability method on a geometrically nonlinear suspended truss system. It was found that linearly modelling a geometrical nonlinear structural system will lead to a conservative result in the tension state and unconservative in compression, and the effect of the correlation of loads is more obvious than resistances. The material behavior has significant effect on the structure system while not on the individual components.

Val et al [200] created a probabilistic method for reliability evaluation of RC frames in the context of nonlinear analysis. His method combines the nonlinear finite element structural model and the first order reliability method(FORM), Petryna [201] proposed a rational computer

framework for time-variant reliability analysis of RC structures,which balances the accuracy of mechanical and stochastic models with maintainable computing costs. It concludes new material models for time-invariant and fatigue behaviour of concrete. He found influence of temporal uncertainties in the evaluation of long-term life history including sequence effects and path-dependence in nonlinear systems, and the influence of spatial scatter of material properties and loads significantly affect the reliability estimates.

Kiyohiro [203] used a probabilistic finite element geometrically nonlinear analysis approach to undertake reliability analysis of suspension bridges, in which, different loading and damage senarios are considered as the main uncertainty. The optimal maintenance for suspension bridges designed according to allowable stress method will be decided based on the result from the reliability analysis. He proposed a general approach to evaluate the system reliability of structures exhibiting geometrically nonlinear elastic behavior.

Numerous fabric structures have been designed and constructed over last recent several decades, and many new fabric materials have been developed and applied in the industry. However a general reliability analysis tool to predict the possibility of fabric structural failure is still absent, because most attention has been paid to predicting the material strengths and load effects not their uncertainties. Single failure point of a fabric structure could be estimated according to given load, geometry and material with constant values by deterministic analysis methods, but the confidence of structural safety is still unknown when a true load and material case are applied. Compromising the efficiency and accuracy, a finite element reliability formulation coupled with FORM is proposed in Chapter.5 based on an efficient deterministic analysis formulation, demonstrated in Chapter.3.

2.4.4 Conclusion

A reliability analysis may possibly include numerous uncertainties, depending on the situations and conditions of the given structures. Some uncertainties like material uncertainties can be assessed using statistical approaches, and the others (e.g human skills) may be analyzed by other methods like fuzzy theory. The literature about the uncertainties involved in a reliability analysis give a general scope of uncertainties for this research, and also a direction of modelling these uncertainties, not only for the uncertainties like fabric material properties included in this research, but also for those excluded due to the limit of a single PhD research scope.

There are many structural reliability methods like Monte-Carlo, FORM, SORM, and full probabilistic methods. FORM is found to be efficient and accurate, and has been successfully applied in a wide range of structural types. SORM can provide a second order failure boundary which may give better simulation of the real cases, however their solution procedures may not be efficient and convergent results are difficult to produce in some cases. The Monte-Carlo method is very easy to apply to the reliability analysis of most structural types, however only efficiently for simple structures. Full probabilistic methods can provide generally correct

reliability answers, but they have high requirements in the uncertainty information which may not be available in a lot of cases.

The finite element reliability methods are generally made by combining the existing reliability methods like FORM and the finite element formulations, and these methods have been applied successfully in a series of geometrically nonlinear materials. Though these reliability methods may not be directly used for fabric structures, they provide good examples for the integration of the finite element method and reliability approaches. If an efficient finite element method is developed specific for fabric structures, then FORM can work out the structural reliabilities based on the given uncertainties within the power of finite element formulations.

2.5 Summary & Conclusion

The conclusions on the literature are given at the ends of each section. The general conclusion of this chapter is given as that the reliability analysis can be a large complicated system work, which include a large mount of uncertainty investigation and probabilistic analysis, and also an suitable reliability philosophy with the efficient computing engine dealing with the structural response due to the uncertainties. Especially for the fabric structures with the geometrical nonlinear structural performance and high material variability, a full-range reliability work is too large for a PhD research work. Therefore in this thesis, the main target of the reliability work should be focus on a good methodology to estimate structural safety based on the obtained or published data of the uncertainties. The uncertainty investigation and analysis of fabric in Chapter 4 are only limited in one type of fabric material, as an example to apply the statistical investigation and probability assessment. And only several random variables are involved in the reliability formulation Chapter 5 to demonstrate the application of the reliability approach using finite element formulation.

Chapter 3

Finite Element Formulation For Fabric Structures

The 3-node constant strain triangular element is the simplest and most widely used in the industry. It is based on a geometrically nonlinear cable analogy approach with a linear strain function and an assumption of small strains. However this approach is shown to be deficient in representing the behavior of a continuum in the presence of shear strains in particular. A modified version of this basic element is proposed based on including higher-order strain terms. The revised element is shown to perform better than the original version, but as not all higher-order terms can be included, large strains fail to be represented accurately. This element is, here, denoted as a meso-strain formulation.

It should be noted that strictly, neither of the aforementioned formulations pass the patch test. Therefore, to achieve this most fundamental of requirement, the cable-analogy principle is retained, but the relationship between the element strains and side lengths is completely revised. A classical finite element approach is adopted in defining the strain-displacement relations, that is equivalent to Green's strain, and therefore applicable to large strain deformations. The cable analogy approach is maintained by relating the nodal displacements, element side lengths and the large strain definitions. Therefore, from a practical perspective, the implementation of the new element formulation can be achieved by modifying existing analysis codes. To this end, Dynamic Relaxation is also adopted to solve the resulting state equations.

Recognizing the limitations of the constant strain triangle, a linear strain triangle formulation is presented, also linked to Dynamic Relaxation as well as the conventional Newton-Raphson procedure. This element is based on the original work of Ye [217] and the formulation revised to improve the mathematical consistency. The main advantage of this type of element over the CST element is the higher efficiency in the stress representation using the same type of degrees of freedom(D.O.F). The additional element curvatures depend on the element geometry and not additional rotational D.O.F and provide an explicit link between out-of-plane loads and corresponding membrane stresses. However in the presence of geometric nonlinearity, the

Newton-Raphson method becomes computationally inefficient with a slow convergence rate using this type of element. In contrast, when coupled with with the Dynamic Relaxation algorithm, a highly efficient analysis tool is developed

The derivation of the formulations and solution procedures of CSTs and LST are detailed in sections 3.1 and 3.2 with wrinkling issues covered in section 3.4. Numerical examples and comparison of these finite element formulations are illustrated and discussed in section 3.5.

3.1 Constant Strain Triangular Element (CST)

Unlike the finite element formulation of the typical CST, in this section the element strains will be expressed as functions of the deformation of pseudo cables or increments of the element side lengths. Based on different strain-displacement functions, the CST element formulation is separated into three types as listed below and detailed in the subsequent sections:

- CST small strain formulation [208]:
  Under the assumption of small strains, the linear cable analogy formulation is developed, but neglects the high order terms in the relation between element strains and pseudo cable strains.

- CST meso-strain formulation [209]:
  The original small strain formulation approach enhanced by inclusion of some higher order terms whilst maintaining the cable analogy introduced from [208].

- CST with large strain formulation:
  A new formulation that abandons the original strain-displacement approach and is based on a typical finite element philosophy, with all high order terms included in a nonlinear continuum framework.

3.1.1 CST small strains formulation

The original form of the CST was, arguably, motivated by a requirement for computational efficiency and also by a desire to analyse a membrane as a cable net, for which the computational mechanics was more straightforward and available at the time. Consequently, the CST became a good candidate element because of the characteristic of having constant values of strain along each of its three sides, meaning if the triangular element could be represented by a set of three bars (or cables), then the membrane could indeed be analysed as a cable net/ geometrically nonlinear truss. In what follows we detail the development of the element in its original form to demonstrate the principle of the formulation.

Referring to Figure 3.1 (A′C′-AC)/AC gives the strain normal to the plane FB related to the normal stress σ_n.Considering the triangles ACD and A′C′D′ and du as the increase in length from AD to A′D′, and dv the increase in length from CD to C′D′, then

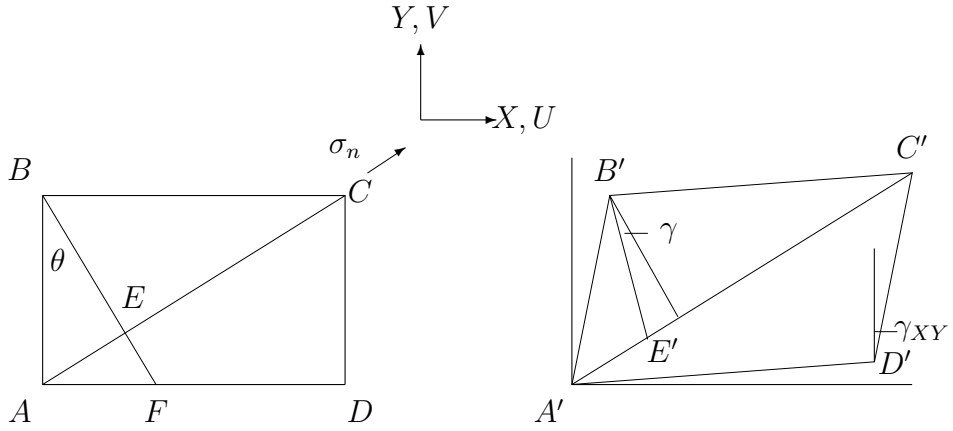

(a) *Unstrained* (b) *strained*

Figure 3.1: Plane element subject to displacement vector

$$\begin{aligned} A'D' &= AD + dU = AD\left(1 + \frac{dU}{AD}\right) = AD(1 + \varepsilon_X) \\ C'D' &= CD + dV = CD\left(1 + \frac{dV}{CD}\right) = CD(1 + \varepsilon_Y) \end{aligned} \tag{3.1}$$

in which, $\varepsilon_X = \frac{\partial U}{\partial X}$ and $\varepsilon_Y = \frac{\partial V}{dY}$

Similarly

$$A'C' = AC(1 + \varepsilon_n) \tag{3.2}$$

In the triangle A′C′D′ we have:

$$A'C'^2 = A'D'^2 + C'D'^2 - 2A'D' \cdot C'D' cos(\frac{\pi}{2} + \gamma_{XY}) \tag{3.3}$$

or

$$AC^2(1 + \varepsilon_n)^2 = AD^2(1 + \varepsilon_X)^2 + CD^2(1 + \varepsilon_Y)^2 + 2AD(1 + \varepsilon_X)CD(1 + \varepsilon_Y)sin(\gamma_{XY}) \tag{3.4}$$

If it is assumed that strains are very small, $sin(\gamma_{XY}) \approx \gamma_{XY}$ and second order powers may be neglected, we obtain:

$$AC^2(1 + 2\varepsilon_n) = AD^2(1 + 2\varepsilon_X) + CD^2(1 + 2\varepsilon_Y) + 2AD \cdot CD\gamma_{XY} \tag{3.5}$$

which, with $AC^2 = AD^2 + CD^2$, reduces to

$$AC^2(2\varepsilon_n) = AD^2(2\varepsilon_X) + CD^2(2\varepsilon_Y) + 2AD \cdot CD\gamma_{XY} \tag{3.6}$$

Dividing through by $2AC^2$ and introducing $cos^2\theta = \frac{AD^2}{AC^2}$ and $sin^2\theta = \frac{CD^2}{AC^2}$,

$$\varepsilon_n = \varepsilon_X cos^2\theta + \varepsilon_Y cos^2\theta + \gamma_{XY} cos\theta sin\theta \tag{3.7}$$

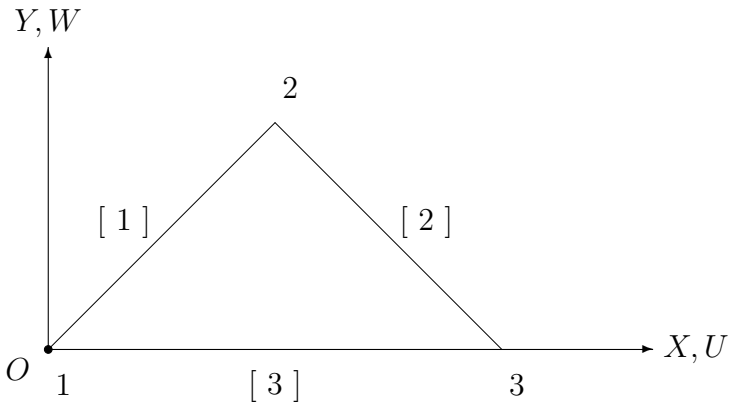

Figure 3.2: Triangular Element made of 3-Cable

If the direct strain in the element side i is denoted as ε_i , and local orthogonal strains defined as $\{\varepsilon\}^T = \{\varepsilon_X \quad \varepsilon_Y \quad \gamma_{XY}\}$,then :

$$\varepsilon_i = \varepsilon_X cos^2\theta_i + \varepsilon_Y sin^2\theta_i + \gamma_{XY} sin\theta_i cos\theta_i \tag{3.8}$$

where, θ_i is the anti-clockwise angle between the element side i and the local X axis, and $i = 1 \rightarrow 3$, and ε_X and ε_Y are the direct strains in the local X and Y directions respectively with the local shear stress γ_{XY}. The extension of side lengths can thus be expressed:

$$\{\delta^{tr}\} = \begin{Bmatrix} \delta_1 \\ \delta_2 \\ \delta_3 \end{Bmatrix} = \begin{Bmatrix} L_1\varepsilon_1 \\ L_2\varepsilon_2 \\ L_3\varepsilon_3 \end{Bmatrix} \tag{3.9}$$

Writing Eqn. 3.8 for each side of the triangular element leads to:

$$\begin{aligned} \varepsilon_1 &= \varepsilon_X cos^2\theta_1 + \varepsilon_Y sin^2\theta_1 + \gamma_{XY} sin\theta_1 cos\theta_1 = \frac{\delta_1}{L_1} \\ &= \varepsilon_X a_1 + \varepsilon_Y b_1 + \gamma_{XY} c_1 \end{aligned}$$

$$\begin{aligned} \varepsilon_2 &= \varepsilon_X a_2 + \varepsilon_Y b_2 + \gamma_{XY} c_2 = \frac{\delta_2}{L_2} \\ \varepsilon_3 &= \varepsilon_X a_3 + \varepsilon_Y b_3 + \gamma_{XY} c_3 = \frac{\delta_3}{L_3} \end{aligned} \tag{3.10}$$

or

$$\begin{Bmatrix} \varepsilon_1 \\ \varepsilon_2 \\ \varepsilon_3 \end{Bmatrix} = \begin{Bmatrix} \frac{\delta_1}{L_1} \\ \frac{\delta_2}{L_2} \\ \frac{\delta_3}{L_3} \end{Bmatrix} = \begin{bmatrix} a_1 & b_1 & c_1 \\ a_2 & b_2 & c_2 \\ a_3 & b_3 & c_3 \end{bmatrix} \begin{Bmatrix} \varepsilon_X \\ \varepsilon_Y \\ \gamma_{XY} \end{Bmatrix} \tag{3.11}$$

Solving for the continuum strains, then:

$$\varepsilon = \begin{Bmatrix} \varepsilon_X \\ \varepsilon_Y \\ \gamma_{XY} \end{Bmatrix} = \frac{1}{det\ [A]} \begin{bmatrix} (b_2c_3 - b_3c_2)L_1^{-1} & (b_3c_1 - b_1c_3)L_2^{-1} & (b_1c_2 - b_2c_1)L_3^{-1} \\ (a_3c_2 - a_2c_3)L_1^{-1} & (a_1c_3 - a_3c_1)L_2^{-1} & (a_2c_1 - a_1c_2)L_3^{-1} \\ (a_2b_3 - a_3b_2)L_1^{-1} & (a_3b_1 - a_1b_3)L_2^{-1} & (a_1b_2 - a_2b_1)L_3^{-1} \end{bmatrix} \begin{Bmatrix} \delta_1 \\ \delta_2 \\ \delta_3 \end{Bmatrix} \tag{3.12}$$

or

$$\{\varepsilon\} = [B^{tr}]\{\delta\}^{tr} \tag{3.13}$$

where $\det[A] = \begin{vmatrix} a_1 & b_1 & c_1 \\ a_2 & b_2 & c_2 \\ a_3 & b_3 & c_3 \end{vmatrix}$

$[B^{tr}]$ can be recognised as the classically expressed strain-displacement relationship which can be used to define the element elastic stiffness matrix $[K_E^{tr}]$, the geometric stiffness matrix $[K_\delta^{pc}]$, and the element force vector $\{T_c\}$ as follows.

The element local stresses are defined as:

$$\{\sigma\} = \begin{Bmatrix} \sigma_X \\ \sigma_Y \\ \tau_{XY} \end{Bmatrix} = \begin{bmatrix} d_{11} & d_{12} & 0 \\ d_{21} & d_{22} & 0 \\ 0 & 0 & d_{33} \end{bmatrix} \cdot \begin{Bmatrix} \varepsilon_X \\ \varepsilon_Y \\ \gamma_{XY} \end{Bmatrix} = [E][B^{tr}] \begin{Bmatrix} \delta_1 \\ \delta_2 \\ \delta_3 \end{Bmatrix} \tag{3.14}$$

where for an isotropic material:

$$d_{11} = d_{22} = \frac{E}{(1-\nu^2)}, d_{12} = d_{21} = \nu \cdot d_{11}, d_{33} = \frac{E}{2(1+\nu)}$$

in which, E is Young's Modulus and ν Possion's ratio, and for an orthotropic material

$$d_{11} = \frac{E_X \cdot E_Y}{E_Y - E_X \cdot \nu_{YX}^2}, \quad d_{12} = d_{21} = \frac{E_X \cdot E_Y \cdot \nu_{XY}}{E_Y - \nu_{XY}^2 \cdot E_X}, \quad d_{22} = \frac{E_Y^2}{E_Y - E_X \cdot \nu_{YX}^2}, \quad d_{33} = G_{XY}$$

in which, E_X,E_Y are Young's Modulus along orthogonal axes X and Y, and G_{XY} is the shear modulus across X and Y, and ν_{YX} is the Possion's ratio in Y direction etc.

For a 3 node CST element, the elastic stiffness matrix is easily shown to be:

$$[K^{tr}] = [B^{tr}]^T[E][B^{tr}] \times V \tag{3.15}$$

where V is the volume of the element. $[K_E^{tr}]$ is a 3×3 matrix acting on the D.O.F δ_1,δ_2 and δ_3 (e.g the side extensions of the element). Knowing $[B^{tr}]$ (e.g Eqn. 3.13) the element elastic stiffness matrix can be readily obtained. Acting on the 3 D.O.F δ_1,δ_2 and δ_3, means that the triangular element has effectively been replaced by a set of three bars. It can be considered that diagonal terms of $[K_E^{tr}]$ are effectively terms of the type EA/L , with A - the cross-section area of the pseudo bar/cable.

It is convenient to develop this analogy further in the derivation of the geometric stiffness matrix. The geometric stiffness is derived from a combination of the pseudo-cable natural (axial) force and a change in orientation in the form of rigid-body rotation. Without the need to provide a full derivation in this chapter, it suffices to state the geometric stiffness of the bar/cable element shown in Fig.3.3 is:

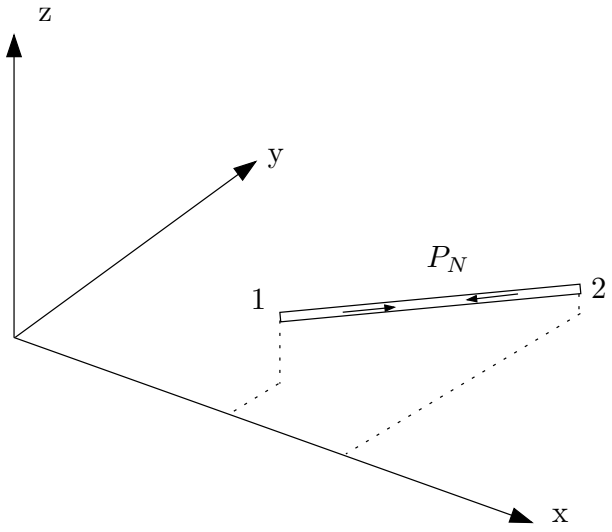

Figure 3.3: Geometry of the bar Element

$$[K_\sigma^{pc}] = \frac{P_N}{L}\begin{bmatrix} [I_3] - [C][C]^T & -[I_3] + [C][C]^T \\ -[I_3] + [C][C]^T & [I_3] - [C][C]^T \end{bmatrix} \tag{3.16}$$

where P_N is the axial force in the bar/cable of length L, $[I_3]$ is a 3×3 identity matrix, and

$$[C] = \begin{bmatrix} c_x \\ c_y \\ c_z \end{bmatrix} = \frac{1}{L}\begin{bmatrix} x_2 - x_1 \\ y_2 - y_1 \\ z_2 - z_1 \end{bmatrix} \tag{3.17}$$

Clearly, what is required is the relationship between the natural force P_N of the three pseudo

cables/bars describing the triangular element and the continuum stresses σ_x,σ_y and τ_{xy} in order to be able to make use of the Eqn. 3.16.

Combing the elastic stiffness matrix $[K_E^{tr}]$ (Eqn. 3.15) with the element side extensions δ_1,δ_2 and δ_3 leads to the element side force T_1, T_2 and T_3 as in:

$$\{T\} = \begin{Bmatrix} T_{c1} \\ T_{c2} \\ T_{c3} \end{Bmatrix} = [B^{tr}][E][B^{tr}]V \begin{Bmatrix} \delta_1 \\ \delta_2 \\ \delta_3 \end{Bmatrix} \tag{3.18}$$

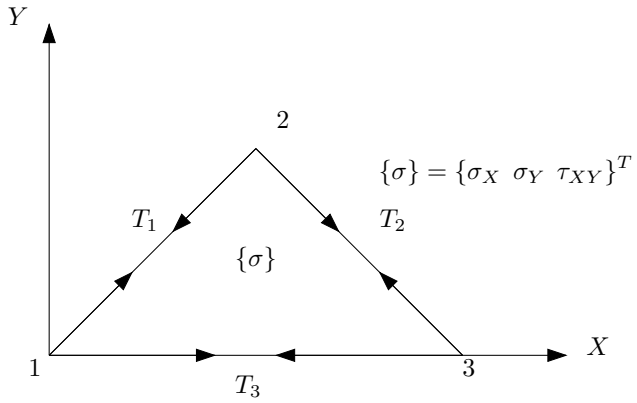

Figure 3.4: The pseudo cable forces

(See also Fig. 3.4). Noting Eqn. 3.14 and pre-multiplying it by $[B^{tr}]^T$ and V, then:

$$V \times [B^{tr}]^T\{\delta\} = V \times [B^{tr}]^T[E][B^{tr}] \begin{Bmatrix} \delta_1 \\ \delta_2 \\ \delta_3 \end{Bmatrix} \tag{3.19}$$

The right-hand-side of Eqn. 3.19 is then identical to the right-hand-side of the Eqn. 3.18, such that we have the definition:

$$\{T\} = \begin{Bmatrix} T_{c1} \\ T_{c2} \\ T_{c3} \end{Bmatrix} = V \times [B^{tr}]^T \begin{Bmatrix} \sigma_X \\ \sigma_Y \\ \tau_{XY} \end{Bmatrix} \tag{3.20}$$

Eqn. 3.20 provides the link between the pseudo cable element forces T_{c1}, T_{c2} and T_{c3}(viz. P_N in Eqn. 3.16) and the triangular element continuum stresses σ_X, σ_Y and τ_{XY}.

It should be noted at this point that both the elastic stiffness and geometric stiffness matrices are functions of the strain-displacement matrix $[B^{tr}]$. For the original CST formulation $[B^{tr}]$ is defined in Eqn. 3.13 with Eqn. 3.12. The limitations of this particular form of $[B^{tr}]$ have been previously stated and are demonstrated in section 3.5. To improve the CST-pseudo cable element formulation it, therefore, remains to establish "better" forms of $[B^{tr}]$. Two alternatives are described in sections 3.1.2 and 3.1.3, and assessed in section 3.5.

3.1.2 Enhanced CST meso strains formulation

As identified in the section 3.1.1, in deriving the formulation $\varepsilon_i = \varepsilon_X \cdot cos^2\theta_i + \varepsilon_Y \cdot sin^2\theta_i + \gamma_{XY} sin\theta_i \cdot cos\theta_i$, high order terms are neglected. A revised formulation is presented in this section that endeavours to include these missing terms with the aim of enhancing the resulting CST. Basing the formulation on the pseudo-cable approach, only the derivation of $[B^{tr}]$ is required to use in Eqns. 3.15 and 3.20.

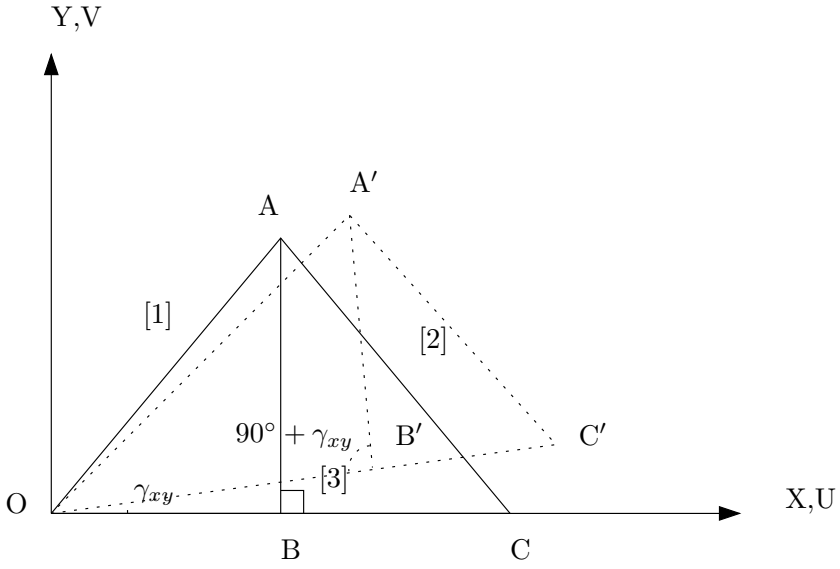

Figure 3.5: 3-node Triangular Element

Considering the triangular element illustrated in the figure 3.5, then the length of side [1] in the deformed (depicted with a dotted line) state is:

$$OA^2[1+\varepsilon_1]^2 = OB^2[1+\varepsilon_X]^2 + AB^2[1+\varepsilon_Y]^2 - 2OB \cdot AB[1+\varepsilon_X][1+\varepsilon_Y] \cdot cos(90^\circ + \gamma_{XY}) \quad (3.21)$$

while the original length is:

$$OA^2 = OB^2 + AB^2$$

With the definitions: $cos\theta = \frac{OB}{OA}, sin\theta = \frac{AB}{OA}$, and using the necessary simplifying assumption as in section 3.1.1: $(sin(\gamma_{XY}) \approx \gamma_{XY})$, then:

$$2\varepsilon_1 + \varepsilon_1^2 = cos^2\theta_1(2\varepsilon_X + \varepsilon_X^2) + sin^2\theta_1(2\varepsilon_Y + \varepsilon_Y^2) + 2cos\theta_1 \cdot sin\theta_1 \cdot (1 + \varepsilon_X + \varepsilon_Y + \varepsilon_X \cdot \varepsilon_Y)\gamma_{XY} \quad (3.22)$$

If we assume that the formulation follows the same form as Eqn. 3.8, then:

$$\varepsilon_1 = \varepsilon_X cos^2\theta_1 + \varepsilon_Y cos^2\theta_1 + \gamma_{XY} sin\theta_1 cos\theta_1 + \Delta \tag{3.23}$$

where Δ represents all the higher order terms.
The significance of Δ can be approximately examined as follows. Equation 3.23 can be used in the first term on the left side of Eqn. 3.22. In substituting Eqn. 3.23 into the second term of left side of Eqn. 3.22, it is mathematically necessary to omit the higher order terms. Consequently,

$$\varepsilon_1^2 = (\varepsilon_X \cdot cos^2\theta_1 + \varepsilon_Y \cdot sin^2\theta_1 + \gamma_{XY} \cdot sin\theta_1 \cdot cos\theta_1 + \Delta)^2 \approx (\varepsilon_X \cdot cos^2\theta_1 + \varepsilon_Y \cdot sin^2\theta_1 + \gamma_{XY} \cdot sin\theta_1 \cdot cos\theta_1)^2 \tag{3.24}$$

or,

$$\varepsilon_1^2 \approx cos^4\theta_1 \cdot \varepsilon_X^2 + sin^4\theta_1 \cdot \varepsilon_Y^2 + sin^2\theta_1 \cdot cos^2\theta_1 \cdot \gamma_{XY}^2 + 2\varepsilon_X \cdot \varepsilon_Y \cdot sin^2\theta_1 \cdot cos^2\theta_1 + 2\varepsilon_Y \cdot \gamma_{XY} \cdot sin^3\theta_1 \cdot cos\theta_1 \tag{3.25}$$

$$+2\gamma_{XY} \cdot \varepsilon_X \cdot cos^3\theta_1 \cdot sin\theta_1$$

We substitute Eqn. 3.25 into the second term on the left side of Eqn. 3.22. Therefore, using equation 3.23 and 3.25 as described above, then:

$$2\Delta \approx cos^2\theta_1 \cdot \varepsilon_X^2 + sin^2\theta_1 \cdot \varepsilon_Y^2 + 2(\varepsilon_X + \varepsilon_Y + \varepsilon_X \cdot \varepsilon_Y) \cdot \gamma_{XY} \cdot sin\theta_1 \cdot cos\theta_1 - \varepsilon_1^2$$

$$\approx (cos^2\theta_1 - cos^4\theta_1) \cdot \varepsilon_X^2 + (sin^2\theta_1 - sin^4\theta_1) \cdot \varepsilon_Y^2 + 2(1 - sin^2\theta_1) \cdot sin\theta_1 \cdot cos\theta_1 \cdot \gamma_{XY} \cdot \varepsilon_X$$

$$+2(1 - cos^2\theta_1) \cdot sin\theta_1 \cdot cos\theta_1 \cdot \gamma_{XY} \cdot \varepsilon_Y + 2(\gamma_{XY} - sin\theta_1 \cdot cos\theta_1) \cdot \varepsilon_X \cdot \varepsilon_Y \cdot sin\theta_1 \cdot cos\theta_1$$

$$-\gamma_{XY}^2 \cdot cos^2\theta_1 \cdot sin^2\theta_1$$

$$\approx sin^2\theta_1 \cdot cos^2\theta_1 \cdot \varepsilon_X^2 + sin^2\theta_1 \cdot cos^2\theta_1 \cdot \varepsilon_Y^2 + 2cos^3\theta_1 \cdot sin\theta_1 \cdot \gamma_{XY} \cdot \varepsilon_X + 2sin^3\theta_1 \cdot cos\theta_1 \cdot \varepsilon_Y$$

$$+2(\gamma_{XY} - sin\theta_1 \cdot cos\theta_1) \cdot \varepsilon_X \cdot \varepsilon_Y \cdot sin\theta_1 \cdot cos\theta_1 - \gamma_{XY}^2 \cdot cos^2\theta_1 \cdot sin^2\theta$$

$$\approx \tfrac{1}{4}(\varepsilon_X^2 + \varepsilon_Y^2) sin^2 2\theta_1 + \gamma_{XY} \cdot (\varepsilon_y \cdot cos^2\theta_1 + \varepsilon_X \cdot sin^2\theta_1) sin2\theta_1 + \varepsilon_X \cdot \varepsilon_Y (\gamma_{XY} - \tfrac{1}{2} sin2\theta_1) sin2\theta_1$$

$$-\tfrac{1}{4}\gamma_{XY}^2 \cdot sin^2 2\theta_1$$

$$\approx [\tfrac{1}{4}(\varepsilon_X - \varepsilon_Y)^2 - \tfrac{1}{4}\gamma_{XY}^2] \cdot sin^2 2\theta_1 + \gamma_{XY} \cdot (\varepsilon_Y \cdot cos^2\theta_1 + \varepsilon_X \cdot sin2\theta_1 + \varepsilon_X \cdot \varepsilon_Y) \sin 2\theta_1$$

such that

$$\Delta \approx [\frac{1}{8}(\varepsilon_X - \varepsilon_Y)^2 - \frac{1}{8}\gamma_{XY}^2] \cdot sin^2 2\theta_1 + \frac{1}{2}\gamma_{XY} \cdot (\varepsilon_Y \cdot cos^2\theta_1 + \varepsilon_X \cdot sin^2\theta_1 + \varepsilon_X \cdot \varepsilon_Y) \cdot sin2\theta_1 = \Delta(o^2)$$

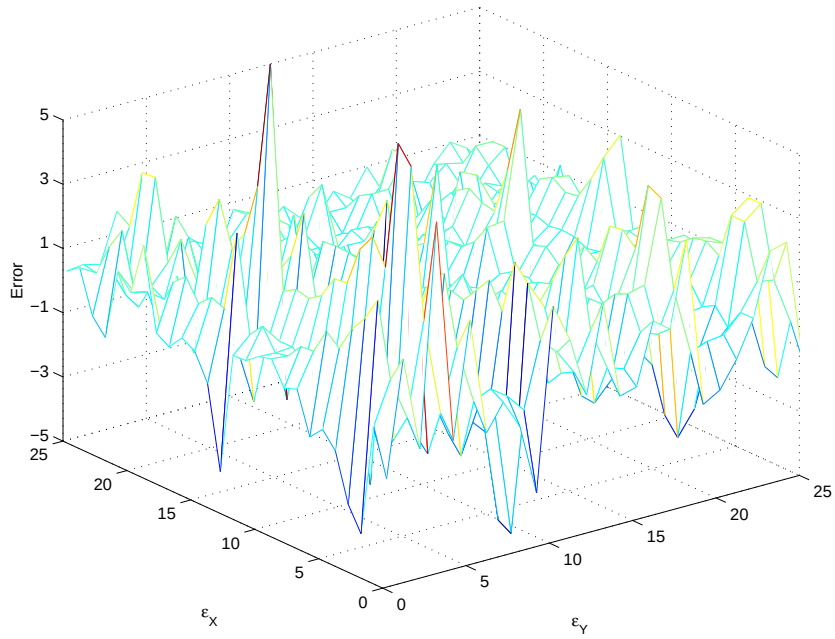

Figure 3.6: Error of linear cable analogy formulation under large strains

and, therefore,

$$\begin{aligned}\varepsilon_i \quad &\approx \quad \varepsilon_X cos^2\theta_i + \varepsilon_Y sin^2\theta_i + \gamma_{XY} sin\theta_i cos\theta_i \\ &\quad +[\frac{1}{8}(\varepsilon_X - \varepsilon_Y)^2 - \frac{1}{8}\gamma_{XY}^2] \cdot sin^2 2\theta_i + \frac{1}{2}\gamma_{XY} \cdot (\varepsilon_Y \cdot cos^2\theta_i + \varepsilon_X \cdot sin^2\theta_i + \varepsilon_X \cdot \varepsilon_Y) \cdot sin2\theta_i \\ (3.26)\end{aligned}$$

Eqn. 3.8 describes a linear relationship between cartesian strains ε_X, ε_Y, and γ_{XY} and a strain orientated in a direction θ from the local X axis. Eqn. 3.26 attempts to capture second order components of strains, whilst the omission of o^3(third order and above) strains and above is a necessary simplication. Subtracting Eqn. 3.8 from Eqn. 3.26 and representing the result graphically for a range of strains (see fig. 3.6), the simplification of the o^2 strain terms can be visualized. Quantitatively, the error is significant. For example, with direct strains ε_X and ε_Y up to 25% and a shear strain of 0.25 or 14^o, the maximum difference between Eqn. 3.8 and 3.26 is of the order of 500%.

Whilst the nonlinear formulation Eqn. 3.26 clearly improves the prediction of the values of strains at arbitrary values of θ, its use in generating the $[B^{tr}]$ matrix is not appropriate, because of its complicated nonlinear form. Instead it is necessary to return to the fundamental definitions.

From figure 3.5, obviously, $\varepsilon_X = \varepsilon_3$ and from Eqn. 3.21, we have:

$$OA^2(1+\varepsilon_1)^2 = OB^2(1+\varepsilon_3)^2 + AB^2(1+\varepsilon_Y)^2 - 2OB \cdot AB(1+\varepsilon_3) \cdot (1+\varepsilon_Y) cos(\gamma_{XY} + 90^\circ) \quad (3.27)$$

If $OA^2 = OB^2 + AB^2$, and $OC = OA \cdot cos\theta_1, AC = OA \cdot sin\theta_1$

then

$$(1+\varepsilon_1)^2 = cos^2\theta_1 \cdot (1+\varepsilon_3)^2 + sin^2\theta_1 \cdot (1+\varepsilon_y)^2 + 2(1+\varepsilon_3)(1+\varepsilon_y)sin\gamma_{xy}sin\theta_1 cos\theta_1 \quad (3.28)$$

Similarly,

$$(1+\varepsilon_2)^2 = cos^2\theta_2 \cdot (1+\varepsilon_3)^2 + sin^2\theta_2 \cdot (1+\varepsilon_y)^2 + 2(1+\varepsilon_3)(1+\varepsilon_y)sin\gamma_{xy}sin\theta_2 cos\theta_2 \quad (3.29)$$

To obtain a strain-displacement relationship that is linear in ε_X, ε_Y, γ_{XY}, then it is necessary to assume that $sin\gamma_{XY} \approx \gamma_{XY}$ and

$$\begin{aligned}(1+\varepsilon_Y)^2 &= 1 + 2\varepsilon_Y + \alpha^c \cdot \varepsilon_Y \\ &= 1 + (2+\alpha^c)\varepsilon_Y \end{aligned} \quad (3.30)$$

Using the notation in Eqn. 3.30, then, Eqns. 3.28 and 3.29 become

$$2\varepsilon_1 + \varepsilon_1^2 = cos^2\theta_1 \cdot (2\varepsilon_3 + \varepsilon_3^2) + sin^2\theta_1 \cdot (2+\alpha^c) \cdot \varepsilon_Y + 2\gamma_{XY}(1+\varepsilon_3)(1+\varepsilon_Y)sin\theta_1 cos\theta_1 \quad (3.31)$$

$$2\varepsilon_2 + \varepsilon_2^2 = cos^2\theta_2 \cdot (2\varepsilon_3 + \varepsilon_3^2) + sin^2\theta_2 \cdot (2+\alpha^c) \cdot \varepsilon_Y + 2\gamma_{xy}(1+\varepsilon_3)(1+\varepsilon_Y)sin\theta_2 cos\theta_2 \quad (3.32)$$

Solving Eqns. 3.31 and 3.32 simultaneously for ε_Y, then,

$\varepsilon_Y =$

$$\frac{(2\varepsilon_1 + \varepsilon_1^2)sin\theta_2 cos\theta_2 - (2\varepsilon_2 + \varepsilon_2^2)sin\theta_1 cos\theta_1 - (2\varepsilon_3 + \varepsilon_3^2) \cdot (cos^2\theta_1 sin\theta_2 cos\theta_2 - cos^2\theta_2 sin\theta_1 cos\theta_1)}{(sin^2\theta_1 sin\theta_2 cos\theta_2 - sin^2\theta_2 sin\theta_1 cos\theta_1)(2+\alpha^c)} .$$

Defining

$a_2 = sin\theta_2 cos\theta_2, b_2 = -sin\theta_1 cos\theta_1, c_2 = cos^2\theta_2 sin\theta_1 cos\theta_1 - cos^2\theta_1 sin\theta_2 cos\theta_2$

$A^c = sin^2\theta_1 sin\theta_2 cos\theta_2 - sin^2\theta_2 sin\theta_1 cos\theta_1$

then

$$\varepsilon_Y = \frac{a_2(2\varepsilon_1 + \varepsilon_1^2) + b_2(2\varepsilon_2 + \varepsilon_2^2) + c_2(2\varepsilon_3 + \varepsilon_3^2)}{A^c(2+\alpha^c)}$$

Similarly, solving Eqns (31) and (32) for γ_{XY}, then

$$\gamma_{XY} = \frac{a_3(2\varepsilon_1 + \varepsilon_1^2) + b_3(2\varepsilon_2 + \varepsilon_2^2) + c_3(2\varepsilon_3 + \varepsilon_3^2)}{2(1+\varepsilon_3)[a_2(2\varepsilon_1 + \varepsilon_1^2) + b_2(2\varepsilon_2 + \varepsilon_2^2) + c_2(2\varepsilon_3 + \varepsilon_3^2) + (2+\alpha^c)A^c]}$$

with,

$a_3 = sin_2^\theta, b_3 = -sin^2\theta_1, c_3 = -[cos^2\theta_1 sin^2\theta_2 - cos^2\theta_2 sin^2\theta_1]$

Finally

$$\begin{Bmatrix} \varepsilon_x \\ \varepsilon_y \\ \gamma_{xy} \end{Bmatrix} = \begin{bmatrix} 0 & 0 & 1 \\ \frac{a_2(2+\varepsilon_1)}{A^c(2+\alpha^c)} & \frac{b_2(2+\varepsilon_2)}{A^c(2+\alpha^c)} & \frac{c_3(2+\varepsilon_3)}{A^c(2+\alpha^c)} \\ \frac{a_3(2+\varepsilon_1)}{2(1+\varepsilon_3)B} & \frac{b_3(2+\varepsilon_2)}{2(1+\varepsilon_3)B} & \frac{c_3(2+\varepsilon_3)}{2(1+\varepsilon_3)B} \end{bmatrix} \begin{Bmatrix} \varepsilon_1 \\ \varepsilon_2 \\ \varepsilon_3 \end{Bmatrix} \tag{3.33}$$

or $\{\varepsilon\} = [B^{tr}]\{\delta\}^{tr}$, where

$$[B^{tr}] = \begin{bmatrix} 0 & 0 & L_3^{-1} \\ \frac{a_2(2+\varepsilon_1)\cdot L_1^{-1}}{A^c(2+\alpha^c)} & \frac{b_2(2+\varepsilon_2)\cdot L_2^{-1}}{A^c(2+\alpha^c)} & \frac{c_3(2+\varepsilon_3)\cdot L_3^{-1}}{A^c(2+\alpha^c)} \\ \frac{a_3(2+\varepsilon_1)\cdot L_1^{-1}}{2(1+\varepsilon_3)B^c} & \frac{b_3(2+\varepsilon_2)\cdot L_2^{-1}}{2(1+\varepsilon_3)B^c} & \frac{c_3(2+\varepsilon_3)\cdot L_3^{-1}}{2(1+\varepsilon_3)B^c} \end{bmatrix} \tag{3.34}$$

in which, collecting all definitions together,

$a_2 = sin\theta_2 cos\theta_2, b_2 = -sin\theta_1 cos\theta_1, c_2 = cos^2\theta_2 sin\theta_1 cos\theta_1 - cos^2\theta_1 sin\theta_2 cos\theta_2$ $a_3 = sin^2\theta_2, b_3 = -sin^2\theta_1, c_3 = -[cos^2\theta_1 sin^2\theta_2 - cos^2\theta_2 - cos^2\theta_2 sin^2\theta_1]$ $A = sin^2\theta_1 sin\theta_2 cos\theta_2 - sin^2\theta_2 sin\theta_1 cos\theta_1$

$B^c = \frac{a_2(2\varepsilon_1+\varepsilon_1^2)+b_2(2\varepsilon_2+\varepsilon_2^2)+c_3(\varepsilon_3+\varepsilon_3^2)+(2+\alpha_i^c)A^c}{A^c(2+\alpha_i^c)}$

α^c is an iteration coefficient, which has an initial value of zero and is subsequently updated according to,

$$\alpha_i^c = \frac{a_2(2\varepsilon_1^{i-1} + \varepsilon_1^{i-1^2}) + b_2(2\varepsilon_2^{i-1} + \varepsilon_2^{i-1^2}) + c_3(2\varepsilon_3^{i-1} + \varepsilon_3^{i-1^2})}{A(2+\alpha_{i-1}^c)}$$

Eqn. 3.31 is in a suitable form to be used in Eqns. 3.15 and 3.16 to define the element stiffness matrices and associated Eqn. 3.18. It should be noted that this formulation relies upon the assumption in Eqn. 3.1 that $\varepsilon_X = \frac{\partial U}{\partial X}$ and $\varepsilon_Y = \frac{\partial V}{\partial Y}$. No assumption is made about the form of γ_{XY}, but it is reasonably assumed that $sin(\gamma_{XY}) = \gamma_{XY}$.

3.1.3 CST with large strain formulation

The preceding CST formulations are characterized by the element strains ε_X and ε_Y defined as a linear deformation gradient (e.g. $\frac{\partial U}{\partial X}$) as in Eqn. 3.1, and the shear strain γ_{XY} approximated by $sin\gamma_{XY} = \gamma_{XY}$. These assumptions may no longer be valid under large strains where Green's deformation of strains is more appropriate, as in:

$$\begin{aligned}
\varepsilon_X &= \frac{dU}{dX} + 0.5\left(\left(\frac{dU}{dX}\right)^2 + \left(\frac{dV}{dX}\right)^2 + \left(\frac{dW}{dX}\right)^2\right) \\
\varepsilon_Y &= \frac{dV}{dY} + 0.5\left(\left(\frac{dU}{dY}\right)^2 + \left(\frac{dV}{dY}\right)^2 + \left(\frac{dW}{dY}\right)^2\right) \\
\gamma_{XY} &= \frac{dU}{dY} + \frac{dV}{dX} + \left(\frac{dU}{dX}\frac{dU}{dY} + \frac{dV}{dX}\frac{dV}{dY} + \frac{dW}{dX}\frac{dW}{dY}\right)
\end{aligned} \tag{3.35}$$

in which, ε_X, ε_Y and γ_{XY} are element strains, and U, V, W are displacements of the element in the local coordinate system XY.

Deriving the element equations using a "standard" finite element philosophy, displacements are interpolated from nodal values using shape functions $[N]$ as in

$$U(X,Y) = \sum_{i=1}^{3} N_i U_i, \quad V(X,Y) = \sum_{i=1}^{3} N_i V_i, \quad W(X,Y) = \sum_{i=1}^{3} N_i W_i \tag{3.36}$$

where $N_1 = \xi_1$, $N_2 = \xi_2$, $N_3 = \xi_3$, and ξ_1, ξ_2, ξ_3 are area co-ordinates of a given point P as defined in figure 3.7:

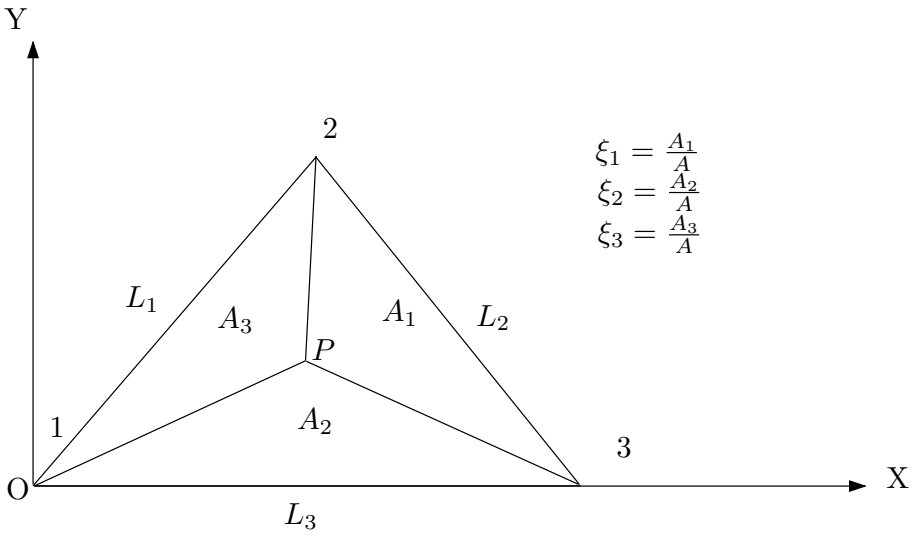

Figure 3.7: Area coordinate system

Given that,

$$\frac{d\xi_1}{dX} = \frac{Y_{23}}{2A} \quad \frac{d\xi_2}{dX} = \frac{Y_{31}}{2A} \quad \frac{d\xi_3}{dX} = \frac{Y_{12}}{2A}$$
$$\frac{d\xi_1}{dY} = \frac{X_{32}}{2A} \quad \frac{d\xi_2}{dY} = \frac{X_{13}}{2A} \quad \frac{d\xi_3}{dY} = \frac{X_{21}}{2A}$$

where A is the area of the element triangle, and for example $Y_{23} = Y_2 - Y_3$, then displacement derivatives are:

$$\begin{aligned}
\frac{dU}{dX} &= \frac{Y_{32}}{2A}U_1 + \frac{Y_{13}}{2A}U_2 + \frac{Y_{21}}{2A}U_3 \qquad \frac{dU}{dY} = \frac{X_{23}}{2A}U_1 + \frac{X_{31}}{2A}U_2 + \frac{X_{12}}{2A}U_3 \\
\frac{dV}{dX} &= \frac{Y_{32}}{2A}V_1 + \frac{Y_{13}}{2A}V_2 + \frac{Y_{21}}{2A}V_3 \qquad \frac{dV}{dY} = \frac{X_{23}}{2A}V_1 + \frac{X_{31}}{2A}V_2 + \frac{X_{12}}{2A}V_3 \\
\frac{dW}{dX} &= \frac{Y_{32}}{2A}W_1 + \frac{Y_{13}}{2A}W_2 + \frac{Y_{21}}{2A}W_3 \qquad \frac{dW}{dY} = \frac{X_{23}}{2A}W_1 + \frac{X_{31}}{2A}W_2 + \frac{X_{12}}{2A}W_3
\end{aligned} \tag{3.37}$$

If node 1 is set at the origin of the local XY coordinate system in which the element is coplanar, and the local X axis is aligned with the base of the triangular element, then $U_1 = V_1 = W_1 = 0$ and $U_3 = \delta_3$,$W_2 = 0$,$V_3 = W_3 = 0$. Consequently Eqns. 3.37 simplify to:

$$\frac{dU}{dX} = \frac{Y_{13}}{2A}U_2 + \frac{Y_{21}}{2A}\delta_3 \qquad \frac{dU}{dY} = \frac{X_{31}}{2A}U_2 + \frac{X_{12}}{2A}\delta_3 \tag{3.38}$$

$$\frac{dV}{dX} = \frac{Y_{13}}{2A}V_2 \qquad \frac{dV}{dY} = \frac{X_{31}}{2A}V_2 \tag{3.39}$$

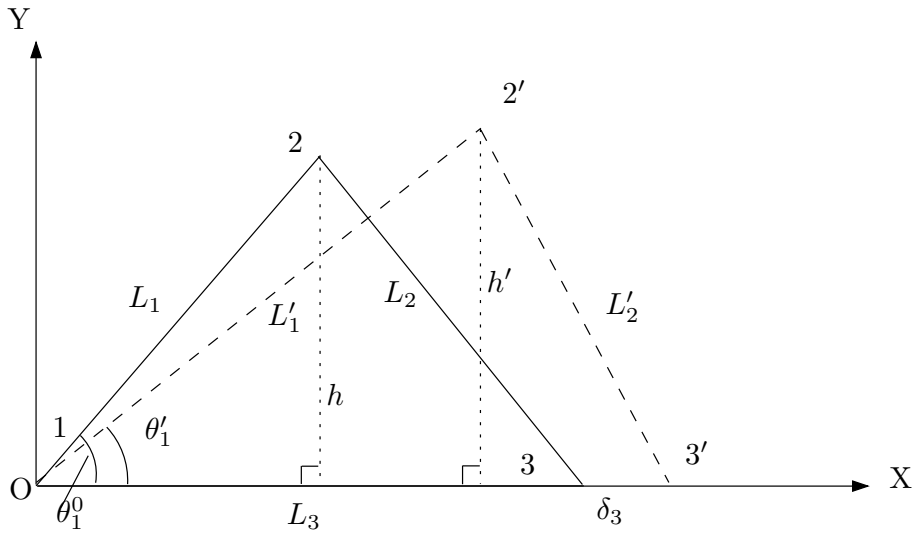

Figure 3.8: Local coordinate system for large strain CST formulation

To ensure consistency with Eqns. 3.15 and 3.18, nodal displacements U_i and V_i are rewritten as functions of the element side extensions δ_1,δ_2, and δ_3 as in:

$$U_2 = L'_1 \cdot cos\theta'_1 - L_1 \cdot cos\theta_1$$

$$\begin{aligned}
&= L'_1 \frac{L'^2_1 + L'^2_3 - L'^2_2}{2L'_1 \cdot L'_3} - L_1 \frac{L_1^2 + L_3^2 - L_2^2}{2L_1 \cdot L_3} \\
&= \frac{(L_1 + \delta_1)^2 + (L_3 + \delta_3)^2 - (L_2 + \delta_2)^2}{2(L_3 + \delta_3)} - \frac{L_1^2 + L_3^2 - L_2^2}{2L_3}
\end{aligned}$$

$$
\begin{aligned}
&= \frac{\delta_1 + 2L_1}{2(L_3+\delta_3)}\delta_1 - \frac{\delta_2 + 2L_2}{2(L_3+\delta_3)}\delta_2 + \frac{L_3^2 - L_1^2 + L_2^2 + \delta_3 \cdot L_3}{2(L_3+\delta_3)L_3}\delta_3 \\
&= a_1 \cdot \delta_1 + a_2 \cdot \delta_2 + a_3 \cdot \delta_3 \qquad (3.40)
\end{aligned}
$$

$$
\begin{aligned}
V_2 &= h' - h \\
&= \frac{2Area_{12'3'}}{L_3'} - \frac{2Area_{123}}{L_3} \\
&= \frac{\sqrt{L_2'^2 L_3'^2 - (\frac{L_2'^2+L_3'^2-L_1'^2}{2})^2}}{L_3'} - \frac{\sqrt{L_2^2 L_3^2 - (\frac{L_2^2+L_3^2-L_1^2}{2})^2}}{L_3} \\
&= \frac{L_3\sqrt{L_2'^2 L_3'^2 - (\frac{L_2'^2+L_3'^2-L_1'^2}{2})^2} - L_3'\sqrt{L_2^2 L_3^2 - (\frac{L_2^2+L_3^2-L_1^2}{2})^2}}{L_3 L_3'} \\
&= \frac{L_3^2[L_2'^2 L_3'^2 - (\frac{L_2'^2+L_3'^2-L_1'^2}{2})^2] - L_3'^2[L_2^2 L_3^2 - (\frac{L_2^2+L_3^2-L_1^2}{2})^2]}{L_3 L_3'[L_3\sqrt{L_2'^2 L_3'^2 - (\frac{L_2'^2+L_3'^2-L_1'^2}{2})^2} + L_3'\sqrt{L_2^2 L_3^2 - (\frac{L_2^2+L_3^2-L_1^2}{2})^2}]} \\
&= \frac{L_3^2 L_3'^2(L_2'-L_2)(L_2'+L_2) - [L_3\frac{L_2'^2+L_3'^2-L_1'^2}{2} - L_3'\frac{L_2^2+L_3^2-L_1^2}{2}]\cdot[L_3\frac{L_2'^2+L_3'^2-L_1'^2}{2} + L_3'\frac{L_2^2+L_3^2-L_1^2}{2}]}{L_3' L_3(L_3\cdot 2A' + L_3'\cdot 2A)} \\
&= \frac{L_3^2 L_3'^2(L_2'+L_2)\delta_2 - [L_3\frac{L_2'^2+L_3'^2-L_1'^2}{2} - L_3'\frac{L_2^2+L_3^2-L_1^2}{2}]\cdot BB}{L_3' L_3(L_3\cdot 2A' + L_3'\cdot 2A)} \\
&= \frac{L_3^2 L_3'^2(L_2'+L_2)\delta_2 - \delta_3\frac{L_2^2+L_3^2-L_1^2}{2}\cdot BB}{L_3' L_3(L_3\cdot 2A' + L_3'\cdot 2A)} \\
&\quad - \frac{[\frac{L_3}{2}((L_2'-L_2)(L_2'+L_2) + (L_3'-L_3)(L_3'+L_3) - (L_1'-L_1)(L_1'+L_1))]\cdot BB}{L_3' L_3(L_3\cdot 2A' + L_3'\cdot 2A)} \\
&= \frac{L_3^2 L_3'^2(L_2'+L_2)\delta_2 - [\frac{L_3}{2}((L_2'+L_2)\delta_2 + (L_3'+L_3)\delta_3 - (L_1'+L_1)\delta_1) - \delta_3\frac{L_2^2+L_3^2-L_1^2}{2}]\cdot BB}{L_3' L_3(L_3\cdot 2A' + L_3'\cdot 2A)} \\
&= \frac{\frac{L_3}{2}(L_1'+L_1)BB\delta_1 + (L_3'^2 L_3^2 - \frac{L_3}{2}\cdot BB)(L_2+L_2')\delta_2 + (\frac{L_2^2+L_3^2-L_1^2}{2} - \frac{L_3(L_3'+L_3)}{2})BB\cdot\delta_3}{L_3' L_3(L_3\cdot 2A' + L_3'\cdot 2A)} \\
&= \frac{\frac{L_3}{2}(L_1'+L_1)BB\delta_1 + (L_3'^2 L_3^2 - \frac{L_3}{2}\cdot BB)(L_2+L_2')\delta_2 + (L_2^2 - L_1^2 - L_3' L_3)\frac{BB}{2}\cdot\delta_3}{AA} \\
&= \frac{BB(2L_1 L_3 + L_3\delta_1)}{2AA}\cdot\delta_1 + [\frac{L_3'^2\cdot L_3^2(L_2'+L_2)}{AA} - \frac{BB(2L_2 L_3 + \delta_2\cdot L_3)}{2AA}]\cdot\delta_2 \\
&\quad + \frac{BB(L_2^2 - L_1^2 - L_3^2 - L_3\cdot\delta_3)}{2AA}\cdot\delta_3 \\
&= b_1\cdot\delta_1 + b_2\cdot\delta_2 + b_3\cdot\delta_3 \qquad (3.41)
\end{aligned}
$$

Substituting Eqn.3.38-3.41 into 3.35, we can get:

$$\{\varepsilon\} = [B]\{\delta\} = \begin{bmatrix} B_{11} & B_{12} & B_{13} \\ B_{21} & B_{22} & B_{23} \\ B_{31} & B_{32} & B_{33} \end{bmatrix} \begin{Bmatrix} \delta_1 \\ \delta_2 \\ \delta_3 \end{Bmatrix} \tag{3.42}$$

in which,

$B_{11} = B_{12} = 0 \qquad B_{13} = \frac{1}{L_3} + \frac{\delta_3}{2L_3^2}$

$B_{21} = E_1 \cdot b_1 + E_2 \cdot a_1 \quad B_{22} = E_1 \cdot b_2 + E_2 \cdot a_2 \quad B_{23} = E_1 \cdot b_3 + E_2 \cdot a_3 + E_3$

$B_{31} = F_1 \cdot a_1 \qquad B_{32} = F_1 \cdot a_2 \qquad B_{33} = F_1 \cdot a_3 + F_2$

The coefficients are defined as:

$L_1' = L_1 + \delta_1 \qquad L_2' = L_2 + \delta_2 \qquad L_3' = L_3 + \delta_3$

$AA = L_3' \cdot L_3(L_3\sqrt{L_3'^2 \cdot L_2'^2 - 0.25(L_2'^2 + L_3'^2 - L_1'^2)^2}$

$\quad + L_3' \cdot \sqrt{L_2^2 \cdot L_3^2 - 0.25(L_2^2 + L_3^2 - L_1^2)^2}$

$BB = 0.5L_3(L_2'^2 + L_3'^2 - L_1'^2) + 0.5L_3'(L_2^2 + L_3^2 - L_1^2)$

$a_1 = \frac{\delta_1 + 2L_1}{2L_3'} \qquad b_1 = \frac{BB(2L_1L_3 + L_3\delta_1)}{2AA}$

$a_2 = -\frac{\delta_2 + 2L_2}{2L_3'} \qquad b_2 = \frac{L_3'^2 \cdot L_3^2(L_2' + L_2)}{AA} - \frac{BB(2L_2L_3 + \delta_2 \cdot L_3)}{2AA}$

$a_3 = \frac{L_3^2 - L_1^2 + L_2^2 + \delta_3 \cdot L_3}{2L_3' \cdot L_3} \qquad b_3 = \frac{BB(L_2^2 - L_1^2 - L_3^2 - L_3 \cdot \delta_3)}{2AA}$

$U_2 = a_1\delta_1 + a_2\delta_2 + a_3\delta_3 \quad V_2 = b_1\delta_1 + b_2\delta_2 + b_3\delta_3 \quad U_3 = \delta_3$

$E_1 = \frac{X_{31}}{2A} + \frac{X_{31}^2}{8A^2}V_2 \qquad E_2 = \frac{X_{31}X_{12}}{4A^2}U_3 + \frac{X_{31}^2}{8A^2}U_2 \qquad E_3 = \frac{X_{12}^2}{8A^2}\delta_3$

$F_1 = \frac{X_{31}}{2A} \qquad F_2 = \frac{X_{12}}{2A} + \frac{Y_{21}}{2A}(\frac{X_{31}}{2A}U_2 + \frac{X_{12}}{2A}\delta_3) \qquad F = L_3'^2 \cdot L_3^2 \cdot L_1'$

where A and A' are the areas of the undeformed and deformed trinagles respectively.

Eqn. 3.42 may be substituted into Eqn. 3.15 and 3.18 to define the element characteristic matrices.

3.1.4 Stiffness Matrix Definitions

Since Dynamic Relaxation will be used as the solution procedure, only the diagonal terms of the stiffness matrices $[K_E^{tr}]$ $[K_\sigma^{pc}]$ are required.

$[K_E^{tr}]$ is the 3×3 elastic stiffness matrix defined in Eqn. 3.15 acting on the side extension δ_1, δ_2 and δ_3, and written symbolically as:

$$[K_E^{tr}] = \begin{bmatrix} K_{11}^{tr} & K_{12}^{tr} & K_{13}^{tr} \\ K_{21}^{tr} & K_{22}^{tr} & K_{23}^{tr} \\ K_{31}^{tr} & K_{32}^{tr} & K_{33}^{tr} \end{bmatrix} \tag{3.43}$$

The diagonal terms of the global elastic stiffness matrix $[K_E^t]$ acting on nodal displacements $\{u_1 \;\; v_1 \;\; w_1 \;\; u_2 \;\; v_2 \;\; w_2 \;\; u_3 \;\; v_3 \;\; w_3\}$ are:

$$[K_E^{t1}] = K_{11}^{tr} \cdot \begin{bmatrix} c_{x1}^2 \\ c_{y1}^2 \\ c_{z1}^2 \end{bmatrix} + K_{33}^{tr} \cdot \begin{bmatrix} c_{x3}^2 \\ c_{y3}^2 \\ c_{z3}^2 \end{bmatrix} \tag{3.44}$$

$$[K_E^{t2}] = K_{11}^{tr} \cdot \begin{bmatrix} c_{x1}^2 \\ c_{y1}^2 \\ c_{z1}^2 \end{bmatrix} + K_{22}^{tr} \cdot \begin{bmatrix} c_{x2}^2 \\ c_{y2}^2 \\ c_{z2}^2 \end{bmatrix} \tag{3.45}$$

$$[K_E^{t3}] = K_{22}^{tr} \cdot \begin{bmatrix} c_{x2}^2 \\ c_{y2}^2 \\ c_{z2}^2 \end{bmatrix} + K_{33}^{tr} \cdot \begin{bmatrix} c_{x3}^2 \\ c_{y3}^2 \\ c_{z3}^2 \end{bmatrix} \tag{3.46}$$

From the Eqn. 3.16, the diagonal terms of $[K_\sigma^{pc}]$ are:

$$[K_{\sigma 11}^{pc}] = \frac{T_{ci}}{l_i} - \frac{T_{ci}}{l_i} c_{xi}^2 \tag{3.47}$$

$$[K_{\sigma 22}^{pc}] = \frac{T_{ci}}{l_i} - \frac{T_{ci}}{l_i} c_{yi}^2 \tag{3.48}$$

$$[K_{\sigma 33}^{pc}] = \frac{T_{ci}}{l_i} - \frac{T_{ci}}{l_i} c_{zi}^2 \tag{3.49}$$

where c_{xi}, c_{yi} andc_{zi} are the direction cosines of the pseudo cable i in the global x, y, z coordinate system, and $i = 1 \rightarrow 3$. The values of T_{c1},T_{c2},T_{c3} are calculated from Eqn. 3.18

In a similar format to the elastic stiffness terms, the diagonal terms of the global geometric stiffness matrix $[K_{pc}^t]$ may be written as:

$$[K_{pc}^{t1}] = [I_3](\frac{T_{c1}}{L_1} + \frac{T_{c3}}{L_3}) - \frac{T_{c1}}{L_1} \cdot \begin{bmatrix} c_{x1}^2 \\ c_{y1}^2 \\ c_{z1}^2 \end{bmatrix} - \frac{T_{c3}}{L_3} \cdot \begin{bmatrix} c_{x3}^2 \\ c_{y3}^2 \\ c_{z3}^2 \end{bmatrix} \tag{3.50}$$

$$[K_{pc}^{t2}] = [I_3](\frac{T_{c1}}{L_1} + \frac{T_{c2}}{L_2}) - \frac{T_{c1}}{L_1} \cdot \begin{bmatrix} c_{x1}^2 \\ c_{y1}^2 \\ c_{z1}^2 \end{bmatrix} - \frac{T_{c2}}{L_2} \cdot \begin{bmatrix} c_{x2}^2 \\ c_{y2}^2 \\ c_{z2}^2 \end{bmatrix} \tag{3.51}$$

$$[K_{pc}^{t3}] = [I_3](\frac{T_{c2}}{L_2} + \frac{T_{c3}}{L_3}) - \frac{T_{c2}}{L_2} \cdot \begin{bmatrix} c_{x2}^2 \\ c_{y2}^2 \\ c_{z2}^2 \end{bmatrix} - \frac{T_{c3}}{L_3} \cdot \begin{bmatrix} c_{x3}^2 \\ c_{y3}^2 \\ c_{z3}^2 \end{bmatrix} \tag{3.52}$$

The total global stiffness matrix $[K_T^t]$ can be expressed as the summation of $[K_E^t]$ and $[K_{pc}^t]$:

$$[K_T^t] = [K_E^t] + [K_{pc}^t] \tag{3.53}$$

where the nine diagonal terms are given by summing the corresponding components of Eqn. 3.44-3.46 and 3.50-3.52.

Similarly the nodal forces of the CST element in the coordinate system xyz can be calculated from:

$$f_1 = \begin{Bmatrix} f_1^x \\ f_1^y \\ f_1^z \end{Bmatrix} = -T_{c1} \cdot \begin{bmatrix} c_{x1} \\ c_{y1} \\ c_{z1} \end{bmatrix} - T_{c3} \cdot \begin{bmatrix} c_{x3} \\ c_{y3} \\ c_{z3} \end{bmatrix} \tag{3.54}$$

$$f_2 = \begin{Bmatrix} f_2^x \\ f_2^y \\ f_2^z \end{Bmatrix} = T_{c1} \cdot \begin{bmatrix} c_{x1} \\ c_{y1} \\ c_{z1} \end{bmatrix} + T_{c2} \cdot \begin{bmatrix} c_{x2} \\ c_{y2} \\ c_{z2} \end{bmatrix} \tag{3.55}$$

$$f_3 = \begin{Bmatrix} f_3^x \\ f_3^y \\ f_3^z \end{Bmatrix} = -T_{c2} \cdot \begin{bmatrix} c_{x2} \\ c_{y2} \\ c_{z2} \end{bmatrix} + T_{c3} \cdot \begin{bmatrix} c_{x3} \\ c_{y3} \\ c_{z3} \end{bmatrix} \tag{3.56}$$

with Eqn. 3.18 defining values of T_{c1}, T_{c2},T_{c3}

3.2 Six-node Linear Strain Triangular Element with Element Curvatures

In addition to the obvious difference in strain-deformation capabilities, the six-node LST element described in this section may also have a curved geometry and nodes that are not necessarily located in a single plane. Furthermore, the concept of the cable-analogy is not adopted. Instead the element is formulated using a classical finite element theory approach. Consequently, only the derivations specific to this particular element are described in this section. The concept of the element formulation was originally described in a very brief paper published in Chinese by Ye [217]. However his formulation is not consistant with the standard finite element formulation. In this section, a new formulation with the application of the curvatures is presented. The formulation described in this chapter, therefore, largely constitutes original work.

3.2.1 Fundamental geometric

Local coordinate system

For a curved plane element, the local tangent co-ordinate system XY is assumed to be aligned with the membrane material direction, and the Z axis is normal to the plane XY. For any point on the surface, the coordinate vector may be expressed as $\overline{R} = \overline{R}(X, Y, Z)$

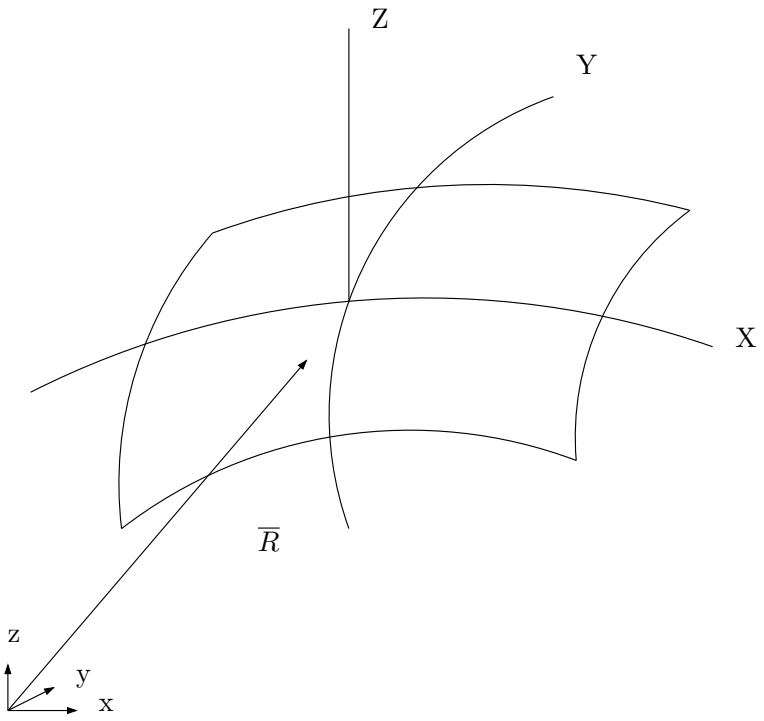

Figure 3.9: Local Curved Co-ordinate System

To facilitate transformation of the local to the global system , a second local coordinate system

$\overline{X}, \overline{Y}, \overline{Z}$ is introduced, in which the plane $\overline{X}, \overline{Y}$ is defined by the position of the apex nodes $1, 2, 3$ as shown in figure 3.10

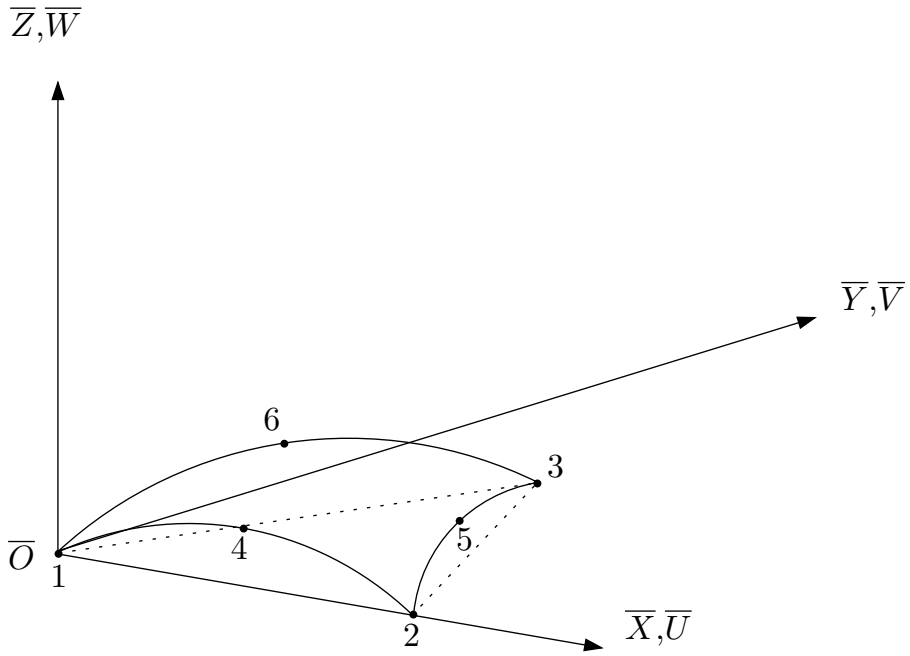

Figure 3.10: Curvilinear coordinate system

The transformation matrix between these two local coordinate systems is expressed as:

$$\begin{Bmatrix} F_{\overline{X}} \\ F_{\overline{Y}} \\ F_{\overline{Z}} \end{Bmatrix} = \overline{T}^c \begin{Bmatrix} F_X \\ F_Y \\ F_Z \end{Bmatrix}, \begin{Bmatrix} \overline{U} \\ \overline{V} \\ \overline{W} \end{Bmatrix} = \overline{T}^c \begin{Bmatrix} U \\ V \\ W \end{Bmatrix} \tag{3.57}$$

where

$$\overline{T}^c = \begin{bmatrix} \frac{1}{\sqrt{1+(\overline{Z},_{\overline{X}})^2}} & 0 & \frac{-\overline{Z},_{\overline{X}}}{\sqrt{1+(\overline{Z},_{\overline{X}})^2}} \\ 0 & \frac{1}{\sqrt{1+(\overline{Z},_{\overline{Y}})^2}} & \frac{-\overline{Z},_{\overline{Y}}}{\sqrt{1+(\overline{Z},_{\overline{Y}})^2}} \\ \frac{\overline{Z},_{\overline{X}}\sqrt{(1+(\overline{Z},_{\overline{X}})^2)(1+(\overline{Z},_{\overline{Y}})^2)}}{\sqrt{1+(\overline{Z},_{\overline{X}})^2+(\overline{Z},_{\overline{Y}})^2}} & \frac{\overline{Z},_{\overline{Y}}\sqrt{(1+(\overline{Z},_{\overline{X}})^2)(1+(\overline{Z},_{\overline{Y}})^2)}}{\sqrt{1+(\overline{Z},_{\overline{X}})^2+(\overline{Z},_{\overline{Y}})^2}} & \frac{\sqrt{(1+(\overline{Z},_{\overline{X}})^2)(1+(\overline{Z},_{\overline{Y}})^2)}}{\sqrt{1+(\overline{Z},_{\overline{X}})^2+(\overline{Z},_{\overline{Y}})^2}} \end{bmatrix} \tag{3.58}$$

in which $\overline{Z},_{\overline{X}}$ and $\overline{Z},_{\overline{Y}}$ are the derivatives of $\overline{Z}$ with respect to $\overline{X}$ and $\overline{Y}$ respectively. Consistent with the number of nodes describing the element, we assume the curved surface can be represented by:

$$\overline{Z} = a_1 + a_2\overline{X} + a_3\overline{Y} + a_4\overline{X}^2 + a_5\overline{XY} + a_6\overline{Y}^2 \tag{3.59}$$

Substituting the coordinates of the 6 nodes into Eqn. 3.59, we obtain the equation array:

$$\begin{bmatrix} 1 & \overline{X}_1 & \overline{Y}_1 & \overline{X}_1^2 & \overline{X}_1\overline{Y}_1 & \overline{Y}_1^2 \\ 1 & \overline{X}_2 & \overline{Y}_2 & \overline{X}_2^2 & \overline{X}_2\overline{Y}_2 & \overline{Y}_2^2 \\ 1 & \overline{X}_3 & \overline{Y}_3 & \overline{X}_3^2 & \overline{X}_3\overline{Y}_3 & \overline{Y}_3^2 \\ 1 & \overline{X}_4 & \overline{Y}_4 & \overline{X}_4^2 & \overline{X}_4\overline{Y}_4 & \overline{Y}_4^2 \\ 1 & \overline{X}_5 & \overline{Y}_5 & \overline{X}_5^2 & \overline{X}_5\overline{Y}_5 & \overline{Y}_5^2 \\ 1 & \overline{X}_6 & \overline{Y}_6 & \overline{X}_6^2 & \overline{X}_6\overline{Y}_6 & \overline{Y}_6^2 \end{bmatrix} \cdot \begin{Bmatrix} a_1 \\ a_2 \\ a_3 \\ a_4 \\ a_5 \\ a_6 \end{Bmatrix} = \begin{Bmatrix} \overline{Z}_1 \\ \overline{Z}_2 \\ \overline{Z}_3 \\ \overline{Z}_4 \\ \overline{Z}_5 \\ \overline{Z}_6 \end{Bmatrix} \tag{3.60}$$

or

$$[\overline{A}] \cdot \{a\} = \{\overline{Z}\}$$

Solving Eqn. 3.60, then

$$\{a\} = [\overline{A}]^{-1}\{\overline{Z}\} \tag{3.61}$$

where the values of a_1–a_6 are calculated numerically.

The curvilinear coordinates (X,Y) are defined with the original at the geometric centre of the element (see fig. 3.9) as:

$$\begin{aligned} X &= \int_0^{\overline{X}} \sqrt{1 + (\frac{\partial \overline{Z}}{\partial \overline{X}})^2} \quad d\overline{X} \\ &= \int_0^{\overline{X}} \sqrt{1 + (a_2 + 2a_4\overline{X} + a_5\overline{Y})^2} \quad d\overline{X} \\ &= (\frac{a_2 + a_5\overline{Y}}{4a_4} + \frac{\overline{X}}{2}) \cdot \sqrt{1 + (a_2 + 2a_4\overline{X} + a_5\overline{Y})^2} + \frac{arcsinh(a_2 + 2a_4\overline{X} + a_5\overline{Y})}{4a_4} \end{aligned} \tag{3.62}$$

$$\begin{aligned} Y &= \int_0^{\overline{Y}} \sqrt{1 + (\frac{\partial \overline{Z}}{\partial \overline{Y}})^2} \quad d\overline{Y} \\ &= \int_0^{\overline{Y}} \sqrt{1 + (a_3 + a_5\overline{X} + 2a_6\overline{Y})} \quad d\overline{Y} \\ &= (\frac{a_3 + a_5\overline{X}}{4a_6} + \frac{\overline{Y}}{2}) \cdot \sqrt{1 + (a_3 + a_5\overline{X} + 2a_6\overline{Y})^2} + \frac{arcsinh(a_3 + a_5\overline{X} + 2a_6\overline{Y})}{4a_6} \end{aligned} \tag{3.63}$$

Element Curvatures

Element curvatures in each element are defined with respect to the local flat plane coordinate system $\overline{X}$, $\overline{Y}$, $\overline{Z}$. With the out-of-plane geometry of the 6-node triangular element written as $\overline{Z} = f(\overline{X}, \overline{Y})$, then the curvatures about the local $\overline{X}$ and $\overline{Y}$ axes, are:

$$K_{\overline{X}} = -\frac{\partial^2 \overline{Z}}{\partial \overline{X}^2}, K_{\overline{Y}} = -\frac{\partial^2 \overline{Z}}{\partial \overline{Y}^2} \tag{3.64}$$

and the torsion between $\overline{X}$ and $\overline{Y}$ axis is:

$$K_{\overline{XY}} = -\frac{\partial^2 \overline{Z}}{\partial \overline{X} \partial \overline{Y}} \tag{3.65}$$

3.2.2 Relationship between element strains and element curvatures

The extra force vectors normal to the element surface are assumed to contribute to the element curvatures and in-plane stresses.

$$\begin{aligned} \Delta f_{\overline{Z}} &= K_{\overline{X}} \times \sigma_{\overline{X}} + K_{\overline{Y}} \times \sigma_{\overline{Y}} + K_{\overline{XY}} \times \tau_{\overline{XY}} = \{K_{\overline{X}} \quad K_{\overline{Y}} \quad K_{\overline{XY}}\} \begin{Bmatrix} \sigma_{\overline{X}} \\ \sigma_{\overline{Y}} \\ \tau_{\overline{XY}} \end{Bmatrix} \\ &= [C_v] \cdot \{\sigma\} \end{aligned} \tag{3.66}$$

Where $[C_v] = [K_{\overline{X}}\ K_{\overline{Y}}\ K_{\overline{XY}}]$ and $\{\sigma\} = \{\sigma_{\overline{X}}\ \sigma_{\overline{Y}}\ \tau_{\overline{XY}}\}^T$

From Eqn. 3.66, it is apparent that if the element curvatures (Eqn 3.64) are zero, e.g a flat surface, then no strains are induced due to to displacements normal to the surface. In that case, the elastic stiffness to normal loads is zero. However the elastic stiffness in the direction normal to the element surface becomes greater as the element curvatures increase.

3.2.3 Finite Element Formulation

Strain-displacement relations

Nodal coordinates in local curved coordinate system are defined in the section 3.2.1. The area coordinate system(ξ_1,ξ_2,ξ_3) introduced in Fig.3.7, is defined for the six node curved triangular element, by the shape functions:

$$\begin{aligned} N_1 = \xi_1(2\xi_1 - 1), N_2 = \xi_2(2\xi_2 - 1), N_3 = \xi_3(2\xi_3 - 1) \\ N_4 = 4\xi_1\xi_2, N_5 = 4\xi_2\xi_3, N_6 = 4\xi_3\xi_1 \end{aligned} \tag{3.67}$$

The displacement fields are approximated by:

$$U(X,Y) = \sum_{i=1}^{6} N_i U_i, \quad V(X,Y) = \sum_{i=1}^{6} N_i V_i, \quad W(X,Y) = \sum_{i=1}^{6} N_i W_i \tag{3.68}$$

and the cartesian co-ordinate X and Y of the unstrained initial configuration are approximated by:

$$X = \sum_{i=1}^{6} N_i X_i, \quad Y = \sum_{i=1}^{6} N_i Y_i \tag{3.69}$$

in which, U_i V_i W_i and X_i Y_i are nodal displacements and nodal coordinates respectively.

The expressions for Green's strains are:

$$\begin{aligned}
\varepsilon_X &= \frac{\partial U}{\partial X} + \frac{1}{2}\left[\left(\frac{\partial U}{\partial X}\right)^2 + \left(\frac{\partial V}{\partial X}\right)^2 + \left(\frac{\partial W}{\partial X}\right)^2\right] \\
\varepsilon_Y &= \frac{\partial V}{\partial Y} + \frac{1}{2}\left[\left(\frac{\partial U}{\partial Y}\right)^2 + \left(\frac{\partial V}{\partial Y}\right)^2 + \left(\frac{\partial W}{\partial Y}\right)^2\right] \\
\gamma_{XY} &= \frac{\partial U}{\partial Y} + \frac{\partial V}{\partial X} + \left(\frac{\partial U}{\partial X}\right)\left(\frac{\partial U}{\partial Y}\right) + \left(\frac{\partial V}{\partial X}\right)\left(\frac{\partial V}{\partial Y}\right) + \left(\frac{\partial W}{\partial X}\right)\left(\frac{\partial W}{\partial Y}\right)
\end{aligned} \tag{3.70}$$

Derivation of Stiffness Matrix and Equilibrium Equation

A virtual displacement δd is defined at the nodes.This results in virtual displacements and strains within the element of:

$$\delta u = N\ \delta d \quad and \quad \delta\epsilon = B\ \delta d \tag{3.71}$$

respectively.

The work done by the nodal forces is :

$$\delta d^T \cdot f \tag{3.72}$$

Similarly, the internal work per unit volume done by the stresses δ, the extra out-of-plane force, and distributed forces:

$$\delta\epsilon^T \cdot \sigma + \delta d \cdot \Delta f_{\overline{Z}} - \delta u^T \cdot b \tag{3.73}$$

or

$$\delta d(B^T \cdot \sigma + C_v \cdot \sigma - N^T \cdot b) \tag{3.74}$$

in which $b = \begin{Bmatrix} b_x \\ b_y \end{Bmatrix}$ is the distributed load,b_x, b_y are the "body force" components. Equating the external work with the total internal work obtained by integrating over the volume of the element,V^e ,we have:

$$\delta d^T \cdot f = \delta d(\int_{V^e} (B^T + C_v)\sigma\ dV - \int_{V^e} N^T b\ dV) \tag{3.75}$$

$$f = \int_{V^e} (B^T + C_v)\sigma\ dV - \int_{V^e} N^T b\ dV \tag{3.76}$$

If we assume general linear elastic behavior, the relationship between stresses and strains will be linear and of the form:

$$\sigma = E(\epsilon - \epsilon_0) + \sigma_0 \tag{3.77}$$

where E is an elasticity matrix containing the appropriate material properties.

Then we can write:

$$f = \int_{V^e} (B^T + C_v) \cdot E \cdot B \cdot d \;\; dV + \int_{V^e} (B^T + C_v)\sigma_0 dV - \int_{V^e} (B^T + C_v) \cdot E \cdot \epsilon_0 dV - \int_{V^e} N^T b \;\; dV \tag{3.78}$$

If assuming zero "body force" and initial strains, then we can get:

$$f = \int_{V^e} (B^T + C_v) \cdot E \cdot B \cdot d \;\; dV + \int_{V^e} (B^T + C_v) \cdot \sigma_0 \;\; dV \tag{3.79}$$

Defining

$$B = B_0 + B_L \tag{3.80}$$

where B_0 is independent of nodal displacement, and B_L is a linear function of the nodal displacements, then

$$f = \int_{V^e} (B^T + C_v) \cdot E \cdot B \cdot d \;\; dV + \int_{V^e} C_v \cdot \sigma_0 \;\; dV + \int_{V^e} B_0^T \cdot \sigma_0 \;\; dV + \int_{V^e} B_L^T \cdot \sigma_0 \;\; dV \tag{3.81}$$

From the Eqn. 3.70, element strains are:

$$\begin{aligned} \epsilon &= \begin{Bmatrix} \epsilon_X \\ \epsilon_Y \\ \gamma_{XY} \end{Bmatrix} \\ &= \begin{Bmatrix} \frac{\partial U}{\partial X} \\ \frac{\partial V}{\partial Y} \\ \frac{\partial V}{\partial X} + \frac{\partial U}{\partial Y} \end{Bmatrix} + \frac{1}{2} \cdot \begin{Bmatrix} (\frac{\partial U}{\partial X})^2 + (\frac{\partial V}{\partial X})^2 + (\frac{\partial W}{\partial X})^2 \\ (\frac{\partial U}{\partial Y})^2 + (\frac{\partial V}{\partial Y})^2 + (\frac{\partial W}{\partial Y})^2 \\ 2 \cdot \{\frac{\partial U}{\partial X} \cdot \frac{\partial V}{\partial Y} + \frac{\partial V}{\partial X} \cdot \frac{\partial V}{\partial Y} + \frac{\partial W}{\partial X} \cdot \frac{\partial W}{\partial Y}\} \end{Bmatrix} \\ &= (B_0 + B_L) \cdot d \end{aligned} \tag{3.82}$$

We define $\epsilon_L = B_0 \cdot d$ and $\epsilon_{NL} = B_L \cdot d$. As they are somewhat cumbersome, the detailed expressions of B_0 and B_L matrix and their derivation are given in Appendix B.1.

ϵ_{NL} can be written as:

$$\begin{aligned}\epsilon_{NL} &= \frac{1}{2}\begin{bmatrix} \frac{\partial U}{\partial X} & \frac{\partial V}{\partial X} & \frac{\partial W}{\partial X} & 0 & 0 & 0 \\ 0 & 0 & 0 & \frac{\partial U}{\partial Y} & \frac{\partial V}{\partial Y} & \frac{\partial W}{\partial Y} \\ \frac{\partial U}{\partial Y} & \frac{\partial V}{\partial Y} & \frac{\partial W}{\partial Y} & \frac{\partial U}{\partial X} & \frac{\partial V}{\partial X} & \frac{\partial W}{\partial X} \end{bmatrix} \cdot \begin{Bmatrix} \frac{\partial U}{\partial X} \\ \frac{\partial V}{\partial X} \\ \frac{\partial W}{\partial X} \\ \frac{\partial U}{\partial Y} \\ \frac{\partial V}{\partial Y} \\ \frac{\partial W}{\partial Y} \end{Bmatrix} \\ &= \frac{1}{2} A \cdot \Delta \end{aligned} \tag{3.83}$$

so

$$\epsilon^T = \frac{1}{2}\Delta^T \cdot A^T \tag{3.84}$$

and

$$A^T = \begin{bmatrix} \frac{\partial U}{\partial X} & 0 & \frac{\partial U}{\partial Y} \\ \frac{\partial V}{\partial X} & 0 & \frac{\partial V}{\partial Y} \\ \frac{\partial W}{\partial X} & 0 & \frac{\partial W}{\partial Y} \\ 0 & \frac{\partial U}{\partial Y} & \frac{\partial U}{\partial X} \\ 0 & \frac{\partial V}{\partial Y} & \frac{\partial V}{\partial X} \\ 0 & \frac{\partial W}{\partial Y} & \frac{\partial W}{\partial X} \end{bmatrix} \tag{3.85}$$

If the initial stress vector

$$\sigma_0 = \begin{Bmatrix} \sigma_{X0} \\ \sigma_{Y0} \\ \tau_{XY0} \end{Bmatrix} \tag{3.86}$$

then

$$A^T \cdot \sigma_0 = \begin{bmatrix} \frac{\partial U}{\partial X} & 0 & \frac{\partial U}{\partial Y} \\ \frac{\partial V}{\partial X} & 0 & \frac{\partial V}{\partial Y} \\ \frac{\partial W}{\partial X} & 0 & \frac{\partial W}{\partial Y} \\ 0 & \frac{\partial U}{\partial Y} & \frac{\partial U}{\partial X} \\ 0 & \frac{\partial V}{\partial Y} & \frac{\partial V}{\partial X} \\ 0 & \frac{\partial W}{\partial Y} & \frac{\partial W}{\partial X} \end{bmatrix} \cdot \begin{Bmatrix} \sigma_{X0} \\ \sigma_{Y0} \\ \tau_{XY0} \end{Bmatrix}$$

$$= \begin{Bmatrix} \frac{\partial U}{\partial X}\cdot\sigma_{X0} + \frac{\partial U}{\partial Y}\cdot\tau_{XY0} \\ \frac{\partial V}{\partial X}\cdot\sigma_{X0} + \frac{\partial V}{\partial Y}\cdot\tau_{XY0} \\ \frac{\partial W}{\partial X}\cdot\sigma_{X0} + \frac{\partial W}{\partial Y}\cdot\tau_{XY0} \\ \frac{\partial U}{\partial Y}\cdot\sigma_{Y0} + \frac{\partial U}{\partial X}\cdot\tau_{XY0} \\ \frac{\partial V}{\partial Y}\cdot\sigma_{Y0} + \frac{\partial V}{\partial X}\cdot\tau_{XY0} \\ \frac{\partial W}{\partial Y}\cdot\sigma_{Y0} + \frac{\partial W}{\partial X}\cdot\tau_{XY0} \end{Bmatrix} \tag{3.87}$$

$$= \begin{bmatrix} \sigma_{X0} & 0 & 0 & \tau_{XY} & 0 & 0 \\ 0 & \sigma_{X0} & 0 & 0 & \tau_{XY} & 0 \\ 0 & 0 & \sigma_{X0} & 0 & 0 & \tau_{XY} \\ \tau_{XY} & 0 & 0 & \sigma_{Y0} & 0 & 0 \\ 0 & \tau_{XY} & 0 & 0 & \sigma_{Y0} & 0 \\ 0 & 0 & \tau_{XY} & 0 & 0 & \sigma_{Y0} \end{bmatrix} \cdot \begin{Bmatrix} \frac{\partial U}{\partial X} \\ \frac{\partial V}{\partial X} \\ \frac{\partial W}{\partial X} \\ \frac{\partial U}{\partial Y} \\ \frac{\partial V}{\partial Y} \\ \frac{\partial W}{\partial Y} \end{Bmatrix}$$

$$= M \cdot \Delta \tag{3.88}$$

in which

$$M = \begin{bmatrix} \sigma_{X0}[I_3] & \tau_{XY0}[I_3] \\ \tau_{XY0}[I_3] & \sigma_{Y0}[I_3] \end{bmatrix}$$

With $\epsilon_{NL} = B_L \cdot d$, then:

$$\begin{aligned} \epsilon_{NL}^T \cdot \sigma_0 &= d^T \cdot B_L^T \cdot \sigma_0 \\ &= \frac{1}{2}\Delta^T \cdot A^T \cdot \sigma_0 \end{aligned} \tag{3.89}$$

While from Eqn. 3.87:

$$\Delta = G \cdot d$$

in which $d = \{U_1 \;\; V_1 \;\; W_1 \;\; U_2 \;\; V_2 \;\; W_2 \;\; U_3 \;\; V_3 \;\; W_3 \;\; U_4 \;\; V_4 \;\; W_4 \;\; U_5 \;\; V_5 \;\; W_5 \;\; U_6 \;\; V_6 \;\; W_6\}$ and G is a 6×18 matrix detailed in Appendix B.2.

Therefore,

$$d^T \cdot B_L^T \cdot \sigma_0 = \frac{1}{2} \cdot d^T \cdot G^T \cdot M \cdot G \cdot d \tag{3.90}$$

$$B_L^T \cdot \sigma_0 = \frac{1}{2} \cdot G^T \cdot M \cdot G \cdot d \tag{3.91}$$

substituting Eqn. 3.91 into Eqn. 3.78, then:

$$f = (K_E + \frac{1}{2}K_\sigma)d + f_e = Kd + f_e \tag{3.92}$$

in which,

$$K_E = \int_{V^e} B^T E B \; dV \tag{3.93}$$

$$K_\sigma = \int_{V^e} G^T \cdot M \cdot G \;\; dV \tag{3.94}$$

and

$$f_e = \int_{V^e} (B_0^T + C_v) \cdot \sigma_0 \;\; dV \tag{3.95}$$

If assuming zero body forces, then from Eqn. 3.76, we can get

$$\int_{V^e} (B^T + C_v)\sigma - f = 0 \tag{3.96}$$

or

$$f = \int_{V^e} (B^T + C_v)\sigma d\ V \tag{3.97}$$

The out-of-balance force vector, denoted by ψ, can then be written as:

$$\psi(u) = \int_{V^e} (B^T + C_v)\sigma - F \; dV \tag{3.98}$$

where F external force vector, B is defined from the strain definition as:

$$d\epsilon = Bdu$$

If the element nodal displacements are large, the strains depend non-linearly on displacements, such that :

$$B = B_0 + B_L(u)$$

If strains are reasonably small, we can still write the general elastic relation:

$$\sigma = E(\epsilon - \epsilon_0) + \sigma_0$$

in which E is the usual set of elastic constants. Then

$$d\psi = \int_{V^e} dB^T + dC_v\sigma \; dV + \int_{V^e} (B^T + C_v) \; d\sigma = K_T \cdot du$$

with $d\sigma = E \cdot d\epsilon = E \cdot B \cdot du$, $dB = dB_L$ and $dC_v = 0$

Therefore

$$d\psi = \int_{V^e} dB_L^T \sigma \cdot dV + K \cdot du \tag{3.99}$$

where

$$K = \int_{V^e} (B^T + C_v) E B \; dV$$

The first term can be generally written as $\int_V dB_L^T \sigma \; dV = K_\sigma \; du$

where K_σ is a symmetric matrix dependent on the stress level. This matrix is known as initial stress matrix or geometric matrix. Therefore:

$$d\psi = (K_E + K_\sigma) \cdot du = K^T \cdot du \tag{3.100}$$

Numerical integration, element distortion and numerical instability

As Eqns. 3.93-3.95 are relatively complex and difficult to integrate analytically, numerical integration techniques are used instead in the form of Gauss quadrature. An integral is evaluated as follows:

$$\int_{\omega A} \phi(\xi_{1i}, \xi_{i2}, \xi_{i3}) dA = \frac{1}{2} \sum_{i=1}^{n} W_i J_i \phi_i \tag{3.101}$$

in which, ϕ_i and J_i are the value of ϕ and Jacobian matrix J, and calculated respectively at the specific sampling point location ξ_i with W_i the corresponding weight factor.

Since area coordinates are not independent but must satisfy the constraint:

$$\xi_1 + \xi_2 + \xi_3 = 1,$$

we define:

$$\begin{aligned} \xi_1 &= \zeta \\ \xi_2 &= \eta \\ \xi_3 &= 1 - \zeta - \eta \end{aligned}$$

To evaluate the shape function derivatives, we invoke the chain rule:

$$\begin{aligned} \frac{\partial N_i}{\partial \zeta} &= \frac{\partial N_i}{\partial \xi_1}\frac{\partial \xi_1}{\partial \zeta} + \frac{\partial N_i}{\partial \xi_2}\frac{\partial \xi_2}{\partial \zeta} + \frac{\partial N_i}{\partial \xi_3}\frac{\partial \xi_3}{\partial \zeta} \\ &= \frac{\partial N_i}{\partial \xi_1} - \frac{\partial N_i}{\partial \xi_3} \end{aligned} \tag{3.102}$$

Similarly

$$\frac{\partial N_i}{\eta} = \frac{\partial N_i}{\xi_2} - \frac{\partial N_i}{\partial \xi_3} \tag{3.103}$$

and

$$\begin{Bmatrix} \frac{\partial N_i}{\partial \zeta} \\ \frac{\partial N_i}{\partial \eta} \end{Bmatrix} = \begin{Bmatrix} \frac{\partial X}{\partial \zeta} & \frac{\partial Y}{\partial \zeta} \\ \frac{\partial X}{\partial \eta} & \frac{\partial Y}{\partial \eta} \end{Bmatrix} \begin{Bmatrix} \frac{\partial N_i}{\partial X} \\ \frac{\partial N_i}{\partial Y} \end{Bmatrix} = J \begin{Bmatrix} \frac{\partial N_i}{\partial X} \\ \frac{\partial N_i}{\partial Y} \end{Bmatrix} \tag{3.104}$$

Substituting Eqn.3.102, 3.103 and 3.67 into Eqn. 3.104 gives,

$$\begin{aligned} J &= \begin{bmatrix} \frac{\partial N_1}{\partial \zeta} & \frac{\partial N_2}{\partial \zeta} & \frac{\partial N_3}{\partial \zeta} & \frac{\partial N_4}{\partial \zeta} & \frac{\partial N_5}{\partial \zeta} & \frac{\partial N_6}{\partial \zeta} \\ \frac{\partial N_1}{\partial \eta} & \frac{\partial N_2}{\partial \eta} & \frac{\partial N_3}{\partial \eta} & \frac{\partial N_4}{\partial \eta} & \frac{\partial N_5}{\partial \eta} & \frac{\partial N_6}{\partial \eta} \end{bmatrix} \begin{Bmatrix} X_1 & Y_1 \\ X_2 & Y_2 \\ X_3 & Y_3 \\ X_4 & Y_4 \\ X_5 & Y_5 \\ X_6 & Y_6 \end{Bmatrix} \\ &= \begin{bmatrix} 4\xi_1 & 0 & -4\xi_3+1 & 4\xi_2 & -4\xi_2 & 4(\xi_3-\xi_2) \\ 0 & 4\xi_2 & -4\xi_3+1 & 4\xi_1 & 4(\xi_3-\xi_2) & -4\xi_1 \end{bmatrix} \begin{Bmatrix} X_1 & Y_1 \\ X_2 & Y_2 \\ X_3 & Y_3 \\ X_4 & Y_4 \\ X_5 & Y_5 \\ X_6 & Y_6 \end{Bmatrix} \\ &= [D_N] \cdot \begin{Bmatrix} X_1 & Y_1 \\ X_2 & Y_2 \\ X_3 & Y_3 \\ X_4 & Y_4 \\ X_5 & Y_5 \\ X_6 & Y_6 \end{Bmatrix} \end{aligned} \tag{3.105}$$

Normally if the function ψ is a polynomial, then integration using Eqn 3.101 can be achieved accurately with an adequate number of Gauss points as listed in table 3.1 based on the highest order terms of the function ψ. For the undistorted LST element, $|J|$ is constant, making ψ a polynomial. With the highest order term in the LST formulation is power four, six Gauss points are sufficient for accurate integration for the undistorted LST.

Highest order	1	2	3	4	5	6
Gauss point required	1	3	4	6	7	12

Table 3.1: The necessary Gauss point number according the highest order

However, geometric distortion produces a [J] matrix whose terms are not polynomials but rather the ratio of two polynomials, so inexact integration is expected using six Gauss points for elements with edges that are not straight and nodes that are not at the midpoints. Therefore it is proposed to use more Gauss points in anticipating element distortion, and twelve Guass points are used here without compromising the accuracy and computational efficiency.

The coefficients in the numerical integration using 12 Gauss points are listed in the table 3.2, and the detailed positions of these Gauss points are shown in figure 3.11.

Points	Area Coordinates ξ_1, ξ_2, ξ_3			Weight W_i
1	0.8738219710	0.0630890144	0.0630890144	0.0508449063
2	0.0630890144	0.8738219710	0.0630890144	0.0508449063
3	0.0630890144	0.0630890144	0.8738219710	0.0508449063
4	0.5014265096	0.2492867451	0.2492867451	0.1167862757
5	0.2492867451	0.5014265096	0.2492867451	0.1167862757
6	0.2492867451	0.2492867451	0.5014265096	0.1167862757
7	0.6365024991	0.3103524510	0.0531450498	0.0828510756
8	0.0531450498	0.6365024991	0.3103524510	0.0828510756
9	0.3103524510	0.0531450498	0.6365024991	0.0828510756
10	0.6365024991	0.0531450498	0.3103524510	0.0828510756
11	0.0531450498	0.3103524510	0.6365024991	0.0828510756
12	0.3103524510	0.6365024991	0.0531450498	0.0828510756

Table 3.2: Coefficients of numerical integration by 12 Gauss points

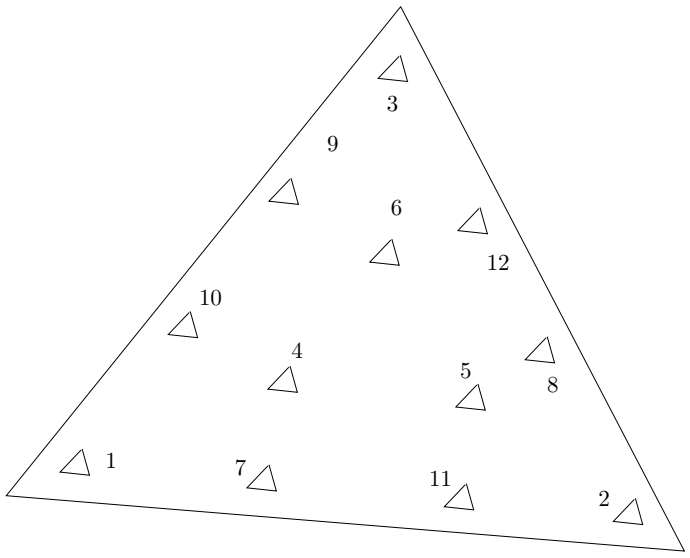

Figure 3.11: Gauss point position of numerical integration

During load analysis, and in particular during form-finding, nodal displacements may induce significant element distortion.

As illustrated in fig. 3.12, the main severe distortion modes of the 6 node curved triangular element are:

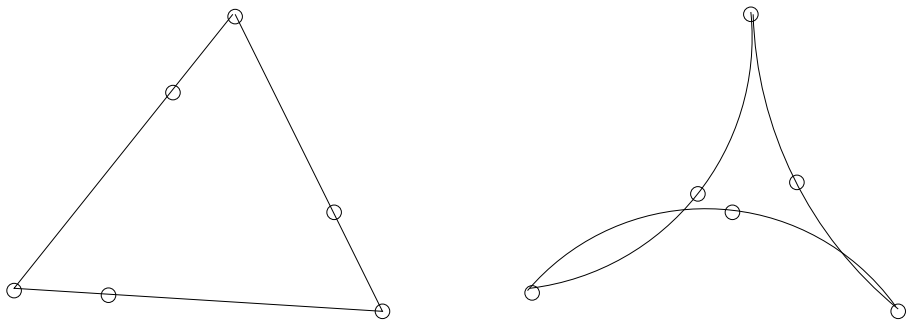

Mid node distortion Inversion

Figure 3.12: Distortion of 6 node curved triangular element

(1) Mid-side nodes remote from the middle position of the element side.

(2) Inversion.

Measures of these types of distortion have been proposed. For example,

(1) Mid point coefficient μ, defined as the maximum distance from mid nodes to the middle position of the element side.

(2) Curvature coefficient β, which is a function of element shape factor and curvatures of the element sides.

If the apex nodes of the triangular element are denoted as ABC, then the shape factor is ([233, 234]),

$$\beta_1 = 2\sqrt{3}\frac{||CA \times CB||}{||AB^2|| + ||BC^2|| + ||CA^2||} \tag{3.106}$$

Example scenarios of β_1 are illustrated in fig. 3.13

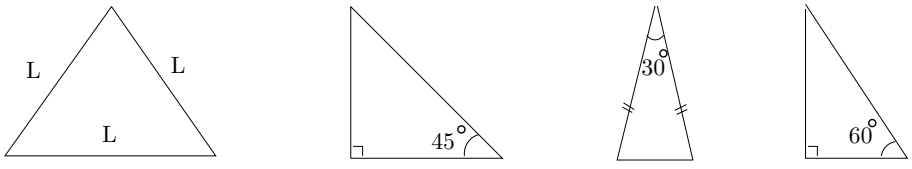

β_1=1 β_1=0.866 β_1=0.764 β_1=0.75

Figure 3.13: The relationship between the element shape and coefficient β_1

The contribution of the element curvatures (e.g. fig. 3.14) to the distortion measure is defined as,

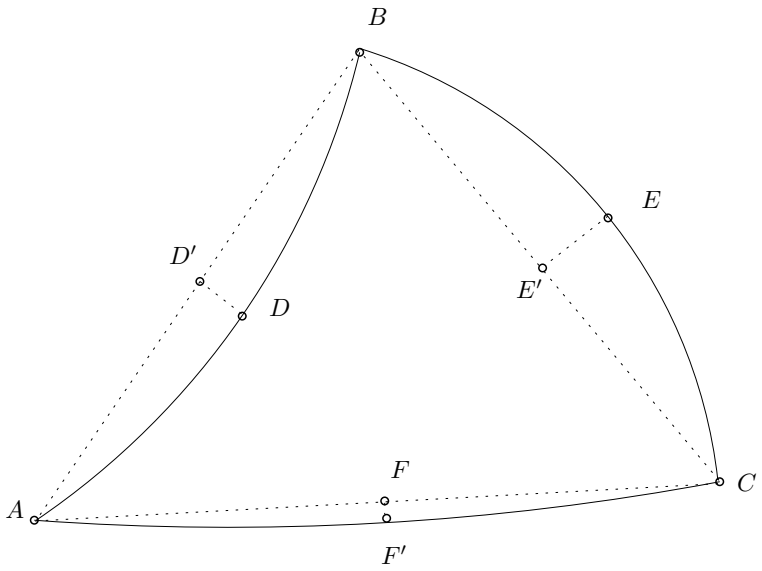

Figure 3.14: Definition of element side curvature coefficient β_2

$$\beta_2 = Max(K_i)^{i=1\rightarrow 3} \tag{3.107}$$

where

$$\begin{aligned} K_1 &= K_{AB} = \frac{DD'}{AB} \\ K_2 &= K_{AC} = \frac{FF'}{AC} \\ K_3 &= K_{BC} = \frac{EE'}{BC} \end{aligned}$$

Finally, the curvature coefficient is stated as:

$$\beta = \frac{\beta_2}{\beta_1}, \quad \beta_1 > 0 \tag{3.108}$$

For the purpose of interpretation, when $\beta_1 \rightarrow 1$,$\beta_2 \rightarrow 0$, the element is undistorted.

Particularly with regard to the calculation of β, the associated computational cost to check for element distortion is relatively high. Furthermore, providing general guidelines, for α_1, β_1, β_2 and β proves almost to be impossible because of the combination of potential geometries.

Judgement of the seriousness of the element distortion can also be based on the point at which the value of the Jacobian ($|J|$) becomes zero at the Gauss points ([219], [220]).

For example, using the numerical integration to calculate the area of the 6 node triangular element with shape 1 and shape 2 shown in figure 3.15, the errors are shown in the table 3.3. It is not obvious from the figures illustrating the element geometry that the second shape is seriously distorted.

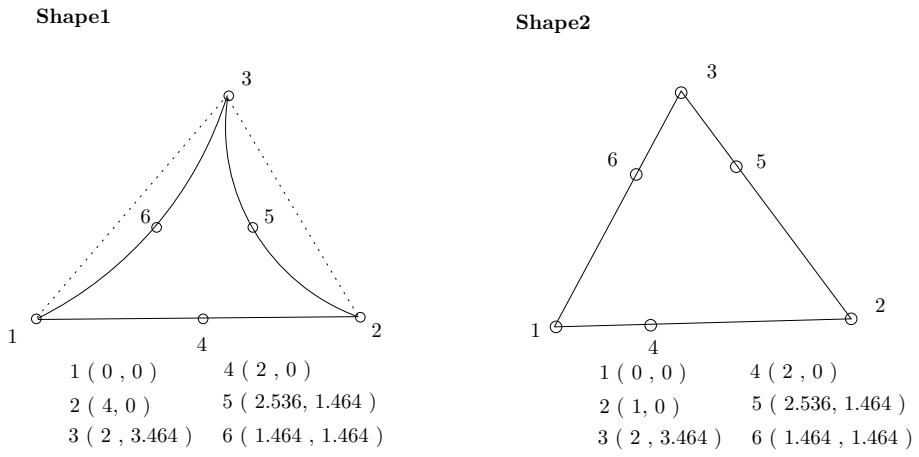

Figure 3.15: Numerical Integration for distorted element

Element shape	6 Gauss points	12 Gauss points	Real Area	Min $\|J_{GP}\|$
Shape 1	4.52	4.07	4.028	> 0
Shape 2	9.531	9.237	6.928	< 0 at GP(4,5,6)

Table 3.3: Error of numerical integration for distorted element

The key advantage of using $|J|$ at each Gauss point to assess distortion is that the calculation carries no computational overhead since the determination of $|J|$ is required to calculate the element stiffness matrix and out-of-balance-force-vector. It also provides an unequivocal check no matter the type of distortion as clearly all values of $|J|$ at the Gauss points must be positive definite.

3.3 Solution Algorithm

The geometric nonlinearity associated with fabric structure analysis makes it necessary to adopt an iterative strategy to solve the equilibrium equations derived in section 3.2.3. In classic finite element non-linear analysis, it would be normal and expected to adopt the Newton-Raphson method. However, in fabric structure analysis where the CST is represented by pseudo cables, the solution algorithm of choice is Dynamic Relaxation. Given that the philosophy of the development of the CST has been maintained using the pseudo cable approach, only the Dynamic Relaxation algorithm has been implemented for this element. In contrast, the Newton-Raphson and Dynamic Relaxation algorithm have been used to solve the LST discretisations. Both methods are summarized below.

3.3.1 Dynamic Relaxation Algorithm

The Dynamic Relaxation algorithm is based on the principle that any body which is in motion will come to rest only when it is at a state of equilibrium. The system is forced into a

pseudo oscillation, with equal amplitude about the equilibrium position. Both the frequency and the amplitude of the fictitious dynamic motion are controlled artificially. As illustrated subsequently, this is achieved through the components of stiffness and of out-of-balance force at each node of the discretization, and by the associated nodal mass.

The motion of the system is described by the D' Alembert principle, written as,

$$\underline{P_{pq}} = M_{pq}\ddot{\delta_{pq}} + C\dot{\delta pq} + \underline{K_{pq}}\delta_{pq} \tag{3.109}$$

or,

$$\underline{P_{pq}} - \underline{K_{pq}}\delta_{pq} = M_{pq}\ddot{\delta_{pq}} + C\dot{\delta_{pq}} \tag{3.110}$$

and

$$\underline{R_{pq}} = M_{pq}\ddot{\delta_{pq}} + C\dot{\delta_{pq}} \tag{3.111}$$

where the subscripts pq refer to the p^{th} node in the q^{th} direction. q can take the values $1 \rightarrow 3$, corresponding to the global axis directions { x, y, z }, respectively. The remaining coefficients are defined below.

$\underline{P_{pq}}$ is the external load vector, including terms representing the effects of surface prestress or initial strains,

$\underline{K_{pq}}$ is the nodal stiffness selected from the terms of the element stiffness matrix

$\underline{R_{pq}}$ is the out-of-balance nodal force (or residual),

M_{pq} is the fictitious nodal mass,

$\ddot{\delta_{pq}}$ is the nodal acceleration.

$\cdot\delta_{pq}$ is the nodal velocity,

δ_{pq} is the nodal displacement.

Kinetic Damping has been shown to be a more stable and a more rapidly convergent technique of damping the pseudo dynamic oscillations of the discretized system, when compared with the Viscous Damp approach (Eqn. 3.109). Using this technique the system is allowed to vibrate freely without attenuation of displacement or frequency. During this motion the kinetic energy of the entire system is monitored. As the system passes the equilibrium configuration the kinetic energy of the system is maximized.

When a maximum value is observed the current oscillation is halted. The pseudo motion is then restarted from this new configuration. As more peaks in the kinetic energy of the system are detected, the proximity of the system to the true equilibrium configuration is increased. The procedure culminates in the minimisation of the sum of the kinetic and potential energies

of the system at equilibrium. Using this approach, Eqn. 3.110 may be written more simply as:

$$\underline{P_{pq}} - \underline{K_{pq}}\delta_{pq} = \underline{R_{pq}} = M_{pq}\ddot{\delta_{pq}} \tag{3.112}$$

The acceleration term given in the right side of Eqn. 3.112 is written as the variation of the velocity over the time increment δt using a central difference approximation, such that,

$$\ddot{\delta_{pq}} = \frac{\dot{\delta_{pq}}^{t+\frac{\delta_t}{2}} - \dot{\delta_{pq}}^{\frac{t-\delta}{2}}}{\delta t} \tag{3.113}$$

substitution of Eqn. 3.113 into Eqn. 3.112 leads to the following recurrent equation for the nodal velocity, $\dot{\delta_{pq}}^{t+\frac{\delta t}{2}}$, as,

$$\dot{\delta_{pq}}^{t+\frac{\delta}{2}} = \dot{\delta_{pq}}^{t-\frac{\delta}{2}} + \underline{R_{pq}}^{t}\frac{\delta t}{M_{pq}} \tag{3.114}$$

In order to ensure numerical stability of the solution algorithm, the following expression has been suggested,

$$\delta t \leq \sqrt{2\frac{M_{pq}}{K_{pq}}} \tag{3.115}$$

or

$$M_{pq} \geq \frac{\underline{K_{pq}}}{2} \cdot \delta t^2 \tag{3.116}$$

Substitution of Eqn. 3.116 into Eqn. 3.114 gives,

$$\dot{\delta_{pq}}^{t+\frac{\delta}{2}} = \dot{\delta_{pq}}^{t-\frac{\delta}{2}} + \underline{R_{pq}}^{t}\left[\frac{2}{\delta t \cdot K_{pq}}\right] \tag{3.117}$$

The velocities at time $t + \frac{\delta t}{2}$ can be used to calculate the current nodal displacement as in,

$$\delta_{pq}^{t+\frac{\delta_t}{2}} = \dot{\delta_{pq}}^{t+\frac{\delta t}{2}} \cdot \delta t \tag{3.118}$$

Therefore, through the recurrent use of Eqn. 3.112, Eqn. 3.117 with 3.118, the pseudo dynamic behaviour of the structure is defined. During each iterative cycle, the current kinetic energy of the system, $U^{t+\frac{\delta t}{2}}$ is monitored and compared with the preceding value, denoted respectively as,

$$U_k^{t+\frac{\delta t}{2}} = \frac{1}{2}\sum_{p=1}^{p=N}\sum_{q=1}^{q=3} M_{pq}(\dot{\delta_{pq}}^{t+\frac{\delta t}{2}})^2 \tag{3.119}$$

$$U_k^{t-\frac{\delta t}{2}} = \frac{1}{2}\sum_{p=1}^{p=N}\sum_{q=1}^{q=3} M_{pq}(\dot{\delta_{pq}}^{t-\frac{\delta t}{2}})^2 \tag{3.120}$$

An energy peak is deemed to have occurred during the time interval $t - \frac{\delta t}{2} \leq t \leq t + \frac{\delta t}{2}$ when

the magnitude of ${U_k}^{t+\frac{\delta t}{2}}$ is less than that of ${U_k}^{t-\frac{\delta t}{2}}$. If it is assumed that the kinetic energy peak occurs at the time t^*, where $t - \frac{\delta t}{2} \leq t^* \leq t + \frac{\delta t}{2}$, it may be estimated that t^* is at the mid point of the interval, $t - \frac{\delta t}{2} \leq t^* \leq t + \frac{\delta t}{2}$, such that $t^* = t$.

Alternatively, a parabola may be fitted through the current and the two previous values of the kinetic energy $({U_k}^{t-\frac{\delta t}{2}}, {U_k}^{t-\frac{3\delta t}{2}})$, yielding an improves estimate of the true position of the kinetic energy peak, written as:

$$t^* = t - \rho.\delta t = t - \delta t^* \tag{3.121}$$

where

$$\rho = \frac{{U_k}^{t+\frac{\delta t}{2}} - {U_k}^{t-\frac{\delta t}{2}}}{{U_k}^{t-\frac{3\delta t}{2}} - 2{U_k}^{t-\frac{\delta t}{2}} + {U_k}^{t+\frac{\delta t}{2}}} \tag{3.122}$$

The pseudo dynamic motion may be restarted therefore, from the configuration described by the following expression

$$\delta^{t^*} = \delta^{t+\frac{\delta t}{2}} - \dot{\delta}^{t+\frac{\delta}{2}} \cdot \delta t - \dot{\delta}^{t-\frac{\delta t}{2}} \cdot \delta t^* \tag{3.123}$$

Through the recurrent use of Eqn. 3.112, 3.117 and 3.118, the condition of static equilibrium of a system can be satisfied by damping its pseudo dynamic behaviour. The pseudo dynamic behaviour of the system has been shown to be controlled by the components of both stiffness and of out-of-balance force at each node of this discretization.

Solution Procedure for CST formulation

The solution procedure for the three types of CST formulation described in section 3.1 using the Dynamic Relaxation Algorithm is summarized below and also presented as fig.3.16:

1) Discretize the membrane with an appropriate mesh.

2) Calculate equivalent nodal loads related to any uniformly applied external loads

3) Establish the local system of co-ordinates and transformation coefficients. For each element, it is further required to:

4) Calculate the $[B^{tr}]$ matrix (Eqn. 3.12, 3.34 or 3.42) and the pseudo cable forces(Eqn.3.18) based on the stress from the initial conditions or the preceding iteration.

5) Calculate the elasticity modulus matrix [E] in the local coordinate system and build the local elastic stiffness matrix K_E^{tr}(Eqn.3.15). Extract the diagonal terms and calculate the global elastic stiffness matrix K^E(Eqn. 3.44,3.45,3.46).

6) Calculate the diagonal terms of local element geometric stiffness matrix K_σ^{pc} (Eqn.3.47,3.48,3.49), and the global geometric stiffness matrix K_{pc}^t (Eqn.3.50,3.51,3.52)

7) Calculate the nodal force of each element (Eqn. 3.54, 3.55, 3.56).

8) Assemble the structure stiffness vector using the terms obtained from step **5** and **6**.

9) Calculate the out-of-balance force for the whole structure. If the out-of-balance force vector, at every node, is less than or equal to the error residual Er, then goto step **12**.

10) Calculate the nodal velocities and the displacements, in the global $\{x \quad y \quad z\}$ co-ordinate directions.

11) Calculate the total kinetic energy of the system, and update the surface geometry, If a kinetic energy peak is detected, return to 3), else 9).

12) Output the equilibrated geometry, nodal displacements and element stresses.

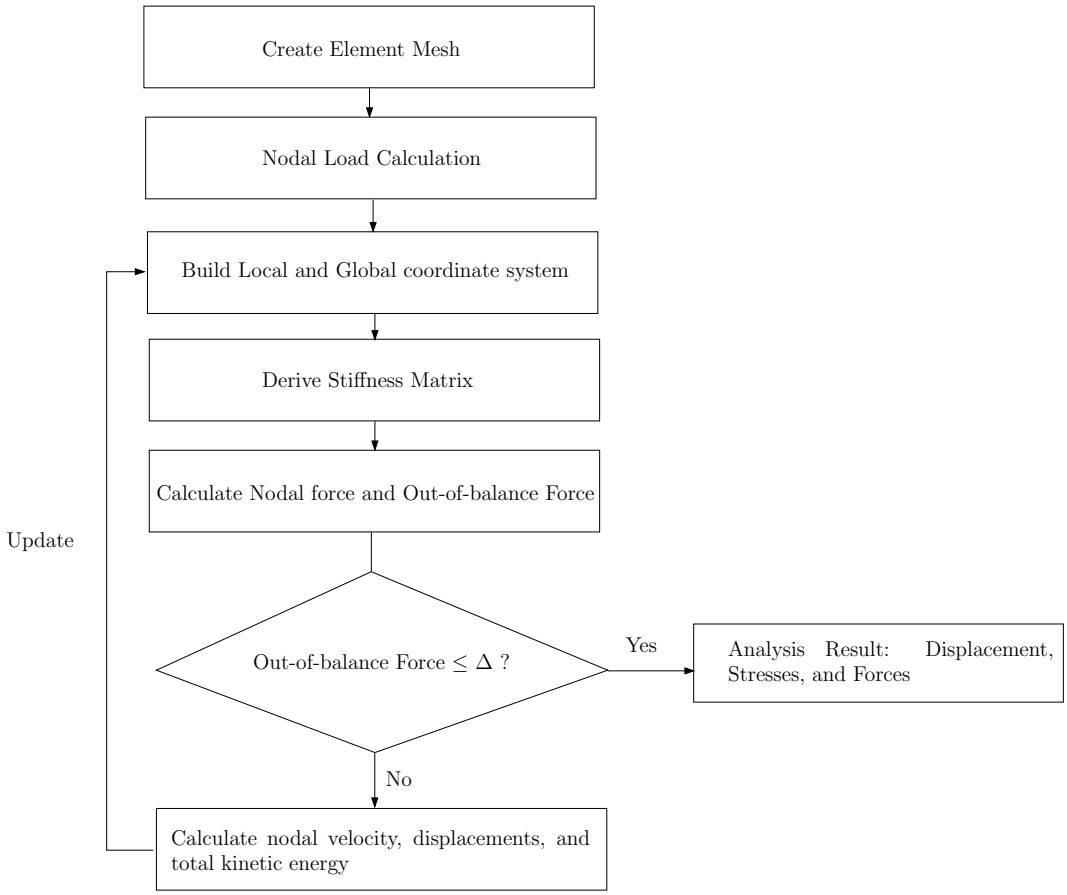

Figure 3.16: CST solution algorithm

Solution Procedure for LST element

The solution procedure using Dynamic Relaxation algorithm of LST element considering the element distortion is presented as below and also in figure 3.17:

(1) Discretise the membrane with an appropriate and undistorted mesh.

(2) Calculate equivalent nodal loads related to any uniformly applied external load (e.g transfer uniform loads σ to nodal loads F_i).

(3) Establish the local coordinates, build the transformation matrix (Eqn.3.57) and calculate the element curvatures (Eqn. 3.64).

(4) For each element, build elastic stiffness matrix K_E (Eqn.3.93), geometric stiffness K_σ (Eqn. 3.94), and element stiffness K (Eqn. 3.92)

(5) Calculate the reaction forces based on the stress from the initial conditions or the preceding iteration. (Eqn. 3.97).

(6) Build the structure stiffness and reaction forces, then calculate the out-of-balance force. If the out-of-balance force $<$ allowable error Δ, then Goto step **14**.

(7) Extract the diagonal terms of K, as the mass for each node (Eqn. 3.116).

(8) Set the dynamic initial conditions as $t = 0$, $V_0 = 0$.

(9) Calculate the node velocities (Eqn. 3.117) and the kinetic energy of the system (Eqns. 3.119 and 3.120).

(10) Calculate the nodal displacements (Eqn. 3.118).

(11) Update geometry by adding nodal displacements, and calculate the out-of-balance force F in updated geometry configuration.

(12) Repeat steps 8-11 until an energy peak is detected.

(13) Go back to Step 3 with updated geometry configuration.

(14) Calculate the output membrane stresses and displacements.

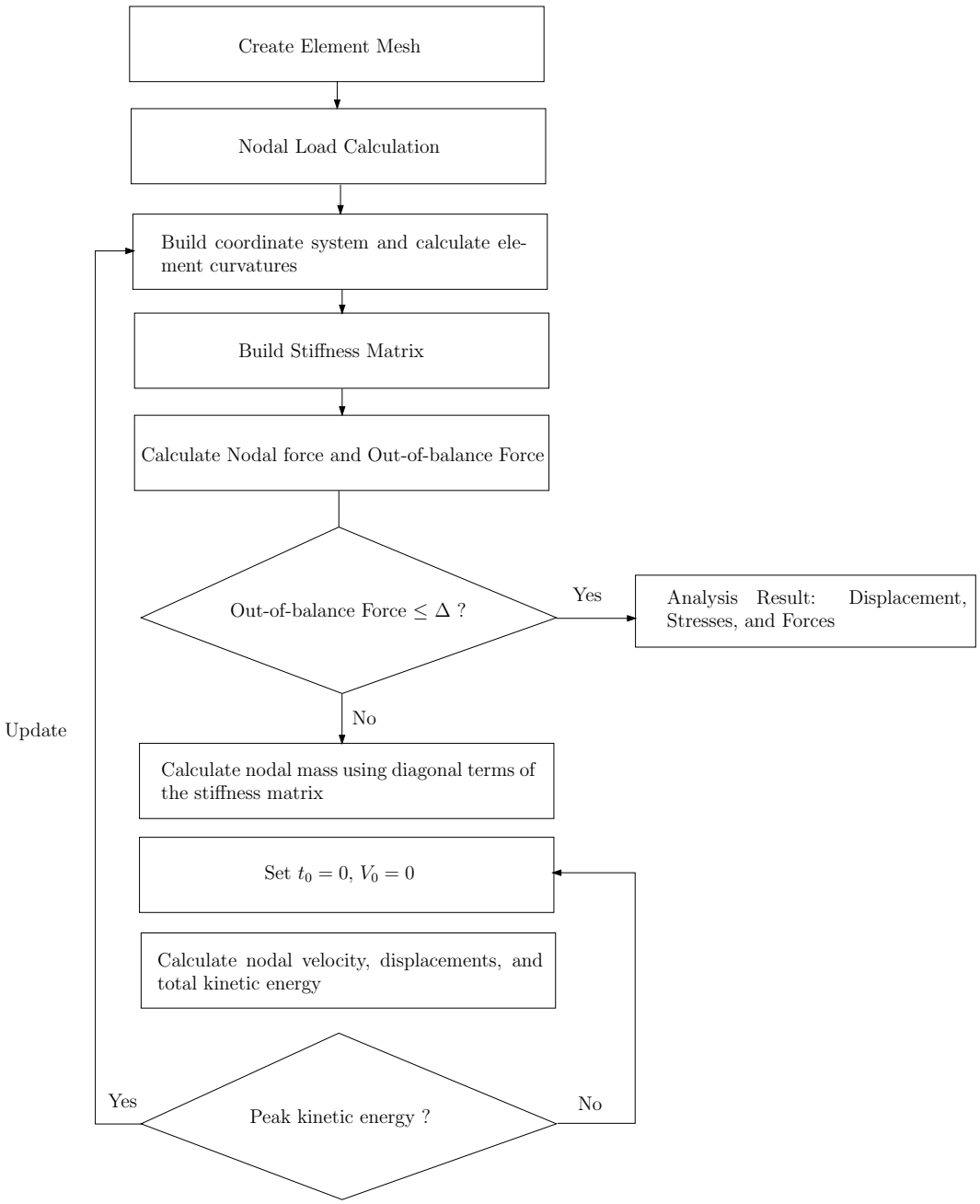

Figure 3.17: LST solution algorithm

The key advantage of the Dynamic Relaxation algorithm is that matrix operations are kept to a minimum along with storage requirements and data transfer is also small. However, the associated disadvantage is that by using only the diagonal stiffness terms there is a level of uncoupling that can lead to undesireable element distortion. For example, when loads are applied to the membrane, the solution algorithm results in some nodal displacements lagging behind neighbouring nodes (e.g. see fig. 3.18).

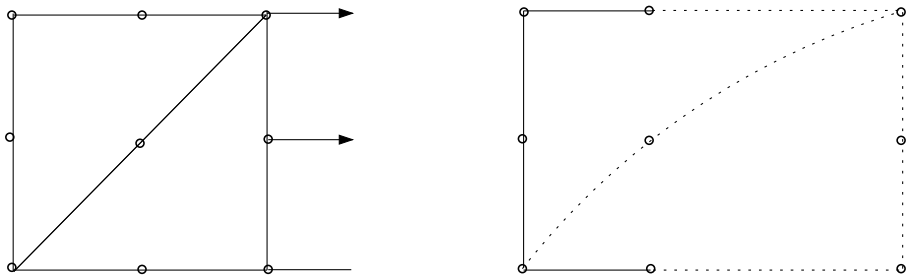

Figure 3.18: The Element Distortion Problem by using Dynamic Relaxation with coarse mesh

With mesh refinement, the problem will be compounded, because the distortion will be more serious as the element size reduces as shown in figure 3.19. When a very refined mesh is used, a smoothly convergent solution procedure is not guaranteed, and accurate results are only obtained when elements are not seriously distorted.

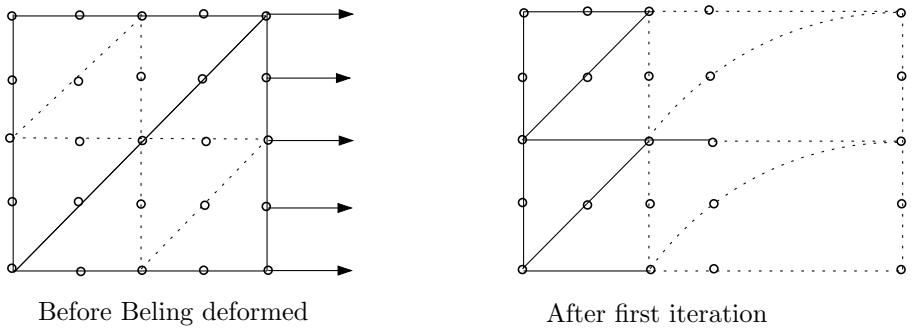

Figure 3.19: The Element Distortion Problem by using Dynamic Relaxation with refine mesh

In the absence of geodesic strings, this problem may be solved by using a mesh-refinement procedure. Form-finding can start with a very coarse mesh, including a small number of elements, whose sizes are comparatively large and unlikely to become too distorted. The mesh is refined by replacing each distorted element with several undistorted elements using the geometrical configuration obtained from the last form-finding analysis. Form-finding and mesh-refinement are repeated until convergence.

3.3.2 Newton-Raphson Method

The Newton-Raphson method is one of the most widely used methods for solving nonlinear equations. Using first derivatives of the nonlinear function with respect to the variable, the root for the nonlinear equation may be approached smoothly and quadratically.For example, a force vector P_A is the nonlinear function of the displacement u_A, and we have

$$(k_0 + k_{NA})u_A = P_A \tag{3.124}$$

where k_0 is constant, and k_{NA} is a function of the displacement u_A:

$$k_{NA} = f(u_A)$$

The load is now increased to a value P_B and the corresponding displacement u_B is sought. A truncated Taylor series expansion of $P = f(u)$ in $(u_B - u_A)$ is:

$$f(u_B) = f(u_A) + (\frac{dP}{du})_A(u_B - u_A) \tag{3.125}$$

Defining $\Delta u_1 = u_B - u_A$ then the Eqn. 3.125 can be written as:

$$f(u_A + \Delta u_1) = f(u_A) + (\frac{dP}{du})_A \Delta u_1 \tag{3.126}$$

where

$$\frac{dP}{du} = \frac{d}{du}(k_0 u + k_N u) = k_0 + \frac{d}{du}(k_N u) = k_t \tag{3.127}$$

k_t is called the tangent stiffness. We seek δu_1 for which $f(u_A + \Delta u_1) = P_B$. Thus, with $f(u_A) = P_A$ and k_t evaluated at A, then,

$$P_B = P_A + (k_t)_A \Delta u_1 \tag{3.128}$$

or,

$$(k_t)_A \Delta u_1 = P_B - P_A \tag{3.129}$$

where $P_B - P_A$ can be interpreted as a load imbalance.

The solution process is depicted in the figure 3.20. After computing Δu_1, we update the displacement estimate to $u_1 = u_A + \Delta u_1$. For the next iteration, we obtain a new tangent stiffness (k_t) by use of :

$$\frac{dP}{du} = \frac{d}{du}(k_0 u + k_N u) = k_0 + \frac{d}{du}(k_N u) = k_t \tag{3.130}$$

with $u = u_1$ and obtain a new load imbalance $P_B - P_1$, where P_1 comes from

$$(k_0 + k_N)u = P \tag{3.131}$$

where, $k_N = f(u)$ with $u = u_1$. The updated displacement estimate is $u_2 = u_1 + \Delta u_2$, where Δu_2 is obtained by solving

$$(k_t)_1 \Delta u_2 = P_B - P_1 \tag{3.132}$$

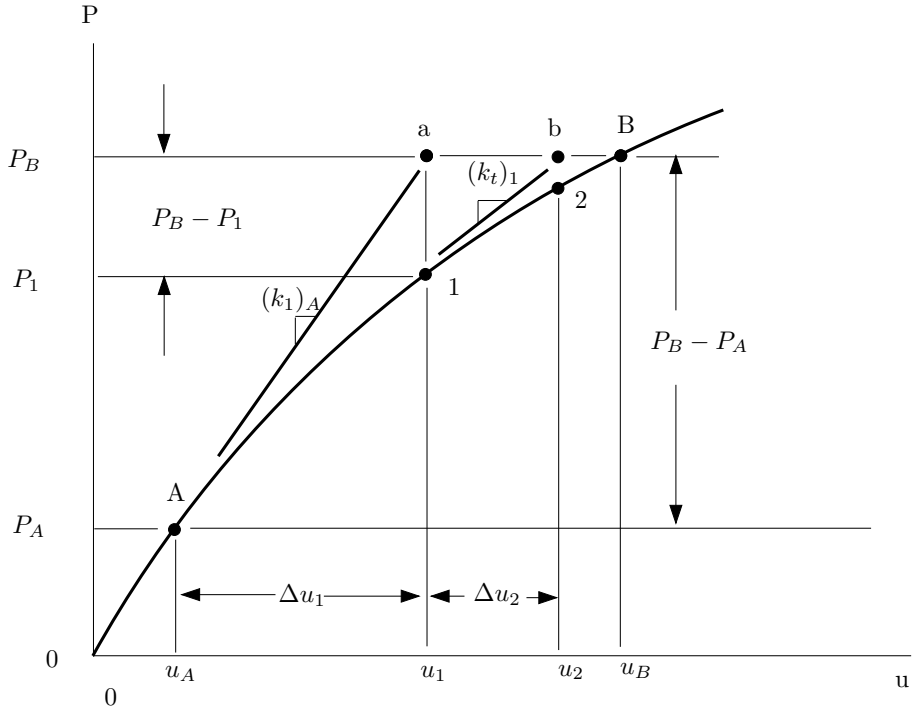

Figure 3.20: N-R solution for u_B caused by P_B starting from point A

The solution procedure continues until convergence of the displacement increments or the load increments is achieved.

Solution Procedure for LST element

Using Newton-Raphson method, the equilibrium state of membrane surface can be obtained by the following procedure:

(1) Discretize the membrane with an appropriate and undistorted mesh

(2) Establish the local element coordinate systems, calculate the transformation matrix and element curvatures.

(3) Build the element elastic stiffness K_E (Eqn. 3.93), geometric stiffness K_σ (Eqn. 3.94) and tangent stiffness matrix (Eqn. 3.100).

(4) Calculate the element reaction force vector (Eqn. 3.97)

(5) Assemble the structure tangent stiffness and reaction nodal force, then evaluate the out-of-balance force. If out-of-balance force $< \Delta$ then Goto **10**.

(6) Calculate the nodal displacements.

(7) Based on the displacement evaluated from last iteration, calculate the out-of-balance force, if the out-of-balance force $< \Delta$ then goto step **9**, else step **8**.

(8) Update the tangent stiffness matrix and return to **step 6**.

(9) Update the coordinate by Eqn. 3.133 and Repeat **Step 2 - 5**.

$$\{X\}_i = \{X\}_{i-1} + \{\Delta U\}_i \tag{3.133}$$

in which, $\{X\}_i$ and $\{X\}_{i-1}$ are geometry in ith and $(i-1)$th iteration, $\{\Delta U\}_i$ is corresponding displacement increment.

(10) Output the nodal displacements, membrane stresses, and element curvatures.

3.3.3 Potential of "floating" mid side nodes

The form-finding procedure is independent of the material properties meaning that, for each element, the stresses are constant in two different directions. In this case, the mid side nodes may seem to be "free" to move if this type of movement does not change the geometry of the element and the stresses.

If we have two elements with the same stress and shape as shown in figure 3.21, the equivalent nodal force is:

$$f = \int_v B \cdot \sigma dv = \sum_{i=1}^{12} B(\xi_1^i, \xi_2^i, \xi_3^i, J^i) \cdot \sigma \cdot |J| \tag{3.134}$$

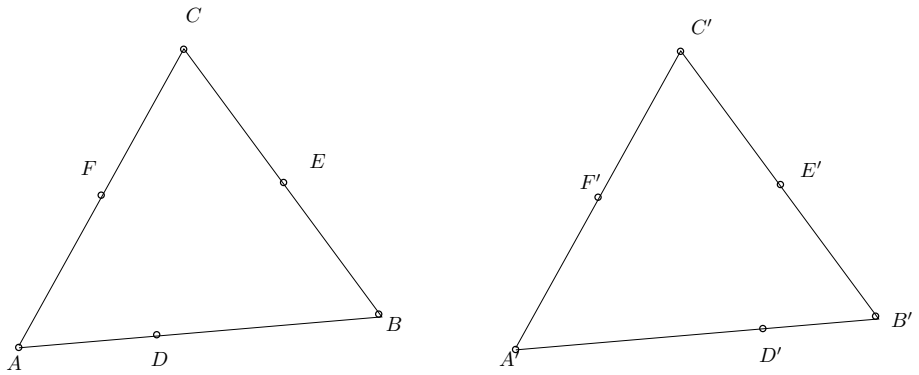

Figure 3.21: Possibility of "Free" Movement of mid side node of the 6 node element

in which, ξ_1^i,ξ_2^i,ξ_3^i are area coordinates, and J^i is the 2×2 Jacobian Matrix. J is made up of terms of including nodal coordinates in the element local coordinate system. For example,

$$[J] = \begin{bmatrix} J_{11} & J_{12} \\ J_{21} & J_{22} \end{bmatrix} \tag{3.135}$$

in which,

$$\begin{aligned} J_{11} &= X_1(4\xi_1 - 1) - X_3(4\xi_3 - 1) + 4\xi_2(X_4 - X_5) + 4(\xi_3 - \xi_1)X_6 \\ J_{12} &= Y_1(4\xi_2 - 1) - Y_3(4\xi_3 - 1) + 4\xi_2(Y_4 - Y_5) + 4(\xi_3 - \xi_1)Y_6 \\ J_{21} &= X_2(4\xi_2 - 1) - X_3(4\xi_3 - 1) + 4\xi_1(X_4 - X_6) + 4(\xi_3 - \xi_2)X_5 \\ J_{22} &= Y_2(4\xi_2 - 1) - Y_3(4\xi_3 - 1) + 4\xi_1(Y_4 - Y_6) + 4(\xi_3 - \xi_2)Y_5 \end{aligned}$$

In the numerical integration of Eqn. 3.134, ξ_1,ξ_2,ξ_3 are the same for element ΔABC and $\Delta A'B'C'$. However apparently $X_D \neq X_{D'}$,$Y_D \neq Y_{D'}$, meaning that $J_{ABC} \neq J_{A'B'C'}$. Therefore the equivalent nodal forces of these two element are different, so such "free" movement of mid side nodes will cause a change of the nodal forces from those defined by the initial stresses.

A further possibility of "free movement" of the mid-side nodes is that the force increments of the mid side shared by two adjacent elements are zero, because the equivalent nodal force produced from one element may be eliminated by the other.

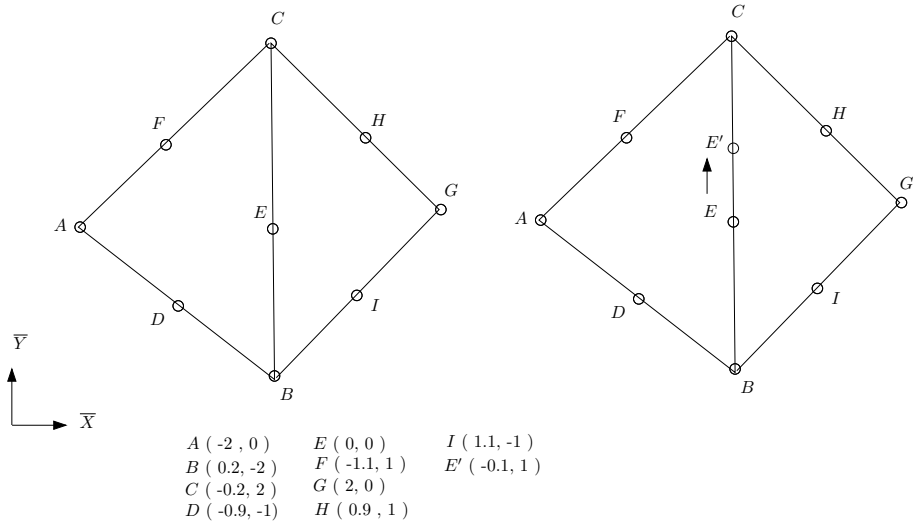

Figure 3.22: Possibility of "Free" Movement of mid-side node of the 6 node element

For example, if there are two adjacent element ABC and CBG shown in figure 3.22 in a form-finding analysis, with initial stresses $\sigma_{\overline{X}0} = 1.0kN/m$, $\sigma_{\overline{Y}0} = 1.0kN/m$ and $\tau_{\overline{XY}0} = 0$. We assume E is the balance point, and if E "floats" to position E', the nodal force increment can be calculated by Eqn. 3.134. The nodal force increment from the element ABC is,

$$\begin{aligned} \Delta F_y(B) &= 0.27kN \\ \Delta F_y(C) &= 0.27kN \end{aligned}$$

Similarly, the nodal force increment from the element GBC is:

$$\begin{aligned} \Delta F'_y(B) &= 0.27kN \\ \Delta F'_y(C) &= 0.27kN \end{aligned}$$

Therefore, the out-of balance force at B, and C generated by the "floating" of E to E' are:

$$\begin{aligned} \Delta F_y(B) &= 0.54kN \\ \Delta F_y(C) &= 0.54kN \end{aligned}$$

Consequently, if E moves to E', nodal force increments from each element are additive, meaning that the movement from E to E' is not "free" (i.e. nodal forces are induced).

Finally, therefore, the two cases of potential "floating" mid-side nodes are shown to be unlikely to be manifested in the analysis.

3.4 Wrinkling procedure

Since the membrane material has no flexural stiffness, vanishing of tensile stresses in an arbitrary position or direction of the membrane surface will immediately lead to buckling in the form of wrinkles. In this case, the membrane will lose or partially lose the stiffness and load resistance in the wrinkled area. From a view point of either aesthetics or structural safety, wrinkling can be regarded as one type of structural failure, and should be inadmissible during membrane structural design.

Structural analysis taking into account wrinkling is sophisticated because the detailed wrinkling pattern not only depends on the stress state but the imperfections of fabric material during the fabrication process. Therefore in this chapter, the main aim of the finite element formulation taking into account wrinkling concentrates on the prediction of wrinkling under

loading for an idealized fabric.

Different wrinkling criteria developed by Otto [87], Miller [88] and Roddeman [89] as shown in Table 2.4, 2.5 and 2.6 are based on principal stress , strain or combined principal strain and stress. According to these criteria, the membrane state can be described as taut(no wrinkle), wrinkled(uniaxial wrinkling) or slack(biaxial wrinkling).

For the local stresses σ_X,σ_Y,τ_{XY},the major principal stress σ_{11} and minor principal stress σ_{22} are,

$$\sigma_{11} = \frac{\sigma_X + \sigma_Y}{2} + \sqrt{(\frac{\sigma_X - \sigma_Y}{2})^2 + \gamma_{XY}^2} \tag{3.136}$$

$$\sigma_{22} = \frac{\sigma_X + \sigma_Y}{2} - \sqrt{(\frac{\sigma_X - \sigma_Y}{2})^2 + \gamma_{XY}^2} \tag{3.137}$$

and the principal strains are obtained from:

$$\varepsilon_{11} = \frac{\varepsilon_X + \varepsilon_Y}{2} + \sqrt{(\frac{\varepsilon_X - \varepsilon_Y}{2})^2 + (\frac{\gamma_{XY}}{2})^2} \tag{3.138}$$

$$\varepsilon_{22} = \frac{\varepsilon_X + \varepsilon_Y}{2} - \sqrt{(\frac{\varepsilon_X - \varepsilon_Y}{2})^2 + (\frac{\gamma_{XY}}{2})^2} \tag{3.139}$$

(1) If the major principal stress $\sigma_{11} < 0$, the membrane is slack.

(2) If the minor principal stress $\sigma_{22} > 0$, wrinkle does not occur.

(3) If $\varepsilon_{11} > 0$, $\sigma_{22} < 0$, wrinkling occurs.

In wrinkled areas, the major principal strain (ε_{11}) direction is the wrinkle direction at that location.
If θ_p is the angle between wrinkle direction and local X axis, then:

$$\theta_p = \frac{1}{2} tan^{-1}(\frac{2\gamma_{XY}}{\varepsilon_X - \varepsilon_Y}) \tag{3.140}$$

When calculating the element stiffness matrix, the existence of wrinkling must be considered. In this case it is not sufficient to use

$$\{\sigma\} = \begin{Bmatrix} \sigma_X & \sigma_Y & \tau_{XY} \end{Bmatrix}^T = [E] \begin{Bmatrix} \varepsilon_X \\ \varepsilon_Y \\ \gamma_{XY} \end{Bmatrix} = [E][B]\{U\} \tag{3.141}$$

in which, $\{U\}$ is nodal displacements.

If compressive stresses are not permitted and therefore the stiffness normal to the wrinkle direction is zero, solution convergence is not always smooth and sometimes not achieved due

to wrinkling [235–237]. Riccardo Rossi [237] proposed an algorithm for the stabilization of the material manipulation. Using his method, if the membrane is in a "wrinkled state", a modified elastic stiffness matrix $[E_{mod}]$ is defined as:

$$[E_{mod}] = \begin{bmatrix} E_{rot,11} & P \cdot E_{rot,12} & E_{rot,13} \\ P \cdot E_{rot,21} & P \cdot E_{rot,22} & P \cdot E_{rot,23} \\ E_{rot,31} & P \cdot E_{rot,32} & E_{rot,33} \end{bmatrix} = [E_{rot}] \times [P] \tag{3.142}$$

in which, P is the penalization parameter, and

$$[E_{rot}] = [R]^T [E][R] \tag{3.143}$$

[R] is the transformation matrix. If the orientation of the principal stress to the local X axis is α_w, then

$$c = cos(\alpha_w); s = sin(\alpha_w); [R] = \begin{bmatrix} c^2 & s^2 & -2cs \\ s^2 & c^2 & 2sc \\ sc & -sc & c^2 - s^2 \end{bmatrix} \tag{3.144}$$

If the penalization is constant, the performace of the wrinkling procedure may be compromised. An alternative definition of P to improve the stability is to make P a function of the maximum (σ_{max}) and effective compressive stresses (σ_2) [237]:

$$P_\sigma = \frac{\sigma_{max}}{\sigma_2} \rightarrow \begin{Bmatrix} P_\sigma > P & \rightarrow P = P_\sigma \\ P_\sigma > 1 \quad or \quad P_\sigma < 0 & \rightarrow P = 1.0 \end{Bmatrix} \tag{3.145}$$

If the modification makes the state change (from wrinkled or slack to taut), then a reduced penalization may be applied as:

$$New\ state\ is\ "taut" \rightarrow \begin{Bmatrix} old\ state\ is\ "taut" \rightarrow & [E_{mod}] = [E] \\ old\ state\ isn't\ "taut" \rightarrow & P = P \cdot \omega; new\ state\ =\ old\ state \end{Bmatrix} \tag{3.146}$$

where $\omega = 10$ is recommended by reference [237].

The elastic stiffness matrix then becomes:

$$K_{E,mod} = \int_v B^T [E_{mod}] B dv \tag{3.147}$$

In addition to the obvious change in the element stiffness matrix, the equivalent nodal load vector is also changed to be of the form:

$$f_e = \int_V B_0 (E_{mod} \cdot \varepsilon + \sigma_0) dV \tag{3.148}$$

In this method, a small compressive stress is allowed in the analysis to enhance the stability of solution procedure and the accuracy. It is necessary to note that there is no guarantee that the "fictitious" compressive stresses are removed during each iteration and at the final configuration, but wrinkling can be predicted with an acceptable accuracy and economical computational cost using this approach [237].

The wrinkling procedures is summarised as follows and presented as figure.3.23:

1) Evaluate the element stresses using the solution procedure described in section 3.3.

2) Judge the element state by the criteria described as table **??**.

3) Calculate the modification coefficient P (Eqn. 3.145), then modify the constitutive matrix $[E]$ to E_{mod} (Eqn. 3.142-3.142).

4) Calculate the updated stiffness matrix and out-of-balance force vectors.

5) If out-of-balance force $< \Delta$ then goto step **6**, else **1**.

6) Output the position of the wrinkles in the membrane and their direction.

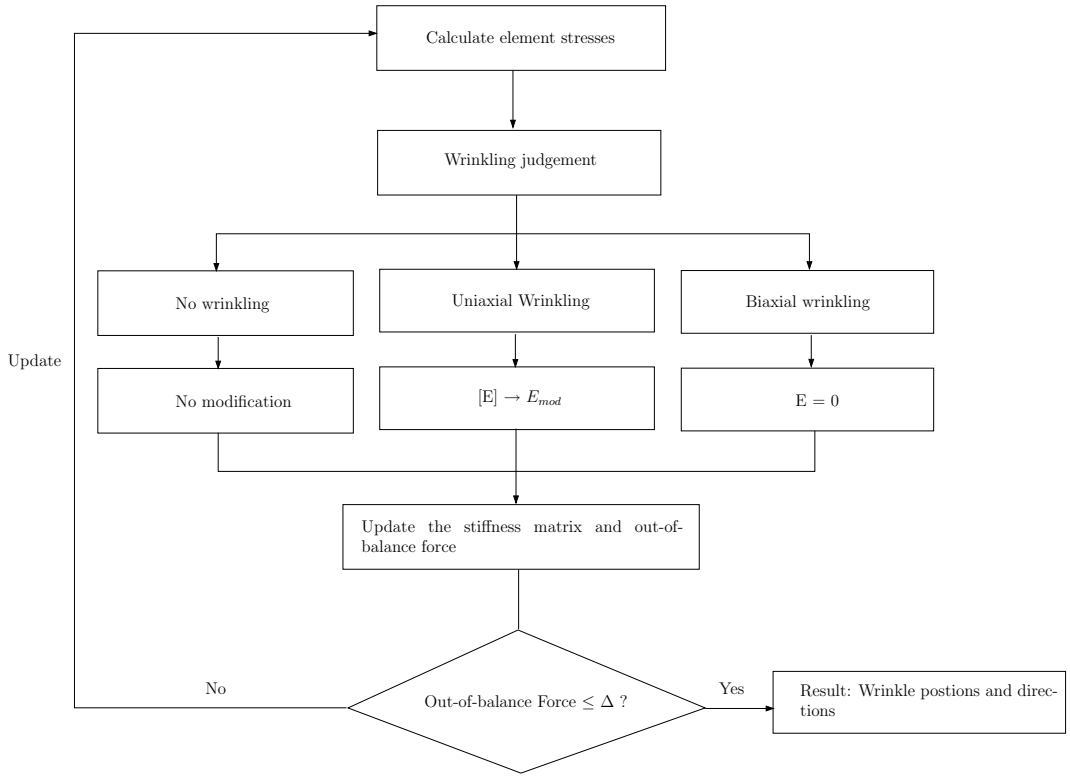

Figure 3.23: Wrinkling solution algorithm

3.5 Numerical Examples and Comparison of CSTs and LST

3.5.1 Hypar Test

The first numerical example is the saddle shape membrane supported by tensioned boundary cables shown in figure 3.24. A and B are two high points, and C, D are two low points. The warp direction is along AB, and fill direction is normal to the warp direction in the membrane element plane:

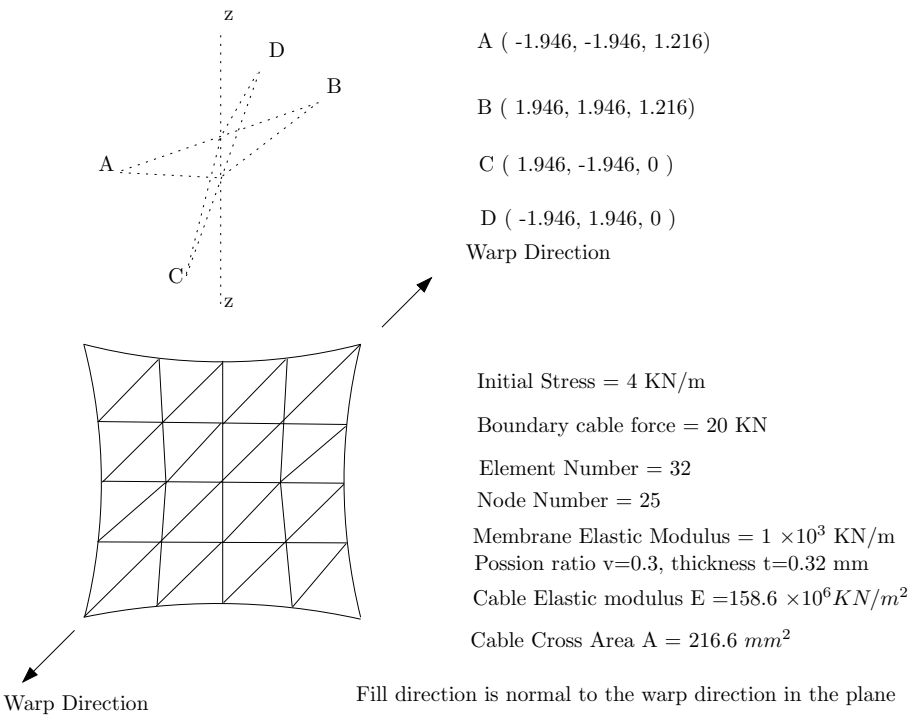

Figure 3.24: A Saddle membrane supported by boundary cables

Form-finding

The form-finding is originated from a shape made of two flat planes as shown in figure 3.25(a). The resulting equilibrated and prestressed geometry is a hypar, indicated in figure 3.25(b) and the form-finding results using 256 CST elements and 128 LST elements are illustrated in Fig.3.26 and Fig.3.27.

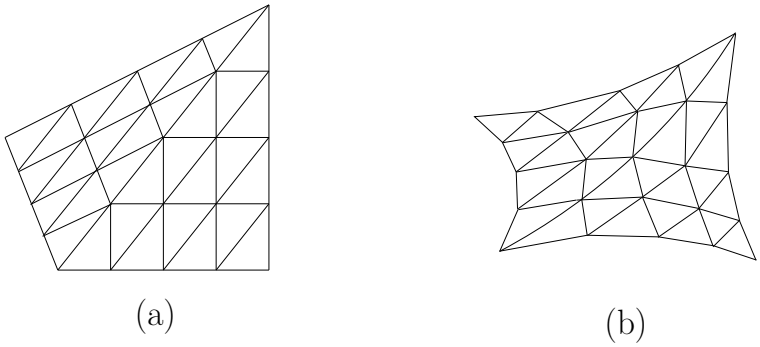

Figure 3.25: Initial and balanced geometry with initial stress $\sigma_x = \sigma_y = 4kN/m$ and boundary cable forces $N = 20kN$

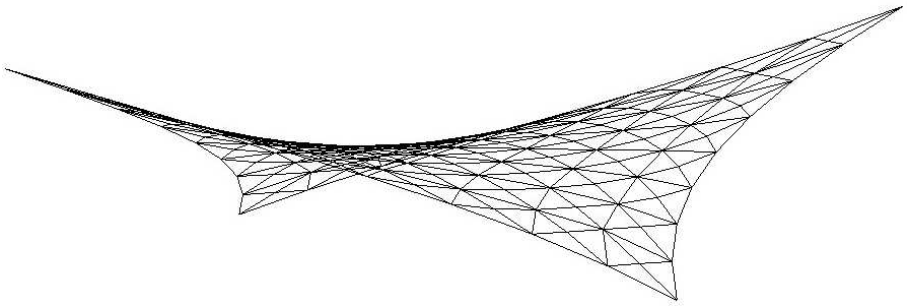

Figure 3.26: Formfinding of the Hypar membrane using 256 CST elements

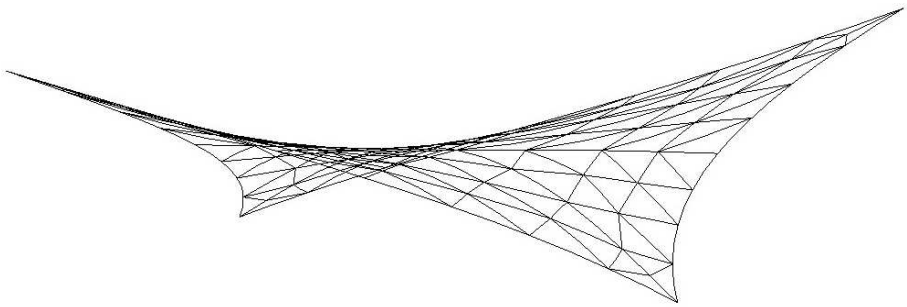

Figure 3.27: Formfinding of the Hypar membrane using 128 LST elements

Loading Analysis

A uniform load $N = 1kN/m^2$ is applied to the hypar membrane in the z direction (defined in figure 3.24). Load analysis solutions using 3 node CST and 6 node LST with Dynamic Relaxation are shown in figures 3.28-3.33. In this case, the membrane strains are small, resulting in little difference between solutions of the three types of CST models. The comparison

is focused therefore on the difference between the large strain CST and LST finite element models.

Figure 3.28-3.30 illustrate the membrane stress distributions using 256 large strain CST elements, and figure 3.31-3.33 using 128 large strain LST finite elements. The shear stresses shown in figure 3.30 , 3.33 are the absolute values, recognizing that the positive and negative shear stresses represent the shear forces in clockwise and anticlockwise directions separately. The same stress ranges are used for the CST and LST results to enable direct visual comparison.

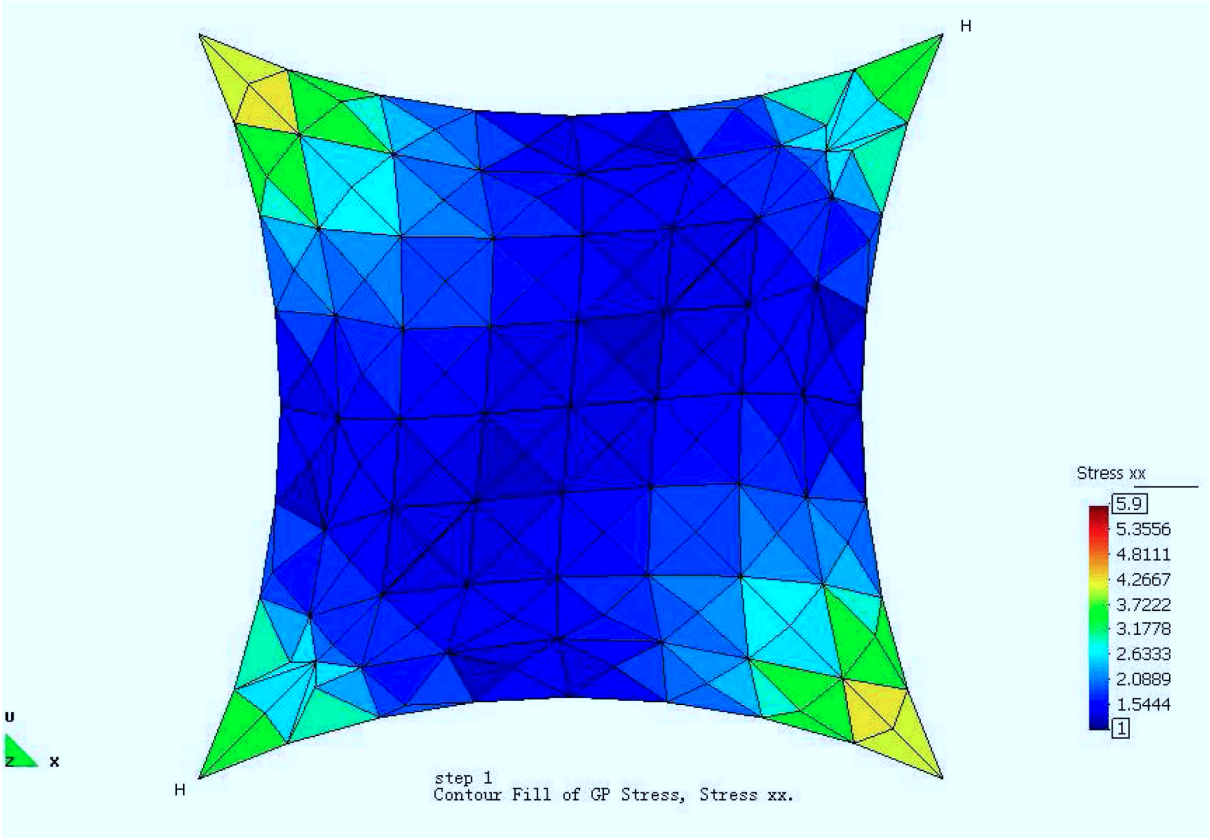

Figure 3.28: Stress along the warp direction — large strain CST

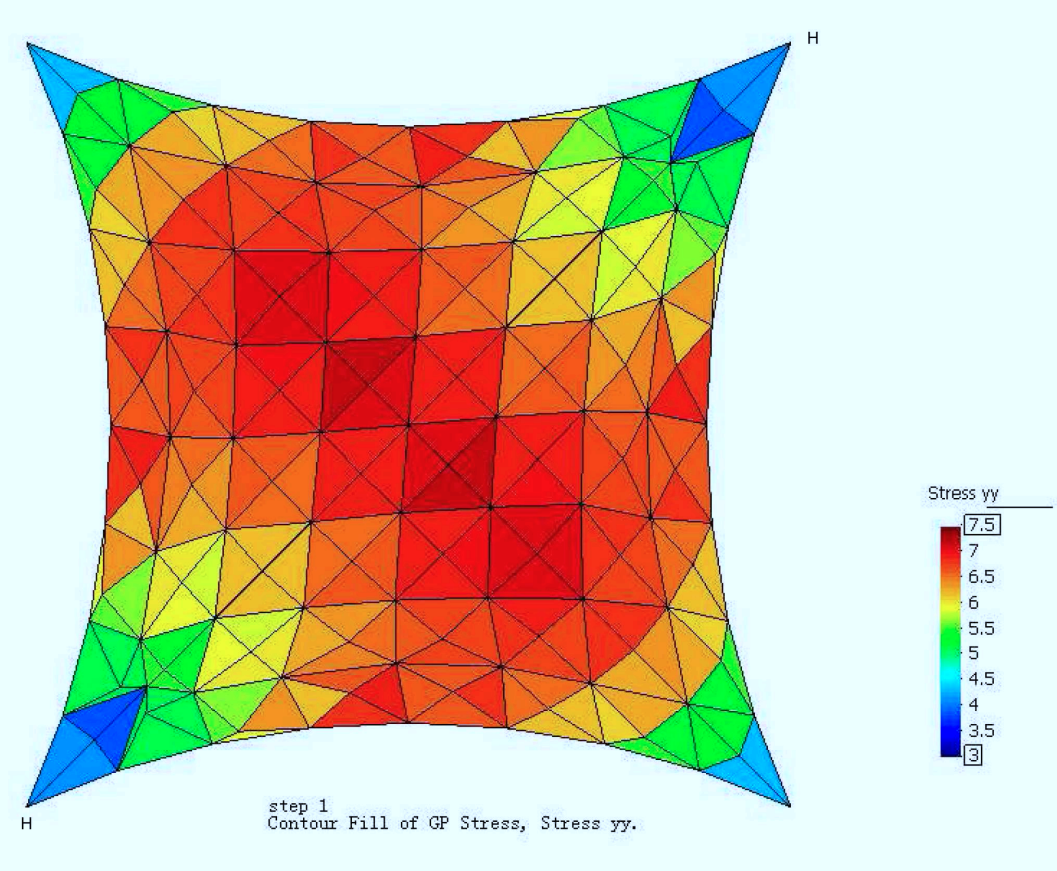

Figure 3.29: Stress along the fill direction — large strain CST

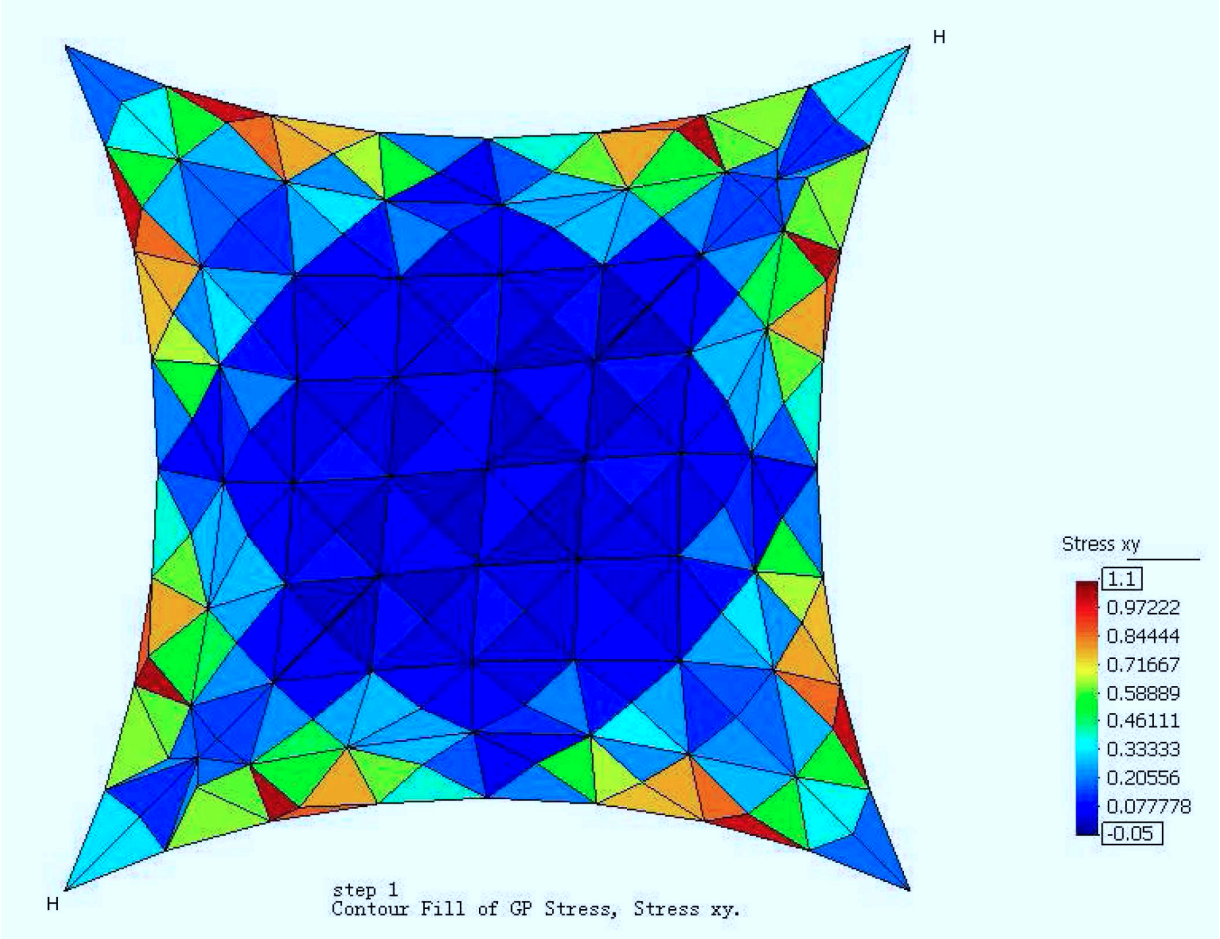

Figure 3.30: Shear stress across the warp and fill direction — large strain CST

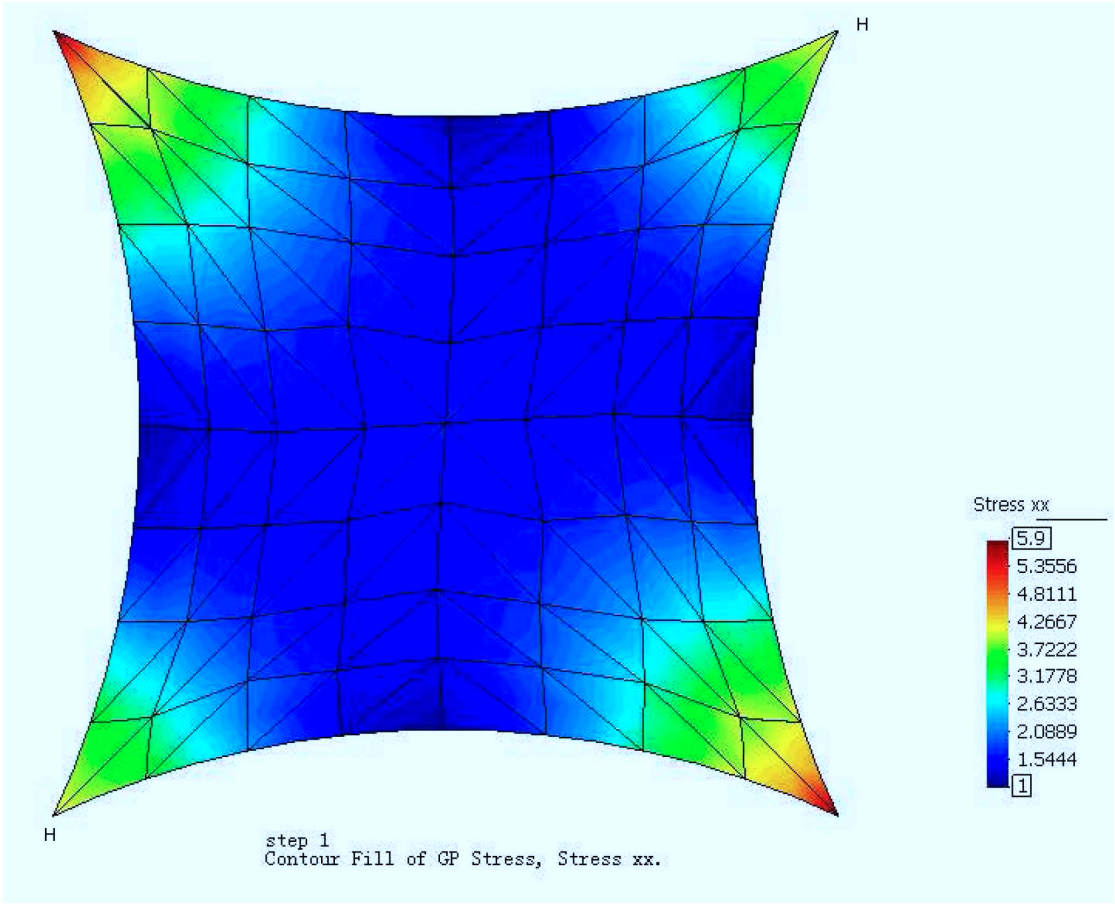

Figure 3.31: Stress along the warp direction — large strain LST

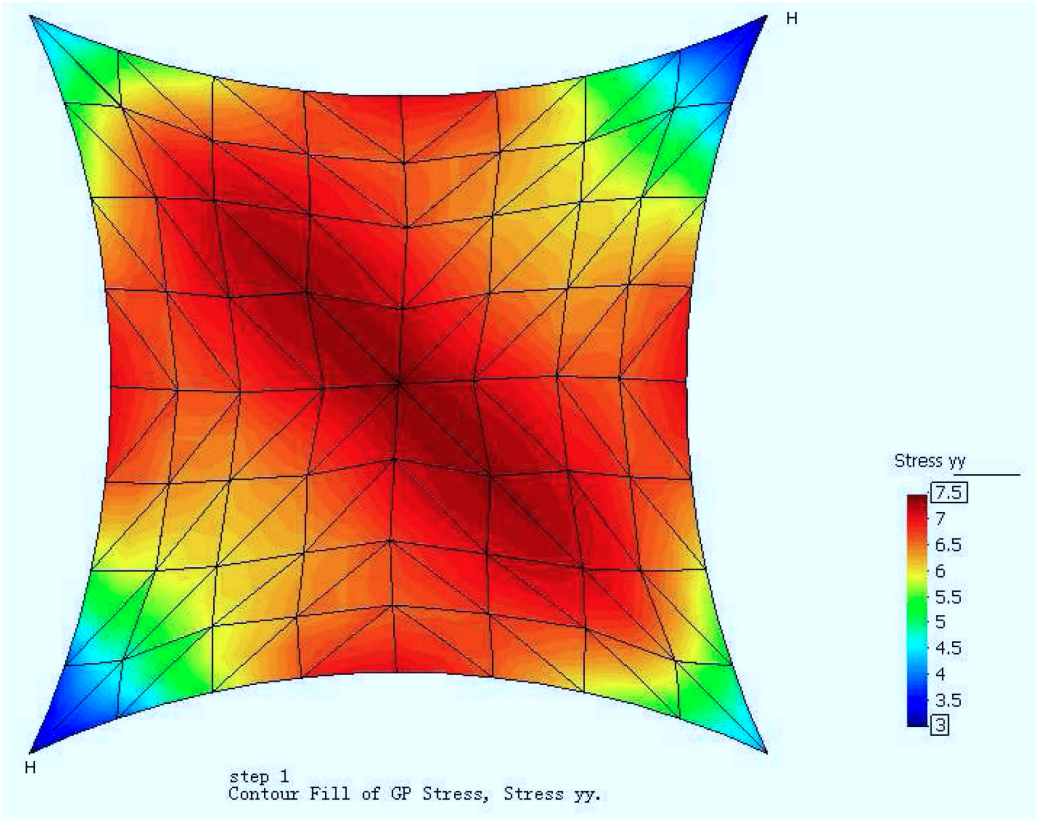

Figure 3.32: Stress along the fill direction — large strain LST

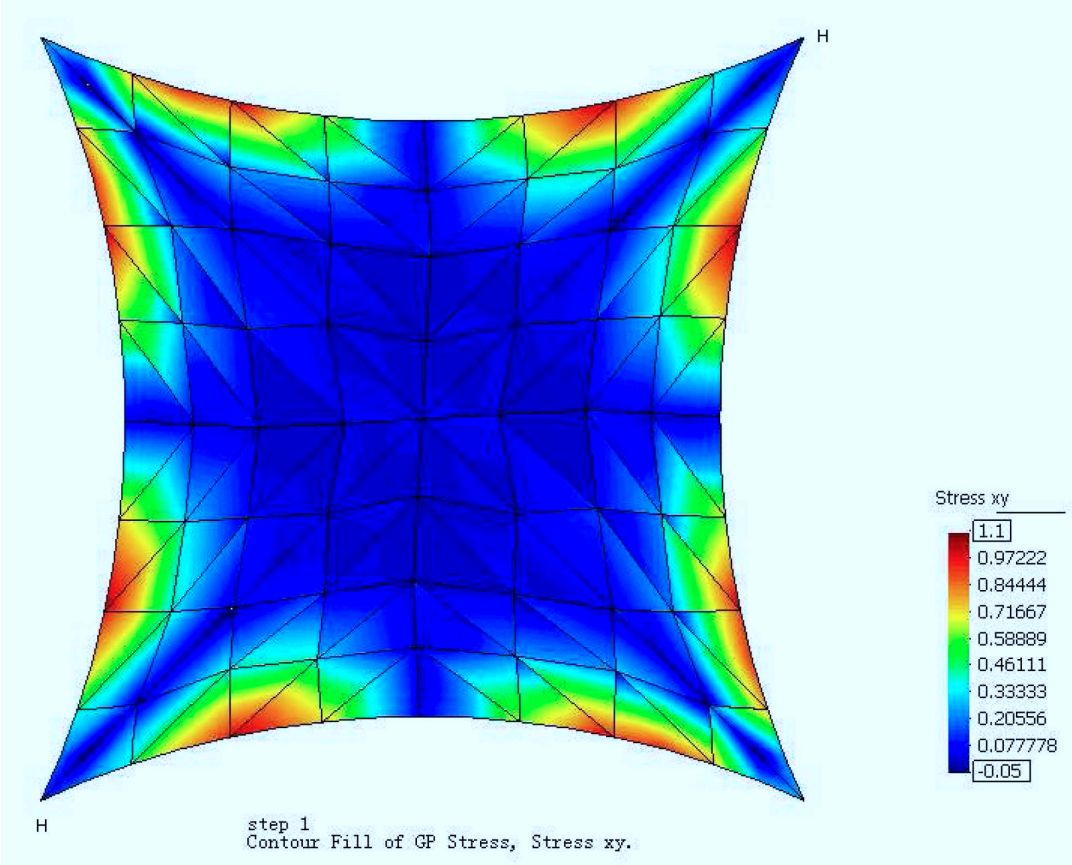

Figure 3.33: Shear stress across the warp and fill direction — large strain LST

Both CST and LST formulations predict that, in the warp direction, the membrane stresses decrease from two low points C,D to the symmetrical axis across two high points A,B (figures 3.28-3.33). Conversely in the fill direction, the stresses increase from the two low points A,B to the symmetrical axis across C,D. The shear stresses are generally uniformly distributed and close to zero. Pockets of shear stress appear at points along the boundary cables.

Comparison between CST and LST

The ranges of the membrane stress obtained from CST and LST models (illustrated in fig. 3.34-3.36 converge to similar values.

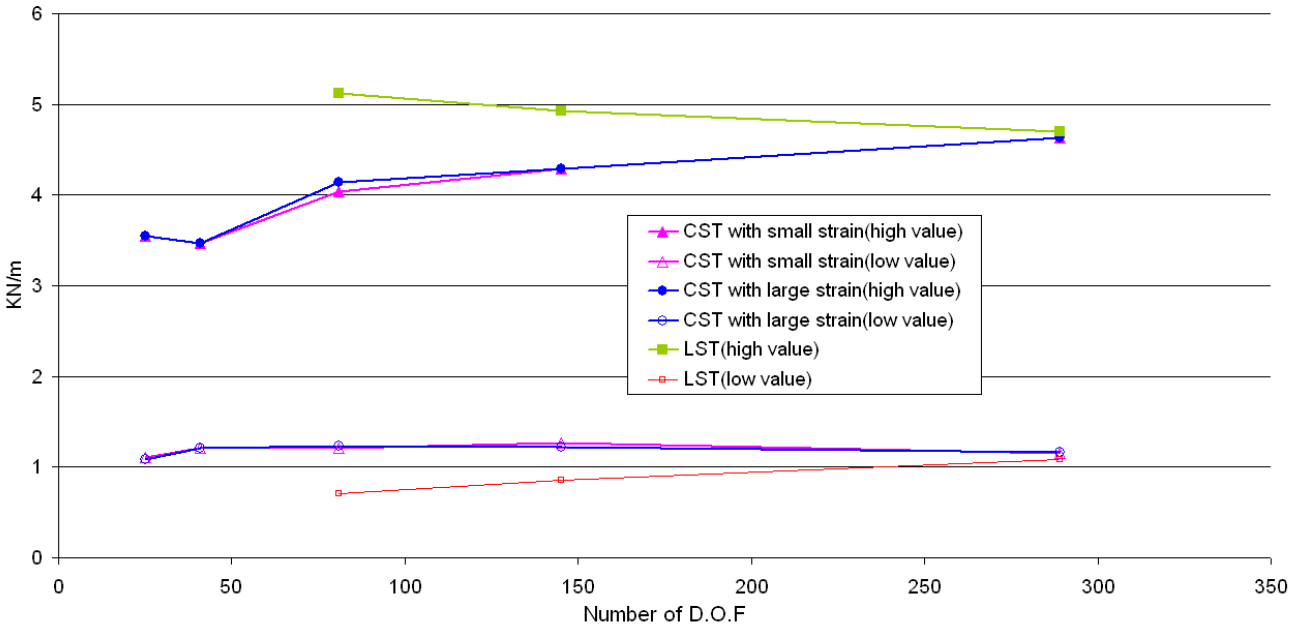

Figure 3.34: Warp stress as a function of the number of D.O.F

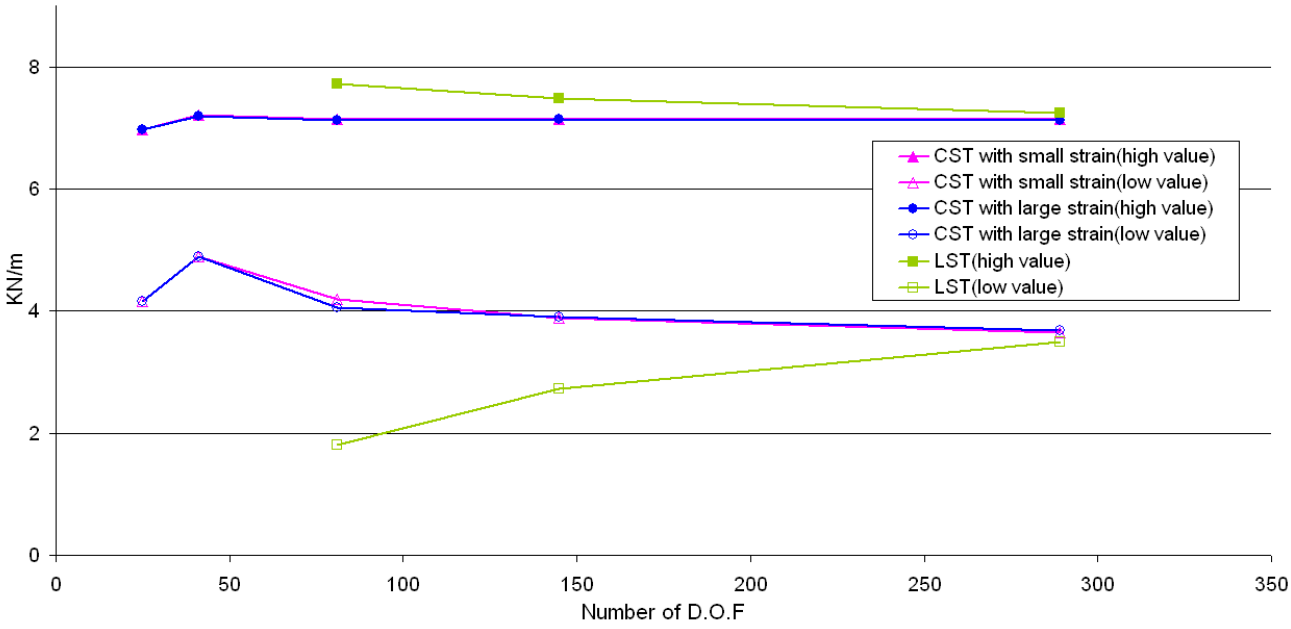

Figure 3.35: Fill stress as a function of the number of D.O.F

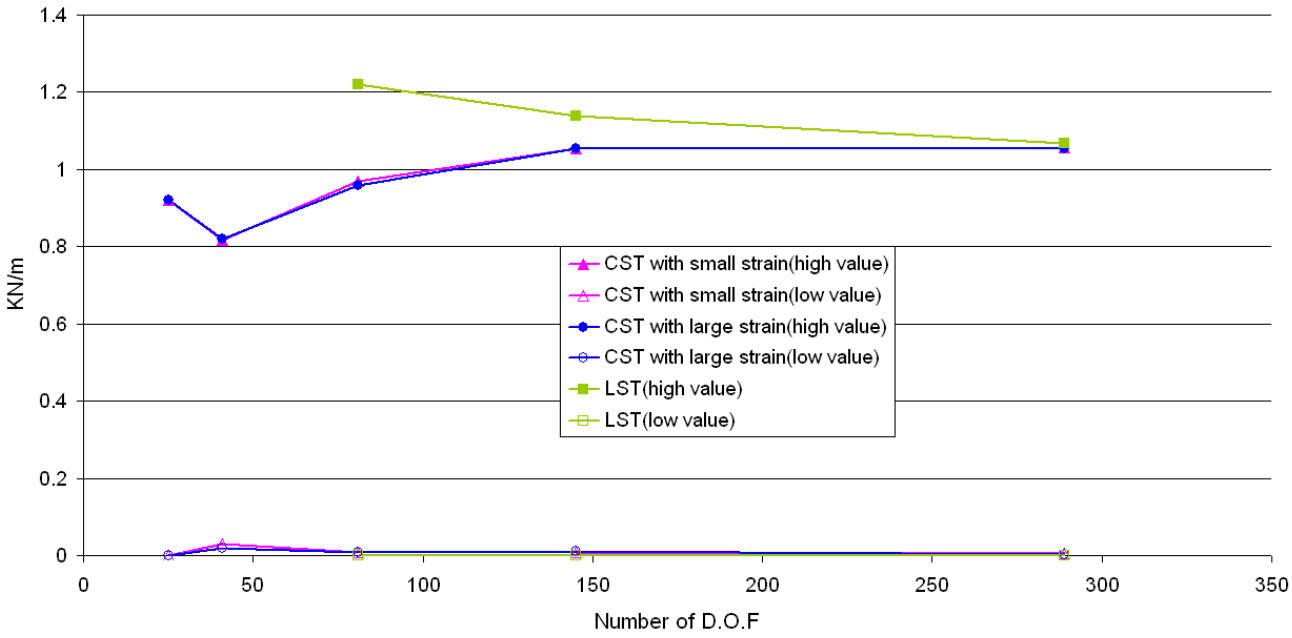

Figure 3.36: Shear stress as a function of the number of D.O.F Number

This characteristic is repeated with respect to the central nodal displacement, as inferred by fig. 3.37, where the LST is shown to converge at a relatively slower rate in this Hypar example, but from an initial solution (coarse mesh) which were representative of the solution from the referred mesh compared with the CST results.

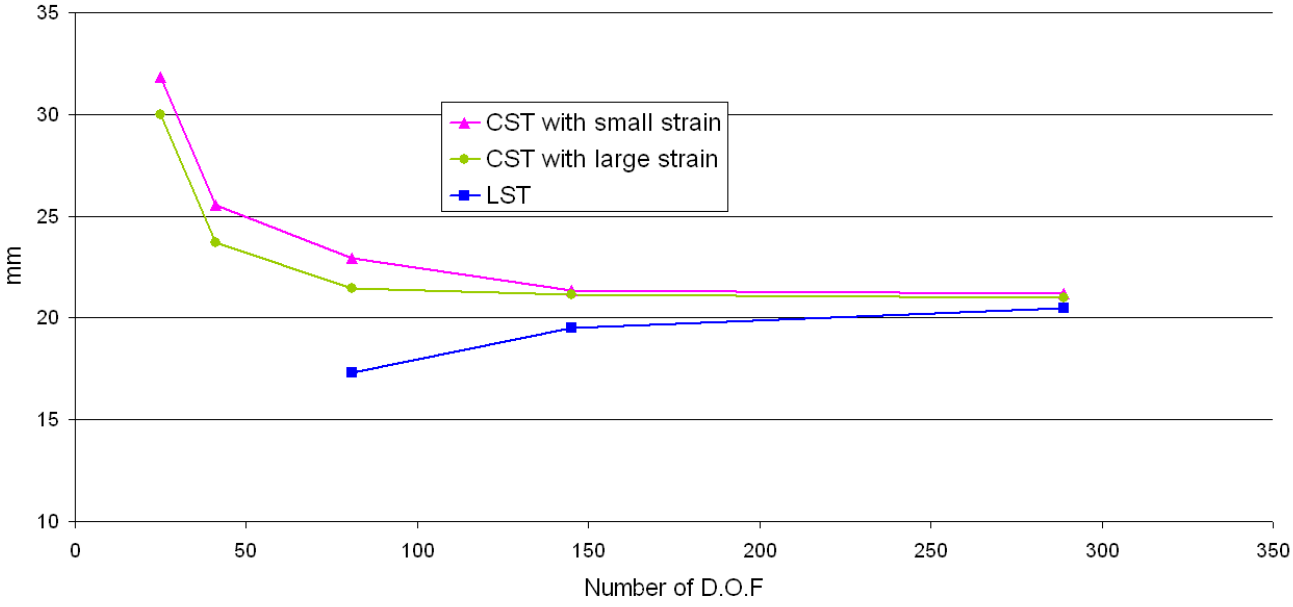

Figure 3.37: Central node displacement as a function of the number of D.O.F Number

In the dominant area of the Hypar, due to upward loads, membrane stresses develop along the fill direction and decline along the warp direction. In contrast, the membrane stresses near

the fixed points increase along the warp direction and decrease along the fill direction (figure 3.28 and 3.29). This phenomenon results from the integrated structural response of membrane surface and boundary cables near the boundary area, where membrane stress is associated with the deformation of both membrane and cable elements. With the narrowing of the fabric in these regions, the effect from cable elements is more pronounced. For example, near the low points, even with reduced curvature along the warp direction of the membrane surface, the enhanced membrane stress along the warp direction is dominated by the stretching and deformation of the boundary cables.

It is notable that the membrane stresses along the warp direction represented by LST (Fig. 3.31) change rapidly near the two low points of the hypar, while even with same D.O.F as figure 3.38, such detailed information of membrane stress in that area is not easy to obtain using large strain CST as in figure 3.28, because the membrane stress of interest is constant across every element. Therefore, a refined mesh is required to enable CST to provide a more accurate estimate of the structure response. An indication of any required mesh refinement is obviously only obtained after an initial analysis. Whilst stress gradients with a LST at the element boundaries can be used to imply adequacy of the mesh density, it is more difficult to demonstrate convergence with the CST.

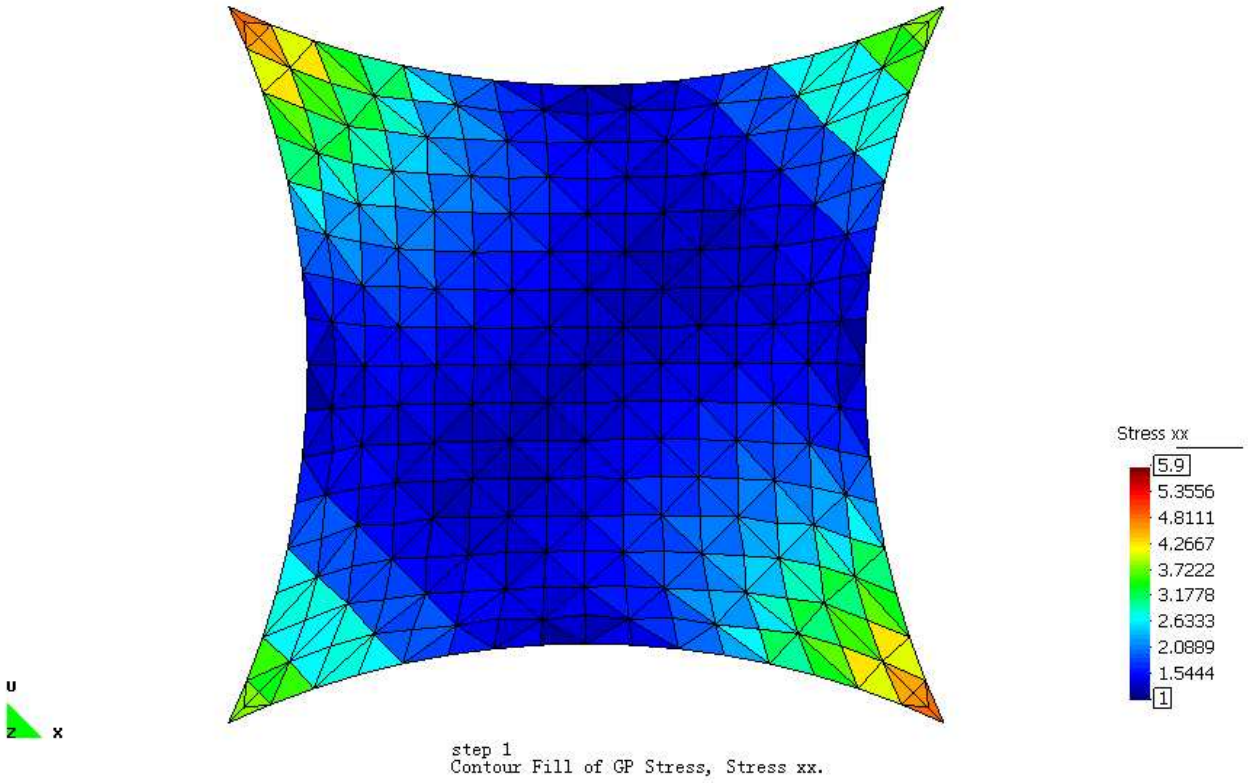

Figure 3.38: Stress along warp direcion - large strain CST with refined mesh

3.5.2 Shear Patch Test

This patch test (Details in fig. 3.39) compares the performance of the three types of CST and LST formulations under conditions of severe shear strains. The Elastic modulus of the patch is $E_x = E_y = 600kN/m$, $G = 30kN/m$, Possion's ratio $v = 0.3$ and thickness $t = unit$, and the patch is discretized with a mesh of 192 elements both for CST and LST . The resulting deformation is illustrated in figure 3.40 below:

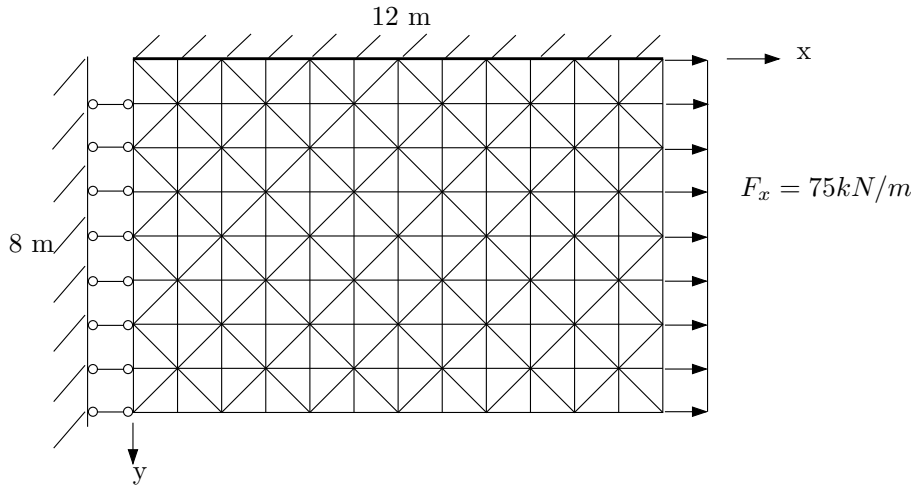

Figure 3.39: Shear patch test and the element mesh

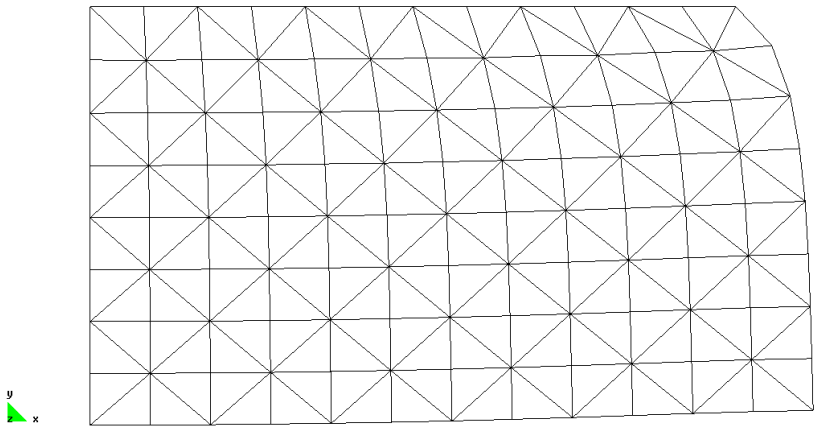

Figure 3.40: Deformed mesh — large CST with F_x=75 kN/m

Fig. 3.41-3.44 illustrate the stress $\sigma_x$obtained from CST and LST formulations. The continuity of σ_x equivalent from large strain CST and LST formulations (as in fig. 3.43 and 3.44) is better than that from the small strain CST(as in fig. 3.41 and 3.42). With increasing distance from the top boundary, the trends of stress σ_x from CST and LST are very similar, but as shown in fig. 3.45, near the bottom line of the patch, the two small strain CST models produce much lower value of σ_x , which is expected to be close to the applied load $F_x = 75kN/m$ due to pure tension in the x direction at the lower boundary.

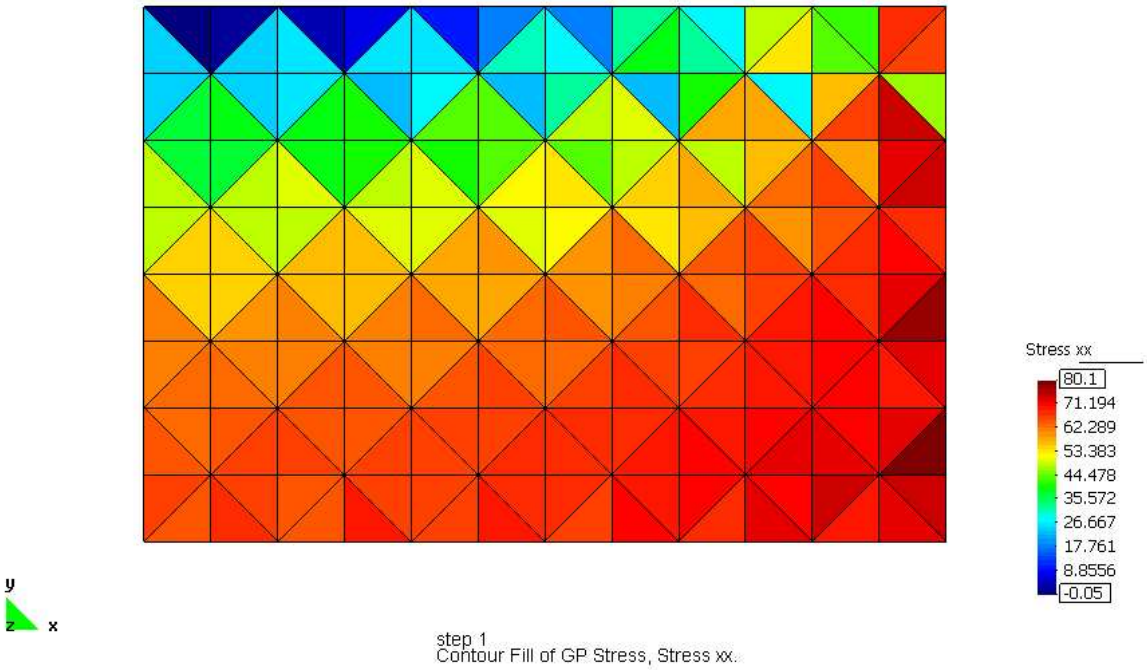

Figure 3.41: Stress σ_x — small strain CST

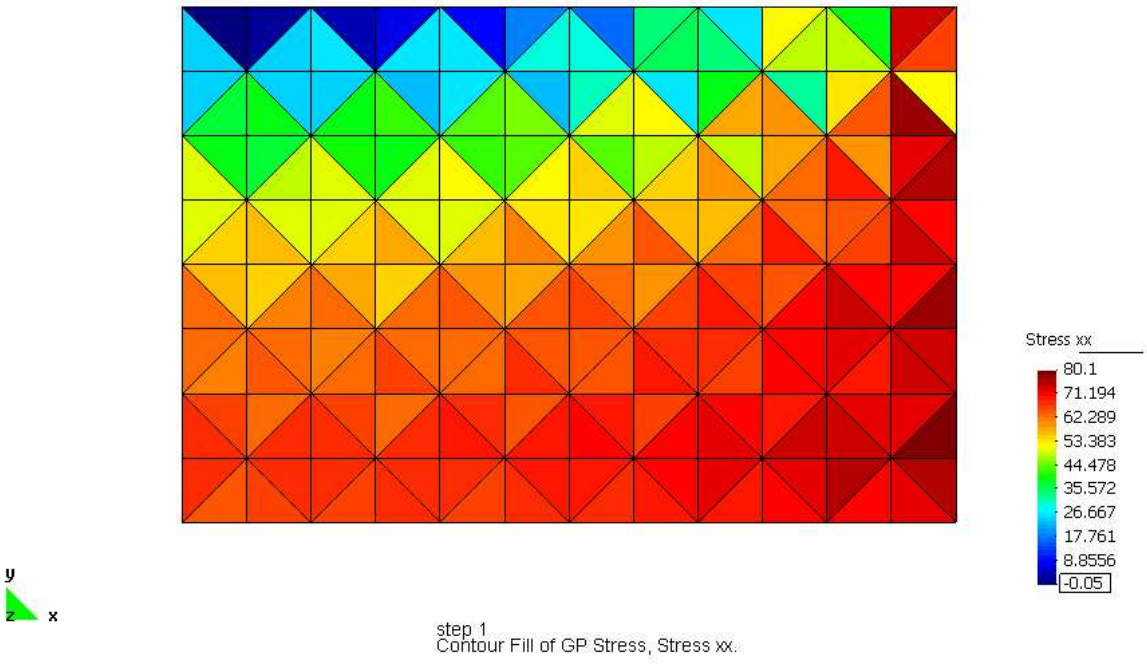

Figure 3.42: Stress σ_x — meso-strain CST

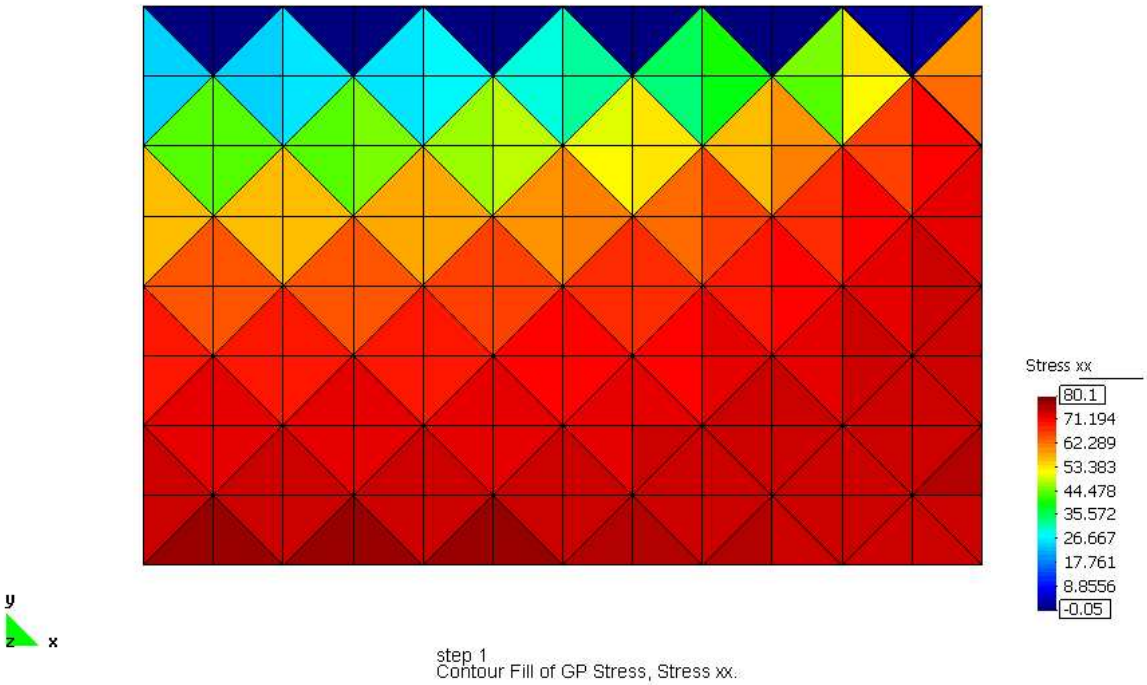

Figure 3.43: Stress σ_x — large strain CST

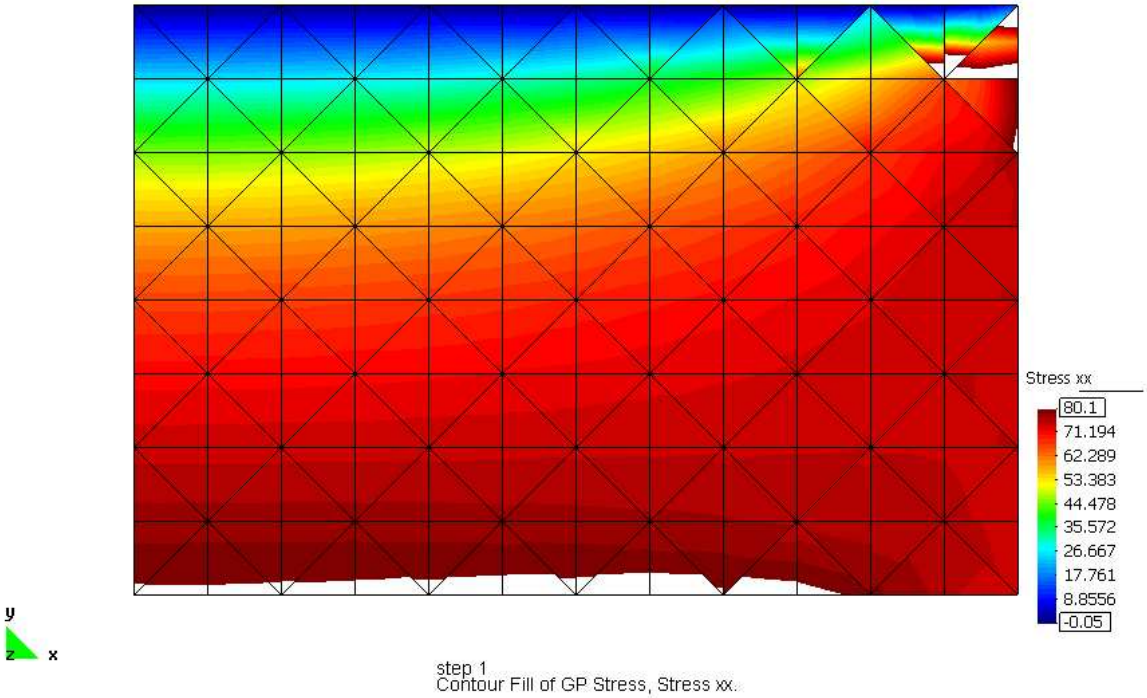

Figure 3.44: Stress σ_x – LST

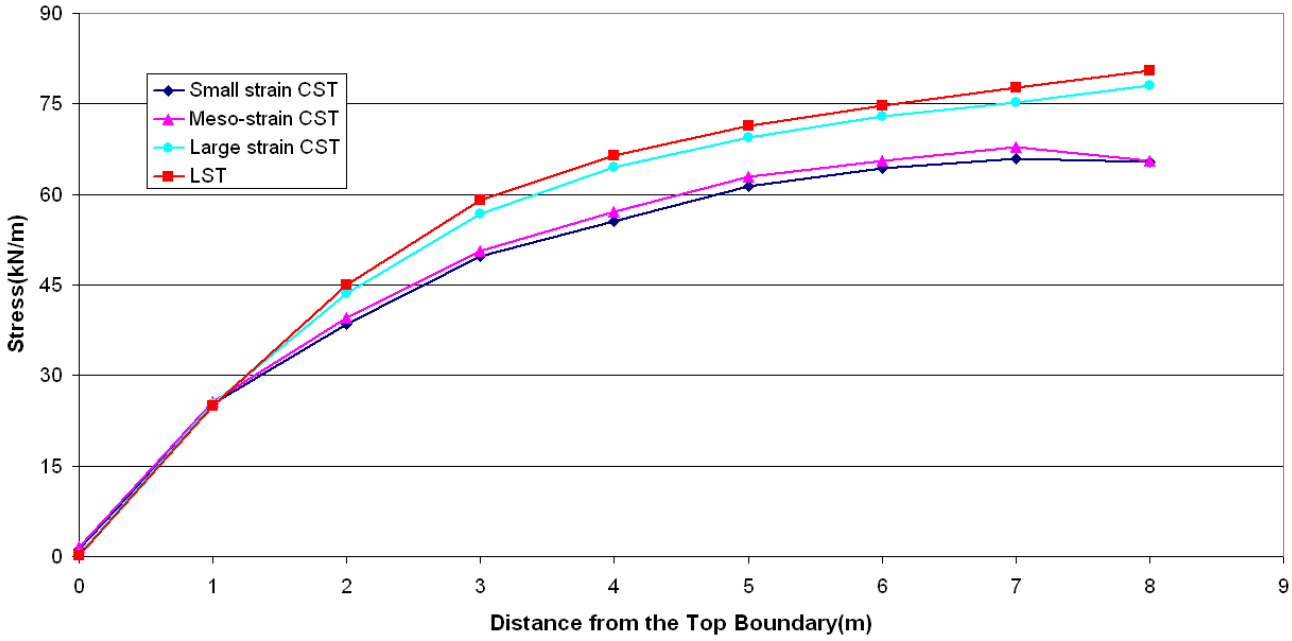

Figure 3.45: Stress σ_x along y axis from the left edge of the patch

It is shown in Fig. 3.46-3.49 ,that compared with σ_x, in most areas, σ_y produced by the CST and LST are similarly small, but near the top boundary, large discontinous element stresses can be observed from the small strain CST results (fig. 3.46 and 3.47).

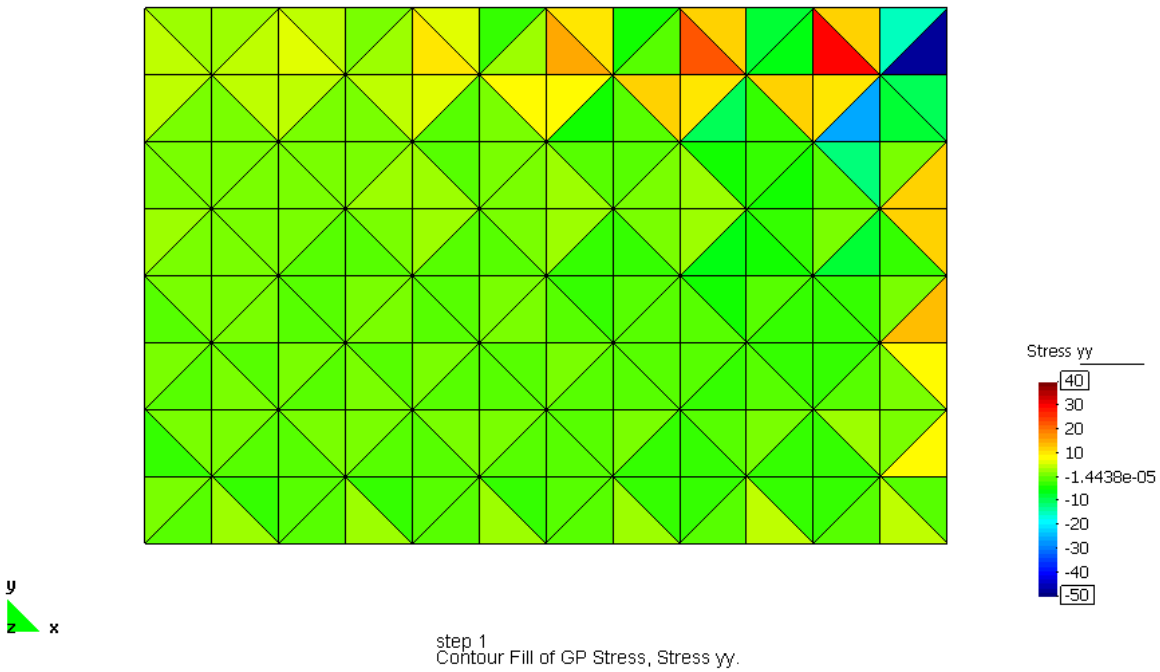

Figure 3.46: Stress σ_y — small strain CST

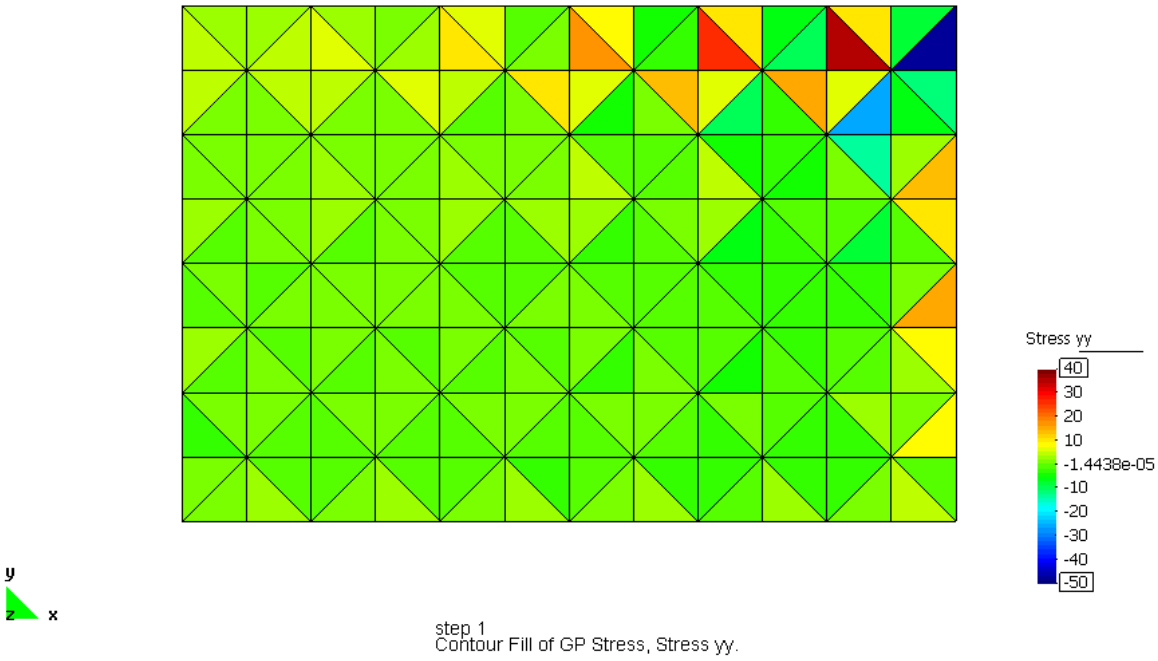

Figure 3.47: Stress σ_y — meso-strain CST

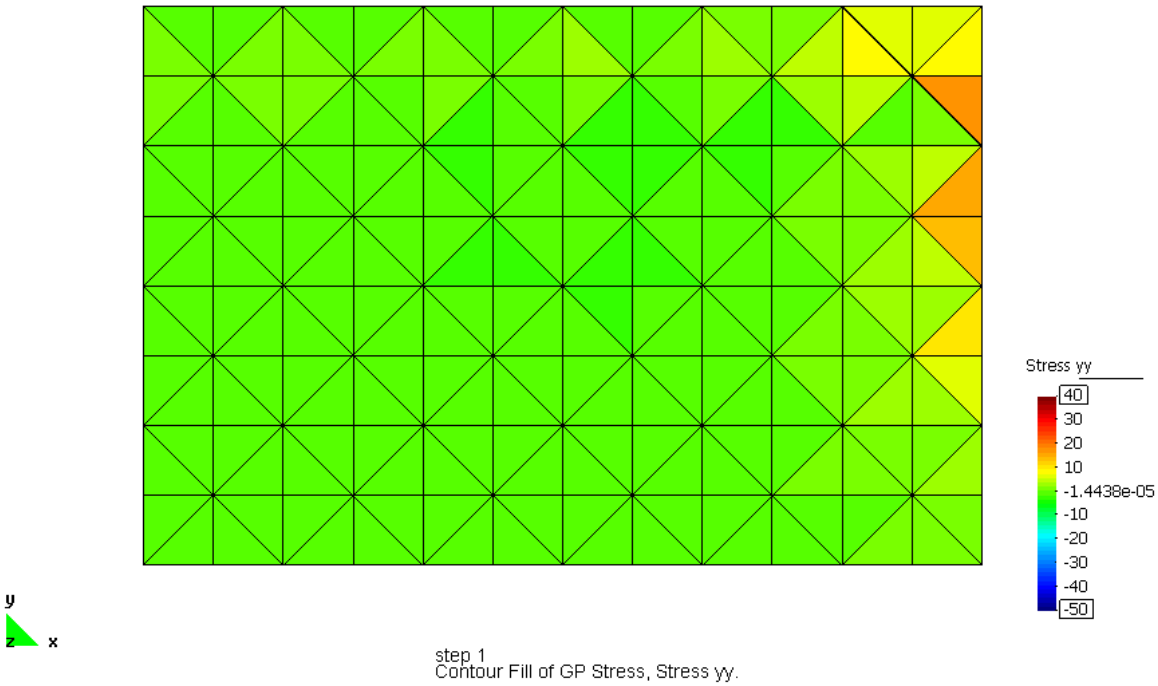

Figure 3.48: Stress σ_y — large strain CST

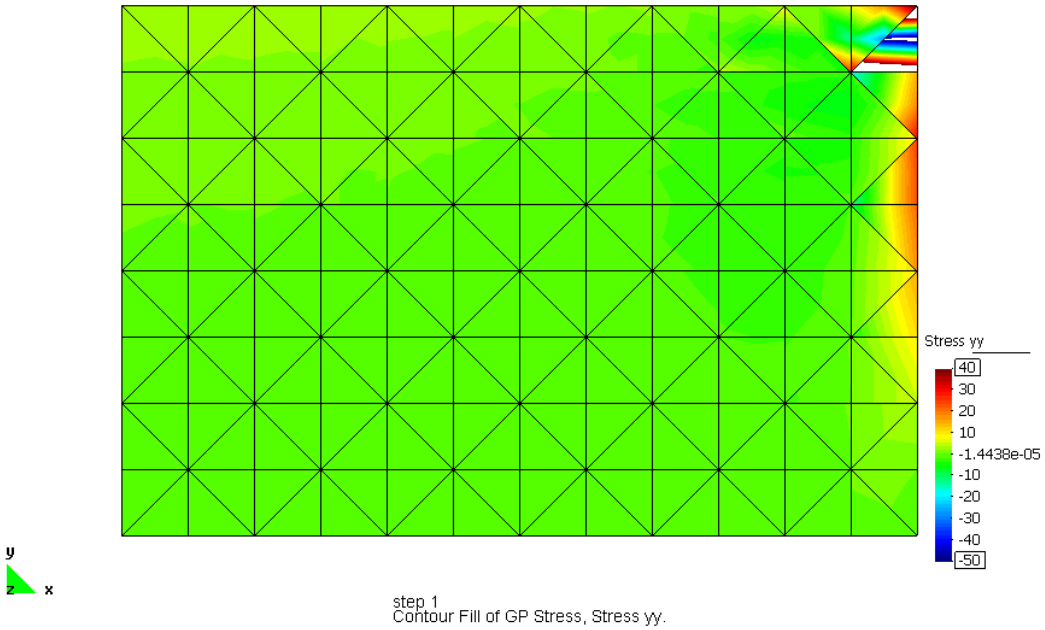

Figure 3.49: Stress σ_y — LST

It is notable that the shear stresses illustrated in fig.3.50-3.53 are of absolute value, then maximum shear stresses from CST and LST can be directly compared visually. The significant errors from the two small strain CST can be found in fig. 3.50 and 3.51, because the maximum shear strains are large(63^o distortion), and serve to illustrate and emphasize the errors introduced by these two formulations.

Whilst the applied load of 75 kN/m is clearly high, this numerical example is used to represent potential scenarios around the edges of clamp plates, for example. It is also interesting to note how the small-strain and meso-strain CST formulations produce a chequerboard style stress distribution. This phenomenon is erroneous and is symptomatic of a type of solution instability, in this case introduced by assumptions within cable-analogy formulation. Similar undesirable solution characteristics are not reproduced by the CST triangle based on a large strain formulation.

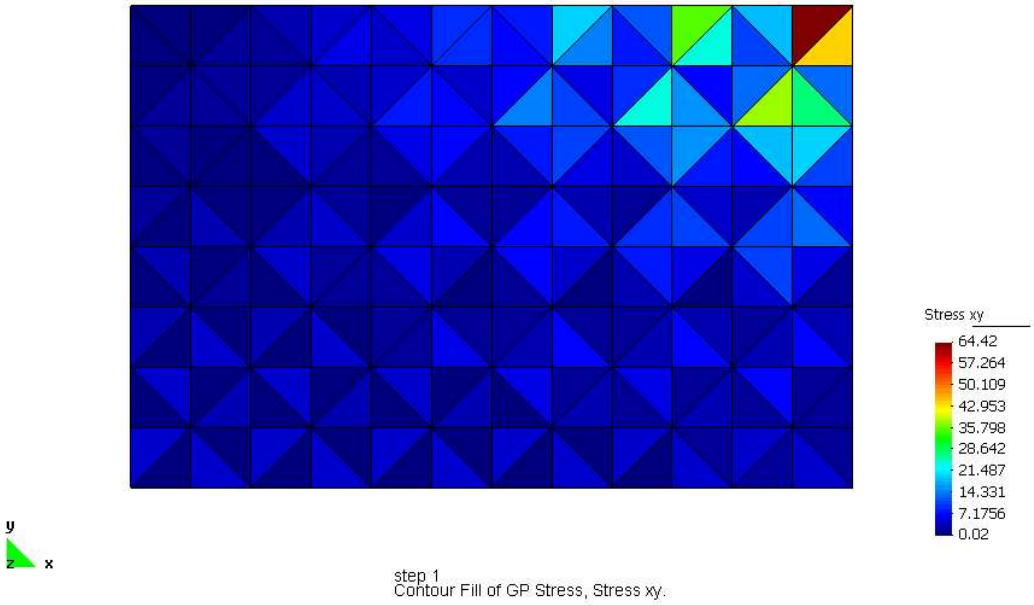

Figure 3.50: Shear τ_{xy} — small strain CST

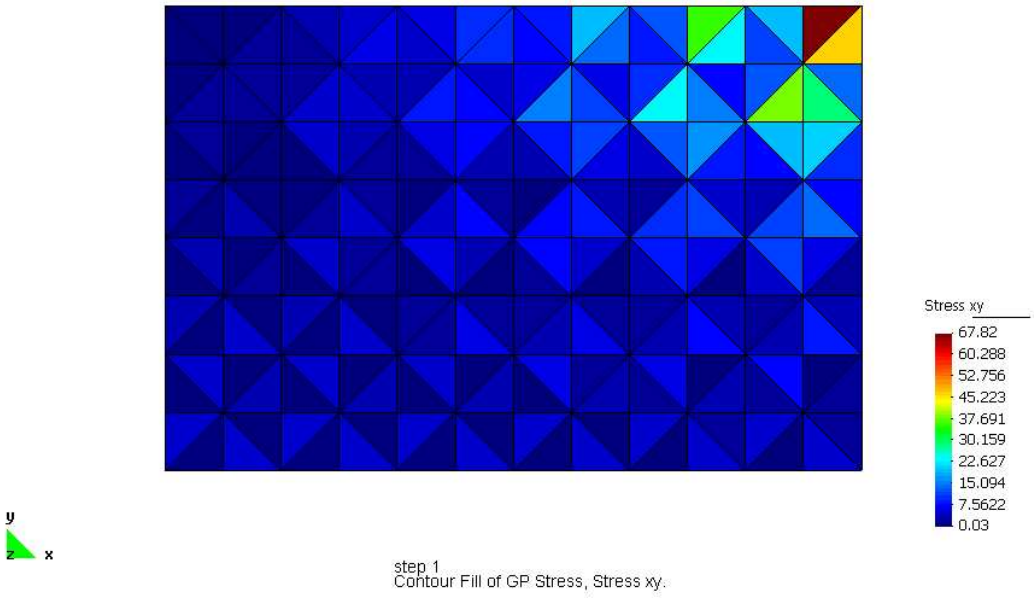

Figure 3.51: Shear τ_{xy} — meso-strain CST

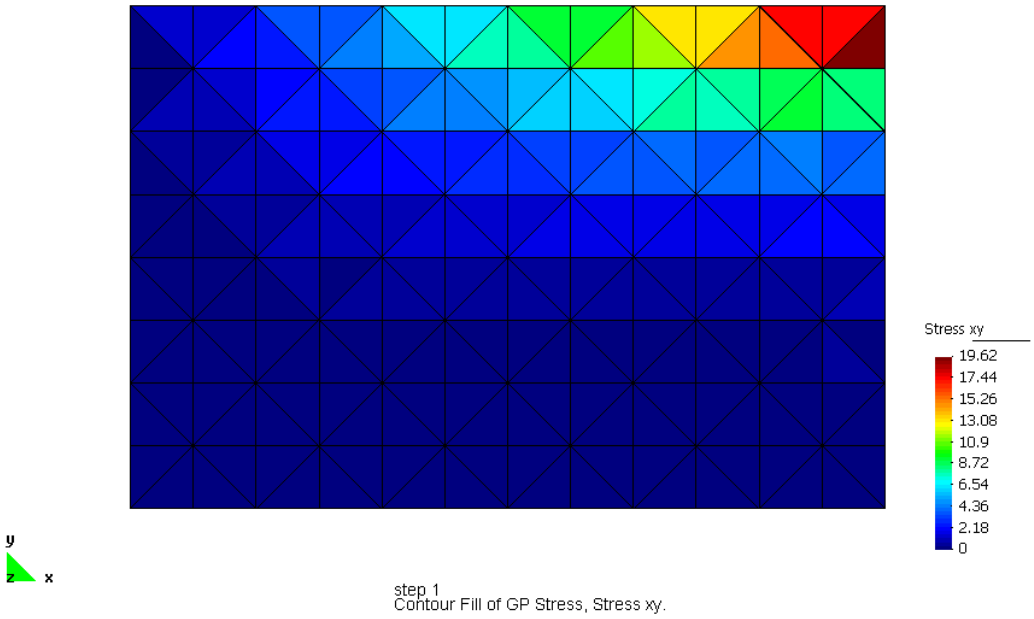

Figure 3.52: Shear τ_{xy} — large strain CST

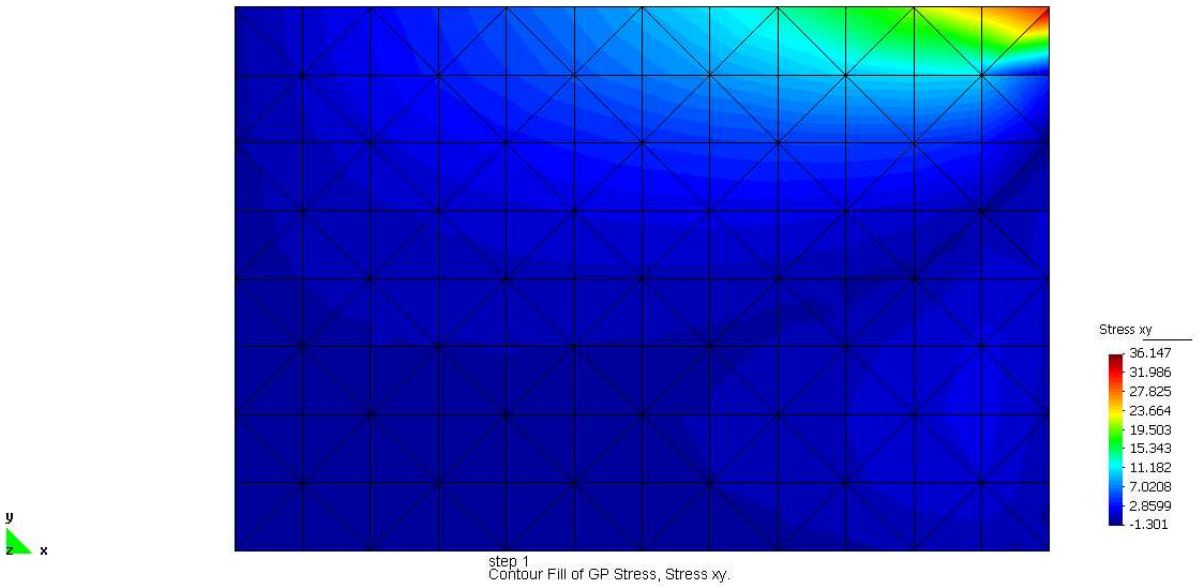

Figure 3.53: Shear τ_{xy} — LST

3.5.3 Verification of the Shear "Patch Test"

The shear problem described in section 3.5.2, has been re-analyzed using a commercially available finite element code – LUSAS. The purpose of this exercise is to demonstrate that the formulation independently developed as part of this research project is correct. The comparison is not intended to lead to exactly the same result since the element formulations and solvers are different (e.g total or updated lagrange , Eulerian). However, similar magnitudes of stresses and distribution should be expected if the two sets of solution are to be verified. Similarities are required (as opposed to exactly matching magnitudes etc), when analysing potentially discontinuous solutions arising from stress concentration, as in this example. LUSAS solutions have been obtained using the same mesh but an alternative six-node plane stress triangular finite element formulation, without geometric stiffness (unavailable). An incremental solution procedure with ten equal load increments has been used with an Eulerian framework. Only the linear strain triangle is used as the basis of the comparison since this formulation is the most comprehensive and commercial finite element codes do not normally permit geometrically nonlinear analysis with the constant strain triangle formulation.

The solutions of the stress σ_x predicted by LST and LUSAS appear to be very similar (fig. 3.54 and 3.55). It is notable that from both LST and LUSAS models, discontinuous stresses are observed in the elements near the right corner point (denoted by C). The discontinuity is of the same type. Interestingly, in both models, if the mesh is refined or coarsened, the discontinuity always appears in the penultimate element next to the boundary discontinuity at the far edge of the patch (at C).

The stresses σ_y and τ_{xy} predicted by the LST and LUSAS models exhibit similar characteristics, though not to the same level, especially in the case of σ_y. It should be noted that the σ_y stress is predominantly a secondary induced stress in that it arises from Poisson's effects as there is no externally applied load in the y direction. Thus qualitative comparison of solutions from the proposed formulation(LST) and a commercially available finite element code(LUSAS) indicates the former is appropriate, correctly formulated and implemented.

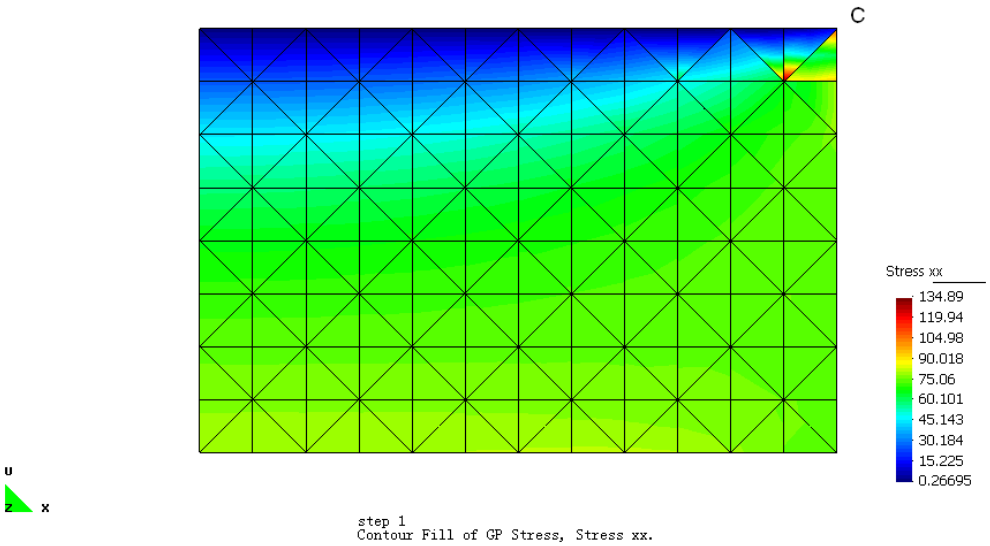

Figure 3.54: Stress σ_x — LST

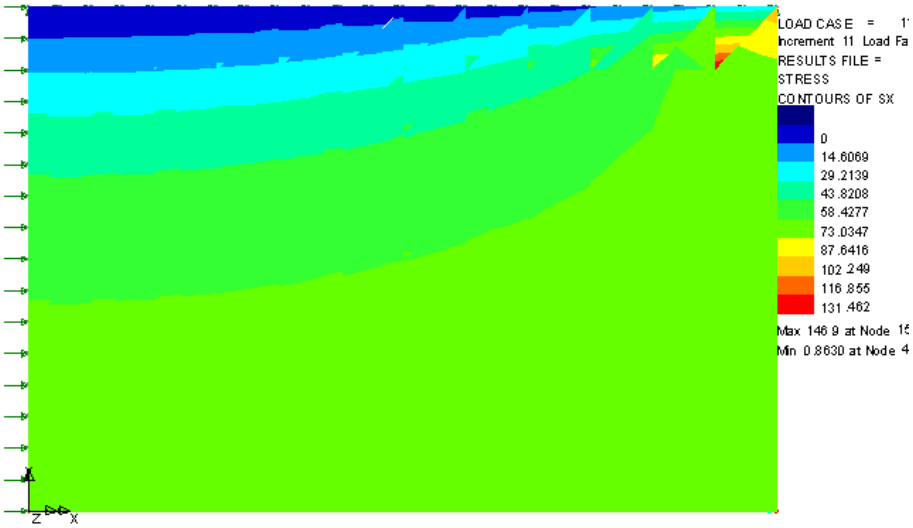

Figure 3.55: Stress σ_x — LUSAS

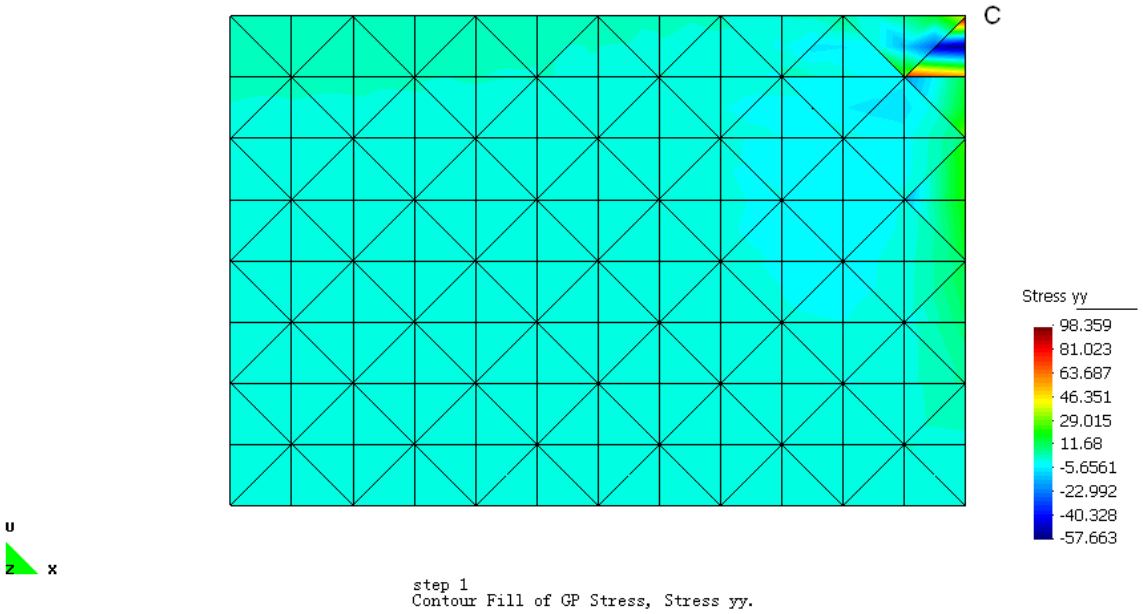

Figure 3.56: Stress σ_y — LST

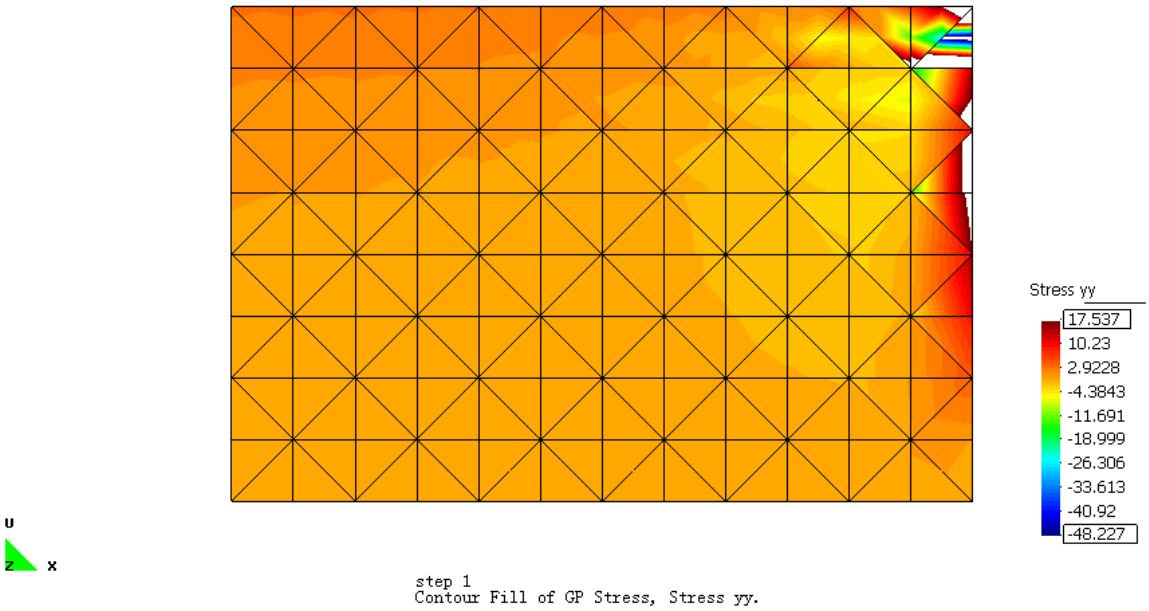

Figure 3.57: Stress σ_y — LST with a similar scale range as that of the equivalent LUSAS solution(fig. 31)

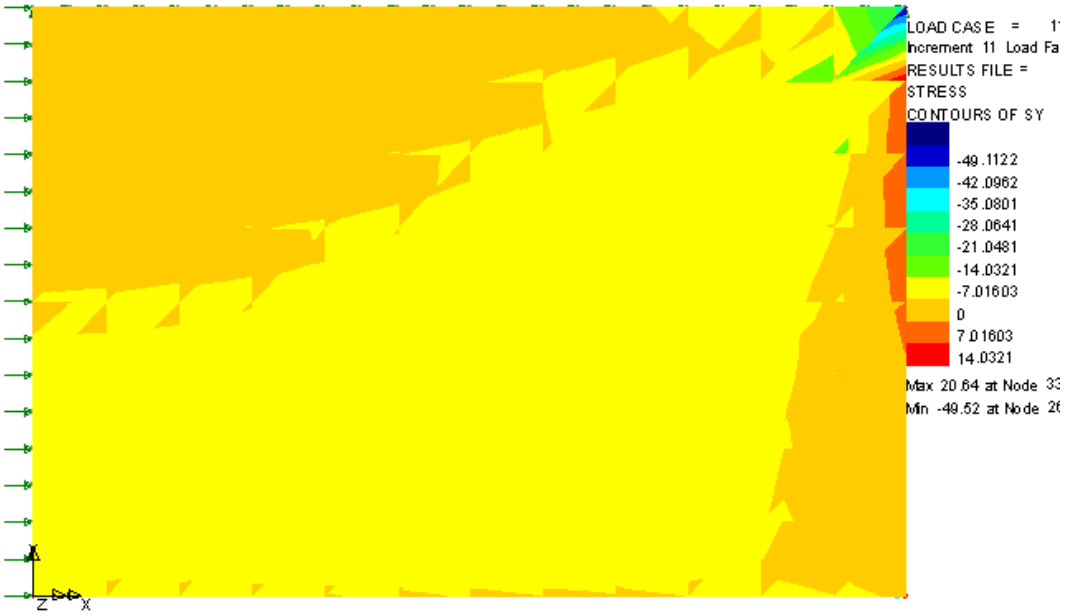

Figure 3.58: Stress σ_y — LUSAS

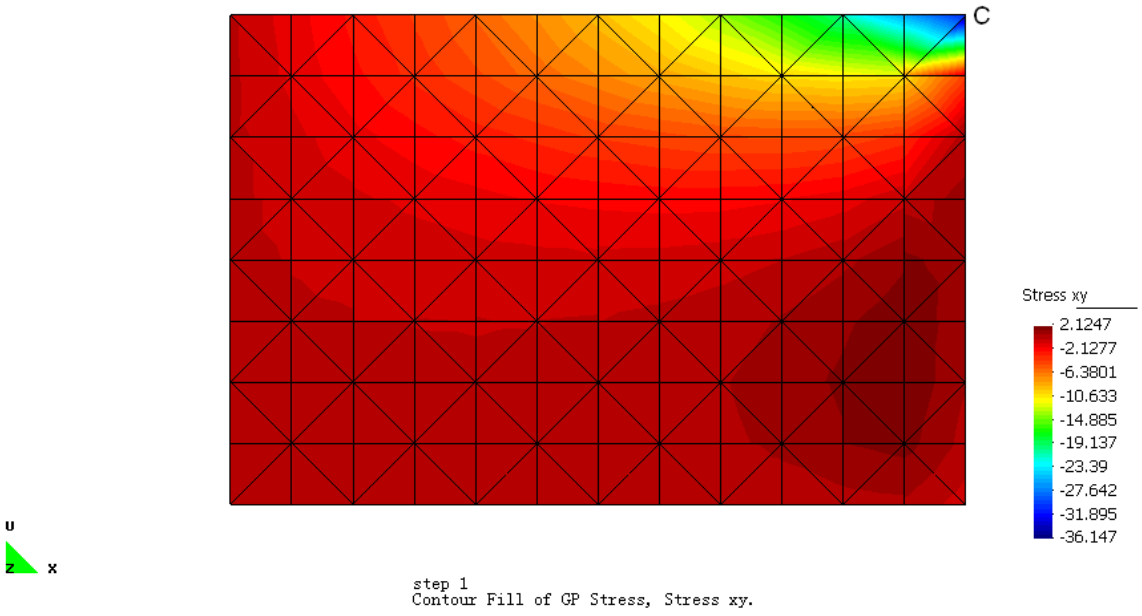

Figure 3.59: Shear stress τ_{xy} — LST

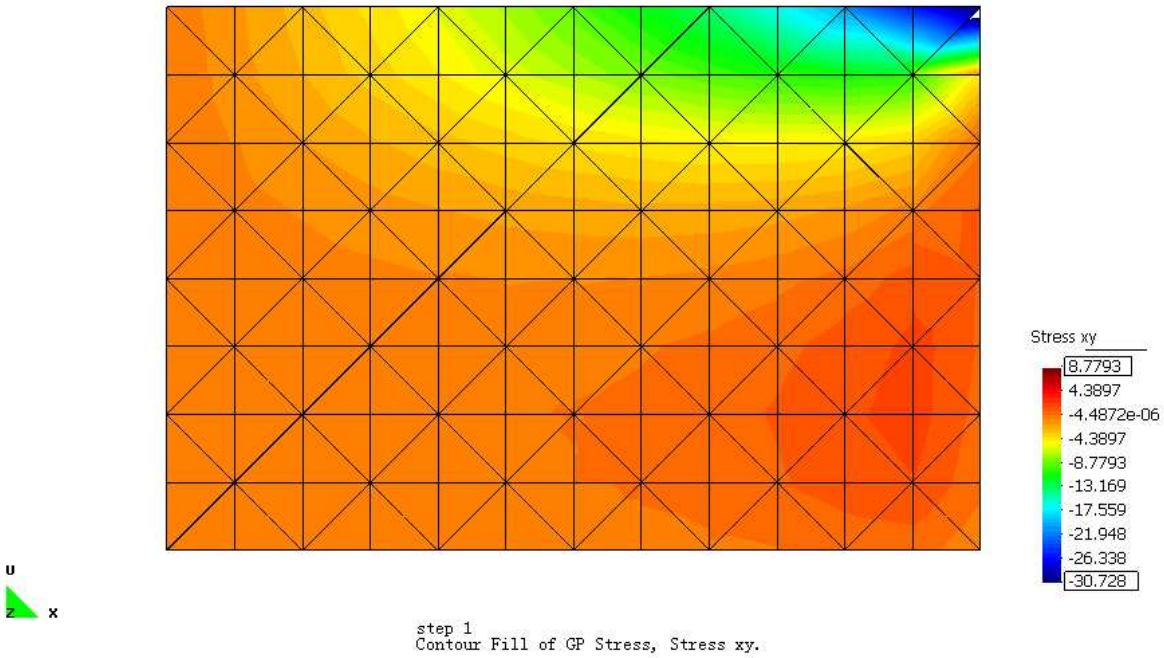

Figure 3.60: Shear stress τ_{xy} — LST with a similar scale range as that of the equivalent LUSAS solution(fig. 34)

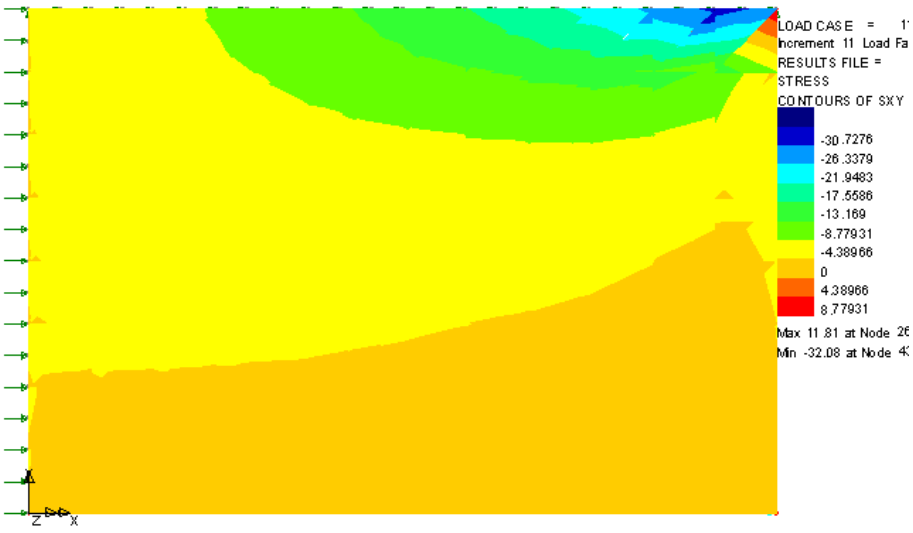

Figure 3.61: Shear stress τ_{xy} — LUSAS

3.5.4 Simulation of The Newcastle University Biaxial Cruciform Test

In the simulation of the membrane biaxial test illustrated in fig. 3.62, the material properties are: $E_x = 600kN/m$, $E_y = 600kN/m$, $G = 30kN/m$, and Poisson's ratio $v = 0.3$. The loads and mesh are shown in the following figures 3.62 and 3.63. There are eleven slits in each of the four strips around the central square, and the length of the slit is 150mm from the central square:

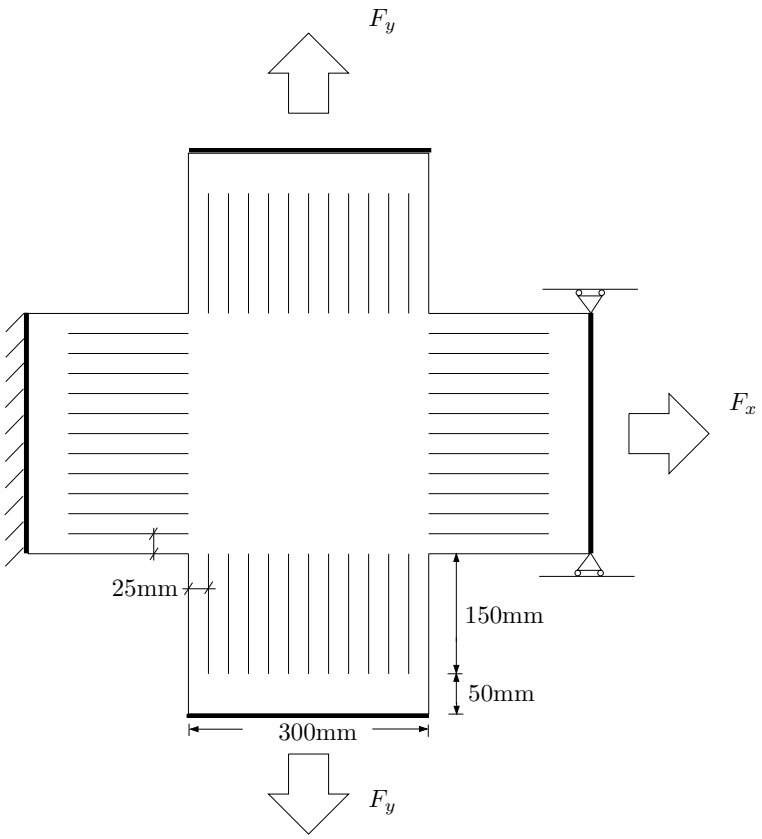

Figure 3.62: Numerical example of membrane biaxial test

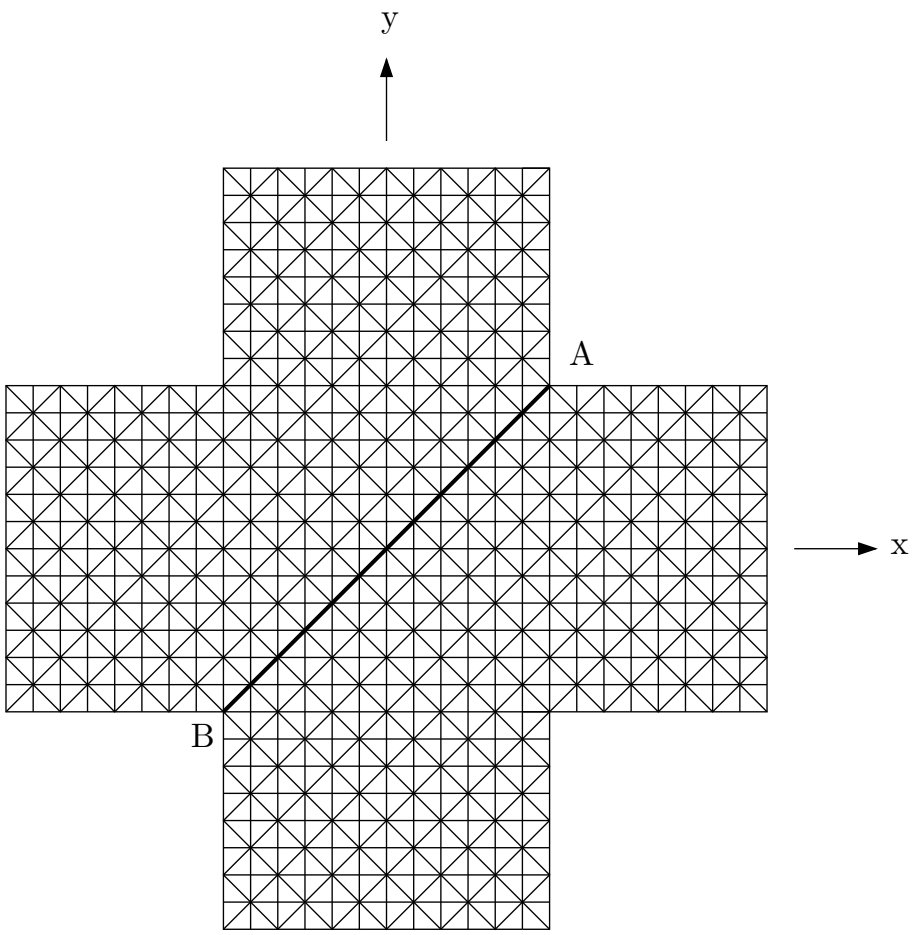

Figure 3.63: Mesh of biaxial cruciform

1) CST Small Strain Cable Analogy Formulation

The distribution of the maximum principal stress σ_x of the biaxial cruciform membrane under the load $F_x = 30kN/m$,$F_y = 30kN/m$, is depicted in fig. 3.64, with the same solution , but with the displayed range limited to the range 28-30 kN/m (in fig. 3.65) for clarity. It is clear in fig. 3.65 and 3.66 that the solutions of both σ_x and τ_{xy} to this symmetrical problem are not symmetrical.

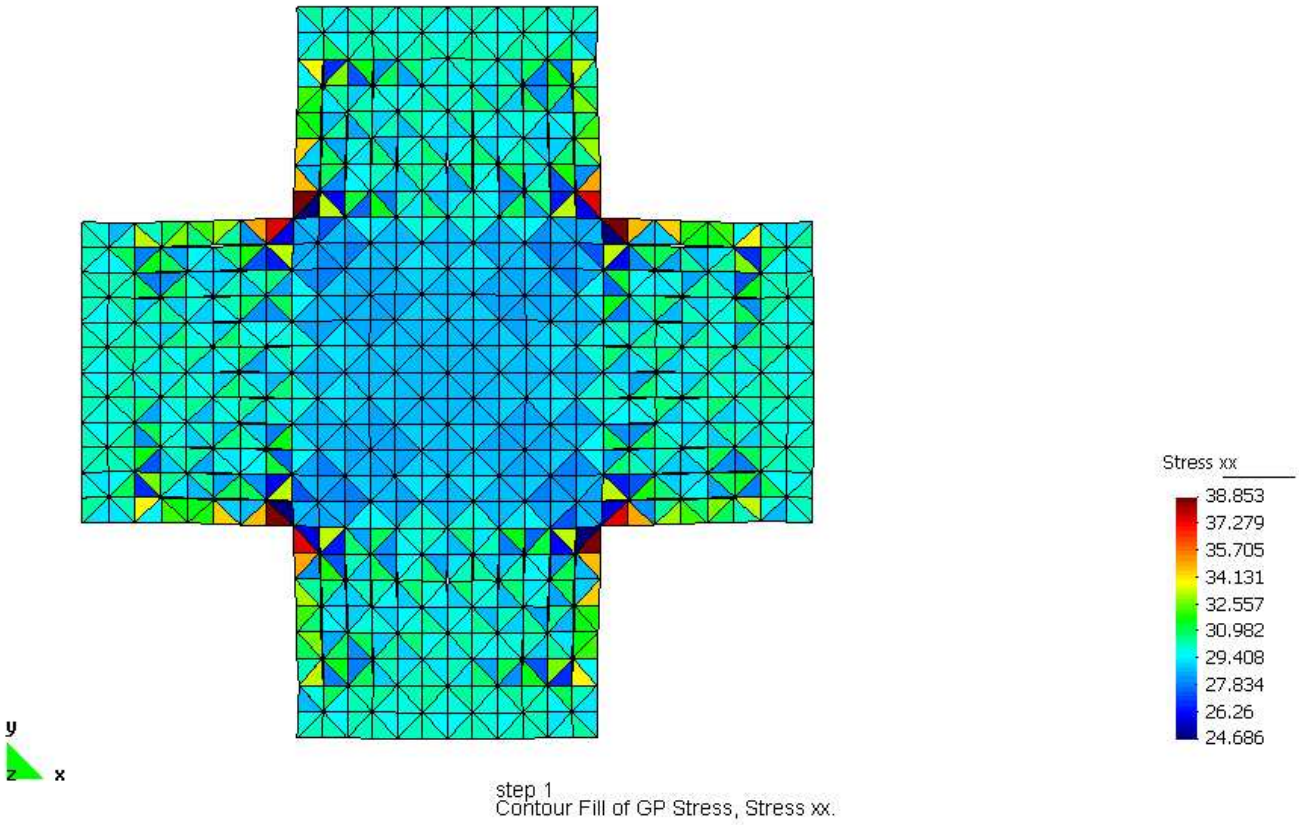

Figure 3.64: Max principal stress σ_x of biaxial cruciform with $F_x = F_y = 30kN/m$

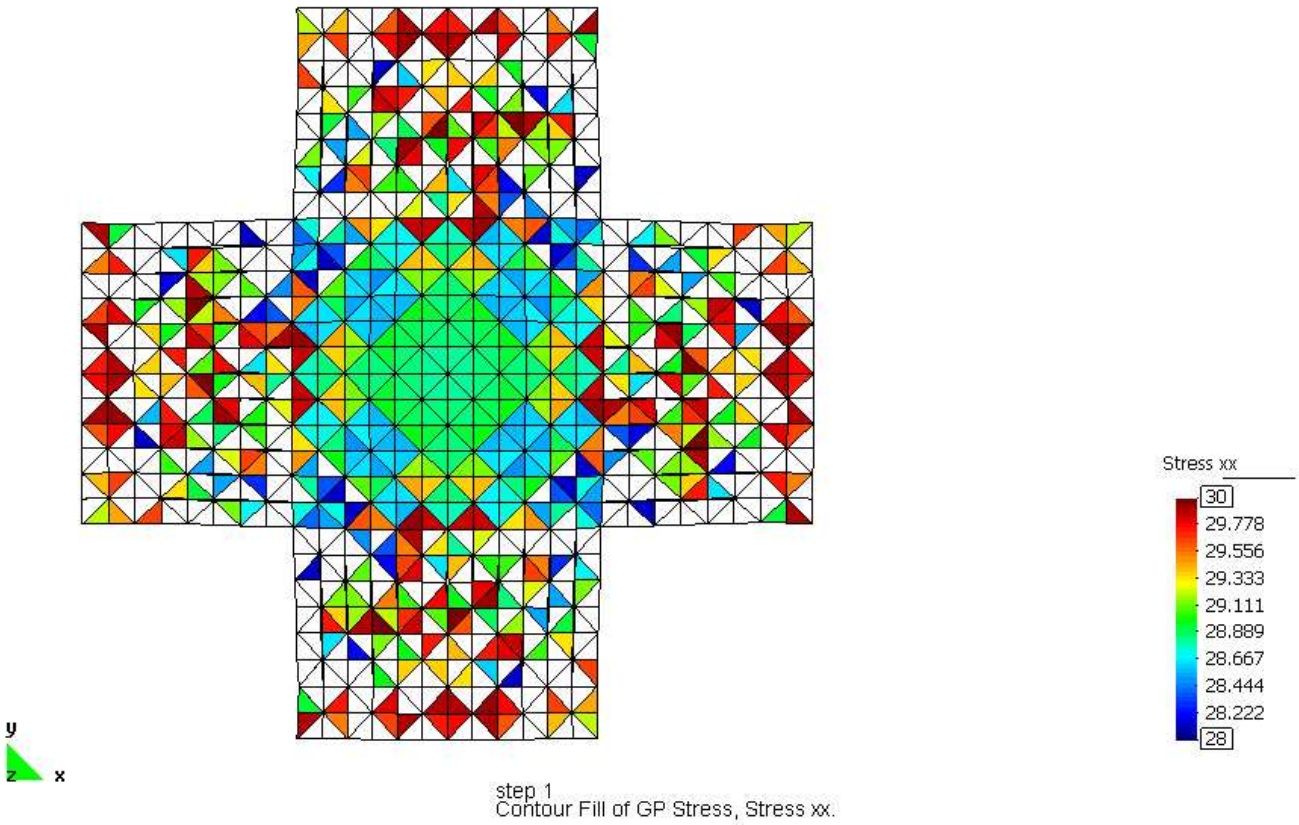

Figure 3.65: Central selected principal stress σ_x of biaxial cruciform with $F_x = F_y = 30kN/m$

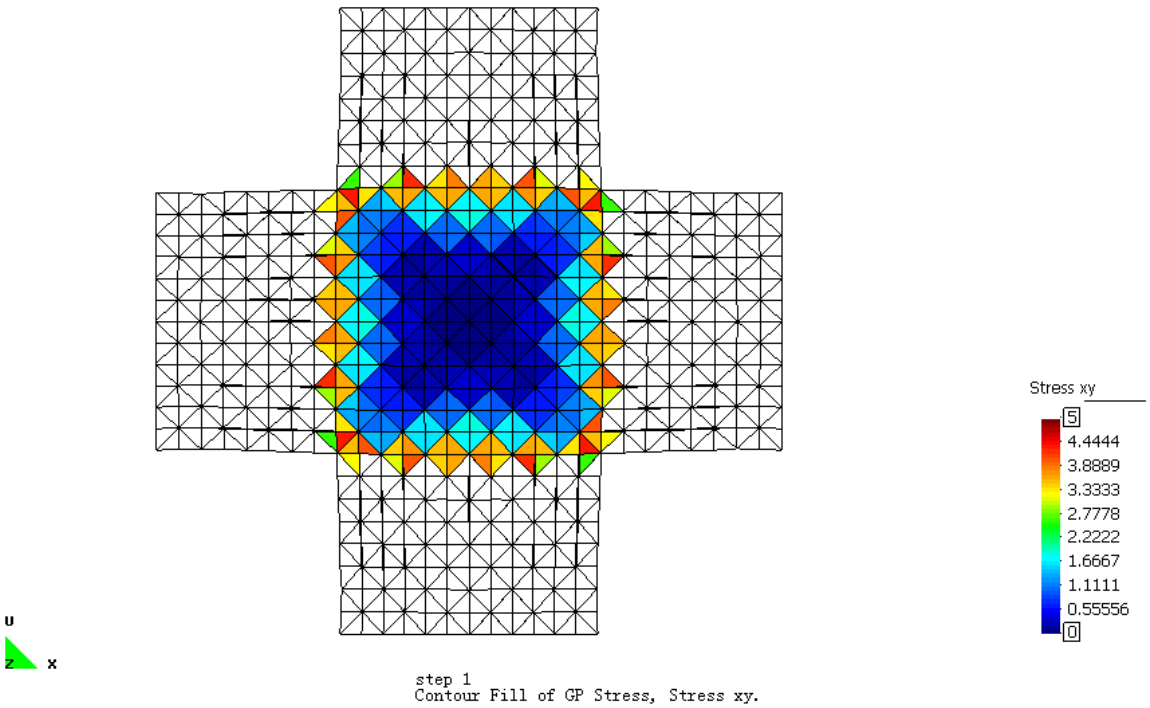

Figure 3.66: Central selected shear stress τ_{xy} of biaxial cruciform with $F_x = F_y = 30kN/m$

As shown in figures 3.67 and 3.68, with the load increased to $F_x = F_y = 60kN/m$ and hence the strains similarly increased, the asymmetry of the geometrically nonlinear result is reinforced.

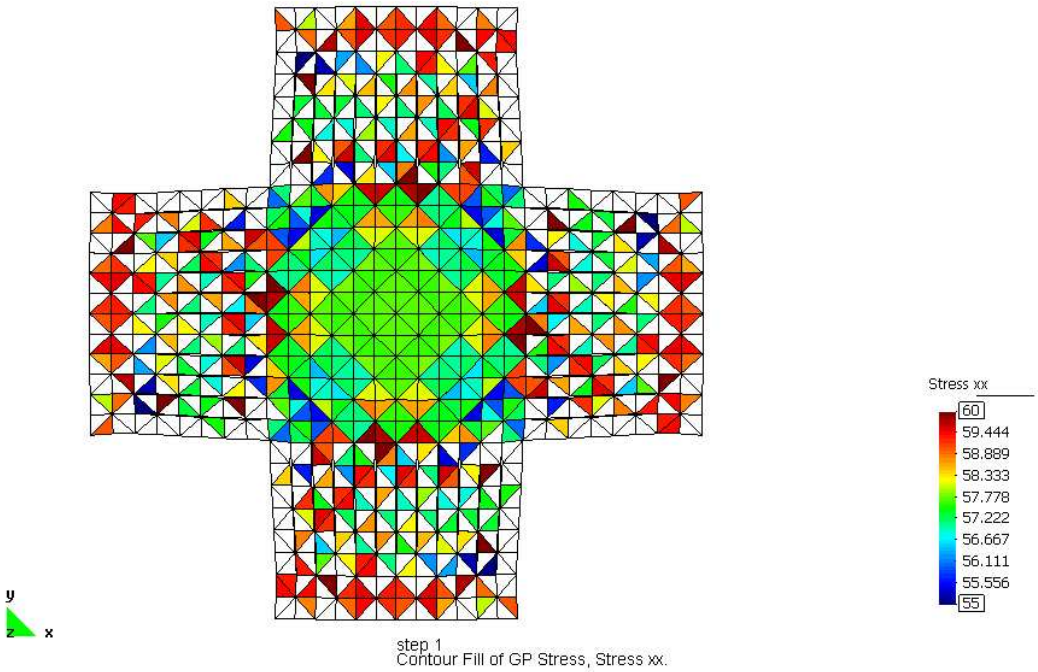

Figure 3.67: Central selected principal stress σ_x of biaxial cruciform with $F_x = F_y = 60kN/m$

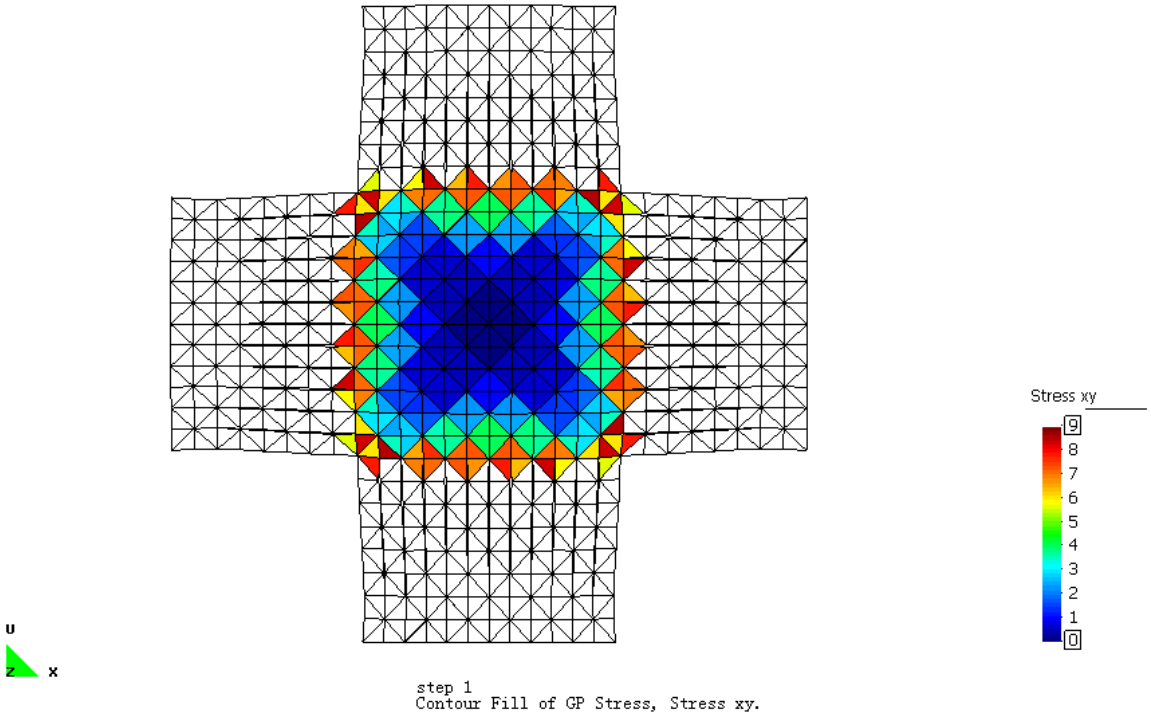

Figure 3.68: Central selected shear stress τ_{xy} of biaxial cruciform with $F_x = F_y = 60kN/m$

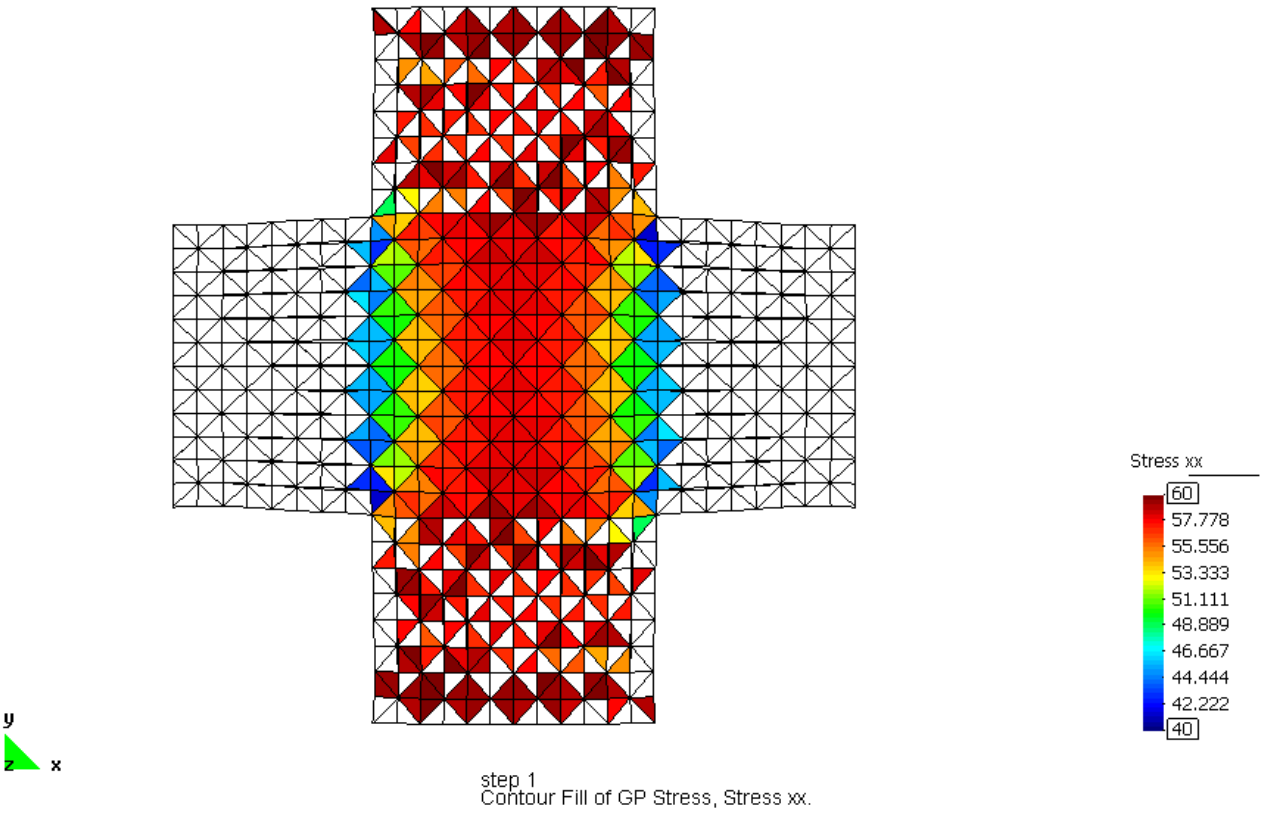

Figure 3.69: Central selected principal stress σ_x of biaxial cruciform with $F_x = 30kN/m$,$F_y = 60kN/m$

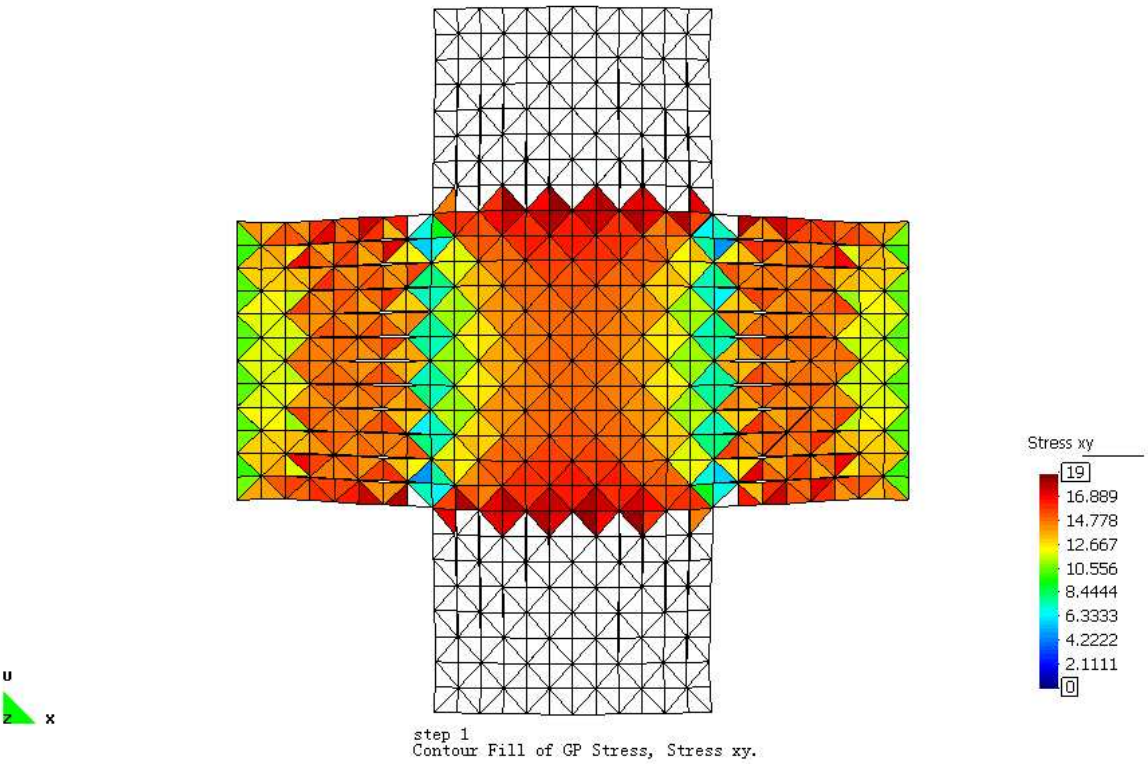

Figure 3.70: Central selected shear stress τ_{xy} of biaxial cruciform with $F_x = 30kN/m$,$F_y = 60kN/m$

2) CST Large Strain Finite Element Formulation

Figures 3.71-3.78 present the maximum principal results obtained from the CST formulation with large strains. From the large strain CST model, the maximum principal stress in the biax cruciform is approximately close to that predicted by the small strain formulation, but it is fully symmetrical, not only about x,y axis, but also about the diagonal line A-B. The solution also remains fully symmetrical for higher values of strain (e.g. when $F_x = 60kN/m$, fig.3.74-3.76).

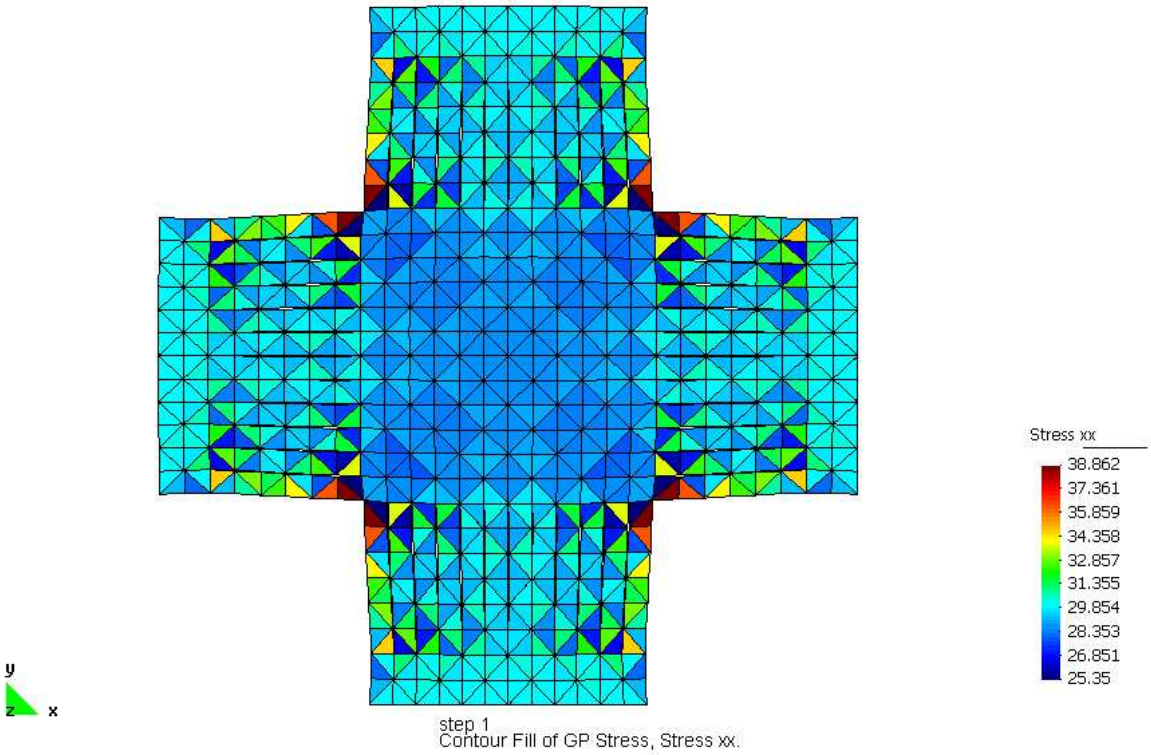

Figure 3.71: Max principal stress σ_x of biaxial cruciform with $F_x = F_y = 30kN/m$

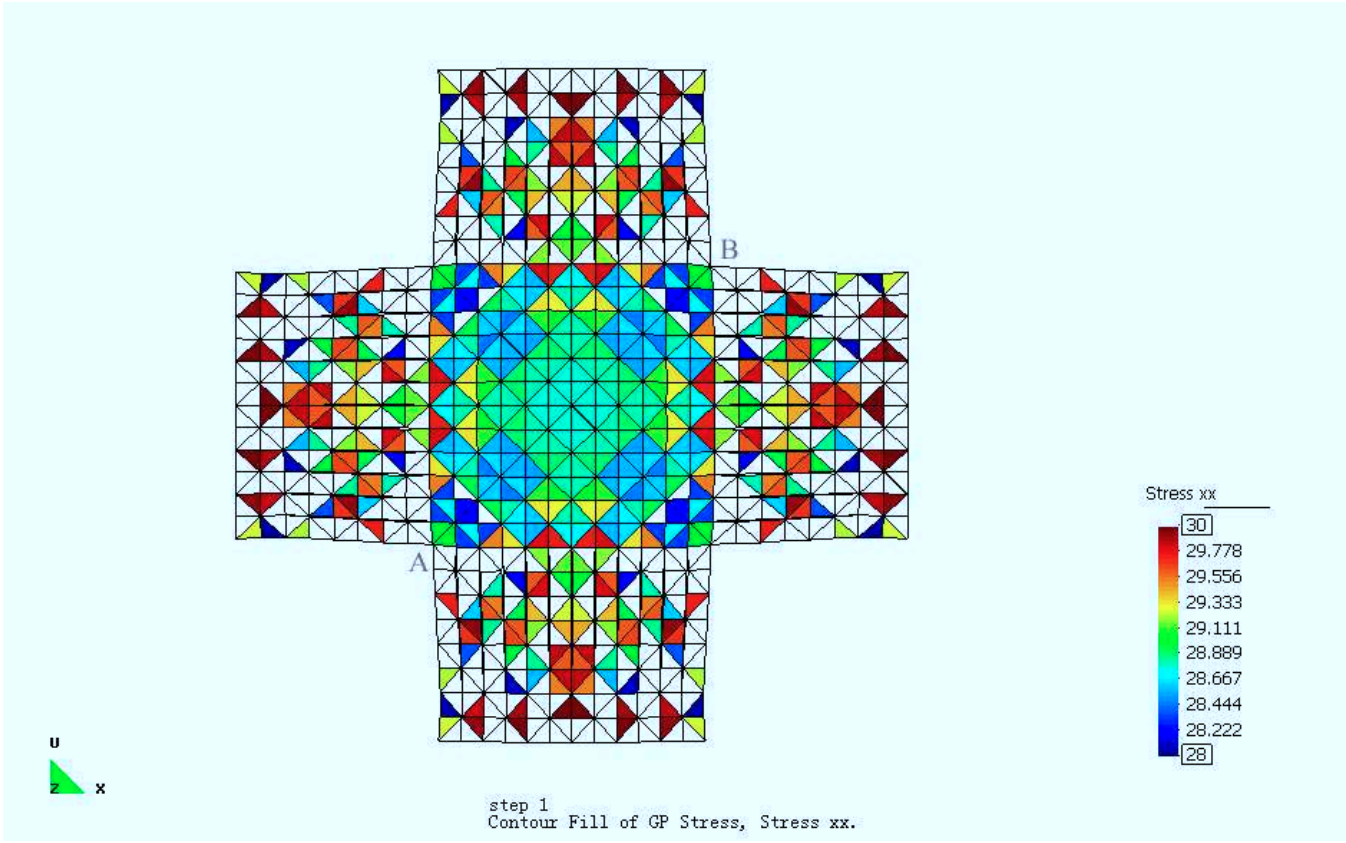

Figure 3.72: Central selected principal stress σ_x of biaxial cruciform with $F_x = F_y = 30kN/m$

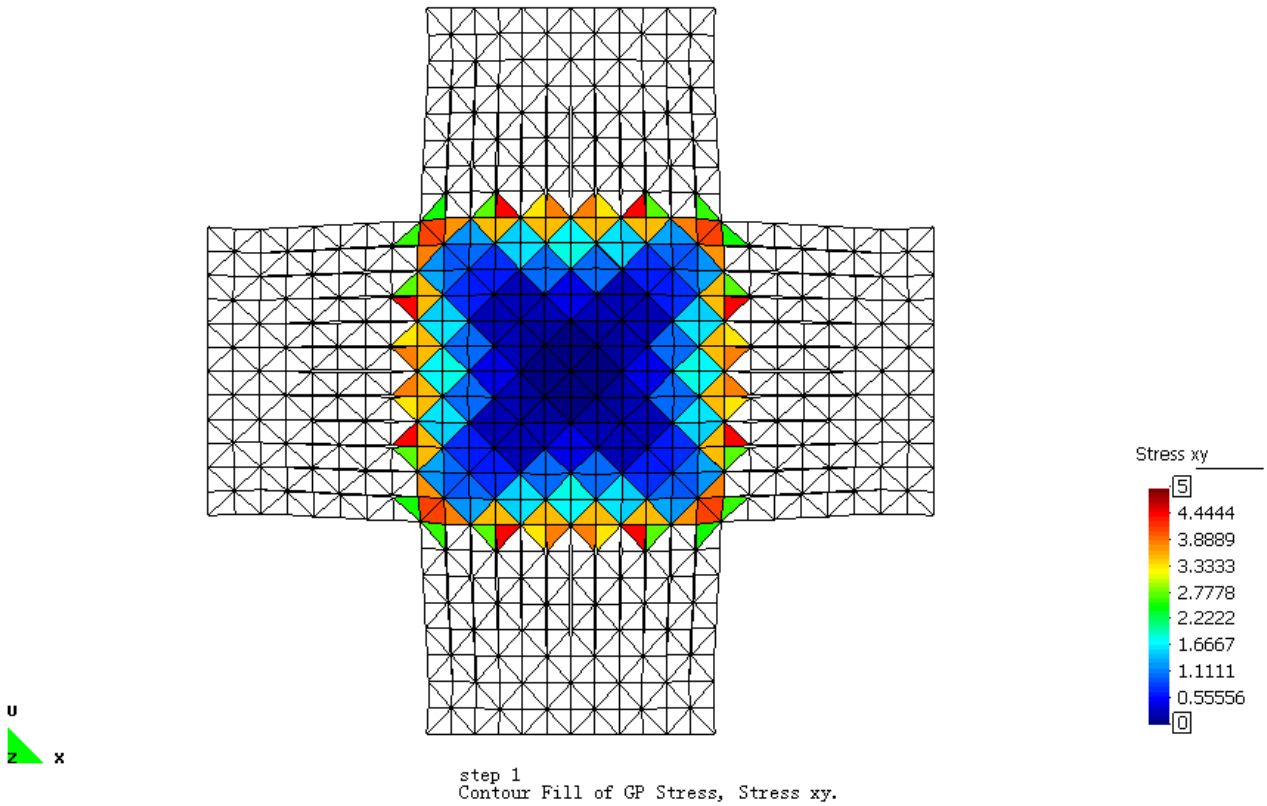

Figure 3.73: Central selected shear stress τ_{xy} of biaxial cruciform with $F_x = F_y = 30kN/m$

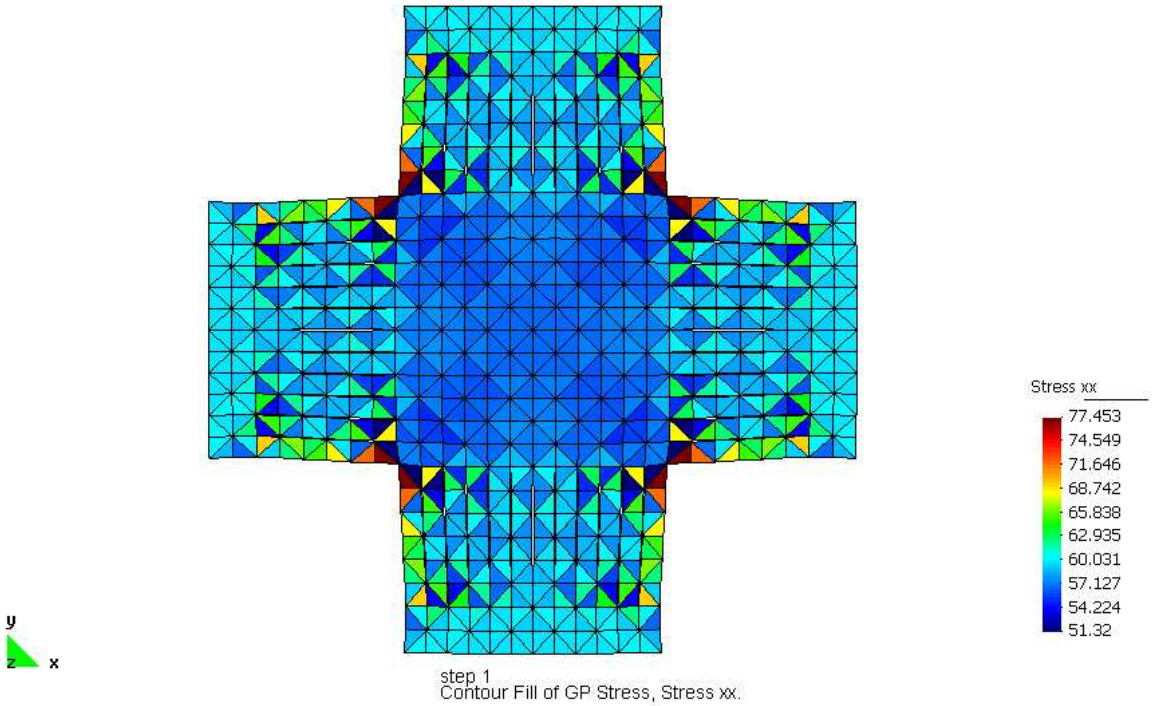

Figure 3.74: Max principal stress σ_x of biaxial cruciform with $F_x = F_y = 60kN/m$

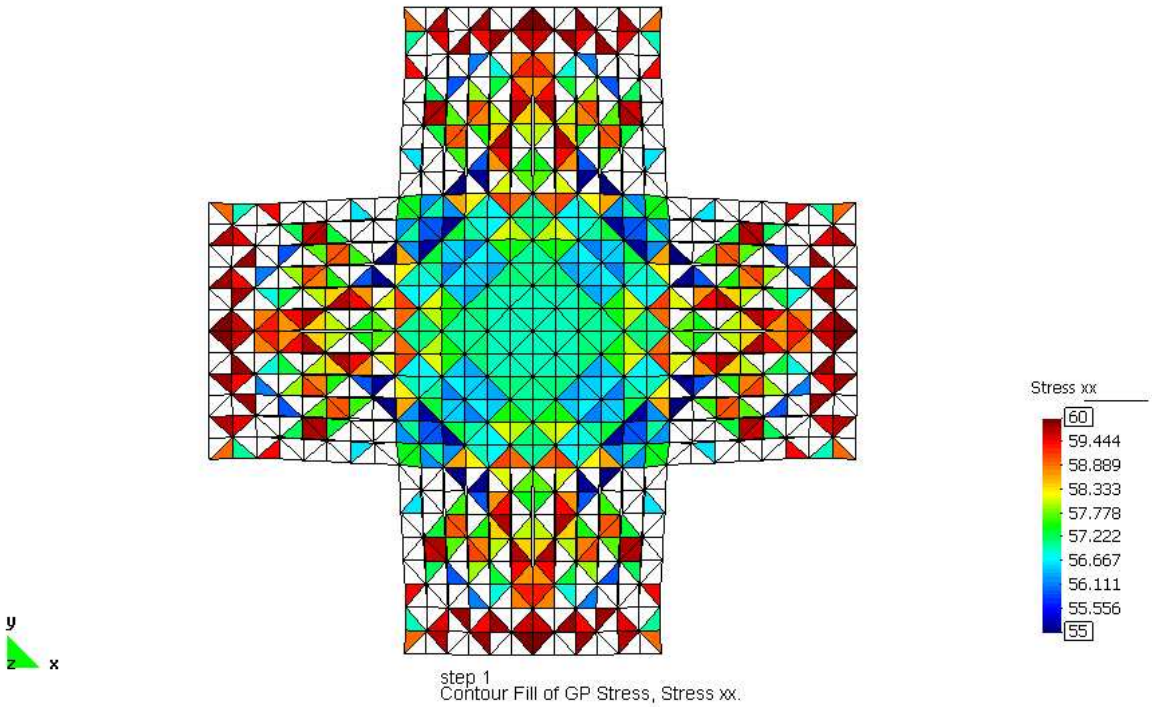

Figure 3.75: Central selected principal stress σ_x of biaxial Cruciform with $F_x = F_y = 60kN/m$

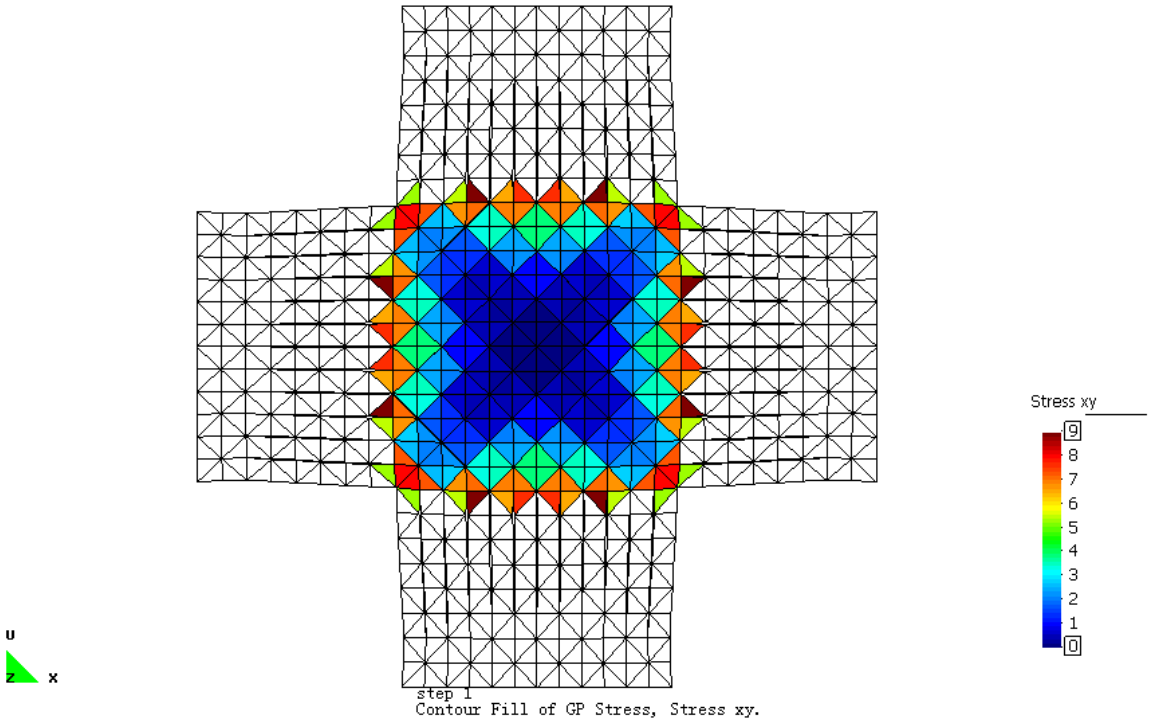

Figure 3.76: Central selected shear stress τ_{xy} of biaxial Cruciform with $F_x = F_y = 60kN/m$

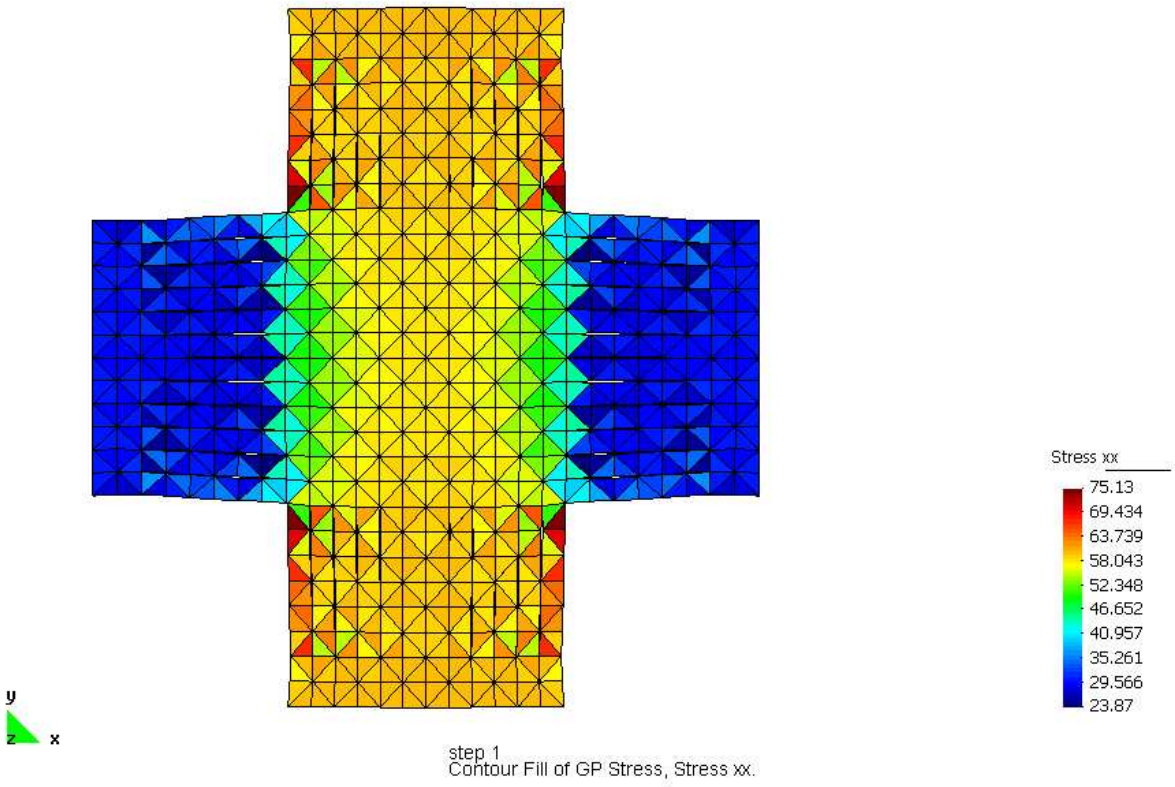

Figure 3.77: Max Principal Stress σ_x of biaxial cruciform with $F_x = 30kN/m$,$F_y = 60kN/m$

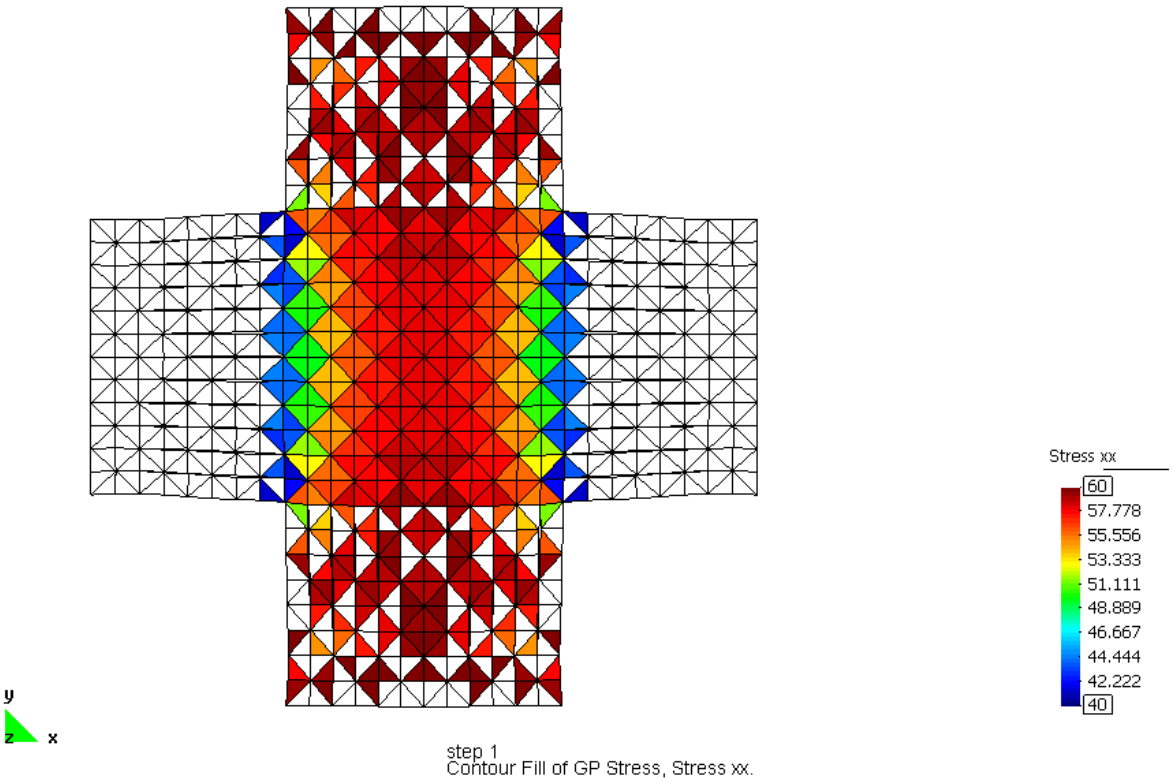

Figure 3.78: Central selected principal stress σ_x of biaxial Cruciform with $F_x = 30kN$,$F_y = 60kN/m$

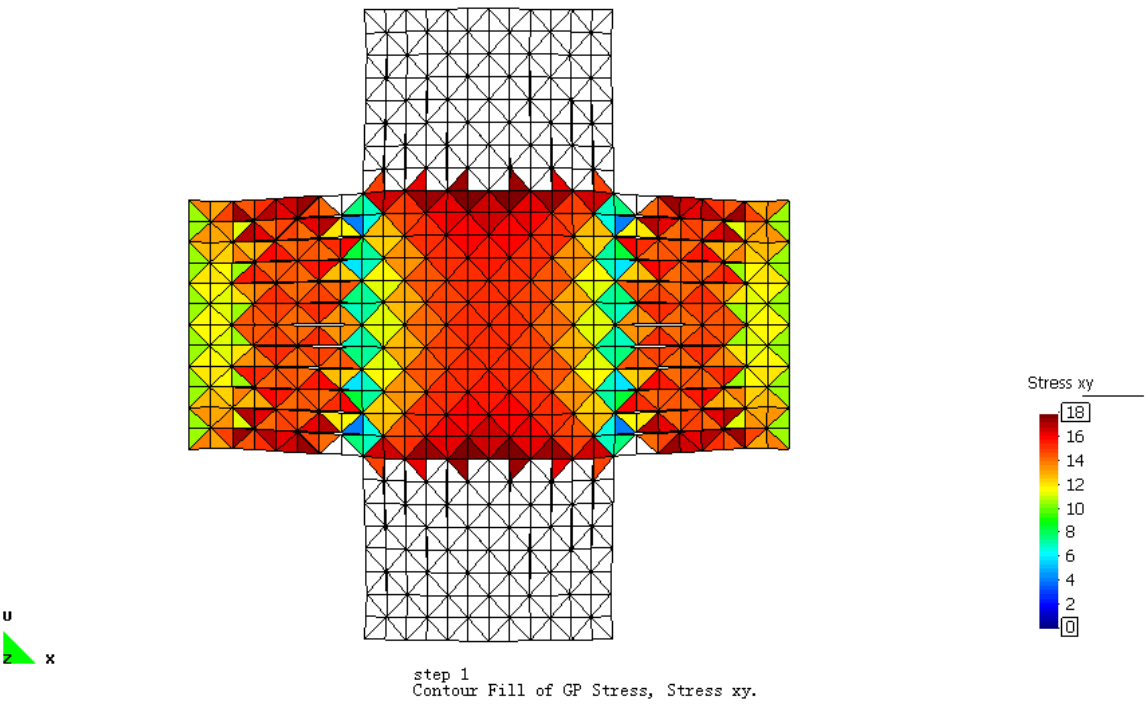

Figure 3.79: Central selected shear stress τ_{xy} of biaxial Cruciform with $F_x = 30kN$,$F_y = 60kN/m$

3) LST Finite Element Model

Modelling the same cruciform sample using the linear strain finite element formulation results in the expected symmetrical solution, but also produces considerably more detailed information. It is conceded that a larger number of D.O.F are used to obtain the additional information, but as demonstrated subsequently, the computational cost increase is relatively minor. The underlying characterstics of the CST solution can be identified, and these solutions are validated against an independent plane stress finite element approximation obtained from [238] and as compiled in figure 3.86. Since, along the centreline, the direct strain is small(about 5%) and the shear strain almost negligible, the results from all the models appear to be very similar (approximately 0.3% variance).

It is interesting to note, that in the corners of the cruciform (e.g at A and B for example) where there is both a geometric and strain discontinuity and significant shear strains, the same stress peak is exhibited by the simulation at the interior of the first element as identified in the shear patch test (e.g fig 3.54), denoted C)

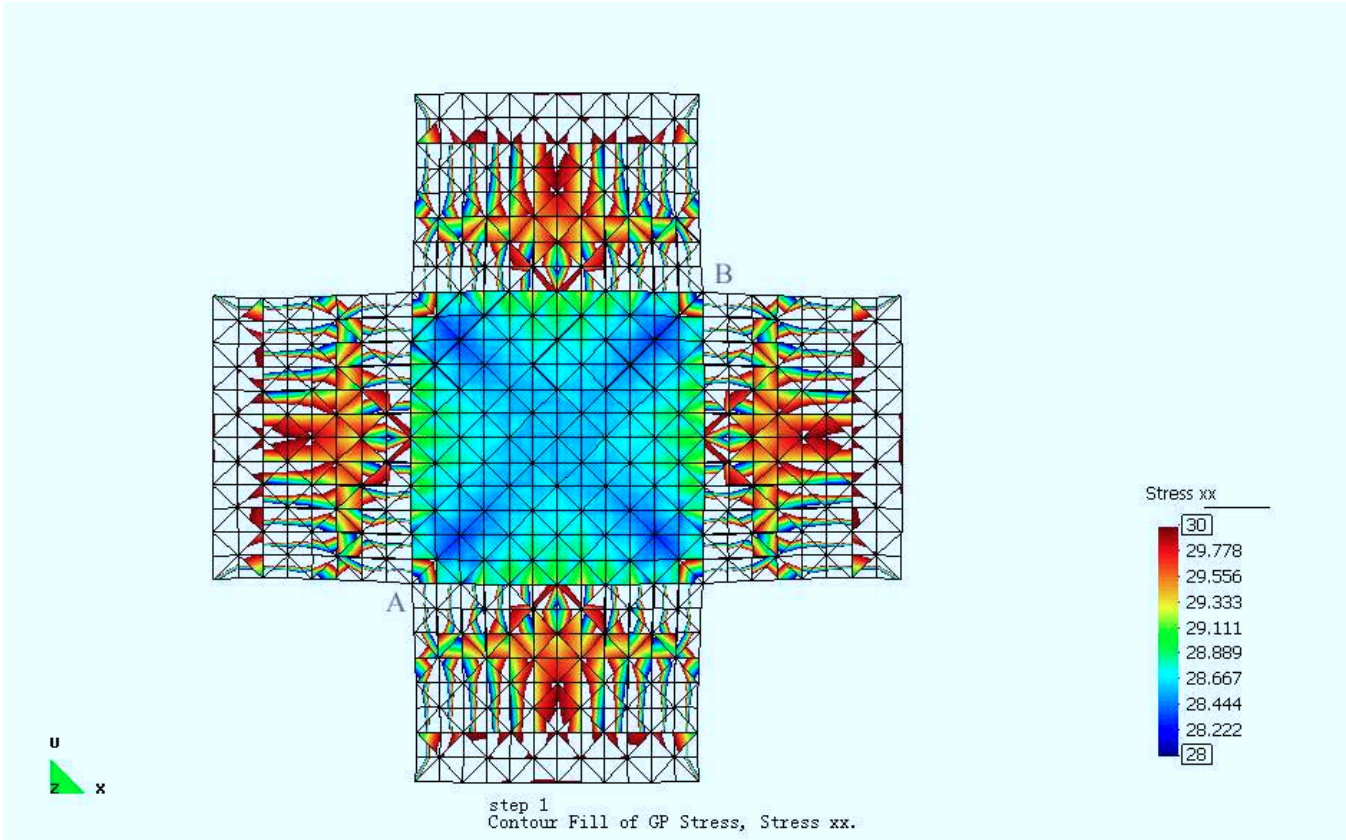

Figure 3.80: Central selected principal stress σ_x of biaxial cruciform with $F_x = F_y = 30kN/m$

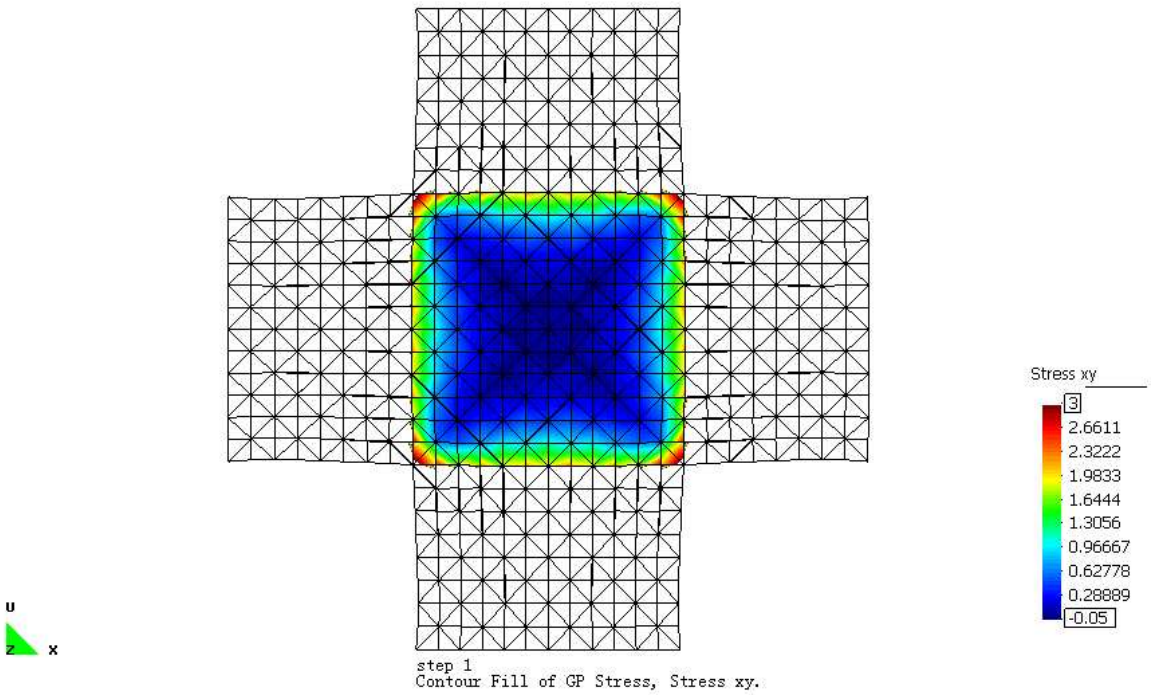

Figure 3.81: Central selected shear stress τ_{xy} of biaxial cruciform with $F_x = F_y = 30kN/m$

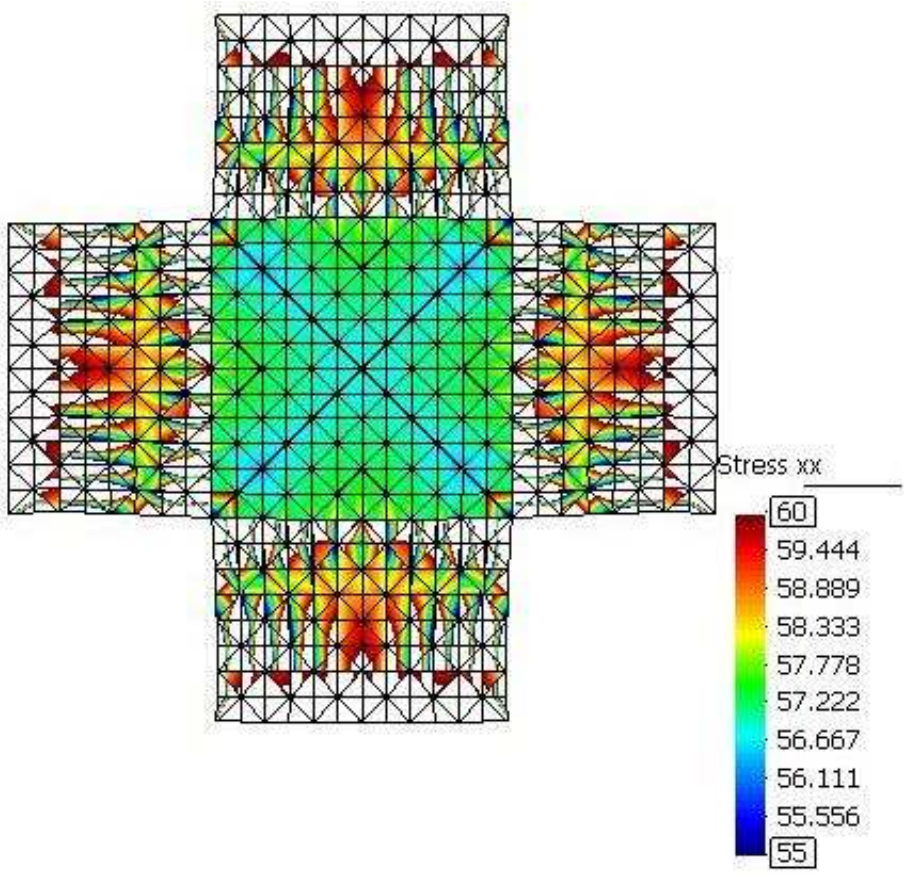

Figure 3.82: Central selected principal stress of biaxial cruciform with $F_x = F_y = 60kN/m$

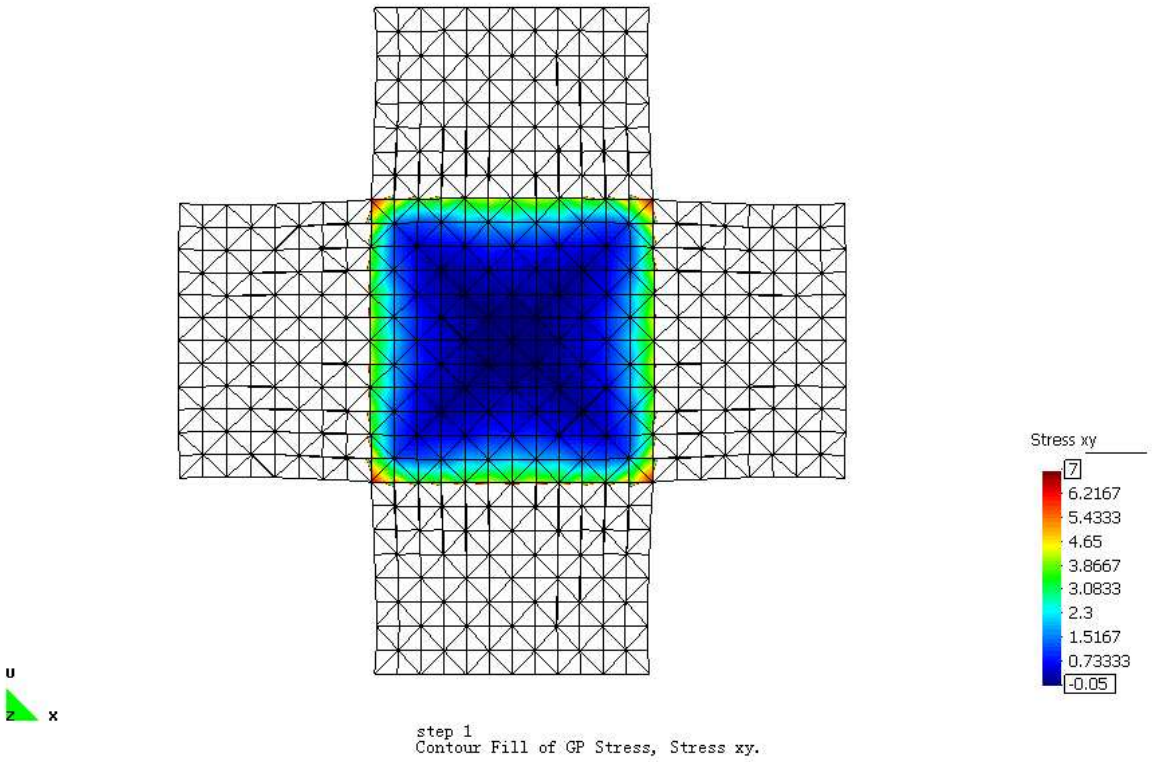

Figure 3.83: Central selected shear stress of biaxial cruciform with $F_x = F_y = 60kN/m$

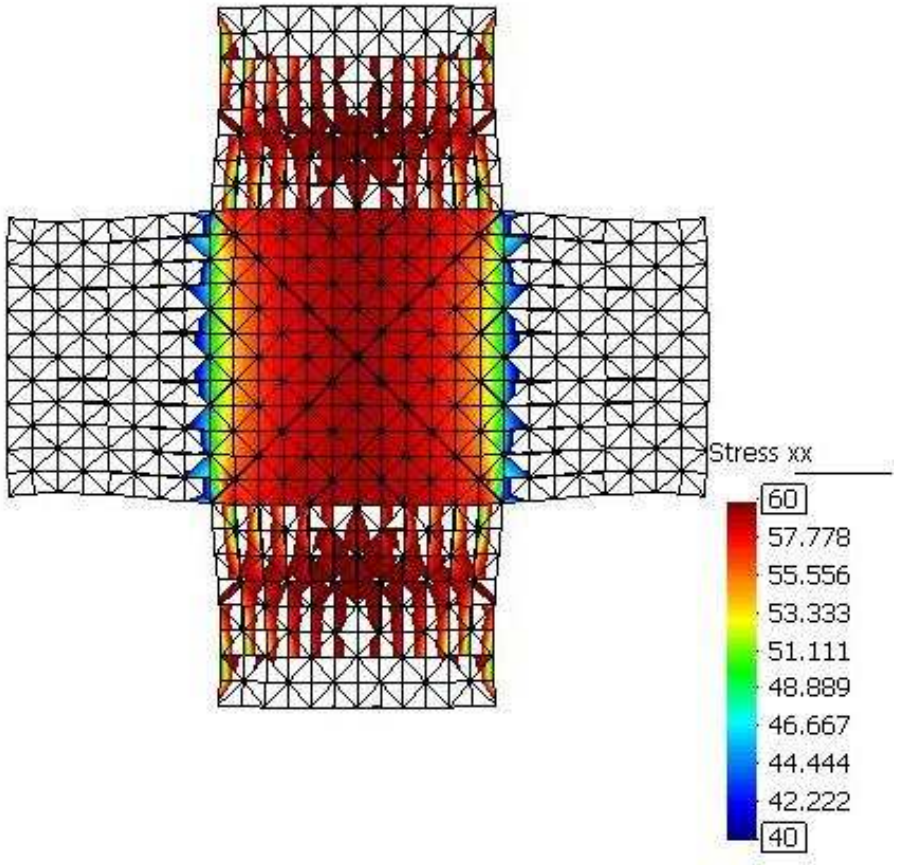

Figure 3.84: Central selected principal stress of biaxial cruciform with $F_x = 30kN/m$,$F_y = 60kN/m$

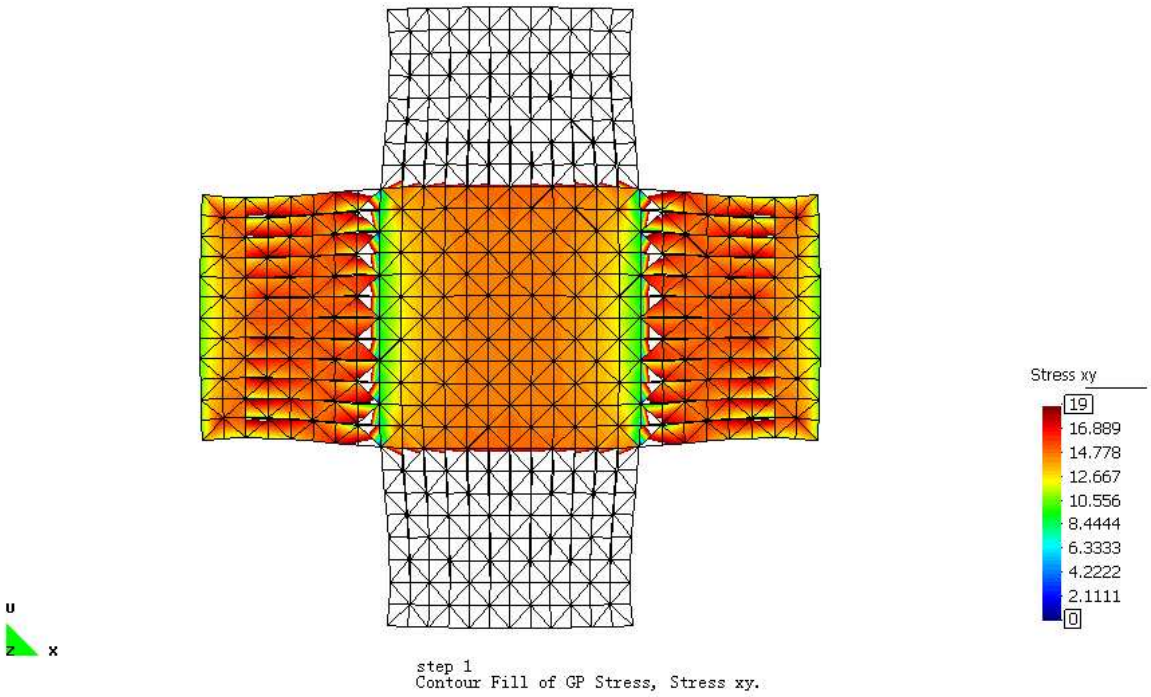

Figure 3.85: Central selected shear stress of biaxial cruciform with $F_x = 30kN/m$,$F_y = 60kN/m$

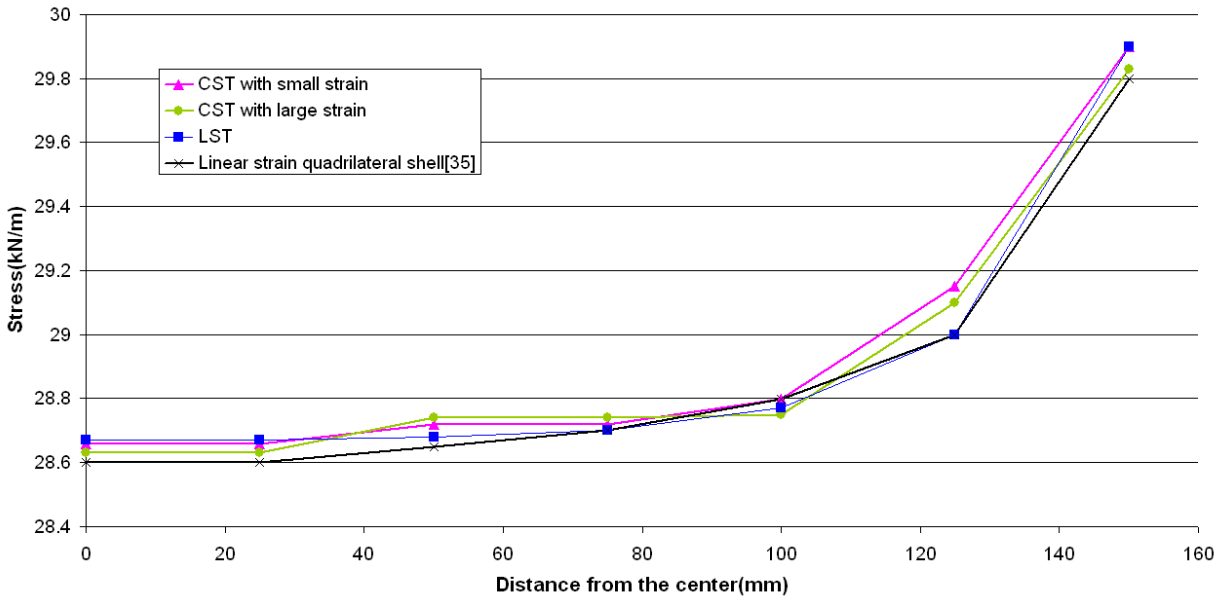

Figure 3.86: Stress along the centreline with $F_x = 30kN/m$,$F_y = 30kN/m$

3.5.5 Wrinkling procedure – shear test demonstration

To demonstrate the potential of the developed wrinkling criterion(stress-strain combined) and calculation algorithm, a reference shear test [229] is defined in fig. 3.87. The shear test is performed as follows: firstly the membrane is pre-stressed in the x-direction by a displacement of $u_x = 1mm$. This displacement is held fixed for the subsequent shear loading inducing up to $u_y = 10mm$. An isotropic ET-foil membrane material is assumed (ET-foil thickness $t = 200\mu$, Young's modulus is $E = 600N/mm^2$ and the Poisson's ration is $\mu = 0.45$).

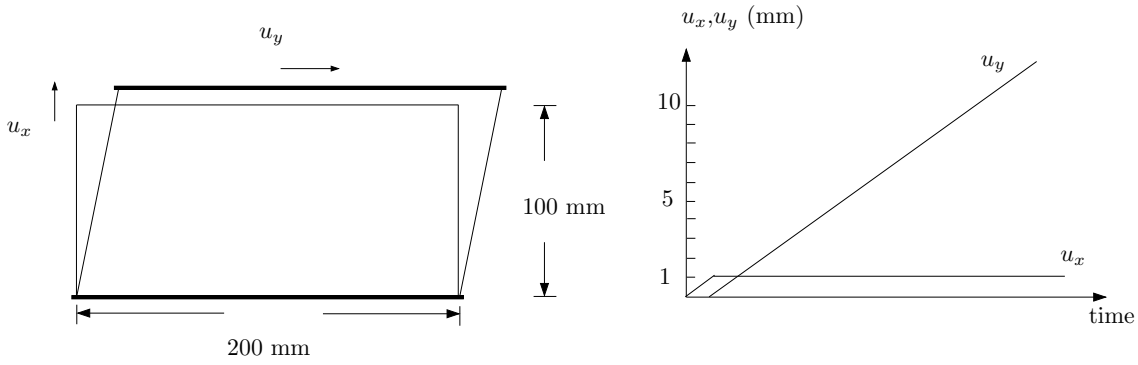

Figure 3.87: Geometry, boundary and loading conditions for the shear test calculation

The corresponding numerical results from reference [229] are shown in fig. 3.88, in which, u_x and u_y denote the orthogonal displacements in the membrane plane respectively, and u_z reflects the depth of the wrinkles in the membrane.

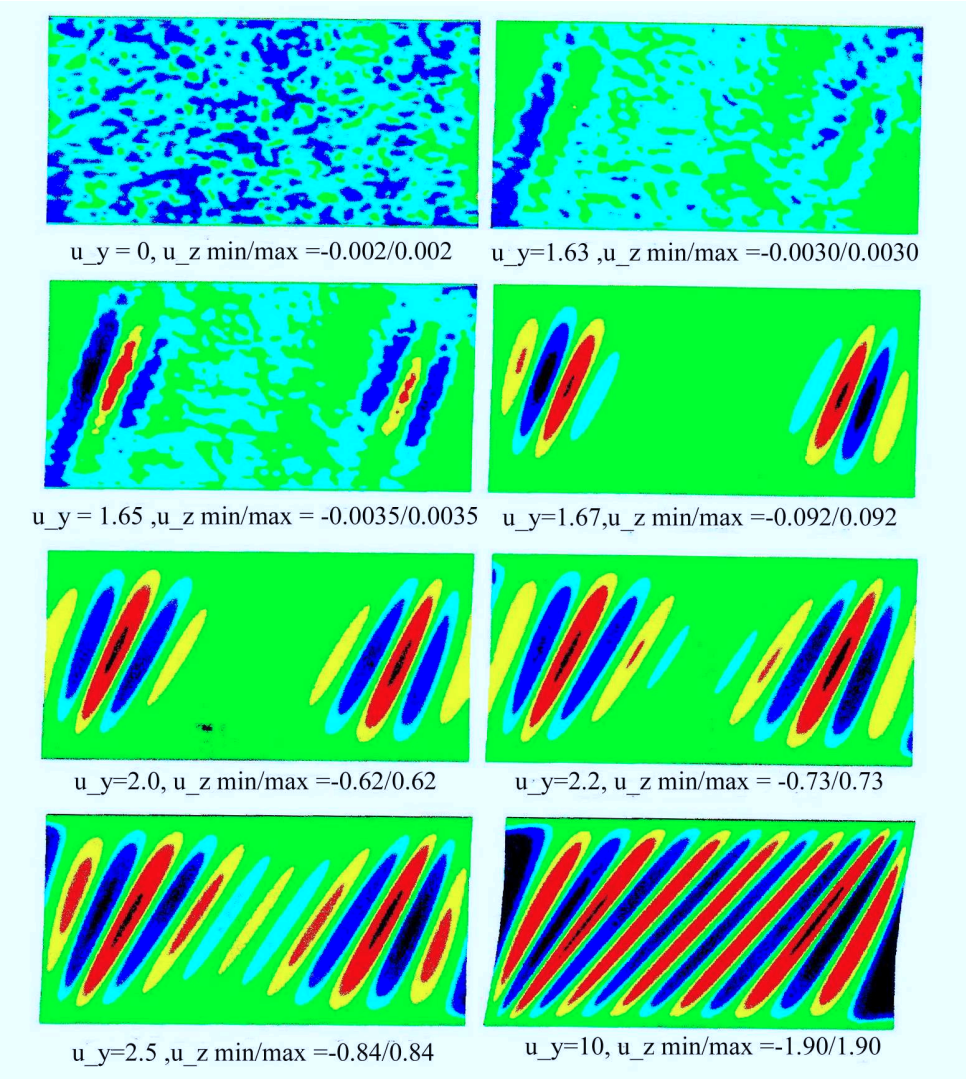

Figure 3.88: Displacement u_z [mm] normal to the membrane plane for the development of wrinkles for selected shear displacements u_y in reference test

As presented in fig. 3.88, the wrinkles start to arise at the two ends, then propagate to the middle of the patch. It is also observed that wrinkling develops before the lateral displacement u_y reaches 1.65 mm, with the wrinkle depths u_z less than 0.0035mm, subsequently from $u_y = 1.65mm$ the wrinkles start to develop dramatically, and the maximum wrinkle depth increases up to $0.62mm$ with a small increment ($\Delta u_y = 2.0 - 1.65 = 0.35mm$) in the lateral displacement. After $u_y = 2.0mm$, the wrinkles develop proportionally, and propagate to the majority of the foil when $u_y = 2.2mm$.

This numerical test is simulated using the large strain CST and LST finite element discretisations using either 16 LST elements or 64 CST elements as shown in fig. 3.89 and 3.90 respectively. The element meshes are coarse compared with the meshs used in the reference solution [229] (at least 10×20) which aimed at determining the details of the wrinkles (e.g depths) using hexahedral elements. It is notable that in the reliability analysis of fabric structures using membrane finite elements, wrinkling may be regarded as one type of the structural failure, with the main target to predict the existence of wrinkles accurately and immediately,

and not the wrinkle details. It is expected to be unnecessary to use a dense mesh to assess the LST and CST capabilities in predicting wrinkling based on the criterion and the algroithm described in section 3.4.

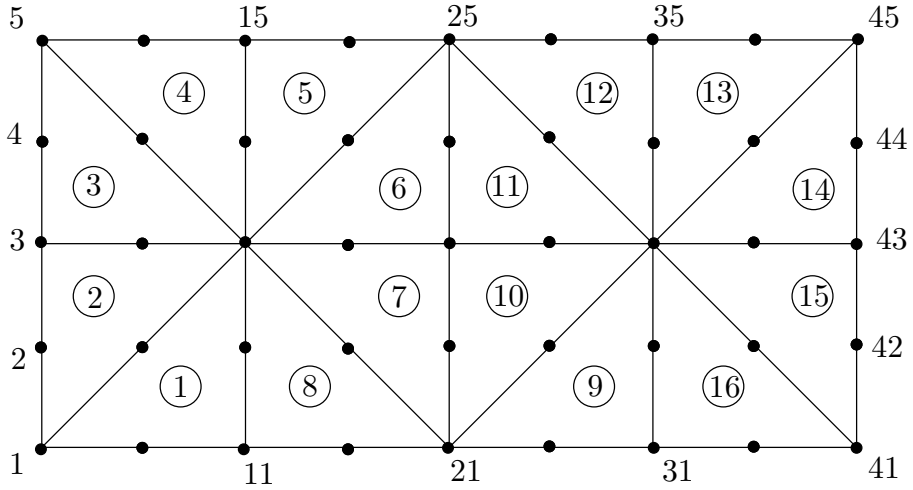

Figure 3.89: LST F.E Mesh for the wrinkle patch

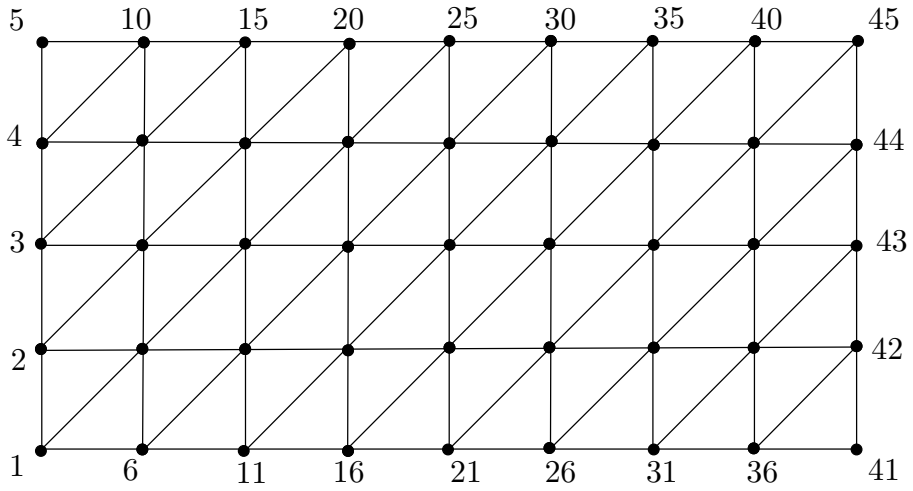

Figure 3.90: CST F.E Mesh for the wrinkle patch

The positions and their directions of wrinkles predicted using these two elements are presented in fig. 3.91 and 3.92 with the short lines to represent wrinkles. For LST elements, the existence of wrinkles and directions are assessed and calculated based on the principal stresses at the twelve element Gauss points, the positions of which have been described in section 3.2.3. Wrinkling information may, therefore, be provided at each Gauss point. In contrast, in the case of the CST, the principal stresses are constant across the element, meaning that the wrinkling point and direction are single valued for each element as shown in fig. 3.92.

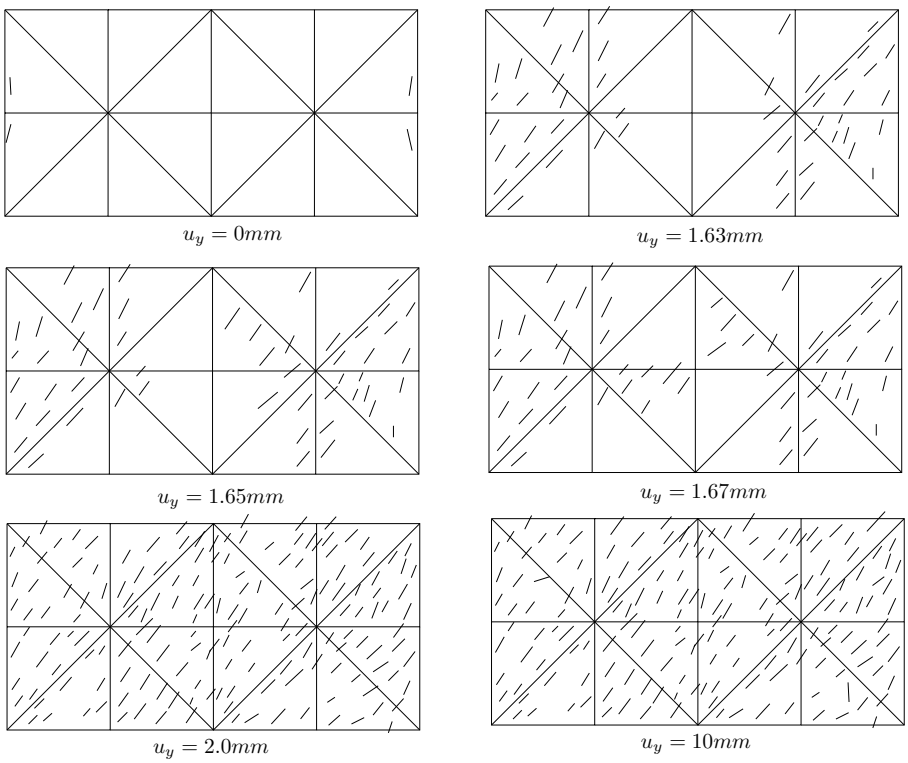

Figure 3.91: Detected wrinkle points and directions for selected shear displacement u_y - LST

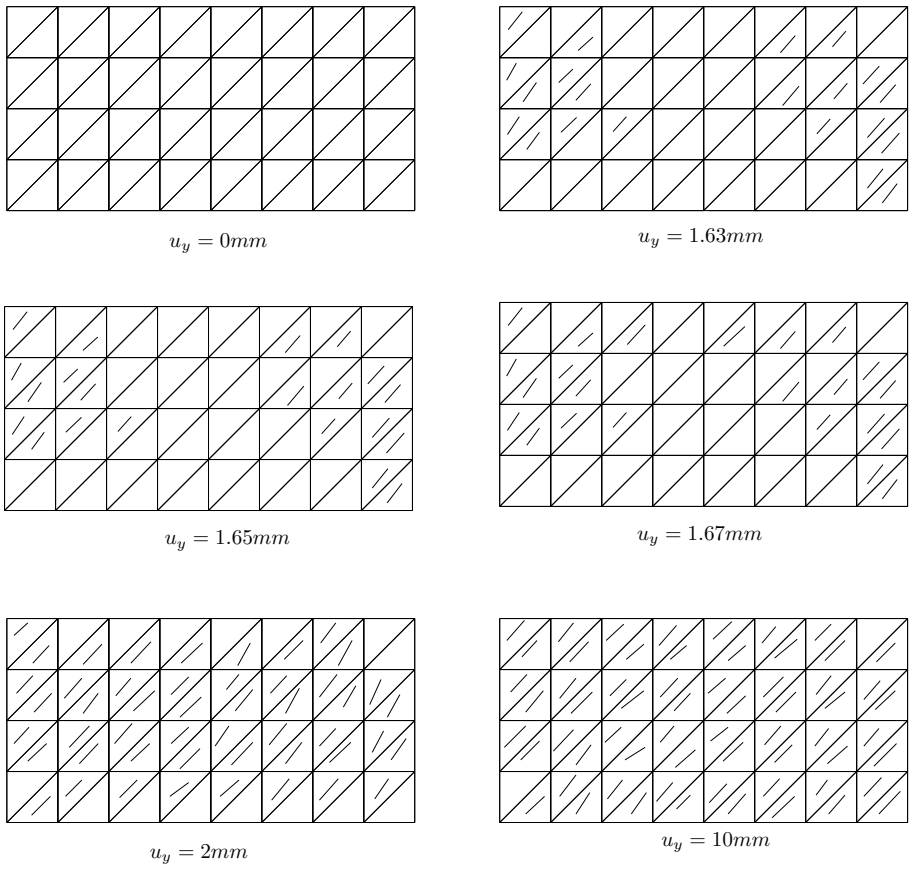

Figure 3.92: Detected wrinkle points and directions for selected shear displacement u_y - CST with mesh I

Given the invariance of stress within each of the CST elements, the dependency of the prediction of the wrinkling solution on the mesh description may be an issue. Therefore the test foil has been remeshed using the same number of D.O.F used in the mesh shown in fig. 3.90 (denote mesh I) to create the mesh depicted in fig. 3.93 (mesh II). The corresponding results are presented in fig. 3.94. Comparing the wrinkles predicted using CST mesh I and II, the general wrinkling distributions and directions are similar, but the wrinkling propagation during $u_y = 1.65 - 1.67mm$ is not predicted by the CST mesh II, suggesting a certain level of mesh dependency.

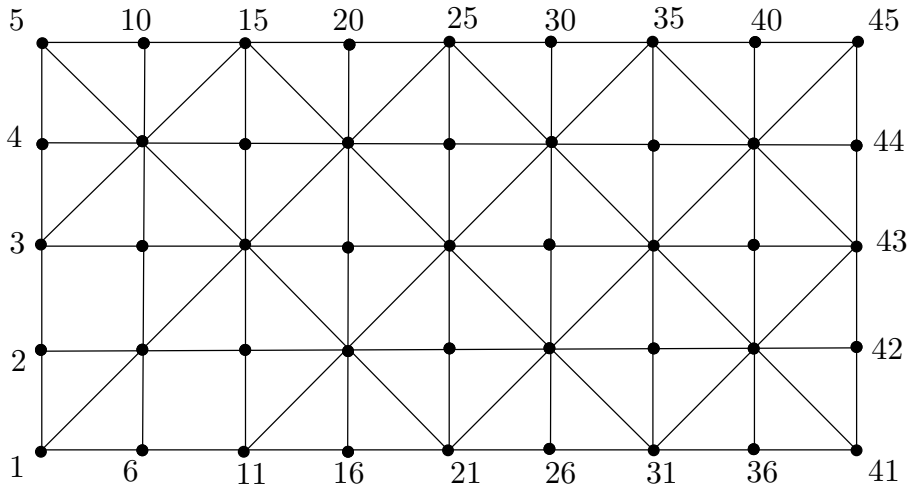

Figure 3.93: CST F.E Mesh for wrinkle patch

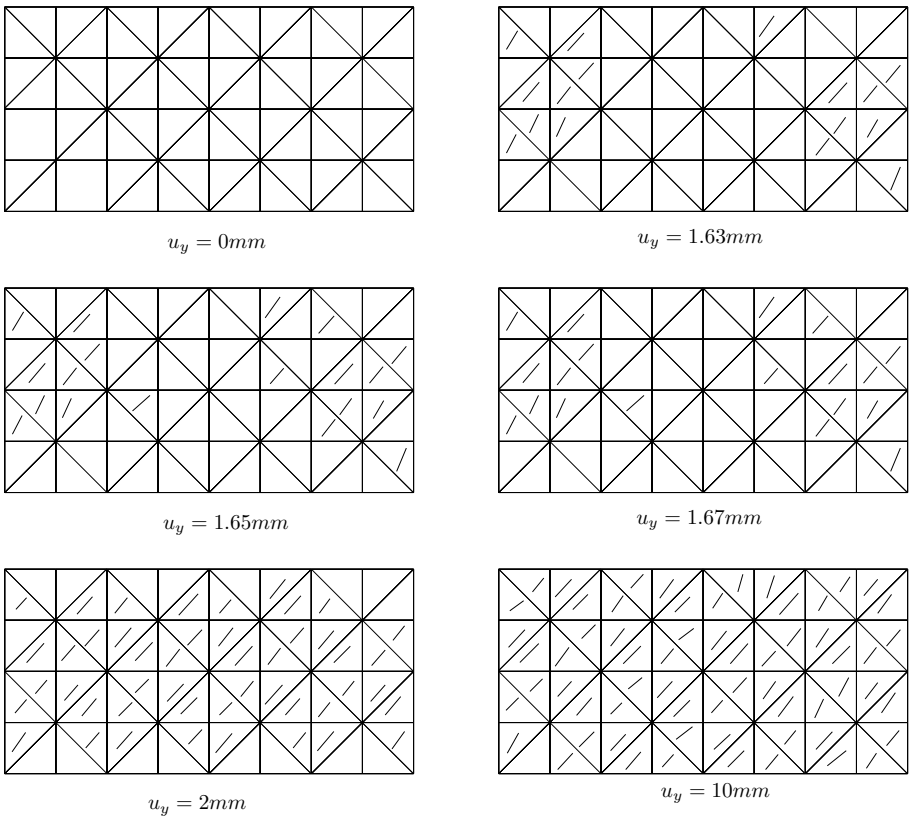

Figure 3.94: Detected Wrinkle points and directions for selected shear displacement u_y -CST with the mesh II

Comparisons of figs. 3.91, 3.92 and 3.94 with fig. 3.88, suggest that the existence of the wrinkling in the patch can be predicted by both LST and CST models accurately, even when they are not easy to observe in three-dimensional (hexahedral) simulation (fig. 3.88) with wrinkle depths in the range $u_z = 0.002 - 0.0035mm$. The general propagation trend of the wrinkles can be approximately predicted using the CST and LST models. For example, during the procedure $u_y = 1.65mm$ to $u_y = 2.00mm$, wrinkles develop rapidly and tend to propagate within most elements. However the detailed wrinkling distribution predicted by CST and LST discretisation are different to the reference result. As anticipated, using a membrane element it is not possible to predict the directions of a continuous or complete wrinkle.

With twelve Gauss points, more detailed wrinkle information can be produced within the LST element compared with the CST element, since in the CST elements there are only constant (average) element principal stresses. With a comparatively coarse mesh, wrinkling information may be misleading because the principal stresses are possibly underestimated. For example, CST element model failed to detect the wrinkling when $u_y = 0$ with the wrinkle depth $u_z = 0.002mm$. Furthermore, as described in section 3.4, the proposed wrinkling procedure permitted some "fictitious" compressive stresses in the analysis. Only when the minimum principal stresses exceed some limit (e.g one tenth of the maximum principal stress), the elasticity modulus of wrinkled membrane will be modified, while the principal stresses calculated using CST element are often smaller than those predicted by the LST under the same

deformation. In this case the material properties may be modified based on the LST results but may be unchanged according to the CST results. For example, during the deformation $u_y = 0$ to $u_y = 1.67mm$, using CST, the material properties have not been modified because the produced minimum principal stresses are not sufficiently large, though wrinkling is indicated.

3.5.6 Computing Cost Comparison

The computing costs of LST element using Dynamic Relaxation(DR) and Newton-Raphson(NR) are initially compared as Table.3.4. Compared with NR solution algorithm, Dynamic Relaxation can achieve much better efficiency. Especially in the Hypar case, the advantage of Dynamic Relaxation seems more obvious when more D.O.F are involved in the analysis. As demonstrated in section.3.3, the Dynamic Relaxation algorithm can avoid large matrix operations and was found to be very efficient for geometrically nonlinear structures. Therefore for the hypar case - a typical geometrically nonlinear surface, the increased cost using Dynamic Relaxation for more D.O.F is much less than using the Newton-Raphson method.

Case		Hypar		Cruciform
D.O.F	81	145	289	2709
Dynamic Relaxation	4 mins	10 mins	23 mins	990 mins
Newton-Raphson	15mins	49 mins	197 mins	1200 mins

Table 3.4: Computing costs of LST elements using Dynamic Relaxation and Newton-Raphson Algorithms

Figure 3.96 and 3.97 illustrate comparisons of the computing costs of the CST and LST formulations to the hypar model(e.g fig. 3.28-3.33) comprising the first three data points, and the cruciform simulation (e.g fig.3.64) as the isolated data points. The most striking impact of these results is that the computational cost of the LST using DR is at least competitive with the CST. For example, the data points D,D1 and D2 in fig.3.96 and 3.97 respectively show that the LST using DR is considerably, more efficient than the CST. Also, for a much more detailed solution to the cruciform simulation, the additional cost of using the LST using DR with the same number of elements as the CST mesh (but considerably more, e.g. $\times 5$ D.O.F) is around 10%. As the computing time using the Dynamic Relaxation algorithm scales linearly with the number of D.O.F (as a result of its uncoupled/vector solution procedure), it appears how these limited data points that the increase in computational cost associated with increased the number of D.O.F in using the LST using DR is offset by the more efficient calculation of the stress and load vector terms in comparison with the CST. This hypothesis is supported by the reversal of the LST using DR being cheaper to analyze the hypar (data point D1 and D2) when compared with using the same number of each element type to analyze the cruciform example.

Furthermore, it has been established that the solution using the LST using DR takes far fewer iterations to achieve convergence at equilibrium than the CST for the same level of accuracy.

Nevertheless, these initial findings are encouraging in terms of the compromise normally associated with the order of the formulation and its corresponding computational cost.

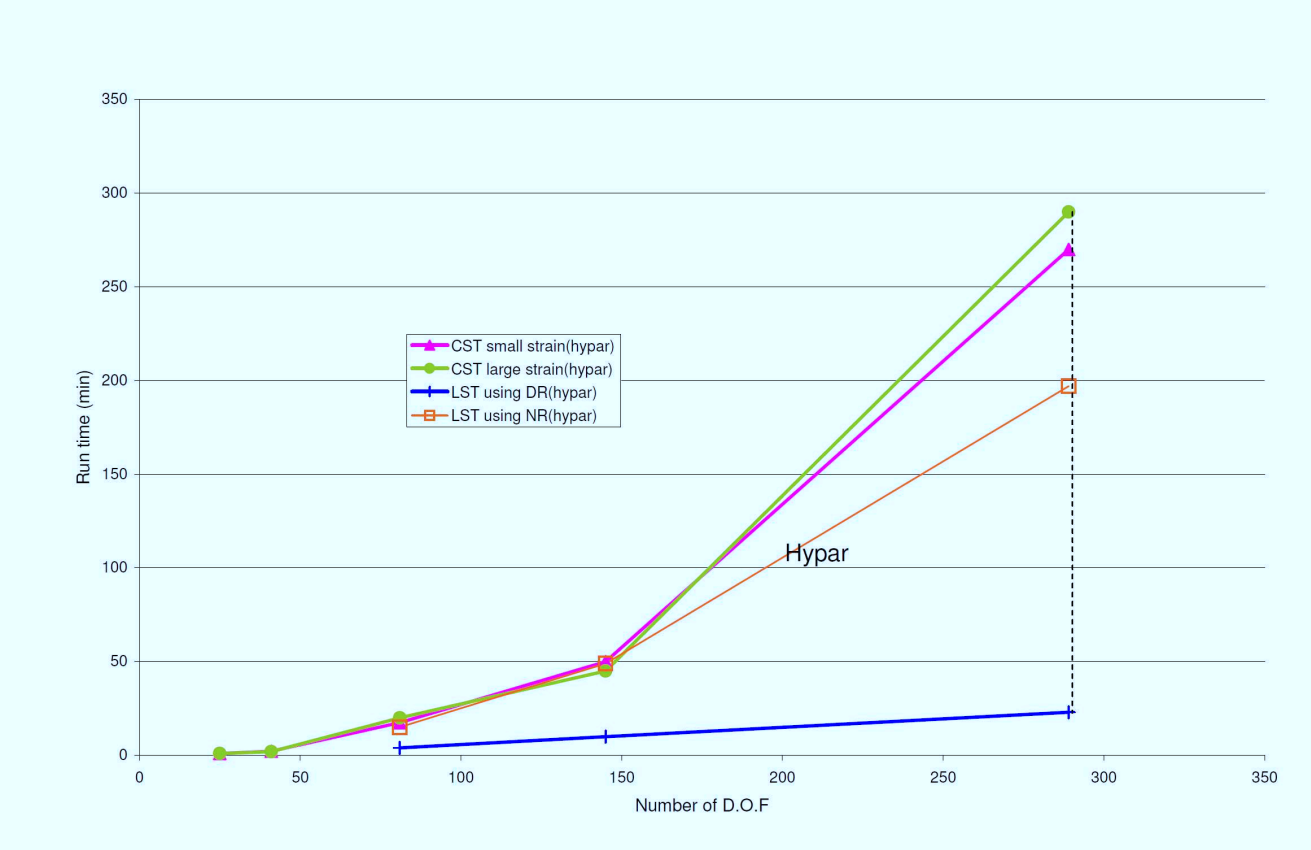

Figure 3.95: Comparison of computing cost between CST and LST formulations with D.O.F – Hypar

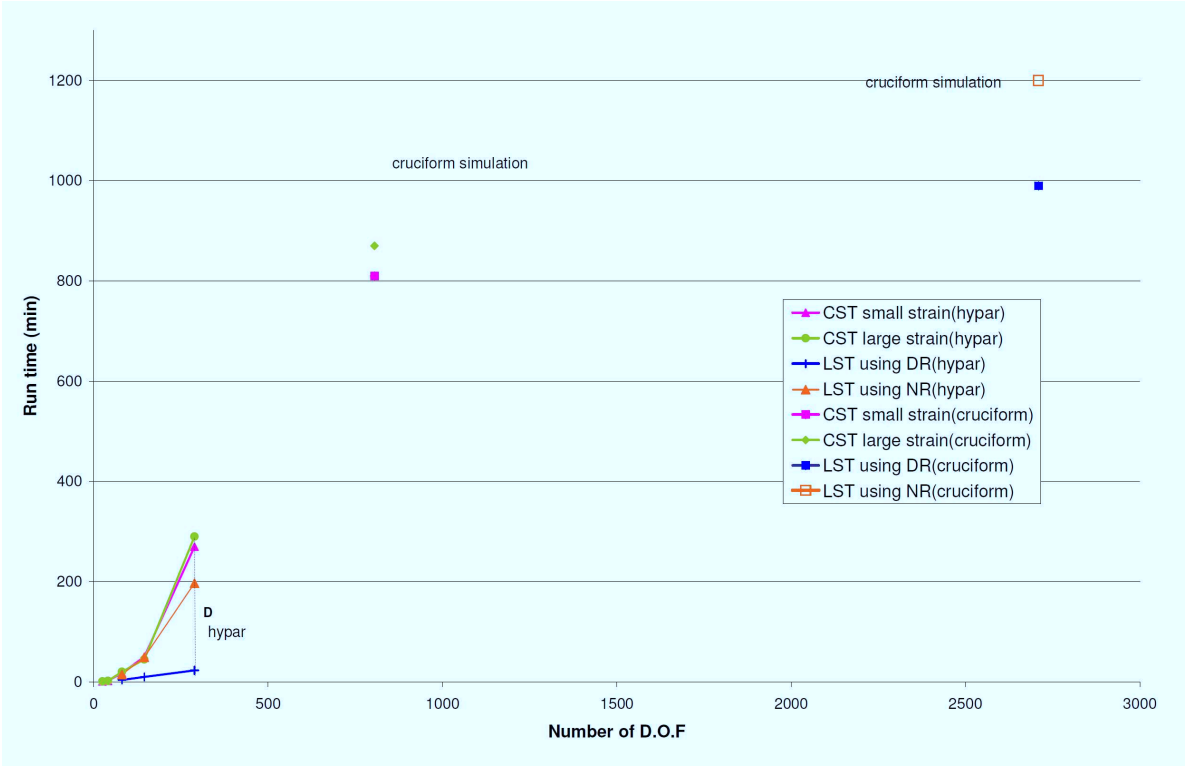

Figure 3.96: Comparison of computing cost between CST and LST formulations with D.O.F – Hypar and Cruciform test

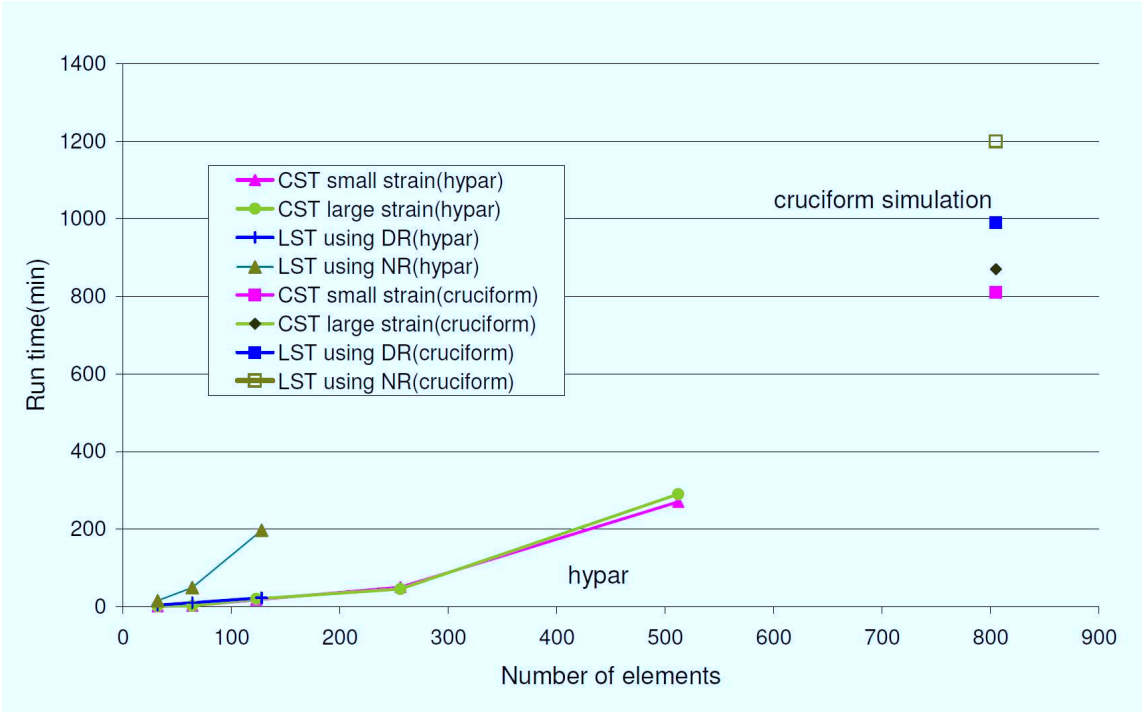

Figure 3.97: Comparison of computing cost between CST and LST formulations with element number – Hypar and Cruciform test

3.6 Conclusions

- The existing (original) CST formulation using the cable-analogy has been examined. The basis of the formulation is shown to assume small strains (e.g $\varepsilon_X = \frac{\partial U}{\partial X}$, $\varepsilon_Y = \frac{\partial V}{\partial Y}$ and $sin(\gamma_{XY}) = \gamma_{XY}$). Furthermore, to ensure a linear strain-displacement (D.O.F) relationship, a second simplifying assumption is made to limit the inclusion of only first-order strain components(Eqn. 3.8). The adoption of the cable-analogy leads to a compact formulation in which the element continuum strains are written as a function of the element side extensions. As such, the continuum is effectively replaced by a triangulated truss. However, when applying standard quality checks often used in finite element technologies, the formulation is shown to be deficient. For example, it does not pass a basic uniaxial patch test. Under moderate strains (5%-10% strains in the biax cruciform example), the deficiency of the existing CST formulation is implied by the development of non-symmetric stresses in the analysis of a symmetric problem.

- A revised formulation – meso-strain CST has been derived by adding high order terms to the small strain CST from Eqn 3.4 - 3.7. Whilst maintaining the small strain assumption ($\varepsilon_X = \frac{\partial U}{\partial X}$ etc.), the modifications to the element aim to explore the significance of second assumption referred to above. It should be noted that the small strain assumption appears only once (at the beginning) in the formulation. The adoption of the element side lengths as D.O.F help to introduce higher-order effects that are otherwise missing. The so-called meso-strain CST formulation shows some improvements over the original form of the element. However, it fails to pass the same patch test and produces significant errors at large strains, again manifested as unexpected asymmetry.

- From the perspective of computational compactness and ease of implementation of a new element into an existing code, it was considered to be expedient to try and maintain the element side-lengths as D.O.F. when endeavoring to formulate a CST that complied with finite element technonolgy standards. Based on Green's strains and classical finite element philosophies, a large strain CST formulation has been successfully derived that fulfils these criteria. Furthermore, it successfully passes the patch test and achieves other expected results. This completely new formulation, therefore, demonstrates the significance of assuming small strains in the existing CST element whilst also showing that it is possible to maintain the same "computational architecture" in the form of side-length D.O.F. However, being a CST, the strains and stresses across every element are constant (average) values. As the membrane stresses are often found to change rapidly, especially in boundary areas, detailed information of the membrane stresses is often difficult and computational expensive to obtain using a CST. Furthermore, in an analysis involving wrinkling, the CST formulation may be misleading in judging the wrinkling areas, with the peak element principal stresses often underestimated.

- To overcome the clear limitations of the CST, a six node LST formulation has been

developed using finite element principles. This is also based on Green's strains, but also makes use of inferred element curvatures. No additional rotational D.O.F are included, so the element remains C_0 continuous. This element formulation is shown to pass the patch and other tests of element quality. The advantage of having the capability of strains and stresses that can vary linearly across the element has been clearly demonstrated by a number of solutions compared with the equivalent CST results. This type of element may exhibit particular forms of element distortion that have the potential compromise numerical stability and solution accuracy, with specific reference to the form-finding analysis. A number of element distortion coefficients have been identified in the literature. However, all of these have some or a considerable computational overhead. They are also difficult to interpret in combination. A better measure has been shown to be the criterion that the Jacobian at each of the element Gauss Points remains positive definite. The possibility of "floating" mid-side nodes (e.g. a type of nodal rigid-body motion) has also been examined and deemed to be unlikely to happen in an analysis.

- From a normal finite element technology viewpoint associated with Newton-Raphson as the solver it would be expected that the LST would be considerably more computationally expensive than the CST. However, when coupled with Dynamic Relaxation algorithm, the LST element has been shown to be extremely competitive, producing much higher quality solutions for very little additional computational effort. It has been concluded for the relatively small number of examples examined, that a mesh of LSTs is very well-suited to the the Dynamic Relaxation algorithm and that characteristics of the formulation coupled with this algorithm do not lead to the computational scaling normally seen when moving from a basic to a higher-order element.

Chapter 4

Probabilistic Properties of Structural Fabric

4.1 Introduction

The materials used for fabric structures generally consist of coated woven fabric, cables and belts, supporting steel and connections. From the viewpoint of statistics, the mechanical properties of all these materials can be regarded as random variables with uncertainties. Theoretically, an accurate structural reliability analysis requires the full uncertainty information in all the corresponding materials. That would require a probabilistic investigation to be undertaken for all these materials for a complete reliability analysis. However, that is beyond the scope of this thesis. In this chapter, the probabilistic investigation focuses on coated woven fabrics used for structural membranes, with the purpose of developing a practical and efficient probabilistic testing and analysis methodology for series of fabric materials.

Coated woven fabric is the main component in a fabric structure. As a composite of inelastic materials(i.e. yarns and coating), it has obviously nonlinear mechanical behaviour which may complicate a probability analysis. The fabric is often assumed to be an orthotropic materials in which yarns are straight along the primary axis, and the fill and warp are normal to each other. However due to the coating process this assumption may not be valid, and an anisotropic composite structure may exist as the fabric material. Therefore the coated woven fabric cannot be simply regarded as a combination of yarn assemblies and coated material. The yarn distribution may become a very important factor affecting the mechanical properties of the fabric, and a key randomness existing in the coated woven fabric.

When the yarns and coating materials are individually manufactured, they may have highly uniform material properties with small randomness. However when they are formed into a composite as a fabric, the randomness of the fabric properties over the material space appears more obvious owing to the manufacturing process. Because of the nonlinearity of the fabric, its elastic properties are not constants under different stress states. The calculation of Young's modulus is normally derived using a regression model. However the model itself

can also appear as an important source of uncertainty. In the analysis and design of fabric structures, the variability in the fabric material is normally accounted for in the application of an additional component to the factor of safety. For example, it is common practice to apply a factor of 1.5 to the tear propagation factor of 4 to produce an overall factor of 6 [3].

Different test methods including specimen cutting and loading procedures, may lead to different test results, from which, a non-unique, probabilistic analysis result for the same type of material may be produced. Since the test method itself is a source of uncertainty, it may appear to increase the randomness of the test samples as one of epistemic uncertainty types.

The probabilistic investigation of the fabric properties is only effective when a large quantity of statistical tests are made. Owing to resource limitation, the randomness of the fabric strength and stress-strain relations are seldom accurately investigated, and the most efforts([122]-[144]) are taken in creating mathematical models to predict the mechanic behavior of the fabric which is often based on a limited test data. Even though the quantity of test samples is always limited by the available time and resources, a larger test number is always preferred to increase statistical confidence.

To acquire more accurate statistical information of the fabric materials, more than 300 samples prepared using two different cutting procedures have been tested. Prior to making the detailed statistical investigation strategy, a small number of material tests have been performed to explore the basic characteristics of the fabric material(e.g yarn distribution, stress-strain curves). Subsequently a suitable mathematical model may then be created and a probabilistic methodologies specific for the given fabric samples is proposed to reduce the systematic uncertainty from the development of the probabilistic model.

The probabilistic analysis starts with a basic statistical investigation of the test data, which can give an approximate range of randomness for different statistical variables. The detailed probabilistic analysis (i.e statistical distributions) is undertaken based on candidate distributions and a non-interval data-fitting test (Kolmogorov-Smirnov test). The selection of the data-fitting distribution is taken to be a function of the maximum difference between the CDFs of candidate distributions and sample data, and the general fitness of the distributions.

In this chapter, the principal methodology of the probabilistic investigation of the fabric material follows a step-by-step procedure. The initial deterministic material tests are described in section 4.3. Subsequently the mathematical representation of the test data and statistical methodology for a large number of tests are determined as described in section.4.4. The probabilistic results and analysis are given in section.4.5.

4.2 Deterministic(uniaxial) test procedure and statistical models

The uncertainty existing in fabric mechanical properties can be statistically determined based on a number of experimental results. According to the statistical principle as "the law of large numbers" [10], a certain amount of test data is required for a valid uncertainty investigation. However, existing published experimental data are far fewer than the required. Therefore, it is necessary to obtain additional test data to satisfy the statistical criteria as sufficiently as possible by undertaking a number of tests.

There are a series of material test procedures for measuring the mechanical properties of coated woven fabrics including the material strengths (tensile and tear), stress-strain relation (biaxial and shear modulus), and other properties(e.g. creep), which have been proposed by national bodies, research institutes and professional bodies [1–3]. In this chapter, the probabilistic analysis is demonstrated based on the data obtained from tests on a Ferrari PVC/polyester 1002, as an example to demonstrate how to apply the probabilistic investigation methodology to a given fabric material or test data.

Currently, the biaxial strength of the fabric is difficult to obtain in most cases [3]. The Uniaxial tensile test remains the primary method to measure the strength of coated woven fabrics. This type of test measures the uniaxial rupture strength of the fabric along the warp or fill direction.

As regulated in BS3424, EN ISO 1421 [3], for uniaxial tension tests, the test specimens should be cut into 1100 $\times$ 50 mm strips along the warp and fill directions. As shown in figure.4.1, all the specimens are cut from fabric rolls, which are commonly used for fabric structure construction. The warp yarns are woven in the coated woven fabric along the roll direction, and the fill yarns across the roll width. The yarns in the fabric roll are assumed to be orthogonal, and yarns are approximately regarded as straight lines. However principally owing to the coating process, this assumption is violated to varying degrees. The yarns may not be straight in the warp, and the fill and warp yarns may not be not orthogonal. This violation will cause inconsistency in the definition of the test specimen in which yarns may not be complete along the length of the specimen near the cut edges. Therefore two cutting methods emerged, one strictly following the 50mm width regulation by simple cutting, and the other one follows the principle of specimen preparation along yarn directions.

Figure 4.1: Fabric roll (Ferrari precontraint 1002)

In the second industry proposed method, a consistent specimen is obtained by cutting the specimen initially wider than finally required, then stripping the yarns from two sides until all the yarns in the strip are continuous between two ends and the specimen width reduces to 50 mm. The initial and extracted specimen are illustrated as fig. 4.3.

When the yarns are distributed orthogonally in the woven fabric, there is little difference between these two cutting methods. However if the yarn distribution is non-orthogonal, the tensile capacities of the samples cut by different methods will be different, because the number of effective yarns in the samples are different. These differences depend on the distortion severity of the yarn distribution over the sample.

The second method ensures that all the yarns are effective when the sample is fully tensioned. When the continuity of all yarns in the specimen are assured, the strength of the sample will not be affected if the yarn distribution is severely non-orthogonal. Therefore the second cutting method is able to provide a measurement of the strength of a fabric sample and to be representative of the parent roll. The first method is more capable of measuring combined effect of the strength and distribution of the yarns.

To reduce qualitative uncertainty associated with determining the statistical content of the strength of a fabric, the second method namely "yarn strippping" is preferred and recommended.

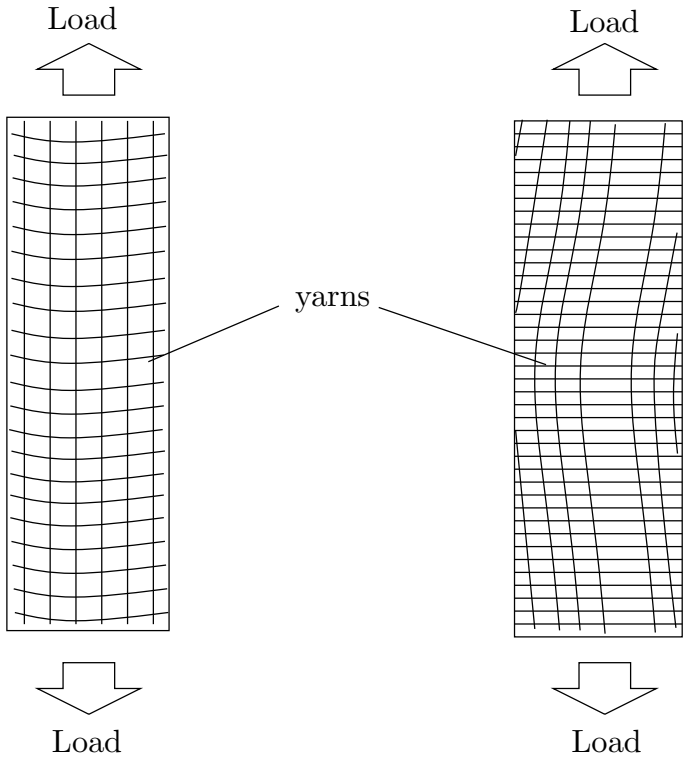

Figure 4.2: Possible distribution of Yarns in the specimen cut by direct method owing to the imperfections

The test equipment is illustrated as fig.4.4. The loading machine is a Shimadzu AG-250KNE, which has capacity from 0.01 N to 250 kN with an accuracy $\leq 0.5 \pm \%$ of the indicated value. The maximum loading speed of the Shimadzu is 250 mm/min, and the accuracy of the loading speed is $\pm 0.1\%$. The fabric strain is measured by a laser extesionmeter Laser Housefield 500L, which indicates the strain based on the increment of the gap between the reflective taps adhered to the sample. Both the load and strain are digitally recorded.

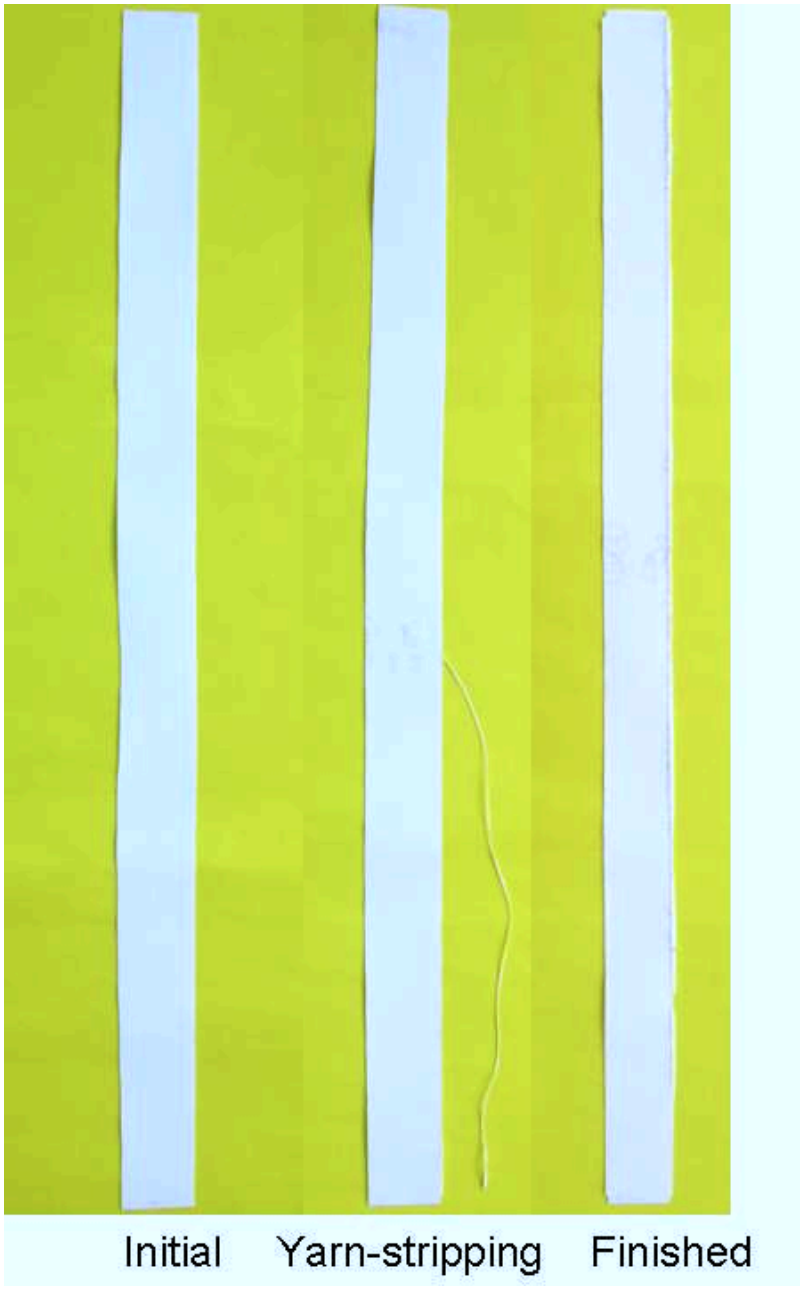

Figure 4.3: Initial, yarn-stripping and trimmed test specimen

Figure 4.4: Test equipment: Shimadzu AG-250KNE and Laser Housefield 500L

4.2.1 Strength measurement

The uniaxial tension strength of the fabric is normally higher than its biaxial tension strength owing to the crimp interaction [3]. However, because the biaxial strength is complicated and not easy to measure requiring specialized equipment of limited availability, the uniaxial strength has become the main parameter representing the material strength. The ultimate uniaxial strength can be computed according to the failure load of the specimens as:

$$\sigma_{ult} = \frac{F_f}{D} \tag{4.1}$$

where, F_f is failure load and D is the specimen width(50mm for standard uniaxial tension test).

4.2.2 Stress-strain relations

The coated woven fabric has clear nonlinear mechanical performance during the full external loading process. The deformation due to a load will depend on the magnitude of the load, and also the previous loading history. Therefore the stress-strain ratio (modulus) of the test samples is not only related to both their inherent mechanical property, but also the loading procedure. Besides the monotonic loading procedure(fig.4.5 (a) in which loading is added gradually until the sample ruptures, a cyclic loading procedure (fig.4.5 (b)) is also specified to obtain the fabric modulus for a different loading history in which the fabric properties are effectively, stabilized to a given load range. This has an averaging affect.

The loading speed of the linear loading test is 10mm/min, and with the same loading rate, the cyclic loading procedure comprises 5 and 3 cycles in two zones separately as illustrated in fig.4.5 (b). The first cyclic loading starts when the load reaches and attains for a short period time the designed prestress F_{pre} advised in "European Design Guide for Tensile Surface Structure" [12]. The second cycle starts at F_1, 12-15% of the ultimate tension strength(UTS) as given in the production information of the fabric roll, and ends at F_2= 25% of UTS.

Unlike uniaxial strength, the stress-strain relations of the fabric are normally nonlinear and difficult to be accurately represented by constant values of Young's modulus. A curve-fitting model may be used to compute the modulus for the statistical analysis based on the stress-strain curves of the test samples.

The accuracy of the fabric modulus estimated by the mathematical model will depend on the model accuracy and efficiency and may be wholly different for different fabric materials and loading conditions. A suitable methodology to model the stress-strain relation of a given fabric material may be determined based on the corresponding test result, but a single model containing a range of variables suitable for all types of fabric may not exist. Therefore, in this thesis, a specific model will be proposed based on the data from the test.

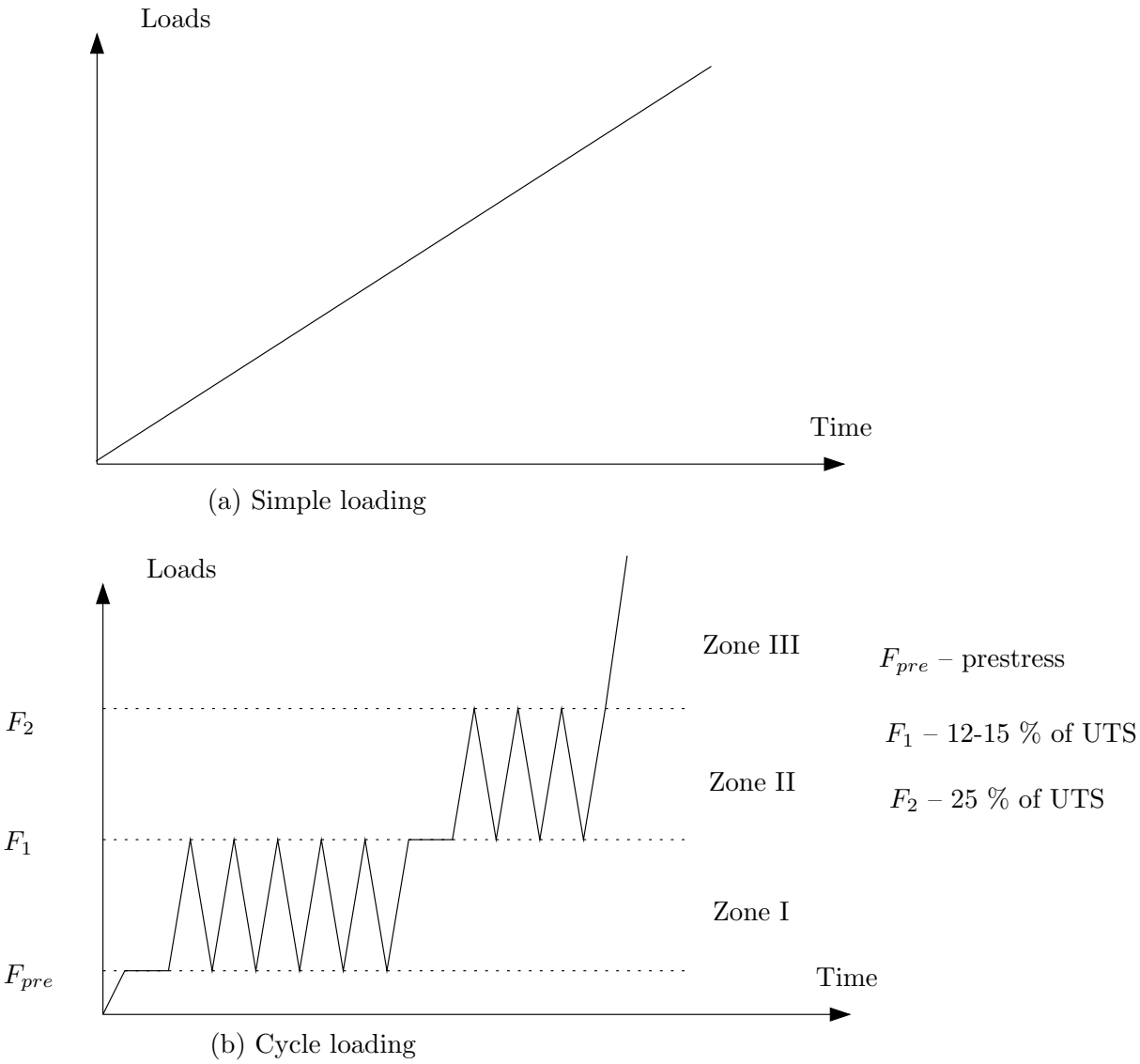

Figure 4.5: Different loading procedure for observing stress-strain relations

4.3 Test investigation for statistical analysis methodology

As a composite material, a variety of coated woven fabrics made of different coatings and yarns are available. These materials may have wholly different mechanical and chemical properties, and their probabilistic chacteristics may need to be presented using different methods(e.g randomness magnitude or distribution). It may not be possible to develop the same probabilistic test or analysis approach suitable for all types of coated woven fabrics. A practical approach is to establish a specific test procedure and analysis methodology suitable for several given fabric material types, and then to modify the methodology to other types of fabric materials.

Therefore, before undertaking a large number of material tests, a small number of specimens were tested to obtain a basic understanding of the mechanical characteristics of these fabric materials for the purpose of developing a test methodology suitable for establishing the probabilistic characteristics of the fabrics.

4.3.1 Uniaxial strength

Initially, a small set of Ferrari 1002 uniaxial specimens produced using the preparation procedures as described in section 4.2 were tested to investigate the characteristics of the uniaxial strength of the fabric. For each set of samples representing different preparation procedures, ten specimens (five for fill and five for warp) were tested. The test results are given in Table.4.1 and 4.2.

A comparison between Table.4.1 and 4.2 suggests that the two types of specimens may not be represented using same statistical variable, since the samples prepared by the yarn-stripping method have a higher uniaxial strength with all yarns working efficiently in the loaded direction, while the uniaxial strength values of the sample obtained by plain cutting represent the combination of the effects of the yarn strength and their incomplete composite structure in the fabric material. A t-test [92] for these two groups of samples can be undertaken as Eqn.4.2:

Sample number	1	2	3	4	5	Mean	S.D.
Fill	80.2	81.6	83.2	80.2	76	80.24	2.67
Warp	78.4	76.6	75.6	76.2	76.4	76.64	1.05

Table 4.1: Uniaxial strength of test sample made by plain cut preparation

Sample number	1	2	3	4	5	Mean	S.D.
Fill	89.6	99.6	98.4	94.6	94.4	95.32	3.93
Warp	87.0	90.4	76.6	85.2	85.2	84.88	5.09

Table 4.2: Uniaxial strength of test sample made by yarn-stripping preparation

$$\begin{aligned} t_{fill} &= \frac{\overline{X}_1 - \overline{X}_2}{\sqrt{(SD_1^2 + SD_2^2)/n}} \\ &= \frac{95.32 - 80.24}{\sqrt{(3.93^2 - 2.67^2)/5}} = 11.693 > t_{n=5}^{0.05} = 2.015 \end{aligned} \tag{4.2}$$

$$\begin{aligned} t_{warp} &= \frac{\overline{X}_1 - \overline{X}_2}{\sqrt{(SD_1^2 + SD_2^2)/n}} \\ &= \frac{84.88 - 76.64}{\sqrt{(5.09^2 - 1.05^2)/5}} = 3.699 > t_{n=5}^{0.05} = 2.015 \end{aligned} \tag{4.3}$$

When using the yarn-stripping cutting procedure, the yarns in the Ferrari 1002 fabric roll appear to be parallel along bow shaped lines in the fill direction and wave lines in the warp direction as fig.4.6. This phenomenon will lead to an obvious difference in the samples made by the two cutting methods, since the yarn distribution is far from othotropic distribution. The test results in Table.4.1 and 4.2 suggest that the samples made by yarn-stripping cutting have about 10-20% higher uniaxial strength than those made by plain cutting preparation. However, the standard deviations of the yarn-stripping samples are larger than those made by plain cut, and the COV values of these two types of samples are similar. That may suggest that the variation of the tension strength of the fabric is more relevant to the randomness of the individual yarns than the cutting method, which has more obvious effects on the magnitude of the material strength rather than its variance.

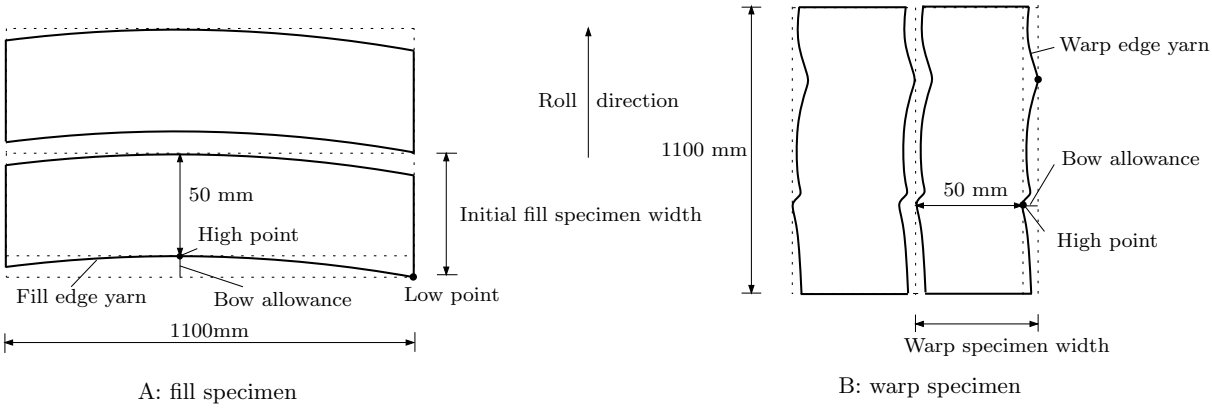

Figure 4.6: Ferrari cutting and bow allowances

4.3.2 Stress-strain relationship

For stress-strain relations, a full stress-strain relationship will be investigated in the specimen by plain cutting preparation, and an elastic stress-strain investigation is carried in the samples by yarn-stripping cutting procedure. Since such these tests aim at a basic probabilistic investigation methodology of the stress-strain in relation of the fabric, the comparison and relation between full stress-strain and elastic stress-strain performance is out of this research scope, therefore full stress-strain performance of yarn-stripping samples and elastic stress-strain performance of plain cut samples are not analyzed considering the capability of this reliability research and material costs.

The typical uniaxial stress-strain curves along fill and warp directions of two types of samples from the test results seemed similar and is presented in fig.4.7.Here considering the statistical requirement, a linear statistical formulation is created to quantify the nonlinear stress-strain relations of the two types of samples to modulus values(e.g Young's modulus) by linearizing the stress-strain curves in different loading zones. A tri-linear model is established for the linear loading samples based on the observed phenomena that the fabrics have significantly

different load-deformation performance in the three loading zones. While Young's modulus of cyclic loading samples are calculated in the cyclic loading zones by the linear regression.

This model is applicable to both linear loading and cycle loading procedures, but different linearizing intervals will be used to obtain the modulus.

Trilinear mathematical model for stress-strain relation

As shown in fig.4.8 and 4.9, in the simulation of stress-strain relation of both two group samples, the load spaces are divided into three zones. In each zone, the stress is assumed to increase linearly with strain giving a constant gradient, which is defined as Young's modulus. The stress-strain relation in the whole loading space is mathematically simulated by a trilinear model with a set of Young's moduli in each zone (e.g. EI, EII, and EIII). These are derived as,

$$E_I, E_{II}, E_{III} = \frac{\sum_{i=1}^{n}(\varepsilon_i - \overline{\varepsilon})(F_i - \overline{F})}{\sum_{i=1}^{n}(\varepsilon_i - \overline{\varepsilon})^2} \tag{4.4}$$

where ε_i and $\overline{\varepsilon}$ are the observed strain value and its mean value respectively in the zone, and F_i and $\overline{F}$ are applied load and mean value of the load in the zone.

For the samples under the linear loading procedure, Young's modulus in each zone is derived based on the linear regression of the entire sample data in the zone interval. While for the samples under the cyclic loading procedure, in the cycling loading zone, linear simulation is only made to the test data describing the cyclic loading, meaning that Young's moduli in zone I&II represents the stress-strain relation in the corresponding part of the loading space. A comparison between fig.4.8 and 4.9 suggests such a different definition of Young's modulus may lead to significant difference in the values of EI and EII for the samples under different loading procedures. Clearly, different stress-strain behaviour are observed in the cyclic loading and non-cylic loading zones.

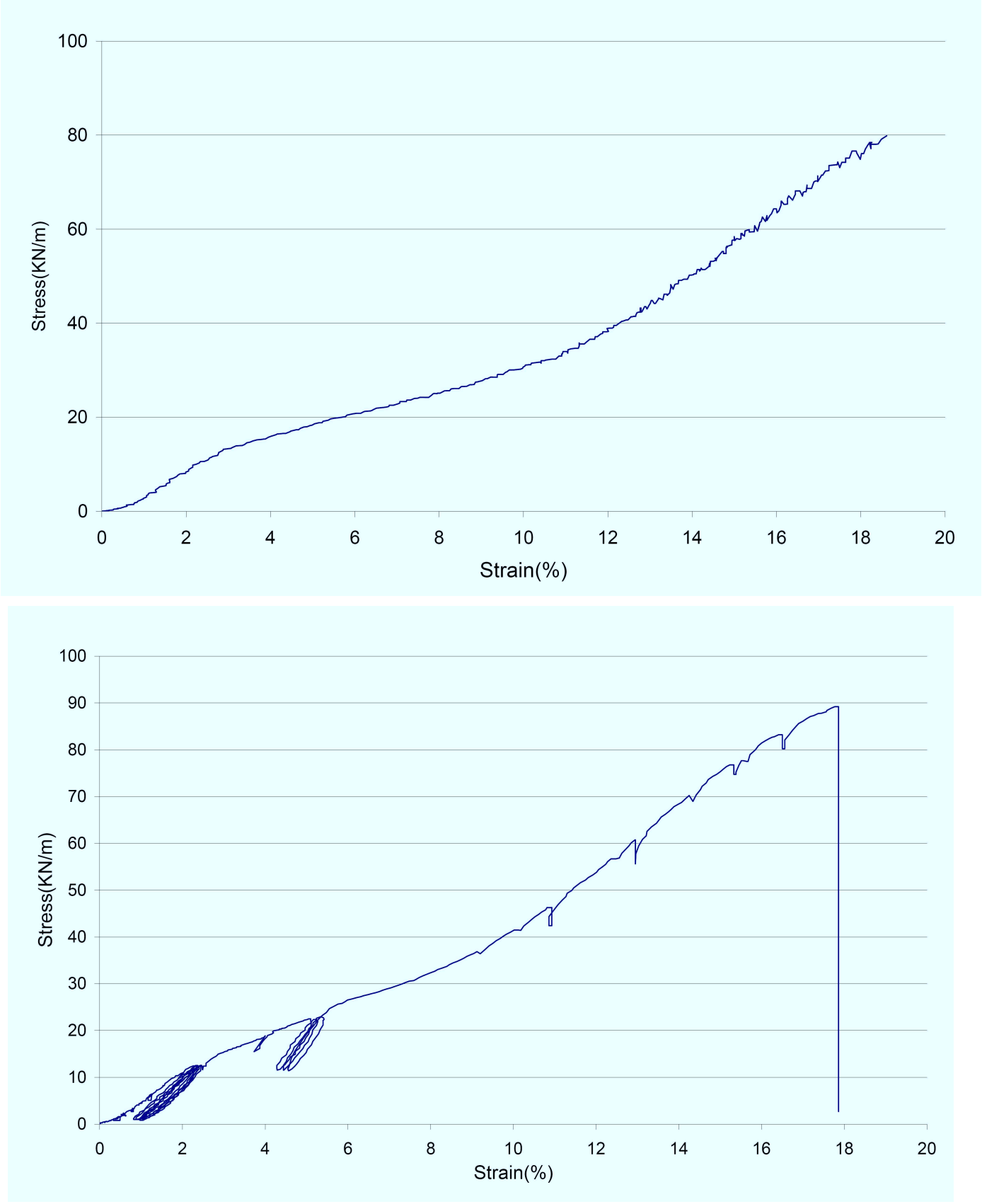

Figure 4.7: Typical uniaxial stress-strain curves of linear and cycle loading samples(fill and warp)

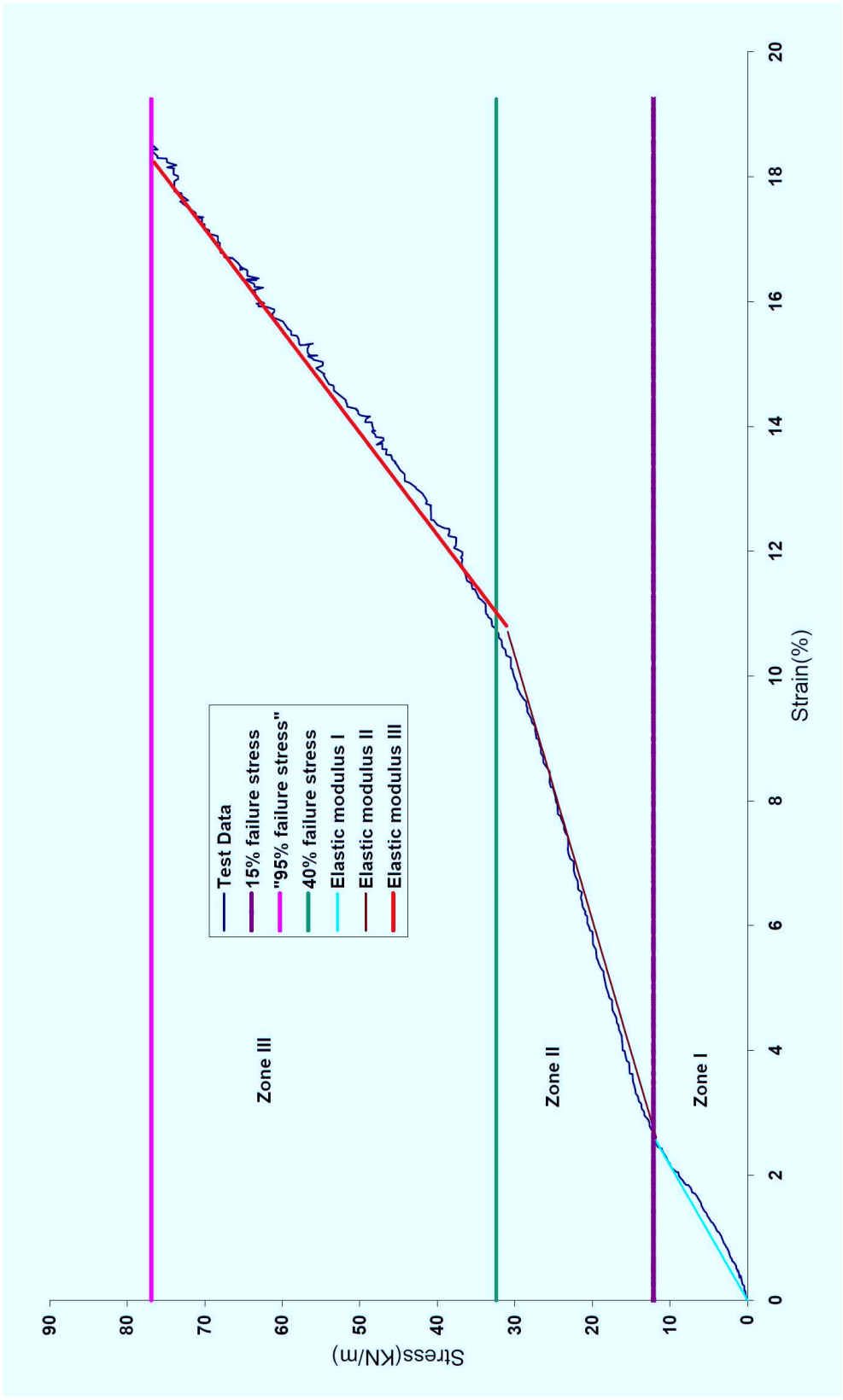

Figure 4.8: Trilinear model for Young's modulus of the samples under linear loading

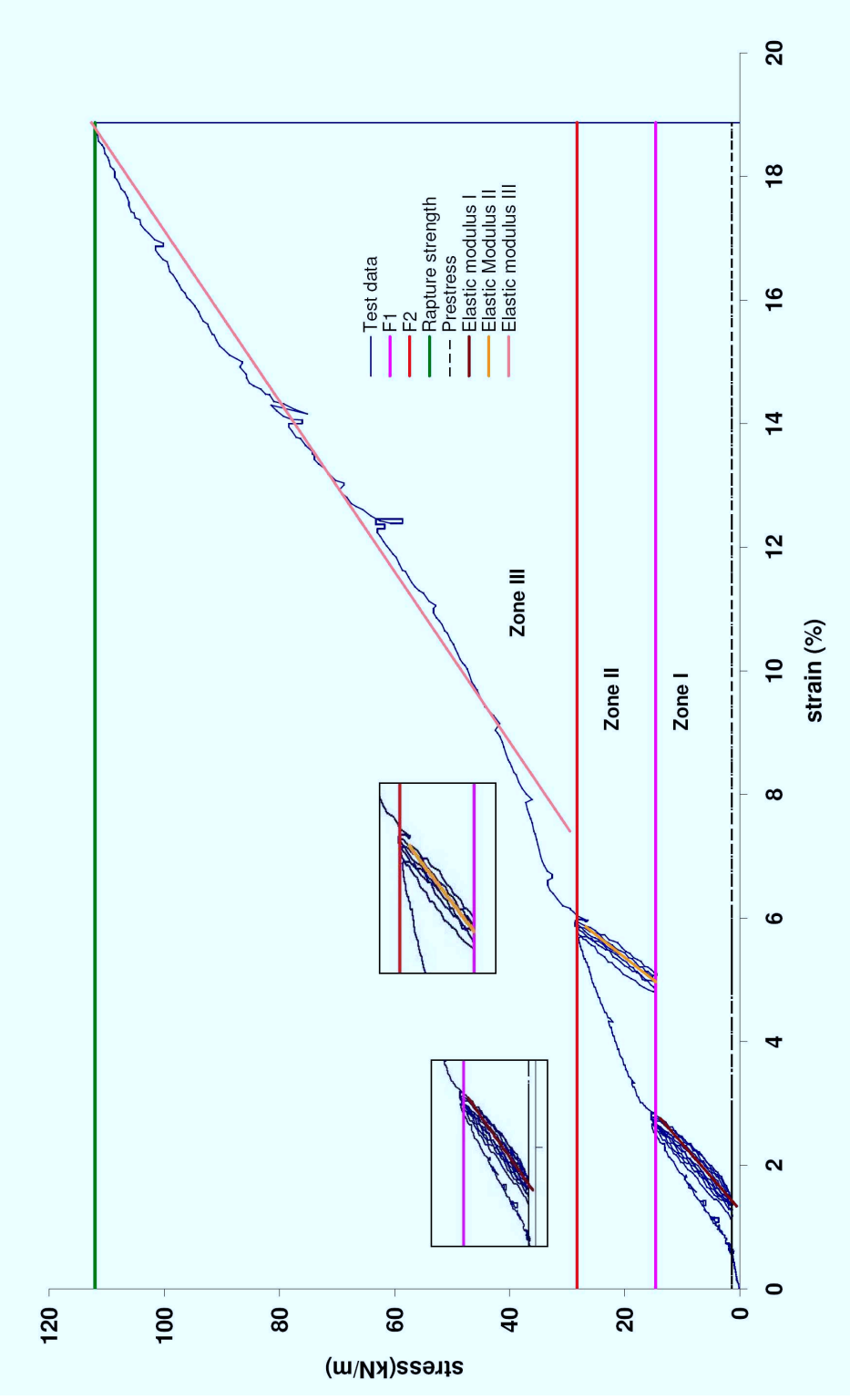

Figure 4.9: Trilinear model for Young's modulus of the samples under cycle loading

4.4 Statistical investigation methodology

Accurate probabilistic properties of the fabric material cannot be identified by just a few tests. Normally it requires a comparatively large quantity of experiments, and the feasible quantity size will also depend on the available resource and time. After hundreds of the test data have been obtained either directly from the measuring equipment or the trilinear regression models, the variations of these data can be analyzed through a statistical investigation, and the probabilistic properties of the mechanical behaviours of the fabric materials can be also identified and summarized with neat statistical descriptions.

4.4.1 General statistical investigation principal

When a random physical quantity is of concern, the possible outcomes are usually a range of measured or observed values, and some of these values may occur more frequently than others. To quantify a random variable, the systematic mathematical modelling or representation of the data is required. Generally, the essential steps to quantify a random variable are:

1 Data collection and modelling – Collect the available relevant information from the published test or experiments and evaluate the statistical information of interest using mathematical modelling.

2 Description of randomness – Describe the value variation and shape of random variables mathematically and graphically.

3 Determination of distributions and parameters – Select a particular distribution for a random variable and estimate its parameters to describe its randomness.

4.4.2 Description of randomness

In deterministic fabric design and analysis, *average* or *mean* values of test samples are normally applied to represent levels and strengths of fabric material. The mean value alone does not provide complete random information, and the dispersion of the values with respect to the mean is necessary to be represented mathematically in terms of *variance*, *standard deviation*, or *coefficient of variation*. Suppose X_s is a random variable and n observations of X_s are available. The mean or expected value of X_s, a measure of central tendency in the data, also known as the first central moment and denoted as $E(X_s)$ or μ_{Xs}, can be calculated for n observations x_{si} as

$$\text{Mean} = E(X_s) = \mu_{Xs} = \frac{1}{n}\sum_{i=1}^{n} x_{si} \tag{4.5}$$

The variance of X_s, a measure of spread in the data about the mean, also known as the second central moment and denoted as $\text{Var}(X_s)$, can be estimated as

$$\text{Variance} = Var(X_s) = \frac{1}{n-1}\sum_{i=1}^{n}(x_{si} - \mu_{Xs})^2 \tag{4.6}$$

Var(X_s) is expressed in different units from the mean value. For example, if the unit of the random variable X_s is kN/m, then the unit of variance will be in $(kN/m)^2$. The dimensional problem can be avoided by using standard deviation, denoted as σ_{Xs}, which is the square root of the variance.

$$\sigma_{Xs} = \sqrt{Var(X_s)} \tag{4.7}$$

Var(X_s) and σ_{Xs} are absolute values and cannot indicate the degree of dispersion in the random variable, without referring to the mean value. Since the mean and the standard deviation are expressed in the same units, a non-dimensional term - coefficient of variation(COV), denoted as $COV(X_s)$ or $\delta_(Xs)$, is introduced by taking the ratio of the standard deviation and the mean as:

$$COV(X_s) = \delta_{Xs} = \frac{\sigma_{Xs}}{\mu_{Xs}} \tag{4.8}$$

The value of the COV indicates the amount of uncertainty or randomness in the variable. For deterministic variables, the COV(X_s) is zero and in many engineering problems, the values of COV varies commonly between 0.1 and 0.3 for a random variable [204].

The asymmetry of the randomness can be measured by the skewness coefficient, denoted as θ_{Xs}, calculated as:

$$\theta_{Xs} = \frac{\gamma_s}{\sigma_{Xs}^3} \tag{4.9}$$

in which, γ_s is the third central moment of the variable, and calculated as:

$$\gamma_s = \frac{1}{n}\sum_{i=1}^{n}(x_{si} - \mu_{Xs})^3 \tag{4.10}$$

As shown in fig.4.10, when θ_{Xs} is zero, the randomness is symmetric; if θ_{Xs} is positive, the dispersion is more above the mean, and if it is negative the dispersion is less above the mean.

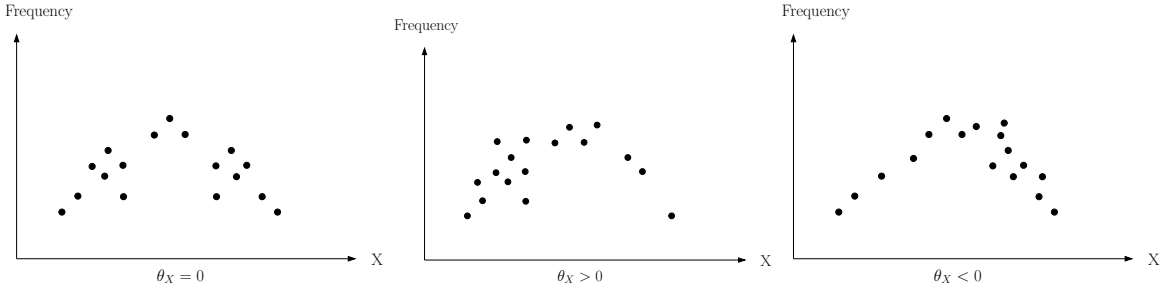

Figure 4.10: Measurement of randomness asymmetry using the skew coefficient θ_{Xs}

In the probabilistic theory, another statistical parameter is median which is defined as the value to separate the population to two halves. The median of the population $X_s(X_{si})$ has,

$$\begin{aligned} P(X_{s(i)} < \text{median}) &\leq 50\% \\ P(X_{s(i)} > \text{median}) &\leq 50\% \end{aligned} \tag{4.11}$$

For a finite sample group X with size n, and if there is $X_{s(1)} < X_{s(2)} < \cdots < X_{s(n)}$, then the median can be calculated by,

$$\begin{aligned} \text{median} &= X_{s(\frac{n+1}{2})}, \qquad \text{if } n \text{ is odd} \\ \text{median} &= 0.5(X_{s(\frac{n}{2})} + X_{s(\frac{n}{2}+1)}), \qquad \text{if } n \text{ is even} \end{aligned} \tag{4.12}$$

Besides the mathematical descriptions of the randomness introduced above, a more complete description can be obtained by plotting the information graphically in the form of a histogram. A histogram can be developed as the following procedure:

Step 1. Arrange the data in increasing order

Step 2. Subdivide the data into several equal intervals and count the number of observations in each interval.

Step 3. Compute the sample frequency of each interval by taking the ratio of sample numbers in each intervals and sample size.

Step 4. Plot the sample frequency in each interval versus the random variable, producing a histogram indicating the randomness

The number of the intervals can be estimated empirically [205] as:

$$k = 1 + 3.3log_{10}n \tag{4.13}$$

where k is the number of intervals and n is the number of samples.

For example, suppose there are a series of random values of the fill strength as listed in Table. 4.3.

Test no.	Fill strength, σ^f_{ult}(kN/m)	Test no.	Fill strength, σ^f_{ult}(kN/m)
1	81.6	17	83.6
2	83.2	18	81.0
3	76.0	19	80.6
4	83.6	20	86.2
5	81.2	21	73.8
6	84.0	22	84.4
7	80.2	23	86.4
8	71.6	24	83.0
9	78.2	25	81.6
10	83.4	26	87.0
11	85.4	27	77.6
12	84	28	80.2
13	83.6	29	79.0
14	84.2	30	80.0
15	74.4	31	78.6
16	77	32	83.2

Table 4.3: Example of fabric test data (n=32)

Then, the number of intervals $k = 1 + 3.3log_{10}32 = 5.97 \approx 6$. Considering the minimum and maximum values of test data, and rounding them to 70 kN/m and 88 kN/m, we use six intervals with a width of 3kN/m each as listed in Table. 4.4, to develop the histogram shown in fig 4.11.

Interval(kN/m)	No. of observations	Sample frequency
70-73	1	1/32=0.0313
73-76	2	0.0625
76-79	5	0.1563
79-82	9	0.2813
82-85	11	0.3438
85-88	4	0.1250

Table 4.4: Data for Histogram and Frequency Diagrams

The primary objective of a frequency diagram(histogram) is to model the pattern or behavior of the randomness by fitting a curve to the diagram. A data-fitting test can then be made both quantitatively and qualitatively to verify whether the fitted curve represents one of many commonly used distributions, such as the normal and log-normal. The modelling of the randomness of fabric mechanical behaviours will be discussed in section. 4.4.3.

The material test data presented in this PhD thesis is only a very small contribution to the whole probabilistic analysis work, but more importantly, is an attempt to establish a methodology to collect and present the probabilistic information of a given fabric material through a set of material tests.

Based on the principle of the statistics, a larger quantity of test data is always desired. These data may be assembled from different institutions and companies with different facilities and

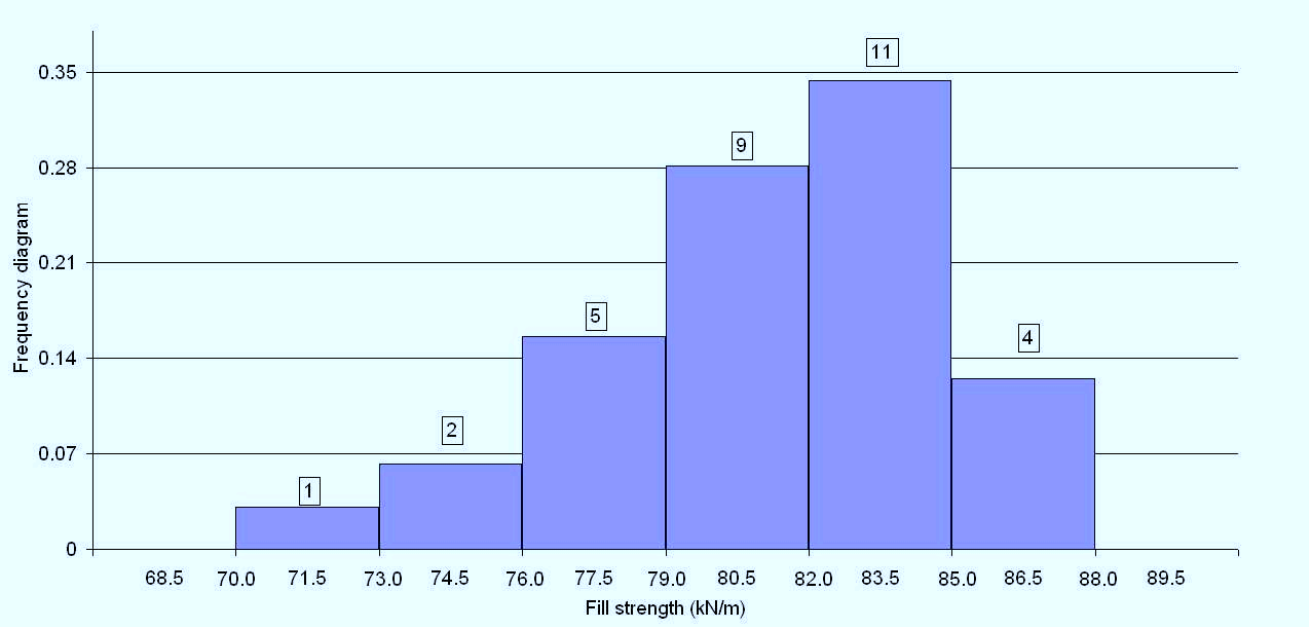

Figure 4.11: Histogram and Frequency Diagram of material test data

test machines. Temperature and other environmental factors (e.g. humidity) may also become important uncertainty sources affecting the test results. Therefore the probabilistic property of the fabric material obtained from the test data may not only reflect the uncertainty that exists in the fabric, but also in other uncertainty sources including:

- Test equipment and operator.
- Environment and temperature.
- Analysis method and assumed mathematical model.

The effects of these uncertainties should be taken into account in the data analysis. The test should be designed to try to reduce their contribution epistemic to the uncertainty content inherent in the fabric (aleatory).

Material strength and load-displacement relationships are the two main mechanical characteristics in the fabric structural design and analysis. Thus their uncertainties also become the main emphasis for probabilistic investigation of the fabric. As noted in the "European Design Guide for Tensile Surface structures,p 295" [13], the fabric tensile strength can be determined from uniaxial tension tests. The load-displacement relationship of fabric materials is nonlinear and normally described using mathematical models, which may have a complex form and bring more difficulties for the probabilistic analysis. In this section, a multi-linear model introduced in section 4.2.2 and 4.3.2 will be applied to represent the load-displacement relationship of the test samples in order to avoid large uncertainty due to the design of experiments.

Test procedure

The uncertainties of the fabric material: PVC-coated polyester Ferrari 1002 as described in Table 4.5 is investigated through uniaxial tension tests. These tests are taken in three individual periods with different quantities and temperatures as listed in Table 4.6.

Tested fabric type	Mass density	Strength (warp/fill)
Ferrari PVC 1002	1050 g/m^2	4.2/4.0 kN /5 cm

Table 4.5: Ferrari 1002 Manufacturer's information of the test fabric material

Cutting method	Loading procedure	Fabric Type	Quantity(warp/fill)	Temperature
Plain	Linear	Ferrari PVC 1002	126/112	23°
Yarn-stripping	Cycle	Ferrari PVC 1002	62/42	23°

Table 4.6: Temperatures and quantities of the fabric test

The cutting procedure of plain cutting samples is illustrated in fig. 4.12. A 15 metre long fabric roll was cut into uniaxial and biaxial test specimens. The uniaxial specimens along the fill direction were mainly cut from the first four blocks while warp specimens, were distributed along the whole roll length. While the yarn-stripping samples were cut from 1.8 × 4.0 m blocks in the fabric roll as figure 4.13.

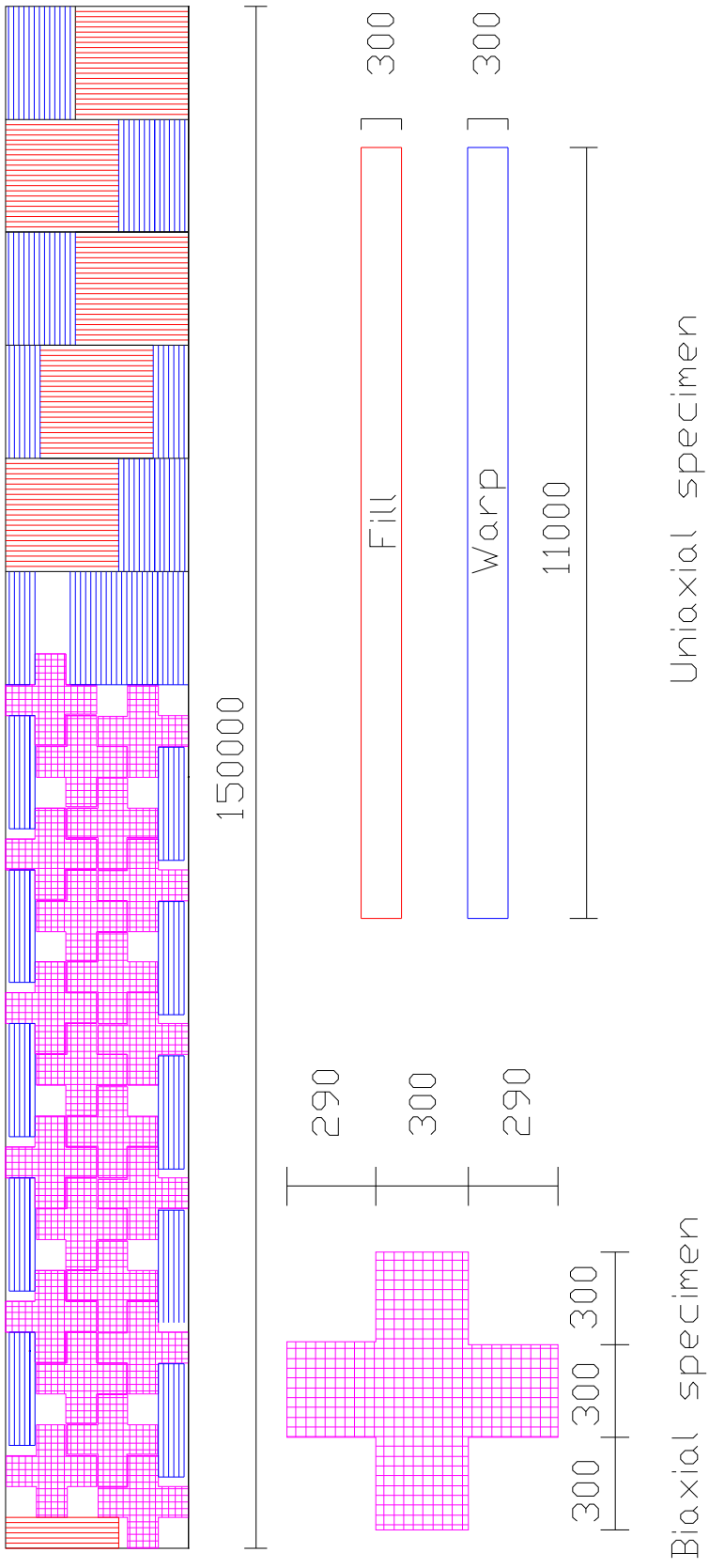

Figure 4.12: Cutting plan of the plain cutting samples

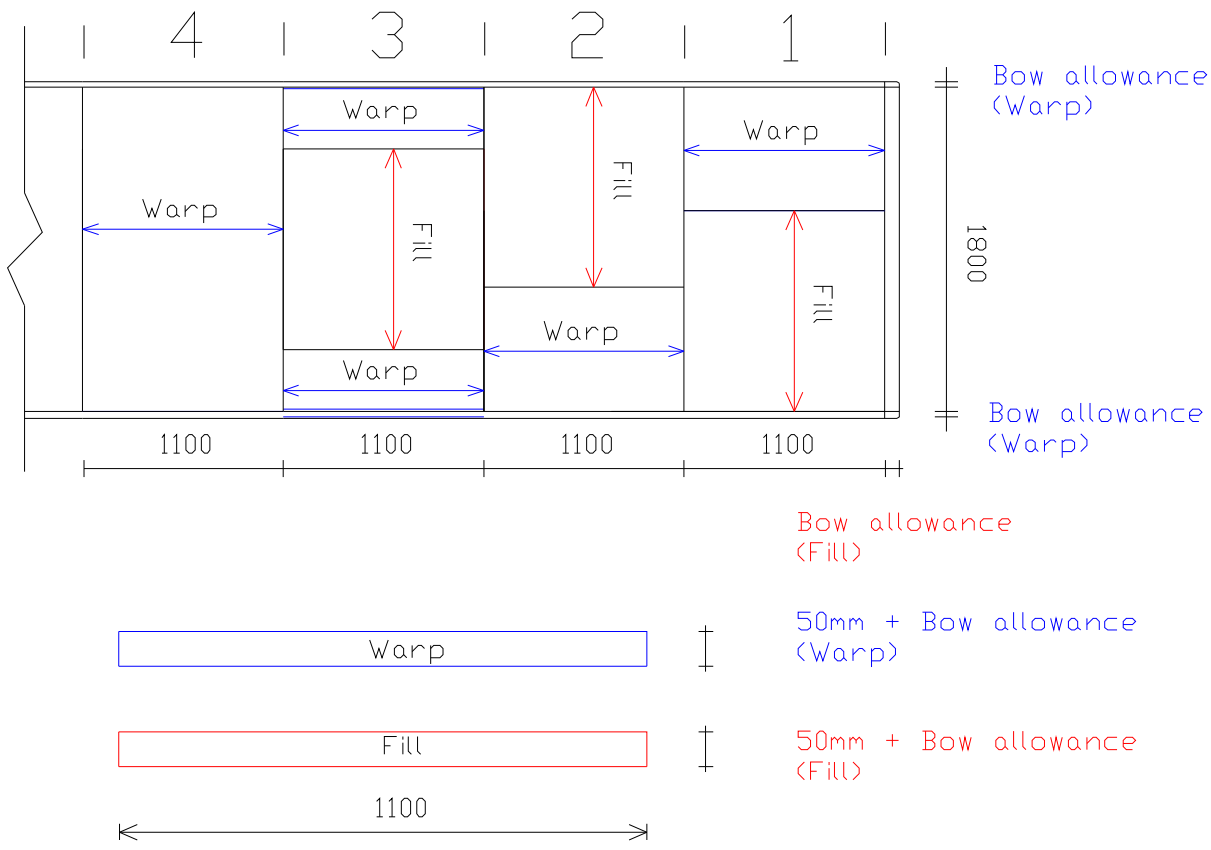

Figure 4.13: Cutting plan of the yarn-stripping samples

To facilitate the stochastic investigation on the variation in material properties over the fabric space, the tested part of the fabric rolls are divided into different blocks defined as fig.4.14. Group I samples are cut from 6 blocks with the dimension 1.1× 1.8m, and both two types of samples of group II are from 4 blocks of different fabric rolls. These blocks present the rough position of the test samples in the fabric roll.

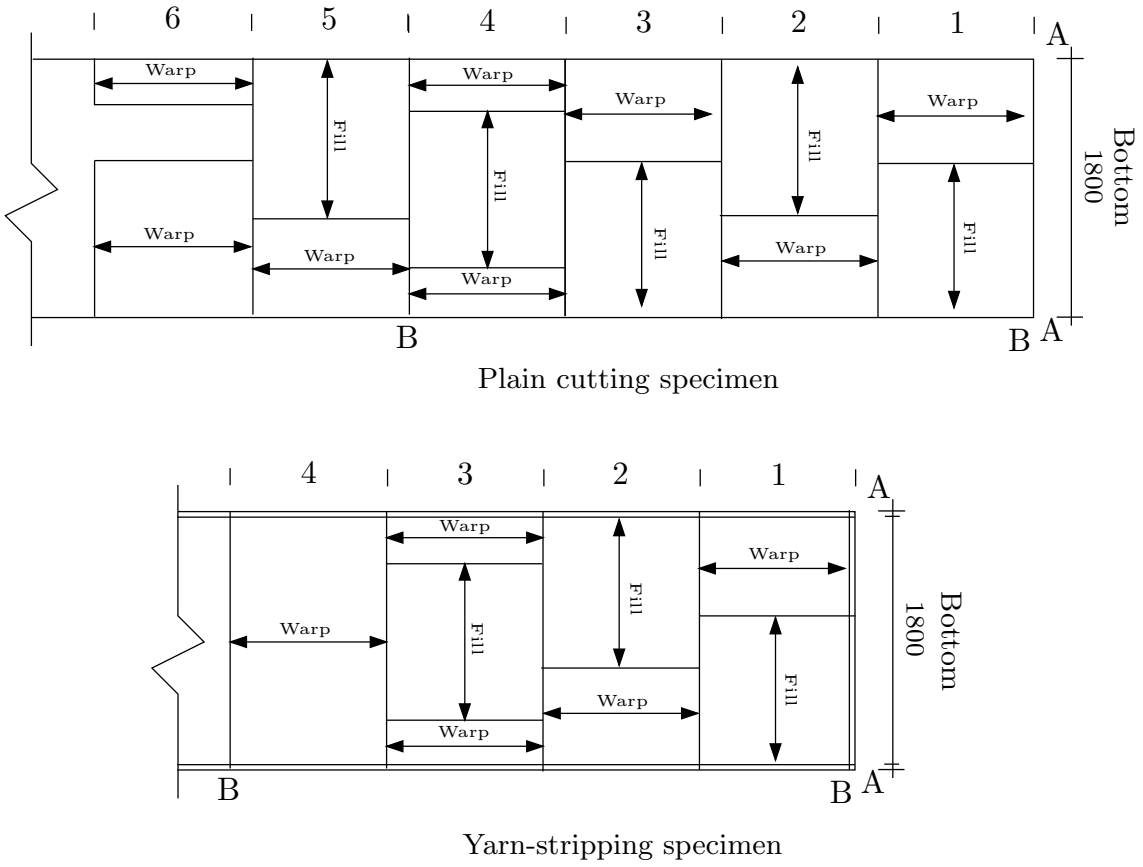

Figure 4.14: Block definition for plain cutting and yarn-stripping fabric

4.4.3 Determination of distributions and parameters

Besides the basic random parameters described in section 4.4.2, the detailed distributions of the random variables were estimated based on a quantitative data-fitting test. Normally, the random variables of interest (e.g ultimate strength or Young's modulus) are distributed continuously in a definite range.

It is notable that the uncertainty sources of the material strength and Young's modulus are different. Material strength can be directly obtained as discrete values from uniaxial tension tests, and it seems that the strength uncertainty may be more dependent to the randomness of the individual yarn strength. While to describe the nonlinear stress-strain behaviour, the Young's modulus has to be estimated using a mathematical model based on the test data. The modelling may become another important uncertainty source to affect the probabilistic results, in another words, a different modelling approach may lead to distinct analysis results.

More complicated models may produce more accurate and detailed descriptions of stress-strain relationships, but the quantification of this relationship is more difficult. Therefore the randomness in the stress-strain relationship of coated woven fabric may be more complex than the strength, with uncertainties combining from the yarns and the weaving composition.

4.4.4 Candidate distributions and the parameter estimation

The initial candidate distributions for the material statistical analysis include:

1 Normal Distribution

2 Log-normal Distribution

3 Exponential Distribution

4 Gumbel Distribution

5 Frenchet Distribution

6 Weibull Distribution

7 Laplace Distribution

8 Rectangular Distribution

9 Pareto Distribution

10 Rayleigh Distribution

Fundamental descriptions of these distributions are given as in Appendix.A:

4.4.5 Goodness-of-fit tests

After the parameters of the assumed candidate distribution are determined based on the general shape of the histogram, the validity of the assumed distribution needs to be verified statistically by goodness-of-fit tests. There are two such tests, which are generally used to check the validity of the assumed distributions, based on the general shape of the histogram : Chi-square and the Kolmogorov-Smirnov method.

Chi-square test

For a sample of n observed values of a random variable, the Chi-square test verifies the goodness-of-fit between the sample data and the assumed theoretical distribution by comparing the observed frequencies $n_1, n_2, \cdots, n_k$ of k values(or in k intervals) with the frequencies $e_1, e_2, \cdots, e_3$ from the distribution. The judgment will be made based on the value of the function of n_i and e_i,

$$\sum_{i=1}^{k} \frac{(n_i - e_i)^2}{e_i}$$

which follows the chi-square (χ_f^2) distribution with ($f = k - 1$) degrees of freedom as $n \to \infty$ for a pre-defined distribution. When the parameters of the assumed distribution are estimated from sample data, such a statement will be valid with ($f = k - 1 - s$), where s is the number of unknown parameters to be estimated.

On this basis, if an assumed distribution satisfies

$$\sum_{i=1}^{k} \frac{(n_i - e_i)^2}{e_i)} < c_{1-\alpha,f}$$

where $c_{1-\alpha,f}$ is the value of the appropriate χ_f^2 distribution at the cumulative probability $(1 - \alpha)$, the assumed theoretical distribution is an acceptable model, at the significance level α. Otherwise, the assumed distribution is not substantiated by the data at the α significant level.

In applying the χ^2 test for goodness of fit,it is generally necessary(for satisfactory results) to have $k \geq 5$ and $e_i \geq 5$.

Kolmogorov-Smirnov test

The Kolmogorov-Smirnov(K-S) test is a widely used goodness-of-fit test, in which, the comparison is made between the cumulative frequencies of the experimental sample data and the assumed theoretical distribution model. The theoretical model is only acceptable if the discrepancy is small with respect to what is normally expected from a given sample size.

For a sample of size n, rearranging the sample data in increasing magnitude to obtain a ordered sample data, which has $x_{s(i)} \leq x_{s(i+1)}$, a stepwise cumulative frequency function is then developed as,

$$S_n(x) = \begin{cases} 0 & x < x_{s(1)} \\ \frac{k}{n} & x_{s(k)} \leq x < x_{s(k+1)} \\ 1 & x \geq x_{s(n)} \end{cases}$$

where $x_{s(1)}, x_{s(2)}, \cdots, x_{s(n)}$ denote values of the ordered sample data, and n is the sample size. In the K-S test, the maximum difference between $S_n(X_s)$ and $F(X_s)$ over the entire range of X_s is the measure of discrepancy between the theoretical model and the observed data. The maximum difference can be written as:

$$D_n = max|F(x_s) - S_n(x_s)|$$

Theoretically, D_n is a random variable whose distribution depends on n. For a given significance level α, the K-S test compares the maximum difference D_n with the critical value D_n^α, whic is defined by:

$$P(D_n \leq D_n^\alpha) = 1 - \alpha$$

Critical values D_n^α at various significance levels α are tabulated in Table.4.7 for various values of n. If the observed D_n is less than the critical value D_n^α,the proposed distribution is acceptable at the specified significance level α; otherwise,the assumed distribution would be rejected.

$n \setminus \alpha$	0.20	0.10	0.05	0.01
5	0.45	0.10	0.05	0.01
10	0.32	0.51	0.56	0.67
15	0.27	0.30	0.34	0.40
20	0.23	0.26	0.29	0.36
25	0.21	0.24	0.27	0.32
30	0.19	0.22	0.24	0.29
35	0.18	0.20	0.23	0.27
40	0.17	0.19	0.21	0.25
45	0.16	0.18	0.20	0.24
50	0.15	0.17	0.19	0.23
> 50	$1.07/\sqrt{n}$	$1.22/\sqrt{n}$	$1.36/\sqrt{n}$	$1.63/\sqrt{n}$

Table 4.7: Critical Value of D_n^α in the Kolmogorov-Smirnov Test

Comparison between K-S test and Chi square

Comparing the two data-fitting tests, the K-S test is shown to be more stable and accurate to judge the best fitting distribution for a given data, because there is no interval required in the test and the comparison between test data and the corresponding distributions is actually taken at every data point. The Chi-square test requires the setting of a suitable interval, that endeavours to create the most detailed histogram as possible, with not many intervals resulting in an indeterminate histogram, and not too few intervals insufficient to distinguish the statistical information of the test data. For example, the sample data listed in Table.4.3 can be represented by different histograms with 4 and 8 intervals as fig.4.15 and 4.16.

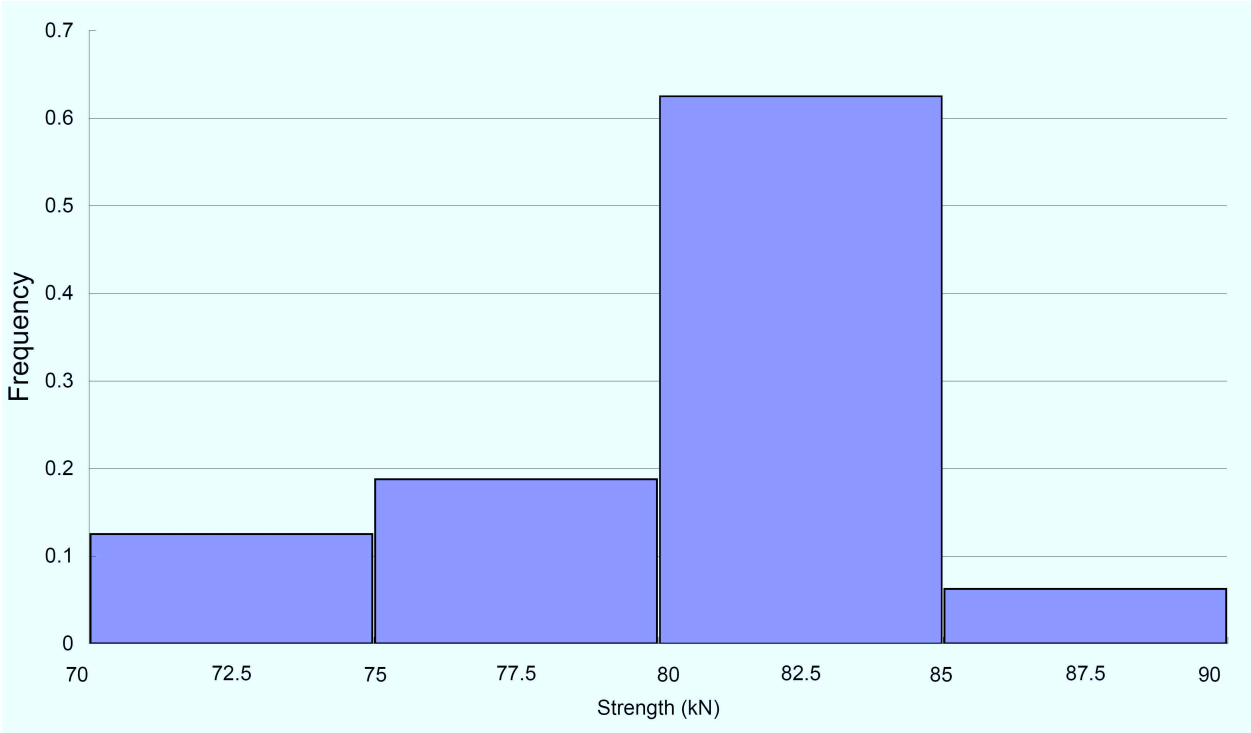

Figure 4.15: Histograms with 4 interval for the same data

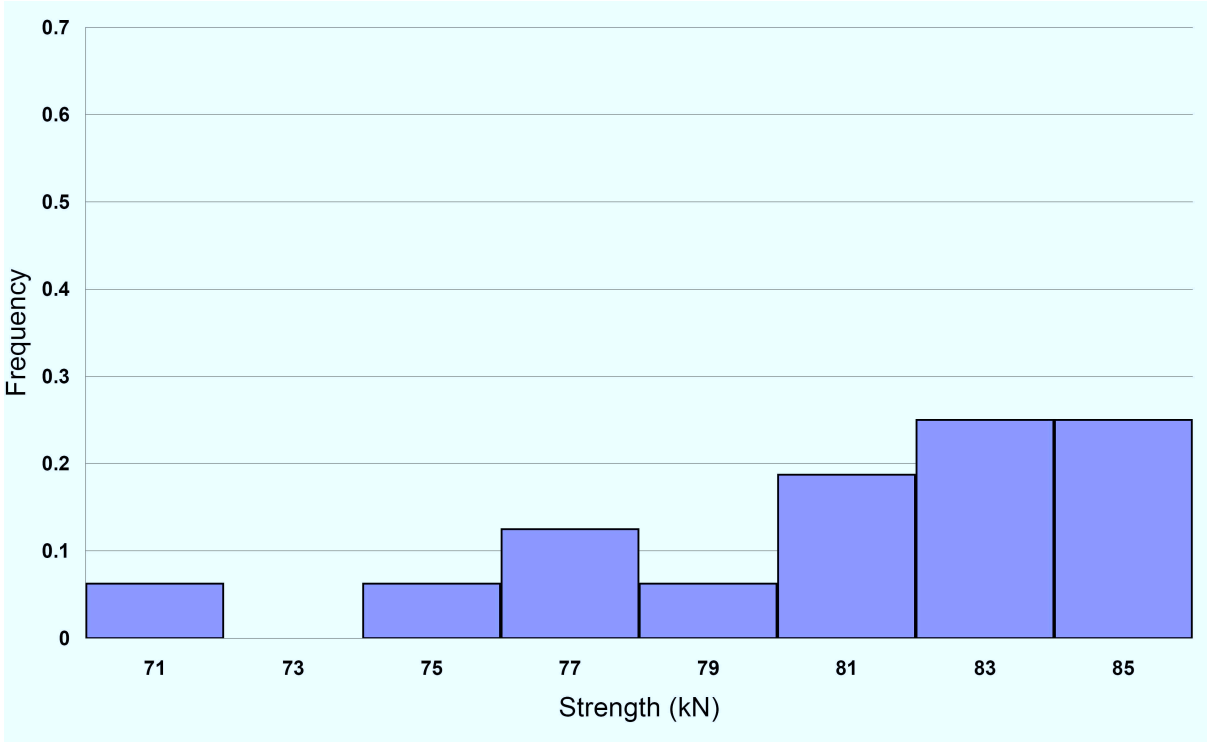

Figure 4.16: Histograms with 8 interval for the same data

However there is no fixed formulation to obtain the optimal interval setting, meaning that corresponding to different interval states the same test data can be transformed to different shape histograms, which consequently leads to a variety of Chi-square results. Even if the optimal interval state is achieved, the judgment of the Chi-square test is based on the difference of the test data and corresponding distributions on a number of intervals which is often deficient unless the data quantity is huge. For example, for a set of test data with 100 values, the Chi-square test only compares about the difference between the experimental data and assumed theoretical distribution in 8 intervals (i.e. $\sum_{i=1}^{8} \frac{n_i - e_i}{e_i}$), while the K-S test is based on the maximum difference D_n possibly over almost 100 sample values(i.e. $D_n = max|F(x_{s(i)}) - S_n(x_{s(i)})|, i = 1 \rightarrow 100$). Therefore the K-S test is more appropriate to judge the best-fitting distributions for the test data, and in the following sections of this chapter, only K-S test will be applied in the statistical examinations.

4.5 Probabilistic analysis of the mechanical properties

From the perspective of statistics, a large sample size will lead to a comparatively accurate probabilistic analysis result. However the quantity of statistical sample tests is always limited by the corresponding available resources, such as time and cost. Balancing the need of statistical accuracy and efficiency, and the available resources, a total of 342 samples of coated woven fabric have been tested as part of this PhD research project to identify the randomness in their mechanical properties.

4.5.1 Randomness analysis with basic statistical parameters

The specimen failure strengths and Young's modulus estimated from the stress-strain curves are listed in Appendix. A.1. Based on these data, the four basic statical quantities: mean value, standard deviation(S.D or σ_s), skewness and the coefficient of variation(COV) are calculated using the formula in section. 4.4.2. In this section, all the test data are initially assumed to be normally distributed with the corresponding estimated mean value and standard deviation. As shown in fig.4.17, for a normal distributed variable, the probability interval between $\mu \pm \sigma$ is 68%, and 95% between $\mu \pm 2\sigma$. In another words, the probability to be (1±COV)% more or less of the mean value is 32%, and there is only 5% probability out of the range of (1±COV)% of the mean value.

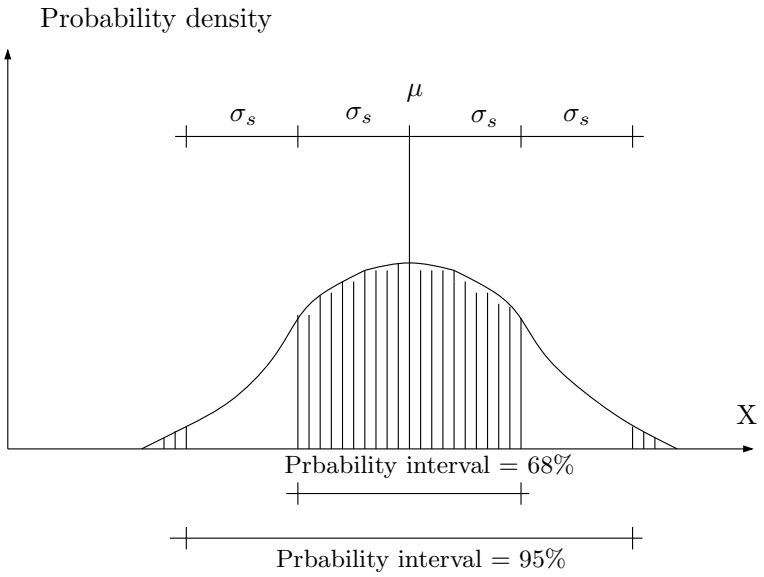

Figure 4.17: Probability interverals of normal distribution

Uniaxial strength

As listed in Table.4.8, the mean strength along the fill direction of plain cutting samples is 81.2kN/m, slightly higher than the corresponding value along the warp direction, and also has a little higher value in standard deviation. The COV values in Table.4.8 suggest that the standard deviation of the fill strength of plain cutting samples is 3.8% of the mean value, and in warp direction, this ratio is 3.5%. These COV values mean that the fill strength has 5% probability of being 7.6% (2×COV) more or less than its mean value, and the warp strength has a 95% probability to be in 1 ± 7% of its mean value of 77.3kN/m. These data can be included as Eqn.4.14,

$$\begin{aligned} S_{fs}^{0.95} &= [(1-7.6\%)\mu_{fs}^{L},\ (1+7.6\%)\mu_{fs}^{L}] = [75.2,\ 87.6] \\ S_{ws}^{0.95} &= [(1-7\%)\mu_{ws}^{L},\ (1+7\%)\mu_{w}^{L}s] = [73.1,\ 82.3] \end{aligned} \tag{4.14}$$

Where $S_{fs}^{0.95}$ and $S_{ws}^{0.95}$ are the unaxial strength interval with 95% probability along the fill and warp directions respectively, and μ_{fs}^{L} and μ_{ws}^{L} are the mean values of fill and warp strength of the linear loading samples.

The skewness values in Table.4.8 suggest the data of fill and warp strengths are skewed in different directions. The fill strength has a large negative skewness meaning that the data has obvious skewness to the right side, while the data of the warp strength has a smaller incline to left compared with the ones of the fill strength. Normally, for a highly skewed sample histogram, symmetrical distribution (e.g normal distribution) may be not valid to represent such data. However in some case, a normal distributed variable can produce a highly skewed histogram when the sample size is small.

Description	mean	S.D.	Skewness	COV	Median	P($X_i < \mu_i$)
Fill strength	81.2	3.1	-1.554	0.038	81.6	43.9%
Warp strength	77.3	2.7	0.411	0.035	77.2	53.6%

Table 4.8: Basic statistical description of the uniaxial strength of samples by plain cut

The dispersion of the sample values can be further detailed using median and $P(X_i < \mu)$ - probability of that sample value is less than the mean value. As listed in Table. 4.8, there are 43.9% sample value below the mean values of the fill strength, 50% sample values are over 81.6 kN/m. While for the warp strength, the median and mean values are very close, and 53.6% sample values are less than the mean value. This means there are about 3.6% sample values are between between the mean(77.2kN/m) and median(77.3 kN/m).

The basic statistical description of the unaixial strength of the samples made by yarn-stripping cutting preparation is stated in Table.4.9. Higher values are observed in both mean values and standard deviations of the unaixial strengths along either fill or yarn direction compared with plain cutting samples. The yarn-stripping cutting can effectively avoid weakening from the bow shape yarn distribution, however the COV values in Table.4.9 suggest that the uncertainties of these samples may not be reduced. For example, the fill strength of yarn-stripping samples has higher variance than normal-cutting samples, and varies ± 8.8% of the mean value with 95% confidence. This phenomenon suggests that reducing the uncertainty factor from cutting may not be able to improve the consistency of the unaixial strength when the sample number is limited, even though the mean values may appear increased.

The skewness of Table.4.9 states both fill and warp strength data are skewed toward the same direction, but the skewness of fill strength data is obviously higher than the warp equivalently. This is similar to the plain-cutting samples. The warp strength has a small skewness value -0.245, meaning that it has a comparatively symmetrical data distribution.

Description	mean	S.D.	Skewness	COV	Median	P($S_i < \mu_i$)
Fill strength	96.9	4.3	-1.342	0.044	97.5	41%
Warp strength	87.2	3.6	-0.245	0.032	87.4	47%

Table 4.9: Basic statistical description of the unaixial of samples by yarn-stripping cut

Comparision between the plain and yarn-stripping cutting samples

The comparison of the unaxial strength of two groups of test samples suggests that significant differences exist in the sample mean value and stand deviations, and the yarn-stripping cutting samples have much higher strength than the plain cutting ones. However these two group samples made of the same types of materials have several similiar probabilistic characteristics such as:

- Their COV values are close compared with their mean values, indicating that their dispersion about the mean values are approximately similar.
- The dispersion of fill samples in each group is slightly larger than the warp.
- Both fill sample values are positive skewed, while warp samples are almost symmetrical.

Stress strain relationship

The basic statistical descriptions of the sample Young's modulus under monotonic loading are calculated and listed in Table.4.10. The mean values suggest that the Young's modulus in both fill and warp direction reduce in loading interval Zone II, then increase in Zone III. The fill Young's modulus has a higher standard deviation in Zone I than the ones in Zone II and Zone III, in which the large COV values are observed. The standard deviations of Young's modulus in Zone I & II are 13.5% and 17.3% of their means respectively, meaning that there is 64% probability that the values of Young's modulus are in the range of 0.8655 - 1.135× mean value of Young's modulus Zone I, and there is 5% probability to be out of the range 0.73 - 1.27 × the mean values of Young's modulus in Zone I and 0.65 - 1.35 × the mean in Zone II.

For Young's modulus in the warp direction as listed in Table.4.10 , large values of mean and standard deviation are found in the first loading Zone, and the COV value suggest large variabilities exist in the Young's modulus of first two zones. In Zone I, the standard deviation is 21.1% of the mean values, and in zone II, this ratio even higher, about 25.9%, indicating that there is 5% probability that the Young's modulus can be 51.8%(2× COV) more or less than their mean value. The warp Young's modulus in zone III has the largest mean value while the standard deviation is low, resulting in a COV value of 0.033, with significantly less variability than the warp Young's modulus in first two loading zones

The skewness in Table.4.10 state that the fill Young's modulus in all three loading zones are highly skewed, and the data are skewed to the left in Zone I, and in the other zones,

the data are skewed to the right. The warp Young's modulus data are skewed to the same direction, and only the data in Zone II has large skewness, while in Zone I & III, the data are approximately symmetrical with the same skewness values 0.223 in Zone I and 0.162 in Zone III. The medians and P($S_i < \mu_i$) of fill Young's modulus listed in Table. 4.10 indicate that the fill Young's modulus in all three zones have high skewed distributions, and especially in Zone I, the significant difference between the mean and median suggests that serious asymmetry and large dispersion exist in the Young's modulus, and that 50% of the sample values are less than 239kN/m, with the mean value 377 kN/m. The warp Young's modulus has high skewness in Zone II, where 63.2% sample values are below the mean 216 kN/m, meaning that 13.2% sample values fall in the interval between the mean 216 kN/m and the median 204 kN/m.

Direction	Interval	mean	S.D.	Skewness	COV	Median	P($S_i < \mu_i$)
fill	Zone I	377	51	1.519	0.135	239	59.5%
	Zone II	237	41	-1.853	0.173	276	45.2%
	Zone III	638	41	-1.046	0.064	642	46%
warp	Zone I	512	108	0.223	0.211	504	49.1%
	Zone II	216	56	1.71	0.259	204	63.2%
	Zone III	612	20	0.162	0.033	615	50.9%

Table 4.10: Basic statistical description of Young's modulus of samples under linear loading

The basic statistical information of Young's modulus under cyclic loading is shown in Table.4.11 , from which, it can be seen that the stress-strain relationship of the fabric samples under uniaxial cyclic loading are wholly different from those under linear uniaxial loading. The mean Young's modulus in both fill and warp direction in zone I are as large as 833kN/m and 804 kN/m, and even higher in Zone II, 1198 kN/m in the fill and 1141kN in the warp. Compared with the mean values, the standard deviations in fill direction listed in Table.4.11, are low, only 30kN/m and 40kN/m in Zone I & II respectively, comparatively large S.D values 71kN/m in Zone I and 90kN/m in Zone II are observed. The COV values listed in Table.4.11 suggest that in the fill, Young's modulus in Zone I has 95% probability to be valued within (±3.7%) of the mean value, and in Zone II there is 5% probability to be 6.6% more or less than the mean. Compared with the fill Young's modulus, the Young's modulus in the warp is much larger such that ratios of S.D and mean are 8.8% in Zone I and 7.9% in Zone II, indicating that vary only within ± 17.6%(2× COV) of the mean in Zone I, and the Young's modulus in Zone II has 95% probability of varying within ± 15.8%(2× COV) of the mean.

The skewness listed in Table.4.11 suggest that the fill Young's modulus data in both zones are skewed to the right, while the Young's modulus in the fill are skewed to left. The comparison between skewness in Zone I and Zone II indicates the distribution of Youngs modulus data in Zone I are more obviously skewed rather than the ones in Zone II, which can be approximately regarded as symmetric with the skewness of -0.025 in fill and 0.022 in warp.

Comparision between the linear loading and cyclic loading samples

Direction	Interval	mean	S.D.	Skewness	COV	Median	P($S_i < \mu_i$)
Fill	cycling Zone I	833	31	-0.655	0.037	844	55.1%
	cycling Zone II	1198	40	-0.025	0.033	1208	47.9%
Warp	cycling Zone I	804	71	0.497	0.088	793	48.3%
	cycling Zone II	1141	90	0.022	0.079	1129	49.4%

Table 4.11: Basic statistical description of Young's modulus of samples under cycle loading

Unlike the uniaxial strength, few similarities between linear and cyclic loading samples can be observed, even though they are made of the same type of materials. The significant difference in the Young's modulus between these two samples are found in,

- The Young's modulus evaluated based on the stress-strain relation under the cyclic loading are much higher than those from the linear loading sample data.
- The variances of Young's modulus in Zone I and II derived from the linear loading sample values are obviously large, while comparatively small evaluated based on the sample values under the cyclic loading.
- The dispersions and skewness of the Young's modulus under these two set of loading conditions are different. Under the linear loading, the fill Young's modulus in Zone I & II and the warp Young's modulus in Zone II are obviously skewed, and the dispersions between the means and medians are significantly large compared with those obtained under the cyclic loading. The fill and warp Young's modulus under the cyclic loading condition have approximately symmetric distributions with small skewness values and the small distance between the means and medians.

4.5.2 Mathematical presentation of the randomness of the test samples

The statistical distribution of a variable normally can be represented mathematically by the random density functions(i.e. PDF and CDF) associated with a given statistical distribution which can fit the characteristic of the sample data approximately.

The first step to select the best-fitting distribution is to calculate the data interval and build the histogram for each quantity of interest as described in Section. 4.4.2. Shape-like distributions are then further selected from the initial candidate distributions aforementioned in section. 4.4.4. Subsequently, the parameters of candidate distributions are evaluated and the best-fitting distributions is judged using the K-S test which is based on the differences in the cumulative probabilities between the test data and candidate distributions.

Regarding the fact that for most quantities of interest, their corresponding histograms follow approximately bell-like shapes, 6 types of distributions are further selected from the initial candidate distributions:

- Normal Distribution
- Log-normal Distribution
- Laplace Distribution
- Gumbel Distribution
- Frechet Distribution
- Weibull Distribution

The PDF and CDF of the distributions are commonly functions of two types of parameters: location and shape. The PDF and CDF formulations of the candidate distributions are listed in Table.4.12 with the corresponding parameters.

Distribution	Parameters	Random density function
Normal	Mean: μ Standard deviation: σ	PDF: $f(x) = \frac{1}{\sigma\sqrt{2\pi}} e^{-0.5(\frac{x-\mu}{\sigma})^2}$ CDF: $\int_{-\infty}^{x} \frac{1}{\sigma\sqrt{2\pi}} e^{-0.5(\frac{x-\mu}{\sigma})^2}$
LogNormal	Location: a, Shape: b	PDF: $f(x) = \frac{1}{bx\sqrt{2\pi}} e^{-0.5(\frac{lnx-a}{b})^2}$ CDF: $\int_{-\infty}^{x} f(x) = \frac{1}{bx\sqrt{2\pi}} e^{-0.5(\frac{lnx-a}{b})^2}$
Laplace	Location: a, Shape: b	PDF: $f(x) = \frac{1}{2b} exp(-\frac{\lvert a-x \rvert}{b})$ CDF: $F(x) = \frac{1}{2} exp(-\frac{a-x}{b})$, $x < a$ $1 - \frac{1}{2} exp(-\frac{x-a}{b})$, $x > a$
Gumbel	Location: a, Shape: b	PDF: $f(x) = \frac{1}{b} exp[-\frac{x-a}{b}] exp[exp(-\frac{x-a}{b})]$ CDF: $F(x) = 1 - exp\{-exp[-\frac{x-a}{b}]\}$
Frechet	Location: a, Shape: b	PDF: $f(x) = -\frac{a}{b}(\frac{a}{x})^b exp[-(\frac{a}{x})^b]$ CDF: $F(x) = 1 - exp[-(\frac{a}{x})^b]$
Weibull	Location: a, Shape: b, c	PDF: $f(x) = \frac{b}{c}(\frac{x-a}{c})^{b-1} exp[-(\frac{x-a}{c})]^b$ CDF: $F(x) = 1 - exp[-(\frac{x-a}{c})^b]$

Table 4.12: The PDF and CDF functions of location and shape parameters.

Subsequently, for each statistical variable (e.g fill strength), these parameters are estimated based on the following descriptions,

Normal distribution

$$\begin{aligned} \mu &= \frac{\sum_{i=1}^{n} X_i}{n} \\ \sigma_s &= \frac{1}{n} \sum_{i=1}^{n} (X_i - \mu)^2 \end{aligned} \tag{4.15}$$

Log-Normal distribution

$$\begin{aligned} a &= \frac{\sum_{i=1}^{n} ln(X_i)}{n} \\ b &= \frac{1}{n}\sum_{i=1}^{n}(ln(X_i) - a)^2 \end{aligned} \tag{4.16}$$

Laplace distribution

$$\begin{aligned} a &= \frac{\sum_{i=1}^{n} ln(X_i)}{n} \\ b &= \frac{1}{n}\sum_{i=1}^{n}|X_i - a| \end{aligned} \tag{4.17}$$

Gumbel distribution

The parameters of the Gumbel distribution can be obtained by solving the equation 4.18.

$$\begin{aligned} b &= \frac{\sum_{i=1}^{n} X_i}{n} - \frac{\sum_{i=1}^{n} X_i exp(\frac{-X_i}{b})}{\sum_{i=1}^{n} exp(\frac{-X_i}{b})} \\ a &= -b\ log[\frac{1}{n}\sum_{i=1}^{n} exp(\frac{-x_i}{b})] \end{aligned} \tag{4.18}$$

Frechet distribution

If a Frechet distribution has the location and shape parameters denoted as a and b, then the distribution of $ln\ Y - n$ will have the the pertinent parameters for the Type II asymptotic distribution:

$$a = e^{u_n}; \quad b = \alpha_n$$

Therefore, the parameters of the Type II asymptotic distribution of the largest value may be obtained by first estimating $\hat{u}_n$ and $\hat{\alpha}_n$ for the logarithms of the sampled data, that is, $ln\ y_1, ln\ y_2, \cdots, ln\ y_n$, using for example the order statistics method, which is introduced in Appendix.A. The estimates of a and b may then be obtained as:

$$\hat{a} = e^{\hat{u}_n}; \quad \hat{b} = \hat{\alpha}_n$$

Similarly,for the parameters of the Type II asymptotic distribution of the smallest value, we obtain $\hat{u}$, and $\hat{\alpha}_1$ as the sample parameters using the sample values $ln\ y_1, ln\ y_2, \cdots, ln\ y_n$; and then the relevant parameters for the Type II asymptotic distribution of the smallest value are:

$$\hat{a}_1 = e^{\hat{u}_1}; \quad \hat{b}_1 = \hat{\alpha}_1$$

Weibull distribution

The Weibull distribution with three parameters can be determined using the first three sample moments; the sample mean $\overline{x}$, the sample standard deviation σ_x, and the sample skewness, $\hat{\theta}_x$. The three extremal parameters of the Weibull distribution may be estimated as follows.

The values of θ_x,as well as $A(b)$ and $B(b)$,may be evaluated as functions of $1/b$ from Relation Among Parameters of Type III Asymptotic Distribution Table.A.11.
Then

$$a = B(\hat{b})\sigma_x$$

and

$$c = A(b)\sigma_x + \overline{x} - a$$

Uniaxial strength

Samples by plain cutting

Based on the sample data and the PDF of the distributions with the estimated parameters in Table.4.12, the D_n values of all candidate distributions attempting to fit the uniaxial strength data of samples by plain cutting are calculated as listed in Table.4.13.

Direction	Normal (μ,σ)	Log-normal (a,b)	Laplace (a,b)	Gumbel (a,b)	Frechet (a,b)	Weibull (a,b,c)
Fill	81.2, 3.1	4.40, 0.039	81.2, 0.15	80.4, 3.129	79.40, 23.87	63.2, 6.817, 0.3782
Warp	77.3, 2.746	4.32, 0.013	77.3, 0.11	75.6, 0.13	74.4, 33.8	70.2, 2.633, 0.3782

Table 4.13: Estimated distribution parameters for uniaxial strength of samples by plain cutting

Based on the definition in section.4.4.5, the n are found to be 55 and 40 for fill and yarn data respectively, and the critical values of D_n^α with 0.05 significance coefficient(95% confidence interval) are respectively,

$$D_{n=55}^{0.05} = 1.36/\sqrt{55} = 0.183, \qquad D_{n=40}^{0.05} = 0.21 \tag{4.19}$$

Compared with the D_n values listed in Table.4.14, for fill strength data, all the candidate distributions pass the K-S test, but the maximum difference between sample data and estimated distributions are different. The Normal distribution has the smallest D_n value, meaning that the gap between the sample data and the normal distribution are smallest out of all the distributions. It is notable that there are two distributions, Log-normal and Weibull distributions having quite close D_n values, 0.044 for log-normal and 0.046 for Weibull distribution to that of the normal distribution, 0.042. In that case, the judgement of best fitting distribution cannot be decided only by D_n values, and the data fitting in the whole are required to be reviewed. As shown in fig.4.18, generally all these three distributions are similarly well-fitted to the sample data, but the Weibull distribution seems to be more fitted especially in the tail.

Such information cannot be reflected by D_n value. Therefore the Weibull distribution may be recommended as the best fitting distribution of the fill strength data of the plain cutting samples.

Direction	Normal	Log-normal	Laplace	Gumbel	Frechet	Weibull
Fill	0.042	0.044	0.066	0.102	0.131	0.046
Warp	0.090	0.082	0.092	0.088	0.519	0.074

Table 4.14: K-S test D_n^{α} values for uniaxial strength of samples by plain cutting

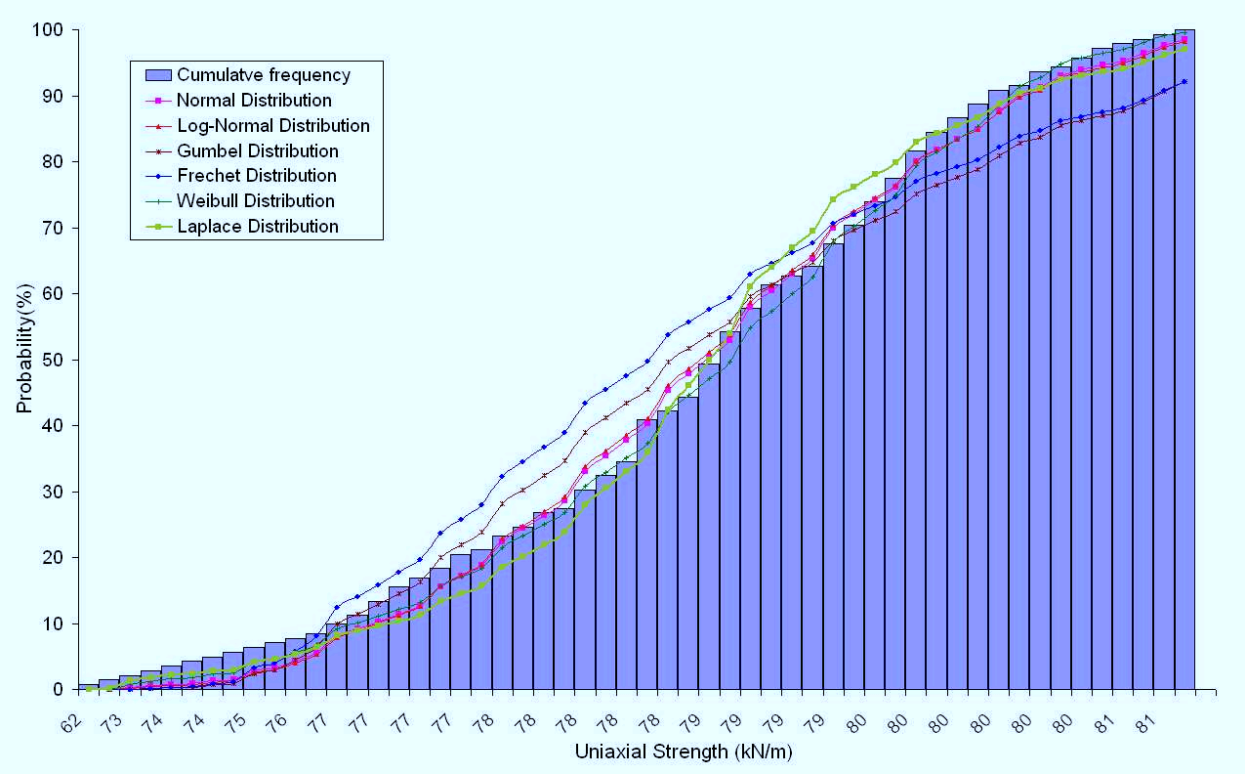

Figure 4.18: KS test result of different distributions for fill strength of sample by plain cutting

A comparison between D_n of the warp strength data listed in Table.4.14 and the critical value given in Eqn.4.19 suggests that only the Frechet distribution failed the K-S test, and all other candidate distributions passed. The Weibull distribution may be considered as the best distribution with a D_n value obviously smaller than the ones of other distributions.

Samples by yarn-stripping

Based on the sample data, n of the uniaxial strength of samples made by yarn-stripping cutting are 42 for fill data and 61 for warp data, the corresponding critical values with 0.05 significance coefficient are,

$$D_{42}^{0.005} = 0.208, \qquad D_{61}^{0.005} = 1.36/\sqrt{61} = 0.174 \tag{4.20}$$

Based on the comparison between D_n values listed in Table.4.16 and the critical D_n^{α} given in Eqn.4.20, the Gumbel distribution for both fill and warp strength data of the samples

prepared by yarn-stripping failed the K-S test. All the other candidate distributions passed the test. The Weibull distribution gives the best fit for both fill and warp directions, with corresponding D_n values significantly lower than those of the other distributions.

Direction	Normal (μ,σ)	Log-normal (a,b)	Laplace (a,b)	Gumbel (a,b)	Frechet (a,b)	Weibull (a,b,c)
Fill	96.9, 4.3	4.58, 0.046	96.9, 3.2	95.2, 5.91	87.3, 37.2	81.5, 5.817, 17.8
Warp	87.2, 2.8	4.47, 0.032	87.2, 2.082	88.5, 3.5	86.5, 40.1	76.1, 5.5, 12.2

Table 4.15: Estimated distribution parameters for uniaxial strength of samples by yarn-stripping cutting

Direction	Normal	Log-normal	Laplace	Gumbel	Frechet	Weibull
Fill	0.171	0.172	0.195	0.271	0.156	0.106
Warp	0.114	0.116	0.143	0.397	0.110	0.071

Table 4.16: K-S test D_n^α values for uniaxial strength of samples by yarn-stripping cutting

It is found that the tensile failure strengths follow the Weibull distribution. Considering that, in the physical failure process of the specimens, rupture always occurs in the weakest yarns of the fabric specimen and then propagate to other yarns quickly until the whole cross-section breaks, then the tensile capacity of the fabric specimen can be clearly seen to be dependent to the minimal yarn strength of the specimen. The randomness in the tension strength is then mainly controlled by the instability of the weakest yarn within the fabric of every 50 mm width (specimen width). With the Weibull distribution known to represent the randomness of extreme values of yarn strength [46], and now the best data-fitting distribution for the fabric strength, the statistical relationship between the strength of the fabric and its yarns is implied for this limited test data.

Stress-strain relation

The parameters of the candidate distributions attempting to fit Young's modulus under linear loading in different loading zones are given in Table.4.17. The K-S test is applied to determine the best data-fitting distribution based on the D^n values calculated and listed in Table.4.7. The critical D^α values can be calculated based on the n values which are obtained from the number of different values in each sample set. For the fill specimen data, the n values are 104 for Zone I & II, and 66 for Zone III, giving the critical values with 0.05 significance coefficient in the three zones for fill Young's modulus under linear loading calculated using Table.4.7 ,

$$D_{104}^{0.05} = 1.36/\sqrt{104} = 0.133, \quad \text{Zone I\& II}, \qquad D_{66}^{0.05} = 1.36/\sqrt{66} = 0.167, \quad \text{Zone III} \tag{4.21}$$

While in the warp direction, the n are 95, 22 and 62 for Zone I, II & III, the corresponding

critical values with 0.05 significance coefficient for K-S test are computed as,

$$D_{95}^{0.05} = 1.36/\sqrt{95} = 0.131, \quad , D_{22}^{0.05} = 0.282 \quad , D_{62}^{0.05} = 1.36/\sqrt{62} = 0.172 \tag{4.22}$$

Linear loading

Direction	Inteval	Normal (μ,σ)	Log-normal (a,b)	Laplace (a,b)	Gumbel (a,b)	Frechet (a,b)	Weibull (a,b,c)
Fill	Zone I	377.0, 51.1	5.93, 0.11	377.0, 31.16	366.0, 35.8	465.1, 5.3	282.0, 2.2, 109.2
	Zone II	237.2, 41.0	5.47, 0.048	273.2, 7.94	234.2, 15.9	250.2, 15.8	181.0, 7.8, 60
	Zone III	638.1, 41.0	6.46, 0.075	638.1, 38.61	627.4, 58.8	607.4, 46.8	440.0, 4.6, 220
Warp	Zone I	512, 108	6.21, 0.24	512, 86.3	454.6, 116.7	465.1, 5.3	220.0, 3.7, 350.0
	Zone II	216, 56	5.38,0.0257	216.4, 4.3	213.7, 4.9	212.0, 46.5	202.0, 3.2, 16.0
	Zone III	612, 20	6.416, 0.032	612.3, 18.95	602.4, 18.9	600.0, 35.0	569.0, 1.9, 50.1

Table 4.17: Estimated distribution parameters for Young's modulus of samples under linear loading

Direction	Inteval	Normal	Log-normal	Laplace	Gumbel	Frechet	Weibull
Fill	Zone I	0.119	0.079	0.157	0.051	0.12	0.091
	Zone II	0.109	0.123	0.094	0.28	0.239	0.082
	Zone III	0.18	0.169	0.202	0.236	0.17	0.144
Warp	Zone I	0.055	0.11	0.084	0.089	0.636	0.058
	Zone II	0.079	0.071	0.111	0.129	0.246	0.091
	Zone III	0.043	0.057	0.068	0.088	0.147	0.096

Table 4.18: K-S test D_n^α values of Young's modulus of samples under linear loading

As shown in Table.4.18 , the Laplace and Weibull distributions fail the K-S test for fitting the data of fill Young's modulus in Zone I, and the other distribution passed the test. For the data of Young's modulus in Zone II, four distributions: Normal, log-normal, Laplace and Weibull pass the K-S test, and Laplace and Weibull distributions have a better fitness of the data with comparatively smaller D_n values. The best-fitting distributions for the data of the fill Young's modulus under linear loading can be simply determined in Zone I and II, based on the minimum D_n values. Gumbel and Weibull distributions with the relevant parameters represent the data best for Zone I and Zone II respectively. However in the case of the Zone III fill Young's modulus, only the Weibull distribution, passes the K-S test, and the gap between the Weibull distribution and sample data is not insignificant. In this case, it is necessary to check the detailed distribution of sample data. As shown in fig.4.19 , the cumulative sample frequency has a significantly different increase with the sample data, that the cumulative frequency of about the first 30% data interval achives as high as 50%,. Such that a unbalance shape make it difficult to fit using the candidate distributions with the smoothly changed CDF.

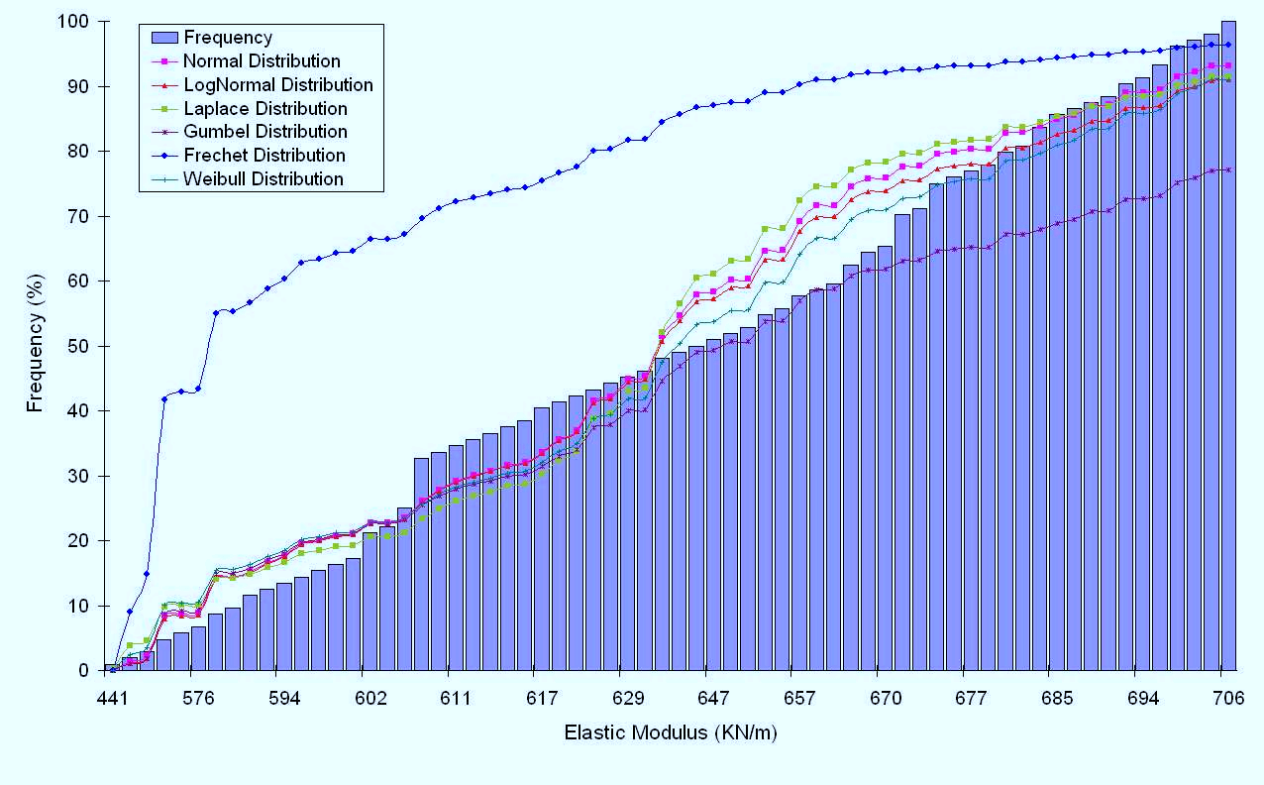

Figure 4.19: KS test for Young's modulus in Zone III of sample by plain cutting

The PDF of the sample data with all candidate distributions is presented in fig.4.20 , which gives clearer information above the sample data distribution. The data forms a double-peak shape, bi-modal and the majority of Young's modulus values around $586kN/m^2$ and $655kN/m^2$, while few data exist in the values between the peaks. There are two possible reason to obtain this data shape. One is because the test sample number is not sufficient to form a representative histogram, which has a mono-peak shape. The other possible reason is that the double-peak shape distribution is the inherent characteristic of the sample data, and as such this shape will be maintained even with more test data. In that case, the candidate distributions with monopothetic peak shapes are difficult to fit the test data. It may then be necessary to separate the data into two parts with each part of the data are distributed around one peak value, as shown in fig. 4.21 and 4.22. An attempt may then be made to find a data-fitting distribution for both part as follows.

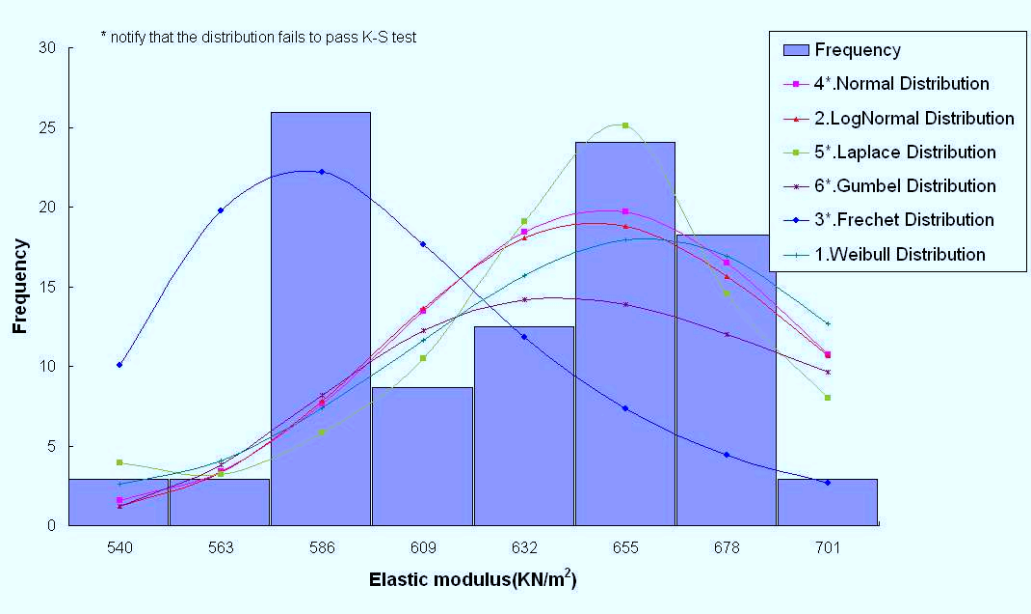

Figure 4.20: Distributions for fill Young's modulus in Zone III of Sample under linear loading

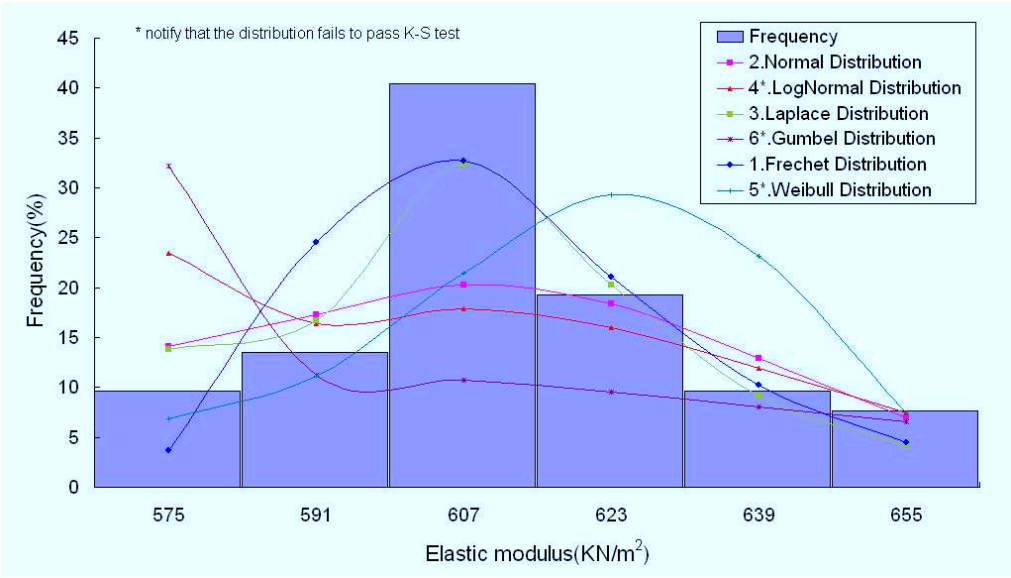

Figure 4.21: Distributions for warp Young's modulus in Zone III of samples by linear loading (part I)

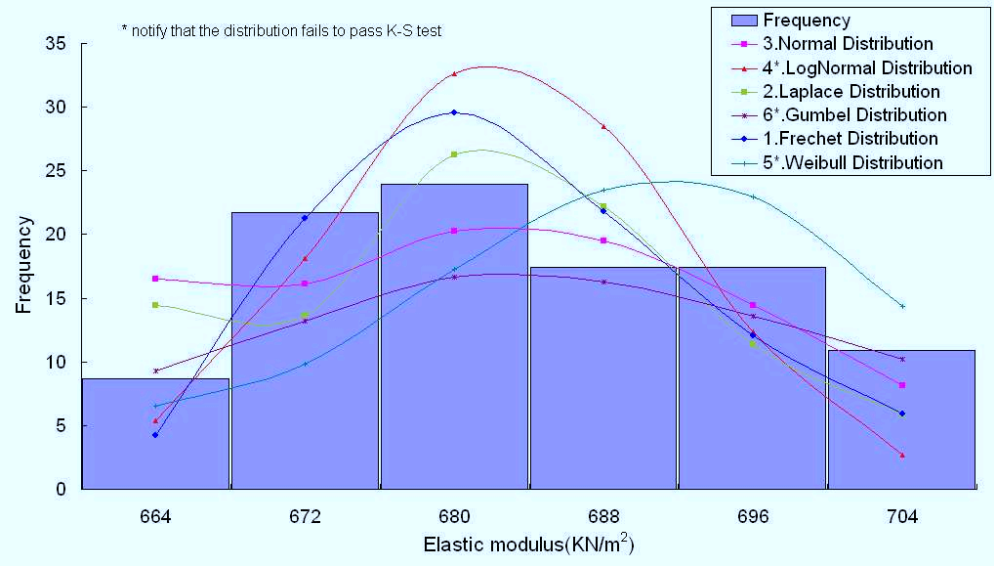

Figure 4.22: Distributions for fill Young's modulus in Zone III of samples by linear loading (part II)

Distribution	Fill Young's modulus in Zone III (Linear loading)	
	Part I	Part II
Normal	0.051	0.139
Log-normal	0.149	0.171
Laplace	0.067	0.107
Gumbel	0.271	0.219
Frechet	0.042	0.072
Weibull	0.162	0.199
Critical value	0.145	0.164

Table 4.19: K-S test D_n^α values of fill Young's modulus under linear loading in Zone III

Even though only three candidate distributions pass K-S test, D_n^α values corresponding to these qualified distributions are comparative small as listed in Table.4.19, indicating a good fit between the sample data and the approximating distribution.

As discussed in this section, most statistical variables fluctuate about the mean values, and the test data will form bell-shape histograms. There is one exception: EIII of Ferrari 1002 - linear loading(fig. 4.20), which has remarkable change over material space. In that case, it is necessary to look at the data corresponding to the Young's modulus variation over the material space.

As shown as fig. 4.23, the Zone III Young's modulus does not fluctuate equally about one value while oscillate about one value along 3m long, then increase and start to swing about another value along the rest of the fabric roll. In that case, the uncertainty information of the fabric cannot be represented by COV values accurately because in the most place of the fabric, the variance is not much and the changing over the fabric roll is smooth and gradual while high COV value may be evaluated because of the large variance range. Therefore the test data can be separated into two group with different mean value and standard deviation

so that the stochastic information of the fabric can be more accurately described. Therefore, the data is separated into two sets with the division line at the 3m distance from A-A line. Data-fitting tests then are taken separately for the two sets data, and demonstrated by fig. 4.21 and 4.22.

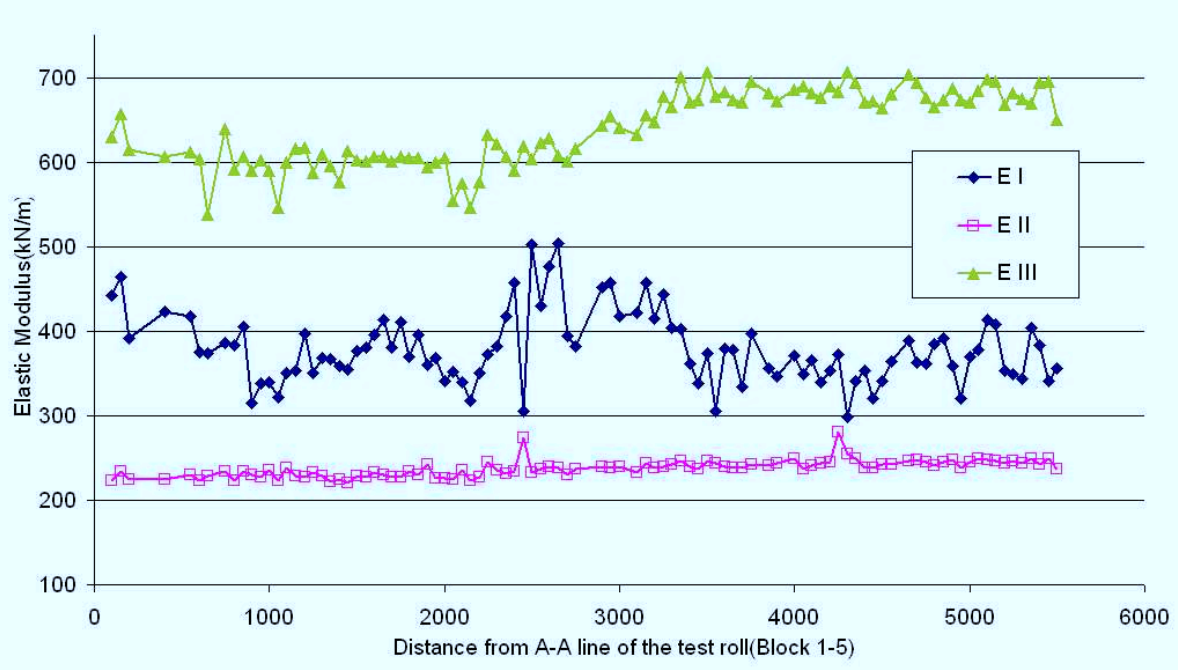

Figure 4.23: Fill Young's modulus along the longitude direction of the fabric roll(Ferrari 1002 - Group I)

For both parts, the Frechet Distributions are the best data-fitting distributions. Despite the fact that the representative distribution types for both parts are the same, the data in these two parts follow two individual Frechet distributions with different PDF and CDF functions as,

For part I:

$$\begin{aligned} PDF: \ f(x) &= \frac{1}{35.1} exp[-\frac{x-595.1}{35.1}] exp[exp(-\frac{x-595.1}{35.1})] \\ CDF: \ F(x) &= 1 - exp\{-exp[-\frac{x-595.1}{35.1}]\} \end{aligned} \tag{4.23}$$

For part II:

$$\begin{aligned} PDF \ f(x) &= \frac{1}{70.2} exp[-\frac{x-675.1}{70.2}] exp[exp(-\frac{x-675.1}{70.2})] \\ CDF \ F(x) &= 1 - exp\{-exp[-\frac{x-675.1}{70.2}]\} \end{aligned} \tag{4.24}$$

As listed in Table.4.18 , the data for the warp Young's modulus under linear loading in Zone I can be represented by Normal and Weibull distributions since both of them have small values of D_n compared with the critical values given in Eqn.4.22 . However the best-fitting distribution cannot be directly determined because these two distribution have very similar

D_n values. Judgement should once again take account of the data fit in the entire data zone. As shown in fig.4.24, in the first small part of the accumulative sample data, the normal distribution is slightly better than the normal distribution in data-fitting, however in the most subsequent data area, Weibull distribution seems to have better fittness rather than Normal distribution. So Weibull distribution should be considered as best fitting distribution based on the graphic comparison.

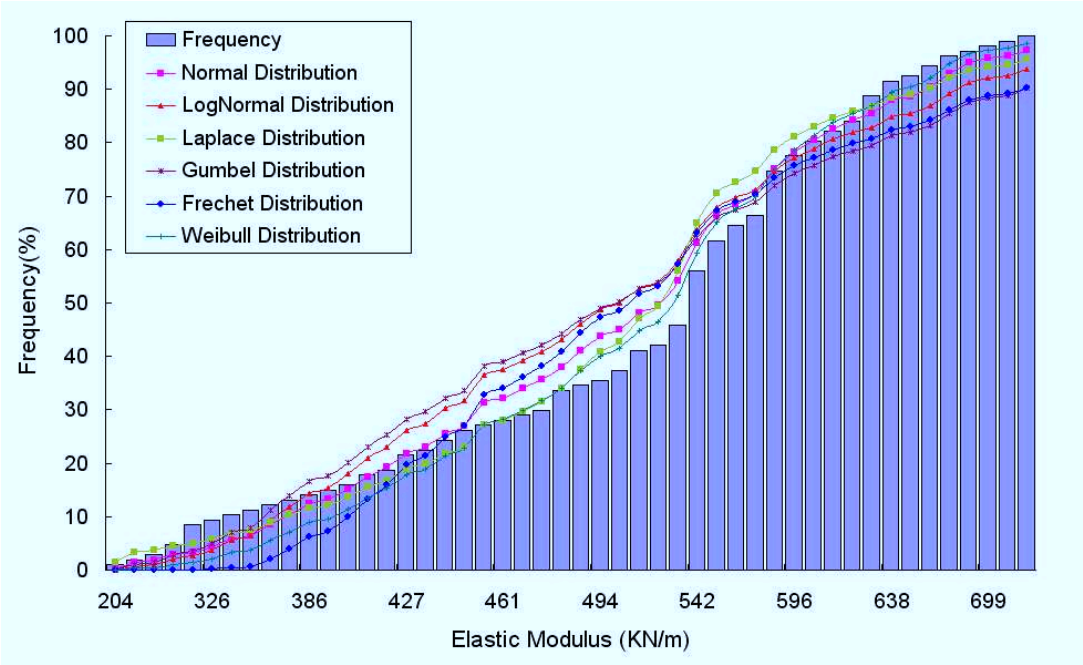

Figure 4.24: KS test of warp Young's modulus in Zone I of sample by linear loading)

The decision of the best distribution for the warp Young's modulus under linear loading in Zone II may also require a review of the CDF and corresponding fit as close D_n values are found for the normal and log-normal distributions as listed in Table.4.18. The log-normal distribution fits the test data better than the others in the most data area(fig.4.25). For the warp Young's modulus data in Zone III, the best fitting distribution is the normal distribution, since it has a obviously lower D_n value rather than other qualified distributions.

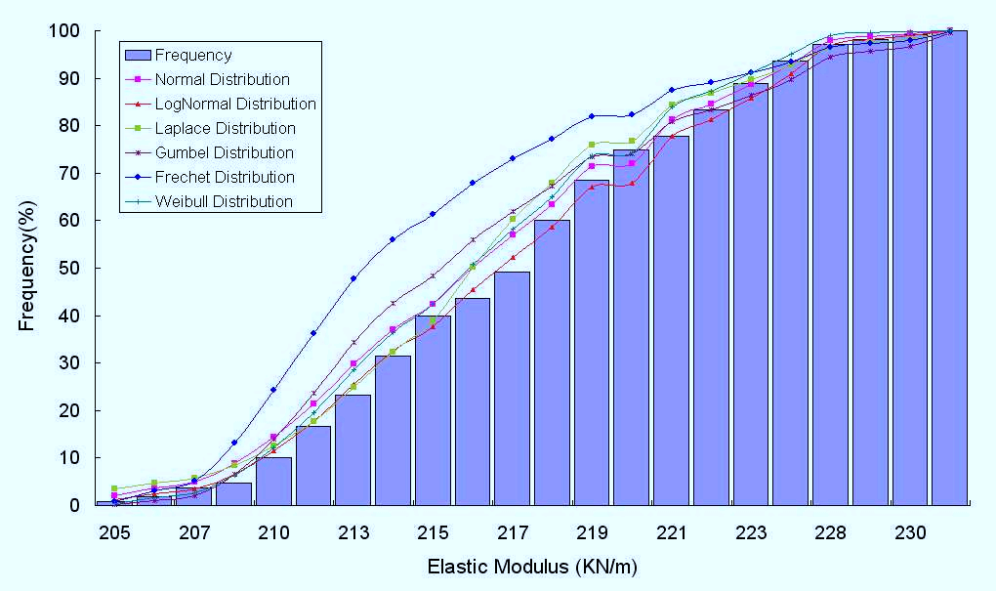

Figure 4.25: KS test of warp Young's modulus in Zone II of sample by linear loading)

Cyclic loading

Based on the number of different sample values, the n values of the K-S test for the sample data of Young's modulus under cyclic loading have $n = 42$ for the fill modulus, and $n = 61$ for the warp modulus in cycle loading zones, the critical D_n^{α} value with 0.05 significance coefficient for the data of the fill modulus under cycle loading are,

$$\begin{aligned} D_{42}^{0.005} &= 0.208 \quad \text{For fill Young's modulus in Zone I and II} \\ D_{61}^{0.005} &= 1.36/\sqrt{61} \\ &= 0.174 \quad \text{For warp Young's modulus in Zone I and II} \end{aligned} \tag{4.25}$$

Based on the comparison between the D_n values listed in Table.4.21 and the critical values given in Eqn.4.25, the best fitting distributions for the data of fill Young's modulus under cyclic loading can be determined. The Frechet distributions with the estimated parameters given in Table.4.20 are best-fitting distributions for the sample data of the fill Young's modulus in Zone I, and in Zone II, the log-normal distribution with a minimum D_n value can be concluded as best-fitting distribution.

Direction	Interval	Normal (μ,σ)	Log-normal (a,b)	Laplace (a,b)	Gumbel (a,b)	Frechet (a,b)	Weibull (a,b,c)
Fill	Zone I	832.6, 31.2	6.73, 0.040	823.6, 26.4	818.8, 29.8	819.5, 32.2	769.5, 2.81, 73.3
	Zone II	1197.9, 40.5	7.09, 0.047	1197.9, 47.7	1171.7, 55.4	1181.7, 22.1	1080.5, 2.2, 137.3
Warp	Zone I	804.1, 70.5	6.69, 0.096	804.1, 49.8	842.0, 98.6	781.0, 15.2	640.0, 350.0, 3.7
	Zone II	1140.8, 87.6	7.04, 0.079	1140.8, 71.1	1163.5, 86.5	1103.5, 13.2	926.1, 2.81, 241.3

Table 4.20: Estimated distribution parameters for Young's modulus of samples under cycle loading

Direction	Interval	Normal	Log-normal	Laplace	Gumbel	Frechet	Weibull
Fill	Zone I	0.089	0.11	0.107	0.09	0.062	0.099
	Zone II	0.141	0.075	0.098	0.114	0.115	0.084
Warp	Zone I	0.091	0.119	0.06	0.4	0.066	0.096
	Zone II	0.059	0.053	0.056	0.286	0.086	0.045

Table 4.21: K-S test D_n^α values of Young's modulus of samples under cycle loading

A graphical comparison is necessary when judging the best distributions for warp Young's modulus in both cyclic zones. For the Young's modulus in Zone I, both Laplace and Frechet distribution can achieve good fits. When comparing these two distributions in fig.4.26, it is found that the two distributions seem approximately equivalent in certain parts. The Laplace distribution seems to have a better fit in the left half of the sample data, while the Frechet distribution provides a good-fit to the rest of the data. From either statistical or mechanical aspect, there is no evidence to identify if the data-fitting in the first half part of CDF is more important than the other. Therefore in that case, it's difficult to decide which one is the best data-fitting distribution, since they have very close D_n values and similar fitting goodness in general. So either of the Laplace or Frechet distribution can be regarded as the best distribution for the sample data.

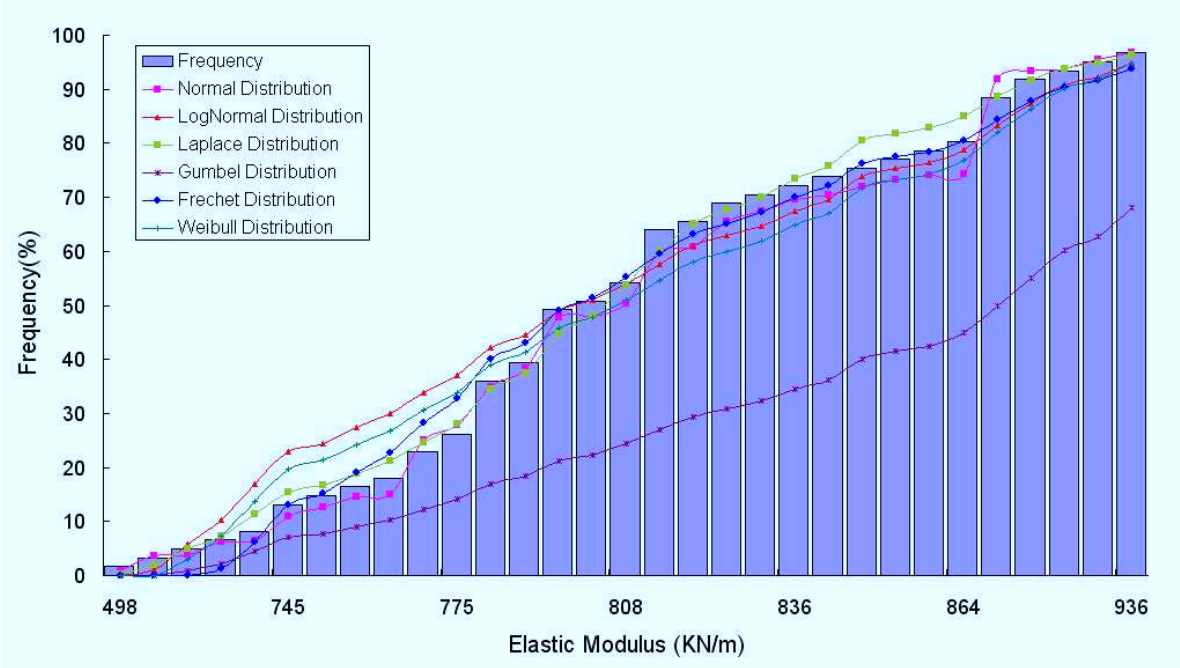

Figure 4.26: KS test of warp Young's modulus in Zone I of sample by cycle loading)

For the sample data of warp Young's modulus under cyclic loading in Zone II, Table.4.21 suggests that most distributions except the Gumbel distribution pass the K-S test with very small D_n values compared with the critical D_n^α. Three distributions following the very similar fitting lines as shown in fig.4.27. However Table.4.21 indicates that the Weibull distribution is closest distribution to the sample data.

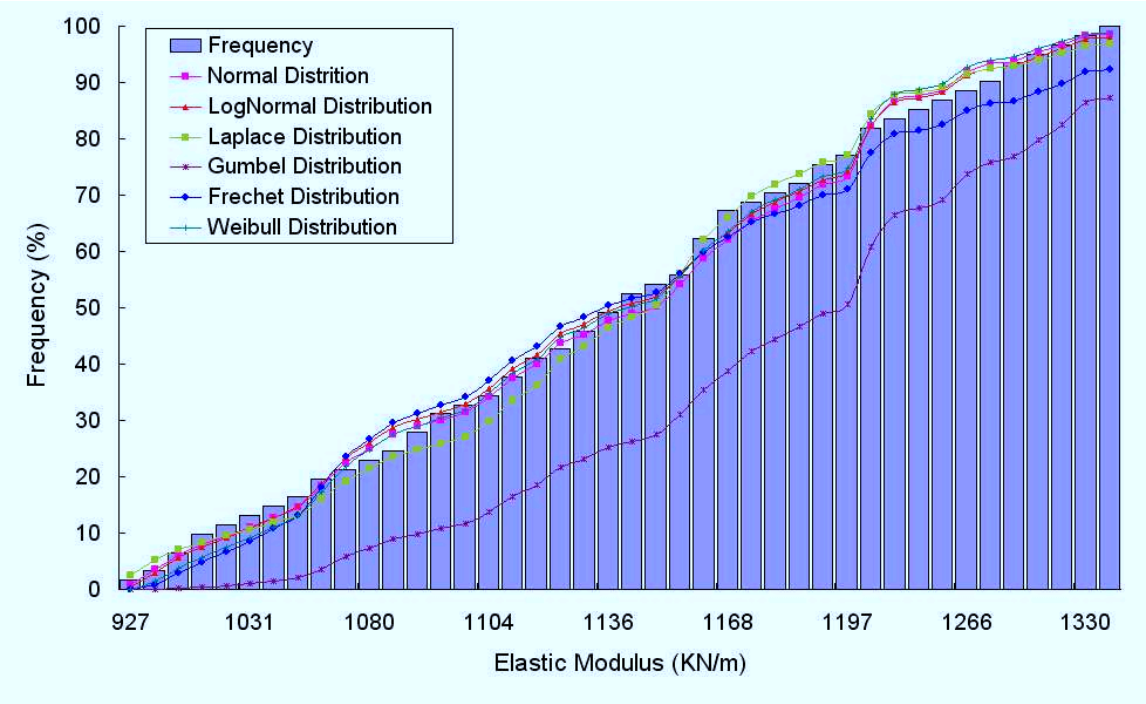

Figure 4.27: KS test of warp Young's modulus in Zone II of sample by cycle loading)

Summary of the best distributions representing the sample data

Uniaxial strength

As shown in Table.4.22, it is found that the tensile failure strengths of all the test data including plain-cut and yarn-stripping samples are best presented by the Weibull distribution, and that different distributions may be used to represent the Young's modulus data of the fabrics.

Considering that in the physical failure process of the specimens, rupture may occur in the weakest yarns of the fabric specimen, then propagate to other yarns quickly until the whole cross-section breaks. The tensile capacity of the fabric specimen may depend on the extreme low value of yarn strength of the specimen, and that the randomness in the tension strength may be mainly contributed by the instability of the weakest yarn strength within the fabric of every 50 mm width (specimen width).

Given that the Weibull distribution, is known to represent the randomness of extreme values of yarn strength [46], and is also found to be best data-fitting distribution, the statistical relations between the strength of the fabric and its yarns is implied.

	Plain-cut	Yarn-stripping
uniaxial Strength	Weibull	Weibull

Table 4.22: Summary of best data-fitting distribution for the uniaxial strength

Uniaxial stress-strain relationship

In contrast, the uncertainty content of the stress-strain relation in the fabric is complex in that the uncertainty in both the manufacture and material test process increase the randomness

of the Young's modulus estimate. It is notable that the data for Young's modulus are not directly read from the test machine, but as presented here, through a tri-linear regression formulation. The choice of the mathematical model is, therefore also a source of uncertainty. Consequently, the randomness of the Young's modulus data is the combination of a number of different uncertainty sources, which may each follow different distributions. When their effects on test data are evenly assembled, it's very hard to use a uniform distribution to describe the variation of the stress-strain relationship for both types of fabric samples as presented in Table.4.23 and 4.24.

Direction	Zone I	Zone II	Zone III
Fill	Gumbel distribution	Weibull distribution	Bi-modal Frechet distribution
Warp	Weibull distribution	Log-normal distribution	Normal distribution

Table 4.23: Summary of best data-fitting distribution for the linear testing data

Direction	Zone I	Zone II
Fill	Frechet distribution	Log-normal distribution
Warp	Laplace distribution	Frechet distribution

Table 4.24: Summary of best data-fitting distribution for the cycle loading data

4.6 Summary

The assumption of orthotropy between fill and warp may not be valid for a coated woven fabric. The distribution of the yarns in the fabric may be very important for affecting the structural performance such as strength and stress-strain relationship. The fabric sample prepared by different cutting procedure can display wholly different characteristics in the mechanical properties, should be considered as two different types of statistical variable in the probabilistic investigation and analysis.

An initial small number of tests suggests that the yarn-stripping samples have higher mean strength and also standard deviation than those made by plain-cut. Their similar COV value may imply that the uncertainty of the fabric strength is more relevant to the randomness of the individual yarn strength rather than the composite structure. That may be further demonstrated by the more probabilistic similarities (e.g. skewness) for these two types of test samples subsequently observed in the large number of tests

The stress-strain relationship under monotonic and cyclic loads are distinctive in both deterministic and probabilistic aspects. The Young's modulus values obtained based on cyclic loading have obviously higher values in magnitude and less randomness compared with those from monotonic loading, indicating that large plastic strain with high randomness may occur when a monotonic load is applied to the fabric.

The determination of the best-fit distributions for the test data may start with the initial candidate distributions selected based on the data histogram, then further judgement can be made using the K-S test. To take account of the calculation tolerance, the graphic comparison may be required when several distributions are equivalent in fitting the test data. When few distributions seem to fit the test data, further procedures (e.g. bi-modal model) may be required for a valid representation of the test data.

The analysis of the test data suggests that Weibull distribution seems to be the best-fitting distribution for the uniaxial strength of both types of test samples made by plain cut and yarn-stripping. While a uniform distribution fitting the data of Young's moduli has not been observed. It seems that the Young's moduli under monotonic and cyclic loads have different distributions. In each loading zone, distinctive best-fitting distributions are observed under the same type of load condition.

Chapter 5

Reliability Analysis of Fabric Structures

In the majority of national and European codes, the "limit state" approach with safety coefficients is used to obtain an optimal safe design, which is regarded as a trade-off between reliability and cost. The safety coefficients correspond to the uncertainty in structural form and materials, and are obtained through experiments or estimated empirically. In traditional structural design (e.g. concrete structures), both the material strength and the loads are factored to achieve a sufficient safety margin. However, in fabric structure analysis and design, increased loading normally changes both the magnitude and distribution of the stresses significantly owing to geometric non-linearity. "A limit state approach(with partial safety factors applied to the loading conditions as well as material strengths) may not be appropriate since the geometry of the structure is dependent on both the magnitude and the distribution of loading"(see European Design Guide for Tensile Surface Structures, 2004,p178). Therefore in fabric structure design, a permissible stress design philosophy is used in which safety factors are applied to the material strength. Maximum factors are 7.0 in IASS code, 8.0 in Japan code and and 9.5 in the German code.

These safety factors are recommended in fabric design codes corresponding to material variability(e.g consistency and degradation) and uncertainty in loading, load effects(e.g. tearing) and analysis/simulation accuracy, but their influence on the structural reliability is ambiguous and cannot represent the randomness in fabric structures accurately. Thus, there is a strong motivation to develop a structural reliability method to analyze fabric structures using probabilistic information describing loads, material properties, and geometry, which may then be used to calibrate new factors or confirm existing factors of safety.

A objective target in structural reliability analysis is the estimation of the probability of failure to achieve a prescribed structural performance. In a finite element-based reliability analysis, the input parameters for the finite element model are defined as a set of random variables X, leading to a unique response vector for a given realization of X. A set of continuous and differentiable limit-state functions $G(X)$ are defined, where $G(X) < 0$ indicates the structural

failure of the components or partial component of the system. Here, it is essentially assumed that fabric structures have several modes of failure and that each failure mode can be described in terms of a single limit state function.

For complicated structures, explicit solutions of the probability of the structural failure are difficult to obtain. Therefore, approximate reliability methods are required to make the problem tractable. These include first and second-order reliability methods (FORM and SORM) [239] and other approximation methods, such as Response Surface approaches [240, 241]. Incorporating with the Hasofer-Lind method [184], FORM has emerged as one of the most effective reliability methods to evaluate the probability of structural failure.

The Hasofer-Lind method, which linearizes the limit state function at the most probable failure point (MPP) and characterizes all the random variables with mean values and standard deviations only, was extended by Rackwitz and Fiessler [242] by including detailed random variable information with different(non-normal) distributions. This led to an efficient safety index algorithm was developed with the advantage that only the values of the limit state functions and their derivatives were needed to be computed instead of solving the limit state function explicitly. The value of the limit state functions can be obtained through a deterministic structural analysis, with the derivatives of $G(X)$ calculated either analytically or numerically, forming effectively a sensitivity analysis of the structural performance with respect to uncertainty.

Apart from an immediate application to FORM, the sensitivity analysis is also important in enabling the effects of the random variables on the fabric structure response to be observed and quantified. For variables with large effects on structural failure, their uncertainty may be reduced by collecting additional information through testing or by making design changes at structural, material and manufacturing levels. For those variable having little influence on structural reliability, they may be simplified as deterministic values to save computational effort, without compromising the accuracy of the reliability estimate. It is possible to derive different design safety factors for random variables individually based on their uncertainties and their influence on structure behavior. Two methods of sensitivity analysis, namely finite difference and analytic approach are introduced and detailed in section 5.3.1 and 5.3.2.

Combining sensitivity analyse and FORM to estimate the probability of failure of a system with an implicit limit state function uses information about the value and gradient of the limit state function at the checking point(or design point), and an iterative optimization scheme to determine to the safety index.

5.1 Safety criterion and limit state functions

The first step in evaluating the reliability of fabric structure is to identify and quantify the uncertainties existing in the realization of the structure. Generally, the main sources of uncertainty can be separated into several categories: material properties, manufacturing or fabrication and construction conditions, environmental impact(load), human effects. However the information of some type of uncertainties (e.g human effects) are case-dependent and not easy to obtain accurately. The reliability analysis in this chapter is limited to include uncertainty in the material properties and loads. A typical membrane structure comprises several materials: fabric, cables, supporting steelwork. Uncertainty of each type of material can be identified by individual statistical variables X. Six statistical variables are defined to represent the uncertainty information of fabric properties:

$$X_1 = E_f,\ X_2 = E_w,\ X_3 = v_{wf},\ X_4 = G_{wf},\ X_5 = \sigma_{ult}^{fill},\ X_6 = \sigma_{ult}^{warp} \tag{5.1}$$

where E_f,E_w are Young's modulus in the fill and warp directions, G_{wf} is the shear modulus across the fill and warp direction, v_{wf} is Possion's ratio, and σ_{ult} is ultimate strength of fabric (rupture strength).

An additional statistical variable is identified with the imposed load coefficient t_{load} with unit mean value:

$$X_7 = t_{load} = \frac{F}{F_c} \tag{5.2}$$

where F is the applied load, F_c is the deterministic value of design load.

Each statistical variable can be characterized by mean value μ, standard derivation σ, and a probability density function (PDF), which can be estimated by material tests combined with formal statistical analysis including the transformation of non-normal distributions.

Unlike traditional construction materials, a structural fabric material is a type of tension-only composite, which is made of fibres in two directions: fill and warp. Therefore material failure of a fabric includes the rupture of the yarns in either direction and the appearance of wrinkles which indicates the disappearance of a positive minimum principal stress, for example (other criteria exist- see wrinkling section in the chapter.3 "Deterministic Fabric Structure Analysis").

The safety criterion related to material stress can be expressed using three functions $G_1(X_s)$, $G_2(X_s)$, and $G_3(X_s)$ defined in Eqn.5.3, in which material failure occurs when $G_i < 0$, $i = 1, 2, 3$.

$$G_1(X_{si}) = \sigma_{per}^{f} - \sigma_{max}^{f},\quad G_2(X_{si}) = \sigma_{per}^{w} - \sigma_{max}^{w},\quad G_3(X_{si}) = \sigma_{min}^{p} - \sigma_{per}^{p} \tag{5.3}$$

where σ_{per}^{f} and σ_{per}^{w} are permissible stresses in fill and warp direction respectively, and normally computed as products of ultimate strength and safety factors:

$$\sigma^f_{per} = \sigma^f_{ult}, \qquad \sigma^w_{per} = \sigma^w_{ult} \tag{5.4}$$

in which, f_f and f_w are safety factors for ultimate strength of fill and warp. These safety factors are normally defined and estimated to taken into account the material degradation due to the environmental impacts [4]. σ^f_{max} and σ^w_{max} are maximum tension stresses in the fabric along fill and warp direction separately. σ^p_{min} is the minimum principal stress of the membrane, and σ^p_{per} is the predefined lower limit which normally corresponds to a percentage of the fabric pre-stress, and X_{si} is the relevant statistical variable.

One basic serviceability requirement in structural design is that the deformation should be controlled to a reasonable level, as in

$$G_4(X_s) = D_{al} - D_{max} \tag{5.5}$$

in which, D_{al} is the deformation allowance, and D_{max} is the maximum deformation.

The fabric structure surface should avoid excessive deformation to ensure adequate structural performance related to phenomena such as ponding - with the structural geometry such that there is positive drainage from all areas. An undeformed pretensioned membrane normally has an anticlastic shape, which provides effective drainage, but large membrane deformation especially in the vertical direction may lead to ponding in some local areas. Therefore, the allowable deformation D_{al} in Eqn.5.5 must be set not only based on the general serviceability requirement, but also allowing for the ponding mitigation.

The failure surface or the limit state i is defined as $G_i = 0$. This represents the boundary between the safe and unsafe regions in the design parameter space, and also identifies states beyond which the structure can no longer fulfill the function for which it was intended. The failure surface and the safe and unsafe regions in respect of statistical variables X_{s1} and X_{s2} are shown in Fig.5.1.
In n variable parameters space, the probability of structural failure p_f can be calculated using Eqn. 5.6

$$p_f = \int \cdots \int_{g(X_s)<0} f_X(x_{s1}, x_{s2}, \cdots, x_{s7}) dx_1 dx_2 \cdots dx_n \tag{5.6}$$

in which $f_X(x_{s1}, x_{s2}, \cdots, x_{sn})$ is the joint probability density function for the statistical variables $X_{s1}, X_{s2}, \cdots, X_{sn}$ and the integration is performed over the failure region $G(X_s) < 0$. If it is assumed that the random variables are statistically independent and the limit state function is a simple combination of design variables, then the joint probability density function may be replaced by the product of the individual probability density functions in the integral.

The computation of p_f by Eqn. 5.6 is the fundamental equation of reliability analysis. The joint probability density function of random variables f_{Xs} is often not available in practice and the multiple integral is also extremely complicated to estimate. The first-order reliability

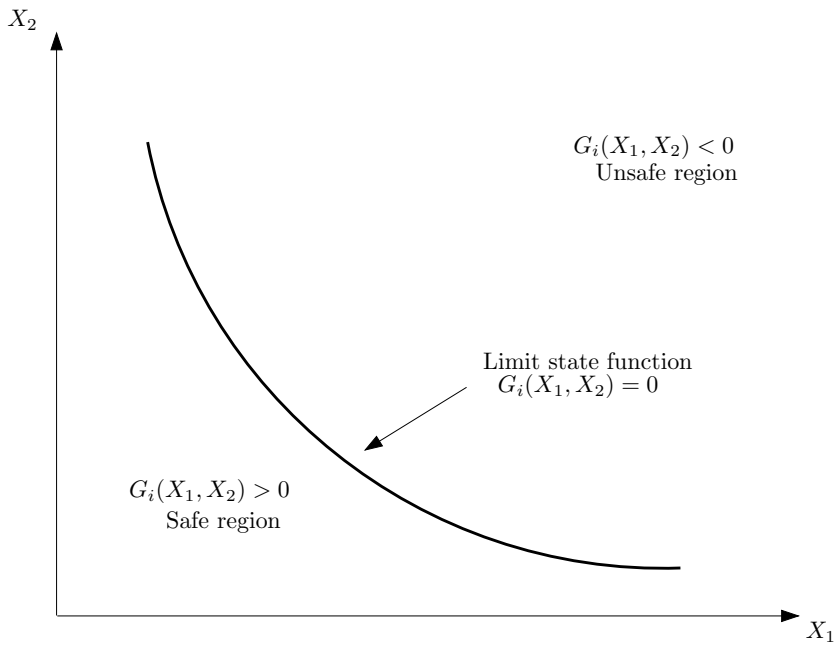

Figure 5.1: Illustrative limit state function ,safe and unsafe regions

method(FORM) uses analytical approximations of this integral that are simpler to compute, making Eqn.5.6 more tractable.

5.2 FORM analysis - principles

Using a first-order approximation with equivalent normal variables, FORM can be used to estimate the probability of structural failure based on the information of the first and second moments of the random variables. Generally, the limit state function G_i can be written as:

$$G_i = f_i(X_{s1}, X_{s2}, \cdots, X_{sn}), \quad i = 1 \rightarrow 4 \tag{5.7}$$

in which, f_i is the function of the random variables for ith limit state function.

A Taylor series expansion of the limit state function about the mean value gives:

$$G_i = f_i(\mu_{Xs}) + \sum_{i=1}^{n} \frac{\partial f_i}{\partial X_{si}}(X_{si} - \mu_{X_{si}}) + \frac{1}{2}\sum_{i=1}^{n}\sum_{j=1}^{n} \frac{\partial^2 f_i}{\partial X_{si}\partial X_{sj}}(X_{si} - \mu_{X_{si}})(X_{sj} - \mu_{X_{sj}}) + \cdots \tag{5.8}$$

where the derivatives are evaluated at the mean values of the random variables $(X_{s1}, X_{s2}, \cdots, X_{sn})$, and μ_{Xsi} is the mean value of variable X_{si}. Truncating the series at the linear terms, we obtain the first-order approximation function:

$$G_i \approx f_i(\mu_X s) + \sum_{i=1}^{n} \frac{\partial f_i}{\partial X_{si}}(X_{si} - \mu_{Xsi}) \tag{5.9}$$

Assuming that $X_{s1}, X_{s2}, \cdots, X_{sn}$ are statistically independent normally distributed random

variables, the function G_i is also normally distributed, and the approximate mean and variance of G_i are:

$$\mu_{G_i} \approx f_i(\mu_{X_{s1}}, \mu_{X_{s2}}, \cdots, \mu_{X_{sn}}) \tag{5.10}$$

and

$$\sigma^2_{G_i} \approx \sum_{i=1}^{n} \left(\frac{\partial G_i}{\partial X_{si}} \right)^2 Var(X_{si}) \tag{5.11}$$

The probability of structural failure is defined as:

$$p_f = P(G_i < 0) \tag{5.12}$$

or

$$p_f = \Phi \left(\frac{0 - \mu_{G_i}}{\sigma_{G_i}} \right) = 1 - \Phi \left(\frac{\mu_{G_i}}{\sigma_{G_i}} \right) = 1 - \Phi(\beta) \tag{5.13}$$

where Φ denotes the CDF of the standard normal variate.

The probability of structure failure calculated by Eqn. 5.13 depends on the ratio of the mean and standard deviation of G_i. This ratio is called the safety index or reliability index and is denoted as β:

$$\beta = \frac{\mu_{G_i}}{\sigma_{G_i}} \tag{5.14}$$

When calculating the safety index using Eqn. 5.14, explicit information about the mean and standard deviation of the limit state function is required. This information is normally not known explicitly, particularly when using simulation techniques such as the finite element method. The problem arises that the safety indices depend on the formulation of the limit state equation as well as the underlying assumption about the distribution of the limit state. This problem was overcome by the Hasofer-Lind method [184], in which, a reduced coordinate system and reduced variables are defined first as:

$$X'_{si} = \frac{X_{si} - \mu_{Xsi}}{\sigma_{Xsi}} (i = 1, 2, \cdots, n) \tag{5.15}$$

Where X'_{si} is a random variable with zero mean and unit standard deviation. Eqn. 5.15 is used to transform the original limit state $G(X_s) = 0$ to the reduced limit state, $G(X'_s) = 0$. The X_s coordinate system is referred to as the original coordinate system and the X'_s coordinate system is referred to as the reduced coordinate system. The safety index is redefined as the minimum distance from the origin of the axes in the reduced coordinate system to the limit state surface. It can be expressed as:

$$\beta_{H-L} = \sqrt{(x'^*_s)^t (x'^*_s)} \tag{5.16}$$

The minimum distance point on the limit state surface is called the design point or checking point. It is denoted by the vector x_s^* in the original coordinate system and by vector $x_s'^*$ in the reduced coordinate system. These vectors represent the values of all the random variables $(X_{s1}, X_{s2}, \cdots, X_{s7})$ at the design point corresponding to the coordinate system being used.

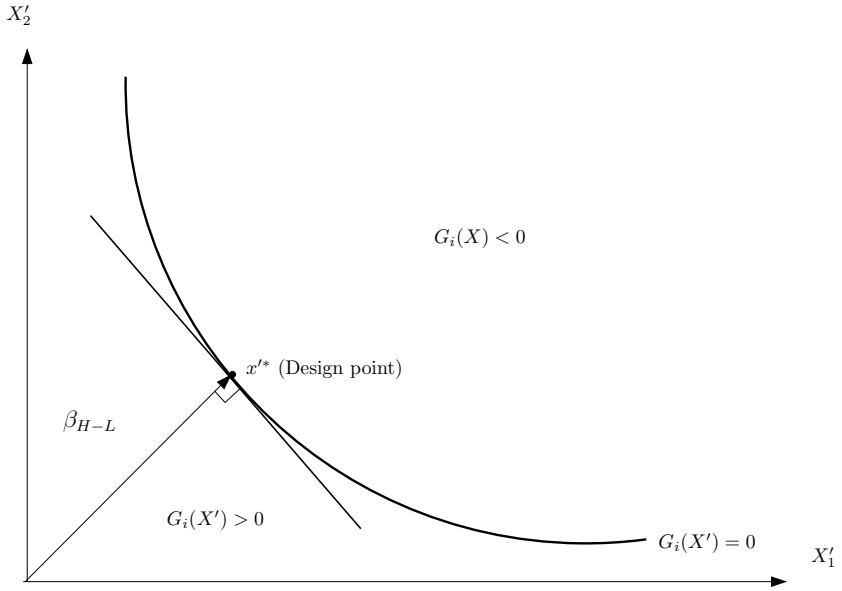

Figure 5.2: Hasofer-Lind reliability index: nonlinear limit state function [184]

As illustrated in fig. 5.2 , it is clear that the nearer $x_s'^*$ is to origin, the larger is the failure probability. Thus, the minimum distance point on the limit state surface also locates the most probable failure point. The point of minimum distance from the origin to the limit state surface, $x_s'^*$, represents the most onerous combination of the stochastic variables. For nonlinear limit state functions, the computation of the minimum distance becomes an optimization problem:

$$\begin{aligned} &\text{Minimize} \quad D = \sqrt{x_s'^t x_s'} \\ &\text{Subject to the constraint} \quad G_i(X_s) = G_i(X_s') = 0 \end{aligned} \tag{5.17}$$

where x_s' represents the coordinates of the checking point on the limit state function in the reduced coordinates. Using the method of Lagrange multipliers, the minimum distance can be found at the point where the gradients of the safety index $\beta = \sqrt{x_s'^t x_s'}$ equal the gradients of the constraint function $G(X_s) = f_i(X_{s1}, X_{s2}, \cdots, X_{sn}) = 0$. Therefore the safety index can be obtained as:

$$\beta_{H-L} = -\frac{\sum_{i=1}^{n} x_{si}'^* \left(\frac{\partial f_i}{\partial X_{si}'}\right)^*}{\sqrt{\sum_{i=1}^{n} \left(\frac{\partial f_i}{\partial X_{si}'}\right)^{2*}}} \tag{5.18}$$

where $(\partial g / \partial X_{si}')^*$ is the ith partial derivative evaluated at the design point with coordinates

$(x'^{*}_{s1}, x'^{*}_{s2}, \cdots, x'^{*}_{sn})$. The design point in the reduced coordinates is given by

$$x'^{*}_{s} = -\alpha_i \beta_{H-L} \quad \text{(i=1,2,...,n)} \tag{5.19}$$

where

$$\alpha_i = \frac{\left(\frac{\partial f_i}{\partial X'_{si}}\right)^{*}}{\sqrt{\sum_{i=1}^{n}\left(\frac{\partial f_i}{\partial X'_{si}}\right)^{2*}}} \tag{5.20}$$

are the direction cosines along the coordinate axes X'_{si}. In the space of the original coordinates and using Eqn 5.20, we find the design point to be

$$x^{*}_{si} = \mu_{X_{si}} - \alpha_i \sigma_{x_{si}} \beta_{H-L} \tag{5.21}$$

The basic algorithm to compute β_{H-L} and x'^{*}_{si} as formulated by Rackwitz(1976) is given as following procedure and presented as figure.5.3:

1) Define the appropriate limit state equation.

2) Assume initial values of the design point $x^{*}_{si}, i = 1, 2, \cdots, n$. Typically, the initial design point may be assumed to be at the mean values of the random variables. Obtain the reduced variates $x'^{*}_{si} = (x^{*}_{si} - \mu_{X_{si}})/\sigma_{X_{si}}$.

3) Evaluate $(\partial f/\partial X_{si})'^{*}$ and α_i at x'^{*}_{si}.

4) Obtain the new design point x'^{*}_{s} in terms of β_{H-L}, as in Eqn. 5.19.

5) Substitute the new x'^{*}_{s} in the limit state equation $G(x'^{*}_{s}) = 0$ and solve for β_{H-L}.

6) Using the β_{H-L} value obtained in step 5, re-evaluate $x'^{*}_{si} = -\alpha_i \beta_{H-L}$.

7) Repeat Steps 3 through 6 until β_{H-L} converges.

This algorithm is illustrated graphically in Fig. 5.3. The starting design point B (normally the mean value) may not be on the limit state surface $G_i(x'_s) = 0$. The line BC represents the tangent to the limit state equation $G_i(x'_s) = C$, and the design point x'^{*}_{s1} at first iteration can be evaluated through step 5. The tangent to the limit state equation $G_i(x'_s) = 0$ at the updated design point is calculated from Eqn. 5.20 leading to the new design point x'^{*}_{s2} and so on until convergence of the safety index value to a minimum.

In the basic FORM solution procedure, the variables are assumed to be normally distributed. When random variables with non-normal distributions are involved in a reliability analysis using FORM, these variables must be transformed to equivalent normal distributed variables. The Rackwitz-Fiessler transformation method has been used extensively in reliability analyse to transform non-normally distributed variables to normal equivalent with the satisfaction of two conditions: the cumulative distribution function(CDF) and the probability density functions(PDF) of the actual variables and the equivalent normal variables should be equal at the checking point $(x^{*}_{s1}, x^{*}_{s2}, \cdots, x^{*}_{sn})$ on the failure surface.

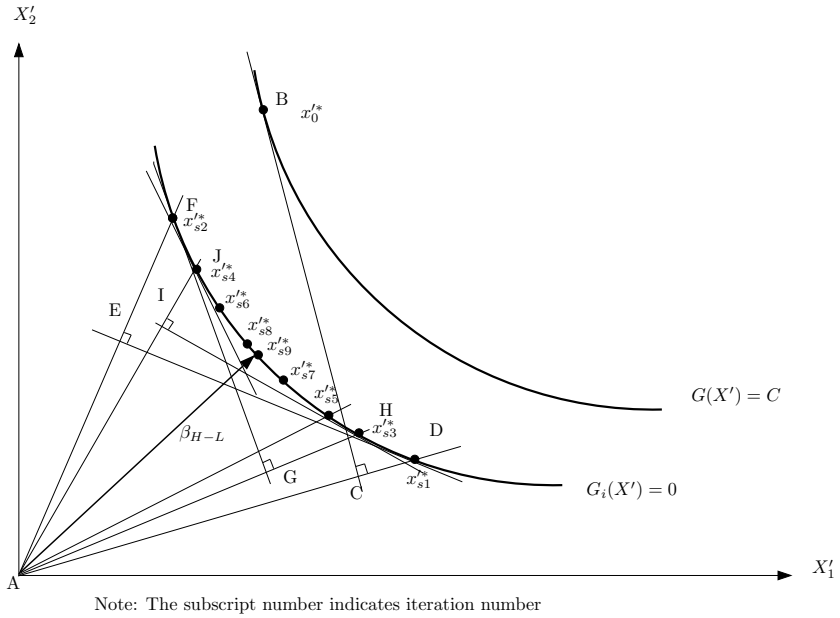

Figure 5.3: Basic algorithm to compute the safety index using FORM [70]

If the mean and standard deviation of the equivalent normal variables at the checking point are denoted by $\mu^N_{X_{si}}$ and $\sigma^N_{X_{si}}$, then based on the equivalent CDF condition, we have:

$$\Phi\left(\frac{x^*_{si} - \mu^N_{X_{si}}}{\sigma^N_{X_{si}}}\right) = F_{X_{si}}(x^*_{si}) \tag{5.22}$$

in which $\Phi(\ )$ is the CDF of the standard normal variate, and $F_{X_{si}}(x^*_{si})$ is the CDF of the original non-normal variable. Eqn. 5.22 can be rewritten as:

$$\mu^N_{X_{si}} = x^*_{si} - \Phi^{-1}[F_{X_{si}}(x^*_{si})]\sigma^N_{X_{si}} \tag{5.23}$$

Based on the condition that the PDFs of original and transformed variables are equal at the checking points, then:

$$\frac{1}{\sigma^N_{X_{si}}}\phi\left(\frac{x^*_{si} - \mu^N_{X_{si}}}{\sigma^N_{X_{si}}}\right) = f_{X_{si}}(x^*_{si}) \tag{5.24}$$

in which, $\phi(\ )$ and $f_{X_{si}}(x^*_{si})$ are the PDFs of the equivalent standard normal and the original non-normal random variables. Substituting Eqn. 5.22 into Eqn. 5.24,we obtain:

$$\sigma^N_{X_{si}} = \frac{\phi\{\Phi^{-1}[F_{X_{si}}(x^*_{si})]\}}{f_{X_{si}}(x^*_{si})} \tag{5.25}$$

This transformation looses accuracy for increasingly skewed distributions such as Frechet. In this case, the mean value and the standard deviation of equivalent normal distributed variables are re-defined as[Rackwitz and Fiessler,1978]:

$$\mu^N_{X_{si}} = F^{-1}_{X_{si}}(0.5) = \text{median of} X_{si} \tag{5.26}$$

and

$$\sigma_{X_{si}}^{N} = \frac{x_{si}^{*} - \mu_{X_{si}}^{N}}{\Phi^{-1}[F_{X_{si}}(x_{si}^{*})]} \tag{5.27}$$

in which $F_{X_{si}}^{-1}(\ )$ is the inverse of the non-normal CDF of X_{si}.

From a practical point of view, the application of the basic FORM algorithm is limited to limit state functions with simple forms, because in many cases, it is very difficult to solve the equation $G_i(x_s'^{*}) = 0$ for design point $x_s'^{*}$ when it is highly nonlinear, and in certain cases is not explicit. For example, in the reliability analysis of fabric structures, the limit state is evaluated through a deterministic finite element analysis with external random variables, making it impossible to perform step 5 in the basic FORM algorithm.

An alternative Newton-Raphson type recursive algorithm was developed by Rackwitz and Fiessler, in that, it linearizes the limit state function at each iteration point, and only requires the derivatives of the limit state function instead of solving the limit state equation explicitly. As shown in Fig. 5.4, initially the starting point $x_s'^{*}$ may not be on the limit state function $G(X_s') = 0$, but on a parallel line $G(X_s') = k$. The linear limit state function $G(X_s')$ may be expressed as,

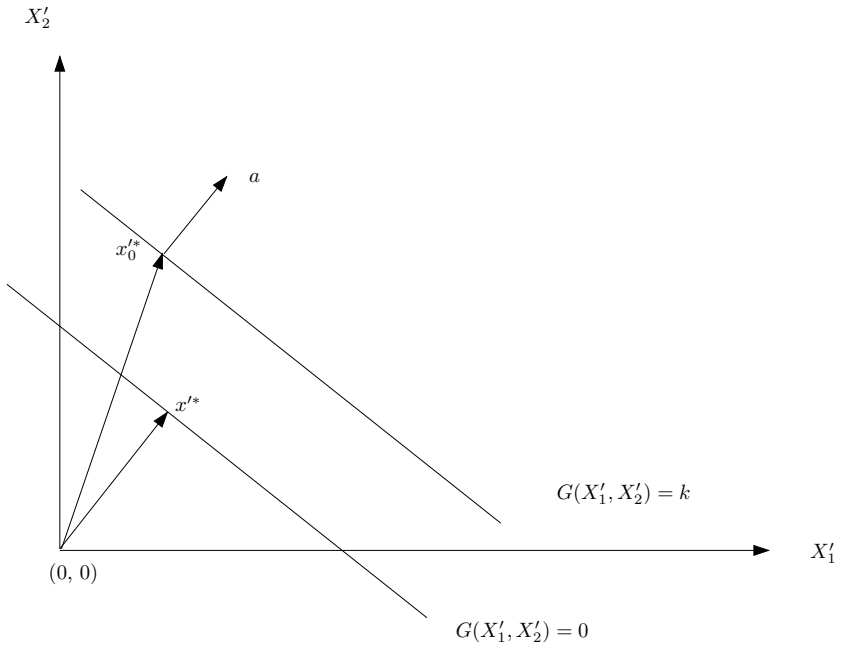

Figure 5.4: Linearized limit state function in HL-RF(Hasofer-Lind and Rackwitz-Fiossler) algorithm

$$G(X_s') = b + a^t x_s' \tag{5.28}$$

or, for example, using two variables,

$$G(X_s') = b + a_1 x_{s1}' + a_2 x_{s2}' \tag{5.29}$$

Here $a^t = (a_1, a_2)$ is the transpose of the gradient vector (i.e., vector of first derivative) of the limit state function. The magnitudes of the vectors x'^*_{s0} and x'^*_s denote the distance from the origin to starting point and to the limit state $G(X'_s) = 0$, respectively. From geometry, x'^*_s can be expressed in terms of x'^*_{s0} as:

$$x'^*_s = \frac{1}{|a|^2}[a^t x'^*_{s0} - G(x'^*_{s0})]\{a\} \tag{5.30}$$

Eqn. 5.30 can be rewritten as:

$$\begin{Bmatrix} x'^*_{s1} \\ x'^*_{s2} \end{Bmatrix} = \frac{1}{a_1^2 + a_2^2}[a_1 x'^*_{s01} + a_2 x'^*_{s02} - G(x'^*_{s01}, x'^*_{s02})] \begin{Bmatrix} a_1 \\ a_2 \end{Bmatrix} \tag{5.31}$$

and for the limit state function with random variables $(x'_{s1}, x'_{s2}, \cdots, x'_{sn})$, it becomes:

$$\begin{Bmatrix} x'^*_{s1} \\ x'^*_{s2} \\ \vdots \\ x'^*_{sn} \end{Bmatrix} = \frac{1}{a_1^2 + a_2^2 + \cdots + a_n^2}[a_1 x'^*_{s(01)} + a_2 x'^*_{s(02)} + \cdots a_n x'^*_{s0n}) - G(x'^*_{s01}, x'^*_{s02}, \cdots, x'^*_{s0n})] \begin{Bmatrix} a_1 \\ a_2 \\ \vdots \\ a_n \end{Bmatrix} \tag{5.32}$$

If the limit state function is linear, then the derivative vector a is constant, and the distance to the limit state from the origin can be obtained in one step. If the limit state function is nonlinear, the gradient is not constant but varies from point to point. Therefore the point of minimum distance will be searched through the recursive formulation as Eqn. 5.33:

$$x'^*_{s(k+1)} = \frac{1}{|\nabla G(x'^*_{s(k)})|^2}[\nabla G(x'^*_{s(k)})^t x'^*_k - G(x'^*_{s(k)})]\nabla G(x'^*_{s(k)}) \tag{5.33}$$

where $\nabla G(x'^*_{s(k)})$ is the gradient vector of the limit state function at $x'^*_{s(k)}$, the kth iteration checking point.

This formula is represented diagrammatically interpreted in fig. 5.5, and the optimization algorithm seeks the minimum distance to the point x'^*_s on the limit state. Therefore the solution convergence can be demonstrated when satisfying the following two criteria:

1. $|x'^*_{s(k)} - x'^*_{s(k-1)}| \leq \delta$
2. $|G(x'^*_{s(k)})| \leq \epsilon$

Both δ and ϵ are allowable error approximations to zero, usually 0.001.

Using this type of recursive algorithm, an alternative FORM solution procedure that permits random variables with any type of distribution is generated as:

1) Define the appropriate limit state function and failure criterion.

2) Assume initial values of the design point $x^*_{si}, i = 1, 2, \cdots, n$(normally mean value), and calculate the corresponding value of the limit state functions $G_i(\ )$.

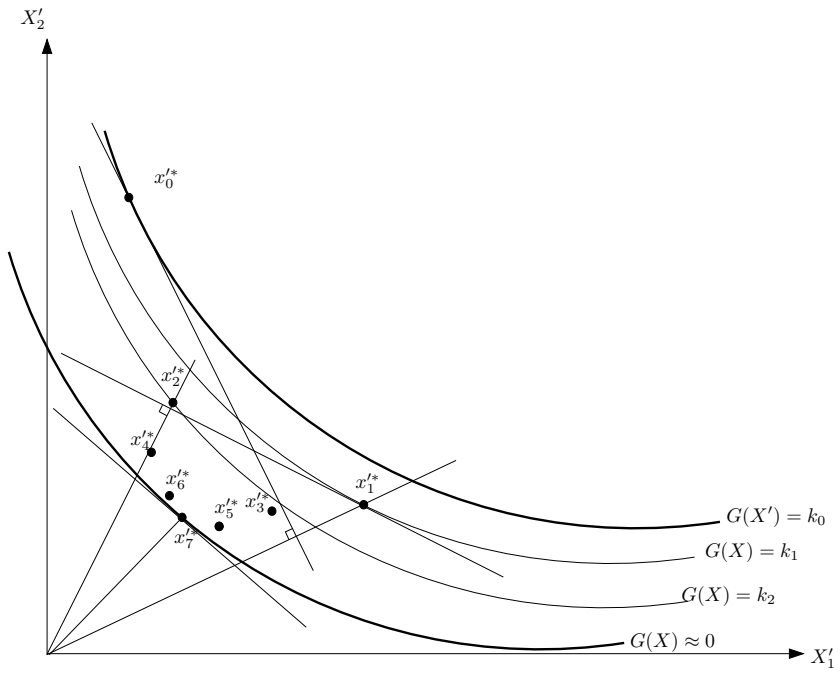

Figure 5.5: Illustrative solution procedure of safety index using HL-RF(Hasofer-Lind and Rackwitz-Fiossler) algorithm [70]

3) For those non-normal distributed variables, compute the mean and standard deviation at the design point of the equivalent normal distribution using Eqn.5.26 and Eqn.5.27. Then transform the random variables to the reduced coordinate system using Eqn.5.34

$$x_{si}'^* = \frac{x_{si}^* - \mu_{X_{si}}^N}{\sigma_{X_{si}}^N} \tag{5.34}$$

4) Compute the partial derivative $\partial G/\partial X_{si}$ evaluated at the design point x_{si}^*.

5) Compute the partial derivative $\partial G/\partial X_{si}'$ using the chain rule of differentiation as

$$\frac{\partial G}{\partial X_{si}'} = \frac{\partial G}{\partial X_{si}} \frac{\partial X_{si}}{\partial X_{si}'} = \frac{\partial G}{\partial X_{si}} \sigma_{X_{si}}^N \tag{5.35}$$

6) Compute the new values of design points ($x_{si}'^*$) in the reduced space using Eqn.5.33.

7) Compute the safety index β based on the values of the design points calculated in step 6 as:

$$\beta = \sqrt{\sum_{i=1}^{n} (x_{si}'^*)^2} \tag{5.36}$$

Check the convergence of β.

8) Compute the new values of the design point (x_s^*)in the original space as:

$$x_{si}^* = \mu_{X_{si}}^N + \sigma_{X_{si}}^N x_{si}'^* \tag{5.37}$$

then update the value of the limit state function $G(\ )$ for this new design point and check if the design points are on the limit state function(i.e. $|G(\ )|$ is very close to zero, say within 0.001). If the convergence criteria in step 7 is satisfied and $|G(\ )|$ is approximately zero(e.g. less than 0.001), then stop. Otherwise, repeat steps 3 through 8 until convergence.

The advantage of this solution algorithm is that solving limit state equation $G(\ ) = 0$ is avoided, so that the reliability analysis can be undertaken for a structure with a complicated or implicit limit state function, given that the partial derivatives of $G(\ )$ with respect to the random variables are available. This algorithm is a general procedure for the reliability analysis of most types of structures, without consideration of the specific characteristics of a specific structure type. For each problem it is necessary to compute the partial derivatives of $G(\ )$ (or sensitivities) with respect to the statistical variables for fabric structures analyzed using a particular finite element formulation. These formulation are detailed in section 5.3.

5.3 Sensitivity Analysis

The FORM introduced in section 5.2 requires the value and gradients of the performance function. The value of the performance function can be obtained from a deterministic structural analysis(e.g finite element analysis) and the gradients of the limit state functions can be derived as:

$$\partial G_1/\partial X_{si} = \partial(\sigma^f_{per} - \sigma^f_{max})/\partial X_{si} = \partial\sigma^f_{per}/\partial X_{si} - \partial\sigma^f_{max}/\partial X_{si} \tag{5.38}$$

$$\partial G_2/\partial X_{si} = \partial(\sigma^w_{per} - \sigma^w_{max})/\partial X_{si} = \partial\sigma^w_{per}/\partial X_{si} - \partial\sigma^w_{max}/\partial X_{si} \tag{5.39}$$

$$\partial G_3/\partial X_{si} = \partial(\sigma^p_{min} - \sigma^p_{per})/\partial X_{si} = \partial\sigma^p_{min}/\partial X_{si} - \partial\sigma^p_{per}/\partial X_{si} \tag{5.40}$$

$$\partial G_4/\partial X_{si} = \partial(D_{al} - D_{max})/\partial X_{si} = \partial D_{al}/\partial X_{si} - \partial D_{max}/\partial X_{si} \tag{5.41}$$

where X_{si} are random variables defined in section 5.2, $i = 1, 2 \cdots, 7$.

The computation of the gradients of limit state functions 5.38 to 5.41 is effectively a sensitivity analysis of the structural response with respect to the random variables. This type of structural sensitivity analysis can be undertaken either numerically (finite difference method) or analytically (classical analytical differentiation).

5.3.1 Finite Difference Method

The response sensitivity can be estimated using the finite difference method by perturbing each variable X_{si} and computing the corresponding change ΔZ in response through multi deterministic analyses, as in,

$$\frac{dZ}{dX_s} = \lim_{\Delta X_s \to 0} \frac{\Delta Z}{\Delta X_s} \tag{5.42}$$

in which, ΔX_s is the perturbation of the random variable.

The variables Z represent any of the structural responses described in section 5.2 (i.e. σ^f_{max}, σ^w_{max}, σ^p_{min}, and D_{max}) and are implicit functions of the random variables $X_s(X_{s1}, X_{s2}, \cdots, X_{sn})$.

The finite difference approach is potentially computationally expensive as the number of variables and limit states increase, and the suitable perturbation is needed to be considered and determined for any different case. However it is the simplest and most straightforward method to compute the sensitivities of structural responses from a deterministic analysis, where sufficiently detailed information about the formulation is not available. In the present context it can be most usefully applied to the checking of analytically derived sensitivities.

5.3.2 Classical Analytical Method

In a deterministic finite element analysis with the stochastic input variables, every quantity computed in the deterministic analysis also becomes stochastic. A deterministic structural response is normally obtained through a numerical model, then an efficient way to calculate variation of structural response with respect to random variables is to compute the variation of the components of the numerical model within the deterministic analysis in terms of the basic random variables. In practical terms, this is simply the application of the chain rule of differentiation to define the derivatives of structural response with respect to the random variables.

Based on the discussion in Chapter 3, the LST formulation has been verified and proved to have better performance than the CST. The reliability formulation will be established based on the LST formulation.

The simplest form of a general deterministic linear finite element structural analysis may be expressed as:

$$KU = F \text{ or } U = K^{-1}F \tag{5.43}$$

in which, K is stiffness matrix, and U and F are nodal displacements and load vectors respectively. If the derivative of nodal displacement is computed with respect to the random variable X_{sj}, we have:

$$\frac{\partial U}{\partial X_{sj}} = K^{-1}\frac{\partial F}{\partial X_{sj}} + \frac{\partial K^{-1}}{\partial X_{sj}}F \tag{5.44}$$

Since

$$KK^{-1} = I \tag{5.45}$$

differentiating this equation with respect X_{sj} gives:

$$\frac{\partial K^{-1}}{\partial X_{sj}} = -K^{-1}\frac{\partial K}{\partial X_{sj}}K^{-1} \tag{5.46}$$

Substituting this result into Eqn.5.44 then,

$$\begin{aligned}\frac{\partial U}{\partial X_{sj}} &= K^{-1}\frac{\partial F}{\partial X_{sj}} - K^{-1}\frac{\partial K}{\partial X_{sj}}K^{-1}F \\ &= K^{-1}\frac{\partial F}{\partial X_{sj}} - K^{-1}\frac{\partial K}{\partial X_{sj}}U \end{aligned} \tag{5.47}$$

Since K and U can be obtained from a deterministic analysis, then the derivatives of nodal displacement can be computed using Eqn. 5.47 if $\frac{\partial F}{\partial X_{sj}}$ and $\frac{\partial K}{\partial X_{sj}}$ are known. Other structural response vectors (e.g. stresses) can be expressed as a function of nodal displacement:

$$\sigma = E\varepsilon = EBU \tag{5.48}$$

Where E is the elastic modulus matrix, ε is element strain, B is the strain-displacement matrix, and U is the nodal displacement. Therefore, the derivative of the stress vector with respect to X_{sj} is

$$\frac{\partial \sigma}{\partial X_{sj}} = \frac{\partial E}{\partial X_{sj}}BU + E\frac{\partial B}{\partial X_{sj}}U + EB\frac{\partial U}{\partial X_{sj}} \tag{5.49}$$

in which, for a nonlinear structural analysis, the B matrix is a function of nodal displacements U, such that:

$$\frac{\partial B}{\partial X_{sj}} = \frac{\partial B}{\partial U}\frac{\partial U}{\partial X_{sj}} = dB\frac{\partial U}{\partial X_{sj}} \tag{5.50}$$

Substituting Eqn. 5.50 into Eqn.5.49, we obtain:

$$\frac{\partial \sigma}{\partial X_{sj}} = \frac{\partial E}{\partial X_{sj}}BU + EdB\frac{\partial U}{\partial X_{sj}}U + EB\frac{\partial U}{\partial X_{sj}} \tag{5.51}$$

Since the minimum principal stress σ^p_{min} can be expressed as:

$$\sigma^p_{min} = 0.5(\sigma_f + \sigma_w) - \sqrt{(\frac{\sigma_w - \sigma_f}{2})^2 + (\sigma_{wf})^2} \tag{5.52}$$

in which, σ_f and σ_w are element stresses in fill and warp, and σ_{wf} is the shear stress, then the derivative of σ^p_{min} can be computed based on $\frac{\partial \sigma}{\partial X_{sj}}$ as:

$$\frac{\partial \sigma^p_{min}}{\partial X_{sj}} = 0.5(\frac{\partial \sigma_f}{\partial X_{sj}} + \frac{\partial \sigma_w}{\partial X_{sj}}) + \frac{0.5(\sigma_f - \sigma_w)(\frac{\partial \sigma_f}{\partial X_{sj}} - \frac{\partial \sigma_f}{\partial X_{sj}}) + 2\sigma_{wf}\frac{\sigma_{wf}}{\partial X_{sj}}}{2\sqrt{\frac{1}{4}(\sigma_f - \sigma_w)^2 + \sigma^2_{wf}}} \tag{5.53}$$

Equations 5.44 to 5.53 illustrate the application of the chain rule of differentiation to the finite element formulations. It is apparent that once the derivative of elastic modulus matrix and nodal displacements are obtained, the derivatives of other structural responses can be readily

evaluated.

In the deterministic analysis of fabric structures, the structure of interest is discretized into a number of two types of elements: membrane and cable elements, and at the final balanced geometry configuration, if the structure to be analyzed is discretized into n membrane elements and s cable elements, the assembled reaction force vector of the elements equals the applied load vector:

$$F = \sum_{i=1}^{n} T_i^m R_i^m + \sum_{k=1}^{s} T_k^c R_k^c \tag{5.54}$$

where T_i^m and T_k^c are the transformation matrix for membrane and cable element between local and global coordinate systems respectively, and R_i^m and R_k^c are the reaction force vectors of membrane and cable element in the local coordinate system separately. As introduced in chapter.3 "Deterministic Fabric analysis", these element reaction force vectors are defined as:

$$R_i^m = \int_V B\sigma dV \tag{5.55}$$

and

$$R_k^c = T_k^c P \tag{5.56}$$

Therefore, Eqn.5.54 becomes

$$F = \sum_{i=1}^{n} T_i \int_V B\sigma dV + \sum_{k=1}^{s} T_k^c P_k \tag{5.57}$$

in which σ is the membrane element stress vector, and it has the form:

$$\sigma = \sigma_E + \sigma_0 = E\varepsilon + \sigma_0 = EBU + \sigma_0 \tag{5.58}$$

where σ_E and σ_0 are stress vectors from the elastic deformation and pretension respectively, and U represents nodal displacements in the element local coordinate system. If we denote u as the nodal displacements in global coordinate system, then:

$$U = T_i^c u \tag{5.59}$$

Substituting Eqn. 5.58 into 5.57, we obtain:

$$F = \sum_{i=1}^{n} T_i^m \int_V B(EBU + \sigma_0) dV + \sum_{k=1}^{s} T_k^c P_k \tag{5.60}$$

Since σ_0 is a prescribed constant, differentiating Eqn. 5.60 with respect X_{sj} gives

$$\begin{aligned}\frac{\partial F}{\partial X_{sj}} &= \sum_{i=1}^{n}\frac{\partial T_i^m}{\partial X_{sj}}\int_V B(EBU+\sigma_0)dV+\sum_{i=1}^{n}T_i^m\int_V\frac{\partial B}{\partial X_{sj}}(EBU+\sigma_0)dV\\ &\quad+\sum_{i=1}^{n}T_i^m\int_V B(\frac{\partial E}{\partial X_{sj}}BU+E\frac{\partial B}{\partial X_{sj}}U+EB\frac{\partial U}{\partial X_{sj}})dV+\sum_{k=1}^{s}\frac{\partial T_k^c}{\partial X_{sj}}P_k\\ &\quad+\sum_{k=1}^{s}T_k^c\frac{\partial P_k}{\partial X_{sj}}\\ &= \sum_{i=1}^{n}\frac{\partial T_i^m}{\partial X_{sj}}\int_V B(EBU+\sigma_0)dV+\sum_{i=1}^{n}T_i^m\int_V\frac{\partial B}{\partial X_{sj}}(EBU+\sigma_0)dV\\ &\quad+\sum_{i=1}^{n}T_i^m\int_V B(\frac{\partial E}{\partial X_{sj}}BU+E\frac{\partial B}{\partial X_{sj}}U+EB\frac{\partial T_i^c}{\partial X_{sj}}u+EBT_i^c\frac{\partial u}{\partial X_{sj}})dV+\\ &\quad\sum_{k=1}^{s}\frac{\partial T_k^c}{\partial X_{sj}}P_k+\sum_{k=1}^{s}T_k^c\frac{\partial P_k}{\partial X_{sj}}\end{aligned}\tag{5.61}$$

Since F is the load vector which is independent to the membrane material properties and ultimate strength, thus

$$\frac{\partial F}{\partial X_{sj}}=\begin{cases}0 & \text{for variables defined in 5.1, j=1}\rightarrow 6\\ \partial(F_c t_{load})/\partial t_{load}=F_c & \text{for load coefficient(5.2), j=7}\end{cases}\tag{5.62}$$

where F_c is the design load. Similarly E is a function of the membrane material parameters $X_{sj}(j=1\rightarrow 4)$ and is independent of the ultimate strength (X_{s5},X_{s6}) and the applied loads coefficient(X_{s7}). Therefore, with

$$E=\begin{bmatrix}\frac{E_f\cdot E_w}{E_w-E_f\cdot\nu_{wf}^2} & \frac{E_f\cdot E_w\cdot\nu_{wf}}{E_w-\nu^2\cdot E_f} & 0\\ \frac{E_f\cdot E_w\cdot\nu_{wf}}{E_w-\nu^2\cdot E_f} & \frac{E_w^2}{E_w-E_f\cdot\nu_{wf}^2} & 0\\ 0 & 0 & G_{wf}\end{bmatrix},\tag{5.63}$$

then, $\frac{\partial E}{\partial X_{sj}}$ can be derived as:

$$\frac{\partial E}{\partial X_{s1}}=\frac{\partial E}{\partial E_f}=\begin{bmatrix}\partial E_{1,1}^f & \partial E_{1,2}^f & 0\\ \partial E_{2,1}^f & \partial E_{2,2}^f & 0\\ 0 & 0 & 0\end{bmatrix}\tag{5.64}$$

$$\frac{\partial E}{\partial X_{s2}}=\frac{\partial E}{\partial E_w}=\begin{bmatrix}\partial E_{1,1}^w & \partial E_{1,2}^w & 0\\ \partial E_{2,1}^w & \partial E_{2,2}^w & 0\\ 0 & 0 & 0\end{bmatrix}\tag{5.65}$$

$$\frac{\partial E}{\partial X_{s3}}=\frac{\partial E}{\partial \nu_{wf}}=\begin{bmatrix}\partial E_{1,1}^\nu & \partial E_{1,2}^\nu & 0\\ \partial E_{2,1}^\nu & \partial E_{2,2}^\nu & 0\\ 0 & 0 & 0\end{bmatrix}\tag{5.66}$$

$$\frac{\partial E}{\partial X_{s4}} = \frac{\partial E}{\partial G_{wf}} = \begin{bmatrix} 0 & 0 & 0 \\ 0 & 0 & 0 \\ 0 & 0 & 1 \end{bmatrix} \tag{5.67}$$

$$\frac{\partial E}{\partial X_{s5}} = \frac{\partial E}{\partial X_{s6}} = \frac{\partial E}{\partial X_{s7}} = 0 \tag{5.68}$$

where

$\partial E^f_{1,1} = \frac{E_w}{E_w - \nu^2_{wf} E_f} + \frac{E_w E_f \nu^2_{wf}}{(E_w - \nu^2_{wf} E_f)^2}, \quad \partial E^f_{2,2} = \frac{E_w E_f}{(E_w - \nu^2_{wf} E_f)^2}$

$\partial E^f_{1,2} = \partial E^w_{2,1} = \frac{E_w \nu_{wf}}{E_w - \nu^2_{wf} E_f} + \frac{E_w E_f}{(E_w - \nu^2_{wf} E_f)^2}$

$\partial E^w_{1,1} = \frac{E_f}{E_w - \nu^2_{wf} E_f} - \frac{E_w E_f}{(E_w - \nu^2_{wf} E_f)^2}, \quad \partial E^w_{2,2} = \frac{2E_w}{(E_w - \nu^2_{wf} E_f)^2} - \frac{E^2_w}{(E_w - \nu^2_{wf} E_f)^2}$

$\partial E^w_{1,2} = E^w_{2,1} = \frac{E_f \nu_{wf}}{E_w - \nu^2_{wf} E_f} - \frac{E_w E_f \nu_{wf}}{(E_w - \nu^2_{wf} E_f)^2}$

$\partial E^\nu_{1,1} = \frac{\sqrt{E_f E_w}}{2(\sqrt{E_w} - \nu^2_{wf}\sqrt{E_f})^2} + \frac{\sqrt{E_w E_f}}{2(\sqrt{E_w} - \nu^2_{wf}\sqrt{E_f})^2}, \quad \partial E^\nu_{2,2} = \frac{E_w\sqrt{E_f E_w}}{2(\sqrt{E_w} - \nu^2_{wf}\sqrt{E_f})^2} - \frac{\sqrt{E_w E_f}}{2(\sqrt{E_w} - \nu^2_{wf}\sqrt{E_f})^2}$

$\partial E^\nu_{1,2} = \partial E^\nu_{2,1} = \frac{E_f E_w}{E_w - \nu^2_{wf} E_f} + \frac{\sqrt{E_w E_f}\nu_{wf}}{2(\sqrt{E_w} - \nu^2_{wf}\sqrt{E_f})^2} - \frac{\sqrt{E_f E_w}}{2(\sqrt{E_w} - \nu^2_{wf}\sqrt{E_f})^2}$

Using the chain rule of differentiation, the derivatives of T_i and B in Eqn. 5.61 are expanded as:

$$\frac{\partial T^m_i}{\partial X_{sj}} = \frac{\partial T^m_i}{\partial u}\frac{\partial u}{\partial X_{sj}} = dT^m \frac{\partial u}{\partial X_{sj}}, \quad \frac{\partial B}{\partial X_{sj}} = \frac{\partial B}{\partial u}\frac{\partial u}{\partial X_{sj}} = dB\frac{\partial u}{\partial X_{sj}} \tag{5.69}$$

$$\frac{\partial T^c_k}{\partial X_{sj}} = \frac{\partial T^c_k}{\partial u}\frac{\partial u}{\partial X_{sj}} = dT^c \frac{\partial u}{\partial X_{sj}}, \quad \frac{\partial P_k}{\partial X_{sj}} = \frac{\partial P_k}{\partial u}\frac{\partial u}{\partial X_{sj}} = dP\frac{\partial u}{\partial X_{sj}} \tag{5.70}$$

Substituting Eqn.5.69 into Eqn.5.61, we obtain:

$$\begin{aligned} \frac{\partial F}{\partial X_{sj}} \;=\; & \sum_{i=1}^{n} dT^m \frac{\partial u}{\partial X_{sj}} \int_V B^T(EBU + \sigma_0)dV + \sum_{i=1}^{n} T^m_i \int_V dB\frac{\partial u}{\partial X_{sj}}(EBU + \sigma_0)dV \\ & + \sum_{i=1}^{n} T^m_i \int_V B^T\Big(\frac{\partial E}{\partial X_{sj}}BU + E\; dB\frac{\partial u}{\partial X_{sj}}U + EBdT^m\frac{\partial u}{\partial X_{sj}}u + EBT^m_i\frac{\partial u}{\partial X_{sj}}\Big)dV \\ & + \sum_{k=1}^{s} dT^c\frac{\partial u}{\partial X_{sj}}P_k + \sum_{k=1}^{s} T^c_k dP\frac{\partial u}{\partial X_{sj}} \end{aligned} \tag{5.71}$$

To make this equation more tractable, we define

$$[DT_1]\frac{\partial u}{\partial X_{sj}} = dT^m\frac{\partial u}{\partial X_{sj}}\int_V B^T(EBU + \sigma_0)dV \tag{5.72}$$

$$[DT_2]\frac{\partial u}{\partial X_{sj}} = dB\frac{\partial u}{\partial X_{sj}}U \tag{5.73}$$

$$[DT_3]\frac{\partial u}{\partial X_{sj}} = dT^m\frac{\partial u}{\partial X_{sj}}u \tag{5.74}$$

$$[DT_4]\frac{\partial u}{\partial X_{sj}} = dB\frac{\partial u}{\partial X_{sj}}(EBU + \sigma_0) \tag{5.75}$$

$$[DT_5]\frac{\partial u}{\partial X_{sj}} = dT^c\frac{\partial u}{\partial X_{sj}}P_k + T_k^c dP\frac{\partial u}{\partial X_{sj}} \tag{5.76}$$

Then, Eqn. 5.71 can be written as:

$$\begin{aligned}\frac{\partial F}{\partial X_{sj}} &= \sum_{i=1}^{n}[DT_1]\frac{\partial u}{\partial X_{sj}} + \sum_{i=1}^{n}T_i^m\int_V B^T\frac{\partial E}{\partial X_{sj}}BU + \sum_{i=1}^{n}T_i^m\int_V[DT_4]\frac{\partial u}{\partial X_{sj}}dV \\ &\quad + \sum_{i=1}^{n}T_i^m\int_V B^T E([DT_2] + B[DT_3] + BT_i^m)\frac{\partial u}{\partial X_{sj}}\,dV + \sum_{k=1}^{s}[DT_5]\frac{\partial u}{\partial X_{sj}}\end{aligned} \tag{5.77}$$

$\frac{\partial u}{\partial X_{sj}}$ may then be determined from:

$$\frac{\partial u}{\partial X_{sj}} = \frac{\frac{\partial F}{\partial X_{sj}} - \sum_{i=1}^{n}T_i\int_V B\frac{\partial E}{\partial X_{sj}}BU\,dV}{\sum_{i=1}^{n}\left\{[DT_1] + T_i^m\int_V\{B^T E([DT_2] + [DT_3] + BT_i) + [DT_4]\}\,dV\right\} + \sum_{k=1}^{s}[DT_5]} \tag{5.78}$$

For the ith element, we define:

$$df_i = T_i\int_V B\frac{\partial E}{\partial X_{sj}}BU\,dV \tag{5.79}$$

$$dK_i^m = [DT_1] + T_i^m\int_V\{B^T E([DT_2] + [DT_3] + BT_i) + [DT_4]\}\,dV \tag{5.80}$$

and

$$dK_k^c = [DT_5] \tag{5.81}$$

Eqn. 5.78 can be then rewritten as:

$$\frac{\partial u}{\partial X_{sj}} = \frac{\frac{\partial F}{\partial X_{sj}} - \sum_{i=1}^{n}df_i}{\sum_{i=1}^{n}dK_i^m + \sum_{k=1}^{s}dK_k^c} \tag{5.82}$$

From Eqn.5.82, it is implied that the derivative of nodal displacement can be computed through an analogous procedure to the finite element method: calculate element vectors first, then assemble the structure vector prior to solving for the system.

Through a deterministic analysis, the vectors in Eqn. 5.60 can be evaluated leading directly to $\frac{\partial F}{\partial X_{sj}}$ in Eqn. 5.62. Therefore the vector df_i can be computed using $\frac{\partial E}{\partial U}$ as derived in Eqn.5.64 to 5.68. The remaining vectors required in Eqn. 5.61 are derived in the following subsections as shown in Fig. 5.6.

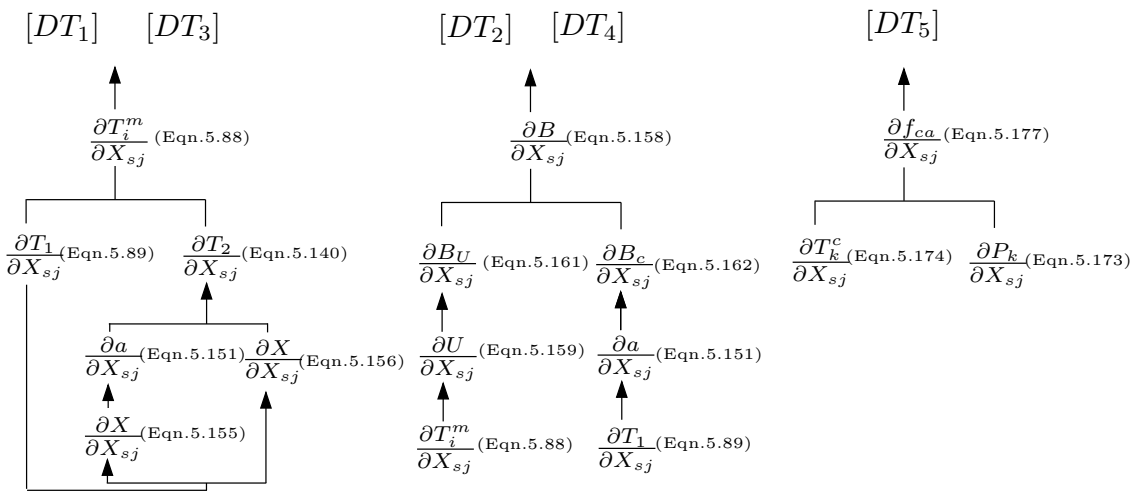

Figure 5.6: Diagram of the structure of sensitivity formulations

Transformation matrix derivatives.

The transformation matrix for membrane element T_i^m can be expressed as:

$$T_i^m = [T_2][T_1] \tag{5.83}$$

where $[T_1]$ is the transformation matrix between the global and local flat coordinate systems, and $[T_2]$ is the transformation matrix between the local flat and local curved coordinate spaces. $[T_1]$ and $[T_2]$ are defined as:

$$[T_1] = \begin{bmatrix} l_1 & l_2 & l_3 \\ m_1 & m_2 & m_3 \\ n_1 & n_2 & n_3 \end{bmatrix} \tag{5.84}$$

and

$$[T_2] = \begin{bmatrix} T_2(1) & 0 & T_2(3) \\ 0 & T_2(2) & T_2(4) \\ T_2(5) & T_2(6) & T_2(7) \end{bmatrix} \tag{5.85}$$

in which, l_i, m_i, n_i are direction cosines between global coordinate and local flat coordinate axis.

$T_2(1) = \frac{1}{\sqrt{1+(\frac{dZ}{dX})^2}}$, $T_2(2) = \frac{1}{\sqrt{1+(\frac{dZ}{dY})^2}}$, $T_2(3) = \frac{\frac{dZ}{dX}}{\sqrt{1+(\frac{dZ}{dX})^2}}$, $T_2(4) = \frac{\frac{dZ}{dY}}{\sqrt{1+(\frac{dZ}{dY})^2}}$,
$T_2(5) = -\frac{\frac{dZ}{dX}\sqrt{(1+\frac{dZ}{dX}^2)(1+\frac{dZ}{dX}^2)}}{1+\frac{dZ}{dX}^2+\frac{dZ}{dY}^2}$, $T_2(6) = -\frac{\frac{dZ}{dY}\sqrt{(1+\frac{dZ}{dX}^2)(1+\frac{dZ}{dX}^2)}}{1+\frac{dZ}{dX}^2+\frac{dZ}{dY}^2}$, $T_2(7) = -\frac{\sqrt{(1+\frac{dZ}{dX}^2)(1+\frac{dZ}{dX}^2)}}{1+\frac{dZ}{dX}^2+\frac{dZ}{dY}^2}$

and $\frac{dZ}{dX}$,$\frac{dZ}{dY}$ are the derivatives of the membrane surface $Z = Z(X, Y)$ with respect to local flat coordinate X and Y. With $Z = Z(X, Y)$ expressed as:

$$Z = Z(X, Y) = a_2X + a_3Y + a_4X^2 + a_5XY + a_6Y^2, \tag{5.86}$$

the derivative of T_i^m is:

$$\frac{\partial T_i^m}{\partial X_{sj}} = \frac{\partial [T_2]}{\partial X_{sj}}[T_1] + [T_2]\frac{\partial [T_1]}{\partial X_{sj}} \tag{5.87}$$

The derivative of $[T_1]$

Differentiating Eqn. 5.84 with respect to X_{sj}, we obtain

$$\frac{\partial [T_1]}{\partial X_{sj}} = \begin{bmatrix} \frac{\partial l_1}{\partial X_{sj}} & \frac{\partial l_2}{\partial X_{sj}} & \frac{\partial l_3}{\partial X_{sj}} \\ \frac{\partial m_1}{\partial X_{sj}} & \frac{\partial m_2}{\partial X_{sj}} & \frac{\partial m_3}{\partial X_{sj}} \\ \frac{\partial n_1}{\partial X_{sj}} & \frac{\partial n_2}{\partial X_{sj}} & \frac{\partial n_3}{\partial X_{sj}} \end{bmatrix} \tag{5.88}$$

If the local flat coordinate axe $\overrightarrow{X}, \overrightarrow{Y}, \overrightarrow{Z}$ are regarded as the vectors in global coordinate system,

$$\overrightarrow{X} = a_x \overrightarrow{i} + a_y \overrightarrow{j} + a_z \overrightarrow{k} \tag{5.89}$$

$$\overrightarrow{Y} = b_x \overrightarrow{i} + b_y \overrightarrow{j} + b_z \overrightarrow{k} \tag{5.90}$$

$$\overrightarrow{Z} = c_x \overrightarrow{i} + c_y \overrightarrow{j} + c_z \overrightarrow{k} \tag{5.91}$$

and,

$$l_1 = \frac{a_x}{\sqrt{a_x^2 + a_y^2 + a_z^2}},\ l_2 = \frac{a_y}{\sqrt{a_x^2 + a_y^2 + a_z^2}},\ l_3 = \frac{a_z}{\sqrt{a_x^2 + a_y^2 + a_z^2}} \tag{5.92}$$

$$m_1 = \frac{b_x}{\sqrt{b_x^2 + b_y^2 + b_z^2}},\ m_2 = \frac{b_y}{\sqrt{b_x^2 + b_y^2 + b_z^2}},\ m_3 = \frac{b_z}{\sqrt{b_x^2 + b_y^2 + b_z^2}} \tag{5.93}$$

$$n_1 = \frac{c_x}{\sqrt{c_x^2 + c_y^2 + c_z^2}},\ n_2 = \frac{c_y}{\sqrt{c_x^2 + c_y^2 + c_z^2}},\ n_3 = \frac{c_z}{\sqrt{c_x^2 + c_y^2 + c_z^2}} \tag{5.94}$$

where $a_x, b_x, c_x, a_y, b_y, c_y, a_z, b_z, c_z$ are the functions of global nodal coordinates, as in:

$$a_x = x_2 - x_1, \quad , a_y = y_2 - y_1, \quad a_z = z_2 - z_1$$

$$b_x = x_p - x_1, \quad , b_y = y_p - y_1, \quad b_z = z_p - z_1$$

$$\begin{aligned} c_x &= (y_2 - y_1)(z_p - z_1) - (z_2 - z_1)(y_p - y_1) \\ c_y &= -(x_2 - x_1)(z_p - z_1) + (z_2 - z_1)(x_p - x_1) \\ c_z &= (x_2 - x_1)(y_p - y_1) - (y_2 - y_1)(x_p - x_1) \end{aligned} \tag{5.95}$$

in which, x_i, y_i, z_i are global nodal coordinates of ith node. x_p, y_p, z_p are the global coordinates

of a single point p along the local Y axis, and there has:

$$\begin{bmatrix} x_2 - x_1 & y_2 - y_1 & z_2 - z_1 \\ \lambda_1 & \lambda_2 & \lambda_3 \\ x_3 - x_1 & y_3 - y_1 & z_3 - z_1 \end{bmatrix} \begin{Bmatrix} x_p \\ y_p \\ z_p \end{Bmatrix} = \begin{Bmatrix} (x_2 - x_1)x_1 + (y_2 - y_1)y_1 + (z_2 - z_1)z_1 \\ \lambda_1 x_1 + \lambda_2 x_2 + \lambda_3 x_3 \\ (x_3 - x_1)x_3 + (y_3 - y_1)y_3 + (z_3 - z_1)z_3 \end{Bmatrix} \tag{5.96}$$

or,

$$\begin{Bmatrix} x_p \\ y_p \\ z_p \end{Bmatrix} = [M_p]^{-1}\{F_p\} \tag{5.97}$$

where $\lambda_1, \lambda_2, \lambda_3$ are functions of global nodal coordinates as:

$$\begin{aligned} \lambda_1 &= (y_2 - y_1)(z_3 - z_1) - (z_2 - z_1)(y_3 - y_1) \\ \lambda_2 &= -(x_2 - x_1)(z_3 - z_1) + (z_2 - z_1)(x_3 - x_1) \\ \lambda_3 &= (x_2 - x - 1)(y_3 - y_1) - (y_2 - y_1)(x_3 - x_1) \end{aligned} \tag{5.98}$$

Therefore the terms in Eqn. 5.88 can be derived as:

$$\begin{aligned} \frac{\partial l_1}{\partial X_{sj}} &= \frac{\partial(\frac{a_x}{\sqrt{a_x^2+a_y^2+a_z^2}})}{\partial X_{sj}} \\ &= \frac{\partial a_x}{\partial X_{sj}} \frac{1}{\sqrt{a_x^2 + a_y^2 + a_z^2}} - \frac{a_x}{2(\sqrt{a_x^2 + a_y^2 + a_z^2})^3} \cdot (2a_x \frac{\partial a_x}{\partial X_j} + 2a_y \frac{\partial a_y}{\partial X_{sj}} + 2a_z \frac{\partial a_z}{\partial X_{sj}}) \end{aligned} \tag{5.99}$$

If we set $B_1 = (\sqrt{a_x^2 + a_y^2 + a_z^2})^3$ and $A_1 = \frac{1}{\sqrt{a_x^2+a_y^2+a_z^2}}$, then Eqn.5.99 becomes

$$\begin{aligned} \frac{\partial l_1}{\partial X_{sj}} &= \frac{\partial a_x}{\partial X_{sj}} A_1 - \frac{a_x}{2B_1}(2a_x \frac{\partial a_x}{\partial X_{sj}} + 2a_y \frac{\partial a_y}{\partial X_{sj}} + 2a_z \frac{\partial a_z}{\partial X_{sj}}) \\ &= \frac{\partial(x_2 - x_1)}{\partial X_{sj}} A_1 - \frac{a_x}{2B_1}(2a_x \frac{\partial(x_2 - x_1)}{\partial X_{sj}} + 2a_y \frac{\partial(y_2 - y_1)}{\partial X_{sj}} + 2a_z \frac{\partial(z_2 - z_1)}{\partial X_{sj}}) \\ &= (\frac{a_x^2}{B_1} - A)\frac{\partial x_1}{\partial X_{sj}} + \frac{a_x a_y}{B_1}\frac{\partial y_1}{\partial X_{sj}} + \frac{a_x a_z}{B_1}\frac{\partial z_1}{\partial X_{sj}} - (\frac{a_x^2}{B} - A_1)\frac{\partial x_2}{\partial X_{sj}} - \frac{a_x a_y}{B_1}\frac{\partial y_2}{\partial X_{sj}} - \frac{a_x a_z}{B_1}\frac{\partial z_2}{\partial X_{sj}} \\ &= (\frac{a_x^2}{B_1} - A)\frac{\partial u_1}{\partial X_{sj}} + \frac{a_x a_y}{B_1}\frac{\partial v_1}{\partial X_{sj}} + \frac{a_x a_z}{B_1}\frac{\partial w_1}{\partial X_{sj}} - (\frac{a_x^2}{B} - A_1)\frac{\partial u_2}{\partial X_{sj}} - \frac{a_x a_y}{B_1}\frac{\partial v_2}{\partial X_{sj}} - \frac{a_x a_z}{B_1}\frac{\partial w_2}{\partial X_{sj}} \end{aligned} \tag{5.100}$$

Similarly,

$$\frac{\partial l_2}{\partial X_{sj}} = \frac{a_x a_y}{B_1}\frac{\partial u_1}{\partial X_{sj}} + (\frac{a_y^2}{B_1} - A_1)\frac{\partial v_1}{\partial X_{sj}} + \frac{a_y a_z}{B_1}\frac{\partial w_1}{\partial X_{sj}} - \frac{a_x a_y}{B_1}\frac{\partial u_2}{\partial X_{sj}} - (\frac{a_y^2}{B_1} - A_1)\frac{\partial v_2}{\partial X_{sj}} - \frac{a_y a_z}{B_1}\frac{\partial w_2}{\partial X_{sj}} \tag{5.101}$$

$$\frac{\partial l_3}{\partial X_{sj}} = \frac{a_x a_z}{B_1}\frac{\partial u_1}{\partial X_{sj}} + \frac{a_y a_z}{B_1}\frac{\partial v_1}{\partial X_{sj}} + (\frac{a_z^2}{B_1} - A_1)\frac{\partial w_1}{\partial X_{sj}} - \frac{a_x a_z}{B_1}\frac{\partial u_2}{\partial X_{sj}} - \frac{a_y a_z}{B_1}\frac{\partial v_2}{\partial X_{sj}} - (\frac{a_z^2}{B_1} - A_1)\frac{\partial w_2}{\partial X_{sj}} \tag{5.102}$$

Writing Eqn.5.100, 5.101 and 5.102 together, we get:

$$\begin{Bmatrix} \frac{\partial l_1}{\partial X_{sj}} \\ \frac{\partial l_2}{\partial X_{sj}} \\ \frac{\partial l_3}{\partial X_{sj}} \end{Bmatrix} = \begin{bmatrix} \frac{a_x^2}{B_1} - A_1 & \frac{a_x a_y}{B_1} & \frac{a_x a_z}{B_1} & -\frac{a_x^2}{B_1} + A_1 & -\frac{a_x a_y}{B_1} & \frac{a_x a_z}{B_1} \\ \frac{a_x a_y}{B_1} & \frac{a_y^2}{B_1} - A_1 & \frac{a_y a_z}{B_1} & -\frac{a_x a_y}{B_1} & -\frac{a_y^2}{B_1} + A_1 & -\frac{a_y a_z}{B_1} \\ \frac{a_x a_z}{B_1} & \frac{a_y a_z}{B_1} & \frac{a_z^2}{B_1} - A_1 & -\frac{a_x a_z}{B_1} & -\frac{a_y a_z}{B_1} & -\frac{a_z^2}{B_1} + A_1 \end{bmatrix} \begin{Bmatrix} \frac{\partial u_1}{\partial X_{sj}} \\ \frac{\partial v_1}{\partial X_{sj}} \\ \frac{\partial w_1}{\partial X_{sj}} \\ \frac{\partial u_2}{\partial X_{sj}} \\ \frac{\partial v_2}{\partial X_{sj}} \\ \frac{\partial w_2}{\partial X_{sj}} \end{Bmatrix}$$

$$= \begin{bmatrix} [dl_1] \\ [dl_2] \\ [dl_3] \end{bmatrix} \begin{Bmatrix} \frac{\partial u_1}{\partial X_{sj}} \\ \frac{\partial v_1}{\partial X_{sj}} \\ \frac{\partial w_1}{\partial X_{sj}} \\ \frac{\partial u_2}{\partial X_{sj}} \\ \frac{\partial v_2}{\partial X_{sj}} \\ \frac{\partial w_2}{\partial X_{sj}} \end{Bmatrix} \tag{5.103}$$

The derivatives of m_i are computed as:

$$\begin{aligned} \frac{\partial m_1}{\partial X_{sj}} &= \frac{\partial(\frac{b_x}{\sqrt{b_x^2+b_y^2+b_z^2}})}{\partial X_{sj}} = \frac{\partial b_x}{\partial X_{sj}}A_2 - \frac{b_x}{2B}(2b_x\frac{\partial b_x}{\partial X_{sj}} + 2b_y\frac{\partial b_y}{\partial X_{sj}} + 2b_z\frac{\partial b_z}{\partial X_{sj}}) \\ &= \frac{\partial(x_p - x_1)}{\partial X_{sj}}A_2 - \frac{b_x}{2B}(2b_x\frac{\partial(x_p - x_1)}{\partial X_{sj}} + 2b_y\frac{\partial(y_p - y_1)}{\partial X_{sj}} + 2b_z\frac{\partial(z_p - z_1)}{\partial X_{sj}}) \end{aligned} \tag{5.104}$$

where $B_2 = (\sqrt{b_x^2 + b_y^2 + b_z^2})^3$ and $A_2 = \frac{1}{\sqrt{b_x^2+b_y^2+b_z^2}}$

Similarly,

$$\frac{\partial m_2}{\partial X_{sj}} = \frac{\partial(y_p - y_1)}{\partial X_{sj}}A_2 - \frac{b_y}{2B}(2b_x\frac{\partial(x_p - x_1)}{\partial X_{sj}} + 2b_y\frac{\partial(y_p - y_1)}{\partial X_{sj}} + 2b_z\frac{\partial(z_p - z_1)}{\partial X_{sj}}) \tag{5.105}$$

$$\frac{\partial m_3}{\partial X_{sj}} = \frac{\partial(z_p - z_1)}{\partial X_{sj}} A_2 - \frac{b_z}{2B}(2b_x \frac{\partial(x_p - x_1)}{\partial X_{sj}} + 2b_y \frac{\partial(y_p - y_1)}{\partial X_{sj}} + 2b_z \frac{\partial(z_p - z_1)}{\partial X_{sj}}) \tag{5.106}$$

The derivatives of x_p, y_p, z_p can be computed by differentiating Eqn. 5.97:

$$\begin{aligned}
\begin{Bmatrix} \frac{\partial x_p}{\partial X_{sj}} \\ \frac{\partial y_p}{\partial X_{sj}} \\ \frac{\partial z_p}{\partial X_{sj}} \end{Bmatrix} &= \frac{\partial [M_p]^{-1}}{\partial X_{sj}} \{F_p\} + [M]^{-1} \{\frac{\partial F_p}{\partial X_{sj}}\} \\
&= -[M_p]^{-1} \frac{\partial [M_p]}{\partial X_{sj}} [M_p]^{-1} \{F\} + [M_p]^{-1} \{\frac{\partial F_p}{\partial X_{sj}}\} \\
&= -[M_p]^{-1} \frac{\partial [M_p]}{\partial X_{sj}} \begin{Bmatrix} x_p \\ y_p \\ z_p \end{Bmatrix} + [M_p]^{-1} \{\frac{\partial F_p}{\partial X_{sj}}\}
\end{aligned} \tag{5.107}$$

From Eqn. 5.96 and 5.97, $[M_p]$ and $\{F_p\}$ are defined as,

$$[M_p] = \begin{bmatrix} x_2 - x_1 & y_2 - y_1 & z_2 - z_1 \\ \lambda_1 & \lambda_2 & \lambda_3 \\ x_3 - x_1 & y_3 - y_1 & z_3 - z_1 \end{bmatrix} \tag{5.108}$$

$$\{F_p\} = \begin{Bmatrix} (x_2 - x_1)x_1 + (y_2 - y_1)y_1 + (z_2 - z_1)z_1 \\ \lambda_1 x_1 + \lambda_2 x_2 + \lambda_3 x_3 \\ (x_3 - x_1)x_3 + (y_3 - y_1)y_3 + (z_3 - z_1)z_3 \end{Bmatrix} \tag{5.109}$$

Therefore, the derivative of $[M_p]$ is,

$$\begin{aligned}
\frac{\partial [M_p]}{\partial X_{sj}} &= \begin{bmatrix} \frac{\partial x_2}{\partial X_{sj}} - \frac{\partial x_1}{\partial X_{sj}} & \frac{\partial y_2}{\partial X_{sj}} - \frac{\partial y_1}{\partial X_{sj}} & \frac{\partial z_2}{\partial X_{sj}} - \frac{\partial z_1}{\partial X_{sj}} \\ \frac{\partial \lambda_1}{\partial X_{sj}} & \frac{\partial \lambda_2}{\partial X_{sj}} & \frac{\partial \lambda_3}{\partial X_{sj}} \\ \frac{\partial x_3}{\partial X_{sj}} - \frac{\partial x_1}{\partial X_{sj}} & \frac{\partial y_3}{\partial X_{sj}} - \frac{\partial y_1}{\partial X_{sj}} & \frac{\partial z_3}{\partial X_{sj}} - \frac{\partial z_1}{\partial X_{sj}} \end{bmatrix} \\
&= \begin{bmatrix} \frac{\partial u_2}{\partial X_{sj}} - \frac{\partial u_1}{\partial X_{sj}} & \frac{\partial v_2}{\partial X_{sj}} - \frac{\partial v_1}{\partial X_{sj}} & \frac{\partial w_2}{\partial X_{sj}} - \frac{\partial w_1}{\partial X_{sj}} \\ \frac{\partial \lambda_1}{\partial X_{sj}} & \frac{\partial \lambda_2}{\partial X_{sj}} & \frac{\partial \lambda_3}{\partial X_{sj}} \\ \frac{\partial u_3}{\partial X_{sj}} - \frac{\partial u_1}{\partial X_{sj}} & \frac{\partial v_3}{\partial X_{sj}} - \frac{\partial v_1}{\partial X_{sj}} & \frac{\partial w_3}{\partial X_{sj}} - \frac{\partial w_1}{\partial X_{sj}} \end{bmatrix}
\end{aligned} \tag{5.110}$$

and the derivative of $\{F_p\}$ is,

$$\frac{\partial\{F_p\}}{\partial X_{sj}} = \begin{Bmatrix} \frac{\partial x_1}{\partial X_{sj}}(x_2-x_1)+x_1(\frac{\partial x_2}{\partial X_{sj}}-\frac{\partial x_1}{\partial X_{sj}})+\frac{\partial y_1}{\partial X_{sj}}(y_2-y_1)+y_1(\frac{\partial y_2}{\partial X_{sj}}-\frac{\partial y_1}{\partial X_{sj}})+\frac{\partial z_1}{\partial X_{sj}}(z_2-z_1) \\ +z_1(\frac{\partial z_2}{\partial X_{sj}}-\frac{\partial z_1}{\partial X_{sj}}) \\ \frac{\partial \lambda_1}{\partial X_{sj}}x_1+\lambda_1\frac{\partial x_1}{\partial X_{sj}}+\frac{\partial \lambda_2}{\partial X_{sj}}y_1+\lambda_2\frac{\partial y_1}{\partial X_{sj}}+\frac{\partial \lambda_3}{\partial X_{sj}}z_1+\lambda_3\frac{\partial z_1}{\partial X_{sj}} \\ \frac{\partial x_3}{\partial X_{sj}}(x_3-x_1)+x_3(\frac{\partial x_3}{\partial X_{sj}}-\frac{\partial x_1}{\partial X_{sj}})+\frac{\partial y_3}{\partial X_{sj}}(y_3-y_1)+y_3(\frac{\partial y_3}{\partial X_{sj}}-\frac{\partial y_1}{\partial X_{sj}})+\frac{\partial z_3}{\partial X_{sj}}(z_3-z_1) \\ +z_3(\frac{\partial z_3}{\partial X_{sj}}-\frac{\partial z_1}{\partial X_{sj}}) \end{Bmatrix}$$

$$= \begin{Bmatrix} \frac{\partial u_1}{\partial X_{sj}}(x_2-x_1)+x_1(\frac{\partial u_2}{\partial X_{sj}}-\frac{\partial u_1}{\partial X_{sj}})+\frac{\partial v_1}{\partial X_{sj}}(y_2-y_1)+y_1(\frac{\partial v_2}{\partial X_{sj}}-\frac{\partial v_1}{\partial X_{sj}})+\frac{\partial w_1}{\partial X_{sj}}(z_2-z_1) \\ +z_1(\frac{\partial w_2}{\partial X_{sj}}-\frac{\partial w_1}{\partial X_{sj}}) \\ \frac{\partial \lambda_1}{\partial X_{sj}}x_1+\lambda_1\frac{\partial u_1}{\partial X_{sj}}+\frac{\partial \lambda_2}{\partial X_{sj}}y_1+\lambda_2\frac{\partial v_1}{\partial X_{sj}}+\frac{\partial \lambda_3}{\partial X_{sj}}z_1+\lambda_3\frac{\partial w_1}{\partial X_{sj}} \\ \frac{\partial u_3}{\partial X_{sj}}(x_3-x_1)+x_3(\frac{\partial u_3}{\partial X_{sj}}-\frac{\partial u_1}{\partial X_{sj}})+\frac{\partial v_3}{\partial X_{sj}}(y_3-y_1)+y_3(\frac{\partial v_3}{\partial X_{sj}}-\frac{\partial v_1}{\partial X_{sj}})+\frac{\partial w_3}{\partial X_{sj}}(z_3-z_1) \\ +z_3(\frac{\partial w_3}{\partial X_{sj}}-\frac{\partial w_1}{\partial X_{sj}}) \end{Bmatrix} \tag{5.111}$$

Differentiating Eqn.5.98, we can obtain the derivaties of $\lambda_1, \lambda_2, \lambda_3$, as in,

$$\begin{aligned} \frac{\partial \lambda_1}{\partial X_{sj}} &= (y_2-y_1)(\frac{\partial z_3}{\partial X_{sj}}-\frac{\partial z_1}{\partial X_{sj}})+(\frac{\partial y_2}{\partial X_{sj}}-\frac{\partial y_1}{\partial X_{sj}})(z_3-z_1)-(z_2-z_1)(\frac{\partial y_3}{\partial X_{sj}}-\frac{\partial y_1}{\partial X_{sj}}) \\ &\quad -(\frac{\partial z_2}{\partial X_{sj}}-\frac{\partial z_1}{\partial X_{sj}})(y_3-y_1) \\ &= \frac{\partial y_1}{\partial X_{sj}}(z_2-z_3)+\frac{\partial y_2}{\partial X_{sj}}(z_3-z_1)+\frac{\partial y_3}{\partial X_{sj}}(z_1-z_2)+\frac{\partial z_1}{\partial X_{sj}}(y_3-y_2) \\ &\quad +\frac{\partial z_2}{\partial X_{sj}}(y_1-z_3)+\frac{\partial z_3}{\partial X_{sj}}(y_2-y_1) \\ &= \frac{\partial v_1}{\partial X_{sj}}(z_2-z_3)+\frac{\partial v_2}{\partial X_{sj}}(z_3-z_1)+\frac{\partial v_3}{\partial u}(z_1-z_2)+\frac{\partial w_1}{\partial X_{sj}}(y_3-y_2) \\ &\quad +\frac{\partial w_2}{\partial X_{sj}}(y_1-z_3)+\frac{\partial w_3}{\partial X_{sj}}(y_2-y_1) \end{aligned} \tag{5.112}$$

$$\begin{aligned} \frac{\partial \lambda_2}{\partial X_{sj}} &= \frac{\partial u_1}{\partial X_{sj}}(z_3-z_2)+\frac{\partial u_2}{\partial X_{sj}}(z_1-z_3)+\frac{\partial u_3}{\partial X_{sj}}(z_2-z_1)+\frac{\partial w_1}{\partial X_{sj}}(x_2-x_3) \\ &\quad +\frac{\partial w_2}{\partial X_{sj}}(x_3-x_1)+\frac{\partial w_3}{\partial X_{sj}}(x_1-x_2) \end{aligned} \tag{5.113}$$

$$\begin{aligned} \frac{\partial \lambda_3}{\partial X_{sj}} &= \frac{\partial u_1}{\partial X_{sj}}(y_2-y_3)+\frac{\partial u_2}{\partial X_{sj}}(y_3-y_1)+\frac{\partial u_3}{\partial X_{sj}}(y_1-y_2)+\frac{\partial v_1}{\partial X_{sj}}(x_3-x_2) \\ &\quad +\frac{\partial v_2}{\partial X_{sj}}(x_1-x_3)+\frac{\partial v_3}{\partial X_{sj}}(x_2-x_1) \end{aligned} \tag{5.114}$$

If we denote,

$$\frac{\partial[M_p]}{\partial X_{sj}}\begin{Bmatrix} x_p \\ y_p \\ z_p \end{Bmatrix} = [MP] \tag{5.115}$$

then $[MP]$ is a 3×1 matrix, and

$$[MP]_{(1,1)} = (\frac{\partial u_2}{\partial X_{sj}} - \frac{\partial u_1}{\partial X_{sj}})x_p + (\frac{\partial v_2}{\partial X_{sj}} - \frac{\partial v_1}{\partial X_{sj}})y_p + (\frac{\partial w_2}{\partial X_{sj}} - \frac{\partial w_1}{\partial X_{sj}})z_p \tag{5.116}$$

$$\begin{aligned}
[MP]_{(2,1)} &= \frac{\partial \lambda_1}{\partial X_{sj}}x_p + \frac{\partial \lambda_2}{\partial X_{sj}}y_p + \frac{\partial \lambda_3}{\partial X_{sj}}z_p \\
&= \frac{\partial u_1}{\partial X_{sj}}[(z_3 - z_2)y_p + (y_2 - y_3)z_p] + \frac{\partial u_2}{\partial X_{sj}}[(z_1 - z_3)y_p + (y_3 - y_1)z_p] \\
&\quad + \frac{\partial u_3}{\partial X_{sj}}[(z_2 - z_1)y_p + (x_2 - x_1)z_p] + \frac{\partial v_1}{\partial X_{sj}}[(z_2 - z_3)x_p + (x_3 - x_2)z_p] \\
&\quad + \frac{\partial v_2}{\partial X_{sj}}[(z_3 - z_1)x_p + (x_1 - x_3)z_p] + \frac{\partial v_3}{\partial X_{sj}}[(z_2 - z_1)x_p + (x_2 - x_1)z_p] \\
&\quad + \frac{\partial w_1}{\partial X_{sj}}[(y_3 - y_2)x_p + (z_3 - z_2)y_p] + \frac{\partial w_2}{\partial X_{sj}}[(y_1 - y_3)x_p + (x_3 - x_1)y_p] \\
&\quad + \frac{\partial w_3}{\partial X_{sj}}[(y_2 - y_1)x_p + (x_1 - x_2)y_p]
\end{aligned} \tag{5.117}$$

$$[MP]_{(3,1)} = (\frac{\partial u_3}{\partial X_{sj}} - \frac{\partial u_1}{\partial X_{sj}})x_p + (\frac{\partial v_3}{\partial X_{sj}} - \frac{\partial v_1}{\partial X_{sj}})y_p + (\frac{\partial w_3}{\partial X_{sj}} - \frac{\partial w_1}{\partial X_{sj}})z_p \tag{5.118}$$

Extracting the terms of the derivatives of nodal displacements from $[MP]$, we get

$$[MP] = [DM]\begin{Bmatrix} \frac{\partial u_1}{\partial X_{sj}} \\ \frac{\partial v_1}{\partial X_{sj}} \\ \frac{\partial w_1}{\partial X_{sj}} \\ \frac{\partial u_2}{\partial X_{sj}} \\ \frac{\partial v_2}{\partial X_{sj}} \\ \frac{\partial w_2}{\partial X_{sj}} \\ \frac{\partial u_3}{\partial X_{sj}} \\ \frac{\partial v_3}{\partial X_{sj}} \\ \frac{\partial w_3}{\partial X_{sj}} \end{Bmatrix} \tag{5.119}$$

$[DM]$ is a 3×9 matrix, whose non-zero terms are,

$DM_{(1,1)} = -x_p$, $DM_{(1,2)} = -y_p$, $DM_{(1,3)} = -z_p$
$DM_{(1,4)} = x_p$, $DM_{(1,5)} = y_p$, $DM_{(1,6)} = z_p$

$$DM_{(2,1)} = (z_2 - z_1)y_p + (y_2 - y_3)z_p, \qquad DM_{(2,2)} = (z_2 - z_3)x_p + (x_3 - x_2)z_p$$
$$DM_{(2,3)} = (y_3 - y_2)x_p + (x_2 - x_3)y_p, \qquad DM_{(2,4)} = (z_1 - z_3)y_p + (y_3 - y_1)z_p$$
$$DM_{(2,5)} = (z_3 - z_1)x_p + (x_1 - x_3)z_p, \qquad DM_{(2,6)} = (y_1 - y_3)x_p + (x_3 - x_1)y_p$$
$$DM_{(2,7)} = (z_2 - z_1)y_p + (x_2 - x_1)z_p, \qquad DM_{(2,8)} = (z_1 - z_2)x_p + (x_2 - x_1)z_p$$
$$DM_{(2,9)} = (y_2 - y_1)x_p + (x_1 - x_2)y_p$$
$$DM_{(3,1)} = -x_p, \qquad DM_{(3,2)} = -y_p, \qquad DM_{(3,3)} = -z_p$$
$$DM_{(3,7)} = x_p, \qquad DM_{(3,8)} = y_p, \qquad DM_{(3,9)} = z_p$$

$\frac{\partial\{F_p\}}{\partial X_{sj}}$ is a 3×1 matrix, and

$$\frac{\partial\{F_p\}}{\partial X_{sj}} = \begin{Bmatrix} \frac{\partial\{F_{p(1,1)}\}}{\partial X_{sj}} \\ \frac{\partial\{F_{p(2,1)}\}}{\partial X_{sj}} \\ \frac{\partial\{F_{p(3,1)}\}}{\partial X_{sj}} \end{Bmatrix} \tag{5.120}$$

in which,

$$\begin{aligned}
\frac{\partial\{F_{p(1,1)}\}}{\partial X_{sj}} &= \frac{\partial x_1}{\partial X_{sj}}(x_2 - 2x_1) + \frac{\partial y_1}{\partial X_{sj}}(y_2 - 2y_1) + \frac{\partial z_1}{\partial X_{sj}}(z_2 - 2z_1) + \frac{\partial x_2}{\partial X_{sj}}x_1 + \frac{\partial y_2}{\partial X_{sj}} + \frac{\partial x_1}{\partial X_j}z_1 \\
\frac{\partial\{F_{p(2,1)}\}}{\partial X_j} &= \frac{\partial x_1}{\partial X_j}\{\lambda_1 + (z_3 - z_2)y_1) + (y_2 - y_3)z_1\} + \frac{\partial x_2}{\partial X_j}\{(z_1 - z_3)y_1 + (y_3 - y_2)z_1\} \\
&\quad + \frac{\partial x_3}{\partial X_j}\{(z_2 - z_1)y_1 + (y_1 - y_2)z_1\} + \frac{\partial y_1}{\partial X_j}\{\lambda_2 + (z_2 - z_3)x_1 + (x_3 - x_2)z_1\} \\
&\quad + \frac{\partial y_2}{\partial X_j}\{(z_3 - z_1)x_1 + (x_1 - x_3)z_1\} + \frac{\partial y_3}{\partial X_j}\{(z_1 - z_2)x_1 + (x_2 - x_1)z_1\} \\
&\quad + \frac{\partial z_1}{\partial X_j}\{\lambda_3 + (y_3 - y_2)x_1 + (x_2 - x_3)y_1\} + \frac{\partial z_2}{\partial X_j}\{(y_1 - y_3)x_1 + (x_1 - x_3)y_1\} \\
&\quad + \frac{\partial z_3}{\partial X_j}\{(y_2 - y_1)x_1 + (x_1 - x_2)y_1\} \\
\frac{\partial\{F_{p(2,1)}\}}{\partial X_j} &= \frac{\partial x_1}{\partial X_j}(-x_3) + \frac{\partial x_3}{\partial u}(2x_3 - x_1) + \frac{\partial y_1}{\partial X_j}(-y_3) + \frac{\partial y_3}{\partial X_j}(2y_3 - y_1) + \frac{\partial z_1}{\partial X_j}(-z_3) \\
&\quad + \frac{\partial z_3}{\partial X_j}(2z_3 - z_1)
\end{aligned} \tag{5.121}$$

Eqn. 5.120 can be rewritten as:

$$\frac{\partial\{F_p\}}{\partial X_j} = [DF]\begin{Bmatrix} \frac{\partial x_1}{\partial X_j} \\ \frac{\partial y_1}{\partial X_j} \\ \frac{\partial z_1}{\partial X_j} \\ \frac{\partial x_2}{\partial X_j} \\ \frac{\partial y_2}{\partial X_j} \\ \frac{\partial z_2}{\partial X_j} \\ \frac{\partial x_3}{\partial X_j} \\ \frac{\partial y_3}{\partial X_j} \\ \frac{\partial z_3}{\partial X_j} \end{Bmatrix} = [DF]\begin{Bmatrix} \frac{\partial u_1}{\partial X_j} \\ \frac{\partial v_1}{\partial X_j} \\ \frac{\partial w_1}{\partial X_j} \\ \frac{\partial u_2}{\partial X_j} \\ \frac{\partial v_2}{\partial X_j} \\ \frac{\partial w_2}{\partial X_j} \\ \frac{\partial u_3}{\partial X_j} \\ \frac{\partial v_3}{\partial X_j} \\ \frac{\partial w_3}{\partial X_j} \end{Bmatrix} \tag{5.122}$$

where $[DF]$ is a 3×9 matrix. The non-zero terms of $[DF]$ are:

$$
\begin{aligned}
&DF_{(1,1)} = x_2 - 2x_1, \qquad DF_{(1,2)} = y_2 - 2y_1, \qquad DF_{(1,3)} = z_2 - 2z_1,\\
&DF_{(1,4)} = x_1, \qquad DF_{(1,5)} = y_1, \qquad DF_{(1,6)} = z_1,\\
&DF_{(2,1)} = \lambda_1 + (z_3 - z_2)x_1 + (y_2 - y_3)y_1, \qquad DF_{(2,2)} = \lambda_2 + (z_2 - z_3)x_1 + (x_3 - x_2)z_1\\
&DF_{(2,3)} = \lambda_3 + (y_3 - y_2)x_1 + (x_2 - x_3)y_1, \qquad DF_{(2,4)} = (z_1 - z_3)y_1 + (y_3 - y_2)z_1\\
&DF_{(2,5)} = (z_2 - z_1)y_1 + (y_1 - y_2)z_1, \qquad DF_{(2,8)} = (z_1 - z_2)x_1 + (x_2 - x_1)z_1\\
&DF_{(2,9)} = (y_2 - y_1)x_1 + (x_1 - x_2)y_1\\
&DF_{(3,1)} = -x_3, \qquad DF_{(3,2)} = -y_3, \qquad DF_{(3,3)} = -z_3,\\
&DF_{(3,7)} = 2x_3 - x_1, \qquad DF_{(3,8)} = 2y_3 - y_1, \qquad DF_{(1,6)} = 2z_3 - z_1,
\end{aligned}
$$

Therefore, Eqn 5.107 can be rewritten as,

$$
\begin{aligned}
\begin{Bmatrix} \frac{\partial x_p}{\partial X_j} \\ \frac{\partial y_p}{\partial X_j} \\ \frac{\partial z_p}{\partial X_j} \end{Bmatrix} &= -[M_p]^{-1}\frac{\partial [M_p]}{\partial X_j}\begin{Bmatrix} x_p \\ y_p \\ z_p \end{Bmatrix} + [M_p]^{-1}\{\frac{\partial F_p}{\partial X_j}\}\\
&= \left\{-[M_p]^{-1}[DM] + [M_p]^{-1}[DF]\right\}\begin{Bmatrix} \frac{\partial u_1}{\partial X_j} \\ \frac{\partial v_1}{\partial X_j} \\ \frac{\partial w_1}{\partial X_j} \\ \frac{\partial u_2}{\partial X_j} \\ \frac{\partial v_2}{\partial X_j} \\ \frac{\partial w_2}{\partial X_j} \\ \frac{\partial u_3}{\partial X_j} \\ \frac{\partial v_3}{\partial X_j} \\ \frac{\partial w_3}{\partial X_j} \end{Bmatrix}\\
&= [DX_p]\begin{Bmatrix} \Delta u_1 \\ \Delta u_2 \\ \Delta u_3 \end{Bmatrix} \qquad (5.123)
\end{aligned}
$$

where $[DX_p]$ is a 3×9 matrix and Δu_i represents the derivatives of nodal displacement vector of the ith node, and

$$
\Delta u_i = \begin{Bmatrix} \frac{\partial u_i}{\partial X_j} \\ \frac{\partial v_i}{\partial X_j} \\ \frac{\partial w_i}{\partial X_j} \end{Bmatrix} \qquad (5.124)
$$

Substituting Eqn.5.123 into Eqn.5.104 to 5.106, we obtain

$$
\frac{\partial m_1}{\partial X_j} = \left[(A_2 - \frac{b_x^2}{B_2})T_1^x + \frac{b_x^2}{B_2} - A_2 - \frac{b_x b_y}{B_2}R_1^x - \frac{b_x b_z}{B_2}S_1^x\right]\frac{\partial u_1}{\partial X_j}
$$

$$
\begin{aligned}
&+\left[(A_2-\frac{b_x^2}{B_2})T_1^y-\frac{b_xb_y}{B_2}R_1^y-\frac{b_xb_z}{B_2}S_1^y+\frac{b_xb_y}{B_2}\right]\frac{\partial v_1}{\partial X_j}\\
&+\left[(A_2-\frac{b_x^2}{B_2})T_1^z-\frac{b_xb_y}{B_2}R_1^z-\frac{b_xb_z}{B_2}S_1^z+\frac{b_xb_z}{B_2}\right]\frac{\partial w_1}{\partial X_j}\\
&+\left[(A_2-\frac{b_x^2}{B_2})T_2^x-\frac{b_xb_y}{B_2}R_2^x-\frac{b_xb_z}{B_2}S_2^x\right]\frac{\partial u_2}{\partial X_j}\\
&+\left[(A_2-\frac{b_x^2}{B_2})T_2^y-\frac{b_xb_y}{B_2}R_2^y-\frac{b_xb_z}{B_2}S_2^y\right]\frac{\partial v_2}{\partial X_j}\\
&+\left[(A_2-\frac{b_x^2}{B_2})T_2^z-\frac{b_xb_y}{B_2}R_2^z-\frac{b_xb_z}{B_2}S_2^z\right]\frac{\partial w_2}{\partial X_j}\\
&\qquad\vdots\\
&+\left[(A_2-\frac{b_x^2}{B_2})T_3^z-\frac{b_xb_y}{B_2}R_3^z-\frac{b_xb_z}{B_2}S_3^z\right]\frac{\partial w_3}{\partial X_j}\\
=\;&[dm_1]\begin{Bmatrix}\Delta u_1\\ \Delta u_2\\ \Delta u_3\end{Bmatrix}
\end{aligned}
\tag{5.125}
$$

where $[dm_1]$ is a 1×9 matrix, and $T_i^x, T_i^y, T_i^z, S_i^x, S_i^y, S_i^z, R_i^x, R_i^y, R_i^z$ are components of the matrix $[DX_p]$ defined in Eqn. 5.123:

$T_1^x = DX_{p(1,1)}$, $T_1^y = DX_{p(1,2)}$, $T_1^z = DX_{p(1,3)}$, $T_2^x = DX_{p(1,4)}$, $T_2^y = DX_{p(1,5)}$, $T_2^z = DX_{p(1,6)}$,
$T_3^x = DX_{p(1,7)}$, $T_3^y = DX_{p(1,8)}$, $T_3^z = DX_{p(1,9)}$, $R_1^x = DX_{p(2,1)}$, $R_1^y = DX_{p(2,2)}$, $R_1^z = DX_{p(2,3)}$,
$R_2^x = DX_{p(2,4)}$, $R_2^y = DX_{p(2,5)}$, $R_2^z = DX_{p(2,6)}$, $R_3^x = DX_{p(2,7)}$, $R_2^y = DX_{p(2,8)}$, $R_2^z = DX_{p(2,9)}$,
$S_1^x = DX_{p(3,1)}$, $S_1^y = DX_{p(3,2)}$, $S_1^z = DX_{p(3,3)}$, $S_2^x = DX_{p(3,4)}$, $S_2^y = DX_{p(3,5)}$, $S_2^z = DX_{p(3,6)}$,
$S_3^x = DX_{p(3,7)}$, $S_3^y = DX_{p(3,8)}$, $S_3^z = DX_{p(3,9)}$.

Similarly,

$$
\begin{aligned}
\frac{\partial m_2}{\partial X_j} =\;&\left[-\frac{b_xb_y}{B_2}T_1^x+(A_2-\frac{b_y^2}{B_2})R_1^x-\frac{b_yb_z}{B_2}S_1^x+\frac{b_xb_y}{B_2}\right]\frac{\partial u_1}{\partial X_j}\\
&+\left[-\frac{b_xb_y}{B_2}T_1^y+(A_2-\frac{b_y^2}{B_2})R_1^y-\frac{b_yb_z}{B_2}S_1^y+\frac{b_y^2}{B_2}-A_2\right]\frac{\partial v_1}{\partial X_j}\\
&+\left[-\frac{b_xb_y}{B_2}T_1^z+(A_2-\frac{b_y^2}{B_2})R_1^z-\frac{b_yb_z}{B_2}S_1^z+\frac{b_yb_z}{B_2}\right]\frac{\partial w_1}{\partial X_j}\\
&+\left[-\frac{b_xb_y}{B_2}T_2^x+(A_2-\frac{b_y^2}{B_2})R_2^x-\frac{b_yb_z}{B_2}S_2^x\right]\frac{\partial u_2}{\partial X_j}\\
&+\left[-\frac{b_xb_y}{B_2}T_2^y+(A_2-\frac{b_y^2}{B_2})R_2^y-\frac{b_yb_z}{B_2}S_2^y\right]\frac{\partial v_2}{\partial X_j}\\
&+\left[-\frac{b_xb_y}{B_2}T_2^z+(A_2-\frac{b_y^2}{B_2})R_2^z-\frac{b_yb_z}{B_2}S_2^z\right]\frac{\partial w_2}{\partial X_j}\\
&\qquad\vdots\\
&+\left[-\frac{b_xb_y}{B_2}T_3^z+(A_2-\frac{b_y^2}{B_2})R_3^z-\frac{b_yb_z}{B_2}S_3^z\right]\frac{\partial w_3}{\partial X_j}
\end{aligned}
$$

$$= [dm_2] \begin{Bmatrix} \Delta u_1 \\ \Delta u_2 \\ \Delta u_3 \end{Bmatrix} \tag{5.126}$$

and,

$$\begin{aligned} \frac{\partial m_3}{\partial X_j} &= \left[-\frac{b_x b_z}{B_2} T_1^x - \frac{b_y b_z}{B_2} R_1^x + (A_2 - \frac{b_z^2}{B_2}) S_1^x + \frac{b_x b_z}{B_2} \right] \frac{\partial u_1}{\partial X_j} \\ &+ \left[-\frac{b_x b_z}{B_2} T_1^y - \frac{b_y b_z}{B_2} R_1^y + (A_2 - \frac{b_z^2}{B_2}) S_1^y + \frac{b_y b_z}{B_2} \right] \frac{\partial v_1}{\partial X_j} \\ &+ \left[-\frac{b_x b_z}{B_2} T_1^z - \frac{b_y b_z}{B_2} R_1^z + (A_2 - \frac{b_z^2}{B_2}) S_1^z + \frac{b_z^2}{B_2} - A_2 \right] \frac{\partial w_1}{\partial X_j} \\ &+ \left[-\frac{b_x b_z}{B_2} T_2^x - \frac{b_y b_z}{B_2} R_2^x + (A_2 - \frac{b_z^2}{B_2}) S_2^x \right] \frac{\partial u_2}{\partial X_j} \\ &+ \left[-\frac{b_x b_z}{B_2} T_2^y - \frac{b_y b_z}{B_2} R_2^y + (A_2 - \frac{b_z^2}{B_2}) S_2^y \right] \frac{\partial v_2}{\partial X_j} \\ &+ \left[-\frac{b_x b_z}{B_2} T_2^z - \frac{b_y b_z}{B_2} R_2^z + (A_2 - \frac{b_z^2}{B_2}) S_2^z \right] \frac{\partial w_2}{\partial X_j} \\ &\vdots \\ &+ \left[-\frac{b_x b_z}{B_2} T_3^z - \frac{b_y b_z}{B_2} R_3^z + (A_2 - \frac{b_z^2}{B_2}) S_3^z \right] \frac{\partial w_3}{\partial X_j} \\ &= [dm_3] \begin{Bmatrix} \Delta u_1 \\ \Delta u_2 \\ \Delta u_3 \end{Bmatrix} \end{aligned} \tag{5.127}$$

The derivatives of the direction cosines n_1, n_2, n_3 are computed by differentiating Eqn. 5.94:

$$\begin{aligned} \frac{\partial n_1}{\partial X_j} &= \frac{\partial c_x}{\partial X_j} A_3 + c_x \frac{c_x \frac{\partial c_x}{\partial X_j} + c_y \frac{\partial c_y}{\partial X_j} + c_z \frac{\partial c_z}{\partial X_j}}{-B_3} \\ &= (A_3 - \frac{c_x^2}{B_3}) \frac{\partial c_x}{\partial X_j} - \frac{c_x c_y}{B_3} \frac{\partial c_y}{\partial X_j} - \frac{c_x c_z}{B_3} \frac{\partial c_z}{\partial X_j} \end{aligned} \tag{5.128}$$

$$\begin{aligned} \frac{\partial n_2}{\partial X_j} &= \frac{\partial c_y}{\partial X_j} A_3 + c_y \frac{c_x \frac{\partial c_x}{\partial X_j} + c_y \frac{\partial c_y}{\partial X_j} + c_z \frac{\partial c_z}{\partial X_j}}{-B_3} \\ &= -\frac{c_x c_y}{B_3} \frac{\partial c_x}{\partial X_j} + (A_3 - \frac{c_y^2}{B_3}) \frac{\partial c_y}{\partial X_j} - \frac{c_x c_z}{B_3} \frac{\partial c_z}{\partial X_j} \end{aligned} \tag{5.129}$$

$$\begin{aligned} \frac{\partial n_3}{\partial X_j} &= \frac{\partial c_z}{\partial u} A_3 + c_z \frac{c_x \frac{\partial c_x}{\partial X_j} + c_y \frac{\partial c_y}{\partial X_j} + c_z \frac{\partial c_z}{\partial X_j}}{-B_3} \\ &= -\frac{c_x c_z}{B_3} \frac{\partial c_x}{\partial X_j} - \frac{c_y c_z}{B_3} \frac{\partial c_y}{\partial X_j} + (A_3 - \frac{c_z^2}{B_3}) \frac{\partial c_z}{\partial X_j} \end{aligned} \tag{5.130}$$

Differentiating Eqn. 5.95 with respect to X_j, we obtain the derivatives of c_x, c_y, c_z:

$$\frac{\partial c_x}{\partial X_j} = \frac{\partial y_p}{\partial X_j}(z_1-z_2)+\frac{\partial z_p}{\partial X_j}(y_2-y_1)+\frac{\partial y_1}{\partial X_j}(z_2-z_p)+\frac{\partial z_1}{\partial X_j}(y_p-y_2)+\frac{\partial y_2}{\partial X_j}(z_p-z_1)+\frac{\partial z_2}{\partial X_j}(y_1-y_p) \tag{5.131}$$

$$\frac{\partial c_y}{\partial X_j} = \frac{\partial x_p}{\partial X_j}(z_2-z_1)+\frac{\partial z_p}{\partial X_j}(x_1-x_2)+\frac{\partial x_1}{\partial X_j}(z_p-z_2)+\frac{\partial z_1}{\partial X_j}(x_2-x_p)+\frac{\partial x_2}{\partial X_j}(z_1-z_p)+\frac{\partial z_2}{\partial X_j}(x_p-x_1) \tag{5.132}$$

$$\frac{\partial c_z}{\partial X_j} = \frac{\partial x_p}{\partial X_j}(y_1-y_2)+\frac{\partial y_p}{\partial X_j}(x_2-x_1)+\frac{\partial x_1}{\partial X_j}(y_2-y_p)+\frac{\partial y_1}{\partial X_j}(x_p-x_2)+\frac{\partial x_2}{\partial X_j}(y_p-y_1)+\frac{\partial y_2}{\partial X_j}(x_p-x_1) \tag{5.133}$$

with,

$$\begin{Bmatrix} \frac{\partial x_p}{\partial X_j} \\ \frac{\partial y_p}{\partial X_j} \\ \frac{\partial z_p}{\partial X_j} \end{Bmatrix} = [DX_p] \begin{Bmatrix} \Delta u_1 \\ \Delta u_2 \\ \Delta u_3 \end{Bmatrix} = \begin{bmatrix} T_1^x & T_1^y & T_1^z & T_2^x & T_2^y & T_2^z & T_3^x & T_3^y & T_3^z \\ R_1^x & R_1^y & R_1^z & R_2^x & R_2^y & R_2^z & R_3^x & R_3^y & R_3^z \\ S_1^x & S_1^y & S_1^z & S_2^x & S_2^y & S_2^z & S_3^x & S_3^y & S_3^z \end{bmatrix} \begin{Bmatrix} \frac{\partial u_1}{\partial X_j} \\ \frac{\partial v_1}{\partial X_j} \\ \frac{\partial w_1}{\partial X_j} \\ \frac{\partial u_2}{\partial X_j} \\ \frac{\partial v_2}{\partial X_j} \\ \frac{\partial w_2}{\partial X_j} \\ \frac{\partial u_3}{\partial X_j} \\ \frac{\partial v_3}{\partial X_j} \\ \frac{\partial w_3}{\partial X_j} \end{Bmatrix} \tag{5.134}$$

then, the derivatives of c_x, c_y, c_z can be written as:

$$\begin{Bmatrix} \frac{\partial c_x}{\partial X_j} \\ \frac{\partial c_y}{\partial X_j} \\ \frac{\partial c_z}{\partial X_j} \end{Bmatrix} = [D_{NN}] \begin{Bmatrix} \frac{\partial u_1}{\partial X_j} \\ \frac{\partial v_1}{\partial X_j} \\ \frac{\partial w_1}{\partial X_j} \\ \frac{\partial u_2}{\partial X_j} \\ \frac{\partial v_2}{\partial X_j} \\ \frac{\partial w_2}{\partial X_j} \\ \frac{\partial u_3}{\partial X_j} \\ \frac{\partial v_3}{\partial X_j} \\ \frac{\partial w_3}{\partial X_j} \end{Bmatrix} \tag{5.135}$$

where $[D_{NN}]$ is a 3×9 matrix, and

$D_{NN(1,1)} = R_1^x(z_1-z_2)+S_1^x(y_2-y_1)$, $\qquad$ $D_{NN(2,1)} = T_1^x(z_2-z_1)+S_1^x(x_1-x_2)+z_p-z_2$,

$$
\begin{aligned}
&D_{NN(3,1)} = T_1^x(y_1-y_2)+R_1^x(x_2-x_1)+y_2-y_p, && D_{NN(1,2)} = R_1^y(z_1-z_2)+S_1^y(y_2-y_1)+z_2-z_p,\\
&D_{NN(2,2)} = T_1^y(z_2-z_1)+S_1^y(x_1-x_2), && D_{NN(3,2)} = T_1^y(y_2-y_1)+R_1^y(x_2-x_1)+x_p-x_2,\\
&D_{NN(1,3)} = R_1^z(z_1-z_2)+S_1^z(y_2-y_1)+y_p-y_2, && D_{NN(2,3)} = T_1^z(z_2-z_1)+S_1^z(x_1-x_2)+x_2-x_p,\\
&D_{NN(3,3)} = T_1^z(y_1-y_2)+R_1^z(x_2-x_1), && D_{NN(1,4)} = R_2^x(z_1-z_2)+S_2^x(y_2-y_1),\\
&D_{NN(2,4)} = T_2^x(z_2-z_1)+S_2^x(x_1-x_2)+z_1-z_p, && D_{NN(3,4)} = T_2^x(z_1-z_2)+R_2^x(x_2-x_1)+y_p-y_1,\\
&D_{NN(1,5)} = R_2^y(z_1-z_2)+S_2^y(y_2-y_1)+z_p-z_1, && D_{NN(2,5)} = T_2^y(z_2-z_1)+S_2^y(x_1-x_2),\\
&D_{NN(3,5)} = T_2^y(y_1-y_2)+R_2^y(x_2-x_1)+x_p-x_1, && D_{NN(1,6)} = R_2^z(z_1-z_2)+S_1^z(y_2-y_1)+y_1-y_p,\\
&D_{NN(2,6)} = T_2^z(z_2-z_1)+S_2^z(x_1-x_2)+x_p-x_1, && D_{NN(3,6)} = T_2^z(y_1-y_2)+R_2^z(x_2-x_1),\\
&D_{NN(1,7)} = R_3^x(z_1-z_2)+S_3^x(y_2-y_1), && D_{NN(1,8)} = R_3^y(z_1-z_2)+S_3^x(y_2-y_1),\\
&D_{NN(1,9)} = R_3^z(z_1-z_2)+S_3^z(y_2-y_1), && D_{NN(2,7)} = T_3^x(z_2-z_1)+S_3^x(x_1-x_2),\\
&D_{NN(2,8)} = T_3^y(z_2-z_1)+S_3^y(x_1-x_2), && D_{NN(2,9)} = T_3^z(z_2-z_1)+S_3^z(x_1-x_2),\\
&D_{NN(3,7)} = T_3^x(y_1-y_2)+R_3^x(x_2-x_1), && D_{NN(3,8)} = T_3^y(y_1-y_2)+R_3^y(x_2-x_1),\\
&D_{NN(3,9)} = T_3^z(y_1-y_2)+R_3^z(x_2-x_1).
\end{aligned}
$$

Substituting Eqn.5.135 into Eqn.5.128 5.129 and 5.130, then

$$
\begin{aligned}
\begin{Bmatrix} \frac{\partial n_1}{\partial X_j} \\ \frac{\partial n_2}{\partial X_j} \\ \frac{\partial n_3}{\partial X_j} \end{Bmatrix} &= \begin{bmatrix} A_3-\frac{c_x^2}{B_3} & -\frac{c_xc_y}{B_3} & \frac{c_xc_z}{B_3} \\ -\frac{c_xc_y}{B_3} & A_3-\frac{c_y^2}{B_3} & -\frac{c_yc_z}{B_3} \\ -\frac{c_xc_z}{B_3} & -\frac{c_yc_z}{B_3} & A_3-\frac{c_z^2}{B_3} \end{bmatrix} \begin{Bmatrix} \frac{\partial c_x}{\partial X_j} \\ \frac{\partial c_y}{\partial X_j} \\ \frac{\partial c_z}{\partial X_j} \end{Bmatrix} \\
&= \begin{bmatrix} A_3-\frac{c_x^2}{B_3} & -\frac{c_xc_y}{B_3} & \frac{c_xc_z}{B_3} \\ -\frac{c_xc_y}{B_3} & A_3-\frac{c_y^2}{B_3} & -\frac{c_yc_z}{B_3} \\ -\frac{c_xc_z}{B_3} & -\frac{c_yc_z}{B_3} & A_3-\frac{c_z^2}{B_3} \end{bmatrix} [D_{NN}] \begin{Bmatrix} \frac{\partial u_1}{\partial X_j} \\ \frac{\partial v_1}{\partial X_j} \\ \frac{\partial w_1}{\partial X_j} \\ \frac{\partial u_2}{\partial X_j} \\ \frac{\partial v_2}{\partial X_j} \\ \frac{\partial w_2}{\partial X_j} \\ \frac{\partial u_3}{\partial X_j} \\ \frac{\partial v_3}{\partial X_j} \\ \frac{\partial w_3}{\partial X_j} \end{Bmatrix} \\
&= [D_N] \begin{Bmatrix} \frac{\partial u_1}{\partial X_j} \\ \frac{\partial v_1}{\partial X_j} \\ \frac{\partial w_1}{\partial X_j} \\ \frac{\partial u_2}{\partial X_j} \\ \frac{\partial v_2}{\partial X_j} \\ \frac{\partial w_2}{\partial X_j} \\ \frac{\partial u_3}{\partial X_j} \\ \frac{\partial v_3}{\partial X_j} \\ \frac{\partial w_3}{\partial X_j} \end{Bmatrix} = \begin{bmatrix} [dn_1] \\ [dn_2] \\ [dn_3] \end{bmatrix} \begin{Bmatrix} \frac{\partial u_1}{\partial X_j} \\ \frac{\partial v_1}{\partial X_j} \\ \frac{\partial w_1}{\partial X_j} \\ \frac{\partial u_2}{\partial X_j} \\ \frac{\partial v_2}{\partial X_j} \\ \frac{\partial w_2}{\partial X_j} \\ \frac{\partial u_3}{\partial X_j} \\ \frac{\partial v_3}{\partial X_j} \\ \frac{\partial w_3}{\partial X_j} \end{Bmatrix}
\end{aligned} \tag{5.136}
$$

in which, $[dn_1], [dn_2], [dn_3]$ are 1×9 matrices.

The product of $\frac{\partial[T_1]}{\partial u}$ and a vector $\{R_1,\ R_2,\ R_3\}$ can be expressed as:

$$\begin{aligned}
\frac{\partial[T_1]}{\partial X_j}\cdot\begin{Bmatrix}R_1\\R_2\\R_3\end{Bmatrix} &= \begin{bmatrix}\frac{\partial l_1}{\partial X_j} & \frac{\partial l_2}{\partial X_j} & \frac{\partial l_3}{\partial X_j}\\ \frac{\partial m_1}{\partial X_j} & \frac{\partial m_2}{\partial X_j} & \frac{\partial m_3}{\partial X_j}\\ \frac{\partial n_1}{\partial X_j} & \frac{\partial n_2}{\partial X_j} & \frac{\partial n_3}{\partial X_j}\end{bmatrix}\begin{Bmatrix}R_1\\R_2\\R_3\end{Bmatrix}\\
&= \begin{Bmatrix}\frac{\partial l_1}{\partial X_j}R_1+\frac{\partial l_2}{\partial X_j}R_2+\frac{\partial l_3}{\partial X_j}R_3\\ \frac{\partial m_1}{\partial X_j}R_1+\frac{\partial m_2}{\partial X_j}R_2+\frac{\partial m_3}{\partial X_j}R_3\\ \frac{\partial n_1}{\partial X_j}R_1+\frac{\partial n_2}{\partial X_j}R_2+\frac{\partial n_3}{\partial X_j}R_3\end{Bmatrix}\\
&= \begin{Bmatrix}[dl_1]R_1+[dl_2]R_2+[dl_3]R_3\\ [dm_1]R_1+[dm_2]R_2+[dm_3]R_3\\ [dn_1]R_1+[dn_2]R_2+[dn_3]R_3\end{Bmatrix}\begin{Bmatrix}\frac{\partial u_1}{\partial X_j}\\ \frac{\partial v_1}{\partial X_j}\\ \frac{\partial w_1}{\partial X_j}\\ \frac{\partial u_2}{\partial X_j}\\ \frac{\partial v_2}{\partial X_j}\\ \frac{\partial w_2}{\partial X_j}\\ \frac{\partial u_3}{\partial X_j}\\ \frac{\partial v_3}{\partial X_j}\\ \frac{\partial w_3}{\partial X_j}\end{Bmatrix}
\end{aligned} \tag{5.137}$$

The derivative of $[T_2]$

Differentiating Eqn. 5.86 with respect X and Y gives:

$$\begin{aligned}
\frac{dZ}{dX} &= a_2+2a_4X+a_5Y\\
\frac{dZ}{dY} &= a_3+a_5X+2a_6Y
\end{aligned} \tag{5.138}$$

The derivative of $[T_2]$ is computed by differentiating Eqn. 5.85:

$$\frac{\partial[T_2]}{\partial X_j}=\begin{bmatrix}\frac{\partial T_2(1)}{\partial X_j} & 0 & \frac{\partial T_2(3)}{\partial X_j}\\ 0 & \frac{\partial T_2(2)}{\partial X_j} & \frac{\partial T_2(4)}{\partial X_j}\\ \frac{\partial T_2(5)}{\partial X_j} & \frac{\partial T_2(6)}{\partial X_j} & \frac{\partial T_2(7)}{\partial X_j}\end{bmatrix} \tag{5.139}$$

If we denote $\sqrt{1+(\frac{dZ}{dX})^2}=A_X$, $\sqrt{1+(\frac{dZ}{dY})^2}=A_Y$ and $B_X=\sqrt{1+(\frac{dZ}{dX})^2+(\frac{dZ}{dY})^2}$, then

$$\frac{\partial dT_2(1)}{\partial X_j} = -\frac{1}{A_X^3}\frac{dZ}{dX}(2a_4\frac{\partial X}{\partial X_j}+a_5\frac{\partial Y}{\partial X_j})-\frac{1}{A_X^3}\frac{dZ}{dX}(\frac{\partial a_2}{\partial X_j}+2X\frac{\partial a_4}{\partial X_j}+Y\frac{\partial a_5}{\partial X_j})$$

$$= [dT_2(1)]_x \begin{Bmatrix} \frac{\partial X}{\partial X_j} \\ \frac{\partial Y}{\partial X_j} \end{Bmatrix} + [dT_2(1)]_a \begin{Bmatrix} \frac{\partial a_2}{\partial X_j} \\ \frac{\partial a_3}{\partial X_j} \\ \frac{\partial a_4}{\partial X_j} \\ \frac{\partial a_5}{\partial X_j} \\ \frac{\partial a_6}{\partial X_j} \end{Bmatrix} \tag{5.140}$$

$$\frac{\partial dT_2(2)}{\partial X_j} = -\frac{1}{A_Y^3}\frac{dZ}{dY}(a_5\frac{\partial X}{\partial X_j} + 2a_6\frac{\partial Y}{\partial X_j}) - \frac{1}{A_Y^3}\frac{dZ}{dY}(\frac{\partial a_3}{\partial X_j} + X\frac{\partial a_5}{\partial X_j} + 2Y\frac{\partial a_6}{\partial X_j})$$

$$= [dT_2(2)]_x \begin{Bmatrix} \frac{\partial X}{\partial X_j} \\ \frac{\partial Y}{\partial X_j} \end{Bmatrix} + [dT_2(2)]_a \begin{Bmatrix} \frac{\partial a_2}{\partial X_j} \\ \frac{\partial a_3}{\partial X_j} \\ \frac{\partial a_4}{\partial X_j} \\ \frac{\partial a_5}{\partial X_j} \\ \frac{\partial a_6}{\partial X_j} \end{Bmatrix} \tag{5.141}$$

$$\frac{\partial dT_2(3)}{\partial X_j} = (-\frac{(\frac{dZ}{dX})^2}{A_X^3} + \frac{1}{A_X})(2a_4\frac{\partial X}{\partial X_j} + a_5\frac{\partial Y}{\partial X_j}) - (\frac{1}{A_X} - \frac{(\frac{dZ}{dX})^2}{A_X^3})(\frac{\partial a_2}{\partial X_j} + 2X\frac{\partial a_4}{\partial X_j} + Y\frac{\partial a_5}{\partial X_j})$$

$$= [dT_2(3)]_x \begin{Bmatrix} \frac{\partial X}{\partial X_j} \\ \frac{\partial Y}{\partial X_j} \end{Bmatrix} + [dT_2(3)]_a \begin{Bmatrix} \frac{\partial a_2}{\partial X_j} \\ \frac{\partial a_3}{\partial X_j} \\ \frac{\partial a_4}{\partial X_j} \\ \frac{\partial a_5}{\partial X_j} \\ \frac{\partial a_6}{\partial X_j} \end{Bmatrix} \tag{5.142}$$

$$\frac{\partial dT_2(4)}{\partial X_j} = (-\frac{(\frac{dZ}{dY})^2}{A_Y^3} + \frac{1}{A_Y})(a_5\frac{\partial X}{\partial X_j} + 2a_6\frac{\partial Y}{\partial X_j}) + (\frac{1}{A_Y} - \frac{(\frac{dZ}{dY})^2}{A_Y^3})(\frac{\partial a_3}{\partial X_j} + X\frac{\partial a_5}{\partial X_j} + 2Y\frac{\partial a_6}{\partial X_j})$$

$$= [dT_2(4)]_x \begin{Bmatrix} \frac{\partial X}{\partial X_j} \\ \frac{\partial Y}{\partial X_j} \end{Bmatrix} + [dT_2(4)]_a \begin{Bmatrix} \frac{\partial a_2}{\partial X_j} \\ \frac{\partial a_3}{\partial X_j} \\ \frac{\partial a_4}{\partial X_j} \\ \frac{\partial a_5}{\partial X_j} \\ \frac{\partial a_6}{\partial X_j} \end{Bmatrix} \tag{5.143}$$

$$\begin{aligned}\frac{\partial dT_2(5)}{\partial X_j} = {} & (\frac{A_X A_Y}{B_X} + \frac{dZ}{dX}k_1)\frac{\partial a_2}{\partial X_j} + \frac{dZ}{dX}k_2\frac{\partial a_3}{\partial X_j} + 2(\frac{A_X A_Y}{B_X} + \frac{dZ}{dX}k_1)X\frac{\partial a_4}{\partial X_j} + [(\frac{A_X A_Y}{B_X} + \frac{dZ}{dX}k_1)Y \\ & + \frac{dZ}{dX}k_2 X]\frac{\partial a_5}{\partial X_j} + 2\frac{dZ}{dX}k_2 Y\frac{\partial a_6}{\partial X_j} + [(\frac{A_X A_Y}{B_X} + \frac{dZ}{dX}k_1)2a_4 + \frac{dZ}{dX}k_2 a_5]\frac{\partial X}{\partial X_j} \\ & + [(\frac{A_X A_Y}{B_X} + \frac{dZ}{dX}k_1)a_5 + \frac{dZ}{dX}k_2 a_6]\frac{\partial Y}{\partial X_j}\end{aligned}$$

$$= [dT_2(5)]_x \begin{Bmatrix} \frac{\partial X}{\partial X_j} \\ \frac{\partial Y}{\partial X_j} \end{Bmatrix} + [dT_2(5)]_a \begin{Bmatrix} \frac{\partial a_2}{\partial X_j} \\ \frac{\partial a_3}{\partial X_j} \\ \frac{\partial a_4}{\partial X_j} \\ \frac{\partial a_5}{\partial X_j} \\ \frac{\partial a_6}{\partial X_j} \end{Bmatrix} \tag{5.144}$$

where $k_1 = \frac{A_Y}{A_X B_X}\frac{dZ}{dX} - 2\frac{A_X A_Y}{B_X^2}\frac{dZ}{dX}$, and $k_2 = \frac{A_X}{A_Y B_X}\frac{dZ}{dY} - 2\frac{A_X A_Y}{B_X^2}\frac{dZ}{dY}$

$$\begin{aligned} \frac{\partial dT_2(6)}{\partial X_j} &= k_1\frac{dZ}{dY}\frac{\partial a_2}{\partial X_j} + (\frac{A_X A_Y}{B_X} + k_2\frac{dZ}{dY})\frac{\partial a_3}{\partial X_j} + 2k_1\frac{dZ}{dY}\frac{\partial a_4}{\partial X_j} + [k_1 Y\frac{dZ}{dY} + (\frac{A_X A_Y}{B_X} + k_2\frac{dZ}{dY})a_5]\frac{\partial a_5}{\partial X_j} \\ &\quad + 2Y(\frac{A_X A_Y}{B_X} + k_2\frac{dZ}{dY})\frac{\partial a_6}{\partial X_j} + [2a_4 k_1 Y\frac{dZ}{dY} + (\frac{A_X A_Y}{B_X} + k_2\frac{dZ}{dY})a_5]\frac{\partial X}{\partial X_j} \\ &\quad + [a_5 k_1 Y\frac{dZ}{dY} + (\frac{A_X A_Y}{B_X} + k_2\frac{dZ}{dY})2a_5]\frac{\partial Y}{\partial X_j} \\ &= [dT_2(6)]_x \begin{Bmatrix} \frac{\partial X}{\partial X_j} \\ \frac{\partial Y}{\partial X_j} \end{Bmatrix} + [dT_2(6)]_a \begin{Bmatrix} \frac{\partial a_2}{\partial X_j} \\ \frac{\partial a_3}{\partial X_j} \\ \frac{\partial a_4}{\partial X_j} \\ \frac{\partial a_5}{\partial X_j} \\ \frac{\partial a_6}{\partial X_j} \end{Bmatrix} \end{aligned} \tag{5.145}$$

$$\begin{aligned} \frac{\partial dT_2(7)}{\partial X_j} &= k_1\frac{\partial a_2}{\partial X_j} + k_2\frac{\partial a_3}{\partial X_j} + 2k_1 X\frac{\partial a_4}{\partial X_j} + (k_1 Y + k_2 X)\frac{\partial a_5}{\partial X_j} + 2k_2 a_6 + (2a_4 k_1 + k_2 a_5)\frac{\partial X}{\partial X_j} \\ &\quad + (a_5 k_1 + 2a_6 k_2)\frac{\partial X}{\partial X_j} \\ &= [dT_2(7)]_x \begin{Bmatrix} \frac{\partial X}{\partial X_j} \\ \frac{\partial Y}{\partial X_j} \end{Bmatrix} + [dT_2(7)]_a \begin{Bmatrix} \frac{\partial a_2}{\partial X_j} \\ \frac{\partial a_3}{\partial X_j} \\ \frac{\partial a_4}{\partial X_j} \\ \frac{\partial a_5}{\partial X_j} \\ \frac{\partial a_6}{\partial X_j} \end{Bmatrix} \end{aligned} \tag{5.146}$$

The product of $\frac{\partial [T_2]}{\partial u}$ and the vector $\{R_1 \;\; R_2 \;\; R_3\}^T$ can be written as:

$$\begin{aligned} \frac{\partial T_2}{\partial X_j}\begin{Bmatrix} R_1 \\ R_2 \\ R_3 \end{Bmatrix} &= \begin{bmatrix} dT_2(1) & 0 & dT_2(3) \\ 0 & dT_2(2) & dT_2(4) \\ dT_2(5) & dT_2(6) & dT_2(7) \end{bmatrix}\begin{Bmatrix} R_1 \\ R_2 \\ R_3 \end{Bmatrix} \\ &= \begin{bmatrix} [dT_2(1)]_x & 0 & [dT_2(3)]_x \\ 0 & [dT_2(2)]_x & [dT_2(4)]_x \\ [dT_2(5)]_x & [dT_2(6)]_x & [dT_2(7)]_x \end{bmatrix}\begin{Bmatrix} R_1 \\ R_2 \\ R_3 \end{Bmatrix}\begin{Bmatrix} \frac{\partial X}{\partial X_j} \\ \frac{\partial Y}{\partial X_j} \end{Bmatrix} \end{aligned}$$

$$+\begin{bmatrix}[dT_2(1)]_a & 0 & [dT_2(3)]_a\\ 0 & [dT_2(2)]_a & [dT_2(4)]_a\\ [dT_2(5)]_a & [dT_2(6)]_a & [dT_2(7)]_a\end{bmatrix}\begin{Bmatrix}R_1\\R_2\\R_3\end{Bmatrix}\begin{Bmatrix}\frac{\partial a_2}{\partial X_j}\\ \frac{\partial a_3}{\partial X_j}\\ \frac{\partial a_4}{\partial X_j}\\ \frac{\partial a_5}{\partial X_j}\\ \frac{\partial a_6}{\partial X_j}\end{Bmatrix} \tag{5.147}$$

in which, $[dT_2(i)]$ are 1×2 matrices:

$$[dT_2(1)]_x=\begin{bmatrix}-2a_4\frac{\frac{dZ}{dX}}{A_x^3} & -a_5\frac{\frac{dZ}{dX}}{A_x^3}\end{bmatrix},[dT_2(2)]_x=\begin{bmatrix}-a_5\frac{\frac{dZ}{dY}}{A_y^3} & -2a_6\frac{\frac{dZ}{dY}}{A_y^3}\end{bmatrix}$$

$$[dT_2(3)]_x=\begin{bmatrix}2a_4(\frac{1}{A_X}-\frac{(\frac{dZ}{dX})^2}{A_Y^3}) & a_5(\frac{1}{A_X}-\frac{(\frac{dZ}{dX})^2}{A_X^3})\end{bmatrix},[dT_2(4)]_x=\begin{bmatrix}a_5(\frac{1}{A_Y}-\frac{(\frac{dZ}{dY})^2}{A_Y^3}) & 2a_6(\frac{1}{A_Y}-\frac{(\frac{dZ}{dY})^2}{A_Y^3})\end{bmatrix}$$

$$[dT_2(5)]_x=\begin{bmatrix}(\frac{A_XA_Y}{B_X}+\frac{dZ}{dX}k_1)a_4+\frac{dZ}{dX}k_2a_5 & (\frac{A_XA_Y}{B_X}+\frac{dZ}{dX}k_1)a_5+\frac{dZ}{dX}k_2a_6\end{bmatrix}$$

$$[dT_2(6)]_x=\begin{bmatrix}\frac{dZ}{dY}k_1a_4+(\frac{A_XA_Y}{B_X}+\frac{dZ}{dY}k_2)a_5 & \frac{dZ}{dY}k_1a_5+(\frac{A_XA_Y}{B_X}+\frac{dZ}{dY}k_2)2a_6\end{bmatrix}$$

$$[dT_2(7)]_x=\begin{bmatrix}2a_4k_1+k_2a_5 & a_5k_1+2a_6k_2\end{bmatrix}$$

$[dT2(i)]_a$ are 1×5 matrices:

$$[dT_2(1)]_a=\begin{bmatrix}\frac{\frac{dZ}{dX}}{A_X^3} & 0 & 2X\frac{\frac{dZ}{dX}}{A_X^3} & 0 & Y\frac{\frac{dZ}{dX}}{A_X^3} & 0\end{bmatrix}$$

$$[dT_2(2)]_a=\begin{bmatrix}0 & -\frac{\frac{dZ}{dY}}{A_Y^3} & 0 & -X\frac{\frac{dZ}{dY}}{A_Y^3} & -2Y\frac{\frac{dZ}{dY}}{A_Y^3}\end{bmatrix}$$

$$[dT_2(3)]_a=\begin{bmatrix}\frac{1}{A_X}-\frac{(\frac{dZ}{dX})^2}{A_X^3} & 0 & (\frac{1}{A_X}-\frac{(\frac{dZ}{dX})^2}{A_X^3})2X & (\frac{1}{A_X}-\frac{(\frac{dZ}{dX})^2}{A_X^3})Y & 0\end{bmatrix}$$

$$[dT_2(4)]_a=\begin{bmatrix}0 & \frac{1}{A_Y}-\frac{(\frac{dZ}{dY})^2}{A_Y^3} & 0 & (\frac{1}{A_Y}-\frac{(\frac{dZ}{dY})^2}{A_X^3})X & 2Y(\frac{1}{A_Y}-\frac{(\frac{dZ}{dY})^2}{A_Y^3})\end{bmatrix}$$

$$[dT_2(5)]_a=\begin{bmatrix}\frac{A_XA_Y}{B_X}+\frac{dZ}{dX}k_1 & \frac{dZ}{dX}k_2 & 2X(\frac{A_XA_Y}{B_X}+\frac{dZ}{dX}k_1) & Y(\frac{A_XA_Y}{B_X}+\frac{dZ}{dX}k_1)+\frac{dZ}{dX}k_2X & 2k_2Y\frac{dZ}{dX}\end{bmatrix}$$

$$[dT_2(6)]_a=\begin{bmatrix}\frac{dZ}{dY}k_1 & \frac{A_XA_Y}{B_X}+\frac{dZ}{dY}k_2 & 2k_1X\frac{dZ}{dY} & k_1Y\frac{dZ}{dY}+(\frac{A_XA_Y}{B_X}+\frac{dZ}{dY}k_2)X & 2Y(\frac{A_XA_Y}{B_X}+\frac{dZ}{dY}k_2)\end{bmatrix}$$

$$[dT_2(7)]_a = \begin{bmatrix} k_1 & k_2 & 2k_1X & k_1Y + k_2X & 2k_2Y \end{bmatrix}$$

The derivative of $\{a\}$

$\{a\}$ can be expressed as:

$$\{a\} = \begin{Bmatrix} a_2 \\ a_3 \\ a_4 \\ a_5 \\ a_6 \end{Bmatrix} = \begin{bmatrix} X_2 & Y_2 & X_2^2 & X_2Y_2 & Y_2^2 \\ X_3 & Y_3 & X_3^2 & X_2Y_3 & Y_3^2 \\ X_4 & Y_4 & X_4^2 & X_2Y_4 & Y_4^2 \\ X_5 & Y_5 & X_5^2 & X_2Y_5 & Y_5^2 \\ X_6 & Y_6 & X_6^2 & X_2Y_6 & Y_6^2 \end{bmatrix}^{-1} \begin{Bmatrix} Z_2 \\ Z_3 \\ Z_4 \\ Z_5 \\ Z_6 \end{Bmatrix} = [XY]^{-1}\{Z\} \tag{5.148}$$

where X_i, Y_i, Z_i are nodal coordinates in local flat coordinate system, and are computed as:

$$\begin{Bmatrix} X_i \\ Y_i \\ Z_i \end{Bmatrix} = [T_1] \begin{Bmatrix} x_i - x_1 \\ y_i - y_1 \\ z_i - z_1 \end{Bmatrix} \tag{5.149}$$

in which, $[T_1]$ is the transformation matrix between local flat and global coordinate system, and x_i, y_i, z_i are global nodal coordinates.

Derivatives of nodal coordinates in the local flat coordinate system

Differentiating Eqn. 5.148 with respect to X_j, we get:

$$\begin{aligned} \frac{\partial a}{\partial X_j} = \begin{Bmatrix} \partial a_2/\partial X_j \\ \partial a_3/\partial X_j \\ \partial a_4/\partial X_j \\ \partial a_5/\partial X_j \\ \partial a_6/\partial X_j \end{Bmatrix} &= \frac{\partial([XY]^{-1})}{\partial X_j}\{Z\} + [XY]^{-1}\frac{\partial Z}{\partial X_j} \\ &= -[XY]^{-1}\frac{\partial [XY]}{\partial X_j}[XY]^{-1}\{Z\} + [XY]^{-1}\frac{\partial Z}{\partial X_j} \\ &= -[XY]^{-1}\frac{\partial [XY]}{\partial X_j}\{a\} + [XY]^{-1}\frac{\partial Z}{\partial X_j} = [XY]^{-1}(\frac{\partial Z}{\partial X_j} - \frac{\partial [XY]}{\partial X_j}\{a\}) \end{aligned} \tag{5.150}$$

in which,

$$\frac{\partial [XY]}{\partial X_j} = \begin{bmatrix} \frac{\partial X_2}{\partial X_j} & \frac{\partial Y_2}{\partial X_j} & 2X_2\frac{\partial X_2}{\partial X_j} & X_2\frac{\partial Y_2}{\partial X_j} + Y_2\frac{\partial X_2}{\partial X_j} & 2Y_2\frac{\partial Y_2}{\partial X_j} \\ \frac{\partial X_3}{\partial X_j} & \frac{\partial Y_3}{\partial X_j} & 2X_3\frac{\partial X_3}{\partial X_j} & X_3\frac{\partial Y_3}{\partial X_j} + Y_2\frac{\partial X_3}{\partial X_j} & 2Y_3\frac{\partial Y_3}{\partial X_j} \\ \frac{\partial X_4}{\partial X_j} & \frac{\partial Y_4}{\partial X_j} & 2X_4\frac{\partial X_4}{\partial X_j} & X_4\frac{\partial Y_4}{\partial X_j} + Y_2\frac{\partial X_4}{\partial X_j} & 2Y_4\frac{\partial Y_4}{\partial X_j} \\ \frac{\partial X_5}{\partial X_j} & \frac{\partial Y_5}{\partial X_j} & 2X_5\frac{\partial X_5}{\partial X_j} & X_5\frac{\partial Y_5}{\partial X_j} + Y_2\frac{\partial X_5}{\partial X_j} & 2Y_5\frac{\partial Y_5}{\partial X_j} \\ \frac{\partial X_6}{\partial X_j} & \frac{\partial Y_6}{\partial X_j} & 2X_6\frac{\partial X_6}{\partial X_j} & X_6\frac{\partial Y_6}{\partial X_j} + Y_2\frac{\partial X_6}{\partial X_j} & 2Y_6\frac{\partial Y_6}{\partial X_j} \end{bmatrix}, \quad \frac{\partial Z}{\partial X_j} = \begin{Bmatrix} \frac{\partial Z_2}{\partial X_j} \\ \frac{\partial Z_3}{\partial X_j} \\ \frac{\partial Z_4}{\partial X_j} \\ \frac{\partial Z_5}{\partial X_j} \\ \frac{\partial Z_6}{\partial X_j} \end{Bmatrix} \tag{5.151}$$

Re-arranging Eqn. 5.150, then:

$$\frac{\partial a}{\partial X_j} = [XY]^{-1}[AN] \begin{Bmatrix} \frac{\partial X_2}{\partial X_j} \\ \frac{\partial Y_2}{\partial X_j} \\ \frac{\partial Z_2}{\partial X_j} \\ \frac{\partial X_3}{\partial X_j} \\ \frac{\partial Y_3}{\partial X_j} \\ \frac{\partial Z_3}{\partial X_j} \\ \vdots \\ \frac{\partial X_6}{\partial X_j} \\ \frac{\partial Y_6}{\partial X_j} \\ \frac{\partial Z_6}{\partial X_j} \end{Bmatrix} \tag{5.152}$$

in which, $[AN]$ is a 5×15 matrix, and:

$$AN(i,j) = \begin{cases} -(a_2 + 2X_i a_4 + a_5 Y_i) & \text{if } j = 3i-2 \\ -(a_3 + X_i a_5 + 2a_6 Y_i) & \text{if } j = 3i-1 \\ 1 & \text{if } j = 3i \\ 0 & \text{others} \end{cases} \tag{5.153}$$

Differentiating Eqn.5.149 with respect to u, we get

$$\begin{Bmatrix} \frac{\partial X_i}{\partial X_j} \\ \frac{\partial Y_i}{\partial X_j} \\ \frac{\partial Z_i}{\partial X_j} \end{Bmatrix} = \frac{\partial [T_1]}{\partial X_j} \begin{Bmatrix} x_i - x_1 \\ y_i - y_1 \\ z_i - z_1 \end{Bmatrix} + [T_1] \begin{Bmatrix} \frac{\partial (x_i - x_1)}{\partial X_j} \\ \frac{\partial (y_i - y_1)}{\partial X_j} \\ \frac{\partial (z_i - z_1)}{\partial X_j} \end{Bmatrix} = \frac{\partial [T_1]}{\partial X_j} \begin{Bmatrix} x_i - x_1 \\ y_i - y_1 \\ z_i - z_1 \end{Bmatrix} + [T_1] \begin{Bmatrix} \frac{\partial u_i}{\partial X_j} - \frac{\partial u_1}{\partial X_j} \\ \frac{\partial v_i}{\partial X_j} - \frac{\partial v_1}{\partial X_j} \\ \frac{\partial w_i}{\partial X_j} - \frac{\partial w_1}{\partial X_j} \end{Bmatrix} \tag{5.154}$$

where u_i, v_i, w_i are nodal displacements along the global coordinate axis x, y, z separately. The derivatives of nodal coordinates in the local flat coordinate system $X_i\ Y_i$ can be computed as:

$$\begin{Bmatrix} \frac{\partial X_i}{\partial X_j} \\ \frac{\partial Y_i}{\partial X_j} \end{Bmatrix} = \frac{\partial ([T_1] \begin{Bmatrix} x_i - x_1 \\ y_i - y_1 \end{Bmatrix})}{\partial u} = \frac{\partial [T_1]}{\partial u} \begin{Bmatrix} x_i - x_1 \\ y_i - y_1 \end{Bmatrix} + [T_1] \{ \begin{matrix} \frac{\partial x_i}{\partial X_j} - \frac{\partial x_1}{\partial X_j} \\ \frac{\partial y_i}{\partial X_j} - \frac{\partial y_1}{\partial X_j} \end{matrix} \}$$

$$= \begin{bmatrix} [dl_1](x_i - x_1) + [dl_2](y_i - y_1) \\ [dm_1](x_i - x_1) + [dm_2](y_i - y_1) \end{bmatrix} \begin{Bmatrix} \frac{\partial u_1}{\partial X_j} \\ \frac{\partial v_1}{\partial X_j} \\ \frac{\partial w_1}{\partial X_j} \\ \frac{\partial u_2}{\partial X_j} \\ \frac{\partial v_2}{\partial X_j} \\ \frac{\partial w_2}{\partial X_j} \\ \frac{\partial u_3}{\partial X_j} \\ \frac{\partial v_3}{\partial X_j} \\ \frac{\partial w_3}{\partial X_j} \end{Bmatrix} + \begin{bmatrix} l_1 & l_2 \\ m_1 & m_2 \end{bmatrix} \begin{Bmatrix} \frac{\partial u_i}{\partial X_j} \\ \frac{\partial v_i}{\partial X_j} \end{Bmatrix} + \begin{bmatrix} l_1 & l_2 \\ m_1 & m_2 \end{bmatrix} \begin{Bmatrix} \frac{\partial u_1}{\partial X_j} \\ \frac{\partial v_2}{\partial X_j} \end{Bmatrix} \tag{5.155}$$

The derivative of B matrix

The B matrix of the six node triangle element is a function of the local displacement of element nodal and element curvatures, which can be expressed as:

$$B = B_U + B_c \tag{5.156}$$

in which, B_U is functioned of local displacements U, and B_c is functioned of element curvatures (K_X,K_Y and K_{XY}). Thus,

$$dB = \frac{\partial B}{\partial X_j} = \frac{\partial B_U}{\partial X_j} + \frac{\partial B_c}{\partial X_j} = \frac{\partial B_U}{\partial U}\frac{\partial U}{\partial X_j} + \frac{\partial B_c}{\partial a}\frac{\partial a}{\partial X_j} \tag{5.157}$$

Differentiating Eqn. 5.59 to obtain:

$$\frac{\partial U}{\partial X_j} = \frac{\partial (T_i^m u)}{\partial X_j} = \frac{\partial T_i^m}{\partial X_j} u + T_i^m \frac{\partial u}{\partial X_j} \tag{5.158}$$

The derivative of B matrix can be written as:

$$\frac{\partial B}{\partial X_j} = \frac{\partial B_U}{\partial X_j} + \frac{\partial B_c}{\partial X_j} \tag{5.159}$$

For each six node triangle element, B_U and B_c are 3×18 matrices as same as B matrix, and the derivatives of B_U and B_c can be shown as:

$$\frac{\partial B_U}{\partial X_j} = \begin{bmatrix} \frac{\partial B_U(1,1)}{\partial X_j} & \frac{\partial B_U(1,2)}{\partial X_j} & \cdots & \frac{\partial B_U(1,18)}{\partial X_j} \\ \frac{\partial B_U(2,1)}{\partial X_j} & \frac{\partial B_U(2,2)}{\partial X_j} & \cdots & \frac{\partial B_U(2,18)}{\partial X_j} \\ \frac{\partial B_U(3,1)}{\partial X_j} & \frac{\partial B_U(3,2)}{\partial X_j} & \cdots & \frac{\partial B_U(3,18)}{\partial X_j} \end{bmatrix} \tag{5.160}$$

$$\frac{\partial B_c}{\partial X_j} = \begin{bmatrix} \frac{\partial B_c(1,1)}{\partial X_j} & \frac{\partial B_c(1,2)}{\partial X_j} & \cdots & \frac{\partial B_c(1,18)}{\partial X_j} \\ \frac{\partial B_c(2,1}{\partial X_j} & \frac{\partial B_c(2,2)}{\partial X_j} & \cdots & \frac{\partial B_c(2,18)}{\partial X_j} \\ \frac{\partial B_c(3,1)}{\partial X_j} & \frac{\partial B_c(3,2)}{\partial X_j} & \cdots & \frac{\partial B_c(3,18)}{\partial X_j} \end{bmatrix} \tag{5.161}$$

where $B_U(i,j)$ and $B_c(i,j)$ are the terms of B_U and B_c respectively as detailed in Appendix C.2. Eqn.5.160 and 5.161 can be rewritten as:

$$\frac{\partial B_U(i,j)}{\partial u} = [dB_u(i,j)] \begin{Bmatrix} \frac{\partial U_1}{\partial X_j} \\ \frac{\partial V_1}{\partial X_j} \\ \frac{\partial W_1}{\partial X_j} \\ \frac{\partial U_2}{\partial X_j} \\ \frac{\partial V_2}{\partial X_j} \\ \frac{\partial W_2}{\partial X_j} \\ \vdots \\ \frac{\partial U_6}{\partial X_j} \\ \frac{\partial V_6}{\partial X_j} \\ \frac{\partial W_6}{\partial X_j} \end{Bmatrix} \tag{5.162}$$

and

$$\frac{\partial B_c(i,j)}{\partial X_j} = [dB_c(i,j)] \begin{Bmatrix} \frac{\partial U_1}{\partial X_j} \\ \frac{\partial V_1}{\partial X_j} \\ \frac{\partial W_1}{\partial X_j} \\ \frac{\partial U_2}{\partial X_j} \\ \frac{\partial V_2}{\partial X_j} \\ \frac{\partial W_2}{\partial X_j} \\ \vdots \\ \frac{\partial U_6}{\partial X_j} \\ \frac{\partial V_6}{\partial X_j} \\ \frac{\partial W_6}{\partial X_j} \end{Bmatrix} \tag{5.163}$$

where, $[dB_U(i,j)]$ and $[dB_c(i,j)]$ are 1×18 matrices.

Therefore, the product of $\frac{\partial B_U}{\partial X_j}$ and $R = \begin{Bmatrix} R_1 & R_2 & \cdots & R_{18} \end{Bmatrix}^T$ can be rewritten as:

$$\frac{\partial B_U}{\partial X_j} R \quad = \quad \begin{bmatrix} \frac{\partial B_U(1,1)}{\partial X_j} & \frac{\partial B_U(1,2)}{\partial X_j} & \cdots & \frac{\partial B_U(1,18)}{\partial X_j} \\ \frac{\partial B_U(2,1)}{\partial X_j} & \frac{\partial B_U(2,2)}{\partial X_j} & \cdots & \frac{\partial B_U(2,18)}{\partial X_j} \\ \frac{\partial B_U(3,1)}{\partial X_j} & \frac{\partial B_U(3,2)}{\partial X_j} & \cdots & \frac{\partial B_U(3,18)}{\partial X_j} \end{bmatrix} \begin{Bmatrix} R_1 \\ R_2 \\ \vdots \\ R_{18} \end{Bmatrix}$$

$$= \begin{bmatrix} [dB_u(1,1)]R_1 + [dB_u(1,2)]R_2 + \cdots + [dB_u(1,18)]R_{18} \\ [dB_u(2,1)]R_1 + [dB_u(2,2)]R_2 + \cdots + [dB_u(2,18)]R_{18} \\ [dB_u(2,1)]R_1 + [dB_u(2,2)]R_2 + \cdots + [dB_u(3,18)]R_{18} \end{bmatrix} \begin{Bmatrix} \frac{\partial U_1}{\partial X_j} \\ \frac{\partial V_1}{\partial X_j} \\ \frac{\partial W_1}{\partial X_j} \\ \frac{\partial U_2}{\partial X_j} \\ \frac{\partial V_2}{\partial X_j} \\ \frac{\partial W_2}{\partial X_j} \\ \vdots \\ \frac{\partial U_6}{\partial X_j} \\ \frac{\partial V_6}{\partial X_j} \\ \frac{\partial W_6}{\partial X_j} \end{Bmatrix} \tag{5.164}$$

While

$$\begin{Bmatrix} U_i \\ V_i \\ W_i \end{Bmatrix} = T_i^m \begin{Bmatrix} u_i \\ v_i \\ w_i \end{Bmatrix} \tag{5.165}$$

Therefore,

$$\begin{Bmatrix} \frac{\partial U_i}{\partial X_j} \\ \frac{\partial V_i}{\partial X_j} \\ \frac{\partial W_i}{\partial X_j} \end{Bmatrix} = \frac{\partial T_i^m}{\partial X_j} \begin{Bmatrix} u_i \\ v_i \\ w_i \end{Bmatrix} + T_j^m \begin{Bmatrix} \frac{\partial u_i}{\partial X_j} \\ \frac{\partial v_i}{\partial X_j} \\ \frac{\partial w_i}{\partial X_j} \end{Bmatrix} \tag{5.166}$$

Cable reaction force derivatives

In the global coordinate space, the reaction forces from cable elements can be expressed as:

$$\{f_{ca}\} = T_k^c P_k \tag{5.167}$$

in which, f_{ca} is the element force vector. T_k^c is a transformation matrix between local and global coordinate system, and P_k is the cable force along the cable axis,

$$P_k = P_0 + \frac{EA}{L}\Delta = P_0 + \frac{EA}{L_0}(L - L_0) \tag{5.168}$$

where P_0 is the pretension in the cable element, and Δ denotes the elastic extension of the cable. $\frac{EA}{L_0}$ represents the elastic modulus of the element, and L and L_0 are the current and initial length. If in the initial configuration the nodal coordinates of the cable element are $P_1(x_1, y_1, z_1)$ and $P_2(x_2, y_1, z_1$ and the nodal displacements for two nodes are u_1, v_1, w_1 and u_2, v_2, w_2 respectively, then:

$$\Delta = L - L_0$$

$$
\begin{aligned}
&= \sqrt{(x_2 - x_1 + u_2 - u_1)^2 + (y_2 - y_1 + v_2 - v_1)^2 + (z_2 - z_1 + w_2 - w_1)^2} \\
&\quad - \sqrt{(x_2 - x_1)^2 + (y_2 - y_1)^2 + (z_2 - z_1)^2} \\
&= \frac{2(x_2 - x_1)(u_2 - u_1) + (u_2 - u_1)^2 + 2(y_2 - y_1)(v_2 - v_1) + (v_2 - v_1)^2}{L + L_0} \\
&\quad + \frac{2(z_2 - z_1)(w_2 - w_1) + (w_2 - w_1)^2}{L + L_0}
\end{aligned} \tag{5.169}
$$

The transformation matrix T_k^c in the deformed configuration can be written as:

$$
T_k^c = \frac{1}{L} \begin{bmatrix} -(x_2 - x_1 + u_2 - u_1) \\ -(y_2 - y_1 + v_2 - v_1) \\ -(z_2 - z_1 + w_2 - w_1) \\ x_2 - x_1 + u_2 - u_1 \\ y_2 - y_1 + v_2 - v_1 \\ z_2 - z_1 + w_2 - w_1 \end{bmatrix} \tag{5.170}
$$

Differentiating Eqn.5.167 with respect to u gives

$$
\frac{\partial f_{ca}}{\partial X_j} = \frac{\partial T_k^c}{\partial X_j} P_k + T_k^c \frac{\partial P_k}{\partial X_j} \tag{5.171}
$$

The derivative of the cable force can be derived by differentiating Eqn.5.168:

$$
\begin{aligned}
\frac{\partial P_k}{\partial X_j} &= \frac{EA}{L_0} \frac{\partial \Delta}{\partial X_j} \\
&= \frac{EA}{L_0(L + L_0)} [2(x_2 - x_1)(\frac{\partial u_2}{\partial X_j} - \frac{\partial u_1}{\partial X_j}) + 2(u_2 - u_1)(\frac{\partial u_2}{\partial X_j} - \frac{\partial u_1}{\partial X_j}) + 2(y_2 - y_1)(\frac{\partial v_2}{\partial X_j} - \frac{\partial v_1}{\partial X_j}) \\
&\quad + 2(y_2 - y_1)(\frac{\partial v_2}{\partial X_j} - \frac{\partial v_1}{\partial X_j}) + 2(z_2 - z_1)(\frac{\partial w_2}{\partial X_j} - \frac{\partial w_1}{\partial X_j}) + 2(w_2 - w_1)(\frac{\partial w_2}{\partial u} - \frac{\partial w_1}{\partial X_j})] \\
&= \frac{2EA}{L_0(L + L_0)} [(x_2 - x_1 + u_2 - u_1)(\frac{\partial u_2}{\partial X_j} - \frac{\partial u_1}{\partial X_j}) + (y_2 - y_1 + v_2 - v_1)(\frac{\partial v_2}{\partial X_j} - \frac{\partial v_1}{\partial X_j}) \\
&\quad + (z_2 - z_1 + w_2 - w_1)(\frac{\partial w_2}{\partial X_j} - \frac{\partial w_1}{\partial X_j})] \\
&= \frac{2EA}{L_0(L + L_0)} \begin{bmatrix} -\Delta x_{ca} & -\Delta y_{ca} & -\Delta z_{ca} & \Delta x_{ca} & \Delta y_{ca} & \Delta z_{ca} \end{bmatrix} \begin{Bmatrix} \frac{\partial u_1}{\partial X_j} \\ \frac{\partial v_1}{\partial X_j} \\ \frac{\partial w_1}{\partial X_j} \\ \frac{\partial u_2}{\partial X_j} \\ \frac{\partial v_2}{\partial X_j} \\ \frac{\partial w_2}{\partial X_j} \end{Bmatrix}
\end{aligned}
$$

$$= [dP] \begin{Bmatrix} \frac{\partial u_1}{\partial X_j} \\ \frac{\partial v_1}{\partial X_j} \\ \frac{\partial w_1}{\partial X_j} \\ \frac{\partial u_2}{\partial X_j} \\ \frac{\partial v_2}{\partial X_j} \\ \frac{\partial w_2}{\partial X_j} \end{Bmatrix} \tag{5.172}$$

in which, $\Delta x_{ca} = x_2 - x_1 + u_2 - u_1$, $\Delta y_{ca} = y_2 - y_1 + v_2 - v_1$, $\Delta z_{ca} = z_2 - z_1 + w_2 - w_1$.

Differentiating Eqn.5.170, we can obtain $\frac{\partial [C]}{\partial u}$ as:

$$\frac{\partial T_k^c}{\partial X_j} = \begin{Bmatrix} -\frac{1}{L}(\frac{\partial u_2}{\partial X_j} - \frac{\partial u_1}{\partial X_j}) + \frac{x_2 - x_1 + u_2 - u_1}{L^2}\frac{\partial L}{\partial X_j} \\ -\frac{1}{L}(\frac{\partial v_2}{\partial X_j} - \frac{\partial v_1}{\partial X_j}) + \frac{y_2 - y_1 + v_2 - v_1}{L^2}\frac{\partial L}{\partial X_j} \\ -\frac{1}{L}(\frac{\partial w_2}{\partial X_j} - \frac{\partial w_1}{\partial X_j}) + \frac{z_2 - z_1 + w_2 - w_1}{L^2}\frac{\partial L}{\partial X_j} \\ \frac{1}{L}(\frac{\partial u_2}{\partial X_j} - \frac{\partial u_1}{\partial u}) - \frac{x_2 - x_1 + u_2 - u_1}{L^2}\frac{\partial L}{\partial X_j} \\ \frac{1}{L}(\frac{\partial v_2}{\partial X_j} - \frac{\partial v_1}{\partial u}) - \frac{y_2 - y_1 + v_2 - v_1}{L^2}\frac{\partial L}{\partial X_j} \\ \frac{1}{L}(\frac{\partial w_2}{\partial X_j} - \frac{\partial w_1}{\partial X_j}) - \frac{z_2 - z_1 + w_2 - w_1}{L^2}\frac{\partial L}{\partial X_j} \end{Bmatrix} = \frac{1}{L}\begin{Bmatrix} -\frac{\partial u_2}{\partial X_j} + \frac{\partial u_1}{\partial X_j} \\ -\frac{\partial v_2}{\partial X_j} + \frac{\partial v_1}{\partial X_j} \\ -\frac{\partial w_2}{\partial X_j} + \frac{\partial w_1}{\partial X_j} \\ \frac{\partial u_2}{\partial X_j} - \frac{\partial u_1}{\partial X_j} \\ \frac{\partial v_2}{\partial X_j} - \frac{\partial v_1}{\partial X_j} \\ \frac{\partial w_2}{\partial X_j} - \frac{\partial w_1}{\partial X_j} \end{Bmatrix} - T_k^c \frac{\partial L}{\partial X_j} \tag{5.173}$$

While,

$$\begin{aligned} \frac{\partial L}{\partial X_j} &= \frac{\partial \sqrt{(x_2 - x_1 + u_2 - u_1)^2 + (y_2 - y_1 + v_2 - v_1)^2 + (z_2 - z_1 + w_2 - w_1)^2}}{\partial X_j} \\ &= \frac{1}{2L}[2(x_2 - x_1 + u_2 - u_1)(\frac{\partial u_2}{\partial X_j} - \frac{\partial u_1}{\partial X_j}) + 2(y_2 - y_1 + v_2 - v_1)(\frac{\partial v_2}{\partial X_j} - \frac{\partial v_1}{\partial X_j}) \\ &\quad +2(z_2 - z_1 + w_2 - w_1)(\frac{\partial w_2}{\partial X_j} - \frac{\partial w_1}{\partial X_j}) \\ &= c_x^p(\frac{\partial u_2}{\partial X_j} - \frac{\partial u_1}{\partial X_j}) + c_y^p(\frac{\partial v_2}{\partial X_j} - \frac{\partial v_1}{\partial X_j}) + c_z^p(\frac{\partial w_2}{\partial X_j} - \frac{\partial w_1}{\partial X_j}) \end{aligned} \tag{5.174}$$

where, $c_x^p = \frac{x_2 - x_1 + u_2 - u_1}{L}$, $c_y^p = \frac{y_2 - y_1 + v_2 - v_1}{L}$, and $c_z^p = \frac{z_2 - z_1 + w_2 - w_1}{L}$.

Substituting Eqn. 5.174 in Eqn. 5.173, we obtain:

$$\frac{\partial T_k^c}{\partial X_j} = \begin{bmatrix} -\frac{1}{L}(\frac{\partial u_2}{\partial X_j} - \frac{\partial u_1}{\partial X_j}) + \frac{c_x^p}{L}[c_x^p(\frac{\partial u_2}{\partial X_j} - \frac{\partial u_1}{\partial X_j}) + c_y^p(\frac{\partial v_2}{\partial X_j} - \frac{\partial v_1}{\partial X_j}) + c_z^p(\frac{\partial w_2}{\partial X_j} - \frac{\partial w_1}{\partial X_j})] \\ -\frac{1}{L}(\frac{\partial v_2}{\partial X_j} - \frac{\partial v_1}{\partial X_j}) + \frac{c_y^p}{L}[c_x^p(\frac{\partial u_2}{\partial X_j} - \frac{\partial u_1}{\partial X_j}) + c_y^p(\frac{\partial v_2}{\partial X_j} - \frac{\partial v_1}{\partial X_j}) + c_z^p(\frac{\partial w_2}{\partial X_j} - \frac{\partial w_1}{\partial X_j})] \\ -\frac{1}{L}(\frac{\partial w_2}{\partial X_j} - \frac{\partial w_1}{\partial X_j}) + \frac{c_z^p}{L}[c_x^p(\frac{\partial u_2}{\partial X_j} - \frac{\partial u_1}{\partial X_j}) + c_y^p(\frac{\partial v_2}{\partial X_j} - \frac{\partial v_1}{\partial X_j}) + c_z^p(\frac{\partial w_2}{\partial X_j} - \frac{\partial w_1}{\partial X_j})] \\ \frac{1}{L}(\frac{\partial u_2}{\partial X_j} - \frac{\partial u_1}{\partial X_j}) - \frac{c_x^p}{L}[c_x^p(\frac{\partial u_2}{\partial X_j} - \frac{\partial u_1}{\partial X_j}) + c_y^p(\frac{\partial v_2}{\partial X_j} - \frac{\partial v_1}{\partial X_j}) + c_z^p(\frac{\partial w_2}{\partial X_j} - \frac{\partial w_1}{\partial X_j})] \\ \frac{1}{L}(\frac{\partial v_2}{\partial X_j} - \frac{\partial v_1}{\partial X_j}) - \frac{c_y^p}{L}[c_x^p(\frac{\partial u_2}{\partial X_j} - \frac{\partial u_1}{\partial X_j}) + c_y^p(\frac{\partial v_2}{\partial X_j} - \frac{\partial v_1}{\partial X_j}) + c_z^p(\frac{\partial w_2}{\partial X_j} - \frac{\partial w_1}{\partial X_j})] \\ \frac{1}{L}(\frac{\partial w_2}{\partial X_j} - \frac{\partial w_1}{\partial X_j}) - \frac{c_z^p}{L}[c_x^p(\frac{\partial u_2}{\partial X_j} - \frac{\partial u_1}{\partial X_j}) + c_y^p(\frac{\partial v_2}{\partial X_j} - \frac{\partial v_1}{\partial X_j}) + c_z^p(\frac{\partial w_2}{\partial X_j} - \frac{\partial w_1}{\partial X_j})] \end{bmatrix}$$

$$
\begin{aligned}
&= \begin{bmatrix}
-\frac{c_x^{p\,2}}{L}+\frac{1}{L} & -\frac{c_x^p c_y^p}{L} & -\frac{c_x^p c_z^p}{L} & -\frac{1}{L}+\frac{c_x^{p\,2}}{L} & \frac{c_x^p c_y^p}{L} & \frac{c_x^p c_z^p}{L} \\
-\frac{c_x^p c_y^p}{L} & -\frac{c_y^{p\,2}}{L}+\frac{1}{L} & -\frac{c_y^p c_z^p}{L} & \frac{c_x^p c_y^p}{L} & \frac{c_y^{p\,2}}{L}-\frac{1}{L} & \frac{c_y^p c_z^p}{L} \\
-\frac{c_x^p c_z^p}{L} & -\frac{c_y^p c_z^p}{L} & -\frac{c_z^{p\,2}}{L}+\frac{1}{L} & \frac{c_x^p c_z^p}{L} & \frac{c_y^p c_z^p}{L} & \frac{c_z^{p\,2}}{L}-\frac{1}{L} \\
\frac{c_x^{p\,2}}{L}-\frac{1}{L} & \frac{c_x^p c_y^p}{L} & \frac{c_x^p c_z^p}{L} & \frac{1}{L}-\frac{c_x^{p\,2}}{L} & -\frac{c_x^p c_y^p}{L} & -\frac{c_x^p c_z^p}{L} \\
\frac{c_x^p c_y^p}{L} & \frac{c_y^{p\,2}}{L}-\frac{1}{L} & \frac{c_y^p c_z^p}{L} & -\frac{c_x^p c_y^p}{L} & -\frac{c_y^{p\,2}}{L}+\frac{1}{L} & -\frac{c_y^p c_z^p}{L} \\
\frac{c_x^p c_z^p}{L} & \frac{c_y^p c_z^p}{L} & \frac{c_z^{p\,2}}{L}-\frac{1}{L} & -\frac{c_x^p c_z^p}{L} & -\frac{c_y^p c_z^p}{L} & -\frac{c_z^{p\,2}}{L}+\frac{1}{L}
\end{bmatrix}
\begin{Bmatrix}
\frac{\partial u_1}{\partial X_j} \\ \frac{\partial v_1}{\partial X_j} \\ \frac{\partial w_1}{\partial X_j} \\ \frac{\partial u_2}{\partial X_j} \\ \frac{\partial v_2}{\partial X_j} \\ \frac{\partial w_2}{\partial X_j}
\end{Bmatrix} \\
&= [dC]\begin{Bmatrix}
\frac{\partial u_1}{\partial X_j} \\ \frac{\partial v_1}{\partial X_j} \\ \frac{\partial w_1}{\partial X_j} \\ \frac{\partial u_2}{\partial X_j} \\ \frac{\partial v_2}{\partial X_j} \\ \frac{\partial w_2}{\partial X_j}
\end{Bmatrix}
\end{aligned} \tag{5.175}
$$

Therefore, the derivative of the cable element force can be written as:

$$
\begin{aligned}
\frac{\partial\{f_{ca}\}}{\partial X_j} &= \frac{\partial T_k^c}{\partial X_j}P + T_k^c\frac{\partial P}{\partial X_j} \\
&= \{[dC]P + T_k^c[dP]\}\begin{Bmatrix}
\frac{\partial u_1}{\partial X_j} \\ \frac{\partial v_1}{\partial X_j} \\ \frac{\partial w_1}{\partial X_j} \\ \frac{\partial u_2}{\partial X_j} \\ \frac{\partial v_2}{\partial X_j} \\ \frac{\partial w_2}{\partial X_j}
\end{Bmatrix}
\end{aligned} \tag{5.176}
$$

5.3.3 Solution procedure of structural sensitivity analysis using analytical method

Using the analytical method, the structural sensitivity analysis of a given membrane structure with cable supports can be undertaken using the following procedure and also presented as figure.5.7:

1) At first, take a deterministic analysis of the membrane structure using the six node LST element formulation (section 3.2) to obtain all the structural response vectors (e.g. nodal displacement, membrane stress, cable forces etc.) at the final balanced geometry configuration.

2) Determine the values of the random variables required in the reliability analysis (i.e. maximum stresses, minimum principal stress, and maximum nodal displacements) and their positions in the membrane.

3) Compute the derivatives of the elastic modulus matrix and loads using Eqn.5.64 to 5.68 and Eqn.5.62 with respect to random variable X_j, then calculate df_i using Eqn.5.79. Initially

$j = 1$.

4) Compute the derivatives of the transformation matrix for membrane element dT^m using Eqn.5.87, then build the matrix $[DT_1]$ and $[DT_3]$ as defined in Eqn.5.72 and 5.76 for every membrane element.

5) Compute the derivatives of B matrix dB using Eqn. 5.157, and build the matrix $[DT_2]$ and $[dT_4]$ as defined in Eqn.5.73 and 5.75 for every membrane element.

6) Compute the derivatives of the transformation matrix and element force of cable element using Eqn.5.175 and 5.172, then build the matrix $[DT_5]$ as defined as Eqn. 5.76 for the cable elements.

7) Build the matrices dK_i^m and dK_k^c for membrane and cable elements using Eqn.5.80 and 5.81, then assemble them for the whole structure.

8) Calculate the derivative of nodal displacement using Eqn.5.82 and find out the derivative of maximum nodal displacement based on the position obtained in step 2, then calculate the derivatives of maximum stresses and minimum principal stresses using Eqn.5.51 and Eqn.5.53.

9) Repeat the process to calculate the derivatives of structural response with respect to the next random variable X_{j+1}.

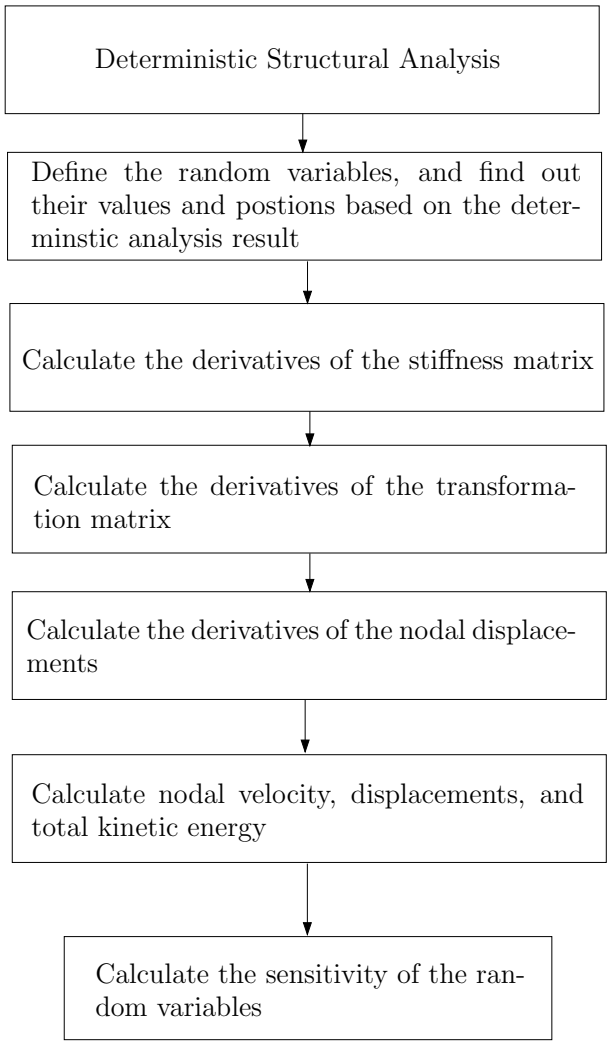

Figure 5.7: Sensitivity solution algorithm

5.3.4 Examples of Structural sensitivity analysis

Structural sensitivity analysis using finite difference and analytical methods are compared using two numerical examples: a patch with only two elements and a hypar with 32 membrane and 32 cable elements .

1) Patch Test:

As detailed in figure 5.8, a lateral load $F = 100kN$ is applied to node 3 of this two-element patch, and using LST finite element formulation, the element stresses and nodal displacements are computed as fig.5.9, and the magnitudes and directions of the extreme values and their positions across the whole patch are obtained. For example, the maximum fill stress $\sigma_{fill} = 285.39$ kN/m^2 is at the Gauss Point 3 in the first element (i.e "EN 1,GP 3"), and the maximum nodal displacement is $D_{max} = 0.46$ at the node 3 along the x direction (i.e. "Node 3,x").

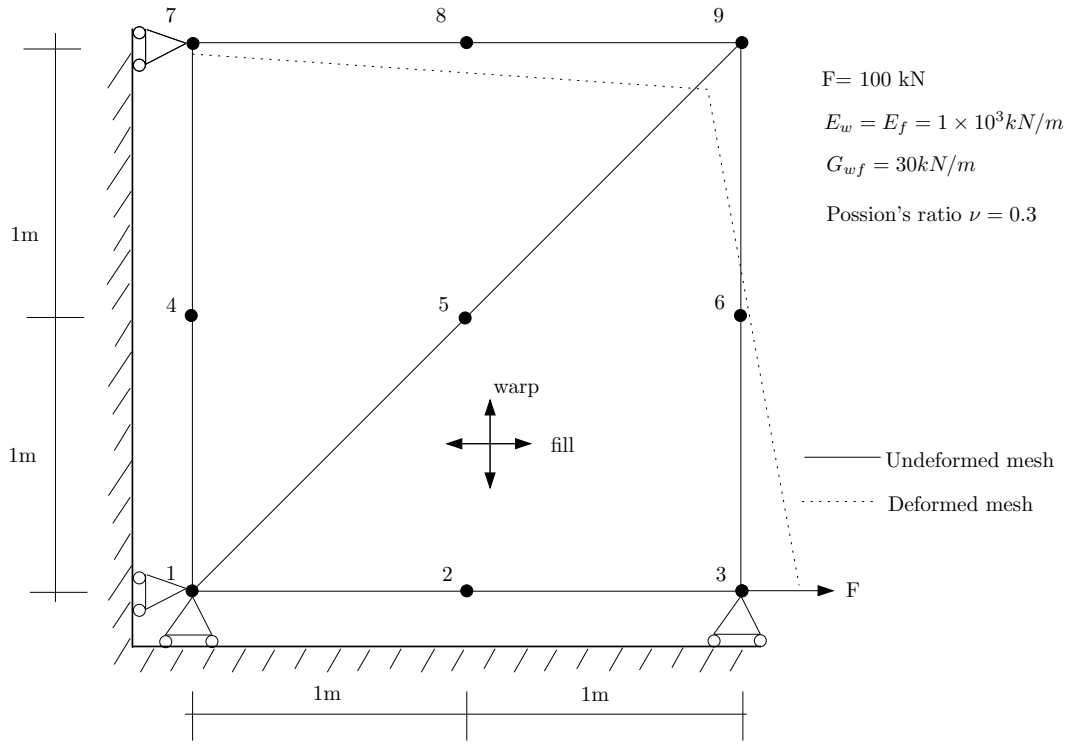

Figure 5.8: Patch test for structural sensitivity analysis

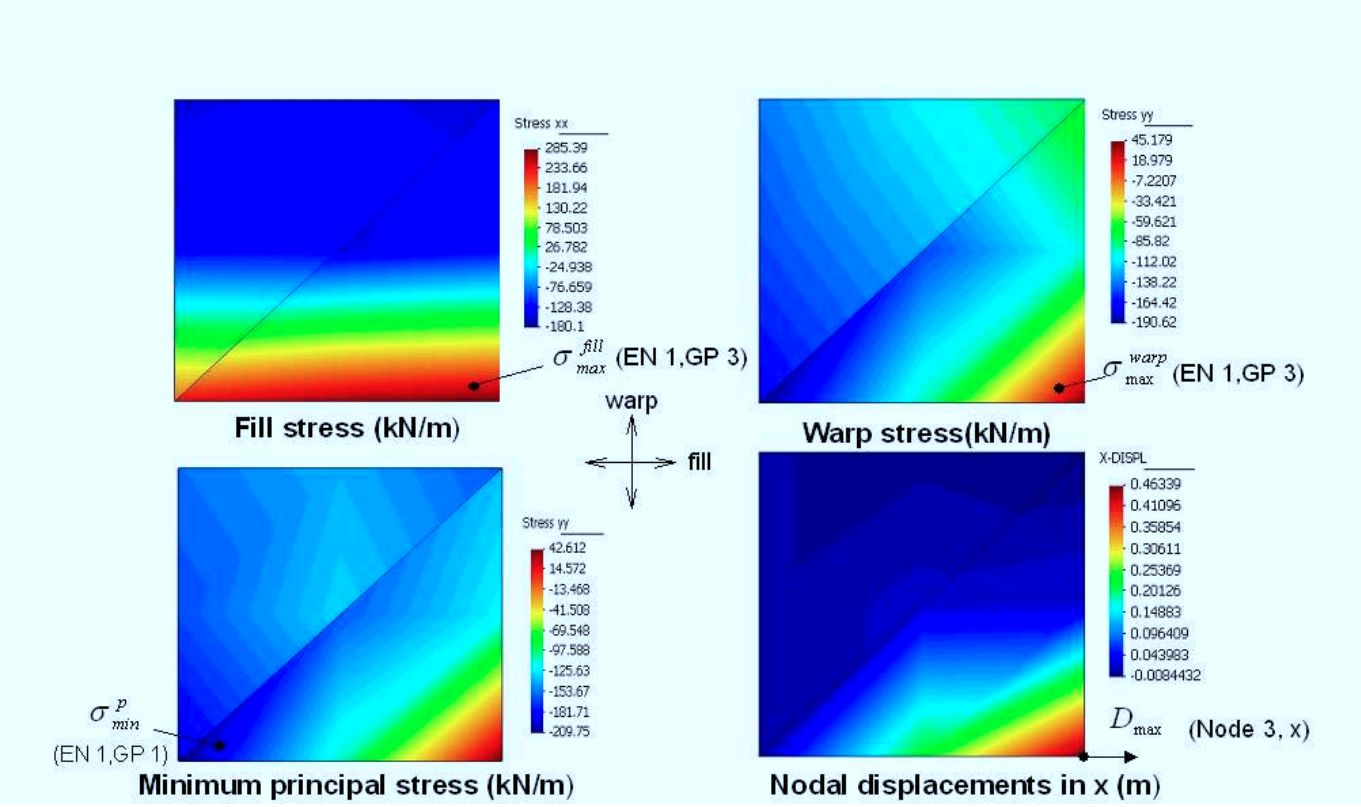

Figure 5.9: Deterministic analysis solution and the positions of the structural responses of interest

Subsequently, the sensitivities of the structural response will be evaluated using finite difference and analytical approaches. When using the finite difference method, the computation is repeated using different perturbation to identify the convergence. For example, as shown in table 5.1, the sensitivities of σ_{max}^{fill} converge when the perturbation approaches 0.1%.

X_j	$\Delta X = 1\%$	$\Delta X = 0.5\%$	$\Delta X = 0.1\%$	$\Delta X = 0.05\%$	$\Delta X = 0.01\%$
t_{load}	6.67	6.54	6.52	6.52	6.52
E_f	-4.63×10^{-2}	-4.74×10^{-2}	-4.78×10^{-2}	-4.79×10^{-2}	-4.78×10^{-2}
E_w	-5.50×10^{-5}	-5.50×10^{-5}	-5.46×10^{-5}	-5.35×10^{-5}	-5.46×10^{-5}
G_{wf}	-0.16	-0.16	-0.15	-0.15	-0.15
v_{wf}	-4.11×10^{-2}	-3.91×10^{-2}	-3.85×10^{-2}	-3.85×10^{-2}	-3.84×10^{-2}

Table 5.1: Convergence verification of the sensitivity of σ_{max}^{fill} using different ΔX

The derivatives of the maximum stresses, minimum principal stresses and maximum nodal displacement from the finite difference method with 0.1% perturbation and the analytical approach are compared in table 5.2. The similarity of the results from these two different sensitivity approaches demonstrates the validation and accuracy of the structural sensitivity analysis results, and also verifies the analytical method formulations derived in section 5.3.2.

	$\partial\sigma_{max}^{fill}/\partial X_j$		$\partial\sigma_{max}^{warp}/\partial X_j$	
X_j	Finite difference	Analytical approach	Finite difference	Analytical approach
t_{load}	6.55	6.55	-22.95	-22.95
E_f	-4.80×10^{-2}	-4.80×10^{-2}	1.94×10^{-2}	1.94×10^{-2}
E_w	-5.38×10^{-5}	-5.39×10^{-5}	-2.59×10^{-4}	-2.59×10^{-4}
G_{wf}	-0.15	-0.15	-0.63	-0.63
v_{wf}	-3.82×10^{-2}	-3.81×10^{-2}	-3.98×10^{-2}	-3.98×10^{-2}

	$\partial\sigma_{min}^{p}/\partial X_j$		$\partial D_{max}/\partial X_j$	
X_j	Finite difference	Analytical approach	Finite difference	Analytical approach
t_{load}	-194.04	-194.04	0.46	0.46
E_f	-0.38	-0.39	-1.92×10^{-4}	-1.93×10^{-4}
E_w	-1.52×10^{-3}	-1.52×10^{-3}	1.23×10^{-6}	1.25×10^{-6}
G_{wf}	11.45	11.37	-1.77×10^{-3}	-1.77×10^{-3}
v_{wf}	70.29	68.97	-6.36×10^{-3}	-6.27×10^{-3}

Table 5.2: Sensitivity analysis using finite difference ($\Delta = 0.1\%$) and analytical approaches

Apparently, the structural responses are most sensitive to the load coefficient t_{load} among the random variables, while the effect from the Young's modulus along the warp direction seems very small, consistent with there being no load in that direction. The deformations are more sensitive to the shear modulus G_{wf} and Possion's ratio v_{wf}. Therefore the minimum principal stress, which is approximately along the warp direction, is more sensitive to G_{wf} and v_{wf} as illustrated by the magnitude of the sensitivities in table 5.2. It is notable that the values in table 5.2 are sensitivities to a unit variation of the random variables, and the influence

on the structural response from uncertainties not only depends on sensitivities but also the magnitude of the uncertainty variance. For example, despite that the sensitivity of Poisson's ratio to minimal principal stress is much higher than E_w and E_f, the structural response from the variance of Poisson's ratio may be still lower, because for regular fabric materials the variance of E_w and E_f can reach 1000kN/m, but Poisson's ratio normally changes within the value about $0 \sim 1$.

When using the finite difference method, results differ based on the corresponding perturbations and an improper perturbation may result in unacceptable errors. From the perspective of the finite difference theory, smaller perturbation will normally lead to more accurate differentiation approximations, within the accuracy of the computer. However, when incorporated with finite element tools, the accuracy of finite difference differentiation will not only depend on the perturbation but also on the accuracy of the finite element analysis. If the increment of structural responses provoked by the perturbation is too small to be recognized in the analysis, and may be regarded as part of residual error in the analysis, the differentiation result will be erroneous. Therefore the differentiation accuracy using the finite different method will be limited by the accuracy of the finite element analysis. For example, as presented in table 5.3, $\partial D_{max}/\partial v_{wf}$ does not converge with the smaller perturbation because of the tiny value of the perturbation ($\Delta = 0.01\%$), and $\partial D_{max}/\partial E_f$ & $\partial D_{max}/\partial E_w$ does not converge to smaller values either due to a low sensitivity value.

	Errors from the finite difference method					Analytical
X_j	$\Delta X = 1\%$	$\Delta X = 0.5\%$	$\Delta X = 0.1\%$	$\Delta X = 0.05\%$	$\Delta X = 0.01\%$	results
t_{load}	0.02053%	0.01561%	0.01167%	0.01117%	0.01078	0.46
E_f	0.7709%	0.2823%	0.09268%	0.04861%	0.1334%	-1.93×10^{-4}
E_w	1.251%	1.262%	1.375%	1.299%	1.238%	1.25×10^{-6}
G_{wf}	0.1972%	0.09316%	0.01404%	0.004555%	0.003033%	-1.77×10^{-3}
v_{wf}	9.808%	4.482%	1.516%	1.531%	1.543%	-6.27×10^{-3}

Table 5.3: Errors of $\partial D_{max}/\partial X_j$ from the finite difference method with different ΔX

2) Hypar membrane:

This numerical example is based on the deterministic analysis of the saddle shape membrane which has been demonstrated in the chapter "Deterministic Fabric Analysis". The hypar membrane supported by tensioned boundary cables is discretized into 32 membrane and cable elements and the analysis results are depicted in fig. 5.10. Following the same procedure in the example "patch test", the positions of the structural responses of interest are initially identified. The sensitivities of these structural responses are then computed using finite difference and analytical approaches separately.

As shown in Table.5.4, the analytical sensitivity formulation is verified by the similarity of the differentiation results from the finite element method to the analytical result. Compared with the patch test solution, the maximum displacement in the hypar is less sensitive to fabric

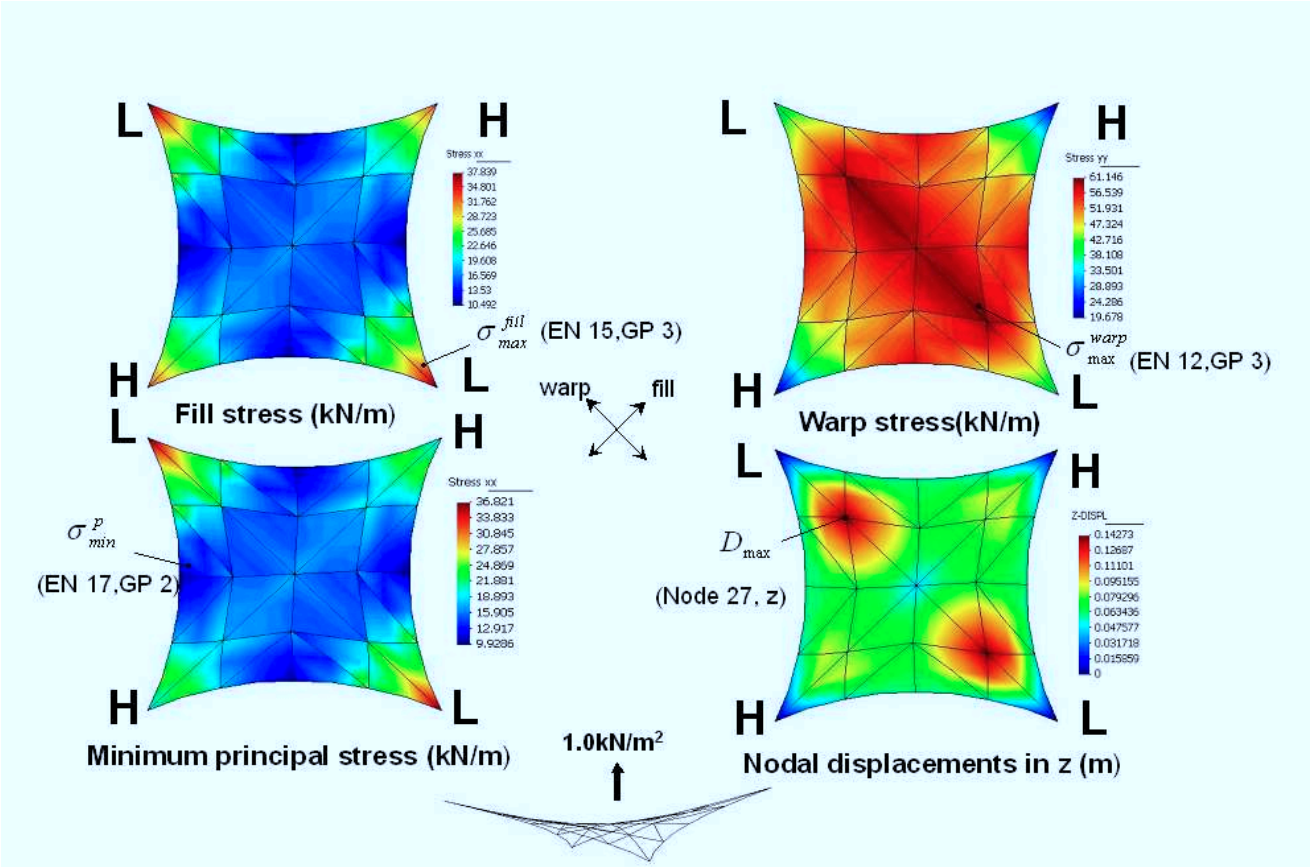

Figure 5.10: Hypar test for sensitivity and reliability analysis

material properties (e.g. $\partial D_{max}/\partial E_f = -2.09 \times 10^{-6}$), because of its geometrically nonlinear structural type. It is also interesting to note that the minimum principal stress drops more than twice rapidly as the maximum stress increases with the same increment of the load. This implies that such this hypar membrane is more prone to fail due to wrinkling rather than by material rupture when the same safety margins are assigned.

From these two numerical examples of structural sensitivity analysis, both the finite difference and analytical methods indicate similar values in estimating the derivatives of the structural response of interest. The finite difference method requires repeating the analytical analysis twice for each derivative quantity, and may be time-consuming when the analytical analysis is complicated. The finite difference method may therefore not be efficient for sensitivity and reliability analysis of large structure systems, but is a useful tool for checking the validity of the analytical formation derived in section.5.3.2. It also proves useful in cases where analytical sensitivities are not available.

X_j	$\partial\sigma^{fill}_{max}/\partial X_j$		$\partial\sigma^{warp}_{max}/\partial X_j$	
	Finite difference	Analytical approach	Finite difference	Analytical approach
t_{load}	7.79	7.92	28.83	29.23
E_f	-2.21×10^{-2}	-2.24×10^{-2}	-5.36×10^{-2}	-5.32×10^{-2}
E_w	1.12×10^{-3}	1.13×10^{-3}	9.40×10^{-5}	9.23×10^{-5}
G_{wf}	2.71×10^{-2}	2.74×10^{-2}	-0.16	-0.16
v_{wf}	0.92	0.93	1.93	1.96

X_j	$\partial\sigma^{p}_{min}/\partial X_j$		$\partial D_{max}/\partial X_j$	
	Finite difference	Analytical approach	Finite difference	Analytical approach
t_{load}	-39.68	-39.60	-1.07×10^{-2}	-1.06×10^{-2}
E_f	-2.73×10^{-2}	-2.80×10^{-2}	-2.08×10^{-6}	-2.09×10^{-6}
E_w	-2.04×10^{-4}	-2.08×10^{-4}	6.81×10^{-7}	6.91×10^{-7}
G_{wf}	0.13	0.13	-3.70×10^{-6}	-3.70×10^{-6}
v_{wf}	16.28	16.40	5.64×10^{-3}	5.68×10^{-3}

Table 5.4: Sensitivity analysis using finite difference and classic perturbation ($\Delta = 0.1\%$)

5.4 Reliability algorithm specific to fabric structural analysis

The reliability of fabric structures with different failure modes can be estimated using the HL-RF(Hasofer-Lind and Rackwitz-Fiossler) algorithm introduced in section 5.2 combined with sensitivity formulations detailed in section 5.3, and can be described as followings and presented as figure.5.11:

1) Obtain the statistical information of the fabric material and applied loads (i.e. distributions and parameters), and calculate the permissible stresses of the fabric(σ^{fill}_{per},σ^{warp}_{per}). (See chapter 4.)

2) Establish the four limit state functions $G_i(i = 1 \rightarrow 4)$ as Eqn. 5.3 and 5.5, and corresponding to each limit state, probability of failure p_f can be estimated as in the following steps:

3) Assume the mean value of the random variables as the initial values of the design point $x^*_i, i = 1, 2, \cdots, 7$.

4) For those non-normal distributed variables, compute the mean and standard deviation at the design point of the equivalent normal distribution using Eqn.5.26 and Eqn.5.27.

5) Calculate the corresponding value of the limit state functions $G_i(\ )$ at the design point based on a finite element deterministic analysis and the corresponding $\partial G_i/\partial X_j$ using analytical sensitivity formulations in section 5.3.2.

6) Calculate gradients of limit state function in the reduced coordinate system $\partial G^*_i/\partial X_j$ using Eqn.5.177.

$$\frac{\partial G_i^*}{\partial X_j} = -\frac{\partial G_i}{\partial X_j}\sigma_{X_i}^N \tag{5.177}$$

7) Compute the new values of design points ($x_i'^*$) in the reduced space using Eqn.5.33.

8) Compute the safety index β based on the values of the design points calculated in step 5 using Eqn. 5.36, Check the convergence of β and $|G(X)_i|$, if β converged and $|G(X)_i|$ is very close to zero, then goto step 10, otherwise step 9.

9) Compute the new values of the design point (x^*)in the original space using Eqn. 5.37 and repeat step 4 to 8.

10) Calculate the probability of failure for next limit states until convergence of β is attained.

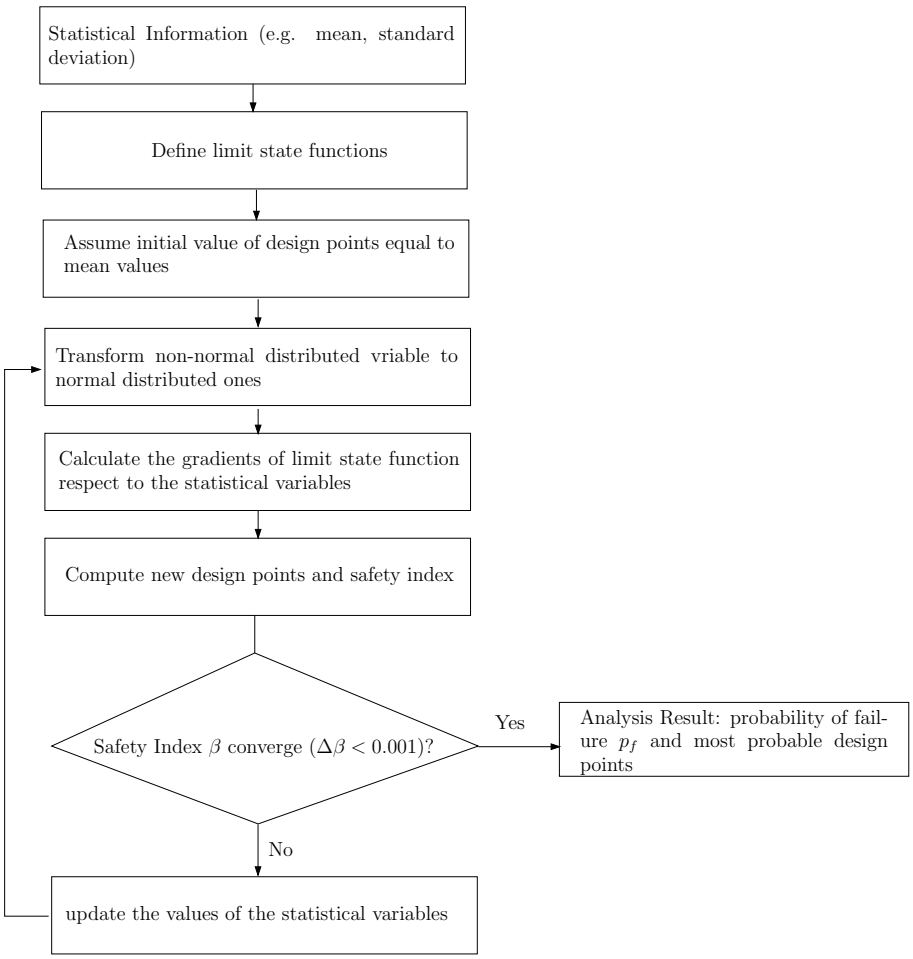

Figure 5.11: Reliability solution algorithm

Using this algorithm, the reliability of the fabric structure corresponding to different limit states can be estimated individually, and a integrated reliability analysis cannot be obtained directly. Normally, for a given fabric structure, structural failure may occur more likely corresponding to one limit state rather than the others. For example, when loading is not uniform, the structure is more prone to fail due to wrinkling rather than the material rupture since the pre-stress in the fabric is normally several percentage of the rupture strength.

5.4.1 Numerical Example of Reliability Analysis

From the discussion in the section 5.3.4, it suggests that not all the random variables involved in the analysis have the same level of effect on the reliability for a specific limit state. In certain cases, only a few random variables (e.g. loads and material strength) play key roles in the reliability analysis, and the reliability is not sensitive to the other variables even though they may have high levels of uncertainty. However in the other case, the reliability is sensitive to the majority of random variables, and the reliability estimation may become difficult since more variables are effective in the reliability calculation.

In this section, two numerical examples are presented. The first is a special case in that most random variables, including loads, material strength, and elastic modulus have approximately the same level of effect on the reliability. The assumed limit states are selected to represent the structural response ranges achievable using these random variables with reasonable COV values. For example, the maximum stress may vary by about 10% of the mean value due to a varying elastic modulus with the COV value of 0.5 while the same performance variable could change up to 200% of the mean with variation in the loads by the same variance. In that case, the limit state will be mainly selected according the structural response ranges by the random variable of elastic modulus to observe and compare the effects of both variables. The main purpose of this example is to verify the reliability formulation with multi-variables, and also to compare the performance effects of these random variables.

The second numerical example is a case study, based on a realistic design case with the probabilistic assumptions. The purpose of the case study is to examine the safety factors currently applied to fabric structure design consistent with the reliability requirement of the Eurocode 0. It also demonstrates how to apply the reliability analysis tool to the realistic design of a fabric structure. Based on the reliability analysis, a tentative suggestion of the corresponding efficient safety factors will be given.

Hypar membrane

The reliability of the Hypar membrane presented in the section 5.3.4 can be evaluated as a fictitious numerical example. In this numerical example, the probability of failure of the pretensioned hypar made of a heavy pvc-polyester fabric material is computed. The statistical design parameters are given in table 5.5. Initially, all random variables are assumed to be normally distributed, and the standard deviation of each variable is 10% of the mean value (i.e $COV = 0.1$)). A high safety factor of 8 based on the European Design Guide [3] is assumed for the materal strength, which was approximately 80kN/m based on the test results in Chapter.4.

Because in this example, the maximum stress in one direction is always higher than the other, i.e $\sigma^w_{max} > \sigma^f_{max}$, therefore the limit states can be assumed as:

$$G_2(X) \quad = \quad \sigma_{per} - \sigma^w_{max}, \qquad \sigma_{per} \sim N(10, 1) \;\; kN/m$$

X_j(kN/m)	Distribution	Mean value	Standard deviation ($COV = 0.1$)
E_f(kN/m)	Normal	1000	100
E_w(kN/m)	Normal	1000	100
G_{wf}(kN/m)	Normal	30	3.0
v_{wf}	Normal	0.1	0.01
t_{load}	Normal	1	0.1
σ_{per}(kN/m)	Normal	10	1.0

Table 5.5: Distributions and parameters of the random variables

$$\begin{aligned} G_3(X) &= \sigma^p_{min} - \sigma^p_{per}, \qquad \sigma^p_{per} = 0 \\ G_4(X) &= D_{al} - D_{max}, \qquad D_{al} = 35mm \end{aligned} \tag{5.178}$$

Where $D_{al} = 35mm$ is assumed to be about 1/120 of the structure span 4m.

The corresponding safety indices with the initial assumption are computed and the values are given in the table 5.6, 5.7 and 5.8 with $COV = 0.1$. To investigate the sensitivity of the random variables to p_f, different safety indices are computed with increasing standard deviation of one random variables whilst maintaining the other initial values. For example, the safety indices with the standard deviation of E_f from 100kN/m ($COV = 0.1$) to 400kN/m ($COV = 0.4$) are calculated in the first rows of table 5.6, 5.7 and 5.8. The probability of structural failures in different failure modes are depicted in figure 5.12, 5.13 and 5.14.

	Safety indices					
X_j	$COV = 0.1$	$COV = 0.15$	$COV = 0.20$	$COV = 0.25$	$COV = 0.30$	$COV = 0.40$
E_f	2.301	2.286	2.251	2.231	2.192	2.089
E_w	2.301	2.271	2.235	2.219	2.146	2.055
G_{wf}	2.301	2.301	2.301	2.300	2.300	2.299
v_{wf}	2.301	2.301	2.301	2.301	2.301	2.301
t_{load}	2.301	2.149	1.984	1.814	1.777	1.403
σ_{per}	2.301	1.596	1.213	0.977	0.817	0.616

Table 5.6: Safety indices for the fabric failure mode with COV

As shown in table 5.6, the safety index in the fabric failure mode seems more sensitive to the uncertainties of the permissible stress and the load rather than the other material properties. The shear modulus and the Possion's ratio appear to have little effect on the safety index, because their variations are comparatively small. As depicted in figure 5.12, it is apparent that the permissible stress is a dominant random variable in evaluating the probability of fabric failure, and the uncertainty of the load may also increase the probability of structural failure.

In the wrinkling and serviceability failure criterion, the permissible stress is not applicable. Therefore only five random variables are involved in the reliability analysis as listed in table

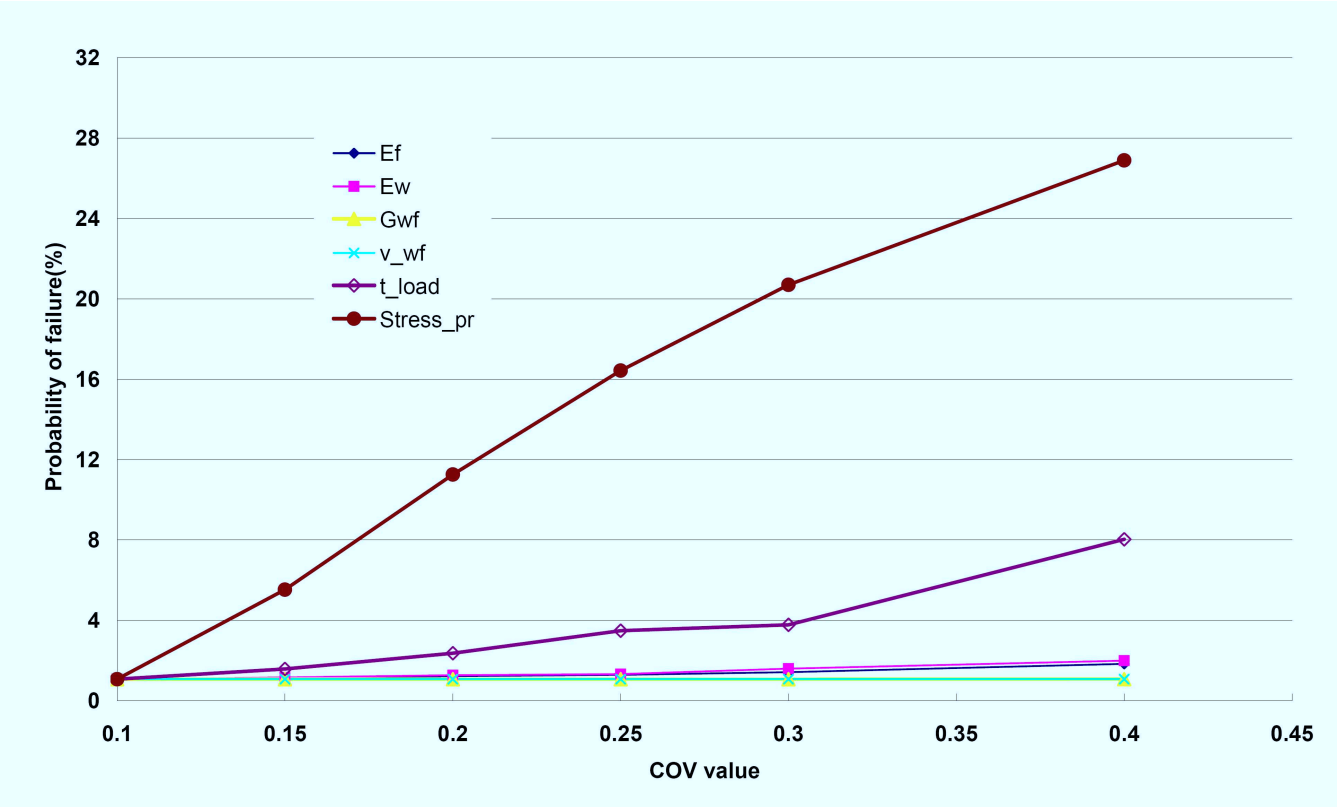

Figure 5.12: p_f of the fabric failure changes with the increasing uncertainties

5.7 and 5.8. As shown in figure 5.13, for the wrinkling failure mode, the load coefficient t_{load} becomes the most important random variable affecting the value of the reliability, and the effects from the Young's modulus of warp and fill are more obvious compared with fabric rupture mode.

	Safety indices					
X_j	$COV = 0.1$	$COV = 0.15$	$COV = 0.20$	$COV = 0.25$	$COV = 0.30$	$COV = 0.40$
E_f	1.976	1.904	1.831	1.662	1.542	1.316
E_w	1.976	1.762	1.563	1.401	1.262	1.041
G_{wf}	1.976	1.976	1.975	1.975	1.973	1.973
v_{wf}	1.976	1.976	1.976	1.976	1.976	1.976
t_{load}	1.976	1.479	1.182	0.971	0.828	0.633

Table 5.7: Safety indices for the wrinkling failure mode with COV values

Considering the serviceability limit state (deformation or ponding), the reliability is implied to be more dependent on the load coefficient t_{load} and Young's modulus in warp direction rather than other material parameters. The relative sensitivities of the limit state function infers the nature of the structural response to the load in which the deflection is effectively controlled clearly by the load or also by the warp stiffness. In this case, a fabric with reduced uncertainty in the warp direction is better suited to increasing the performance of this type

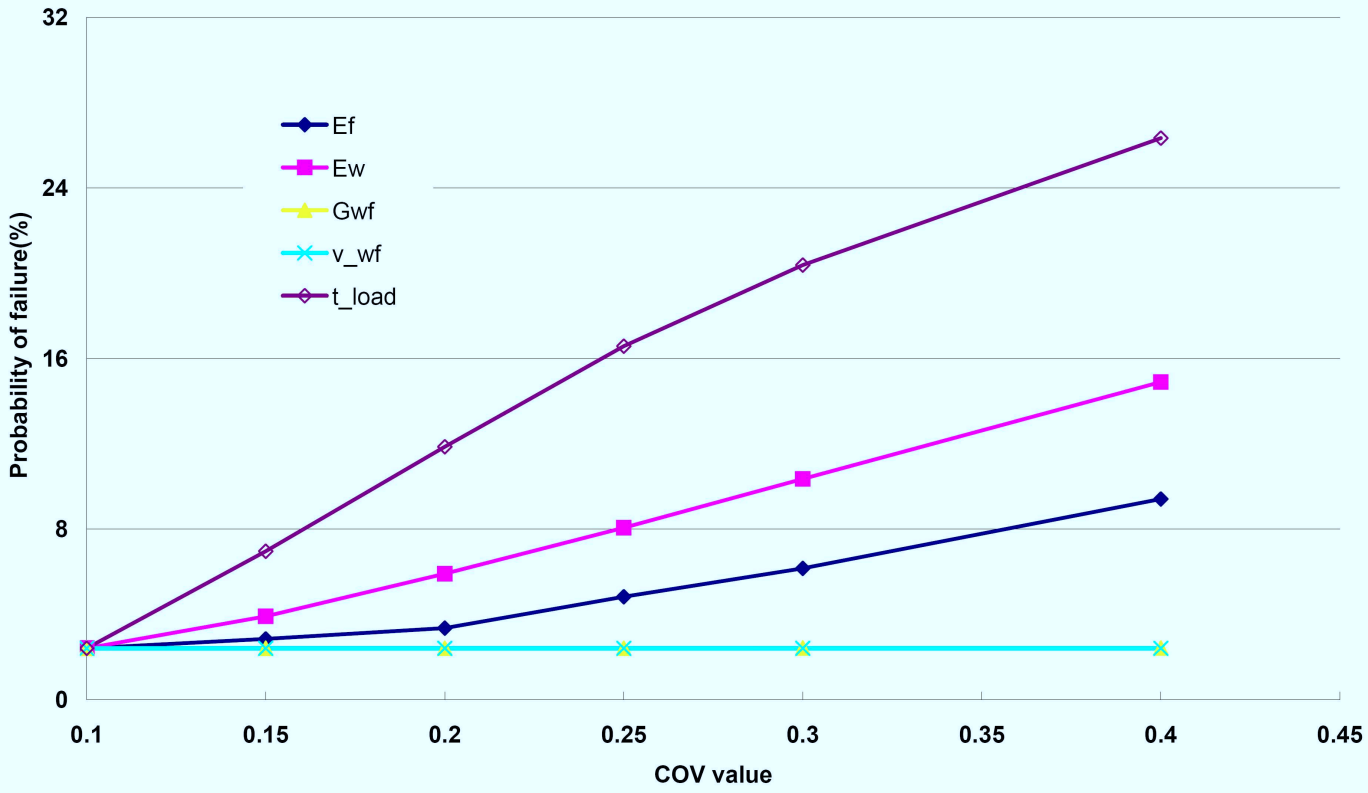

Figure 5.13: p_f of the wrinkling failure changes with the increasing uncertainties

of structure. It is also notable that E_w approaches approximately the same effect as the load coefficient t_{load} on the reliability in serviceability failure.

	Safety indices					
X_j	$COV = 0.1$	$COV = 0.15$	$COV = 0.20$	$COV = 0.25$	$COV = 0.30$	$COV = 0.40$
E_f	3.086	3.067	3.061	3.054	3.045	2.996
E_w	3.086	2.486	2.183	1.725	1.515	1.167
G_{wf}	3.086	3.086	3.084	3.082	3.076	3.071
v_{wf}	3.086	3.084	3.083	3.081	3.079	3.069
t_{load}	3.086	2.382	1.956	1.681	1.426	1.057

Table 5.8: Safety indices for the serviceability failure mode with COV values

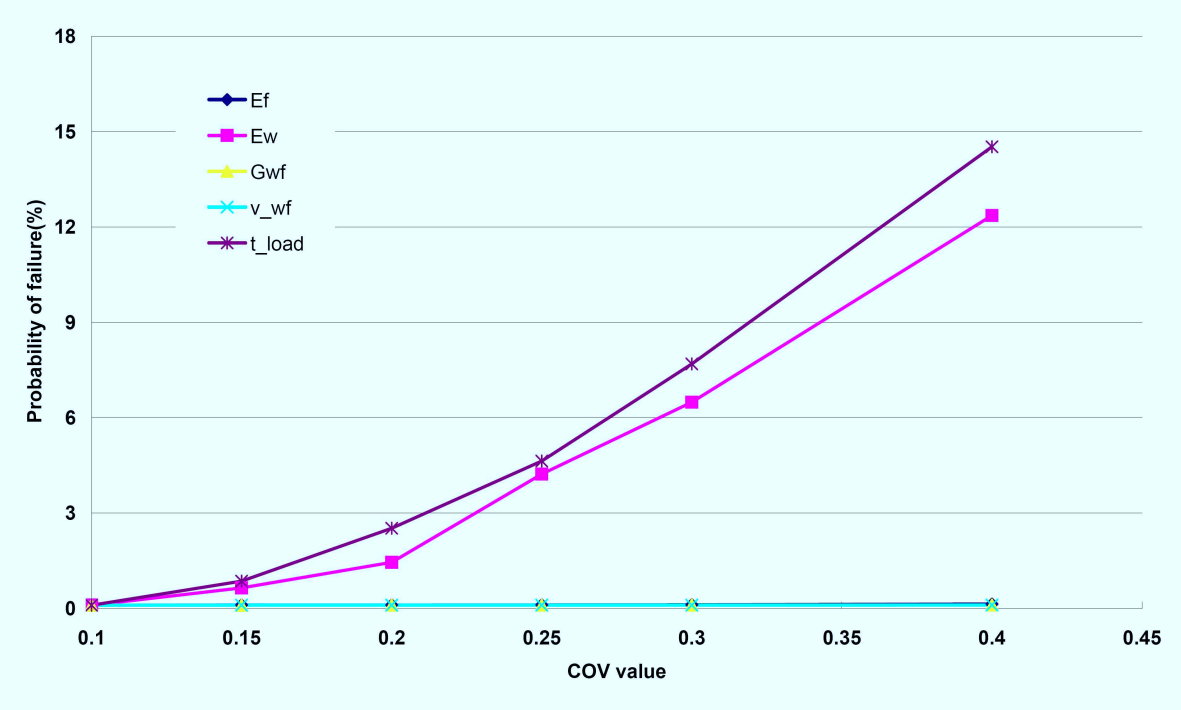

Figure 5.14: p_f of the serviceability failure (deformation) changes with the increasing uncertainties

This numerical example demonstrate a basic reliability estimation of a simple and typical fabric structure form. The emphasis of this example is be focus on the comparison of the influences on the structural reliability from different uncertainty sources. The results in this example demonstrate that for a given structural type, not all uncertainties will affect the structural reliability significantly, and their influences based on different limit states also may be different. In this example, loading and material strength have the greatest affect on the reliability in the material failure mode, while the obvious effects of other material properties are only observed in the serviceability limit states (wrinkling and deformation). The uncertainties in fill and warp elastic modulus also have different influences on the reliability, which depends on the stress and deformation distributions along the membrane surface and inherent load-carrying mechanism.

Recognition of the performances of a range of uncertainties involved in a given fabric structure design and analysis is very important. If one type of uncertainty is found to make a dominant contributing to the reliability, then the variance and distribution of the structural response will largely depend on the randomness and distribution of this type of uncertainty.

Three types of failure modes were discussed in this example. However the three types of failure are unlikely to simultaneity appear. The most common situation is that one type of limit state will be approached first. In that case, the other two types of failure may not be taken into account since the structure will have already "failed" according to the definition of the structural failure. If a given fabric structure always tends to fail in one mode rather than the other two, then it may be reasonable to consider this mode as the main failure mode,

and compute the structural reliability based on the corresponding limit state. However the locations of the failures defined under the different limit states (e.g. deflection and wrinkling) may be not in the same point. When the reliability of local membrane parts are required, the other failures may be still need to be evaluated.

Doncaster Creche canopy

This is a numerical example based on a real fabric structure project: Creche Canopy in Doncaster, UK, designed by Arup as figure.5.15.

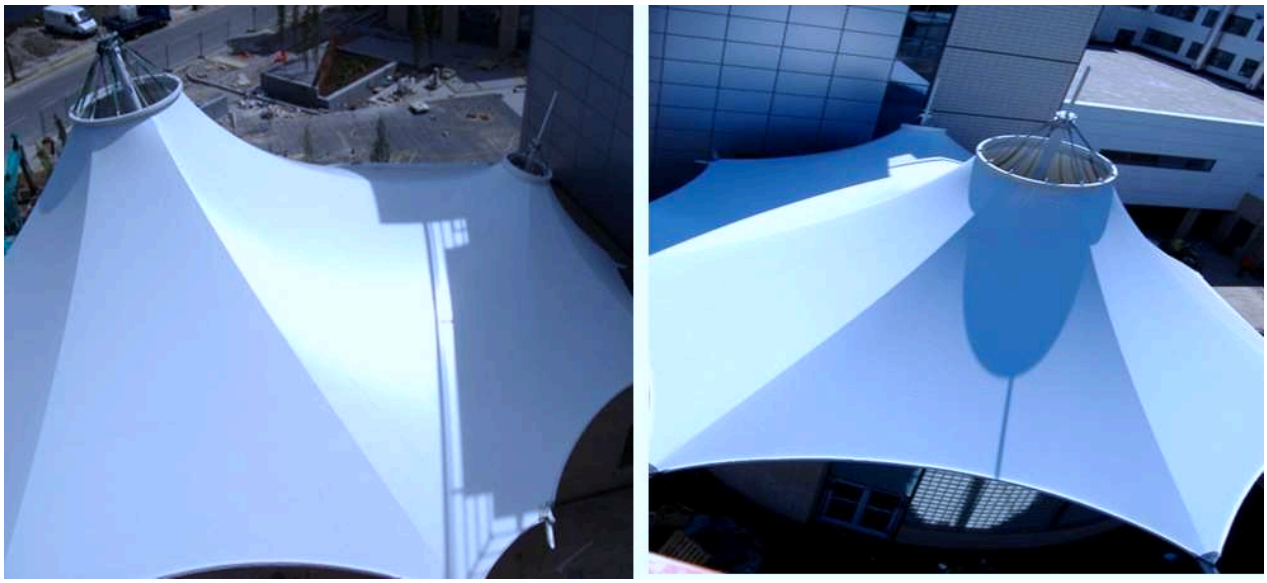

Figure 5.15: Creche Canopy in Doncaster (Arup)

As shown in fig.5.16 and 5.17, the PVC-polyester canopy comprises two conics, supported by masts and steel rings in the central of each cone, booms and tensioned cables including boundary cables and belts at the perimeter and within the fabric.

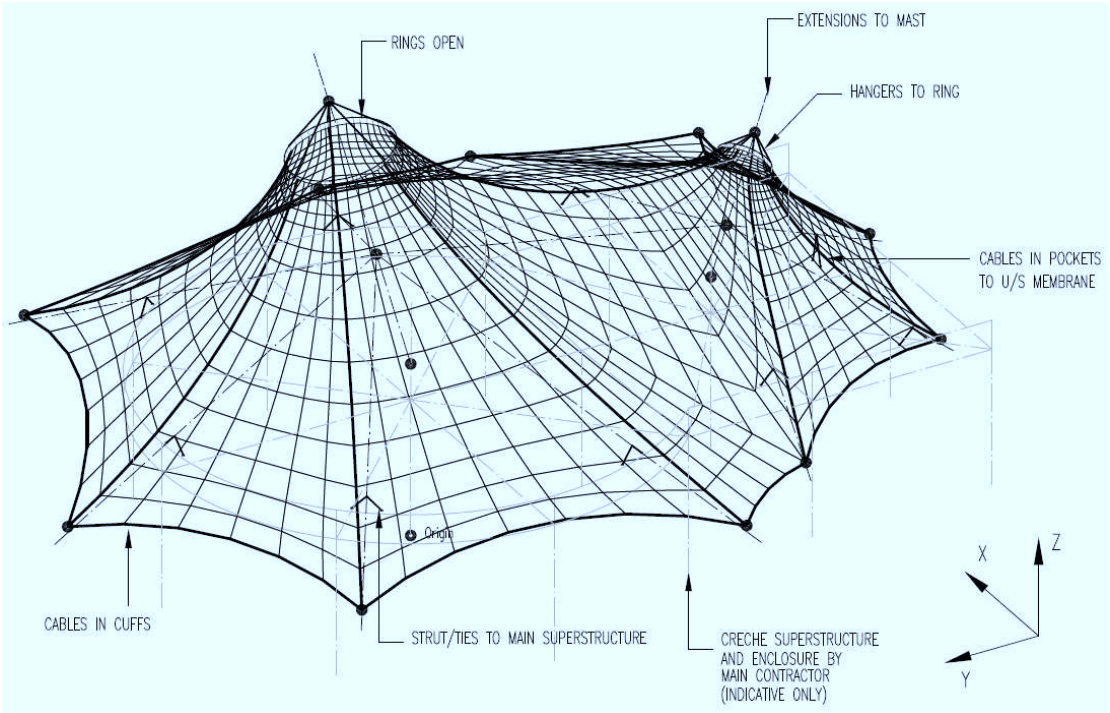

Figure 5.16: Design 3D view of Creche Canopy in Doncaster (Arup)

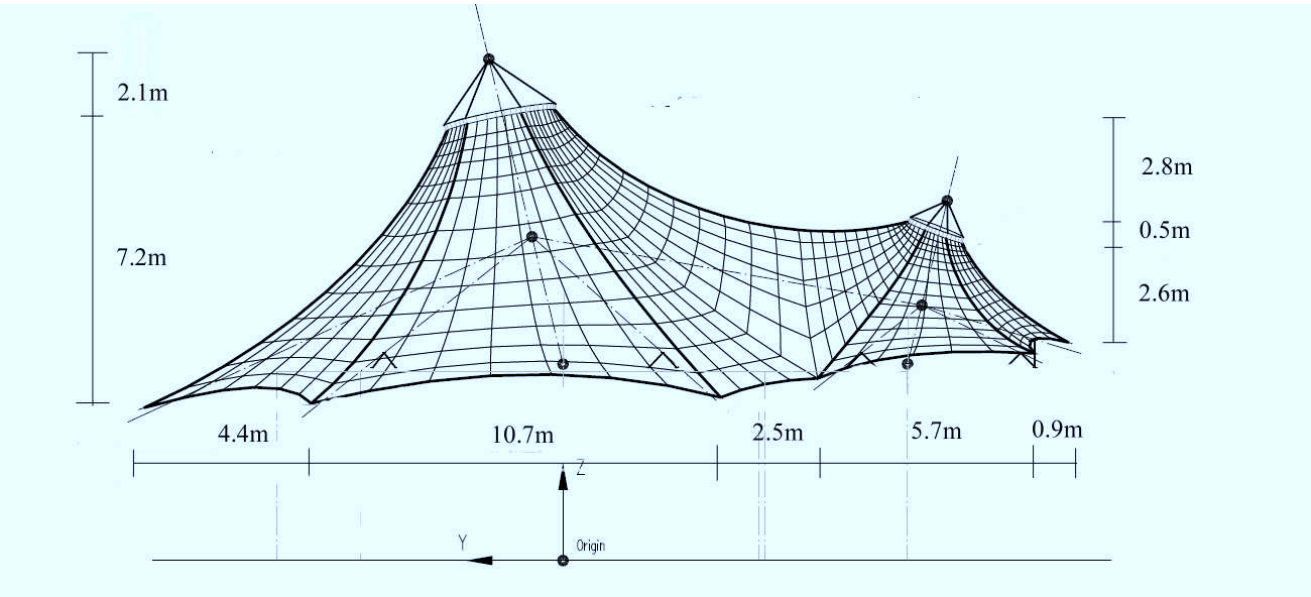

Figure 5.17: Elevation of Creche Canopy in Doncaster (Arup)

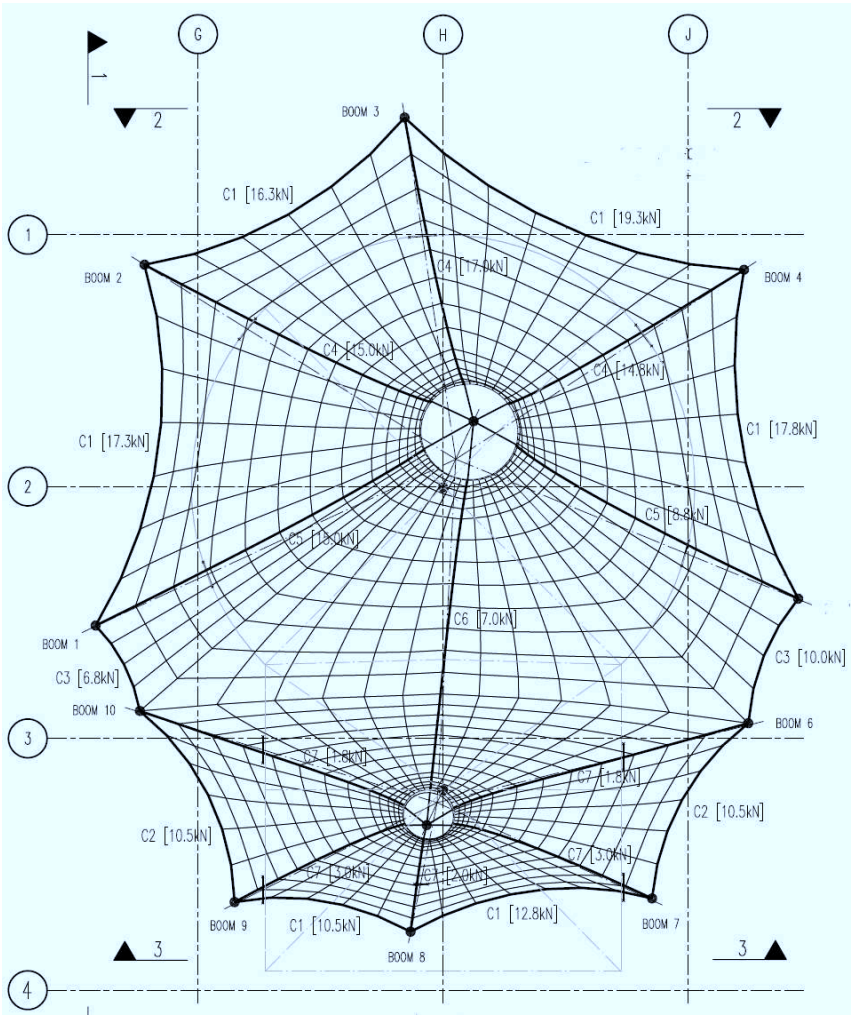

Figure 5.18: Plan showing pretensions in cables of Creche Canopy (Arup)

The prestress of the membrane is 1.5 kN/m along the fill and warp directions. The pretensions of the cables and belts are presented in fig.5.16. The membrane surface is discretized by 166 LST elements. The equilibrated prestressed (form-found) geometry is illustrated in fig.5.19.

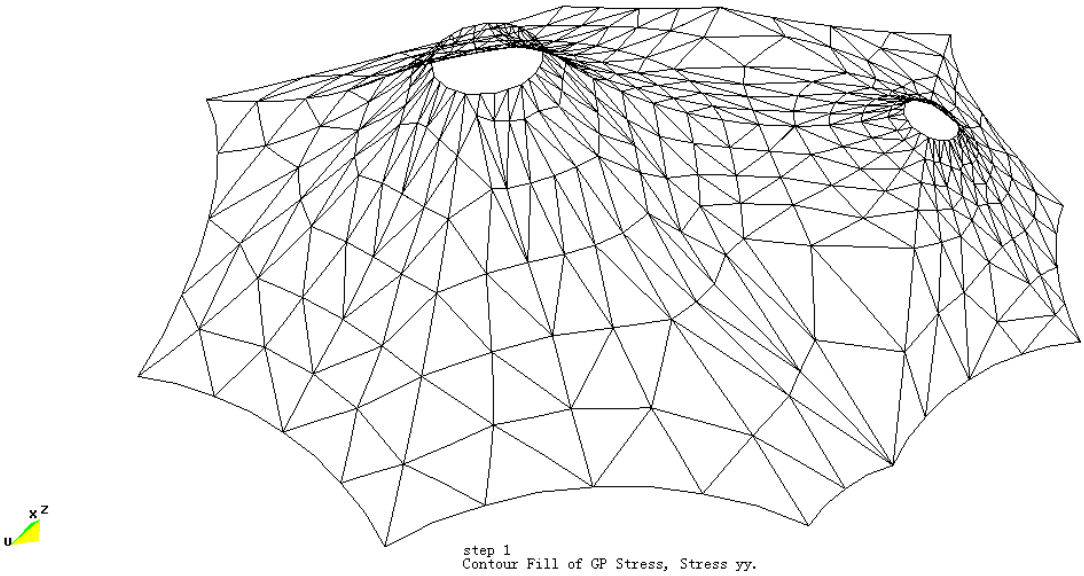

Figure 5.19: Form-finding of Creche Canopy using 656 LST elements

The initial loading analysis assumed the following input parameters:

Fabric elastic modulus: $E_f = E_w = 1000kN/m$,$G_{yx} = 30kN/m$, Possion's ration: $v_{wf} = 0.1$, membrane thickness: $t = 0.32mm$

Cable Elastic modulus: $E = 156.8 \times 10^6 kN/m^2$, cable crosssection area: $A = 216.6mm^2$ (The values are assumed as normal steel cables)

Initial fictional uniform load in vertical direction (Z): $F_z = -0.1kN/m^2$.

The nodal displacements arising from the effect of the uniformly applied load are illustrated in fig.5.20, with the corresponding membrane stress distributions presented in fig.5.20 to fig.5.21. Owing to the strong stiffness of the cables and belts compared with the fabric, the displacement values of nodes near the cables are very low, while large nodal displacements appeared in the membrane remote from the belts. Several displacement "ponds" are formed within the areas defined by the cables. The max displacement is located in the area close to the interface between the two component conics as depicted in fig.5.20.

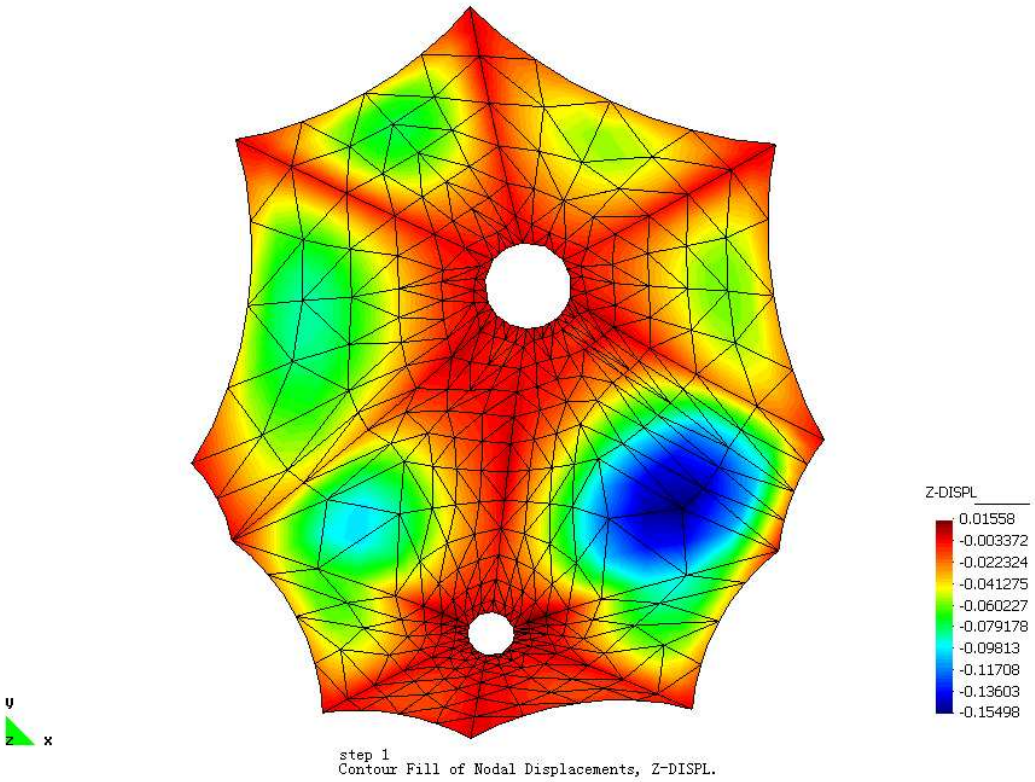

Figure 5.20: Nodal displacement(m) in vertical direction (z is upward direction

As shown in fig.5.21 and 5.22, the membrane stress distribution is clearly related to the belt positions, and smooth stress distributions are limited to the areas between the belts. In the area around the interface of the two cones, generally the maximum or peak stresses are along the Y direction, while in the two outer perimeter areas, most significant stresses along X direction are observed. Maximum stresses along in directions are observed near the support head rings, where the stress distribution appear less smooth because of the integrated effects from belts and rings in these areas.

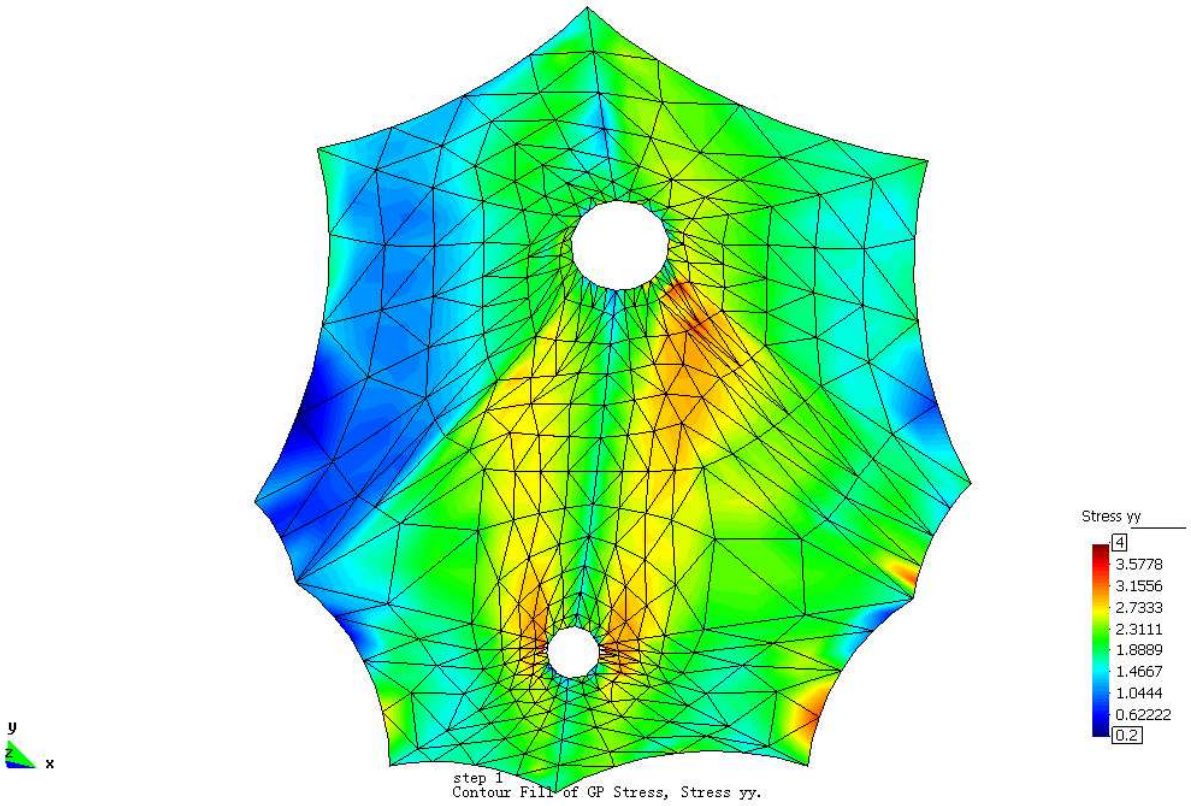

Figure 5.21: Membrane stress along global y axis(kN/m^2)

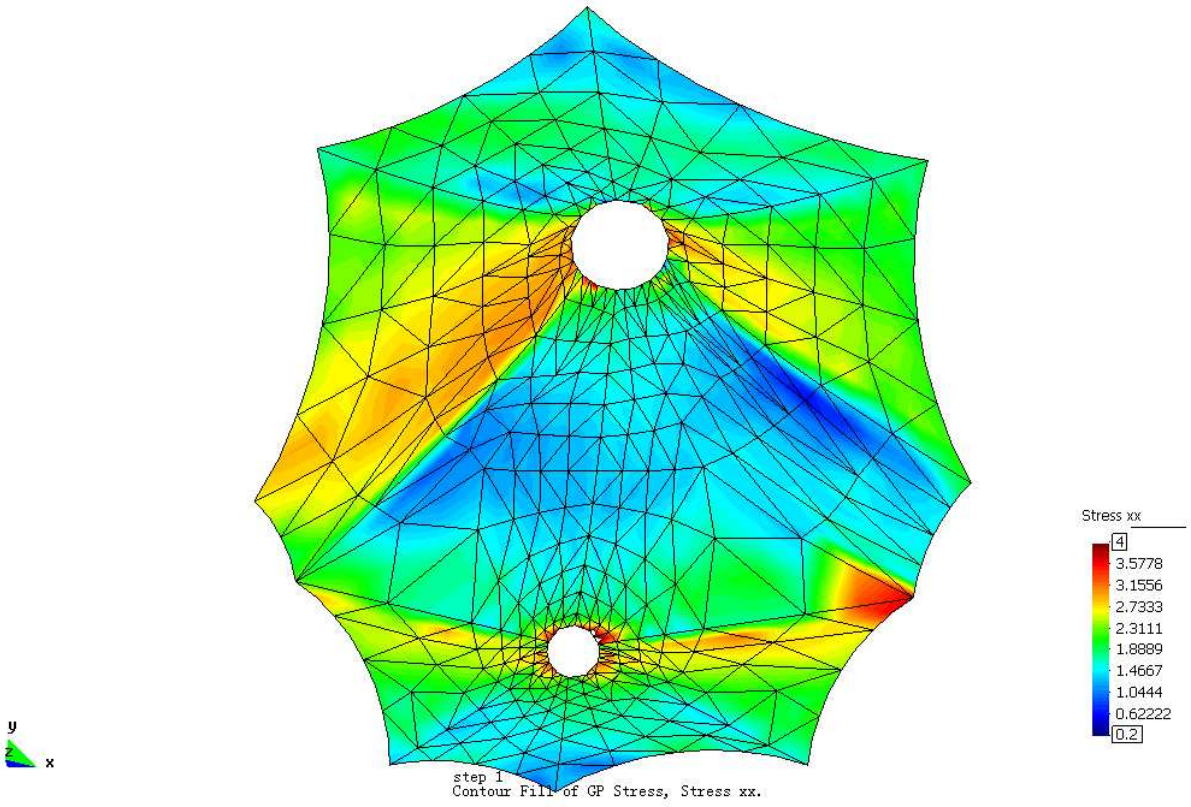

Figure 5.22: Membrane stress along global x axis(kN/m^2)

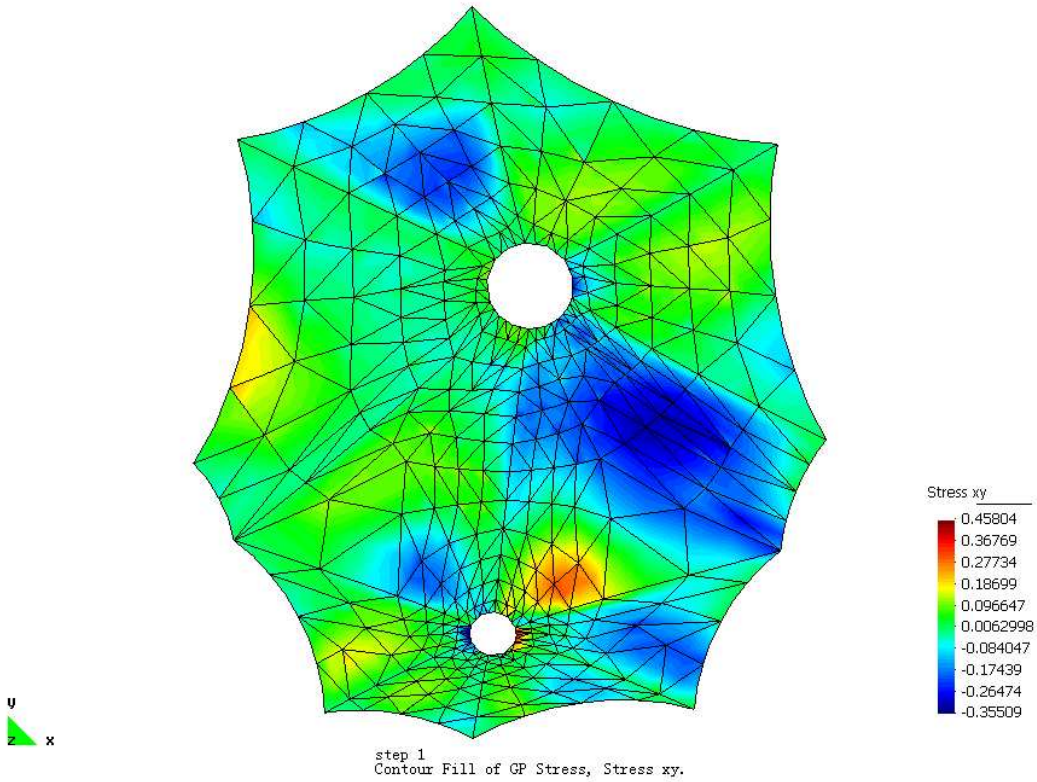

Figure 5.23: Membrane shear stress across global xy axis(kN/m^2)

Fictional Example for the uncertainty comparison

Assuming that similar fabric material as hypar membrane is used in the canopy, the initial statistical input parameters are defined as Table.5.5. Different from the hypar example, the magnitude of the uniform load is only 0.1 kN/m^2, which seems much less than the one in hypar. But the resulting maximum and minimum stresses approach about 4kN/m, and 0.2kN/m, which are suitable for a good analysis of the sensitivity comparison for different variables.

Since the maximum stresses in X and Y directions are close, four limit states will be assumed to judge the structural failure of the canopy as,

$$\begin{aligned} G_1(X) &= \sigma_{per} - \sigma^y_{max}, & \sigma_{per} &\sim N(10,1) \\ G_2(X) &= \sigma_{per} - \sigma^x_{max}, & \sigma_{per} &\sim N(10,1) \quad kN/m \\ G_3(X) &= \sigma^p_{min} - \sigma^p_{per}, & \sigma^p_{per} &= 0 \\ G_4(X) &= D_{al} - D_{max}, & D_{al} &= -160mm \end{aligned} \tag{5.179}$$

The safety index in the material failure mode are computed and listed in Table.5.9 and 5.10, and p_f in fill yarn directions are illustrated in fig.5.24 and 5.25. In the material failure mode, the probabilities of the fabric rupture in both fill and warp direction are strongly dependent to the COV values of the fabric strength, and a significant increase in p_f value is observed with

0.1 increment in the COV value of the strength. The variations in other statistical parameters (e.g load coefficient t_{load}) have a reduced influence on the p_f under the material failure limit state as much as the material strength, meaning that in this case, the material strength is the dominant statistical variable.

Unlike in the hypar example, the variation of the load coefficient t_{load} seems more significant to the value of p_f. For example, the uncertainty with a COV=0.4 only result in a p_f value less than 1%. But it is obversed from Table.5.9 and 5.10, that t_{load} is the second most important randomness variable in the safety index.

The stress contour(fig.5.21-5.23 suggests the maximum stresses in both fill and warp direction are similar under a static load of F=0.1kN/m, indicating that the limit states of material failure may be approached at the same time. However the remarkable difference in safety index corresponding to fill and warp failure demonstrate the rupture failure of the fabric seems more commonly to appear in the fill direction when the variation in the Young's modulus and loads are taken into account.

	Safety indices					
X_j	$COV = 0.1$	$COV = 0.15$	$COV = 0.20$	$COV = 0.25$	$COV = 0.30$	$COV = 0.40$
E_f	3.791	3.750	3.695	3.632	3.581	3.492
E_w	3.791	3.740	3.701	3.601	3.762	3.652
G_{wf}	3.791	3.790	3.789	3.780	3.788	3.786
v_{wf}	3.791	3.791	3.791	3.790	3.790	3.789
t_{load}	3.791	3.640	3.472	3.372	3.203	3.081
σ_{per}	3.791	2.574	1.911	1.543	1.293	0.971

Table 5.9: Safety indices for the fabric failure mode (fill) with $C\hat{O}V$

	Safety indices					
X_j	$COV = 0.1$	$COV = 0.15$	$COV = 0.20$	$COV = 0.25$	$COV = 0.30$	$COV = 0.40$
E_f	4.501	4.451	4.402	4.351	4.304	4.207
E_w	4.501	4.462	4.423	4.381	4.342	4.302
G_{wf}	4.501	4.29	4.289	4.287	4.285	4.281
v_{wf}	4.501	4.499	4.499	4.498	4.498	4.498
t_{load}	4.501	4.321	4.14	3.98	3.82	3.46
σ_{per}	4.501	3.029	2.39	1.812	1.512	1.241

Table 5.10: Safety indices for the fabric failure mode (warp) with $C\hat{O}V$

As shown in fig.5.26, wrinkling failure is more dependent on Young's modulus and loading coefficient. The load coefficient is still the most important basic variable affecting the probability of structural failure. Unlike the hypar case, both warp and fill Young's moduli altered significantly the p_f by wrinkling, meaning that wrinkling may happen in both fill and warp direction within the same probability when the COV is low, but is more probable in the warp direction for an increasing COV. Compared with the hypar, the canopy has more complicated

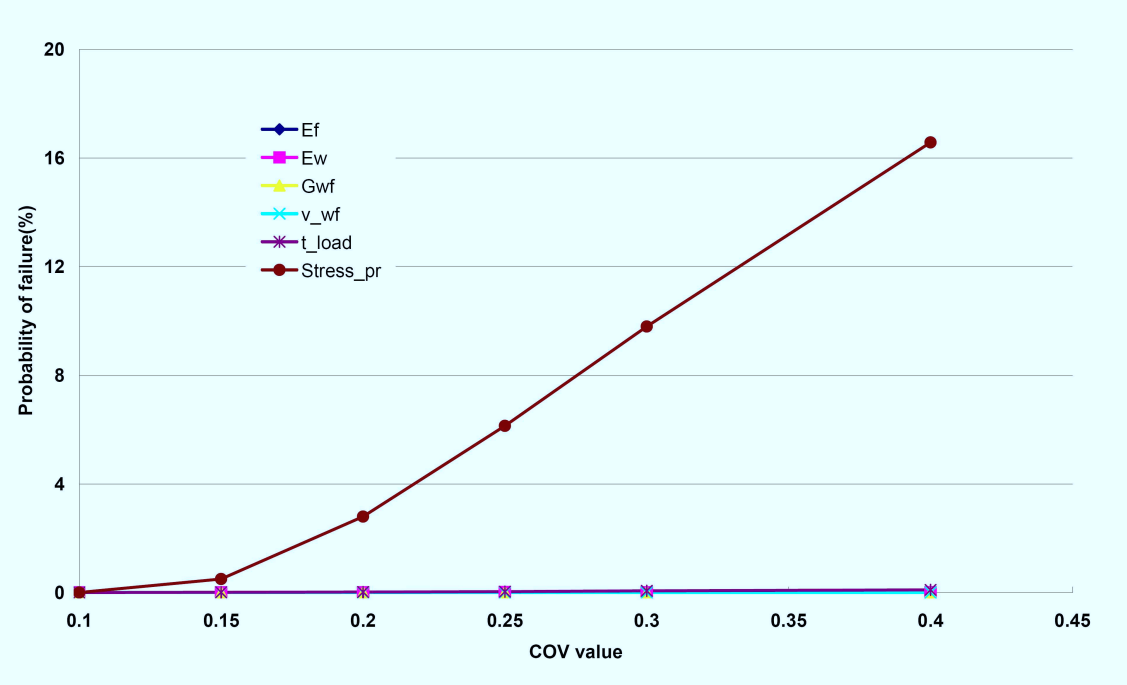

Figure 5.24: p_f of the fabric failure in fill changes with the increasing uncertainties

geometry and boundary conditions, leading to a non-smooth stress distribution, such that wrinkling may appear at different position and along different directions in the fabric surface at same time.

Compared with the material failure mode, the p_f under the wrinkling limit state indicates that the wrinkling is more probable rather than material rupture. The membrane prestress is 1.5kN/m, and a small variation in load and Young's modulus can produce increments of negative strain leading to wrinkles in the local areas of the fabric, whilst theoretically fabric rupture occurs under a large increment in load, or a severe degradation in material strength.

	Safety indices					
X_j	$COV = 0.1$	$COV = 0.15$	$COV = 0.20$	$COV = 0.25$	$COV = 0.30$	$COV = 0.40$
E_f	1.034	0.842	0.735	0.632	0.522	0.375
E_w	1.034	0.821	0.652	0.576	0.490	0.336
G_{wf}	1.034	1.034	1.034	1.034	1.034	1.034
v_{wf}	1.034	1.034	1.034	1.034	1.034	1.034
t_{load}	1.034	0.682	0.523	0.442	0.358	0.274

Table 5.11: Safety indices for the wrinkling failure mode with COV values

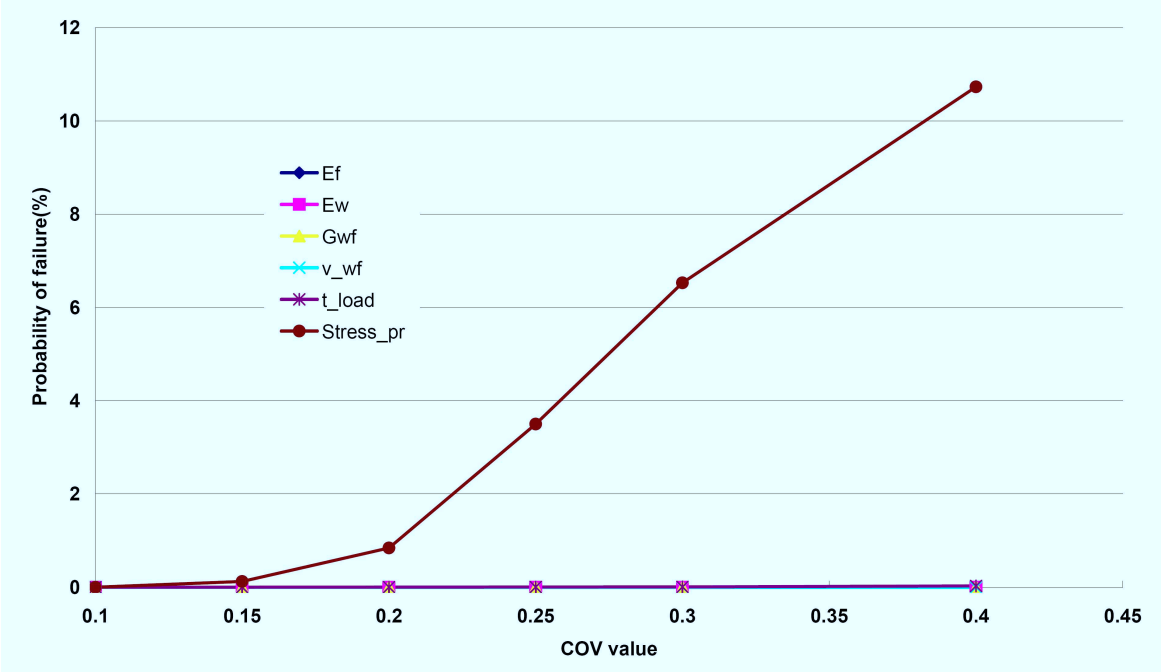

Figure 5.25: p_f of the fabric failure in warp changes with the increasing uncertainties

	Safety indices					
X_j	$COV = 0.1$	$COV = 0.15$	$COV = 0.20$	$COV = 0.25$	$COV = 0.30$	$COV = 0.40$
E_f	1.191	1.157	1.135	1.107	1.087	1.064
E_w	1.191	1.180	1.171	1.159	1.151	1.350
G_{wf}	1.191	1.190	1.189	1.189	1.188	1.186
v_{wf}	1.191	1.191	1.191	1.191	1.191	1.190
t_{load}	1.191	0.841	0.632	0.513	0.426	0.357

Table 5.12: Safety index for the serviceability failure mode with COV values

The safety index under the limit state $G_4(X)$ are calculated as Table.5.12, and the corresponding p_f values are illustrated as fig.5.27. The load coefficient t_{load} is found to be the most important random variable determining the safety index, which is also sensitive to Young's modulus especially in the fill direction. The variation of the shear modulus and Possion's ratio within COV=4.0 seem to have no obvious effect on the safety index and probability of structural failure.

This numerical example demonstrates the importance of the variations in material strength, loads and Young's modulus in the fabric structural reliability. The variation in material strength seems to dominate in the material failure mode, and loads have key roles in both structural and serviceability failure modes, and the instability of Young's modulus has obvious influence on the reliability in serviceability failure modes including wrinkling and large defor-

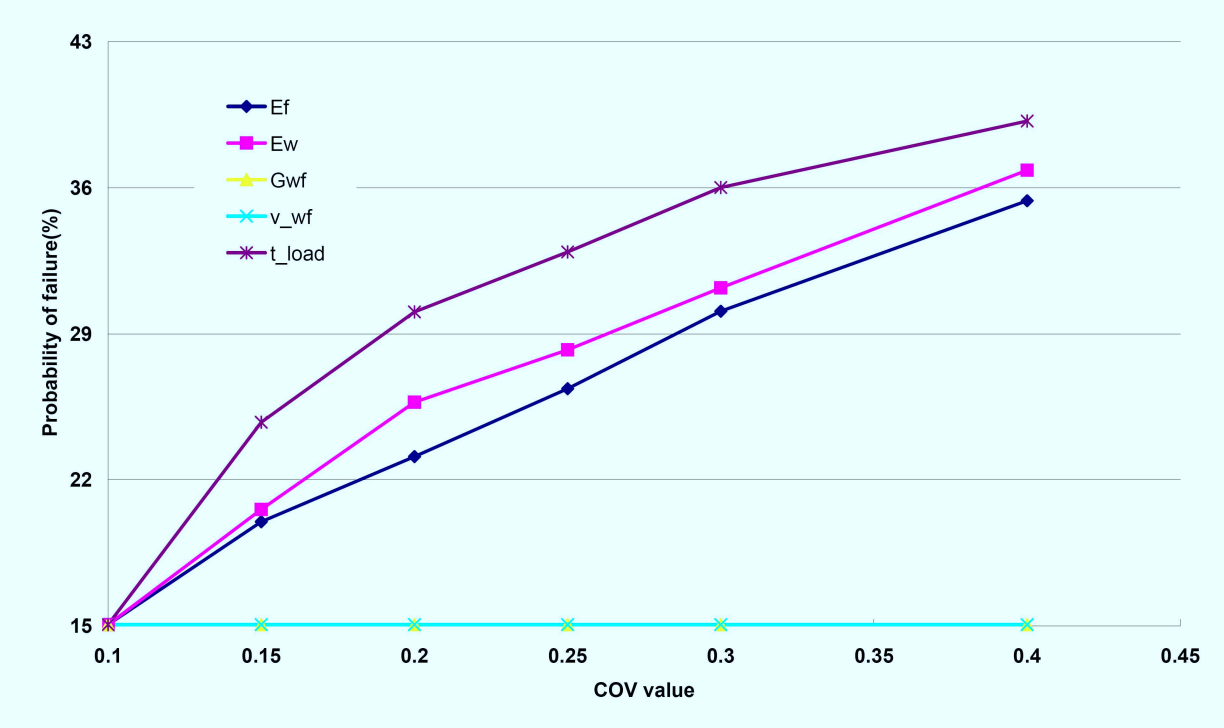

Figure 5.26: p_f of the wrinkling failure changes with the increasing uncertainties

mation. As the important material properties, shear modulus and Possion's ratio do not exhibit strong effect on the structural reliability unless their variations are very large(COV>0.4).

Theoretically, the structural reliability in any failure mode can be exactly estimated only when all uncertainty information are taken into account. However, it's not practicable to obtain the exact stochastic information of all the parameters involved in the reliability analysis under this PhD research, owing to the huge amount of cost and time. Through this numerical example, the sensitivities of statistical input parameters to the structural reliability can be estimated and compared, then the importance of these parameters will be obtained, which may be considered as a guide to the statistical investigation. If one statistical variable is found to be most important to the structural reliability(e.g material strength in the material failure mode), the uncertainty information of this variable should be investigated more carefully and exactly than others. In contrast, if any random variable is found to have little influence on the reliability, very clear statistical information may not be necessary and a huge amount of time and cost can be avoided since the accuracy of the reliability will be little compromised by the limited accuracy of the stochastic information of this statistical variable.

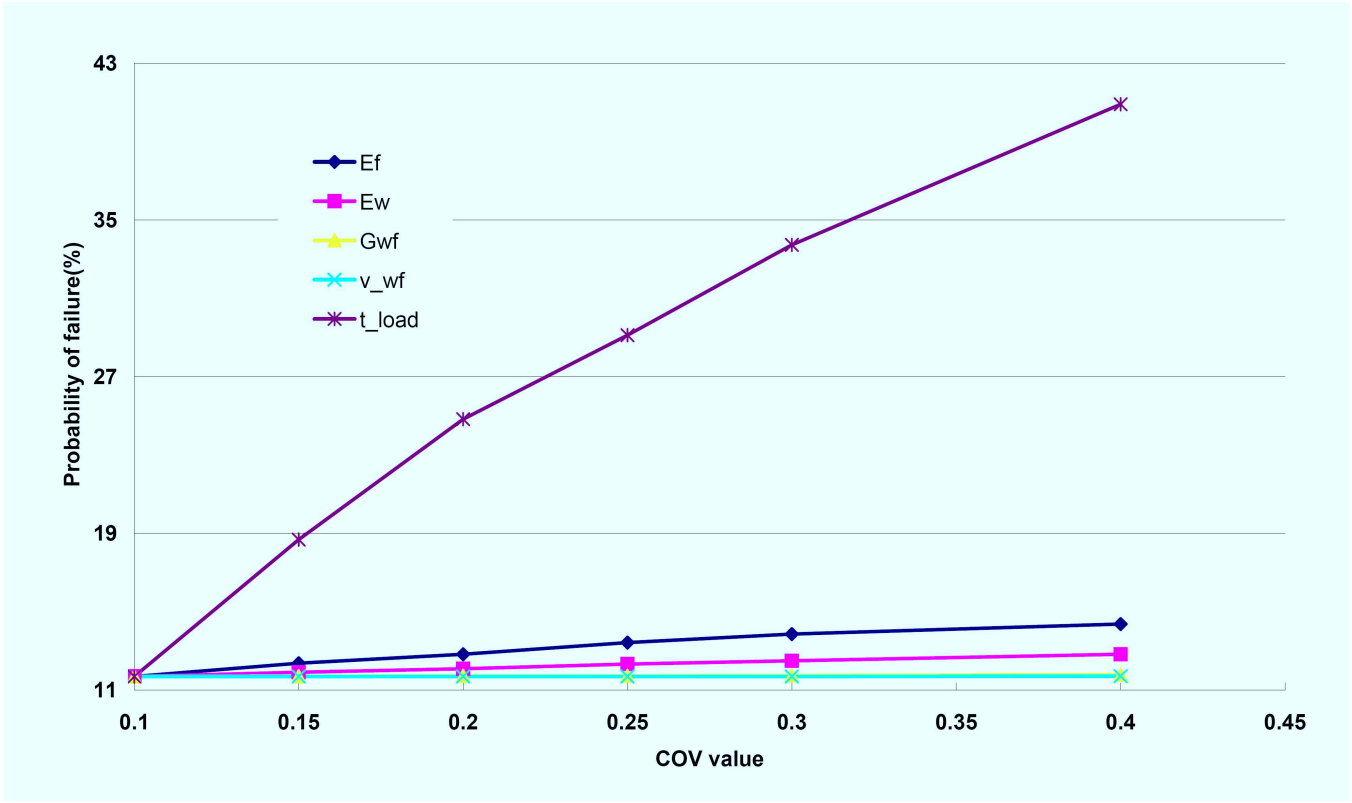

Figure 5.27: p_f of the fabric failure changes with the increasing uncertainties

Realistic analysis for the verification of existing safety factors

In current national design guides for fabric structures, a number of safety factors are advised to make a conservative design which limits the probability structural of failure in a certain degree. British Standard(BS EN 1990:2002,C6) gives a target structural safety index for 50 years $\beta = 3.8$, corresponding to a probability of structural failure $p_f = 0.724\%$. Assuming this safety index as the critical one for fabric structures, then those safety factors should result in a qualified structural reliability with $\beta > 3.8$ or $p_f < 0.724\%$.

There are so many uncertainties that can weaken the material strength. Amongst them, tear propagation is one most important issue to affect the realistic strength of most fabric types. The issue of the tear problem has been presented by European Design Guide for Tensile Surface Structures [3], and it is recommended that a safety factor of 4 should be used to take into account the tearing. Therefore a safety factor of 4 allowing for tear propagation will be applied as one primary safety factor.

In this example, the p_f of the canopy will be calculated with the uncertainty information obtained from chapter.3 and the published references. If we assume the canopy material is Ferrari 1002 PVC-coated polyester (group I), then the material statistical properties in chapter.3 can be used for the input parameters. Considering in the fabric rupture failure mode, the fabric will be highly tensioned, the statistical properties of the elastic modulus in

zone III will be used in the safety estimation, and for conservatively purpose, the warp strength is defined as the allowable strength with a primary safety factor of 4 for tear propagation [3]:

X_j	Distribution	Mean value	Standard deviation
E_f	Weibull	638 kN/m	41 kN/m
E_w	Normal	612 kN/m	20 kN/m
G_{wf}	Normal	30 kN/m	3.0 kN/m
v_{wf}	Normal	0.3	0.05
σ_{per} - initial)	Weibull	76.9 kN/m	2.7 kN/m
σ^*_{per}- Reduced for tearing	Weibull	76.9/4=19.3 kN/m	2.7/4 =0.65 kN/m

Table 5.13: Distributions and parameters of the random variables

In fabric structural design, wind and snow are the main types of load. The design values can be calcualted following "Eurocode 1:Actions on structures" [254, 255]. The effective wind speed is defined as,

$$v_m(z) = C_r(z) \cdot C_0(z) \cdot v_b \tag{5.180}$$

where z is the height of the structure v_b is basic wind speed, and here $z = 10m$. $C_r(z)$ can be computed as,

$$C_r(z) = K_r \cdot ln(\frac{z}{z_0}) \tag{5.181}$$

where $K_r = 0.19(\frac{z_0}{z_{0,11}})^0.07$, following the Eurocode, $z_0 = 1.0$, $z_{0,11} = 0.05m$, then

$$K_r = 0.19 \times (\frac{1.0}{0.05})^{0.07} = 0.254 \tag{5.182}$$

and

$$C_r(z) = 0.234 \times ln(\frac{10}{1}) \tag{5.183}$$

$C_0(z) = 1.0$ is recommended by Eurocode. Substituting $C_r(z)$ and $C_0(z) = 1.0$ into Eqn.5.180,

$$v_m(z) = 0.539 \cdot v_b \tag{5.184}$$

The wind pressure is,

$$q_p(z) = [1 + 7 \cdot l_v(z)]\frac{1}{2} \cdot \rho \cdot V_m^2(z) \tag{5.185}$$

where

$$l_v(z) = \frac{K_1}{C_0(z) \cdot ln(\frac{z}{z_0}} = \frac{1}{1 \cdot ln(\frac{10}{1})} = 0.434 \tag{5.186}$$

and ρ is air density and $\rho = 1.25kg/m^3$, so

$$q_p(z) = [1 + 7 \cdot 0.434]\frac{1}{2} \cdot 1.25 \cdot (0.539)^2 \cdot v_b^2 = 0.733 v_b^2 \tag{5.187}$$

The wind force per area has

$$F_w/Area_f = c_s \cdot c_d \cdot c_f \cdot q_p(z) \tag{5.188}$$

For buildings with a height less than 15m, $c_s \cdot c_d = 1$, and $c_f = -0.8$ assuming the this structure as multi-span open canopy type. For the area around Doncaster, the basic wind speed $v_b = 23m/s$, then

$$F_w/Area_f = c_s \cdot c_d \cdot c_f \cdot q_p(z) = -0.8 \times 0.733 \times v_b^2 = 0.586 \times 23^2 N/m^2 = 0.31 kN/m^2 \tag{5.189}$$

The snowing load is defined as,

$$S = \mu_i \cdot C_e \cdot C_t \cdot S_k \tag{5.190}$$

where $\mu_i = 0.8$ for the multi span roof with slope from 0 to 30 degree. $C_e = C_t = 1$ for normal topography. S_k is the local ground snow load value, and $S_k = 0.3 kN/m^2$ for Doncaster area. Therefore

$$S = 0.8 \cdot 0.3 = 0.24 kN/m^2 \tag{5.191}$$

The load combination F_1 and F_2 for wind and snow:

$$\begin{aligned} F_1 &= 1.5 F_w/Area_f = -0.47 kN/m^2 \\ F_2 &= 1.35 \cdot selfweight + 1.5 cdot S = 0.01 \times 1.35 + 1.5 \times (0.24) = 0.37 kN/m^2 \end{aligned} \tag{5.192}$$

The safety indices are computed based on the different load combinations as:

$\beta_1 = 4.768, \beta_2 = 5.349$

Both these values are larger than the critical safety index 3.8, indicating that the canopy can achieve the target reliability without other safety factors on the material strength. In this reliability computation, the loads are assumed as deterministic, but the traditional load combination F_2 is defined conservatively fully considering the variation of loads, meaning that such a deterministic load combination does not compromise the structural reliability. So the value of β_2 is valid and conservative for the fabric failure of the canopy under such a load combination.

To estimate the safety margin for the uncertainties which are not taken into account, the minimum fabric strengths required for the reliability requirement, are calculated as following

table5.14, and the safety margin can be demonstrated by the ratio of the required minimum strengths and original strength of the fabric material.

Load type	Unfactored combination		factored combination	
	Wind	Snow	Wind	Snow
Minimum strength (kN/m)	12.4	11.3	14.8	14.1
1/safety factor	1/6.2	1/6.8	1/5.2	1/5.45
Safety index(β)	3.8	3.8	3.8	3.8

Table 5.14: The minimum strength and safety margin according to the reliability requirement given by Eurocode 0

Table 5.14 suggests that the total safety factors applied to the material strength should not be over 6.2 for the unfactored load combination in which the variance of loads are not taken into account, and no more than 5.2 for the factored load combination. That means that the fabric will fail if the material strength is degraded to the value less than 1/6.2 or 1/5.2 of its manufactured uniaxial strength. It seems there are quite large safety margin allowing for the relative uncertainties, however, European Design Guide for Tensile Surface Structures [4] proposes a safety factor of 4 for the tearing issue, meaning that only one quarter of the uniaixal strength is possibly achieved due to the tear problem in the real case. Therefore the safety margin requirement for other uncertainties is relatively small. If the general safety factor is assumed a product of different sub-factors, then the products of sub-factors excluding tearing are $6.2/4 = 1.55$ and $5.2/4 = 1.3$ respectively for the unfactored and factored load combinations. In other words, if the remaining effects of the rest uncertainties reduce the material strength by 1.55/1.3, the structural reliability is not qualified to the standards given by Eurocode 0.

As listed in Table.5.15, the European Design Guide for Tensile Surface Structures [4] gives a series of safety factors on fabric strengths proposed by different national codes. Different design conclusion may be drawn with different design codes.

Fabric structures are characterized by unique geometries and may be constructed from a number of different fabrics. The large safety margin in the Doncaster canopy case does not suggest these factors are over-estimated because reliabilities of fabric structures are expected to be different when designed using the safety factor approach. However when using the reliability approach, a single measure of structural safety is defined.

Design Guide or regulation	Safety coefficient	Corresponding consideration
IASS recommendation	4.2 - 6.0 for warp 5.0 - 7.0 for fill	Material unevenness & reliability Calculation accuracy Loading uncertainty Environmental degradation Unforeseen aspects
French Design Guide	5.0 - 7.0	Fabric quality Structure scale Pollution level
German Practice & Italian Code	4.9 - 6.4 Permanent 2.9 - 3.2 Wind storm 4.4 - 5.1 Maximum snow	Loading type Surface information Connection conditions
Japan guide	8/6 for sustained loads 4/3 for temporary loads	Function type
ASCE Standard	3.3 - 4.2	Strength reduction depending on loading combinations Life cycle

Table 5.15: A review of safety coefficients on fabric strength(European Design Guide for Tensile Surface Structures [3])

Reliability check under a higher wind load

The safety factors in Table.5.14 is based on a wind speed $V_b = 23$m/s, which are applied to the normal building. Considering the complicated geometry of the canopy and the effect from the surrounding building, the value of wind speed may be underestimated. For a conservative reason, a high wind speed $V_b = 35m/s$ is applied to check the reliability of the structure and material strength.

$$F_w/Area_f = c_s \cdot c_d \cdot c_f \cdot q_p(z) = -0.8 \times 0.733 \times v_b^2 = 0.586 \times 35^2 = 0.74kN/m^2 \quad (5.193)$$

The factored wind load is,

$$F_1 = 1.5F_w/Area_f = -1.1kN/m^2 \quad (5.194)$$

Table 5.16 suggests that when increasing the wind load from -0.45 kN/m to -1.1kN/m, the required minimum fabric strength increases from 14.8 kN/m to 36.6kN/m. The safety margin of the assumed fabric material - Ferrari 1002 is significantly reduced, and the maximum safety factor applicable on the material strength is only 2.1 for the factored wind load combination. That means that the fabric will fail if the material strength is degraded to the value less than 1/2.1 of its manufactured uniaxial strength.

Obviously, such the small safety margin is not enough for tearing and other uncertainties, which require a safety factor of at least 4. The current fabric material assumed is not strong enough for the wind load combination, and may need to be replaced by a higher strength

fabric type.

Load type	Unfactored combination		factored combination	
	Wind	Snow	Wind	Snow
Minimum strength (kN/m)	24.0	11.3	36.6	14.1
1/safety factor	1/3.2	1/6.8	1/2.1	1/5.45
Safety index(β)	3.8	3.8	3.8	3.8

Table 5.16: The minimum strength and safety margin according to the reliability requirement given by Eurocode 0

The minimum strength achieving the minimum structural safety is 36.6 kN/m, indicating that the required initial strength of the fabric may be larger than $36.6 \times 4 = 146.4$kN/m allowing for tearing, if it has similar variance as the pre-assumed fabric property in Table.5.13. If more safety margins beside tearing are required for other uncertainties like environmental impacts and material degradation, a fabric material of larger value of strength ($\geq$ 150kN/m)(e.g. Ferrari 1502) may be recommended.

5.5 Conclusion

In this chapter, the finite element reliability analysis is achieved through the FORM and a finite element analysis, which is used to calculate the gradients of structural response. Two approaches to calculate the gradient of limit state functions: finite difference and analytical method have been compared. The finite difference method is found to be time-consuming when the limit state function has a complicated form and a number of statistical variables are involved in the analysis, and its accuracy is dependent on the perturbation values. The analytical approach using the differentiation chain rule has good performance in computing efficiency and accuracy without perturbations.

The sensitivities of the statistical variables to the reliability are calculated and compared in two numerical examples under different limit states. The material strength and load coefficient are found to be the most important elements for the probability of material failure, and the variation in Young's modulus seems to have obvious influence on the reliability in serviceability failure modes including wrinkling and large deformation. Whereas the shear modulus and Possion's ratio seems have little affect on the reliability under all failure modes with a increased variation. The sensitivities of the statistical variables to the reliability are highly relative with the stress distribution in the membrane, for example, the probability of wrinkling is always sensitive to Young's modulus in the direction where minimum principal stress is observed. When the membrane presstress is much lower than the material tension strength, wrinkling is found to be prone to appear before fabric rupture.

The reliability based on the practical input parameters in the real design case demonstrates that a large safety margin may be found when the degradation of the material strength is not taken into account. Different design approaches given in a variety of design codes are not consistent and possibly lead to different design judgement about the structural safety. The sub-factors representing some specific uncertainties in these design guides can be helpful for a reliability judgement when the statistical property information is not available.

Reliability analysis can replace the factor of safety approach if all statistical information is available, leading to a single measure of structural safety.

Chapter 6

Conclusion & Recommendations

6.1 Conclusion

Besides the detailed conclusions provided at the end of each chapter/section, the general review of this PhD research work is given in this part.

Reliability assessment for fabric structures is desired for solving the issues around the inconsistent use of safety factors in current fabric structural design, and also encouraged by the requirement in architecture and structural engineering. A safe structural design and optimized use of fabric materials can be achieved by an effective and efficient reliability estimation tool, which normally consists of three main parts: an efficient and accurate structural analysis tool, an applicable methodology for the identification of uncertainties relative to fabric structures and an efficient reliability formulation coupled with the specific failure modes of fabric structures.

A extensive literature review of fabric structural design and analysis, fabric properties and uncertainties, and reliability calculations was carried. The necessity of developing a reliability tool for fabric structures based on the design codes currently used was demonstrated by the literatures, and two types of finite element methods (CST and LST) were recommended for computing the structural response of fabric structures. To obtain a deep knowledge of fabric materials, a number of developed fabric material models and probabilistic analysis methods were reviewed and summarized. Different reliability estimation approaches were discussed and compared, FORM coupled with finite element formulations were initially recommended for the reliability calculation of fabric structures.

Four types of finite elements for the analysis of fabric structures were presented - three types of 3-node constant strain triangular element(CST) and a 6-node linear strain triangle element(LST). For the CST element, the significant error introduced by ignoring second order ('large') strains was defined mathematically and demonstrated numerically. An enhanced nonlinear cable analogy formulation, based on the same principles as the existing element was derived, and shown to be limited in successfully overcoming the effects of assuming small strains in the underlying mathematics. A large strain continuum formulation that continues

to adopt the philosophy of the original cable analogy approach, but that is based on a classical finite element philosophy, was shown to be successful within the constraints of a constant strain field.

A classically-based linear strain triangular finite element was presented, characterised by a modified curved 6-node triangular element with element curvatures and coupled with the Newton-Raphson and Dynamic Relaxation algorithms. The inclusion of curvatures in the numerical representations of membrane surfaces were demonstrated to be important terms which affect the relationship between the membrane strains and nodal displacements and in some special cases, the out-of-balance forces.

Fortran 90 programs of the constant strain triangle and linear strain triangle with curvatures were developed. The effectiveness of these formulations was demonstrated by a number of numerical examples evaluated using the programs. Furthermore, when coupled with Dynamic Relaxation, the linear strain triangular element was shown to be extremely computationally efficient, and highly competitive compared with an equivalent CST mesh.

A probabilistic measurement and analysis methodology was proposed based on the uniaxial test. The variations of the uniaxial strength and Young's modulus were estimated, and the variation details were well represented by suitable distributions. The test data of samples made by different cutting approaches - plain cut and yarn-stripping were compared and discussed, and yarn-striping method is recommended for reducing the variations of the samples especially in assessment of Young's modulus. The strength of both the samples made by plain-cut and yarn-striping follow Weibull distributions, and Young's moduli of the two types of samples do not follow an uniformed type of distributions.

An efficient finite element reliability formulation for fabric structures was established. It combines the first order reliability method(FORM) and linear strain triangle element which was recommended in Chapter 3. The sensitivities of the randomness possibly involved in fabric structural design were analysed and compared. In some design cases, the structural reliability may be more sensitive to some uncertainty types over than others.

A Fortran 90 program of a reliability analysis tool was developed. It is able to compute the structural reliability of fabric structures corresponding to different limit states (e.g. wrinkling or ponding). Both the Normal and non-normal distributed uncertainties are valid for the reliability calculation.

A procedure to verify the current safety factors and estimate the relevant reliability was proposed. Combined with the available uncertainty information and safety factors, the structural reliability can be determined with more accuracy. When all statistical information is available, the factor of safety approach can be replaced by the reliability method. Then a single measure of structural safety can be achieved for a design optimization.

6.2 Recommendations for future work

Further work on the reliability analysis should be focused on the improvement of the efficiency of finite element formulation, obtaining more detailed probabilistic information in fabric structural design and construction, and highly accurate reliability analysis using high order reliability methods.

6.2.1 Finite element formulation

Different finite element types should also be tried for the structural analysis of fabric structures. The six node linear strain element introduced in Chapter 3, has constant curvatures in the element. The curvature terms could be involved in high order surface elements(e.g. eight node quadrilateral) with similar definition. The element surface could be described using a high order polynomial function, and the curvature terms which are defined as second order derivatives of the surface function will not be constant, while varying across the element. That may enable the element to represent highly curved fabric surfaces without a high density mesh, and enhance the efficiency of the structural analysis. More detailed and accurate stress contours may be obtained by using the high order elements with curvatures.

Large displacements may result in element distortions of the mesh discretized by high order elements especially in form-finding. In that case, distortion issues for high order element types may need to be investigated and a good procedure avoiding excessive element distortions should be proposed. Form-finding can be initially carried out by low-order (e.g CST or 4 node quadrilateral) elements, which are subsequently replaced by high order elements. Large deformations will normally occur in the form-finding, where the initial balanced geometry configuration is achieved. After the low-order elements are replaced, the nodal displacements to form final balanced geometry for high element meshes will be comparatively small, and reduce the element distortion to a large extent.

6.2.2 Material investigation

The probabilistic measurement and analysis methodology proposed in Chapter 4, based on the uniaxial testing of PVC-polyester Ferriari 1002, should be applied to different PVC-polyester types(e.g. Ferriari 1202) and other fabric types(e.g. PTFE coated glass fibre). The tri-linear mathematical model presented in Section.4.2.2 is proposed based on the uniaxial stress-strain relation of PVC Ferriari 1202, and may not be applicable for other material types. A distinctive model to represent Young's modulus may need to be developed for other fabric types. High order models may also be developed for an accurate representation of the nonlinear stress-strain curves.

Different material test types like biaxial, shear and tear testing should be involved in the future work. A small number of tests as trials are recommended before large quantity exper-

iments, and different description formulations and models to represent the characteristics of the fabric from the trials could be established based on the trials test results. To investigate the inherent randomness in the fabric of interest, a uniform test procedure and condition is recommended to avoid extra uncertainty sources(e.g. temperature or environmental impacts). After a large number of test data are produced, a candidate distribution list can be selected and determined based on the histogram of test data. To achieve a high efficiency for the statistical investigation, a Fortran program could be developed to evaluate the variation and best distributions, and linked to the program of reliability work.

In some cases, the available experimental data and information are too limited out carry a probabilistic investigation, and an efficient and accurate predictive model could be estimated for producing more valid data based on the available experimental results. The produced "fictitious" data will have the same probabilistic characteristics as the original ones. To reduce the test costs, new test methods could be designed to replace those time-consuming and expensive test methods like biaixial and shear tests. For example, the Young's modulus under biaxial tensile forces could be approximately estimated through a specific uniaxial test using a predictive model.

6.2.3 Reliability Analysis

The high order reliability method(e.g. SORM) could be developed for a better representation of nonlinear limit state functions. In this thesis, the uncertainty source involved in the reliability estimation is only limited in Non-cognitive(quantitative) types. In the future work, the uncertainty source may be expanded to cognitive(qualitative) types including worker skills and experience, existing buildings, human impacts etc. Fuzzy theory could be introduced in combining and analyzing these types of uncertainties. Finally a reliability frame work allowing for both quantitative and qualitative uncertainty sources could be undertaken for a comprehesive reliability analysis.

Bibliography

[1] Guide for Specific Membrane Structures, Membrane Structures Association of Japan,1990.

[2] Tensile Membrane Structures, ASCE Standard,2002

[3] European Design Guide for Tensile Surface Structures,2004

[4] "Structural design bassis and safety criteria", European Design Guide for Tensile Surface Structures,2004,p177-190

[5] Recommendations for the Design of Air Supported Structures, IASS, 1986.

[6] "Recommendaion pour la conception des ouvrages permanents de Couverture Textile." Annals du Batiment Travaux, September 1997 no.4, pp5-16.

[7] Tragluftbauten - DIN 4134, 1983.

[8] Instuctions for the Design, Realisation, Verification, Use and Maintenance of Tents, Tensiles Structures and Air-supported Structures, Italian Norm(draft),1995.

[9] Tensile Membrane Structures, ASCE Standard, 2002.

[10] Qi Minyou, "Probability and Mathematical Statisticas"'(Chinese), Higher Education Press, China. 2002.

[11] D.S.Wakefield, "Engineering analysis of tension structures: theory and practice", Engineering Structures, 21, 1999, p680-690.

[12] "Material property and testing", European Design Guide for Tensile Surface Structures,2004,p219-241

[13] "Testing method and standards", European Design Guide for Tensile Surface Structures,2004,p295

[14] Otto F. Tensile structures . MIT Press, Cambridge, MA. 1971

[15] Barnes,M R. Form finding and analysis of tension structures by Dynamic Relaxation, Int J of Space Structures, 14, No 2,89-104, 1999

[16] Schek, H -J. The Force Density method for form finding and computation of general networks, Computer Methods in Applied Mechanics and Engineering 3, 115-134,1974

[17] J.Bonet, J.Mahaney. Form finding of membrane structures by the updated reference method with minimum mesh distortion. International journal of solids and structures, 2001, vol. 38, no32-33, pp. 5469-5480

[18] Larisa Barnets, Graham F. Carey. Extension of a mesh quality metric for elements with a curved boundary edge or surface. Transactions of the ASME, Vol5. p302-308, 2005.

[19] Mitchell, A. R., Philips, G., and Wachspress, E., Forbidden shapes in the finite element method, J. Inst. Math. Appl., 8,pp. 260-269, 1971.

[20] Baart, M. L., and Mulder, E. J. A note on invertible two-dimensional quadratic finite element transformations. Commun. Appl. Numer. Methods. 3. pp. 535-539,1987.

[21] Frey, A. E., C. A, and Porsching, T. A. Some results on the global inversion of bilinear and quadratic isoprarametric finite element transformations, Math. Comput. 32,pp 725-749, 1978.

[22] A. Caner and R. Hsu, P.E., Member, ASCE. Tension fabric shape finding, Journal of Structural Engineering, September, p1065-1071, 1999.

[23] Richard K. Miller and John M. Hedgepheth. An algorithm for finite element analysis of partly wrinkled membrane. AIAA 4293, p1761-1763, 1982.

[24] S.Babu Aminjikarai, Ala Tabiei. A strain-rate dependent 3-D micromechanical model for finite element simulations of plain weave composite structures. Composite Structures, v81,p407-418, 2007.

[25] M.J.King, P.Jearanaisilawong, S.Socrate. A continuum constitutive model for the mechanical behavior of woven fabrics. International Journal of Solids and Structures, v42, p3867-3896, 2005.

[26] Woong Ryeol Yu, Farhang Pourboghrat, Kwansoo Chung. Non-orthogonal constitutive equation for woven fabric reinforced thermoplastic composites. Composites Part A:applied science and manufacturing. v33,p1095-1105,2002.

[27] P.Potluri, V.S. Thammandra. Influence of uniaxial and biaxial tension on meso-scale geometry and strain fields in a woven composite. Composite Structures, v77, p405-418, 2007.

[28] YI Hong-lei, DING Xin, CHEN Shou-hui. Esitmation of the elastic constraints of architectural membrane under bi-axial tensile loading. Engineering Mechanics(Chinese), v23, No.10 2006.

[29] Alfred M. Freudenthal. The safety of structures. ASCE,1945 Oct, p1157-1198.

[30] Han Ping Hong, Niel C.Lind. Approximate reliability analysis using normal polynomial and simulation results. Structural Safety. v18, No.4, p329-339,1996.

[31] Frank Grooteman, Adaptive radial-based importance sampling method for structural reliability. Structural Safety 30(2008) 533-542.

[32] Jinsuo Nie, Bruce R. Ellingwood, A new directional simulation method for system reliability. Part I: application of deterministic sets. Probabilistic Engineering Mechanics 19(2004) 425-436.

[33] B.F. Song, W.Jiang. An equivalent linear method for structural system reliability with nonlinear safety magins. Computers & Structures, v55, No.6, p1095-1100,1995.

[34] Gert de Cooman. On modeling possibilistic uncertainty in two-state reliability theory. Fuzzy sets and systems, v83, p215-238, 1996.

[35] Dan M.Frangopol, Kiyohiro Imai. Geometrically nonlinear finite element reliability analysis of structural system. II: applications. Computers & Structures, v77, p693-709,2000.

[36] B.N.Bridgens, P.D.Gosling. Direct stress-strain representation for coated woven fabrics. Computer & Structures, v82,p1913-1927, 2004.

[37] Barnes MR. Form-finding and analysis of tension structures by dynamic relaxation. Phd thesis.University of London, 1977

[38] Wakefield DS. Pretensioned networks supported by compression arches. Phd thesis, University of London, 1980

[39] Bucholdt HA, McMillan BR. Iterative methods for the solution of pretensioned cable structures. In : IASS Symposium on Tension Structures and Space Frances, Tokyo, 1971

[40] Maurin B, Motro R. Density methods and minimal forms computation, In: IASS Colloquium on Structural Morphology, Nottingham, 1997,p143-154.

[41] S de Jong, R Postle. Energy optimisation methods in fabric mechanics, Mechanics of Flexible Fibre Assemblies, p277-241, Amsterdan, 1980.

[42] J.W.S. Hearle. The formation of textile structures. Mechanics of Flexible Fibre Assemblies, p1-33,1980.

[43] Ning Pan. Analysis of woven fabric strengths: prediction of fabric strength under uniaxial and biaxial extensions. Composites Science and Technology, v56,p311-327,1996.

[44] S.R. Moghe. From fibers to woven fabrics. Mechanics of Flexible Fibre Assemblies, p159-173,1980.

[45] G.A.V. Leaf. Woven fabric tensile mechanics. Mechanics of Flexible Fibre Assemblies, p179-193,1980.

[46] S.L. Phoenix. Statistical models for the tensile strength of yarns and cables. Mechanics of Flexible Fibre Assemblies, p113-141,1980.

[47] E. Barbero, J.Fernandez-Saez, C.Navarro. Statistical analysis of the mechanical properties of composite materials. Composites:Part B 31,p375-381, 2000.

[48] T. Harth, S.Schwan, J.Lehn, F.G. Kollmann. Identification of material parameters for inelastic constitutive models: statistical analysis and design of experiments. International Journal of Plasticity, v20,p1403-1440,2004.

[49] S.K. Sinha, Reliability and Life Testing, Wiley Easten, New Delhi, 1986

[50] F.T.Peirce. The geometry of cloth structure, J. Text. Inst.28(1937) 45-96

[51] Phelan DG, Harber RB. An integrated design method for cable-reinforced membrane structures. In: Proceedings of IASS Symposium, vol:2. 1986. p. 119-26

[52] Ishii K. On development of curved surface of membrane structures. In: IASS International Symposium on Pneumatic Structures,1972

[53] Ataka N,Kozuka Y.A determination method of geodesic lines on the surface of membrane structures [in Japanese]. In: Summary of technical papers of the Annual Meeting AIJ, 1984. p. 21020-21.

[54] Moncrieff E,Topping BHV. Computer methods for the generation of membrane cutting patterns. Comput. Struct. 1990;37(4):441-50

[55] Moncrieff E,Grundig L, Stroel D. The cutting pattern generation of the pilgrims tents for phase of the Mina Valley Project. In: IASS International Symposium, Madrid ,vol. I .1999.p. C127

[56] Grundig L, Ekert L, Moncrieff E. Geodesic and semi-geodesic line algorithms for cutting pattern generation of architectural textile structures. In: Proceedings of Asia-Pacific Conference on Shell and Spatial Structures. 1996.p. 435-43.

[57] Grundig L, Moncrieff E. Form finding, analysis and patterning of regular and irregular-mesh cable-net structures. In: Proceedings of the IASS-LAS98 Conferences, Sydney,(Austrralia), vol.2.1998. p. 856-65

[58] Suzuki T. An analytical method of geodesic line in membrane structures In: Proc. IASS Symp, vol. 2. 1995.p. 915-22

[59] Tabarrok B.Qin Z.Form finding and cutting pattern generation for fabric tension structures. In:Microcomputers in civil engineering, vol,8 . Amsterdam: Elsevier Science Publishers Ltd;1993.p.337-84.

[60] Tsubota H. Determination of actual initial equilibrium state and optimum cutting patterns for membrane structures [in Japanese]. phD dissertation. Kyoto (Japan): Kyoto University,1991

[61] Tsubota H.Yoshida A. Theoretical analysis of actual initial equilibrium state for membrane structures based on cutting pattern. In: IASS Symposium, India, vol,,1988.p.647-56

[62] Tsubota H,Yoshida A. Theoretical analysis of determining optimum cutting patterns for membrane structures. In: Proc. IASS Symposium, Madrid, vol.3. 1989 p. 11-5.

[63] Yagi T.A simultaneous analysis method for the equilibrium state and the cutting pattern configuration of membrane structures (in Japanese). PhD Dissertation . Nagoya (Japan): Nagoya National University, 1998.

[64] Yagi T, Ohmori H.A new approach for cutting pattern analysis of membrane structures. In: Proceedings of the IASS-LAS98 Conference, Sydney (Australia),vol.2. 1998.p. 895-910.

[65] Armen, H.; Levine, H.; Pifko, A.; Levy, A. NONLINEAR ANALYSIS OF STRUCTURES. Source: NASA Contractor Reports, Mar, 1974,128p

[66] Kyriacou, S.K. (Univ of Maryland); Shah, A.D.; Humphrey, J.D.Inverse finite element characterization of nonlinear hyperelastic membranes, Source: Journal of Applied Mechanics, Transactions ASME, v 64, n 2, Jun, 1997, p 257-262

[67] Jeremic, B. (Dept. of Civil/Environmental Engrg., University of California); Runesson, K.; Sture, S. Finite deformation analysis of geomaterials, Source: International Journal for Numerical and Analytical Methods in Geomechanics, v 25, n 8, July, 2001, p 809-840

[68] Bognar, Gabriella (Univ of Miskolc), Finite element method for a nonlinear problem, Source: Computer Assisted Mechanics and Engineering Sciences, v 7, n 4, 2000, p 471-478

[69] Liu P-L, Der Kiureghian A. Finite element reliability methods for geometrically nonlinear structures. Report No.UCB/SCEMM-89/05. Department of Civil Engineering, University of California, Berkeley, CA, 1989.

[70] Der Kiureghian A,Ke J-B. The stochastic finite element method in structural reliability. Probab Engng Mech 1988;3(2) :83-91.

[71] Teigen JG, Frangopol DM, Sture S, Felippa CA. Probabilistic FEM for nonlinear concrete structures.I:theory. J Struct Engng 1991; 117(9): 2674-89.

[72] Teigen JG, Frangopol DM, Sture S, Felippa CA. Probabilistic FEM for nonlinear concrete structures.I:Application. J Struct Engng 1991; 117(9): 2690-707.

[73] Metropolis, N.; Ulam, S., The Monte Carlo Method. Journal of the American Statistical Association 44 (247): 335-341(1949).

[74] Claudio M. Rocco S. A rule induction approach to improve Monte Carlo system reliability assemssment. Reliability Engineering and System Safety 82(2003) 85-92.

[75] Jose E. ramirez-Marquez, David W. Coit, A Monte-Carlo simulation approach for approximating multi-state two-terminal reliability. Reliability Engineering and System Safety 87(2005) 253-264.

[76] A.Naess, B.J.Leira, O.Batsevych. System reliability by enhanced Monte Carlo simulation. Structural Safety 31 (2009) 349-355.

[77] Frangopol DM, Lee Y-H, William K. Nonlinear finite element reliability analysis of concrete. J Engng Mech 1996;122(12): 1174-82.

[78] Estes AC, Frangopol DM. RELSYS: a computer program for structural system reliability. Strut Engng Mech 1996;6(8): 901-19.

[79] Taylor RL. FEAP- a finite element analysis program, version 6.0. Department of Civil Engineering, University of California, Berkeley, CA, 1996.

[80] Otto.F, Rasch B. Finding form. Deutscher Werkbund Bayern,Edition A.Menges,1995.

[81] J.B Pargana. Realistic modelling of tension fabric structures.PhD thesis, Civil and Environmental Engineering Department.Imperial College London.2005

[82] P.D Gosling. Optimal structural membranes-I.Formulation of a curved quadrilateral element for surface definition. Comput.Structs.Vol 61.No 5.pp 871-883,1996.

[83] Liu P-L,Der Kiureghian A. Finite element reliability of geometrically nonlinear uncertain structures. J Engng Mech 1991;117(8),1806-25.

[84] Kiyohiro Imai. Geometrically nonlinear finite element reliability analysis of structural system,I:theory. Comp. Struct. Vol 77,677-691,2000.

[85] B.Tabarrok, Z.Qin. Nonlinear Analysis of tension structures. Comp. Structs, Vol 45,No 5/6,pp 973-984,1992.

[86] Ye xiaobing. Analysis theory of membrane structure by curved surface finite element method. Journal of Building Structures(Chinese),vol 19,n 5,pp 17-21,1998.

[87] F. Otto. Zugbeanspruchte Konstruktionen, vol. 1 & 2, Ullstein Verlag,1962.

[88] R.K. Miller, J.M. Hedgepeth, V.I. Weingarten, P. Das, S. Kahyai, Finite element analysis of partly wrinkled membranes, Comput.Struct.20(1985) 631-639.

[89] D.G. Roddeman, Force transmission in wrinkled membranes,Ph.D thesis, Eindhoven University of Technology,1987.

[90] J.T. Oden, T.Sato, Finite strains and displacements of elastic membranes by the finite element method, Int. J.Solids Struct, 3(1967) 471-448.

[91] R.k.Miller,Model tests as an aid to design and construction of membrane structures, Proceedings of the IASS Symposium on Shells, Membranes and Space Frames, Osaka, Vol. 2, Elsevier Science Publishers B.V.,Amsterdam, 1986, pp.157-160.

[92] George E.P.Box, Statistics for Experimenters - Design, Innovation, and Discovery, second Edition. ISBN 978-7-111-27258-8, John Wiley & Son, Inc. 2005.

[93] P. Contri, B.A. Schrefler, A geometrically nonlinear finite element analysis of wrinkled membrane surfaces by no-compression material model, Commun. Appl. Numer. Methods 4(1988) 5-15.

[94] K.Ishii, Numerical methods tension structures,Proceedings of the Conference on 10 years of Progress in Shell and Spatial Structures, IASS, Madrid 1989,pp. 3.

[95] M, Fujikake, O. Kojima, S.Fukushima, Analysis of fabric tensions, Comput. Struct.32(1989) 537-547.

[96] T. Raible, K. Tegeler, Development of a wrinkling algorithm for orthotropic membrane materials, Comput, Mechods Appl. Mech. Engrg. 2005

[97] Ramana V.Grandhi, Liping Wang. Reliablity-based structural optimization using improved two-point adaptive nonlinear approximations. Finite Element in Analysis and Design 29(1998) 35-48.

[98] Argyris JH, Dunne PC, Malejannakis G, Schelkle E. A simple triangular facet shell element with application to linear and non-linear equilibrium and elastic stability problems. Computer Methods in Applied Mechanics and Engineering 1977; 11: 97-113.

[99] Bathe K J, Ho LW. A simple and effective element for analysis of general shell structures. Computers and Structures 1980;13 :673-681.

[100] Batoz JL, Bathe KJ, Ho LW. A study of three noded triangular plate bending elements. International Journal for Numerical Methods in Engineering 1980; 15: 1771-812.

[101] Horrigmoe G, Bergan PG. Nonlinear analysis of free-form shells by flat finite elements. Computers Methods in Applied Mechanics and Engineering 1978; 16: 11-35.

[102] Hsiao KM. Nonlinear analysis of general shell structures by flat triangular shell element. Computers and Structures 1978; 13: 555-675.

[103] C.A.Felippa, "Refined Finite Element Analysis of Linear and Nonlinear Two-Dimensional Solids" UCB/SESM Report No. 66/22, University of California, Berkeley, October 1966.

[104] Wilson,E.L."Matrix Finite Analysis of Nonlinear Structures",Proc. 2nd ASCE Conf. on Electronic Computation,Pittsburgh,Ps.,Sept.1960.

[105] Turner,M.J.,Martin, H.C and R.C Weikel. "Further Developments and Applications of the Stiffness Method" in AGARDograph No.72,cited in Ref.18.

[106] Fraeijs de Veubeke.B.M.,"Displacements and Equilibrium Models in Finite Element Method",chapter 9 of "Stress Analysis." edited by O.C.Zienkiewicz and G.S.Holister,John Wiley and Sons,1965.

[107] G.Subramanian and A.Krishnan."On an efficient use of CST Elements".Int. J.Num.method in Eng. Vol.14.1063-1072.1978

[108] N.P.Dario."A Comparison of First and Second Order Axially Symmetric Finite Elements." Int. J.num. Method. in Eng. Vol.5.573-583.

[109] Lawrence L.Durocher. "A Numerical Comparison of Axisymmetric Finite Elements". Int. J. Num. Methods in Eng. Vol.12. 1415-1427(1978).

[110] D.Radaj."Accuracy of the Finite Element Analysis for the Elastic Plate with a Circular hole." International Journal for Numerical Methods in Engineering Volume 6, Issue 3, p443C446, 197.

[111] D.G.Harrison and Y.K.Cheung."A Higher-order Triangular Finite Element for the Solution of Field Problems In Orthotropic Media." Int. J. Num. Methods in Eng. Vol.7. 287-295(1973)

[112] P.Silvester."High-order Polynomial Triangular Finite Elements For Potential Problems".Int. J. Engng Sci Vol. 7.pp 849-861(1969)

[113] Zienkiewicz OC. The finite element method, 3rd ed. New Jersey :McGraw-Hill;1977.

[114] Eugenio Onate, Advances in the formulation of the rotation-free basic shell triangle. Comput. Mechods, Appl. Mech. Engrg. 194 (2005) 2406-2443.

[115] Fernando G.Flores, Eugenio Onate, Improvements in the membrane behavior of the three node rotation-free BST shell triangle using an assumed strain approach. Comput. Mechods, Appl. Mech. Engrg. 194 (2005)907-932.

[116] Houtman, R. & Orpana, M. (2000) Materials for Membrane Structures, Bauen mit Textilien Heft, 4/2000.

[117] Buckley, C.P. (1980) Review of the mechanical properties of fibres, pp 35-49, Mechanics of flexible fibre assemblies, edited by John W.S. Hearle, John J. Thwaites, Jafargholi Amirbayat, Alphen aan den Rijn, Netherlands Germantown, Md. : Sijthoff & Noordhoff

[118] Morris, P.J., Merkin, J.H., Rennell, R.W. (1999) Modelling of yarn properties from fibre properties, Journal of the Textile Institute, 90, Part 1 (3), 323-335

[119] Osswald, T., Menges, G. (1996) Materials Science of Polymers for Engineers, Hanser Publishers

[120] Birkett,D.(2002),Keeping the thread,Education in Chemistry,Royal Society of Chemistry website, http://www.rsc.org/lap/educatio/eic/2002/birkett_mar02.htm

[121] Morton, W.E. and Hearle, J.W.S. (1975) Physical properties of textile fibres, 2nd ed, London, Heinemann

[122] Boisse, P.; Borr, M.; Buet, K.; Cherouat, A. (1997) Finite element simulations of textile composite forming including the biaxial fabric behaviour, Composites Part B:Engineering, v 28B, n 4, p 453-464.

[123] Testa, R.B., Stubbs, N., Spillers, W.R. (1978) Bilinear Model for Coated Square Fabrics, Journal of Engineering Mechanics, 104, 1027-1042.

[124] Testa, R.B., and Yu, L.M., "Stress-strain relation for coated fabrics," J. Eng. Mech., 113(11), 1631-1646 (1987).

[125] Robinson, A. T. C., and Marks, R. (1967). Woven cloth construction. Butterworths, London, England

[126] Peirce, F.T. (1937) The Geometry of cloth structure, Journal of the Textile Institute, 28, 81-88

[127] Freeston, W.D.; Platt, M.M.; Schoppee, M.M. (1967) Stress-strain response of fabrics under two-dimensional loading, Textile Research Journal, 37, 656-682

[128] Pargana, J.B., Lloyd Smith, D., Izzuddin, B.A. (2000) Advanced material model for the analysis of tensioned fabric structures, Computational methods for shell and spatial structures, IASS-IACM 2000, Chania-Crete, Greece

[129] Schock, H.J. (1991) On the structural behaviour and material characteristics of PTFE-coated glass-fibre fabric, Journal of Coated Fabrics, 20, 277-288

[130] Pan, N. (1996) Analysis of woven fabric strengths: prediction of fabric strength under uniaxial and biaxial extensions, Composites Science and Technology, 56 (3) 311-327

[131] T.Ishikawa, Antisymmetric elastic properties of composite plates of satin weave cloth, Fiber Sci. Technol, 15(1981) 127-145

[132] T.Ishikawa, T.W. Chou, Elastic behavior of woven hybrid composites, J. Compos. Mater.16 (1982) 2-19.

[133] Shahpurwala, A.A & Schwartz, P., Modeling woven fabric tensile strength using statistical bundle theory. Textil Rearch Jounal, 59(1989) 26.

[134] T.Ishikawa, T.W.Chou, Stiffness and strength behavior of fabric composites, J. Mater. Sci. 17 (1982) 3211-3220.

[135] T.Ishikawa, T.W. Chou, One-dimensional micromechanical analysis of woven fabric composites, AIAA J. 21 (12) (1983) 1714-1721.

[136] N.K. Naik, P.S. Shembekar, Elastic behavior of woven fabric composites: I lamina analysis J.Compos. Mater.26(15) (1992) 2196-2225.

[137] N.K. Naik, V.K. Ganesh, Failure behavior of plain weave fabric laminates under on-axis uniaxial tensile loading: II analytical prediction J.Compos. Mater. 30(16) (1996) 1779-1822.

[138] H.T. Hahn, S.W. Tsai, Nonlinear elastic behavior of unidirectional composite laminae, J. Compos, Mater. 7(1973) 102-118.

[139] R.A. Naik, Failure analysis of woven and braided fabric reinforced composites, J. Compos. Mater. 29(1995) 2334-2363.

[140] D.M.Blackketter, D.E. Walrath, A.C. Hansen, Modelling damage in a plain weave fabric-reinforced composite material, J.Compos. Technol. Res. 15(2)(1993) 136-142.

[141] A. Tabiei, G. Song, Y. Jiang, Strength simulation of woven fabric composite materials with material non-linearity using micromechanics based model, J.Thermoplastic Compos. 16(2003) 5-20.

[142] I. Ivanov, A. Tabiei, Three-dimensional computational micro-mechanical model for woven fabric composites, Compos. Struct. 54(4)(2001) 489-496.

[143] A.Tabiei,I.Ivanov, Fiber reorientation in unidirectional and woven composites for finite element simulation. Compos. Sci. Technol(2001).

[144] Kawabata, S., Niwa, M.., Kawai, H. (1973a) Finite-deformation theory of plain-weave fabrics. Part I. The biaxial-deformation theory, Journal of the Textile Institute, 64 (1) 21-46

[145] Mott, R., Huber, G. & Leewood, A. (1985) Biaxial test method for characterization of fabric materials used in permanent fabric roof structures, The American Society for Testing and Materials, Journal of Testing and Evaluation, 9-16.

[146] Bassett, R., Postle, R. & Pan N. (1999a) Experimental Methods for Measuring Fabric Mechanical Properties: A Review and Analysis, Textile Research Journal, 69 (11) 866-875

[147] Reichardt, C., Woo, H. & Montgomery, D. (1953), A two-dimensional load-extension tester for woven fabrics, Textile Research Journal, 23, 424-428

[148] Klein, W. (1959) Stress-strain response of fabrics under two-dimensional loading, part I, The biaxial tester, Textile Research Journal, 29, 816-821

[149] Clulow, E.E. and Taylor, H.M. (1963) An experimental and theoretical investigation of biaxial stress-strain relations in a plain-weave cloth, Journal of the Textile Institute, 54, T323-T347

[150] Reinhardt, H. (1976) On the biaxial testing and strength of coated fabrics, Experimental Mechanics, 16 (2) 71-74.

[151] MacRory, B. & McNamara, A. (1977) Experimental Investigation of the biaxial load-extension properties of plain weft-knitted fabrics, Textile Research Journal, 47, 233-239.

[152] Bassett, R., Postle, R. & Pan N. (1999b) Grip point spacing along the edges of an isotropic fabric sheet in a biaxial tensile test, Polymer Composites, 20, 305-313.

[153] Bolotin, V.V. Statistical methods in the nonlinear theory of elastic shells.lzv.Acad. Nauk SSSR Otd.Tekh.Nauk.1958,3(English translation,NASA TTF-85,1962,1-16).

[154] Koiter, W.T. On the stability of elastic equilibrium.PhD Dissertation. Delft. Holland,1945(English translation:NASA Tech.Trans.1967,F10.833).

[155] Roorda. J. Concepts in elastic structural stability.In Mechanics Today.Vol.1.ed.S.Nemat-Nasser.Pergamon.Oxford,1972,pp.332-372.

[156] Ikedan K, Murota K.Random inital imperfections of structures. Int. J.Solids Structures 1991: 28(8):1003-21.

[157] Ikeda K,Murota K. Elishakoff I.Reliability of structures subject to normally distributed initial imperfections.Computers and Structures 1996 :59(3):463-9.

[158] Weibull, W. A statistical theory on the strength of materials. The Royal Swedish Institute for Engineering Research Proceeding,No.151.1939.

[159] Heller R.A.(ed.). Probabilistic Aspects of Fatigue.STEP-511.AM.Soc.for Testing and Materials.Philadelphia,1972.

[160] Hill R.Hutchinson J.W.Bifurcation phenomena in the plane tension test. J.Mech.Phys.Soilds 1975:23:239-64.

[161] Peirce, F.T., 1937. The geometry of cloth structure. Journal of Textile Institute 28 (3), T45T96.

[162] Kawabata, S., Niwa, M., Kawai, H., 1973. The finite deformation theory of plain weave fabrics. Part II: The uniaxial deformation theory. Journal of Textile Institute 64 (2), 4761.

[163] Kato, S., Yoshiro, T., Minami, H., 1999. Formulation of constitutive equations for fabric membranes based on the concept of fabric lattice model. Engineering Structures 21, 691708.

[164] Shockey, D.A., Elrich, D.C., Simons, J.W., 1999. Improved Barriers to Turbine Engine Fragments: Interim Report I. DOT/FAA AR-99/8,I.

[165] Ikeda K.Goto S.Imperfection sensitivity for size effect of granular materials.Soils and Foundations 1993:33(2):157-70.

[166] Ikeda K.Maruyama K.Ishida H.Kagawa S.Bifurcation in compressive behavior of concrete.ACI Materials Journal 1997;94(6);484-91.

[167] Trukstra CJ.Theory of structural design decision .Study No.2. Waterloo(Ontario,Canada): Soild Mechanics Division,Univ Waterloo,1970.

[168] Minimum design loads for buildings and other structures[ASCE 7-98]:Reston(VA):ASCE;1998.

[169] Pearce HT,Wen YK.Stochastic combination of load effects.J Str Div,ASCE 1984;110(7);1613-29.

[170] Ellingwood B,Rosowsky D.Combining snow and earthquake loads for limit state design.J Struc Engng, ASCE 1996;112(11):1364-8..

[171] Ushakov IA,editor.Handbook of reliability engineering.New York: Wiley/Interscience;1994.

[172] Schueller GI,editor.Structural dynamics-recent advances.Berlin:Springer; 1991.

[173] Scheuller GI,Ang AHS.Advances in structural reliability.Nucl Engng Des 1992;134:121-40.

[174] Wen YK.Building reliability and code calibration.Earthquake Spectra 1995;11:269-349.

[175] A.G.Davenport, The application of statistical concepts to the wind loading of structures,Proc.Inst.Civil Eng.19(1961) 449-472.

[176] A.G Davenport,Note on the distribution of the largest value of a random function with application to gust loading. Proc.Inst.Civil Eng.24(1964) 187-196.

[177] A.G Davenport,Gust loading factors, J.Struct.Div.ASCE 93(1967)11-34.

[178] G.Solari, A long wind response estimation:closed form solution, J.Struct. Div.ASCE 108(1982) 225-244.

[179] Dempster AP. A generalization of bayesian inference. J Royal Statistical Society 1969;B30: 205-47.

[180] Achintya Haldar and Sankaran Mahadevan. "Reliability Assessment Using Stochastic Finite Element Analysis", John Wiely& Sons, INC, ISBN 0-471-36961-6,2000.

[181] Jin guo liang ,Chen ling and Dong jia mei .Monte Carlo Finite Element Method of Structural Reliability Analysis.Daqing Petroleum Institute, Anda Heilongjiang, China.(1992)

[182] Madsen HO,Krenk S,Lind NC, Methods of structural safety.Englewood Cliffs(N.J):Prentice-Hall,1986.

[183] Bjerager P.Methods for structural reliability computation. In:Casciati F,editor.Reliability problems:general principles and applications in mechanics of solid and structures.New York:Springer Verlag Wien ,1991.p. 89-136.

[184] Hasofer AM,Lind NC.Exact and invariant second-moment code format. J Engng Mech Division,ASCE 1974;100(1):111-21.

[185] Fiessler B,Neumann H-J,Rackwitz R.Quadratic limit states in structural reliability.J Engrg Mech ASCE 1979;105(4):661-76.

[186] Bucher CG,Adaptive sampling:an iterative fast Monte-Carlo procedure.Structural Safety 1988;5(2):119-26.

[187] Mori Y,Ellingwood B.Time-dependent system reliability analysis by adaptive importance sampling.Structural Safety 1993;12(1):59-73.

[188] Tichy M. First-order third-moment reliability method. Structural Safety 1994;16:189-200.

[189] Bucher CG,Bourgund U. A fast and efficient response surface approach for structural reliability problems. Structural Safety 1990;7:57-66.

[190] Zhao YG,Jiang JR. A structural reliability method based on genetic algorithm earthquake Engineering and Engineering Vibration 1995;15(3)44-58(in Chinese).

[191] Yang-Gang Zhao, Tetsuro Ono, A general procedure for first/second order reliability method(FORM/SORM). Structural Safety 21(1999) 95-112.

[192] Yang-Gang Zhao, Tetsuro Ono, Moment methods for structural reliability. Structural Safety 23(2001) 47-75.

[193] Jean-Claude Mitteau, Error evaluations for the computation of failure probability in static structural reliability problems. Probabilistic Engineer Mechanics 14(1999) 119-135.

[194] Armen D.K., Taleen.D, Multiple design points in first and second-order reliability. Structural Safety 20(1998), 37-49.

[195] Kuschel N,Pieracci A,Rackwitz R.Multiple β-points in structural reliability.In:3rd Int.Conf.on Computational Stochastic Mechanics,Santorini,14-17 June 1998.

[196] Bjerager P. On computation methods for structural reliability analysis. In:Frangopol DM.editor.New directions in structural system reliability.Boulder (CO): University of Colorado,1988.p.52-67.

[197] Ditlevsen O,Melchers R E.Gluver H.General multi-dimensional probability integration by directional simulation.Computers And Structures 1990;36(2);355-68.

[198] Melchers R E.Structural system reliability assessment using directional simulation. Structural Safety 1994;16:23-37.

[199] Moarefzadeh MR, Melchers RE. Directional importance sampling for ill-proportioned spaces. Structural Safety. 21:1-22.1999

[200] Dimitri Val, Fiodor Bljuger,David Yankelevsky. Reliability evaluation in nonlinear analysis of reinforced concrete structures. Structural Safty Vol.19, No.2.pp.203-217,1997

[201] Y.S.Petryna,W.B.Kratzig. Computational framework for long-term reliability analysis of RC structures. Comput. Methods Appl. Mech. Engrg. 194(2005) 1619-1639

[202] Michael Havbro Faber,Jochen Kohler,John Dalsgaard Sorensen. Probabilistic modeling of graded timber material properties. Structural safety ,vol 26,295-309,2000.

[203] Kiyohiro Imai,Dan M. Frangopol. System reliability of suspension bridges. Structural Safety, vol 24,219-299, 2002.

[204] A. Haldar, S. Mahadevan. Probability, Reliability, and Statistical Methods in Engineering Design. John Wiley & Son, Inc. New York(2000), p38.

[205] A. Haldar, S. Mahadevan. Probability, Reliability, and Statistical Methods in Engineering Design. John Wiley & Son, Inc. New York(2000), p39.

[206] J.Argyris, et al., A general method for the shape finding of lightweight tension structures, Comput. methods Appl. Mech. Eng. 3(1974) 135-149.

[207] D.S Wakefield, Numerical modelling in tension structures design and construction, Proceedings of IASS Coll. Structural Morphology: Towards the New Millennium, Nottingham, 1997.

[208] P.D.Gosling, Numerical modelling of stable minimal surfaces. PhD thesis, University of Warwick. 1992

[209] Zhang Lei, A large strain cable-analogy membrane finite element, MSc disertation, Civil Engineering Department, Newcastle University. 2003

[210] Otto.F, Rasch B. Finding form. Deutscher Werkbund Bayern,Edition A.Menges,1995.

[211] J.B Pargana. Realistic modelling of tension fabric structures.PhD thesis, Civil and Environmental Engineering Department.Imperial College London.

[212] P.D Gosling. Optimal structural membranes-I.Formulation of a curved quadrilateral element for surface definition. Comput.Structs.Vol 61.No 5.pp 871-883,1996.

[213] L.Grundig. Minimal surface for finding forms of structural membranes. Computer & Structures Vol. 30, No. 3,pp. 679-683, 1988.

[214] Liu P-L,Der Kiureghian A. Finite element reliability of geometrically nonlinear uncertain structures. J Engng Mech 1991;117(8),1806-25.

[215] Kiyohiro Imai. Geometrically nonlinear finite element reliability analysis of structural system,I:theory. Comp. Struct. Vol 77,677-691,2000.

[216] B.Tabarrok, Z.Qin. Nonlinear Analysis of tension structures. Comp. Structs, Vol 45,No 5/6,pp 973-984.

[217] Ye xiaobing. Analysis theory of membrane structure by curved surface finite element method. Jounal of Building Structures(Chinese),vol 19,n 5,pp 17-21,1998.

[218] Wang Xun Chen. Finite Element Method. Publication of Qinghua University, 2003,pp 138.

[219] A.R. Mitchell, G.Phillips. Forbidden shapes in the finite element method. J.Inst.Maths Applics(1971) 8, 260-269.

[220] M.L.BAART. Quadratic Transformations of Triangular Finite Elements in Two Dimensions. IMA Journal of Numerical Analysis (1986) 6, 475-487.

[221] Robert D.Cook, Davids S. Malkus. Concepts and applications of finite element analysis. Third Edition, University of Wisconsin - Madison (1989), pp 185.

[222] F. OttoZugbeanspruchte Konstruktionen, vol. 1 & 2, Ullstein Verlag,1962.

[223] R.K. Miller, J.M. Hedgepeth, V.I. Weingarten, P. Das, S. Kahyai, Finite element analysis of partly wrinkled membranes, Comput.Struct.20(1985) 631-639.

[224] Roddeman D.G. Drukker J. "Finite element analysis of membrane wrinkling", International Journal for numerical methods in engineering., 2001, vol 50,pp. 1017-1038.

[225] J.T. Oden, T.Sato, Finite strains and displacements of elastic membranes by the finite element method, Int. J.Solids Struct, 3(1967) 471-448.

[226] R.k.Miller,Model tests as an aid to design and construction of membrane structures, Proceedings of the IASS Symposium on Shells, Membranes and Space Frames, Osaka, Vol. 2, Elsevier Science Publishers B.V.,Amsterdam, 1986, pp.157-160.

[227] M. Hideki, O. Kiyoshi, A study on modeling and structural behaviour of membrane structures, Proceedings of the IASS Symposium on Shells, Membranes and Space Frames, Osaka, Vol. 2,1986,pp. 161-167.

[228] P. Contri, B.A. Schrefler, A geometrically nonlinear finite element analysis of wrinkled membrane surfaces by no-compression material model, Commun. Appl. Numer. Methods 4(1988) 5-15.

[229] K.Ishii, Numerical methods tension structures,Proceedings of the Conference on 10 years of Progress in Shell and Spatial Structures, IASS, Madrid 1989,pp. 3.

[230] M, Fujikake, O. Kojima, S.Fukushima, Analysis of fabric tensions, Comput. Struct.32(1989) 537-547.

[231] T. Raible, K. Tegeler, Development of a wrinkling algorithm for orthotropic membrane materials, Comput, Mechods Appl. Mech. Engrg. 2005,p2550-2568.

[232] F. Sindel, T. Nouri-Baranger, Including optimisation in the conception of fabric structures. Comput. struct. 79(2001) 2451-2499.

[233] Lo SH. Generating quadrilateral elements on plane and over curved surfaces. Computers and Structures 1989;31;421-6

[234] Lo SH. A new mesh generation scheme for arbitrary planar domains. International Journal for Numerical Methods in Engineering 1985;21:1403-26.

[235] Riccardo Rossi. Convergence of the modified material model for wrinkling simulation of light-weight membrane structures. Textile composites and inflatables structures 2003,pp148-153.

[236] Xinxiang Liu, Large deflection analysis of pneumatic envelopes using a penalty parameter modified material method. Finite element analysis and design 37(2001) pp233-251.

[237] Riccardo Rossi. Simulation of light-weight membrane structures by wrinkling model. Int. J. Numer. Meth. Engrg. 2005; 62:2177-2153

[238] Bridgens,B.N. Architectural fabric properties: determination, representation & prediction, Chapter 3 ,PhD Thesis in Structural Engineering, University of Newcastle Upon Tyne,UK,2006.

[239] Ditlevsen O,Madsen HO. Structural reliability methods. Chichester, New York, NY: Wiley;1996.

[240] Rubinstein RY, Melamed B. Modern simulation and modeling. New York, NY: Wiley; 1998.

[241] Rajashekhar MR, Ellingwood BR. A response surface approach for reliability analysis. Struct Saf 1993;12:205-20.

[242] R.Rackwitz, B. Fiessler, Structural reliability under combined load sequences, Comput. Struct. 9 (1978) 489-494.

[243] Zhang, Y., and Der Kiureghian, A. Dynamic response sensitivity of inelastic structures." Comput. Meth. Appl. Mech. Engrg., v108, p23-36,1993.

[244] Enrique Castillo, and Jose Manuel Gutierrez, and Ali S.Hadi. "Modeling Probabilistic Networks of Discrete and Continuous Variables". Journal of Multivariate Analysis, v64, p48-65, 1998.

[245] X.L.Guan, and R.E.Melchers. "A load space formulation for probabilistic finite element analysis of structure reliability". Probabilistic Engineering Mechanics v14, p73-81. 1999.

[246] Y.-X. Zhang, and Q.Gao, and J,-N. Wang. "An approach for determing an appropriate assumed distribution of fatigue life under limit data." Reliability Engineering and System Safety, v67, p1-7, 2000.

[247] M.A. Stephens. "EDF Statistics for Goodness of Fit and Some Comparison." Journal of the American Statistical Association, v69, p730-737, 1974.

[248] Lieblein, J. "Two early papers on the relation between extreme values and tensile strength". Biometrika, v41, p559-60.

[249] T.Igusa, S.G. Buonopane, B.R. Ellingwood. "Bayesian analysis of uncertainty for structural engineering applications." Structural Safety, v24, pp165-186, 2002.

[250] Dempster AP. A generalization of bayesian inference. J Royal Statistical Society 1968; B30:205-47.

[251] Beatriz S.L.P. de Lima, Nelson F.F. Ebecken. "A comparison of models for uncertainty analysis by the finite element method". Finite Element in Analysis and Design, v34, pp211-232, 2000.

[252] Ruoxue Zhang, Sankaran Mahadevan. "Model uncertainty and Bayesian updating in reliability-bsed inspection", Structural Safety, v22, pp145-160, 2000.

[253] "Eurocode 0: Basis of Structural Design,BS EN: 1990:2002".

[254] "Eurcode 1:Actions on structrues, Part 1-4: General actions Wind actions, BS EN 1991-1-4:2005"

[255] "Eurcode 1:Actions on structrues, Part 1-3: General actions Snow loads, BS EN 1991-1-3:2003"

Appendix A

Test Data, Statistical Distributions

A.1 Uniaxial Test Data and Estimated Young's Modulus

Label	Strength (kN/m)	Young's modulus (kN/m)			Label	Strength (kN/m)	Young's modulus (kN/m)		
		Zone I	Zone II	Zone III			Zone I	Zone II	Zone III
A-1-F-1	80.2	323	261	598	A-2-F-1	84.4	249	265	595
A-1-F-2	81.6	337	263	612	A-2-F-2	86.4	256	268	598
A-1-F-3	83.2	321	272	638	A-2-F-3	83	211	269	582
A-1-F-4	80.2	258	262	595	A-2-F-4	81.6	245	266	597
A-1-F-5	76	198	264	597	A-2-F-5	87	253	264	588
A-1-F-6	83.6	235	253	583	A-2-F-6	77.6	221	267	580
A-1-F-7	81.2	295	258	582	A-2-F-7	80.2	244	259	606
A-1-F-8	84	280	263	591	A-2-F-8	79	252	266	593
A-1-F-9	61.6	310	266	611	A-2-F-9	80	239	267	591
A-1-F-10	68.2	240	271	613	A-2-F-10	78.6	275	268	596
A-1-F-11	83.4	266	267	591	A-2-F-11	83.2	281	265	593
A-1-F-12	85.4	219	264	586	A-2-F-12	81.4	239	267	591
A-1-F-13	84	243	268	523	A-2-F-13	80.6	278	262	599
A-1-F-14	84.2	177	209	430	A-2-F-14	79.4	275	267	605
A-1-F-15	83.6	220	276	617	A-2-F-15	76.4	271	267	600
A-1-F-16	74.4	261	262	595	A-2-F-16	72.6	228	272	602
A-1-F-17	77	294	270	596	A-2-F-17	81.4	252	264	602
A-1-F-18	83.6	190	270	595	A-2-F-18	84.2	225	264	605
A-1-F-19	81	206	269	593	A-2-F-19	80.6	232	257	560
A-1-F-20	80.6	236	266	584	A-2-F-20	83.4	236	266	586
A-1-F-21	86.2	192	254	549	A-2-F-21	80.6	195	254	549
A-1-F-22	73.8	212	269	602	A-2-F-22	80	227	262	585

Table A.1: Test data of plain-cut specimens (Ferrari 1002 Fill.1)

Label	Strength	Young's modulus (kN/m)			Label	Strength	Young's modulus (kN/m)		
	(kN/m)	Zone I	Zone II	Zone III		(kN/m)	Zone I	Zone II	Zone III
A-3-F-1	86	239	284	610	A-4-F-1	83	268	286	686
A-3-F-2	75.4	286	272	614	A-4-F-2	81.6	222	283	670
A-3-F-3	80.6	313	270	594	A-4-F-3	81.4	213	277	665
A-3-F-4	81.4	397	271	585	A-4-F-4	87.6	217	286	678
A-3-F-5	77.4	180	315	606	A-4-F-5	77.8	164	282	670
A-3-F-6	79	477	268	592	A-4-F-6	80.4	244	278	669
A-3-F-7	77.2	348	273	612	A-4-F-7	81	269	276	663
A-3-F-8	80.6	424	277	612	A-4-F-8	79.6	188	276	661
A-3-F-9	78.4	466	276	594	A-4-F-9	84	276	283	676
A-3-F-10	78.4	294	266	586	A-4-F-10	86.4	217	285	672
A-3-F-11	77.2	287	273	608	A-4-F-11	85.6	218	280	666
A-3-F-12	81.4	315	275	603	A-4-F-12	84.6	213	213	658
A-3-F-13	73.4	315	276	604	A-4-F-13	81.6	213	283	665
A-3-F-14	82.2	342	278	625	A-4-F-14	83.2	219	289	669
A-3-F-15	80.6	391	277	639	A-4-F-15	88.2	204	278	678
A-3-F-16	77.8	331	274	600	A-4-F-16	80.6	221	283	669
A-3-F-17	77.6	325	273	605	A-4-F-17	82.2	204	280	665
A-3-F-18	79.2	324	270	614	A-4-F-18	84.6	214	285	684
A-3-F-19	78.2	358	283	636	A-4-F-19	82.6	239	281	683
A-3-F-20	80	303	276	630	A-4-F-20	84	255	287	686
A-3-F-21	81.4	345	278	658	A-4-F-21	83.4	190	288	678
A-3-F-22	81.6	270	285	645	A-4-F-22	74.6	239	278	666
A-5-F-1	81.6	198	277	661	A-6-F-1	75.6	184	278	666
A-5-F-2	86.2	238	281	662	A-6-F-2	82	232	285	678
A-5-F-3	83	242	279	670	A-6-F-3	83	207	284	671
A-5-F-4	83.4	235	236	682	A-6-F-4	82.2	211	285	671
A-5-F-5	82	266	284	686	A-6-F-5	83	174	282	660
A-5-F-6	82	238	286	688	A-6-F-6	85	268	280	661
A-5-F-7	82.2	237	282	667	A-6-F-7	84	201	279	667
A-5-F-8	85	257	280	655	A-6-F-8	85.6	157	279	681
A-5-F-9	81.6	251	284	661	A-6-F-9	79.4	221	273	658
A-5-F-10	78.4	235	291	678	A-6-F-10	84.4	235	281	661
A-5-F-11	85	198	277	661	A-6-F-11	85.6	261	278	659
A-5-F-12	81.2	246	283	656	A-6-F-12	82	218	282	664
A-5-F-13	86.6	252	289	667	A-6-F-13	84.4	190	282	674
A-5-F-14	83.4	292	286	683	A-6-F-14	77.4	270	279	656
A-5-F-15	83.6	276	289	677	A-6-F-15	80.2	294	273	656

Table A.2: Test data of plain-cut specimens (Ferrari 1002 Fill.2)

Label	Strength	Young's modulus (kN/m)			Label	Strength	Young's modulus (kN/m)		
	(kN/m)	Zone I	Zone II	Zone III		(kN/m)	Zone I	Zone II	Zone III
A-5-F-16	84.2	201	283	661	A-6-F-16	82	241	284	668
A-5-F-17	79.2	205	284	669	A-6-F-17	79	230	280	658
A-5-F-18	82.4	194	283	665	A-6-F-18	84.6	232	278	662
A-5-F-19	77.4	289	286	671	A-6-F-19	79.4	212	281	665
A-5-F-20	84.2	263	285	673	A-6-F-20	80.6	192	276	645
A-5-F-21	82.6	189	288	678	A-6-F-21	82.2	238	276	649
A-5-F-22	80.4	222	274	643	A-6-F-22	78.2	226	268	640
A-12-F-1	77.6	272	271	649	A-12-F-7	82.4	179	282	646
A-12-F-2	83.6	245	279	657	A-12-F-8	84	245	287	669
A-12-F-3	81.4	272	281	665	A-12-F-9	74	251	276	643
A-12-F-4	81.2	219	288	663	A-12-F-10	80	191	279	653
A-12-F-5	83.2	237	283	648	A-12-F-11	80.4	247	285	653
A-12-F-6	77	235	269	631					

Table A.3: Test data of plain-cut specimens (Ferrari 1002 Fill.3)

Label	Strength	Young's modulus (kN/m)			Label	Strength	Young's modulus (kN/m)		
	(kN/m)	Zone I	Zone II	Zone III		(kN/m)	Zone I	Zone II	Zone III
A-1-W-1	78.4	379	249	574	A-2-W-1	79	235	254	581
A-1-W-2	76.6	201	248	572	A-2-W-2	74.6	244	263	435
A-1-W-3	75.6	319	254	595	A-2-W-3	74.4	236	246	565
A-1-W-4	76.2	228	245	560	A-2-W-4	77.4	268	248	576
A-1-W-5	76.4	388	250	588	A-2-W-5	79.2	246	243	573
A-1-W-6	77.2	168	247	574	A-2-W-6	83	235	233	584
A-1-W-7	75.2	131	248	583	A-2-W-7	73.6	265	252	590
A-1-W-8	77.2	216	244	568	A-2-W-8	78	228	247	570
A-1-W-9	73.4	245	243	569	A-2-W-9	77.6	245	247	581
A-1-W-10	79	90	244	577	A-2-W-10	74.4	147	248	588
A-1-W-11	71.4	188	252	608	A-2-W-11	75	239	244	576
A-1-W-12	70.2	219	247	523	A-2-W-12	77.6	238	245	236
A-1-W-13	76.2	92	241	548	A-2-W-13	77.6	157	245	576

Table A.4: Test data of plain-cut specimens (Ferrari 1002 Warp.1)

Label	Strength	Young's modulus (kN/m)			Label	Strength	Young's modulus (kN/m)		
	(kN/m)	Zone I	Zone II	Zone III		(kN/m)	Zone I	Zone II	Zone III
A-3-W-1	80.2	433	259	607	A-7-W-1	79.4	333	264	603
A-3-W-2	81	397	257	604	A-7-W-2	82.6	264	260	617
A-3-W-3	79	218	249	574	A-7-W-3	77.2	254	249	589
A-3-W-4	81.6	391	255	600	A-7-W-4	72.3	298	234	600
A-3-W-5	76.2	209	250	581	A-7-W-5	81.3	295	236	601
A-3-W-6	75.4	451	258	610	A-7-W-6	77.3	337	253	606
A-3-W-7	78.2	307	258	616	A-7-W-7	77.4	285	254	585
A-3-W-8	79.2	260	254	581	A-7-W-8	75.2	326	253	597
A-3-W-9	78.2	181	245	570	A-7-W-9	76.2	292	254	597
A-3-W-10	76.4	309	251	603	A-7-W-10	74.4	246	250	590
A-3-W-11	73.2	545	260	626	A-8-W-1	80.6	247	250	590
A-3-W-12	70.6	315	254	598	A-8-W-2	77.2	176	253	596
A-3-W-13	73.2	289	250	605	A-8-W-3	77.6	319	253	602
A-4-W-1	76.4	361	256	591	A-8-W-4	73.6	268	251	608
A-4-W-2	77.4	400	260	621	A-8-W-5	77.4	363	252	605
A-4-W-3	78.4	410	260	626	A-8-W-6	76	149	253	594
A-4-W-4	78.6	320	252	606	A-8-W-7	76	180	251	603
A-4-W-5	77.4	324	255	613	A-8-W-8	78.6	285	252	598
A-4-W-6	79.4	367	256	619	A-8-W-9	78.6	141	253	590
A-4-W-7	76.4	530	256	599	A-8-W-10	80.6	337	244	582
A-4-W-8	76.2	316	258	615	A-9-W-1	3.72	285	252	598
A-4-W-9	77.4	406	252	610	A-9-W-2	3.73	262	254	592
A-4-W-10	77.4	313	257	614	A-9-W-3	4.01	219	252	590
A-4-W-11	75.2	167	256	615	A-9-W-4	3.9	274	249	587
A-4-W-12	74.4	495	256	613	A-9-W-5	3.88	314	252	611
A-4-W-13	76.4	319	260	614	A-9-W-6	3.72	252	253	608
A-5-W-1	81.6	189	263	623	A-9-W-7	3.82	307	257	609
A-5-W-2	78.4	309	257	611	A-9-W-8	3.57	150	250	608
A-5-W-3	76.6	128	254	602	A-9-W-9	3.68	60	257	601
A-5-W-4	85.4	368	261	620	A-9-W-10	3.78	93	249	591
A-5-W-5	76.6	311	260	627	A-10-W-6	76.4	235	265	605
A-5-W-6	81	311	260	622	A-10-W-7	77.2	233	261	616
A-5-W-7	84	203	263	634	A-10-W-8	77.6	197	255	610
A-5-W-8	78	309	260	620	A-10-W-9	73.6	348	254	591
A-5-W-9	76.6	324	253	613	A-10-W-10	73.2	155	247	586
A-5-W-10	80	298	253	616	A-11-W-1	74.2	363	259	605
A-5-W-11	74.6	311	255	609	A-11-W-2	74.6	282	255	600
A-5-W-12	75.6	378	255	616	A-11-W-3	73.6	286	250	587
A-5-W-13	76.4	381	252	598	A-11-W-4	76.4	473	256	618
A-6-W-1	80.4	496	265	648	A-11-W-5	74.6	369	256	611
A-6-W-2	78.2	435	263	633	A-11-W-6	83	394	255	605
A-6-W-3	76	310	253	627	A-11-W-7	77.8	259	251	597
A-6-W-4	77.2	416	255	617	A-11-W-8	76	98	254	623
A-6-W-5	76.2	304	253	602	A-11-W-9	85.2	265	253	622
A-6-W-6	71.6	422	251	604	A-11-W-10	76.4	260	250	582

Table A.5: Test data of plain cut specimens (Ferrari 1002 Warp.2)

Label	Strength (kN/m)	Young's modulus (kN/m)			Label	Strength (kN/m)	Young's modulus (kN/m)		
		Zone I	Zone II	Zone III			Zone I	Zone II	Zone III
B-1-F-1	89.6	770	1118	598	B-2-F-8	101.3	847	1194	595
B-1-F-2	99.6	881	1119	630	B-2-F-9	95.0	914	1249	612
B-1-F-3	98.4	834	1235	610	B-2-F-10	100.7	841	1146	621
B-1-F-4	94.6	823	1162	603	B-2-F-11	101.4	834	1152	606
B-1-F-5	94.4	808	1224	616	B-2-F-12	97.6	843	1154	601
B-1-F-6	92.6	772	1289	603	B-2-F-13	100.9	882	1189	603
B-1-F-7	97	829	1227	601	B-2-F-14	100.9	842	1220	608
B-1-F-8	101.6	849	1278	612	B-3-F-1	82	824	1225	602
B-1-F-9	96.6	868	1254	628	B-3-F-2	99.2	814	1212	596
B-1-F-10	94.2	892	1200	621	B-3-F-3	91.2	817	1177	619
B-1-F-11	100.6	811	1240	610	B-3-F-4	99.4	804	1238	599
B-1-F-12	98	790	1135	597	B-3-F-5	99.6	862	1107	592
B-1-F-13	95	765	1153	603	B-3-F-6	101	845	1227	616
B-1-F-14	85.2	779	1154	539	B-3-F-7	102	821	1208	603
B-2-F-1	98.5	781	1277	599	B-3-F-8	98.6	901	1191	623
B-2-F-2	97.8	817	1282	604	B-3-F-9	102	830	1228	618
B-2-F-3	96.5	834	1106	612	B-3-F-10	101	888	1300	611
B-2-F-4	99.1	809	1187	611	B-3-F-11	98.6	833	1238	616
B-2-F-5	101.3	840	1249	610	B-3-F-12	100.6	879	1160	619
B-2-F-6	98.6	891	1104	597	B-3-F-13	101.2	814	1224	623
B-2-F-7	98.6	848	1194	627	B-3-F-14	100.4	812	1212	613

Table A.6: Test data of yarn-stripping cut specimens (Ferrari 1002 Fill)

Label	Strength (kN/m)	Young's modulus (kN/m)			Label	Strength (kN/m)	Young's modulus (kN/m)		
		Zone I	Zone II	Zone III			Zone I	Zone II	Zone III
B-1-W-1	87	835	1081	601	B-2-W-1	81.5	705	1237	482
B-1-W-2	90.4	830	1031	544	B-2-W-2	81.7	731	1022	498
B-1-W-3	76.6	795	1152	558	B-2-W-3	79.3	727	1031	500
B-1-W-4	85.2	869	1073	561	B-2-W-4	80.7	734	1153	495
B-1-W-5	85.2	749	1091	528	B-2-W-5	79.8	750	1209	502
B-1-W-6	88.2	735	1035	534	B-2-W-6	80.7	719	1065	492
B-1-W-7	85.2	811	1038	540	B-2-W-7	81.5	734	1196	481
B-1-W-8	84.4	734	1127	508	B-2-W-8	78.7	744	1181	506
B-1-W-9	87.6	641	1168	521	B-2-W-9	77.0	735	1079	520
B-1-W-10	87.6	780	1094	525	B-2-W-10	75.9	755	1231	526
B-1-W-11	81.4	810	1130	553	B-2-W-11	79.1	700	970	511

Table A.7: Test data of yarn-striping cut specimens (Ferrari 1002 Warp.1)

Label	Strength (kN/m)	Young's modulus (kN/m)			Label	Strength (kN/m)	Young's modulus (kN/m)		
		Zone I	Zone II	Zone III			Zone I	Zone II	Zone III
B-3-W-1	88	762	1087	523	B-4-W-11	96.1	830	1253	581
B-3-W-2	88.2	840	1197	540	B-4-W-12	102.4	1011	1378	618
B-3-W-3	83.6	879	1177	574	B-4-W-13	97.0	832	1201	569
B-3-W-4	85.4	798	1200	539	B-4-W-14	95.0	903	1276	581
B-3-W-5	86.2	791	1193	528	B-4-W-15	95.2	805	1178	584
B-3-W-6	86	736	1139	524	B-4-W-16	95.7	991	1294	606
B-3-W-7	88.6	764	1189	523	B-4-W-17	94.0	933	1222	581
B-3-W-8	86.6	808	1266	542	B-4-W-18	95.7	849	1185	564
B-3-W-9	84.2	708	1156	505	B-4-W-19	90.5	937	1167	601
B-3-W-10	83.2	811	1106	571	B-4-W-20	95.4	925	1095	574
B-4-W-1	95.4	743	1340	568	B-4-W-21	97.0	875	1057	585
B-4-W-2	95.5	1015	1083	604	B-4-W-22	96.2	964	1350	585
B-4-W-3	97.7	1014	1130	587	B-4-W-23	97.5	981	1233	596
B-4-W-4	94.4	866	1256	556	B-4-W-24	90.7	939	1105	620
B-4-W-5	95.0	788	1001	593	B-4-W-25	99.5	919	1086	588
B-4-W-6	97.0	837	1175	564	B-4-W-26	94.9	923	1322	580
B-4-W-7	96.1	892	1227	577	B-4-W-27	94.7	888	1226	593
B-4-W-8	95.7	948	1144	574	B-4-W-28	95.5	538	1282	580
B-4-W-9	96.4	839	1060	579	B-4-W-29	95.9	888	1208	596
B-4-W-10	97.9	935	1381	591					

Table A.8: Test data of yarn-stripping cut specimens (Ferrari 1002 Warp.2)

Label	Strength (kN/m)	Young's modulus (kN/m)			Label	Strength (kN/m)	Young's modulus (kN/m)		
		Zone I	Zone II	Zone III			Zone I	Zone II	Zone III
C-1-F-1	5.88	949.34	1387.6	722.15	C-2-F-9	5.706	1029.4	1442.9	739.9
C-1-F-2	5.61	955.07	1345.7	705.54	C-2-F-10	5.968	1132.4	1353.3	723.4
C-1-F-3	5.63	938.7	1530.1	737.43	C-2-F-11	5.975	1142.8	1114.5	760.2
C-1-F-4	5.88	920.2	1134.5	686.86	C-2-F-12	5.775	1037.3	1393.8	752.3
C-1-F-5	5.73	918.95	1308.5	733.36	C-2-F-13	5.912	1107.2	1350.4	798.2
C-1-F-6	5.42	980.83	1319.1	735.18	C-2-F-14	5.911	1037.3	1393.8	752.3
C-1-F-7	5.85	951.61	1297.1	734.48	C-3-F-1	5.887	1055.7	1551.1	739.8
C-1-F-8	5.91	991.21	1244.7	772.45	C-3-F-2	5.825	1037.9	1332.1	726.7
C-1-F-9	5.56	918.7	1240.2	737.24	C-3-F-3	6.035	1064.6	1357.9	764.6
C-1-F-10	5.8	954.96	1387.5	755.08	C-3-F-4	5.718	988.7	1529.7	749.9
C-1-F-11	5.68	910.09	1305.4	761.97	C-3-F-5	5.737	1071.7	1311.7	743.8
C-1-F-12	5.68	956.26	1270.6	739.07	C-3-F-6	5.918	1117.1	1527.2	757.8
C-1-F-13	5.6	916.86	1299.7	727.05	C-3-F-7	5.862	1100.5	1565.9	791.9
C-2-F-1	6.062	1143.9	1212.9	760.9	C-3-F-8	5.868	992.8	1343.1	756.4
C-2-F-2	5.456	1143.6	1195.1	743.6	C-3-F-9	6.118	1089.9	1577.9	761.5
C-2-F-3	5.825	1023.9	1400.4	759.9	C-3-F-10	5.806	1050.6	1379.6	755.5
C-2-F-4	5.65	1023.6	1298.6	717.9	C-3-F-11	6.234	1165.7	1405	764.1
C-2-F-5	5.818	1116.9	1389.9	773.3	C-3-F-12	6.043	1088.9	1400.9	746.1
C-2-F-6	5.887	1154.5	1587.9	746.8	C-3-F-13	5.837	1055.7	1532.1	767.9
C-2-F-7	5.956	1018.3	1206.5	760.3	C-3-F-14	6.1	1093.1	1500.2	783.8
C-2-F-8	6.075	1019.9	1333.3	716.7					

Table A.9: Test data of group II specimens (Ferrari 1202 Fill)

Label	Strength (kN/m)	Young's modulus (kN/m)			Label	Strength (kN/m)	Young's modulus (kN/m)		
		Zone I	Zone II	Zone III			Zone I	Zone II	Zone III
C-1-W-1	6.05	1026.7	1312.1	738.2	C-3-W-10	5.702	1170.9	1445.6	748.3
C-1-W-2	5.68	1019.2	1275.5	736.2	C-4-W-1	5.662	1079.4	1392	726.3
C-1-W-3	5.2	1019.1	1208.8	736.6	C-4-W-2	5.343	1135.4	1371.9	723.8
C-1-W-4	5.86	1063.5	1184.4	757.79	C-4-W-3	5.706	1175.6	1452.6	757
C-1-W-5	5.75	1045.7	1310.5	732.14	C-4-W-4	5.65	1254.6	1404.8	748.1
C-1-W-6	5.81	1006.2	1282.2	729.2	C-4-W-5	5.562	1109.1	1242.7	749.7
C-1-W-7	5.47	1052.2	1274.3	738.82	C-4-W-6	5.675	1187.6	1514.7	726.9
C-1-W-8	5.83	993.23	1283.2	713.4	C-4-W-7	5.706	1169.5	1463.9	751.3
C-1-W-9	5.72	1049.4	1330.7	753.37	C-4-W-8	5.662	1188.8	1496.1	729.5
C-1-W-10	5.36	1033.7	1274.9	729.55	C-4-W-9	5.6	1099.8	1514.1	729.9
C-1-W-11	5.46	925.85	1261.2	722.55	C-4-W-10	5.937	1182.8	1276.2	778.2
C-2-W-1	5.687	1155.5	1441.5	754.08	C-4-W-11	5.806	1068.6	1460.6	752.1
C-2-W-2	5.693	1155.5	1371.3	755.1	C-4-W-12	5.137	1176.8	1289.7	716
C-2-W-3	5.643	1088.5	1470.7	750.9	C-4-W-13	5.825	1194.1	1476.1	763.5
C-2-W-4	5.562	1120.2	1359.8	741.52	C-4-W-14	5.731	1149.3	1299.4	736.1
C-2-W-5	5.712	1109.9	1396	735.9	C-4-W-15	5.818	1048	1413.3	761.6
C-2-W-6	5.237	1071.3	1415.2	713	C-4-W-16	5.725	1070	1356.8	753.7
C-2-W-7	5.631	1123.1	1371.5	747.8	C-4-W-17	5.775	1160.9	1327	745.9
C-2-W-8	5.406	1091.6	1237.9	725.3	C-4-W-18	5.725	1163.1	1349.5	746.8
C-2-W-9	5.364	1078.8	1361	730	C-4-W-19	5.631	1117	1412.1	755.2
C-2-W-10	5.83	1129	1390	740	C-4-W-20	5.837	1081.4	1340	717.5
C-2-W-11	5.631	1097.9	1328.5	736.9	C-4-W-21	5.75	1141.2	1464.9	750.6
C-3-W-1	5.281	1215.4	1477.1	735.2	C-4-W-22	5.481	1261.8	1551.1	755.9
C-3-W-2	5.675	999.6	1467.1	757.7	C-4-W-23	5.556	1120.7	1460.5	754.6
C-3-W-3	5.8	1157.6	1443.2	757.7	C-4-W-24	5.706	1145.7	1440.7	741
C-3-W-4	5.731	1070.1	1478.6	739.3	C-4-W-25	5.612	1106.1	1409.1	748.8
C-3-W-5	5.493	1165.4	1526	735.9	C-4-W-26	5.662	1153.1	1448	736.6
C-3-W-6	5.712	1090.9	1458.5	740.7	C-4-W-27	5.831	1099.9	1482.9	737.4
C-3-W-7	5.731	1213.9	1540.6	758.3	C-4-W-28	5.637	1069.1	1417.9	733.9
C-3-W-8	5.762	1124.4	1388.5	745.8	C-4-W-29	5.456	1054.4	1477.1	737.4
C-3-W-9	5.5	1120.9	1455.6	728.3	C-4-W-30	5.456	1055.1	1353.9	721.5

Table A.10: Test data of group II specimens (Ferrari 1202 Warp)

A.2 Types of Distribution

Some Important Distributions List

Normal Distribution

Log-normal Distribution

Rectangular Distribution

Exponential Distribution

Extreme Value Distribution

Weibull Distribution

Cauchy Distribution

Gamma Distribution

Gompertz Distribution

Laplace Distribution

Logistic Distribution

Pareto Distribution

Rayleigh Distribution

Bernoulli Distributions

Beta Distribution

Binomial Distribution

Possion Distribution

Geometric Distribution

Chi-square Distribution.

F-Distribution.

Student's t distribution.

Normal Distribution

The normal distribution (the "bell-shaped curve" which is symmetrical about the mean) is a theoretical function commonly used in inferential statistics as an approximation to sampling distributions (see also Elementary Concepts). In general, the normal distribution provides a good model for a random variable, when:

1.There is a strong tendency for the variable to take a central value;

2.Positive and negative deviations from this central value are equally likely;

3.The frequency of deviations falls off rapidly as the deviations become larger.

As an underlying mechanism that produces the normal distribution, one may think of an infinite number of independent random (binomial) events that bring about the values of a particular variable. For example, there are probably a nearly infinite number of factors that determine a person's height (thousands of genes, nutrition, diseases, etc.). Thus, height can be expected to be normally distributed in the population.

Variate $N : \mu, \sigma$

Range $-\infty < x < \infty$

Location parameter μ,the mean.

Scale parameter $\sigma > 0$, the standard deviation.

The normal distribution function is determined by the following formula:

$$f(x) = 1/[(2 \times \pi)^{1/2} \times \sigma] \times e^{-1/2 \times [(x-\mu)/\sigma]^2}, \quad for \ -\infty < x < \infty$$

The Cumulative distribution function:

$$F(x) = \int_{-\infty}^{x} 1/[(2 \times \pi)^{1/2} \times \sigma] \times e^{-1/2 \times [(x-\mu)/\sigma]^2}, \quad for \ -\infty < x < \infty$$

where

μ is the mean

σ is the standard deviation

e is the base of the natural logarithm, sometimes called Euler's e

π is the constant Pi (3.14...)

Parameter estimation

Parameter	Estimator	Method/Properties
μ	$\overline{x}$	Unbiased,maximum likelihood
σ^2	$ns^2/(n-1)$	Unbiased
σ^2	s^2	Maximum likelihood

Example

Log-normal Distribution

The log-normal distribution is often used in simulations of variables such as personal incomes, age at first marriage, or tolerance to poison in animals. In general, if x is a sample from

a normal distribution, then $y = e^x$ is a sample from a log-normal distribution. Thus, the probability density function of log-normal distribution is defined as:

Variate $\mathbf{L} : m, \sigma$ or $\mathbf{L} : \mu, \sigma$

Range $0 \leq x < \infty$.

Scale parameter $m > 0$, the median

Alternative parameter μ, the mean of log $\mathbf{L}$

m and μ are related by $m = exp(\mu), \mu = log\ m$

Shape parameter $\sigma > 0$, the standard deviation of log $\mathbf{L}$.

$$f(x) = 1/[x\sigma(2\pi)^{1/2}] \times e^{-[\frac{ln(x)-\mu}{\sigma}]^2/2}, \quad for\ 0 < x < \infty,\ \sigma > 0,\ \xi > 0$$

The cumulative density function:

$$F(x) = \Phi(\frac{lnx - \mu}{\sigma}), \quad x \in R$$

μ is the scale parameter

σ is the shape parameter

e is the base of the natural logarithm, sometimes called Euler's e

The following estimators are derived by transformation to the normal distributions.

Parameter	Estimator
Median,m	$\hat{\mu} = (\frac{1}{n}) \sum_{i=1}^{n}\ logx_i$
Variance of log(L),σ^2	$\hat{\sigma}^2 = (\frac{1}{n-1)}) \sum_{i=1}^{n}\ [log(x_i - \hat{\mu})]^2$

Example

Rectangular (Uniform) Continuous Distribution

The rectangular distribution is useful for describing random variables with a constant probability density over the defined range $a < b$

Variate:$\mathbf{R} : a, b$

Location parameter a,the lower parameters,we imply the standard or unit rectangular variate $\mathbf{R} : 0, 1$

Range $a \leq x \leq b$

LOcation parameter a,the lower limit of the range.

Parameter b,the upper limit of the range.

The probability density function:

$$\begin{aligned} f(x) &= 1/(b-a), \quad for\ a < x < b \\ &= 0, \quad elsewhere \end{aligned}$$

the Cumulative density function:

$$F(x) = (x-a)/(b-a)$$

where

$a < b$ are constants

Parameter	Estimator	Method
Lower limit,a	$\overline{x} - \sqrt{3}/s$	Matching moments
Upper limit,b	$\overline{x} + \sqrt{3}/s$	Matching moments

Exponential Distribution

If T is the time between occurrences of rare events that happen on the average with a rate l per unit of time, then T is distributed exponentially with parameter λ (lambda). Thus, the exponential distribution is frequently used to model the time interval between successive random events. Examples of variables distributed in this manner would be the gap length between cars crossing an intersection, life-times of electronic devices, or arrivals of customers at the check-out counter in a grocery store. The exponential distribution function is defined as:

Variate **E**:b

Range $0 \leq x < +\infty$.

Scale parameter b¿0,the mean.

Alternative parameter λ, the hazard function(hazard rate),$\lambda = 1/b$

$$f(x) = 1/b \times e^{-x/b}, \quad for\ 0 \leq x < \infty, b > 0$$

The cumulative density function:

$$F(x) = 1 - exp(-x/b)$$

where

b is scale parameter.

Parameter estimation

Parameter	Estimator	Method
b	$s^2/\overline{x}$	Unbiased,maximum likelihood

Example

Extreme Value(Gumbel) Distribution

The extreme value distribution is often used to model extreme events, such as the size of floods, gust velocities encountered by airplanes, maxima of stock marked indices over a given year, etc.; it is also often used in reliability testing, for example in order to represent the distribution of failure times for electric circuits (see Hahn and Shapiro, 1967).

Variate $\mathbf{V}$: a, b

Range: $-\infty < x < +\infty$

Location parameter a, the mode.

Scale parameter $b > 0$

The extreme value (Type I) distribution has the probability density function:

$$f(x) = 1/b \times e^{[-(x-a)/b]} \times e^{\{e^{[-(x-a)/b]}\}}, \quad for \ -\infty < x < \infty, \ b > 0$$

The cumulative density function:

$$F(x) = 1 - exp\{-exp[-(x-a)/b]\}$$

where

a is the location parameter

b is the scale parameter

e is the base of the natural logarithm, sometimes called Euler's e

Parameter estimation

By the method of maximum likelihood, the estimator $\hat{a}$,$\hat{b}$ are the solutions of the simultaneous equations:

$$\hat{b} = \overline{x} - \frac{\sum_{i=1}^{n} x_i exp(\frac{-x_i}{\hat{b}})}{\sum_{i=1}^{n} exp(\frac{-x_i}{\hat{b}})}$$

$$\hat{a} = -\hat{b} \ log[\frac{1}{n} \sum_{i=1}^{n} exp(\frac{-x_i}{\hat{b}})]$$

Type II Extreme Value Distribution(Frechet distribution)

Extreme values from an initial distribution with a polynomial tail(in the direction of the appropriate extreme) will converge asymptotically, in distribution to the Type II asymptotic form.For the largest value,the Type II asymptotic PDF is:

$$f(x) = \frac{k}{v_n}(\frac{v_n}{x})^{k+1} exp[-(\frac{v_n}{x})^k]$$

The cumulative density function is:

$$F(x) = exp[-(\frac{v_n}{x})^k]$$

where

v_n: The characteristic largest value of the initial variate X.

k: The shape parameter;1/k is a measure of dispersion.

The Type II asymptotic form for the smallest value as follows:

Probability density function:

$$f(x) = -\frac{k}{v_1}(\frac{v_1}{x})^{k+1} exp[-(\frac{v_1}{x})^k]$$

Cumulative density function:

$$F(x) = 1 - exp[-(\frac{v_1}{x})^k], \quad x \leq 0, \quad v_1 > 0$$

where the parameter v_1 is the characteristic smallest value of the initial variate X and k is the shape parameter;again,$1/k$ is a measure of dispersion.

Parameter estimation

If an extreme variate X_n has the Type II asymptotic distribution with parameters v_n and k_n, then the distribution of $ln\ Y - n$ will have the the pertinent extremal parameters for the Type II asymptotic distribution become:

$$v_n = e^{u_n}; \quad k_n = \alpha_n$$

Therefore, the parameters of the Type II asymptotic distribution of the largest value may be obtained by first estimating $\hat{u}_n$ and $\hat{\alpha}_n$ for the logarithms of the sampled data, that is, $ln\ y_1, ln\ y_2, \cdots, ln\ y_n$, using for example the order statiscs method,therefore obtaining $\hat{u}_n$ and $\hat{\alpha}_n$ .The estimates of v_n and k_n may then be obtained as:

$$\hat{v}_n = e^{\hat{u}_n}; \quad \hat{k}_n = \hat{\alpha}_n$$

Similarly,for the parameters of the Type II asymptotic distribution of the smallest value, we obtain $\hat{u}$, and $\hat{\alpha}_1$ as the sample parameters using the sample values $ln\ y_1, ln\ y_2, \cdots, ln\ y_n$; and then the relevant parameters for the Type II asymptotic distribution of the smallest value are:

$$\hat{v}_1 = e^{\hat{u}_1}; \quad \hat{k}_1 = \hat{\alpha}_1$$

Type III Extreme Value Distribution(Weibull Distribution)

As described earlier, the exponential distribution is often used as a model of time-to-failure measurements, when the failure (hazard) rate is constant over time. When the failure probability varies over time, then the Weibull distribution is appropriate. Thus, the Weibull distribution is often used in reliability testing (e.g., of electronic relays, ball bearings, etc.; see Hahn and Shapiro, 1967).

Variate $\mathbf{W}$: η, β

Range $0 \leq x < \infty$

Scale parameter $\eta > 0$ is the characteristic life.

Shape parameter $\beta > 0$
The PDF of Weibull distribution with 2 parameters is defined as

$$f(x) = \beta/\eta \times (x/\eta)^{\beta-1} \times e^{-(x/\eta)^{\beta}}, \quad for\ 0 \leq x < \infty,\ \eta > 0,\ \beta > 0$$

The CDF of Weibull distributin is:

$$F(x) = 1 - exp[-(x/\eta)^{\beta}]$$

The PDF of Weibull distribution with 3 parameters is:

$$[\beta(x-\gamma)^{\beta-1}/\eta^{\beta}]exp\{-[(x-\gamma)/\eta]^{\beta}\}, x \geq \gamma$$

The CDF of Weibull distribution with 3 parameters is:

$$1 - exp\{-[(x-\gamma)/\eta]^{\beta}\}, x \geq \gamma$$

where

η is the scale parameter

β is the shape parameter

γ is the location coefficient
e is the base of the natural logarithm, sometimes called Euler's e
Parameter estimation

If all three parameters must be estimated from the sampled data,the sample skewness(third moment) will also be needed,in addition to the sample mean and sample variance.If the first three sample moments have been evaluated from a set of sample(smallest(values,namely, the sample mean $\overline{x}$,the sample standard deviation σ_x,and the sample skewness $\hat{\theta}_x$,the three extremal parameters of the Weibull distribution may be estimated as follows.

The values of θ_x,as well as $A(\beta)$ and $B(\beta)$,may be evaluated as functions of $1/\beta$ from Relation Among Parameters of Type III Asymptotic Distribution Table.A.11,
Then

$$\eta = B(\hat{\beta})\sigma_x$$

and

$$\gamma = A(\beta)\sigma_x + \overline{x} - \eta$$

1/k	θ_z	A(k)	B(k)	1/k	θ_z	A(k)	B(k)
0.010	-1.08107	0.44815	78.98172	0.510	0.65781	0.24038	2.11963
0.020	-1.02485	0.44611	39.98904	0.520	0.68445	0.23516	2.08181
0.030	-0.97070	0.44392	26.98621	0.530	0.71103	0.22994	2.04511
0.040	-0.91845	0.44160	20.48081	0.540	0.73755	0.22471	2.00949
0.050	-0.86797	0.43915	16.57435	0.550	0.76404	0.21947	1.97489
0.060	-0.81910	0.43657	13.96734	0.560	0.79049	0.21424	1.94124
0.070	-0.77174	0.43386	12.10286	0.570	0.81690	0.20900	1.90851
0.080	-0.72577	0.43104	10.70245	0.580	0.84330	0.20377	1.87666
0.090	-0.68110	0.42810	9.61140	0.590	0.86968	0.19854	1.84563
0.100	-0.63764	0.42504	8.73689	0.600	0.89605	0.19331	1.81538
0.110	-0.59530	0.42188	8.01986	0.610	0.92241	0.18809	1.78590
0.120	-0.54400	0.41861	7.42093	0.620	0.94877	0.18288	1.75713
0.130	-0.51369	0.41524	6.91285	0.630	0.97514	0.17767	1.72905
0.140	-0.47429	0.41178	6.47613	0.640	1.00153	0.17247	1.70162
0.150	-0.43574	0.40822	6.09651	0.650	1.02793	0.16729	1.67482
0.160	-0.39800	0.40456	5.76326	0.660	1.05435	0.16211	1.64863
0.170	-0.36101	0.40082	5.46821	0.670	1.08081	0.15695	1.62302
0.180	-0.32473	0.39700	5.20498	0.680	1.10730	0.15180	1.59796
0.190	-0.28911	0.39309	4.96856	0.690	1.13382	0.14667	1.57343
0.200	-0.25411	0.38910	4.75490	0.700	1.16039	0.14156	1.54942
0.210	-0.21970	0.38504	4.56077	0.710	1.18701	0.13646	1.52590
0.220	-0.18583	0.38090	4.38350	0.720	1.21368	0.13138	1.50286
0.230	-0.15249	0.37242	4.22088	0.730	1.24042	0.12632	1.48027
0.240	-0.11963	0.35470	4.07108	0.740	1.26721	0.12128	1.45813
0.250	-0.08724	0.35013	3.93258	0.750	1.29401	0.11626	1.43641

1/k	θ_z	A(k)	B(k)	1/k	θ_z	A(k)	B(k)
0.260	-0.05527	0.34551	3.80405	0.760	1.32100	0.11126	1.41511
0.270	-0.02372	0.35922	3.68440	0.770	1.34801	0.10629	1.39420
0.280	0.00746	0.35470	3.57267	0.780	1.37510	0.10134	1.37368
0.290	0.03827	0.35013	3.46806	0.790	1.40228	0.09642	1.35354
0.300	0.06874	0.34551	3.36982	0.800	1.42955	0.09152	1.33375
0.310	0.09889	0.34083	3.27736	0.810	1.45690	0.08664	1.31431
0.320	0.12874	0.33611	3.19015	0.820	1.48436	0.08180	1.29522
0.330	0.15831	0.33135	3.10769	0.830	1.51192	0.07698	1.27645
0.340	0.18761	0.32654	3.02957	0.840	1.53959	0.07219	1.25800
0.350	0.21665	0.32169	2.95543	0.850	1.56736	0.06743	1.23987
0.360	0.24546	0.31681	2.88492	0.860	1.59525	0.06271	1.22203
0.370	0.27405	0.31189	2.81777	0.870	1.62326	0.05801	1.20449
0.380	0.30244	0.30693	2.75370	0.880	1.65140	0.05334	1.18723
0.390	0.33063	0.30195	2.69247	0.890	1.67966	0.05801	1.17026
0.400	0.35863	0.29693	2.63389	0.900	1.70804	0.05334	1.15355
0.410	0.38647	0.29189	2.57775	0.910	1.73657	0.04871	1.13711
0.420	0.41415	0.28683	2.52389	0.920	1.76523	0.04411	1.12092
0.430	0.44168	0.28173	2.47214	0.930	1.79404	0.03954	1.10499
0.440	0.46907	0.27662	2.42236	0.940	1.82299	0.03500	1.08930
0.450	0.49634	0.27149	2.37443	0.950	1.85209	0.03050	1.07385
0.460	0.52349	0.26634	2.32823	0.960	1.88135	0.02604	1.05863
0.470	0.55054	0.26117	2.28365	0.970	1.91077	0.02161	1.04364
0.480	0.57748	0.25599	2.24058	0.980	1.94034	0.01721	1.02888
0.490	0.60434	0.25080	2.19895	0.990	1.97009	0.01285	1.01433
0.500	0.63111	0.24560	2.15866	1.000	2.00000	0.00000	1.00000

Table A.11: Relations Among Parameters of Weibull distribution

Example

The followings is set of fatigue life test data from metals,which is assumed to be represented the weibull distribution(ASTM,1963).Parameter of the distribution could be estimated in light of the sample data.

m	1	2	3	4	5	6	7	8
Cycles to Failure,x_1(in 10^5 cycles)	4.0	5.0	6.0	7.3	8.0	9.0	10.6	13.0

The first three sample moments can be shown to be as follows:

$$\begin{aligned} \overline{x} &= 7.86 \times 10^5 \; cycles \\ \sigma_x &= 2.99 \times 10^5 \; cycles \\ \hat{\theta}_x &= \frac{10.05}{26.73} = 0.376 \end{aligned}$$

with $\hat{\theta} = 0.376$,we obtain from Table.A.11

$$\begin{aligned} 1/\hat{\beta} &= 0.407 \\ A(\hat{\beta}) &= 0.293 \\ B(\hat{\beta}) &= 2.595 \end{aligned}$$

Thus

$$\hat{\beta} = 1/0.407 = 2.46$$

so

$$\begin{aligned} \hat{\eta} &= 2.595 \times 2.99^5 = 7.759 \times 10^5 \\ \hat{\gamma} &= 0.293 \times 2.99 \times 10^5 + 7.86 \times 10^5 - 7.759 \times 10^5 = 0.977 \times 10^5 \end{aligned}$$

Cauchy Distribution

The Cauchy distribution is interesting for theoretical reasons. Although its mean can be taken as zero, since it is symmetrical about zero, the expectation, variance, higher moments, and moment generating function do not exist. The Cauchy distribution is defined as:

C : a, b.

Range: $-\infty < x < \infty$

Location parameter a,the median.

Scale parameter $b > 0$
The Probability density function is:

$$f(x) = 1/(b \times \pi \times 1 + [(x-a)/b]^2), \quad for\ 0 < b$$

The cumulative density function is:

$$F(x) = \frac{1}{2} + \frac{1}{\pi} tan^{-1}(\frac{x-a}{b})$$

where

a is the location parameter (median)

b is the scale parameter
π is the constant Pi(3.1415...)

The Cauchy distribution is often cited as an example of a distribution which has no mean, variance or higher moments defined, although its mode and median are well defined and are both equal to a.

Gamma Distribution

The probability density function of the exponential distribution has a mode of zero. In many instances, it is known a priori that the mode of the distribution of a particular random variable of interest is not equal to zero (e.g., when modeling the distribution of the life-times of a product such as an electric light bulb, or the serving time taken at a ticket booth at a baseball game). In those cases, the gamma distribution is more appropriate for describing the underlying distribution. The gamma distribution is defined as:

Variate $\gamma : b, c$

Range $0 \leq x < \infty$

Scale parameter $b > 0$. Alternative parameter $\lambda, \lambda = 1/b$

Shape parameter $c > 0$

The probability density function is:

$$f(x) = \{1/[b\Gamma(c)]\} \times [x/b]^{c-1} \times e^{-x/b}, \quad for\ 0 \leq x,\ c > 0$$

The cumulative density function is:

$$F(x) = \frac{\Gamma_x(c)}{\Gamma(c)}, \quad \Gamma_x(c) = \int_0^x u^{c-1} e^{-u} du$$

where

Γ is the Gamma function

c is the Shape parameter

b is the Scale parameter

e is the base of the natural logarithm, sometimes called Euler's e

Parameter estimation

Parameter	Estimator	Method
Scale parameter,b	$s^2/\overline{x}$	Matching moments
Shape parameter,c	$(\overline{x}/s)^2$	Matching moments

Maximum-likelihood estimators $\hat{b}$ and $\hat{c}$ are the solutions of the simultaneous equations for $\psi(c)$

$$\hat{b} = \overline{x}/\hat{c}$$

$$log\ \hat{c} - \psi(\hat{c}) = log[\overline{x}/(\Pi_{i=1}^{n}\ x_i)^{1/n}]$$

Gompertz Distribution

The Gompertz distribution is a theoretical distribution of survival times. Gompertz (1825) proposed a probability model for human mortality, based on the assumption that the "average exhaustion of a man's power to avoid death to be such that at the end of equal infinetely small intervals of time he lost equal portions of his remaining power to oppose destruction which he had at the commencement of these intervals" (Johnson, Kotz, Blakrishnan, 1995, p. 25).

The probability density function is:

$$f(x) = \lambda e^{cx} Exp\{-\frac{\lambda}{c}(e^{cx} - 1)\}, \quad forx > 0$$

The cumulative density function is:

$$F(x) = 1 - Exp\{-\frac{\lambda}{c}(e^{cx} - 1)\}, \quad forx > 0$$

where λ and c are parameters

Parameter estimation

By using ML method,the parameters could be obtained by solving the following equations:

$$\hat{c} = -n\sum_{i=1}^{n}(c^{\hat{c}x_i} - 1)(\sum_{i=1}^{n} x_i \sum_{i=1}^{n}(e^{\hat{c}x_i} - 1) - n\sum_{i=1}^{n} x_i e^{\hat{c}x_i})^{-1}$$

$$\hat{\lambda} = -\hat{c}\sum_{i=1}^{n} x_i(\frac{1}{\hat{c}}\sum_{i=1}^{n}(e^{\hat{c}x_i} - 1) - \sum_{i=1}^{n} x_i e^{\hat{c}x_i})^{-1}$$

Laplace Distribution

For interesting mathematical applications of the Laplace distribution see Johnson and Kotz (1995). The Laplace (or Double Exponential) distribution is defined as:

Variate $\mathbf{L}$: a, b

Range $-\infty < x < \infty$

Location parameter $-\infty < a < \infty$,the mean

Scale parameter $b > 0$

The probability density function is:

$$f(x) = 1/(2b) \times e^{-(|x-a|/b)}, \quad for\ -\infty < x < \infty$$

The cumulative density function is:

$$\begin{aligned} F(x) &= \frac{1}{2}exp[-(\frac{a-x}{b})], \quad x < a \\ &= 1 - \frac{1}{2}exp[-(\frac{x-a}{b})], \quad x \geq a \end{aligned}$$

where

a is the location parameter (mean)

b is the scale parameter

e is the base of the natural logarithm, sometimes called Euler's e

Parameter estimation

Parameter	Estimator	Method
a	median,mean	Maximum likelihood
b	$\frac{1}{}\sum_{i=1}^{n} \|x_i - a\|$	Maximum likelihood

Logistic Distribution

The logistic distribution is used to model binary responses (e.g., Gender) and is commonly used in logistic regression. The logistic distribution is defined as:

Range $-\infty < x < \infty$

Location parameter a,the mean

Scale parameter $b > 0$

Alternative parameter $k = \pi b/3^{1/2}$, the standard deviation.

The probability density function is:

$$f(x) = (1/b) \times e^{-(x-a)/b} \times \{1 + e^{-(x-a)/b}\}^{-2}, \quad for \ -\infty < x < \infty, \ 0 < b$$

The cumulative density function is:

$$F(x) = 1 - \{1 + exp[(x-a)/b]\}^{-1}$$

where

a is the location parameter (mean)

b is the scale parameter

e is the base of the natural logarithm, sometimes called Euler's e

Parameter estimation

The maximum-likelihood estimation $\hat{a}$ and $\hat{b}$ of the location and scale parameters are the solution of the simultanous equations:

$$\sum_{i=1}^{n}[1+exp(\frac{x_i-\hat{a}}{\hat{b}})]^{-1}=\frac{n}{2}$$

$$\sum_{i=1}^{n}(\frac{x_i-\hat{a}}{\hat{b}})\frac{1-exp[(x_i-\hat{a})/\hat{b}]}{1+exp[(x_i-\hat{a})/\hat{b}]}=n$$

Pareto Distribution

The Pareto distribution is commonly used in monitoring production processes (see Quality Control and Process Analysis). For example, a machine which produces copper wire will occasionally generate a flaw at some point along the wire. The Pareto distribution can be used to model the length of wire between successive flaws. The standard Pareto distribution is defined as:

Range $a \leq x < \infty$

Location parameter $a > 0$

Shape parameter $c > 0$

The probability density function is:

$$f(x)=ca^c/x^{c+1}, \quad for a \leq x < \infty$$

The cumulative density function is:

$$F(x)=1-(a/x)^c, \quad for a \leq x < \infty$$

where

a is the location parameter, $a > 0$
c is the shape parameter, $c > 0$

Parameter estimation

Parameter	Estimator	Method
1/c	$(\frac{1}{n})\sum_{i=1}^{n} log(\frac{x_i}{\hat{a}})$	Maximum likelihood
a	$minx_i$	Maximum likelihood

Rayleigh Distribution

If two independent variables y1 and y2 are independent from each other and normally distributed with equal variance, then the variable $x=\sqrt{y_1^2+y_2^2}$ will follow the Rayleigh distribution. Thus, an example (and appropriate metaphor) for such a variable would be the distance of darts from the target in a dart-throwing game, where the errors in the two dimensions of the

target plane are independent and normally distributed. The Rayleigh distribution is defined as:

Range $0 < x < \infty$

Scale parameter $b > 0$

The probability density function is:

$$f(x) = x/b^2 \times e^{-\frac{x^2}{2b^2}}, \quad for\ 0 \leq x < \infty,\ b > 0$$

The cumulative density function:

$$F(x) = 1 - exp[-x^2/(2b^2)]$$

where

b is the scale parameter
e is the base of the natural logarithm, sometimes called Euler's e

Parameter estimation

Parameter	Estimator	Method
b	$s^2/(\frac{1}{2n}\sum_{i=1}^{n} x_i^2)$	maximum likelihood

Bernoulli Distribution

This distribution best describes all situations where a "trial" is made resulting in either "success" or "failure," such as when tossing a coin, or when modeling the success or failure of a surgical procedure. The Bernoulli distribution is defined as:

Variate $\mathbf{B} : 1, p$

(The general binomial variate is $\mathbf{B} : n, p$,involving n trials.)

Range $x \in \{0, 1\}$.

Parameter p,the Bernoulli probability parameter, $0 < p < 1$.

The probability density function:

$$f(x) = p^x \times (1-p)^{1-x}, \quad for\ x \in \{0, 1\}$$

The cumulative density function:

$$F(0) = 1 - p; F(1) = 1$$

where p is the probability that a particular event (e.g., success) will occur.

Beta Distribution

The beta distribution arises from a transformation of the F distribution and is typically used to model the distribution of order statistics. Because the beta distribution is bounded on both sides, it is often used for representing processes with natural lower and upper limits.The beta distribution is defined as:

Variate β, ν, ω

Range $0 \leq x \leq 1$

Shape parameters $\nu > 0, \omega > 0$

The probability density function is:

$$f(x) = \Gamma(\nu + \omega)/[\Gamma(\nu)\Gamma(\omega)] \times x^{\nu-1} \times (1-x)^{\omega-1}, \quad for\ 0 < x < 1,\ \nu > 0, \omega > 0$$

The cumulative density function is:

$$F(x) = \frac{\int_0^x u^{\nu-1}(1-u)^{\omega-1}du}{B(\nu,\omega)}$$

where Γ is the Gamma function

ν, ω are the shape parameters(Shape1 and Shape2, respectively)

Definitions

Beta functions:

$$B(\nu,\omega) = \int_0^1 u^{\nu-1}(1-u)^{\omega-1}du$$

Gamma function:

$$\Gamma(c) = \int_0^\infty exp(-u)u^{c-1}du$$

Interrelationships:

$$\begin{aligned} B(\nu,\omega) &= \frac{\Gamma(\nu)\Gamma(\omega)}{\Gamma(\nu+\omega)} \\ \Gamma(c) &= (c-1)\Gamma(c-1) \\ B(\nu+1,\omega) &= \frac{\nu}{\nu+\omega}B(\nu,\omega) \end{aligned}$$

Parameter estimation

Parameter	Estimator	Method
ν	$\overline{x}\{[\overline{x}(1-\overline{x})/s^2]-1\}$	Matching moments
ω	$(1-\overline{x})\{[\overline{x}(1-\overline{x})/s^2]-1\}$	Matching moments

The maximum-likelihood estimators $\hat{\nu}$ and $\hat{\omega}$ are the solutions of the simultaneous equations:

$$\psi(\hat{\nu}) - \psi(\hat{\nu}+\hat{\omega}) = n^{-1}\sum_{i=1}^{n} log\ x_i$$

$$\psi(\hat{\omega}) - \psi(\hat{\nu}+\hat{\omega}) = n^{-1}\sum_{i-1}^{n} log(1-x_i)$$

in which,

$$\psi(c) = \frac{d}{dc}[log\Gamma(c)] = \frac{d\Gamma(c)/dc}{\Gamma(c)}$$

$$\Gamma(c) = \int_0^{\infty} exp(-u)u^{c-1}du$$

Binomial Distribution

The binomial distribution is useful for describing distributions of binomial events, such as the number of males and females in a random sample of companies, or the number of defective components in samples of 20 units taken from a production process. The binomial distribution is defined as:

Variate $\mathbf{B}$: n, p

Quantile x,number of success.

Range $0 \leq x \leq n,\ x$ an integer.

The probability function:

$$F(x) = [n!/(x! \times (n-x)!)] \times p^x \times q^{n-x}, \quad for\ x = 0, 1, 2, ..., n$$

The distribution function:

$$f(x) = \sum_{i=0}^{x}[n!/(i! \times (n-i)!]p^i q^{n-i}$$

where

p is the probability that the respective event will occur

q is equal to 1-p

n is the maximum number of independent trials.

Parameter estimation

Parameter	Estimator	Method
Bernoulli probability,p	x/n	Minimum variance unbiased

Poisson Distribution

The Poisson distribution is also sometimes referred to as the distribution of rare events. Examples of Poisson distributed variables are number of accidents per person, number of sweepstakes won per person, or the number of catastrophic defects found in a production process. It is defined as:

Variate **P** : λ

Range $0 \leq x < \infty, x$ integer.

Parameter the mean,$\lambda > 0$.

The distribution function:

$$f(x) = \sum_{i=1}^{x} \lambda^i exp(-\lambda)/i!$$

The Probability function:

$$F(x) = (\lambda^x \times e^{-\lambda})/x!, \quad for\ x = 0, 1, 2, ...,\ 0 < \lambda$$

where

λ (lambda) is the expected value of x (the mean)

Parameter estimation

Parameter	Estimator	Method
λ	$s^2/\overline{x}$	Minimum variance unbiased,maximum likelihood

Geometic Distribution

If independent Bernoulli trials are made until a "success" occurs, then the total number of trials required is a geometric random variable. The geometric distribution is defined as:

Variate **G** : p.

Quantile n,number of trials.

Range $n \geq 0, n$ an integer.

The distribution function:

$$F(x) = 1 - q^{x+1}, \quad for\ x = 1, 2, ...$$

The probability function:

$$f(x) = p \times (1 - p)^x, \quad for\ x = 1, 2, ...$$

where

p is the probability that a particular event (e.g., success) will occur.

Chi-square Distribution

The sum of ν independent squared random variables, each distributed following the standard normal distribution, is distributed as Chi-square with ν degrees of freedom. This distribution is most frequently used in the modeling of random variables (e.g., representing frequencies) in statistical applications. The Chi-square distribution is defined by:

Variate $\chi^2 : \nu$

Range $0 \leq x < \infty$

Shape parameter ν,degree of freedom.

The probability density function:

$$f(x) = \{1/[2^{\nu/2} \times \Gamma(\nu/2)]\} \times [x^{(\nu/2)-1} \times e^{-x/2}], \quad for\ \nu = 1, 2, ..., 0 < x$$

The cumulative density function:

$$F(x) = \int_0^{\infty} \{1/[2^{\nu/2} \times \Gamma(\nu/2)]\} \times [x^{(\nu/2)-1} \times e^{-x/2}], \quad for\ \nu = 1, 2, ..., 0 < x$$

where

ν is the degrees of freedom

e is the base of the natural logarithm, sometimes called Euler's e

Γ is the Gamma function

F Distribution

Snedecor's F distribution is most commonly used in tests of variance (e.g., ANOVA). The ratio of two chi-squares divided by their respective degrees of freedom is said to follow an F distribution. The F distribution (for x ¿ 0) has the probability density function (for ν = 1, 2, ...; w = 1, 2, ...):

Variate $\mathbf{F}, \nu, \omega, \delta$

Range $0 < x < \infty$

Shape parameter ν, ω positive integers are the degrees of the freedom,and $\delta > 0$ the noncentrality parameter.

The probability density function:

$$f(x) = [\Gamma\{(\nu + \omega)/2\}]/[\Gamma(\nu/2)\Gamma(\omega/2)] \times (\nu/\omega)^{(\nu/2)} \times x^{[(\nu/2)-1]} \times \{1 + [(\nu/\omega) \times x]\}^{-(\nu+\omega)/2},$$

The cumulative density function:

$$F(x) = \int_0^\infty [\Gamma\{(\nu+\omega)/2\}]/[\Gamma(\nu/2)\Gamma(\omega/2)] \times (\nu/\omega)^{(\nu/2)} \times x^{[(\nu/2)-1]} \times \{1+[(\nu/\omega)\times x]\}^{-(\nu+\omega)/2},$$

$$for\ 0 \leq x < \infty \quad \nu = 1, 2, ..., \quad \omega = 1, 2, ...$$

where

ν, ω are the shape parameters, degrees of freedom

Γ is the Gamma function

Student's t Distribution

The student's t distribution is symmetric about zero, and its general shape is similar to that of the standard normal distribution. It is most commonly used in testing hypothesis about the mean of a particular population. The student's t distribution is defined as (for n = 1, 2, . . .):

Variate t, ν

Range $-\infty x < \infty$

Shape parameter ν,degree of freedom, ν a positive integer

The probability density function:

$$f(x) = \Gamma[(\nu+1)/2]/\Gamma(\nu/2) \times (\nu \times \pi)^{-1/2} \times [1 + (x^2/\nu)^{-(\nu+1)/2}]$$

The cumulative density function:

$$\begin{aligned} F(x) &= \frac{1}{2} + \frac{1}{\pi} tan^{-1}(\frac{x}{\nu^{1/2}}) + \frac{1}{\pi}\frac{x\nu^{1/2}}{\nu + x^2} \times \sum_{j=0}^{(\nu-3)/2} \frac{a_j}{(1+x^2/\nu)^j}, \nu \quad odd \\ &= \frac{1}{2} + \frac{x}{2(\nu+x^2)^{1/2}} \times \sum_{j=0}^{(\nu-2)/2} \frac{b_j}{(1+\frac{x^2}{\nu})^j}, \nu \quad even \end{aligned}$$

where

ν is the shape parameter, degrees of freedom

Γ is the Gamma function

π is the constant Pi (3.14 . . .)

Appendix B

Derivation of Finite Element Formulations

B.1 Appendix B1: Derivation of the [B] matrix in the LST element formulation

An arbitarily located point P divides a triangle $1-2-3$ into three subareas A_1, A_2,and,A_3

Area coordinates are defined as ratios of areas:

$$\xi_1 = \frac{A_1}{A} \quad \xi_2 = \frac{A_2}{A} \quad \xi_3 = \frac{A_3}{A} \tag{B.1}$$

where A is the area of triangle $1-2-3$.Since $A = A_1 + A_2 + A_3$, the ξ_i are not independent. They satisfy the constraint equation

$$\xi_1 + \xi_2 + \xi_3 = 1 \tag{B.2}$$

The constraint equation and the linear relation between Cartesian and area coordinate are expressed by equations below:

$$\begin{Bmatrix} 1 \\ X \\ Y \end{Bmatrix} = [A] \cdot \begin{Bmatrix} \xi_1 \\ \xi_2 \\ \xi_3 \end{Bmatrix} and \begin{Bmatrix} \xi_1 \\ \xi_2 \\ \xi_3 \end{Bmatrix} = [A]^{-1} \begin{Bmatrix} 1 \\ x \\ y \end{Bmatrix} \tag{B.3}$$

where,with $x_{ij} = x_i - x_j$ and $y_{ij} = y_i - y_j$

$$[A] = \begin{bmatrix} 1 & 1 & 1 \\ x_1 & x_2 & x_3 \\ y_1 & y_2 & y_3 \end{bmatrix}$$

and

$$[A]^{-1} = \frac{1}{2A}\begin{bmatrix} x_2y_3 - x_3y_2 & y_{23} & x_{32} \\ x_3y_1 - x_1y_3 & y_{31} & x_{13} \\ x_1y_2 - x_2y_1 & y_{12} & y_{21} \end{bmatrix}$$

$2A = det[A] = x_{21}y_{31} - x_{31}y_{21}$

Displacement can be expressed as:

$$U(\xi_1,\xi_2,\xi_3) = U_1\xi_1(2\xi_1-1)+U_2\xi_2(2\xi_2-1)+U_3\xi_3(2\xi_3-1)+U_4\cdot 4\xi_1\xi_2+U_5\cdot 4\xi_2\xi_3+U_6\cdot 4\xi_3\xi_1 \quad \text{(B.4)}$$

$$V(\xi_1,\xi_2,\xi_3) = V_1\xi_1(2\xi_1-1)+V_2\xi_2(2\xi_2-1)+V_3\xi_3(2\xi_3-1)+V_4\cdot 4\xi_1\xi_2+V_5\cdot 4\xi_2\xi_3+V_6\cdot 4\xi_3\xi_1 \quad \text{(B.5)}$$

$$W(\xi_1,\xi_2,\xi_3) = W_1\xi_1(2\xi_1-1)+W_2\xi_2(2\xi_2-1)+W_3\xi_3(2\xi_3-1)+W_4\cdot 4\xi_1\xi_2+W_5\cdot 4\xi_2\xi_3+W_6\cdot 4\xi_3\xi_1 \quad \text{(B.6)}$$

Formulation of element matrices requires that a function ϕ , expressed in terms of area coordinates, be differentiated with respect to Cartesian coordinates. By the chain rule, with $\phi = \phi(\xi_1, \xi_2\xi_3)$

$$\frac{\partial\phi}{\partial X} = \frac{\partial\phi}{\partial\xi_1}\frac{\partial\xi_1}{\partial X} + \frac{\partial\phi}{\partial\xi_2}\frac{\partial\xi_2}{\partial X} + \frac{\partial\phi}{\partial\xi_3}\frac{\partial\xi_3}{\partial X} \quad \text{(B.7)}$$

$$\frac{\partial\phi}{\partial Y} = \frac{\partial\phi}{\partial\xi_1}\frac{\partial\xi_1}{\partial Y} + \frac{\partial\phi}{\partial\xi_2}\frac{\partial\xi_2}{\partial Y} + \frac{\partial\phi}{\partial\xi_3}\frac{\partial\xi_3}{\partial Y} \quad \text{(B.8)}$$

From the former equations:

$$\frac{\partial\xi_1}{\partial X} = \frac{Y_{23}}{2A} \quad \frac{\partial\xi_2}{\partial X} = \frac{Y_{31}}{2A} \quad \frac{\partial\xi_3}{\partial X} = \frac{Y_{12}}{2A} \quad \text{(B.9)}$$

$$\frac{\partial\xi_1}{\partial Y} = \frac{X_{32}}{2A} \quad \frac{\partial\xi_2}{\partial Y} = \frac{X_{13}}{2A} \quad \frac{\partial\xi_3}{\partial Y} = \frac{X_{21}}{2A} \quad \text{(B.10)}$$

where $2A = det[A] = X_{21}Y_{31} - X_{31}Y_{21}, Y_{23} = Y_2 - Y_3$, and so on

We already know:

$$\frac{\partial}{\partial\xi_1}\phi = \phi_1 \quad \frac{\partial}{\partial\xi_2}\phi = \phi_2 \quad \frac{\partial}{\partial\xi_3}\phi = \phi_3 \quad \text{(B.11)}$$

then we have

$$\frac{\partial}{\partial X}U(X,Y) = U_1\frac{Y_{23}}{2A}(4\xi_1 - 1) + U_2\frac{Y_{31}}{2A}(4\xi_2 - 1) + U_3\frac{Y_{12}}{2A}(4\xi_3 - 1) + U_4\frac{1}{2A}4(\xi_2 Y_{23} + \xi_1 Y_{31})$$

$$+U_5\frac{1}{2A}4(\xi_3 Y_{31} + \xi_2 Y_{12}) + U_6\frac{1}{2A}4(\xi_1 Y_{12} + \xi_3 Y_{23})$$

$$\frac{\partial}{\partial X}V(X,Y) = V_1\frac{Y_{23}}{2A}(4\xi_1 - 1) + V_2\frac{Y_{31}}{2A}(4\xi_2 - 1) + V_3\frac{Y_{12}}{2A}(4\xi_3 - 1) + V_4\frac{1}{2A}4(\xi_2 Y_{23} + \xi_1 Y_{31})$$

$$+V_5\frac{1}{2A}4(\xi_3 Y_{31} + \xi_2 Y_{12}) + V_6\frac{1}{2A}4(\xi_1 Y_{12} + \xi_3 Y_{23})$$

$$\frac{\partial}{\partial X}W(X,Y) = W_1\frac{Y_{23}}{2A}(4\xi_1 - 1) + W_2\frac{Y_{31}}{2A}(4\xi_2 - 1) + W_3\frac{Y_{12}}{2A}(4\xi_3 - 1) + W_4\frac{1}{2A}4(\xi_2 Y_{23} + \xi_1 W_{31})$$

$$+W_5\frac{1}{2A}4(\xi_3 Y_{31} + \xi_2 Y_{12}) + W_6\frac{1}{2A}4(\xi_1 Y_{12} + \xi_3 Y_{23})$$

$$\frac{\partial}{\partial Y}U(X,Y) = U_1\frac{X_{32}}{2A}(4\xi_1 - 1) + U_2\frac{X_{13}}{2A}(4\xi_2 - 1) + U_3\frac{X_{21}}{2A}(4\xi_3 - 1) + U_4\frac{1}{2A}4(\xi_2 X_{32} + \xi_1 X_{13})$$

$$+U_5\frac{1}{2A}4(\xi_3 X_{13} + \xi_2 X_{21}) + U_6\frac{1}{2A}4(\xi_1 X_{21} + \xi_3 X_{32})$$

$$\frac{\partial}{\partial Y}V(X,Y) = V_1\frac{X_{32}}{2A}(4\xi_1 - 1) + V_2\frac{X_{13}}{2A}(4\xi_2 - 1) + V_3\frac{X_{21}}{2A}(4\xi_3 - 1) + V_4\frac{1}{2A}4(\xi_2 X_{32} + \xi_1 X_{13})$$

$$+V_5\frac{1}{2A}4(\xi_3 X_{13} + \xi_2 X_{21}) + V_6\frac{1}{2A}4(\xi_1 X_{21} + \xi_3 X_{32})$$

$$\frac{\partial}{\partial Y}W(X,Y) = W_1\frac{X_{32}}{2A}(4\xi_1 - 1) + W_2\frac{X_{13}}{2A}(4\xi_2 - 1) + W_3\frac{X_{21}}{2A}(4\xi_3 - 1) + W_4\frac{1}{2A}4(\xi_2 X_{32} + \xi_1 X_{13})$$

$$+W_5\frac{1}{2A}4(\xi_3 X_{13} + \xi_2 X_{21}) + W_6\frac{1}{2A}4(\xi_1 X_{21} + \xi_3 X_{32}) \tag{B.12}$$

Substituting these to the formulation:

$$\varepsilon_X = U_1\frac{Y_{23}}{2A}(4\xi_1-1)+U_2\frac{Y_{31}}{2A}(4\xi_2-1)+U_3\frac{Y_{12}}{2A}(4\xi_3-1)+U_4\frac{1}{2A}4(\xi_2Y_{23}+\xi_1Y_{31})$$

$$+U_5\frac{1}{2A}4(\xi_3Y_{31}+\xi_2Y_{12})+U_6\frac{1}{2A}4(\xi_1Y_{12}+\xi_3Y_{23})+K_X[W_1\xi_1(2\xi_1-1)+$$

$$W_2\xi_2(2\xi_2-1)+W_3\xi_3(2\xi_3-1)+W_4\cdot 4\xi_1\xi_2+W_5\cdot 4\xi_2\xi_3+W_6\cdot 4\xi_3\xi_1]+$$

$$\frac{1}{2}[U_1\frac{Y_{23}}{2A}(4\xi_1-1)+U_2\frac{Y_{31}}{2A}(4\xi_2-1)+U_3\frac{Y_{12}}{2A}(4\xi_3-1)+U_4\frac{1}{2A}4(\xi_2Y_{23}$$

$$+\xi_1Y_{31})+U_5\frac{1}{2A}4(\xi_3Y_{31}+\xi_2Y_{12})+U_6\frac{1}{2A}4(\xi_1Y_{12}+\xi_3Y_{23})]^2+$$

$$\frac{1}{2}[V_1\frac{Y_{23}}{2A}(4\xi_1-1)+V_2\frac{Y_{31}}{2A}(4\xi_2-1)+V_3\frac{Y_{12}}{2A}(4\xi_3-1)+V_4\frac{1}{2A}4(\xi_2Y_{23}$$

$$+\xi_1Y_{31})+V_5\frac{1}{2A}4(\xi_3Y_{31}+\xi_2Y_{12})+V_6\frac{1}{2A}4(\xi_1Y_{12}+\xi_3Y_{23})]^2+$$

$$\frac{1}{2}[W_1\frac{Y_{23}}{2A}(4\xi_1-1)+W_2\frac{Y_{31}}{2A}(4\xi_2-1)+W_3\frac{Y_{12}}{2A}(4\xi_3-1)+W_4\frac{1}{2A}4(\xi_2Y_{23}$$

$$+\xi_1W_{31})+W_5\frac{1}{2A}4(\xi_3Y_{31}+\xi_2Y_{12})+W_6\frac{1}{2A}4(\xi_1Y_{12}+\xi_3Y_{23})]^2 \tag{B.13}$$

$$\varepsilon_Y = V_1\frac{X_{32}}{2A}(4\xi_1-1)+V_2\frac{X_{13}}{2A}(4\xi_2-1)+V_3\frac{X_{21}}{2A}(4\xi_3-1)+V_4\frac{1}{2A}4(\xi_2X_{32}+\xi_1X_{13})$$

$$+V_5\frac{1}{2A}4(\xi_3X_{13}+\xi_2X_{21})+V_6\frac{1}{2A}4(\xi_1X_{21}+\xi_3X_{32})+K_Y[W_1\xi_1(2\xi_1-1)+$$

$$W_2\xi_2(2\xi_2-1)+W_3\xi_3(2\xi_3-1)+W_4\cdot 4\xi_1\xi_2+W_5\cdot 4\xi_2\xi_3+W_6\cdot 4\xi_3\xi_1]+$$

$$\frac{1}{2}[U_1\frac{X_{32}}{2A}(4\xi_1-1)+U_2\frac{X_{13}}{2A}(4\xi_2-1)+U_3\frac{X_{21}}{2A}(4\xi_3-1)+U_4\frac{1}{2A}4(\xi_2X_{32}$$

$$+\xi_1X_{13})+U_5\frac{1}{2A}4(\xi_3X_{13}+\xi_2X_{21})+U_6\frac{1}{2A}4(\xi_1X_{21}+\xi_3X_{32})]^2+$$

$$\frac{1}{2}[V_1\frac{X_{32}}{2A}(4\xi_1-1)+V_2\frac{X_{13}}{2A}(4\xi_2-1)+V_3\frac{X_{21}}{2A}(4\xi_3-1)+V_4\frac{1}{2A}4(\xi_2X_{32}+$$

$$\xi_1X_{13}+V_5\frac{1}{2A}4(\xi_3X_{13}+\xi_2X_{21})+V_6\frac{1}{2A}4(\xi_1X_{21}+\xi_3X_{32})]^2+$$

$$\frac{1}{2}[W_1\frac{X_{32}}{2A}(4\xi_1-1)+W_2\frac{X_{13}}{2A}(4\xi_2-1)+W_3\frac{X_{21}}{2A}(4\xi_3-1)+W_4\frac{1}{2A}4(\xi_2X_{32}+$$

$$\xi_1X_{13})+W_5\frac{1}{2A}4(\xi_3X13+\xi_2X_{21})+W_6\frac{1}{2A}4(\xi_1X_{21}+\xi_3X_{32})]^2 \tag{B.14}$$

$$\gamma_{XY}=U_1\frac{X_{32}}{2A}(4\xi_1-1)+U_2\frac{X_{13}}{2A}(4\xi_2-1)+U_3\frac{X_{21}}{2A}(4\xi_3-1)+U_4\frac{1}{2A}4(\xi_2X_{32}+\xi_1X_{13})$$

$$+U_5\frac{1}{2A}4(\xi_3X_{13}+\xi_2X_{21})+U_6\frac{1}{2A}4(\xi_1X_{21}+\xi_3X_{32})+V_1\frac{Y_{23}}{2A}(4\xi_1-1)+$$

$$V_2\frac{Y_{31}}{2A}(4\xi_2-1)+V_3\frac{Y_{12}}{2A}(4\xi_3-1)+V_4\frac{1}{2A}4(\xi_2Y_{23}+\xi_1Y_{31})+V_5\frac{1}{2A}4(\xi_3Y_{31}$$

$$+\xi_2Y_{12})+V_6\frac{1}{2A}4(\xi_1Y_{12}+\xi_3Y_{23})+K_{XY}\cdot 2[W_1\xi_1(2\xi_1-1)+W_2\xi_2(2\xi_2-1)$$

$$+W_3\xi_3(2\xi_3-1)+W_4\cdot 4\xi_1\xi_2+W_5\cdot 4\xi_2\xi_3+W_6\cdot 4\xi_3\xi_1]+[U_1\frac{Y_{23}}{2A}(4\xi_1-1)$$

$$+U_2\frac{Y_{31}}{2A}(4\xi_2-1)+U_3\frac{Y_{12}}{2A}(4\xi_3-1)+U_4\frac{1}{2A}4(\xi_2Y_{23}+\xi_1Y_{31})+U_5\frac{1}{2A}4(\xi_3Y_{31}$$

$$+\xi_2Y_{12})+U_6\frac{1}{2A}4(\xi_1Y_{12}+\xi_3Y_{23})]\times[U_1\frac{X_{32}}{2A}(4\xi_1-1)+U_2\frac{X_{13}}{2A}(4\xi_2-1)+$$

$$U_3\frac{X_{21}}{2A}(4\xi_3-1)+U_4\frac{1}{2A}4(\xi_2X_{32}+\xi_1X_{13})+U_5\frac{1}{2A}4(\xi_3X_{13}+\xi_2X_{21})+U_6\frac{1}{2A}4(\xi_1X_{21}$$

$$+\xi_3X_{32})]+[V_1\frac{Y_{23}}{2A}(4\xi_1-1)+V_2\frac{Y_{31}}{2A}(4\xi_2-1)+V_3\frac{Y_{12}}{2A}(4\xi_3-1)+V_4\frac{1}{2A}4(\xi_2Y_{23}$$

$$+\xi_1Y_{31})+V_5\frac{1}{2A}4(\xi_3Y_{31}+\xi_2Y_{12})+V_6\frac{1}{2A}4(\xi_1Y_{12}+\xi_3Y_{23})]\times[V_1\frac{X_{32}}{2A}(4\xi_1-1)$$

$$+V_2\frac{X_{13}}{2A}(4\xi_2-1)+V_3\frac{X_{21}}{2A}(4\xi_3-1)+V_4\frac{1}{2A}4(\xi_2X_{32}+\xi_1X_{13})+V_5\frac{1}{2A}4(\xi_3X_{13}$$

$$+\xi_2X_{21})+V_6\frac{1}{2A}4(\xi_1X_{21}+\xi_3X_{32})]+[W_1\frac{Y_{23}}{2A}(4\xi_1-1)+W_2\frac{Y_{31}}{2A}(4\xi_2-1)+$$

$$W_3\frac{Y_{12}}{2A}(4\xi_3-1)+W_4\frac{1}{2A}4(\xi_2Y_{23}+\xi_1Y_{31})+W_5\frac{1}{2A}4(\xi_3Y_{31}+\xi_2Y_{12})$$

$$+W_6\frac{1}{2A}4(\xi_1Y_{12}+\xi_3Y_{23})]\times[W_1\frac{X_{32}}{2A}(4\xi_1-1)+W_2\frac{X_{13}}{2A}(4\xi_2-1)+W_3\frac{X_{21}}{2A}(4\xi_3-1)$$

$$+W_4\frac{1}{2A}4(\xi_2X_{32}+\xi_1X_{13})+W_5\frac{1}{2A}4(\xi_3X_{13}+\xi_2X_{21})+W_6\frac{1}{2A}4(\xi_1X_{21}+\xi_3X_{32})] \tag{B.15}$$

So the relationship between local principal strains and nodal displacement is:

$$\{\varepsilon\}=\{\varepsilon_X \quad \varepsilon_Y \quad \gamma_{XY}\}^T=[B]\{D\} \tag{B.16}$$

in which $\{D\}=\{U_1\ \ V_1\ \ W_1\ \ U_2\ \ V_2\ \ W_2\ \ U_3\ \ V_3\ \ W_3\ \ U_4\ \ V_4\ \ W_4\ \ U_5\ \ V_5\ \ W_5\ \ U_6\ \ V_6\ \ W_6\ \ \}^T$
The terms of the B matrix are followed:

$$\begin{aligned}B_{1,1} &= \frac{Y_{23}}{2A}(4\xi_1-1)+U_1\frac{Y_{23}^2}{8A^2}(4\xi_1-1)^2+\frac{Y_{23}}{2A}(4\xi_1-1)[U_2\frac{Y_{31}}{2A}(4\xi_2-1)\\ &\quad +U_3\frac{Y_{12}}{2A}(4\xi_3-1)+U_4\frac{4}{2A}(\xi_2Y_{23}+\xi_1Y_{31})+U_5\frac{4}{2A}(\xi_3Y_{31}+\xi_2Y_{12})\\ &\quad +U_6\frac{4}{2A}(\xi_1Y_{12}+\xi_3Y_{23})]\end{aligned}$$

$$\begin{aligned}B_{1,2} &= V_1\frac{Y_{23}^2}{8A^2}(4\xi_1-1)^2+\frac{Y_{23}}{2A}(4\xi_1-1)[V_2\frac{Y_{31}}{2A}(4\xi_2-1)+V_3\frac{Y_{12}}{2A}(4\xi_3-1)\\ &\quad +V_4\frac{4}{2A}(\xi_2Y_{23}+\xi_1Y_{31})+V_5\frac{4}{2A}(\xi_3Y_{31}+\xi_2Y_{12})+V_6\frac{4}{2A}(\xi_1Y_{12}+\xi_3Y_{23})]\end{aligned}$$

$$B_{1,3} = K_{\bar{X}} \cdot \xi_1(2\xi_1 - 1) + W_1 \frac{Y_{23}^2}{8A^2}(4\xi_1 - 1)^2 + \frac{Y_{23}}{2A}(4\xi_1 - 1)[W_2 \frac{Y_{31}}{2A}(4\xi_2 - 1) + W_3 \frac{Y_{12}}{2A}(4\xi_3 - 1) + W_4 \frac{4}{2A}(\xi_2 Y_{23} + \xi_1 Y_{31}) + W_5 \frac{4}{2A}(\xi_3 Y_{31} + \xi_2 Y_{12}) + W_6 \frac{4}{2A}(\xi_1 Y_{12} + \xi_3 Y_{23})]$$

$$B_{1,4} = \frac{Y_{31}}{2A}(4\xi_2 - 1) + \frac{1}{2}U_2 \cdot \frac{Y_{31}^2}{4A^2}(4\xi_2 - 1)^2 + \frac{Y_{31}}{2A}(4\xi_2 - 1)[U_3 \frac{Y_{12}}{2A}(4\xi_3 - 1) + U_4 \cdot \frac{4}{2A}(\xi_2 Y_{23} + \xi_1 Y_{31}) + U_5 \frac{4}{2A}(\xi_3 Y_{31} + \xi_2 Y_{12}) + U_6 \frac{4}{2A}(\xi_1 Y_{12} + \xi_3 Y_{23})]$$

$$B_{1,5} = \frac{1}{2}V_2 \cdot \frac{Y_{31}^2}{4A^2}(4\xi_2 - 1)^2 + \frac{Y_{31}}{2A}(4\xi_2 - 1)[V_3 \frac{Y_{12}}{2A}(4\xi_3 - 1) + V_4 \cdot \frac{4}{2A}(\xi_2 Y_{23} + \xi_1 Y_{31}) + V_5 \frac{4}{2A}(\xi_3 Y_{31} + \xi_2 Y_{12}) + V_6 \frac{4}{2A}(\xi_1 Y_{12} + \xi_3 Y_{23})]$$

$$B_{1,6} = K_{\bar{X}} \cdot \xi_2(2\xi_2 - 1) + \frac{1}{2}W_2 \cdot \frac{Y_{31}^2}{4A^2}(4\xi_2 - 1)^2 + \frac{Y_{31}}{2A}(4\xi_2 - 1)[W_3 \frac{Y_{12}}{2A}(4\xi_3 - 1) + W_4 \cdot \frac{4}{2A}(\xi_2 Y_{23} + \xi_1 Y_{31}) + W_5 \frac{4}{2A}(\xi_3 Y_{31} + \xi_2 Y_{12}) + W_6 \frac{4}{2A}(\xi_1 Y_{12} + \xi_3 Y_{23})]$$

$$B_{1,7} = \frac{Y_{12}}{2A}(4\xi_3 - 1) + \frac{1}{2}U_3 \cdot \frac{Y_{12}^2}{4A^2}(4\xi_3 - 1)^2 + \frac{Y_{12}}{2A}(4\xi_3 - 1)[U_4 \cdot \frac{4}{2A}(\xi_2 Y_{23} + \xi_1 Y_{31}) + U_5 \frac{4}{2A}(\xi_3 Y_{31} + \xi_2 Y_{12}) + U_6 \frac{4}{2A}(\xi_1 Y_{12} + \xi_3 Y_{23})]$$

$$B_{1,8} = \frac{1}{2}V_3 \cdot \frac{Y_{12}^2}{4A^2}(4\xi_3 - 1)^2 + \frac{Y_{12}}{2A}(4\xi_3 - 1)[V_4 \cdot \frac{4}{2A}(\xi_2 Y_{23} + \xi_1 Y_{31}) + V_5 \frac{4}{2A}(\xi_3 Y_{31} + \xi_2 Y_{12}) + V_6 \frac{4}{2A}(\xi_1 Y_{12} + \xi_3 Y_{23})]$$

$$B_{1,9} = K_{\bar{X}} \cdot \xi_3(2\xi_3 - 1) + \frac{1}{2}W_3 \cdot \frac{Y_{12}^2}{4A^2}(4\xi_3 - 1)^2 + \frac{Y_{12}}{2A}(4\xi_3 - 1)[W_4 \cdot \frac{4}{2A}(\xi_2 Y_{23} + \xi_1 Y_{31}) + W_5 \frac{4}{2A}(\xi_3 Y_{31} + \xi_2 Y_{12}) + W_6 \frac{4}{2A}(\xi_1 Y_{12} + \xi_3 Y_{23})]$$

$$B_{1,10} = \frac{4}{2A}(\xi_2 Y_{23} + \xi_1 Y_{31}) + U_4 \cdot \frac{2}{A^2}(\xi_2 Y_{23} + \xi_1 Y_{31})^2 + \frac{4}{2A}(\xi_2 Y_{23} + \xi_1 Y_{31})[U_5 \frac{4}{2A}(\xi_3 Y_{31} + \xi_2 Y_{12}) + U_6 \frac{4}{2A}(\xi_1 Y_{12} + \xi_3 Y_{23})]$$

$$B_{1,11} = V_4 \cdot \frac{2}{A^2}(\xi_2 Y_{23} + \xi_1 Y_{31})^2 + \frac{4}{2A}(\xi_2 Y_{23} + \xi_1 Y_{31})[V_5 \frac{4}{2A}(\xi_3 Y_{31} + \xi_2 Y_{12}) + V_6 \frac{4}{2A}(\xi_1 Y_{12} + \xi_3 Y_{23})]$$

$$B_{1,12} = K_{\bar{X}} 4\xi_1\xi_2 + W_4 \cdot \frac{2}{A^2}(\xi_2 Y_{23} + \xi_1 Y_{31})^2 + \frac{4}{2A}(\xi_2 Y_{23} + \xi_1 Y_{31}) [W_5 \frac{4}{2A}(\xi_3 Y_{31} + \xi_2 Y_{12}) + W_6 \frac{4}{2A}(\xi_1 Y_{12} + \xi_3 Y_{23})]$$

$$B_{1,13} = \frac{4}{2A}(\xi_3 Y_{31} + \xi_2 Y_{12}) + U_5 \frac{2}{A^2}(\xi_3 Y_{31} + \xi_2 Y_{12})^2 + \frac{4}{2A}(\xi_3 Y_{31} + \xi_2 Y_{12}) \cdot U_6 \frac{4}{2A}(\xi_1 Y_{12} + \xi_3 Y_{23})$$

$$B_{1,14} = V_5 \frac{2}{A^2}(\xi_3 Y_{31} + \xi_2 Y_{12})^2 + \frac{4}{2A}(\xi_3 Y_{31} + \xi_2 Y_{12}) \cdot V_6 \frac{4}{2A}(\xi_1 Y_{12} + \xi_3 Y_{23})$$

$$B_{1,15} = K_{\bar{X}} \cdot 4\xi_2\xi_3 + W_5 \frac{2}{A^2}(\xi_3 Y_{31} + \xi_2 Y_{12})^2 + \frac{4}{2A}(\xi_3 Y_{31} + \xi_2 Y_{12}) \cdot W_6 \frac{4}{2A}(\xi_1 Y_{12} + \xi_3 Y_{23})$$

$$B_{1,16} = \frac{4}{2A}(\xi_1 Y_{12} + \xi_3 Y_{23}) + U_6 \frac{2}{A^2}(\xi_1 Y_{12} + \xi_3 Y_{23})^2$$

$$B_{1,17} = V_6 \frac{2}{A^2}(\xi_1 Y_{12} + \xi_3 Y_{23})^2$$

$$B_{1,18} = K_{\bar{X}} \cdot 4\xi_3\xi_1 + W_6 \frac{2}{A^2}(\xi_1 Y_{12} + \xi_3 Y_{23})^2$$

$$B_{2,1} = U_1\frac{X_{32}^2}{8A^2}(4\xi_1-1)^2+\frac{X_{32}}{2A}(4\xi_1-1)[U_2\frac{X_{13}}{2A}(4\xi_2-1)+U_3\frac{X_{21}}{2A}(4\xi_3-1)+ U_4\frac{4}{2A}(\xi_2X_{32}+\xi_1X_{13})+U_5\frac{4}{2A}(\xi_3X_{13}+\xi_2X_{21})+U_6\frac{4}{2A}(\xi_1X_{21}+\xi_3X_{32})]$$

$$B_{2,2} = \frac{X_{32}}{2A}(4\xi_1-1)+V_1\frac{X_{32}^2}{8A^2}(4\xi_1-1)^2+\frac{X_{32}}{2A}(4\xi_1-1)[V_2\frac{X_{13}}{2A}(4\xi_2-1)+V_3\frac{X_{21}}{2A}(4\xi_3-1) +V_4\frac{4}{2A}(\xi_2X_{32}+\xi_1X_{13})+V_5\frac{4}{2A}(\xi_3X_{13}+\xi_2X_{21})+V_6\frac{4}{2A}(\xi_1X_{21}+\xi_3X_{32})]$$

$$B_{2,3} = K_{\bar{Y}}\cdot\xi_1(2\xi_1-1)+W_1\frac{X_{32}^2}{8A^2}(4\xi_1-1)^2+\frac{X_{32}}{2A}(4\xi_1-1)[W_2\frac{X_{13}}{2A}(4\xi_2-1) +W_3\frac{X_{21}}{2A}(4\xi_3-1)+W_4\frac{4}{2A}(\xi_2X_{32}+\xi_1X_{13})+W_5\frac{4}{2A}(\xi_3X_{13}+\xi_2X_{21}) +W_6\frac{4}{2A}(\xi_1X_{21}+\xi_3X_{32})]$$

$$B_{2,4} = \frac{1}{2}U_2\cdot\frac{X_{13}^2}{4A^2}(4\xi_2-1)^2+\frac{X_{13}}{2A}(4\xi_2-1)[U_3\frac{X_{21}}{2A}(4\xi_3-1)+U_4\cdot\frac{4}{2A}(\xi_2X_{32} +\xi_1X_{13})+U_5\frac{4}{2A}(\xi_3X_{13}+\xi_2X_{21})+U_6\frac{4}{2A}(\xi_1X_{21}+\xi_3X_{32})]$$

$$B_{2,5} = \frac{X_{13}}{2A}(4\xi_2-1)+\frac{1}{2}V_2\cdot\frac{X_{13}^2}{4A^2}(4\xi_2-1)^2+\frac{X_{13}}{2A}(4\xi_2-1)[V_3\frac{X_{21}}{2A}(4\xi_3-1)+ V_4\cdot\frac{4}{2A}(\xi_2X_{32}+\xi_1X_{13})+V_5\frac{4}{2A}(\xi_3X_{13}+\xi_2X_{21})+V_6\frac{4}{2A}(\xi_1X_{21}+\xi_3X_{32})]$$

$$B_{2,6} = K_{\bar{Y}}\cdot\xi_2(2\xi_2-1)+\frac{1}{2}W_2\cdot\frac{X_{13}^2}{4A^2}(4\xi_2-1)^2+\frac{X_{13}}{2A}(4\xi_2-1)[W_3\frac{X_{21}}{2A}(4\xi_3-1) +W_4\cdot\frac{4}{2A}(\xi_2X_{32}+\xi_1X_{13})+W_5\frac{4}{2A}(\xi_3X_{13}+\xi_2X_{21})+W_6\frac{4}{2A}(\xi_1X_{21}+\xi_3X_{32})]$$

$$B_{2,7} = \frac{1}{2}U_3\cdot\frac{X_{21}^2}{4A^2}(4\xi_3-1)^2+\frac{X_{21}}{2A}(4\xi_3-1)[U_4\cdot\frac{4}{2A}(\xi_2X_{32}+\xi_1X_{13})+U_5\frac{4}{2A}(\xi_3X_{13}+\xi_2X_{21}) +U_6\frac{4}{2A}(\xi_1X_{21}+\xi_3X_{32})]$$

$$B_{2,8} = \frac{X_{21}}{2A}(4\xi_3-1)+\frac{1}{2}V_3\cdot\frac{X_{21}^2}{4A^2}(4\xi_3-1)^2+\frac{X_{21}}{2A}(4\xi_3-1)[V_4\cdot\frac{4}{2A}(\xi_2X_{32}+\xi_1X_{13})+V_5\frac{4}{2A}(\xi_3X_{13}+\xi_2X_{21})+V_6\frac{4}{2A}(\xi_1X_{21}+\xi_3X_{32})]$$

$$B_{2,9} = K_{\bar{Y}}\cdot\xi_3(2\xi_3-1)+\frac{1}{2}W_3\cdot\frac{X_{21}^2}{4A^2}(4\xi_3-1)^2+\frac{X_{21}}{2A}(4\xi_3-1)[W_4\cdot\frac{4}{2A}(\xi_2X_{32}+\xi_1X_{13})+W_5\frac{4}{2A}(\xi_3X_{13}+\xi_2X_{21})+W_6\frac{4}{2A}(\xi_1X_{21}+\xi_3X_{32})]$$

$$B_{2,10} = U_4\cdot\frac{2}{A^2}(\xi_2X_{32}+\xi_1X_{13})^2+\frac{4}{2A}(\xi_2X_{32}+\xi_1X_{13})[U_5\frac{4}{2A}(\xi_3X_{13}+\xi_2X_{21})+U_6\frac{4}{2A}(\xi_1X_{21}+\xi_3X_{32})]$$

$$B_{2,11} = \frac{4}{2A}(\xi_2X_{32}+\xi_1X_{13})+V_4\cdot\frac{2}{A^2}(\xi_2X_{32}+\xi_1X_{13})^2+\frac{4}{2A}(\xi_2X_{32}+\xi_1X_{13})[V_5\frac{4}{2A}(\xi_3X_{13}+\xi_2X_{21})+V_6\frac{4}{2A}(\xi_1X_{21}+\xi_3X_{32})]$$

$$B_{2,12} = K_{\bar{Y}}4\xi_1\xi_2+W_4\cdot\frac{2}{A^2}(\xi_2X_{32}+\xi_1X_{13})^2+\frac{4}{2A}(\xi_2X_{32}+\xi_1X_{13})[W_5\frac{4}{2A}(\xi_3X_{13}+\xi_2X_{21})+W_6\frac{4}{2A}(\xi_1X_{21}+\xi_3X_{32})]$$

$$B_{2,13} = U_5\frac{2}{A^2}(\xi_3X_{13}+\xi_2X_{21})^2+\frac{4}{2A}(\xi_3X_{13}+\xi_2X_{21})\cdot U_6\frac{4}{2A}(\xi_1X_{21}+\xi_3X_{32})$$

$$B_{2,14} = \frac{4}{2A}(\xi_3X_{13}+\xi_2X_{21})+V_5\frac{2}{A^2}(\xi_3X_{13}+\xi_2X_{21})^2+\frac{4}{2A}(\xi_3X_{13}+\xi_2X_{21})\cdot V_6\frac{4}{2A}(\xi_1X_{21}+\xi_3X_{32})$$

$$B_{2,15} = K_{\bar{Y}}\cdot4\xi_2\xi_3+W_5\frac{2}{A^2}(\xi_3X_{13}+\xi_2X_{21})^2+\frac{4}{2A}(\xi_3X_{13}+\xi_2X_{21})\cdot W_6\frac{4}{2A}(\xi_1X_{21}+\xi_3X_{32})$$

$$B_{2,16} = U_6\frac{2}{A^2}(\xi_1 X_{21} + \xi_3 X_{32})^2$$

$$B_{2,17} = \frac{4}{2A}(\xi_1 X_{21} + \xi_3 X_{32}) + V_6\frac{2}{A^2}(\xi_1 X_{21} + \xi_3 X_{32})^2$$

$$B_{2,18} = K_{\bar{Y}} \cdot 4\xi_3\xi_1 + W_6\frac{2}{A^2}(\xi_1 X_{21} + \xi_3 X_{32})^2$$

$$\begin{aligned} B_{3,1} = {} & \frac{X_{32}}{2A}(4\xi_1 - 1) + \frac{Y_{23}}{2A}(4\xi_1 - 1)[U_1\frac{X_{32}}{2A}(4\xi_1 - 1) + U_2\frac{X_{13}}{2A}(4\xi_2 - 1) + U_3\frac{X_{21}}{2A}(4\xi_3 - 1) \\ & + U_4\frac{4}{2A}(\xi_2 X_{32} + \xi_1 X_{13}) + U_5\frac{4}{2A}(\xi_3 X_{13} + \xi_2 X_{21}) + U_6\frac{4}{2A}(\xi_1 X_{21} + \xi_3 X_{32})] \end{aligned}$$

$$\begin{aligned} B_{3,2} = {} & \frac{Y_{23}}{2A}(4\xi_1 - 1) + \frac{Y_{23}}{2A}(4\xi_1 - 1)[V_1\frac{X_{32}}{2A}(4\xi_1 - 1) + V_2\frac{X_{13}}{2A}(4\xi_2 - 1) + V_3\frac{X_{21}}{2A}(4\xi_3 - 1) \\ & + V_4\frac{4}{2A}(\xi_2 X_{32} + \xi_1 X_{13}) + V_5\frac{4}{2A}(\xi_3 X_{13} + \xi_2 X_{21}) + V_6\frac{4}{2A}(\xi_1 X_{21} + \xi_3 X_{32})] \end{aligned}$$

$$\begin{aligned} B_{3,3} = {} & 2K_{X\bar{Y}} \cdot \xi_1(2\xi_1 - 1) + \frac{Y_{23}}{2A}(4\xi_1 - 1)[W_1\frac{X_{32}}{2A}(4\xi_1 - 1) + W_2\frac{X_{13}}{2A}(4\xi_2 - 1) \\ & + W_3\frac{X_{21}}{2A}(4\xi_3 - 1) + W_4\frac{4}{2A}(\xi_2 X_{32} + \xi_1 X_{13}) + W_5\frac{4}{2A}(\xi_3 X_{13} + \xi_2 X_{21}) \\ & + W_6\frac{4}{2A}(\xi_1 X_{21} + \xi_3 X_{32})] \end{aligned}$$

$$\begin{aligned} B_{3,4} = {} & \frac{X_{13}}{2A}(4\xi_2 - 1) + \frac{Y_{31}}{2A}(4\xi_2 - 1)[U_1\frac{X_{32}}{2A}(4\xi_1 - 1) + U_2\frac{X_{13}}{2A}(4\xi_2 - 1) + U_3\frac{X_{21}}{2A}(4\xi_3 - 1) \\ & + U_4\frac{4}{2A}(\xi_2 X_{32} + \xi_1 X_{13}) + U_5\frac{4}{2A}(\xi_3 X_{13} + \xi_2 X_{21}) + U_6\frac{4}{2A}(\xi_1 X_{21} + \xi_3 X_{32})] \end{aligned}$$

$$\begin{aligned} B_{3,5} = {} & \frac{Y_{31}}{2A}(4\xi_2 - 1) + \frac{Y_{31}}{2A}(4\xi_2 - 1)[V_1\frac{X_{32}}{2A}(4\xi_1 - 1) + V_2\frac{X_{13}}{2A}(4\xi_2 - 1) + V_3\frac{X_{21}}{2A}(4\xi_3 - 1) \\ & + V_4\frac{4}{2A}(\xi_2 X_{32} + \xi_1 X_{13}) + V_5\frac{4}{2A}(\xi_3 X_{13} + \xi_2 X_{21}) + V_6\frac{4}{2A}(\xi_1 X_{21} + \xi_3 X_{32})] \end{aligned}$$

$$\begin{aligned} B_{3,6} &= 2K_{X\bar{Y}} \cdot \xi_2(2\xi_2 - 1) + \frac{Y_{31}}{2A}(4\xi_2 - 1)[W_1\frac{X_{32}}{2A}(4\xi_1 - 1) + W_2\frac{X_{13}}{2A}(4\xi_2 - 1) \\ &\quad + W_3\frac{X_{21}}{2A}(4\xi_3 - 1) + W_4\frac{4}{2A}(\xi_2 X_{32} + \xi_1 X_{13}) + W_5\frac{4}{2A}(\xi_3 X_{13} + \xi_2 X_{21}) \\ &\quad + W_6\frac{4}{2A}(\xi_1 X_{21} + \xi_3 X_{32})] \end{aligned}$$

$$\begin{aligned} B_{3,7} &= \frac{X_{21}}{2A}(4\xi_3 - 1) + \frac{Y_{12}}{2A}(4\xi_3 - 1)[U_1\frac{X_{32}}{2A}(4\xi_1 - 1) + U_2\frac{X_{13}}{2A}(4\xi_2 - 1) + U_3\frac{X_{21}}{2A}(4\xi_3 - 1) \\ &\quad + U_4\frac{4}{2A}(\xi_2 X_{32} + \xi_1 X_{13}) + U_5\frac{4}{2A}(\xi_3 X_{13} + \xi_2 X_{21}) + U_6\frac{4}{2A}(\xi_1 X_{21} + \xi_3 X_{32})] \end{aligned}$$

$$\begin{aligned} B_{3,8} &= \frac{Y_{12}}{2A}(4\xi_3 - 1) + \frac{Y_{12}}{2A}(4\xi_3 - 1)[V_1\frac{X_{32}}{2A}(4\xi_1 - 1) + V_2\frac{X_{13}}{2A}(4\xi_2 - 1) + V_3\frac{X_{21}}{2A}(4\xi_3 - 1) \\ &\quad + V_4\frac{4}{2A}(\xi_2 X_{32} + \xi_1 X_{13}) + V_5\frac{4}{2A}(\xi_3 X_{13} + \xi_2 X_{21}) + V_6\frac{4}{2A}(\xi_1 X_{21} + \xi_3 X_{32})] \end{aligned}$$

$$\begin{aligned} B_{3,9} &= 2K_{X\bar{Y}} \cdot \xi_3(2\xi_3 - 1) + \frac{Y_{12}}{2A}(4\xi_3 - 1)[W_1\frac{X_{32}}{2A}(4\xi_1 - 1) + W_2\frac{X_{13}}{2A}(4\xi_2 - 1) \\ &\quad + W_3\frac{X_{21}}{2A}(4\xi_3 - 1) + W_4\frac{4}{2A}(\xi_2 X_{32} + \xi_1 X_{13}) + W_5\frac{4}{2A}(\xi_3 X_{13} + \xi_2 X_{21}) \\ &\quad + W_6\frac{4}{2A}(\xi_1 X_{21} + \xi_3 X_{32})] \end{aligned}$$

$$\begin{aligned} B_{3,10} &= \frac{4}{2A}(\xi_2 X_{32} + \xi_1 X_{13}) + \frac{4}{2A}(\xi_2 Y_{23} + \xi_1 Y_{31})[U_1\frac{X_{32}}{2A}(4\xi_1 - 1) + U_2\frac{X_{13}}{2A}(4\xi_2 - 1) \\ &\quad + U_3\frac{X_{21}}{2A}(4\xi_3 - 1) + U_4\frac{4}{2A}(\xi_2 X_{32} + \xi_1 X_{13}) + U_5\frac{4}{2A}(\xi_3 X_{13} + \xi_2 X_{21}) \\ &\quad + U_6\frac{4}{2A}(\xi_1 X_{21} + \xi_3 X_{32})] \end{aligned}$$

$$\begin{aligned} B_{3,11} &= \frac{4}{2A}(\xi_2 Y_{23} + \xi_1 Y_{31}) + \frac{4}{2A}(\xi_2 Y_{23} + \xi_1 Y_{31})[V_1\frac{X_{32}}{2A}(4\xi_1 - 1) + V_2\frac{X_{13}}{2A}(4\xi_2 - 1) \\ &\quad + V_3\frac{X_{21}}{2A}(4\xi_3 - 1) + V_4\frac{4}{2A}(\xi_2 X_{32} + \xi_1 X_{13}) + V_5\frac{4}{2A}(\xi_3 X_{13} + \xi_2 X_{21}) \\ &\quad + V_6\frac{4}{2A}(\xi_1 X_{21} + \xi_3 X_{32})] \end{aligned}$$

$$
\begin{aligned}
B_{3,12} &= 2K_{X\bar{Y}} \cdot 4\xi_1\xi_2 + \frac{4}{2A}(\xi_2 Y_{23} + \xi_1 Y_{31})[W_1 \frac{X_{32}}{2A}(4\xi_1 - 1) + W_2 \frac{X_{13}}{2A}(4\xi_2 - 1) \\
&\quad + W_3 \frac{X_{21}}{2A}(4\xi_3 - 1) + W_4 \frac{4}{2A}(\xi_2 X_{32} + \xi_1 X_{13}) + W_5 \frac{4}{2A}(\xi_3 X_{13} + \xi_2 X_{21}) \\
&\quad + W_6 \frac{4}{2A}(\xi_1 X_{21} + \xi_3 X_{32})]
\end{aligned}
$$

$$
\begin{aligned}
B_{3,13} &= \frac{4}{2A}(\xi_3 X_{13} + \xi_2 X_{21}) + \frac{4}{2A}(\xi_3 Y_{31} + \xi_2 Y_{12})[U_1 \frac{X_{32}}{2A}(4\xi_1 - 1) + U_2 \frac{X_{13}}{2A}(4\xi_2 - 1) \\
&\quad + U_3 \frac{X_{21}}{2A}(4\xi_3 - 1) + U_4 \frac{4}{2A}(\xi_2 X_{32} + \xi_1 X_{13}) + U_5 \frac{4}{2A}(\xi_3 X_{13} + \xi_2 X_{21}) \\
&\quad + U_6 \frac{4}{2A}(\xi_1 X_{21} + \xi_3 X_{32})]
\end{aligned}
$$

$$
\begin{aligned}
B_{3,14} &= \frac{4}{2A}(\xi_3 Y_{31} + \xi_2 Y_{12}) + \frac{4}{2A}(\xi_3 Y_{31} + \xi_2 Y_{12})[V_1 \frac{X_{32}}{2A}(4\xi_1 - 1) + V_2 \frac{X_{13}}{2A}(4\xi_2 - 1) \\
&\quad + V_3 \frac{X_{21}}{2A}(4\xi_3 - 1) + V_4 \frac{4}{2A}(\xi_2 X_{32} + \xi_1 X_{13}) + V_5 \frac{4}{2A}(\xi_3 X_{13} + \xi_2 X_{21}) \\
&\quad + V_6 \frac{4}{2A}(\xi_1 X_{21} + \xi_3 X_{32})]
\end{aligned}
$$

$$
\begin{aligned}
B_{3,15} &= 2K_{X\bar{Y}} \cdot 4\xi_2\xi_3 + \frac{4}{2A}(\xi_3 Y_{31} + \xi_2 Y_{12})[W_1 \frac{X_{32}}{2A}(4\xi_1 - 1) + W_2 \frac{X_{13}}{2A}(4\xi_2 - 1) \\
&\quad + W_3 \frac{X_{21}}{2A}(4\xi_3 - 1) + W_4 \frac{4}{2A}(\xi_2 X_{32} + \xi_1 X_{13}) + W_5 \frac{4}{2A}(\xi_3 X_{13} + \xi_2 X_{21}) \\
&\quad + W_6 \frac{4}{2A}(\xi_1 X_{21} + \xi_3 X_{32})]
\end{aligned}
$$

$$
\begin{aligned}
B_{3,16} &= \frac{4}{2A}(\xi_1 X_{21} + \xi_3 X_{32}) + \frac{4}{2A}(\xi_1 Y_{12} + \xi_3 Y_{23})[U_1 \frac{X_{32}}{2A}(4\xi_1 - 1) + U_2 \frac{X_{13}}{2A}(4\xi_2 - 1) \\
&\quad + U_3 \frac{X_{21}}{2A}(4\xi_3 - 1) + U_4 \frac{4}{2A}(\xi_2 X_{32} + \xi_1 X_{13}) + U_5 \frac{4}{2A}(\xi_3 X_{13} + \xi_2 X_{21}) \\
&\quad + U_6 \frac{4}{2A}(\xi_1 X_{21} + \xi_3 X_{32})]
\end{aligned}
$$

$$\begin{aligned} B_{3,17} &= \frac{4}{2A}(\xi_1 Y_{12}+\xi_3 Y_{23})+\frac{4}{2A}(\xi_1 Y_{12}+\xi_3 Y_{23})[V_1\frac{X_{32}}{2A}(4\xi_1-1)+V_2\frac{X_{13}}{2A}(4\xi_2-1) \\ &+V_3\frac{X_{21}}{2A}(4\xi_3-1)+V_4\frac{4}{2A}(\xi_2 X_{32}+\xi_1 X_{13})+V_5\frac{4}{2A}(\xi_3 X_{13}+\xi_2 X_{21}) \\ &+V_6\frac{4}{2A}(\xi_1 X_{21}+\xi_3 X_{32})] \end{aligned}$$

$$\begin{aligned} B_{3,18} &= 2K_{X\bar{Y}}\cdot 4\xi_3\xi_1+\frac{4}{2A}(\xi_1 Y_{12}+\xi_3 Y_{23})[W_1\frac{X_{32}}{2A}(4\xi_1-1)+W_2\frac{X_{13}}{2A}(4\xi_2-1) \\ &+W_3\frac{X_{21}}{2A}(4\xi_3-1)+W_4\frac{4}{2A}(\xi_2 X_{32}+\xi_1 X_{13})+W_5\frac{4}{2A}(\xi_3 X_{13}+\xi_2 X_{21}) \\ &+W_6\frac{4}{2A}(\xi_1 X_{21}+\xi_3 X_{32})] \end{aligned}$$

B.2 Appendix B2: G matrix in LST formulation element

G is a 6×18 matrix,the non-zero terms of G are:

$$G_{1,1}=\frac{Y_{23}}{2A}(4\xi_1-1),\ G_{1,4}=\frac{Y_{31}}{2A}(4\xi_2-1),\ G_{1,7}=\frac{Y_{12}}{2A}(4\xi_3-1)$$

$$G_{1,10}=\frac{2}{A}(\xi_2 Y_{23}+\xi_1 Y_{31}), G_{1,13}=\frac{2}{A}(\xi_3 Y_{31}+\xi_2 Y_{12}), G_{1,16}=\frac{2}{2A}(\xi_1 Y_{12}+\xi_3 Y_{23})$$

$$G_{2,2}=\frac{Y_{23}}{2A}(4\xi_1-1),\ G_{2,5}=\frac{Y_{31}}{2A}(4\xi_2-1),\ G_{2,8}=\frac{Y_{12}}{2A}(4\xi_3-1)$$

$$G_{2,11}=\frac{2}{A}(\xi_2 Y_{23}+\xi_1 Y_{31}), G_{2,14}=\frac{2}{A}(\xi_3 Y_{31}+\xi_2 Y_{12}), G_{2,17}=\frac{2}{2A}(\xi_1 Y_{12}+\xi_3 Y_{23})$$

$$G_{3,3}=\frac{Y_{23}}{2A}(4\xi_1-1),\ G_{3,6}=\frac{Y_{31}}{2A}(4\xi_2-1),\ G_{3,9}=\frac{Y_{12}}{2A}(4\xi_3-1)$$

$$G_{3,12}=\frac{2}{A}(\xi_2 Y_{23}+\xi_1 Y_{31}), G_{3,15}=\frac{2}{A}(\xi_3 Y_{31}+\xi_2 Y_{12}), G_{3,18}=\frac{2}{2A}(\xi_1 Y_{12}+\xi_3 Y_{23})$$

$$G_{4,1}=\frac{X_{32}}{2A}(4\xi_1-1),\ G_{4,4}=\frac{X_{13}}{2A}(4\xi_2-1),\ G_{4,7}=\frac{X_{21}}{2A}(4\xi_3-1)$$

$$G_{4,10}=\frac{2}{A}(\xi_2 X_{32}+\xi_1 X_{13}), G_{4,13}=\frac{2}{A}(\xi_3 X_{13}+\xi_2 X_{21}), G_{4,16}=\frac{2}{2A}(\xi_1 X_{21}+\xi_3 X_{32})$$

$$G_{5,2} = \frac{X_{32}}{2A}(4\xi_1 - 1),\ G_{5,5} = \frac{X_{13}}{2A}(4\xi_2 - 1),\ G_{5,8} = \frac{X_{21}}{2A}(4\xi_3 - 1)$$

$$G_{5,11} = \frac{2}{A}(\xi_2 X_{32} + \xi_1 X_{13}), G_{5,14} = \frac{2}{A}(\xi_3 X_{13} + \xi_2 X_{21}), G_{5,17} = \frac{2}{2A}(\xi_1 X_{21} + \xi_3 X_{32})$$

$$G_{6,3} = \frac{X_{32}}{2A}(4\xi_1 - 1),\ G_{6,6} = \frac{X_{13}}{2A}(4\xi_2 - 1),\ G_{6,9} = \frac{X_{21}}{2A}(4\xi_3 - 1)$$

$$G_{6,12} = \frac{2}{A}(\xi_2 X_{32} + \xi_1 X_{13}), G_{6,15} = \frac{2}{A}(\xi_3 X_{13} + \xi_2 X_{21}), G_{6,18} = \frac{2}{2A}(\xi_1 X_{21} + \xi_3 X_{32})$$

B.3 Transformation between different coordinate systems

From the surface model of fabric strcture,al the node coordinates of element in the global coordinate system can be obtained.

assume a 6-nodes triangular element with six nodes :

$1(x_1, y_1, z_1),\ 2(x_1, y_1, z_1),\ 3(x_3, y_3, z_3),\ 4(x_4, y_4, z_4),\ 5(x_5, y_5, z_5),\ 6(x_6, y_6, z_6)$

The first step is to create a plane local coordinate system $\overline{OXYZ}$,the plane is decided by nodes 1,2,3

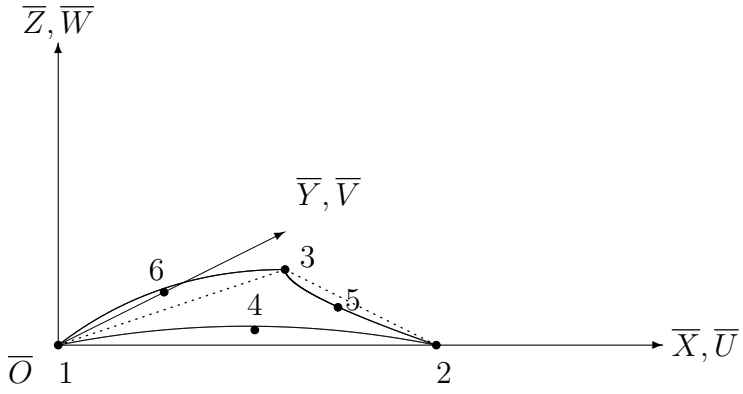

Figure B.1: Local Plane Co-ordinate System

$\overline{X}$ axis is aligned with the side 1-2,then vector $\vec{\overline{X}}$ in global coordinate system oxyz is:

$$\vec{\overline{X}} = (x_2 - x_1)i + (x_2 - y_1)j + (z_2 - z_1)k$$

because $\vec{\overline{Y}}$ axis is normal to $\vec{\overline{X}}$ axis and pass the node $1(\overline{X}_1, \overline{Y}_1, \overline{Z}_1)$, and in the plane $\overline{OXY}$,so we can assume:

$$\vec{\overline{Y}} = x_b \cdot i + y_b \cdot i + z_b \cdot i$$

while the plane made of nodes 1,2,3 could be derived by:

$$\vec{12} = \{x_2 - x_1, y_2 - y_1, z_2 - z_1\}$$

$$\vec{13} = \{x_3 - x_1, y_3 - y_1, z_3 - z_1\}$$

$$\begin{aligned} n &= \vec{12} \times \vec{13} = \begin{vmatrix} i & j & k \\ x_2 - x_1 & y_2 - y_1 & z_2 - z_1 \\ x_3 - x_1 & y_3 - y_1 & z_3 - z_1 \end{vmatrix} \\ &= \{(y_2 - y_1)(z_3 - z_1) - (z_2 - z_1)(y_3 - y_1)\} \cdot i \\ &\quad - \{(x_2 - x_1)(z_3 - z_1) - (z_2 - z_1)(x_3 - x_1)\} \cdot j \\ &\quad + \{(x_2 - x_1)(y_3 - y_1) - (y_2 - y_1)(x_3 - x_1)\} k \\ &= \lambda_1 \cdot i + \lambda_2 \cdot j + \lambda_3 \cdot k \end{aligned}$$

the $\overline{OXYZ}$ plane equation is:

$$\lambda_1(x - x_1) + \lambda_2(y - y_1) + \lambda_3(z - z_1) = 0$$

we assume a point $P(x_p, y_p, z_p)$ in $\overline{Y}$ axis

and $\overline{3 - P}$ normal to $\overline{1 - 3}$

then $\vec{\overline{Y}} = (x_p - x_1)i + (y_p - y_1)j + (z_p - z_1)k = b_x \cdot i + b_y \cdot j + b_z \cdot k$

and

$$(x_p - x_3)(x_3 - x_1) + (y_p - y_3)(y_3 - y_1) + (z_p - z_1) = 0$$

because $\overline{Y}$ normal to $\overline{X}$

then

$$\overline{X} \cdot \overline{Y} = 0$$

that is:

$$(x_2 - x_1)(x_p - x_1) + (y_2 - y_1)(y_p - y_1) + (z_2 - z_1)(z_p - z_1) = 0$$

then we have to solve equation array

$$\begin{array}{ccccccc} (x_2 - x_1)(x_p - x_1) & + & (y_2 - y_1)(y_p - y_1) & + & (z_2 - z_1)(z_p - z_1) & = & 0 \\ \lambda_1(x_p - x_1) & + & \lambda_2(y_p - y_1) & + & \lambda_3(z_p - z_1) & = & 0 \\ (x_3 - x_1)(x_p - x_3) & + & (y_3 - y_1)(y_p - y_1) & + & (z_3 - z_1)(z_p - z_1) & = & 0 \end{array}$$

then we can get :

$$\vec{\overline{Y}} = b_x \cdot i + b_y \cdot j + b_z \cdot k$$

another axis $\overline{Z}$ in $\overline{OXYZ}$ has:

$$\begin{aligned} \vec{\overline{Z}} &= \vec{\overline{X}} \times \vec{\overline{Y}} \\ &= \begin{vmatrix} i & j & k \\ a_x & a_y & a_z \\ b_x & b_y & b_z \end{vmatrix} \\ &= (a_y b_z - a_z b_y)i - (a_x b_z - a_z b_x)j + (a_x b_y - a_y b_x)k \\ &= c_x \cdot i + c_y \cdot j + c_z \cdot k \end{aligned}$$

The cosines between $\overline{X}, \overline{Y}, \overline{Z}$ and x, y, z is :

	$\overline{X}$	$\overline{Y}$	$\overline{Z}$
x	l_1	m_1	n_1
y	l_2	m_1	n_1
z	l_3	m_3	n_3

For the coordinate system $\overline{OXYZ}$
vector $\vec{\overline{X}}$,$\vec{\overline{Y}}$,$\vec{\overline{Z}}$ has :

$$\vec{\overline{X}} = a_x \cdot i + a_y \cdot j + a_z \cdot k$$

$$\vec{\overline{Y}} = b_x \cdot i + b_y \cdot j + b_z \cdot k$$

$$\vec{\overline{Z}} = b_x \cdot i + a_y \cdot j + b_z \cdot k$$

then :

$$l_1 = \frac{a_x}{\sqrt{a_x^2 + a_y^2 + a_z^2}}, l_2 = \frac{a_y}{\sqrt{a_x^2 + a_y^2 + a_z^2}}, l_3 = \frac{a_z}{\sqrt{a_x^2 + a_y^2 + a_z^2}}$$

$$m_1 = \frac{b_x}{\sqrt{b_x^2 + b_y^2 + b_z^2}}, m_2 = \frac{b_y}{\sqrt{b_x^2 + b_y^2 + b_z^2}}, m_3 = \frac{b_z}{\sqrt{b_x^2 + b_y^2 + b_z^2}}$$

$$n_1 = \frac{c_x}{\sqrt{c_x^2 + c_y^2 + c_z^2}}, n_2 = \frac{c_y}{\sqrt{c_x^2 + c_y^2 + c_z^2}}, n_3 = \frac{c_z}{\sqrt{c_x^2 + c_y^2 + c_z^2}}$$

Transformation matrix for node coordinates is

$$\begin{Bmatrix} x_i \\ y_i \\ z_i \end{Bmatrix} = \begin{bmatrix} l_1 & m_1 & n_1 \\ l_2 & m_2 & n_2 \\ l_3 & m_3 & n_3 \end{bmatrix} \cdot \begin{Bmatrix} \overline{X}_i \\ \overline{Y}_i \\ \overline{Z}_i \end{Bmatrix}$$

or

$$\begin{Bmatrix} x_i \\ y_i \\ z_i \end{Bmatrix} = [\Lambda_r] \cdot \begin{Bmatrix} \overline{X}_i \\ \overline{Y}_i \\ \overline{Z}_i \end{Bmatrix}$$

in which

$$[\Lambda_r] = \begin{bmatrix} l_1 & m_1 & n_1 \\ l_2 & m_2 & n_2 \\ l_3 & m_3 & n_3 \end{bmatrix}$$

and $i = 1 \rightarrow 6$

We assume the curved surface can be presented by equation:

$$\overline{Z} = a_1 + a_2\overline{X} + a_3\overline{Y} + a_4\overline{X}^2 + a_5\overline{XY} + a_6\overline{y}^2$$

input coordinates of 6 nodes,we can get equation array:

$$\begin{bmatrix} 1 & \overline{X}_1 & \overline{Y}_1 & \overline{X}_1^2 & \overline{X}_1\overline{Y}_1 & \overline{Y}_1^2 \\ 1 & \overline{X}_2 & \overline{Y}_2 & \overline{X}_2^2 & \overline{X}_2\overline{Y}_2 & \overline{Y}_2^2 \\ 1 & \overline{X}_3 & \overline{Y}_3 & \overline{X}_3^2 & \overline{X}_3\overline{Y}_3 & \overline{Y}_3^2 \\ 1 & \overline{X}_4 & \overline{Y}_4 & \overline{X}_4^2 & \overline{X}_4\overline{Y}_4 & \overline{Y}_4^2 \\ 1 & \overline{X}_5 & \overline{Y}_5 & \overline{X}_5^2 & \overline{X}_5\overline{Y}_5 & \overline{Y}_5^2 \\ 1 & \overline{X}_6 & \overline{Y}_6 & \overline{X}_6^2 & \overline{X}_6\overline{Y}_6 & \overline{Y}_6^2 \end{bmatrix} \cdot \begin{Bmatrix} a_1 \\ a_2 \\ a_3 \\ a_4 \\ a_5 \\ a_6 \end{Bmatrix} = \begin{Bmatrix} \overline{Z}_1 \\ \overline{Z}_2 \\ \overline{Z}_3 \\ \overline{Z}_4 \\ \overline{Z}_5 \\ \overline{Z}_6 \end{Bmatrix}$$

or

$$[\overline{A}] \cdot \{a\} = \{\overline{Z}\}$$

so

$$\{a\} = [\overline{A}]^{-1}\{\overline{Z}\}$$

because in the curved surface of the element,the nodal coordinates are the curved length between nodes and original point along the curved axis,so we have so

$$\begin{aligned} X &= \int_0^{\overline{X}} \sqrt{1+(\frac{\partial \overline{Z}}{\partial \overline{X}})^2} \quad d\overline{X} \\ &= \int_0^{\overline{X}} \sqrt{1+(a_2+2a_4\overline{X}+a_5\overline{Y})^2} \quad d\overline{X} \\ &= (\frac{a_2+a_5\overline{Y}}{4a_4}+\frac{\overline{X}}{2})\cdot\sqrt{1+(a_2+2a_4\overline{X}+a_5\overline{Y})^2}+\frac{arcsinh(a_2+2a_4\overline{X}+a_5\overline{Y})}{4a_4} \end{aligned}$$

$$\begin{aligned} Y &= \int_0^{\overline{Y}} \sqrt{1+(\frac{\partial \overline{Z}}{\partial \overline{Y}})^2} \quad d\overline{Y} \\ &= \int_0^{\overline{Y}} \sqrt{1+(a_3+a_5\overline{X}+2a_6\overline{Y})} \quad d\overline{Y} \\ &= (\frac{a_3+a_5\overline{X}}{4a_6}+\frac{\overline{Y}}{2})\cdot\sqrt{1+(a_3+a_5\overline{X}+2a_6\overline{Y})^2}+\frac{arcsinh(a_3+a_5\overline{X}+2a_6\overline{Y})}{4a_6} \end{aligned}$$

$$\begin{Bmatrix} \overline{U} \\ \overline{V} \\ \overline{W} \end{Bmatrix} = \overline{T}^c \begin{Bmatrix} U \\ V \\ W \end{Bmatrix}$$

where

$$\overline{T}^c = \begin{bmatrix} \frac{1}{\sqrt{1+(\frac{\partial \overline{Z}}{\partial \overline{X}})^2}} & 0 & \frac{-\frac{\partial \overline{Z}}{\partial \overline{X}}}{\sqrt{1+(\frac{\partial \overline{Z}}{\partial \overline{X}})^2}} \\ 0 & \frac{1}{\sqrt{1+(\frac{\partial \overline{Z}}{\partial \overline{Y}})^2}} & \frac{-\frac{\partial \overline{Z}}{\partial \overline{Y}}}{\sqrt{1+(\frac{\partial \overline{Z}}{\partial \overline{Y}})^2}} \\ \frac{\frac{\partial \overline{Z}}{\partial \overline{X}}}{\sqrt{1+(\frac{\partial \overline{Z}}{\partial \overline{X}})^2}} & \frac{\frac{\partial \overline{Z}}{\partial \overline{Y}}}{\sqrt{1+(\frac{\partial \overline{Z}}{\partial \overline{Y}})^2}} & \frac{1}{\sqrt{1+(\frac{\partial \overline{Z}}{\partial \overline{X}})^2+(\frac{\partial \overline{Z}}{\partial \overline{Y}})^2}} \end{bmatrix}$$

then

$$\begin{Bmatrix} U_i \\ V_i \\ W_i \end{Bmatrix} = [\Lambda_r]^{-1}\cdot[\overline{T}^c]_i^{-1} \begin{Bmatrix} u_i \\ v_i \\ w_i \end{Bmatrix} = [T_g]_i \cdot \begin{Bmatrix} u_i \\ v_i \\ w_i \end{Bmatrix}$$

so the final transformation matrix is:

$$[T_G] = \begin{bmatrix} [T_g]_1 & 0 & 0 & 0 & 0 & 0 \\ 0 & [T_g]_2 & 0 & 0 & 0 & 0 \\ 0 & 0 & [T_g]_3 & 0 & 0 & 0 \\ 0 & 0 & 0 & [T_g]_4 & 0 & 0 \\ 0 & 0 & 0 & 0 & [T_g]_5 & 0 \\ 0 & 0 & 0 & 0 & 0 & [T_g]_6 \end{bmatrix}$$

act on $\{u_1\ v_1\ w_1\ u_2\ v_2\ w_2\ u_3\ v_3\ w_3\ u_4\ v_4\ w_4\ u_5\ v_5\ w_5\ u_6\ v_6\ w_6\ \}$

in which $[T_g]_i = [\Lambda_r]^{-1} \cdot [T_c]_i^{-1}$

Example

The surface of the fabric structure in the global coordinate system could be expressed by $z = x^2$

with boundary $-10 \leq x \leq 10$ and $-5 \leq y \leq 5$

one curved element with 6-nodes

$$\begin{array}{cc} 1(0,0,0) & 4(1,-0.5,1) \\ 2(2,-1,4) & 5(1.5,0,2.25) \\ 3(1,1,1) & 6(0.5,0.5.0.25) \end{array}$$

then build the first Local Plane Coordinate System,and the plane is decided by node 1,2,3

vector

$$\begin{aligned} \vec{12} &= \{x_2 - x_1, y_2 - y_1, z_2 - z_1\} \\ &\quad \{2,-1,4\} \end{aligned}$$

$$\begin{aligned} \vec{13} &= \{x_3 - x_1, y_3 - y_1, z_3 - z_1\} \\ &\quad \{1,1,1\} \end{aligned}$$

$$n = \vec{12} \times \vec{13} = \begin{vmatrix} i & j & k \\ 2 & -1 & 4 \\ 1 & 1 & 1 \end{vmatrix} = -5i + 2j + 3k$$

Then the $\overline{OXYZ}$ plane equation is:

$$-5(x - x_1) + 2(y - y_2) + 3(z - z_1) = 0$$

because $x_1 = y_1 = z_1 = 0$
then the equation is:

$$-5x + 2y + 3z = 0 \tag{B.17}$$

assume there is a point $P(x_p, y_p, z_p)$ has $\vec{P1} \perp \vec{12}$ and $\vec{P3} \perp \vec{13}$

while

$$\begin{aligned} \vec{P1} &= (x_p - x_1)i + (y_p - y_1)j + (z_p - z_1)k \\ &= x_p \cdot i + y_p \cdot j + z_p \cdot k \\ &= b_x \cdot i + b_y \cdot j + b_z \cdot k \end{aligned}$$

$$\begin{aligned} \vec{P3} &= (x_p - x_3)i + (y_p - y_3)j + (z_p - z_3)k \\ &= (x_p - 1) \cdot i + (y_p - 1) \cdot j + (z_p - 1) \cdot k \end{aligned}$$

$$\begin{aligned} \vec{13} &= (x_3 - x_1)i + (y_3 - y_1)j + (z_3 - z_1)k \\ &= x_3 \cdot i + y_3 \cdot j + z_3 \cdot k \\ &= i \ + \ j \ + k \end{aligned}$$

For$\vec{P3} \perp \vec{13}$, we have$\vec{P3} \cdot \vec{13} = 0$

$$(x_p - 1) + (y_p - 1) + (z_p - 1) = 0$$

$$x_p + y_p + z_p = 3 \tag{B.18}$$

For $\vec{P1} \perp \vec{12}$

$$\begin{aligned} \vec{12} &= (x_2 - x_1)i + (y_2 - y_1)j + (z_2 - z_1)k \\ &\quad 2i \ - j \ + 4k \end{aligned}$$

$$\vec{P1} \cdot \vec{12} = 0$$

that is:

$$2x_p - y_p + 4z_p = 0 \tag{B.19}$$

solve the equation array (1) (2) (3)

we can get

$$x_p = 0.868, y_p = 2.052, z_p = 0.079$$

Then we can get:

$$\begin{aligned} \vec{\overline{X}} = \vec{12} &= a_x \cdot i + a_y \cdot j + a_z \cdot k \\ &(x_2 - x_1)i + (y_2 - y_1)j + (z_2 - z_1)k \\ &2i \ - \ j \ + \ 4k \end{aligned}$$

$$\begin{aligned} \vec{\overline{Y}} = \vec{1P} &= b_x \cdot i + b_y \cdot j + b_z \cdot k \\ &(x_P - x_1)i + (y_P - y_1)j + (z_P - z_1)k \\ &0.868i \ - \ 2.053j \ + \ 0.079k \end{aligned}$$

$$\begin{aligned} \vec{\overline{Z}} &= \vec{12} \times \vec{13} \\ &c_x \cdot i + c_y \cdot j + c_z \cdot k \\ &-5i \ + \ 2j \ + \ 3k \end{aligned}$$

then

$$l_1 = \frac{a_x}{\sqrt{a_x^2 + a_y^2 + a_z^2}} = \frac{2}{\sqrt{2^2 + 1^2 + 4^2}} = 0.436$$

$$l_2 = \frac{a_y}{\sqrt{a_x^2 + a_y^2 + a_z^2}} = \frac{-1}{\sqrt{2^2 + 1^2 + 4^2}} = -0.218$$

$$l_3 = \frac{a_z}{\sqrt{a_x^2 + a_y^2 + a_z^2}} = \frac{4}{\sqrt{2^2 + 1^2 + 4^2}} = 0.872$$

$$m_1 = \frac{b_x}{\sqrt{b_x^2 + b_y^2 + b_z^2}} = \frac{0.868}{\sqrt{0.868^2 + 2.053^2 + 0.079^2}} = 0.389$$

$$m_2 = \frac{b_y}{\sqrt{b_x^2 + b_y^2 + b_z^2}} = \frac{2.053}{\sqrt{0.868^2 + 2.053^2 + 0.079^2}} = 0.389$$

$$m_3 = \frac{b_x}{\sqrt{b_x^2 + b_y^2 + b_z^2}} = \frac{0.079}{\sqrt{0.868^2 + 2.053^2 + 0.079^2}} = 0.035$$

$$n_1 = \frac{c_x}{\sqrt{c_x^2 + c_y^2 + c_z^2}} = \frac{-5}{\sqrt{(-5)^2 + 2^2 + 3^2}} = -0.812$$

$$n_2 = \frac{c_y}{\sqrt{c_x^2 + c_y^2 + c_z^2}} = \frac{2}{\sqrt{(-5)^2 + 2^2 + 3^2}} = 0.325$$

$$n_3 = \frac{c_z}{\sqrt{c_x^2 + c_y^2 + c_z^2}} = \frac{3}{\sqrt{(-5)^2 + 2^2 + 3^2}} = 0.487$$

$$[\Lambda_r] = \begin{bmatrix} l_1 & m_1 & n_1 \\ l_2 & m_2 & n_2 \\ l_3 & m_3 & n_3 \end{bmatrix} = \begin{bmatrix} 0.436 & 0.389 & -0.812 \\ -0.218 & 0.921 & 0.325 \\ 0.878 & 0.033 & 0.487 \end{bmatrix}$$

$$\begin{Bmatrix} x_i - x_o \\ y_i - y_o \\ z_i - z_o \end{Bmatrix} = [\Lambda_r] \begin{Bmatrix} \overline{X}_i \\ \overline{Y}_i \\ \overline{Z}_i \end{Bmatrix}$$

so

$$\begin{Bmatrix} \overline{X}_i \\ \overline{Y}_i \\ \overline{Z}_i \end{Bmatrix} = [\Lambda_r] \begin{Bmatrix} x_i - x_o \\ y_i - y_o \\ z_i - z_o \end{Bmatrix}$$

in which ,$x_o, y_o, z_o$is the coordinate of point $\overline{O}$ in global coordinate system and $i = 1 \rightarrow 6$ then we can get coordinates of 6 nodes in the $\overline{OXYZ}$ coordinate system

$\overline{X}_1 = \overline{Y}_1 = \overline{Z}_1 = 0$

$\overline{X}_2 = 4.587, \overline{Y}_2 = 0, \overline{Z}_2 = 0$

$\overline{X}_3 = 1.095, \overline{Y}_3 = 1.345, \overline{Z}_3 = 0$

$\overline{X}_4 = 1.419, \overline{Y}_4 = -0.035, \overline{Z}_4 = -0.486$

$\overline{X}_5 = 2.622, \overline{Y}_5 = 0.633, \overline{Z}_4 = -0.121$

$\overline{X}_6 = 0.329, \overline{Y}_4 = 0.663, \overline{Z} - 4 = -0.121$

then

$$\overline{Z} = a_1 + a_2\overline{X} + a_3\overline{Y} + a_4\overline{X}^2 + a_5\overline{XY} + a_6\overline{Y}^2$$

can be satisfied by these 6 nodes, so we have:

$$[\overline{A}] \cdot \{a\} = \left\{\overline{Z}\right\}$$

$$[\overline{A}] = \begin{bmatrix} 1 & \overline{X}_1 & \overline{Y}_1 & \overline{X}_1^2 & \overline{X}_1\overline{Y}_1 & \overline{Y}_1^2 \\ 1 & \overline{X}_2 & \overline{Y}_2 & \overline{X}_2^2 & \overline{X}_2\overline{Y}_2 & \overline{Y}_2^2 \\ 1 & \overline{X}_3 & \overline{Y}_3 & \overline{X}_3^2 & \overline{X}_3\overline{Y}_3 & \overline{Y}_3^2 \\ 1 & \overline{X}_4 & \overline{Y}_4 & \overline{X}_4^2 & \overline{X}_4\overline{Y}_4 & \overline{Y}_4^2 \\ 1 & \overline{X}_5 & \overline{Y}_5 & \overline{X}_5^2 & \overline{X}_5\overline{Y}_5 & \overline{Y}_5^2 \\ 1 & \overline{X}_6 & \overline{Y}_6 & \overline{X}_6^2 & \overline{X}_6\overline{Y}_6 & \overline{Y}_6^2 \end{bmatrix}$$

$$= \begin{bmatrix} 1 & 0 & 0 & 0 & 0 & 0 \\ 1 & 4.587 & 0 & 21.041 & 0 & 0 \\ 1 & 1.095 & 1.345 & 1.199 & 1.473 & 1.809 \\ 1 & 1.419 & -0.035 & 2.014 & -0.050 & 0.001 \\ 1 & 2.622 & 0.663 & 6.875 & 1.738 & 0.440 \\ 1 & 0.329 & 0.663 & 0.108 & 0.218 & 0.44 \end{bmatrix}$$

then we can solve that equation to get:

$$[a] = \begin{Bmatrix} a_1 \\ a_2 \\ a_3 \\ a_4 \\ a_5 \\ a_6 \end{Bmatrix} = \begin{Bmatrix} 0 \\ -0.492 \\ -0.345 \\ 0.107 \\ 0.324 \\ 0.219 \end{Bmatrix}$$

then

$$\overline{Z} = -0.492\overline{X} - 0.345\overline{Y} + 0.107\overline{X}^2 + 0.324\overline{XY} + 0.219\overline{Y}^2$$

so

$$\frac{\partial \overline{Z}}{\partial \overline{Y}} = a_2 + 2a_4\overline{X} + a_5\overline{Y} = -0.492 + 0.213\overline{X} + 0.324\overline{Y}$$

$$\frac{\partial \overline{Z}}{\partial \overline{X}} = a_3 + a_5\overline{X} + 2a_6\overline{Y} = -0.345 + 0.324\overline{X} + 0.438\overline{Y}$$

then

$$\begin{Bmatrix} \overline{U} \\ \overline{V} \\ \overline{W} \end{Bmatrix} = [\overline{T}^c] \begin{Bmatrix} U \\ V \\ W \end{Bmatrix}$$

in which

$$\overline{T}^c = \begin{bmatrix} \frac{1}{\sqrt{1+(\frac{\partial \overline{Z}}{\partial \overline{X}})^2}} & 0 & \frac{-\frac{\partial \overline{Z}}{\partial \overline{X}}}{\sqrt{1+(\frac{\partial \overline{Z}}{\partial \overline{X}})^2}} \\ 0 & \frac{1}{\sqrt{1+(\frac{\partial \overline{Z}}{\partial \overline{Y}})^2}} & \frac{-\frac{\partial \overline{Z}}{\partial \overline{Y}}}{\sqrt{1+(\frac{\partial \overline{Z}}{\partial \overline{Y}})^2}} \\ \frac{\frac{\partial \overline{Z}}{\partial \overline{X}}}{\sqrt{1+(\frac{\partial \overline{Z}}{\partial \overline{X}})^2}} & \frac{\frac{\partial \overline{Z}}{\partial \overline{Y}}}{\sqrt{1+(\frac{\partial \overline{Z}}{\partial \overline{Y}})^2}} & \frac{1}{\sqrt{1+(\frac{\partial \overline{Z}}{\partial \overline{X}})^2+(\frac{\partial \overline{Z}}{\partial \overline{Y}})^2}} \end{bmatrix}$$

so

$$\begin{Bmatrix} U \\ V \\ W \end{Bmatrix} = [\overline{T}^c]^{-1} \begin{Bmatrix} \overline{U} \\ \overline{V} \\ \overline{W} \end{Bmatrix}$$

substituting node coordinates in $\overline{OXYZ}$
then get:

$$[\overline{T}^c]_1 = \begin{bmatrix} 0.898 & 0 & 0.442 \\ 0 & 0.954 & 0.329 \\ -0.442 & 0.349 & 0.857 \end{bmatrix}$$

$$[\overline{T}^c]_2 = \begin{bmatrix} 0.898 & 0 & -0.440 \\ 0 & 0.659 & -0.752 \\ 0.440 & 0..752 & 0.627 \end{bmatrix}$$

$$[\overline{T}^c]_3 = \begin{bmatrix} 0.984 & 0 & -0.175 \\ 0 & 0.858 & -0.514 \\ 0.175 & 0.514 & 0.0.848 \end{bmatrix}$$

$$[\overline{T}^c]_4 = \begin{bmatrix} 0.98 & 0 & 0.196 \\ 0 & 0.995 & 0.099 \\ -0.196 & -0.099 & 0.976 \end{bmatrix}$$

$$[\overline{T}^c]_5 = \begin{bmatrix} 0.962 & 0 & -0.273 \\ 0 & 0.782 & 0.622 \\ 0.273 & -0.622 & 0.627 \end{bmatrix}$$

$$[\overline{T}^c]_6 = \begin{bmatrix} 0.980 & 0 & -0.203 \\ 0 & 0.999 & -0.052 \\ -0.203 & 0.052 & 0.978 \end{bmatrix}$$

then

$$\begin{Bmatrix} U_i \\ V_i \\ W_i \end{Bmatrix} = [\Lambda_r]^{-1} \cdot [\overline{T}^c]_i^{-1} \begin{Bmatrix} u_i \\ v_i \\ w_i \end{Bmatrix} = [T_g]_i \cdot \begin{Bmatrix} u_i \\ v_i \\ w_i \end{Bmatrix}$$

so the final transformation matrix is:

$$[T_G] = \begin{bmatrix} [T_g]_1 & 0 & 0 & 0 & 0 & 0 \\ 0 & [T_g]_2 & 0 & 0 & 0 & 0 \\ 0 & 0 & [T_g]_3 & 0 & 0 & 0 \\ 0 & 0 & 0 & [T_g]_4 & 0 & 0 \\ 0 & 0 & 0 & 0 & [T_g]_5 & 0 \\ 0 & 0 & 0 & 0 & 0 & [T_g]_6 \end{bmatrix}$$

act on $\{u_1\ v_1\ w_1\ u_2\ v_2\ w_2\ u_3\ v_3\ w_3\ u_4\ v_4\ w_4\ u_5\ v_5\ w_5\ u_6\ v_6\ w_6\ \}$

in which $[T_g]_i = [\Lambda_r]^{-1} \cdot [T_c]_i^{-1}$

$$[\overline{T}^g]_1 = \begin{bmatrix} 0.394 & 0.324 & 0.056 \\ 0.794 & 0.654 & 0.113 \\ -0.145 & -0.119 & -0.02 \end{bmatrix}$$

$$[\overline{T}^g]_2 = \begin{bmatrix} 0.701 & -0.279 & 0.682 \\ 1.413 & -0.562 & 1.375 \\ -0.258 & 0.103 & -0.251 \end{bmatrix}$$

$$[\overline{T}^g]_3 = \begin{bmatrix} 0.247 & 0.088 & 0.493 \\ 0.498 & 0.178 & 0.993 \\ -0.091 & -0.033 & -0.181 \end{bmatrix}$$

$$[\overline{T}^g]_4 = \begin{bmatrix} 0.381 & 0.353 & 0.225 \\ 0.768 & 0.712 & 0.453 \\ -0.14 & -0.13 & -0.083 \end{bmatrix}$$

$$[\overline{T}^g]_5 = \begin{bmatrix} 0.304 & 0.527 & 0.134 \\ 0.613 & 1.063 & 0.27 \\ -0.112 & -0.194 & -0.049 \end{bmatrix}$$

$$[\overline{T}^g]_6 = \begin{bmatrix} 0.295 & 0.319 & 0.195 \\ 0.596 & 0.644 & 0.393 \\ -0.109 & -0.118 & -0.072 \end{bmatrix}$$

Use the formulation

$$X = \int_0^{\overline{X}} 1 - \frac{\partial^2 \overline{Z}}{\partial \overline{X}} \cdot \overline{Z} d\overline{X}$$

$$= \int_0^{\overline{X}} (1 - 2a_4)(a_1 + a_2\overline{X} + a_3\overline{Y} + a_4\overline{X}^2 + a_5\overline{XY} + a_6\overline{Y}^2) d\overline{X}$$

$$= \overline{X} - 2a_4(\frac{1}{2}a_2\overline{X}^2 + a_3\overline{XY} + \frac{1}{3}a_4\overline{X}^3 + \frac{1}{2}a_5\overline{X}^2\overline{Y} + a_6\overline{XY}^2)$$

$$Y = \int_0^{\overline{Y}} (1 - 2a_5)(a_1 + a_2\overline{X} + a_3\overline{Y} + a_4\overline{X}^2 + a_5\overline{XY} + a_6\overline{Y}^2 d\overline{Y}$$

$$= \overline{Y} - 2a_6(a_2\overline{XY} + \frac{1}{2}a_3\overline{Y}^2 + a_4\overline{X}^2\overline{Y} + \frac{1}{2}a_5\overline{XY}^2 + \frac{1}{3}a_6\overline{Y}^3$$

we can get node coordinates in the OXYZ coordinate system, because all the nodes are in the surface plane,so $Z_i = 0$,$i = 1 \rightarrow 6$

$$X_1 = Y_1 = 0$$

$$X_2 = 4.958, Y_2 = 0$$

$$X_3 = 1.108, Y_3 = 1.505$$

$$X_4 = 1.502, Y_4 = -0.042$$

$$X_5 = 2.848, Y_5 = 0.766$$

$$X_3 = 0.338, Y_3 = 0.724$$

Appendix C

Derivations of Reliability Formulations

C.1 Appendix C1:Derivation of principal curvatures

Suppose the element surface can be expressed as the equation:

$$\overline{Z} = \overline{Z}(\overline{X}, \overline{Y}) = a_1 + a_2\overline{X} + a_3\overline{Y} + a_4\overline{X}^2 + a_5\overline{XY} + a_6\overline{Y}^2$$

and the element curvatures are:

$$K_{\overline{X}} = -2\frac{\partial^2\overline{Z}}{\partial\overline{X}^2} = -2a_4, \quad , K_{\overline{Y}} = -2\frac{\partial^2\overline{Z}}{\partial\overline{Y}^2} = -2a_6, \quad , K_{\overline{XY}} = -\frac{\partial\overline{Z}^2}{\partial\overline{X}\partial\overline{Y}} = -a_5$$

Assume there is another co-ordinate system $\overline{X'Y'Z}$ with a angle θ between $\overline{X}'$ and $\overline{X}$ along the clockwise direction as shown in fig. C.1.

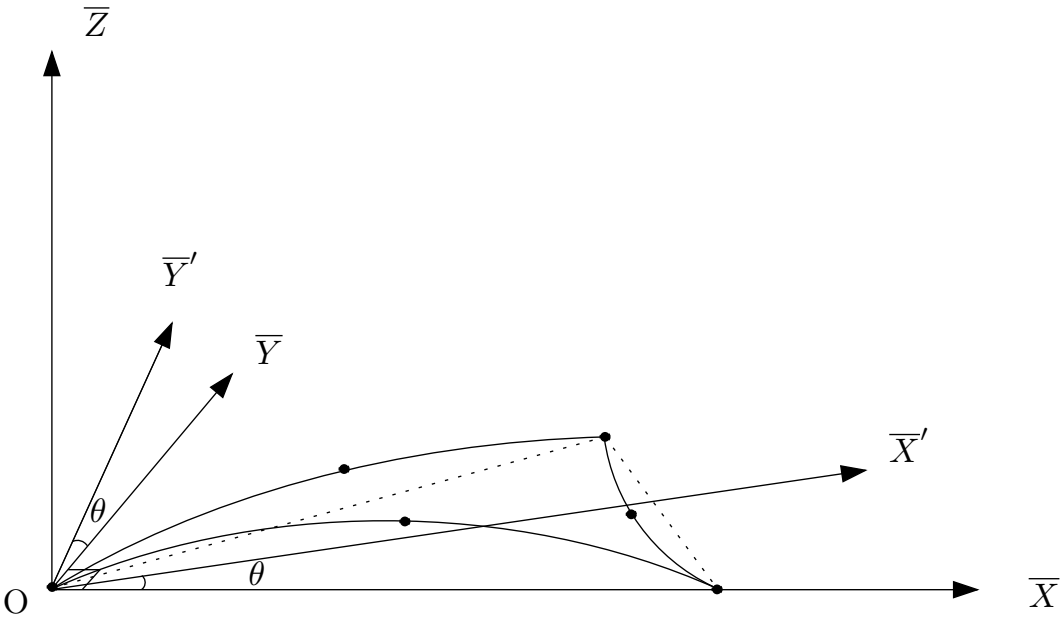

Figure C.1: Co-ordinate systems for the ith element surface

And,

$$\begin{aligned}\overline{X} &= \overline{X}'cos\theta - \overline{Y}'sin\theta \\ \overline{Y} &= \overline{X}'sin\theta - \overline{Y}'cos\theta\end{aligned}$$

then in $\overline{X'Y'Z}$ coordinate system, the element surface equation becomes,

$$\begin{aligned}\overline{Z} &= \overline{Z}(\overline{X}', \overline{Y}') = a_1 + a_2(\overline{X}'cos\theta - \overline{Y}'sin\theta) + a_3(\overline{X}'sin\theta - \overline{Y}'cos\theta) + a_4(\overline{X}'cos\theta - \overline{Y}'sin\theta)^2 \\ &\quad + a_5(\overline{X}'cos\theta - \overline{Y}'sin\theta)(\overline{X}'sin\theta - \overline{Y}'cos\theta) + a_6(\overline{X}'sin\theta - \overline{Y}'cos\theta)^2\end{aligned}$$

The element curvatures in $\overline{X}'Y'Z$ are:

$$\begin{aligned}K_{\overline{X}'} &= \frac{\partial^2 Z}{\partial \overline{X}'^2} = a_4cos^2\theta + a_5cos\theta sin\theta + a_6sin^2\theta \\ &= \frac{a_4}{2}(1 + cos2\theta) + \frac{a_5}{2}sin2\theta + \frac{a_6}{2}(1 - cos2\theta) \\ &= \frac{a_4 + a_6}{2} + \frac{a_4 - a_6}{2}cos2\theta + \frac{a_5}{2}sin2\theta \\ K_{\overline{Y}'} &= \frac{\partial^2 Z}{\partial \overline{Y}'^2} = a_4sin^2\theta + a_5cos\theta sin\theta + a_6cos^2\theta \\ &= \frac{a_4}{2}(1 - cos2\theta) + \frac{a_5}{2}sin2\theta + \frac{a_6}{2}(1 + cos2\theta) \\ &= \frac{a_4 + a_6}{2} + \frac{a_6 - a_4}{2}cos2\theta + \frac{a_5}{2}sin2\theta\end{aligned}$$

The maximum principal curvature is

$$k_1 = max(K_{\overline{X}'} \text{ or } K_{\overline{Y}'}) = \frac{a_4 + a_6}{2} + \sqrt{(\frac{a_4 - a_6}{2})^2 + (\frac{a_5}{2})^2}$$

and the minimum principal curvature is

$$k_2 = min(K_{\overline{X}'} \text{ or } K_{\overline{Y}'}) = \frac{a_4 + a_6}{2} - \sqrt{(\frac{a_4 - a_6}{2})^2 + (\frac{a_5}{2})^2}$$

There, the product of k_1 and k_2 is,

$$k_1k_2 = \left(\frac{a_4 + a_6}{2} + \sqrt{(\frac{a_4 - a_6}{2})^2 + (\frac{a_5}{2})^2}\right)\left(\frac{a_4 + a_6}{2} - \sqrt{(\frac{a_4 - a_6}{2})^2 + (\frac{a_5}{2})^2}\right)$$

$$= (\frac{a_4+a_6}{2})^2 - \left((\frac{a_4-a_6}{2})^2 + (\frac{a_5}{2})^2\right) = a_4a_6 - \frac{a_5^2}{4}$$
$$= \frac{K_{\overline{X}}K_{\overline{Y}} - K_{\overline{XY}}^2}{4}$$

C.2 Appendix C2:B matrix derivatives

Extracting the derivatives of local displacements from $\frac{\partial B_U(i,j)}{\partial X_j}$ and $\frac{\partial B_c(i,j)}{\partial X_j}$, and defining:

$\kappa_{1,1} = S_{1,1}(4\xi_1 - 1)$, $\kappa_{1,2} = S_{1,2}(4\xi_2 - 1)$, $\kappa_{1,3} = (S_{1,1} + S_{1,2})(1 - 4\xi_3)$
$\kappa_{1,4} = S_{1,1} \cdot 4\xi_2 + S_{1,2} \cdot 4\xi_1$, $\kappa_{1,5} = 4S_{1,2}(\xi_3 - \xi_2) - 4\xi_2 S_{1,1}$, $\kappa_{1,6} = 4(\xi_3 - \xi_1)S_{1,1} - 4\xi_1 S_{1,2}$

$\kappa_{2,1} = S_{2,1}(4\xi_1 - 1)$, $\kappa_{2,2} = S_{2,2}(4\xi_2 - 1)$, $\kappa_{2,3} = (S_{2,1} + S_{2,2})(1 - 4\xi_3)$
$\kappa_{2,4} = S_{2,1} \cdot 4\xi_2 + S_{2,2} \cdot 4\xi_1$, $\kappa_{2,5} = 4S_{2,2}(\xi_3 - \xi_2) - 4\xi_2 S_{2,1}$, $\kappa_{2,6} = 4(\xi_3 - \xi_1)S_{2,1} - 4\xi_1 S_{2,2}$

in which, S is a 2×2 matrix as:

$$S = \frac{1}{|J|}\begin{bmatrix} J(2,2) & -J(1,2) \\ -J(2,1) & J(1,1) \end{bmatrix}$$

where J is the Jacobian matrix relating Cartesian and area coordinate systems. Then,

$$\frac{\partial B_U(1,1)}{\partial X_j} = \begin{bmatrix} 0.5\kappa_{1,1}^2 & \kappa_{1,1}\kappa_{1,2} & \kappa_{1,1}\kappa_{1,3} & \kappa_{1,1}\kappa_{1,4} & \kappa_{1,1}\kappa_{1,5} & \kappa_{1,1}\kappa_{1,6} \end{bmatrix} \begin{Bmatrix} \frac{\partial U_1}{\partial X_j} \\ \frac{\partial U_2}{\partial X_j} \\ \frac{\partial U_3}{\partial X_j} \\ \frac{\partial U_4}{\partial X_j} \\ \frac{\partial U_5}{\partial X_j} \\ \frac{\partial U_6}{\partial X_j} \end{Bmatrix}$$

$$\frac{\partial B_U(1,2)}{\partial X_j} = \begin{bmatrix} 0.5\kappa_{1,1}^2 & \kappa_{1,1}\kappa_{1,2} & \kappa_{1,1}\kappa_{1,3} & \kappa_{1,1}\kappa_{1,4} & \kappa_{1,1}\kappa_{1,5} & \kappa_{1,1}\kappa_{1,6} \end{bmatrix} \begin{Bmatrix} \frac{\partial V_1}{\partial X_j} \\ \frac{\partial V_2}{\partial X_j} \\ \frac{\partial V_3}{\partial X_j} \\ \frac{\partial V_4}{\partial X_j} \\ \frac{\partial V_5}{\partial X_j} \\ \frac{\partial V_6}{\partial X_j} \end{Bmatrix}$$

$$\frac{\partial B_U(1,3)}{\partial X_j} = \begin{bmatrix} 0.5\kappa_{1,1}^2 & \kappa_{1,1}\kappa_{1,2} & \kappa_{1,1}\kappa_{1,3} & \kappa_{1,1}\kappa_{1,4} & \kappa_{1,1}\kappa_{1,5} & \kappa_{1,1}\kappa_{1,6} \end{bmatrix} \begin{Bmatrix} \frac{\partial W_1}{\partial X_j} \\ \frac{\partial W_2}{\partial X_j} \\ \frac{\partial W_3}{\partial X_j} \\ \frac{\partial W_4}{\partial X_j} \\ \frac{\partial W_5}{\partial X_j} \\ \frac{\partial W_6}{\partial X_j} \end{Bmatrix}$$

$$\frac{\partial B_U(1,4)}{\partial X_j} = \begin{bmatrix} 0.5\kappa_{1,2}^2 & \kappa_{1,2}\kappa_{1,3} & \kappa_{1,2}\kappa_{1,4} & \kappa_{1,2}\kappa_{1,5} & \kappa_{1,2}\kappa_{1,6} \end{bmatrix} \begin{Bmatrix} \frac{\partial U_2}{\partial X_j} \\ \frac{\partial U_3}{\partial X_j} \\ \frac{\partial U_4}{\partial X_j} \\ \frac{\partial U_5}{\partial X_j} \\ \frac{\partial U_6}{\partial X_j} \end{Bmatrix}$$

$$\frac{\partial B_U(1,5)}{\partial X_j} = \begin{bmatrix} 0.5\kappa_{1,2}^2 & \kappa_{1,2}\kappa_{1,3} & \kappa_{1,2}\kappa_{1,4} & \kappa_{1,2}\kappa_{1,5} & \kappa_{1,2}\kappa_{1,6} \end{bmatrix} \begin{Bmatrix} \frac{\partial V_2}{\partial X_j} \\ \frac{\partial V_3}{\partial X_j} \\ \frac{\partial V_4}{\partial X_j} \\ \frac{\partial V_5}{\partial X_j} \\ \frac{\partial V_6}{\partial X_j} \end{Bmatrix}$$

$$\frac{\partial B_U(1,6)}{\partial X_j} = \begin{bmatrix} 0.5\kappa_{1,2}^2 & \kappa_{1,2}\kappa_{1,3} & \kappa_{1,2}\kappa_{1,4} & \kappa_{1,2}\kappa_{1,5} & \kappa_{1,2}\kappa_{1,6} \end{bmatrix} \begin{Bmatrix} \frac{\partial W_2}{\partial X_j} \\ \frac{\partial W_3}{\partial X_j} \\ \frac{\partial W_4}{\partial X_j} \\ \frac{\partial W_5}{\partial X_j} \\ \frac{\partial W_6}{\partial X_j} \end{Bmatrix}$$

$$\frac{\partial B_U(1,7)}{\partial X_j} = \begin{bmatrix} 0.5\kappa_{1,3}^2 & \kappa_{1,3}\kappa_{1,4} & \kappa_{1,3}\kappa_{1,5} & \kappa_{1,3}\kappa_{1,6} \end{bmatrix} \begin{Bmatrix} \frac{\partial U_3}{\partial X_j} \\ \frac{\partial U_4}{\partial X_j} \\ \frac{\partial U_5}{\partial X_j} \\ \frac{\partial U_6}{\partial X_j} \end{Bmatrix}$$

$$\frac{\partial B_U(1,8)}{\partial X_j} = \begin{bmatrix} 0.5\kappa_{1,3}^2 & \kappa_{1,3}\kappa_{1,4} & \kappa_{1,3}\kappa_{1,5} & \kappa_{1,3}\kappa_{1,6} \end{bmatrix} \begin{Bmatrix} \frac{\partial V_3}{\partial X_j} \\ \frac{\partial V_4}{\partial X_j} \\ \frac{\partial V_5}{\partial X_j} \\ \frac{\partial V_6}{\partial X_j} \end{Bmatrix}$$

$$\frac{\partial B_U(1,9)}{\partial X_j} = \begin{bmatrix} 0.5\kappa_{1,3}^2 & \kappa_{1,3}\kappa_{1,4} & \kappa_{1,3}\kappa_{1,5} & \kappa_{1,3}\kappa_{1,6} \end{bmatrix} \begin{Bmatrix} \frac{\partial W_3}{\partial X_j} \\ \frac{\partial W_4}{\partial X_j} \\ \frac{\partial W_5}{\partial X_j} \\ \frac{\partial W_6}{\partial X_j} \end{Bmatrix}$$

$$\frac{\partial B_U(1,10)}{\partial X_j} = \begin{bmatrix} 0.5\kappa_{1,4}^2 & \kappa_{1,4}\kappa_{1,5} & \kappa_{1,4}\kappa_{1,6} \end{bmatrix} \begin{Bmatrix} \frac{\partial U_4}{\partial X_j} \\ \frac{\partial U_5}{\partial X_j} \\ \frac{\partial U_6}{\partial X_j} \end{Bmatrix}$$

$$\frac{\partial B_U(1,11)}{\partial X_j} = \begin{bmatrix} 0.5\kappa_{1,4}^2 & \kappa_{1,4}\kappa_{1,5} & \kappa_{1,4}\kappa_{1,6} \end{bmatrix} \begin{Bmatrix} \frac{\partial V_4}{\partial X_j} \\ \frac{\partial V_5}{\partial X_j} \\ \frac{\partial V_6}{\partial X_j} \end{Bmatrix}$$

$$\frac{\partial B_U(1,12)}{\partial X_j} = \begin{bmatrix} 0.5\kappa_{1,4}^2 & \kappa_{1,4}\kappa_{1,5} & \kappa_{1,4}\kappa_{1,6} \end{bmatrix} \begin{Bmatrix} \frac{\partial W_4}{\partial X_j} \\ \frac{\partial W_5}{\partial X_j} \\ \frac{\partial W_6}{\partial X_j} \end{Bmatrix}$$

$$\frac{\partial B_U(1,13)}{\partial X_j} = \begin{bmatrix} 0.5\kappa_{1,5}^2 & \kappa_{1,5}\kappa_{1,6} \end{bmatrix} \begin{Bmatrix} \frac{\partial U_5}{\partial X_j} \\ \frac{\partial U_6}{\partial X_j} \end{Bmatrix}$$

$$\frac{\partial B_U(1,14)}{\partial X_j} = \begin{bmatrix} 0.5\kappa_{1,5}^2 & \kappa_{1,5}\kappa_{1,6} \end{bmatrix} \begin{Bmatrix} \frac{\partial V_5}{\partial X_j} \\ \frac{\partial V_6}{\partial X_j} \end{Bmatrix}$$

$$\frac{\partial B_U(1,15)}{\partial X_j} = \begin{bmatrix} 0.5\kappa_{1,5}^2 & \kappa_{1,5}\kappa_{1,6} \end{bmatrix} \begin{Bmatrix} \frac{\partial W_5}{\partial X_j} \\ \frac{\partial W_6}{\partial X_j} \end{Bmatrix}$$

$$\frac{\partial B_U(1,16)}{\partial X_j} = \begin{bmatrix} 0.5\kappa_{1,6}^2 \end{bmatrix} \begin{Bmatrix} \frac{\partial U_6}{\partial X_j} \end{Bmatrix}, \quad \frac{\partial B_U(1,17)}{\partial u} = \begin{bmatrix} 0.5\kappa_{1,6}^2 \end{bmatrix} \begin{Bmatrix} \frac{\partial V_6}{\partial X_j} \end{Bmatrix}, \quad \frac{\partial B_U(1,18)}{\partial u} = \begin{bmatrix} 0.5\kappa_{1,6}^2 \end{bmatrix} \begin{Bmatrix} \frac{\partial W_6}{\partial X_j} \end{Bmatrix}$$

$$\frac{\partial B_U(2,1)}{\partial X_j} = \begin{bmatrix} 0.5\kappa_{2,1}^2 & \kappa_{2,1}\kappa_{2,2} & \kappa_{2,1}\kappa_{2,3} & \kappa_{2,1}\kappa_{2,4} & \kappa_{2,1}\kappa_{2,5} & \kappa_{2,1}\kappa_{2,6} \end{bmatrix} \begin{Bmatrix} \frac{\partial U_1}{\partial X_j} \\ \frac{\partial U_2}{\partial X_j} \\ \frac{\partial U_3}{\partial X_j} \\ \frac{\partial U_4}{\partial X_j} \\ \frac{\partial U_5}{\partial X_j} \\ \frac{\partial U_6}{\partial X_j} \end{Bmatrix}$$

$$\frac{\partial B_U(2,2)}{\partial X_j} = \begin{bmatrix} 0.5\kappa_{2,1}^2 & \kappa_{2,1}\kappa_{2,2} & \kappa_{2,1}\kappa_{2,3} & \kappa_{2,1}\kappa_{2,4} & \kappa_{2,1}\kappa_{2,5} & \kappa_{2,1}\kappa_{2,6} \end{bmatrix} \begin{Bmatrix} \frac{\partial V_1}{\partial X_j} \\ \frac{\partial V_2}{\partial X_j} \\ \frac{\partial V_3}{\partial X_j} \\ \frac{\partial V_4}{\partial X_j} \\ \frac{\partial V_5}{\partial X_j} \\ \frac{\partial V_6}{\partial X_j} \end{Bmatrix}$$

$$\frac{\partial B_U(2,3)}{\partial X_j} = \begin{bmatrix} 0.5\kappa_{2,1}^2 & \kappa_{2,1}\kappa_{2,2} & \kappa_{2,1}\kappa_{2,3} & \kappa_{2,1}\kappa_{2,4} & \kappa_{2,1}\kappa_{2,5} & \kappa_{2,1}\kappa_{2,6} \end{bmatrix} \begin{Bmatrix} \frac{\partial W_1}{\partial X_j} \\ \frac{\partial W_2}{\partial X_j} \\ \frac{\partial W_3}{\partial X_j} \\ \frac{\partial W_4}{\partial X_j} \\ \frac{\partial W_5}{\partial X_j} \\ \frac{\partial W_6}{\partial X_j} \end{Bmatrix}$$

$$\frac{\partial B_U(2,4)}{\partial X_j} = \begin{bmatrix} 0.5\kappa_{2,2}^2 & \kappa_{2,2}\kappa_{2,3} & \kappa_{2,2}\kappa_{2,4} & \kappa_{2,2}\kappa_{2,5} & \kappa_{2,2}\kappa_{2,6} \end{bmatrix} \begin{Bmatrix} \frac{\partial U_2}{\partial X_j} \\ \frac{\partial U_3}{\partial X_j} \\ \frac{\partial U_4}{\partial X_j} \\ \frac{\partial U_5}{\partial X_j} \\ \frac{\partial U_6}{\partial X_j} \end{Bmatrix}$$

$$\frac{\partial B_U(2,5)}{\partial X_j} = \begin{bmatrix} 0.5\kappa_{2,2}^2 & \kappa_{2,2}\kappa_{2,3} & \kappa_{2,2}\kappa_{2,4} & \kappa_{2,2}\kappa_{2,5} & \kappa_{2,2}\kappa_{2,6} \end{bmatrix} \begin{Bmatrix} \frac{\partial V_2}{\partial X_j} \\ \frac{\partial V_3}{\partial X_j} \\ \frac{\partial V_4}{\partial X_j} \\ \frac{\partial V_5}{\partial X_j} \\ \frac{\partial V_6}{\partial X_j} \end{Bmatrix}$$

$$\frac{\partial B_U(2,6)}{\partial X_j} = \begin{bmatrix} 0.5\kappa_{2,2}^2 & \kappa_{2,2}\kappa_{2,3} & \kappa_{2,2}\kappa_{2,4} & \kappa_{2,2}\kappa_{2,5} & \kappa_{2,2}\kappa_{2,6} \end{bmatrix} \begin{Bmatrix} \frac{\partial W_2}{\partial X_j} \\ \frac{\partial W_3}{\partial X_j} \\ \frac{\partial W_4}{\partial X_j} \\ \frac{\partial W_5}{\partial X_j} \\ \frac{\partial W_6}{\partial X_j} \end{Bmatrix}$$

$$\frac{\partial B_U(2,7)}{\partial X_j} = \begin{bmatrix} 0.5\kappa_{2,3}^2 & \kappa_{2,3}\kappa_{2,4} & \kappa_{2,3}\kappa_{2,5} & \kappa_{2,3}\kappa_{2,6} \end{bmatrix} \begin{Bmatrix} \frac{\partial U_3}{\partial X_j} \\ \frac{\partial U_4}{\partial X_j} \\ \frac{\partial U_5}{\partial X_j} \\ \frac{\partial U_6}{\partial X_j} \end{Bmatrix}$$

$$\frac{\partial B_U(2,8)}{\partial X_j} = \begin{bmatrix} 0.5\kappa_{2,3}^2 & \kappa_{2,3}\kappa_{2,4} & \kappa_{2,3}\kappa_{2,5} & \kappa_{2,3}\kappa_{2,6} \end{bmatrix} \begin{Bmatrix} \frac{\partial V_3}{\partial X_j} \\ \frac{\partial V_4}{\partial X_j} \\ \frac{\partial V_5}{\partial X_j} \\ \frac{\partial V_6}{\partial X_j} \end{Bmatrix}$$

$$\frac{\partial B_U(2,9)}{\partial X_j} = \begin{bmatrix} 0.5\kappa_{2,3}^2 & \kappa_{2,3}\kappa_{2,4} & \kappa_{2,3}\kappa_{2,5} & \kappa_{2,3}\kappa_{2,6} \end{bmatrix} \begin{Bmatrix} \frac{\partial W_3}{\partial X_j} \\ \frac{\partial W_4}{\partial X_j} \\ \frac{\partial W_5}{\partial X_j} \\ \frac{\partial W_6}{\partial X_j} \end{Bmatrix}$$

$$\frac{\partial B_U(2,10)}{\partial X_j} = \begin{bmatrix} 0.5\kappa_{2,4}^2 & \kappa_{2,4}\kappa_{2,5} & \kappa_{2,4}\kappa_{2,6} \end{bmatrix} \begin{Bmatrix} \frac{\partial U_4}{\partial X_j} \\ \frac{\partial U_5}{\partial X_j} \\ \frac{\partial U_6}{\partial X_j} \end{Bmatrix}$$

$$\frac{\partial B_U(2,11)}{\partial X_j} = \begin{bmatrix} 0.5\kappa_{2,4}^2 & \kappa_{2,4}\kappa_{2,5} & \kappa_{2,4}\kappa_{2,6} \end{bmatrix} \begin{Bmatrix} \frac{\partial V_4}{\partial X_j} \\ \frac{\partial V_5}{\partial X_j} \\ \frac{\partial V_6}{\partial X_j} \end{Bmatrix}$$

$$\frac{\partial B_U(2,12)}{\partial X_j} = \begin{bmatrix} 0.5\kappa_{2,4}^2 & \kappa_{2,4}\kappa_{2,5} & \kappa_{2,4}\kappa_{2,6} \end{bmatrix} \begin{Bmatrix} \frac{\partial W_4}{\partial X_j} \\ \frac{\partial W_5}{\partial X_j} \\ \frac{\partial W_6}{\partial X_j} \end{Bmatrix}$$

$$\frac{\partial B_U(2,13)}{\partial X_j} = \begin{bmatrix} 0.5\kappa_{2,5}^2 & \kappa_{2,5}\kappa_{2,6} \end{bmatrix} \begin{Bmatrix} \frac{\partial U_5}{\partial X_j} \\ \frac{\partial U_6}{\partial X_j} \end{Bmatrix}$$

$$\frac{\partial B_U(2,14)}{\partial X_j} = \begin{bmatrix} 0.5\kappa_{2,5}^2 & \kappa_{2,5}\kappa_{2,6} \end{bmatrix} \begin{Bmatrix} \frac{\partial V_5}{\partial X_j} \\ \frac{\partial V_6}{\partial X_j} \end{Bmatrix}$$

$$\frac{\partial B_U(2,15)}{\partial X_j} = \begin{bmatrix} 0.5\kappa_{2,5}^2 & \kappa_{2,5}\kappa_{2,6} \end{bmatrix} \begin{Bmatrix} \frac{\partial W_5}{\partial X_j} \\ \frac{\partial W_6}{\partial X_j} \end{Bmatrix}$$

$$\frac{\partial B_U(2,16)}{\partial X_j} = \begin{bmatrix} 0.5\kappa_{2,6}^2 \end{bmatrix} \begin{Bmatrix} \frac{\partial U_6}{\partial X_j} \end{Bmatrix}, \quad \frac{\partial B_U(2,17)}{\partial u} = \begin{bmatrix} 0.5\kappa_{2,6}^2 \end{bmatrix} \begin{Bmatrix} \frac{\partial V_6}{\partial X_j} \end{Bmatrix}, \quad \frac{\partial B_U(2,18)}{\partial u} = \begin{bmatrix} 0.5\kappa_{2,6}^2 \end{bmatrix} \begin{Bmatrix} \frac{\partial W_6}{\partial X_j} \end{Bmatrix}$$

$$\frac{\partial B_U(3,1)}{\partial X_j} = \begin{bmatrix} \kappa_{1,1}\kappa_{2,1} & \kappa_{1,1}\kappa_{2,2} & \kappa_{1,1}\kappa_{2,3} & \kappa_{1,1}\kappa_{2,4} & \kappa_{1,1}\kappa_{2,5} & \kappa_{1,1}\kappa_{2,6} \end{bmatrix} \begin{Bmatrix} \frac{\partial U_1}{\partial X_j} \\ \frac{\partial U_2}{\partial X_j} \\ \frac{\partial U_3}{\partial X_j} \\ \frac{\partial U_4}{\partial X_j} \\ \frac{\partial U_5}{\partial X_j} \\ \frac{\partial U_6}{\partial X_j} \end{Bmatrix}$$

$$\frac{\partial B_U(3,2)}{\partial X_j} = \begin{bmatrix} \kappa_{1,1}\kappa_{2,1} & \kappa_{1,1}\kappa_{2,2} & \kappa_{1,1}\kappa_{2,3} & \kappa_{1,1}\kappa_{2,4} & \kappa_{1,1}\kappa_{2,5} & \kappa_{1,1}\kappa_{2,6} \end{bmatrix} \begin{Bmatrix} \frac{\partial V_1}{\partial X_j} \\ \frac{\partial V_2}{\partial X_j} \\ \frac{\partial V_3}{\partial X_j} \\ \frac{\partial V_4}{\partial X_j} \\ \frac{\partial V_5}{\partial X_j} \\ \frac{\partial V_6}{\partial X_j} \end{Bmatrix}$$

$$\frac{\partial B_U(3,3)}{\partial X_j} = \begin{bmatrix} \kappa_{1,1}\kappa_{2,1} & \kappa_{1,1}\kappa_{2,2} & \kappa_{1,1}\kappa_{2,3} & \kappa_{1,1}\kappa_{2,4} & \kappa_{1,1}\kappa_{2,5} & \kappa_{1,1}\kappa_{2,6} \end{bmatrix} \begin{Bmatrix} \frac{\partial W_1}{\partial X_j} \\ \frac{\partial W_2}{\partial X_j} \\ \frac{\partial W_3}{\partial X_j} \\ \frac{\partial W_4}{\partial X_j} \\ \frac{\partial W_5}{\partial X_j} \\ \frac{\partial W_6}{\partial X_j} \end{Bmatrix}$$

$$\frac{\partial B_U(3,4)}{\partial X_j} = \begin{bmatrix} \kappa_{1,2}\kappa_{2,1} & \kappa_{1,2}\kappa_{2,2} & \kappa_{1,2}\kappa_{2,3} & \kappa_{1,2}\kappa_{2,4} & \kappa_{1,2}\kappa_{2,5} & \kappa_{1,2}\kappa_{2,6} \end{bmatrix} \begin{Bmatrix} \frac{\partial U_1}{\partial X_j} \\ \frac{\partial U_2}{\partial X_j} \\ \frac{\partial U_3}{\partial X_j} \\ \frac{\partial U_4}{\partial X_j} \\ \frac{\partial U_5}{\partial X_j} \\ \frac{\partial U_6}{\partial X_j} \end{Bmatrix}$$

$$\frac{\partial B_U(3,5)}{\partial X_j} = \begin{bmatrix} \kappa_{1,2}\kappa_{2,1} & \kappa_{1,2}\kappa_{2,2} & \kappa_{1,2}\kappa_{2,3} & \kappa_{1,2}\kappa_{2,4} & \kappa_{1,2}\kappa_{2,5} & \kappa_{1,2}\kappa_{2,6} \end{bmatrix} \begin{Bmatrix} \frac{\partial V_1}{\partial X_j} \\ \frac{\partial V_2}{\partial X_j} \\ \frac{\partial V_3}{\partial X_j} \\ \frac{\partial V_4}{\partial X_j} \\ \frac{\partial V_5}{\partial X_j} \\ \frac{\partial V_6}{\partial X_j} \end{Bmatrix}$$

$$\frac{\partial B_U(3,6)}{\partial X_j} = \begin{bmatrix} \kappa_{1,2}\kappa_{2,1} & \kappa_{1,2}\kappa_{2,2} & \kappa_{1,2}\kappa_{2,3} & \kappa_{1,2}\kappa_{2,4} & \kappa_{1,2}\kappa_{2,5} & \kappa_{1,2}\kappa_{2,6} \end{bmatrix} \begin{Bmatrix} \frac{\partial W_1}{\partial X_j} \\ \frac{\partial W_2}{\partial X_j} \\ \frac{\partial W_3}{\partial X_j} \\ \frac{\partial W_4}{\partial X_j} \\ \frac{\partial W_5}{\partial X_j} \\ \frac{\partial W_6}{\partial X_j} \end{Bmatrix}$$

$$\frac{\partial B_U(3,7)}{\partial X_j} = \begin{bmatrix} \kappa_{1,3}\kappa_{2,1} & \kappa_{1,3}\kappa_{2,2} & \kappa_{1,3}\kappa_{2,3} & \kappa_{1,3}\kappa_{2,4} & \kappa_{1,3}\kappa_{2,5} & \kappa_{1,3}\kappa_{2,6} \end{bmatrix} \begin{Bmatrix} \frac{\partial U_1}{\partial X_j} \\ \frac{\partial U_2}{\partial X_j} \\ \frac{\partial U_3}{\partial X_j} \\ \frac{\partial U_4}{\partial X_j} \\ \frac{\partial U_5}{\partial X_j} \\ \frac{\partial U_6}{\partial X_j} \end{Bmatrix}$$

$$\frac{\partial B_U(3,8)}{\partial X_j} = \begin{bmatrix} \kappa_{1,3}\kappa_{2,1} & \kappa_{1,3}\kappa_{2,2} & \kappa_{1,3}\kappa_{2,3} & \kappa_{1,3}\kappa_{2,4} & \kappa_{1,3}\kappa_{2,5} & \kappa_{1,3}\kappa_{2,6} \end{bmatrix} \begin{Bmatrix} \frac{\partial V_1}{\partial X_j} \\ \frac{\partial V_2}{\partial X_j} \\ \frac{\partial V_3}{\partial X_j} \\ \frac{\partial V_4}{\partial X_j} \\ \frac{\partial V_5}{\partial X_j} \\ \frac{\partial V_6}{\partial X_j} \end{Bmatrix}$$

$$\frac{\partial B_U(3,9)}{\partial X_j} = \begin{bmatrix} \kappa_{1,3}\kappa_{2,1} & \kappa_{1,3}\kappa_{2,2} & \kappa_{1,3}\kappa_{2,3} & \kappa_{1,3}\kappa_{2,4} & \kappa_{1,3}\kappa_{2,5} & \kappa_{1,3}\kappa_{2,6} \end{bmatrix} \begin{Bmatrix} \frac{\partial W_1}{\partial X_j} \\ \frac{\partial W_2}{\partial X_j} \\ \frac{\partial W_3}{\partial X_j} \\ \frac{\partial W_4}{\partial X_j} \\ \frac{\partial W_5}{\partial X_j} \\ \frac{\partial W_6}{\partial X_j} \end{Bmatrix}$$

$$\frac{\partial B_U(3,10)}{\partial X_j} = \begin{bmatrix} \kappa_{1,4}\kappa_{2,1} & \kappa_{1,4}\kappa_{2,2} & \kappa_{1,4}\kappa_{2,3} & \kappa_{1,4}\kappa_{2,4} & \kappa_{1,4}\kappa_{2,5} & \kappa_{1,4}\kappa_{2,6} \end{bmatrix} \begin{Bmatrix} \frac{\partial U_1}{\partial X_j} \\ \frac{\partial U_2}{\partial X_j} \\ \frac{\partial U_3}{\partial X_j} \\ \frac{\partial U_4}{\partial X_j} \\ \frac{\partial U_5}{\partial X_j} \\ \frac{\partial U_6}{\partial X_j} \end{Bmatrix}$$

$$\frac{\partial B_U(3,11)}{\partial X_j} = \begin{bmatrix} \kappa_{1,4}\kappa_{2,1} & \kappa_{1,4}\kappa_{2,2} & \kappa_{1,4}\kappa_{2,3} & \kappa_{1,4}\kappa_{2,4} & \kappa_{1,4}\kappa_{2,5} & \kappa_{1,4}\kappa_{2,6} \end{bmatrix} \begin{Bmatrix} \frac{\partial V_1}{\partial X_j} \\ \frac{\partial V_2}{\partial X_j} \\ \frac{\partial V_3}{\partial X_j} \\ \frac{\partial V_4}{\partial X_j} \\ \frac{\partial V_5}{\partial X_j} \\ \frac{\partial V_6}{\partial X_j} \end{Bmatrix}$$

$$\frac{\partial B_U(3,12)}{\partial X_j} = \begin{bmatrix} \kappa_{1,4}\kappa_{2,1} & \kappa_{1,4}\kappa_{2,2} & \kappa_{1,4}\kappa_{2,3} & \kappa_{1,4}\kappa_{2,4} & \kappa_{1,4}\kappa_{2,5} & \kappa_{1,4}\kappa_{2,6} \end{bmatrix} \begin{Bmatrix} \frac{\partial W_1}{\partial X_j} \\ \frac{\partial W_2}{\partial X_j} \\ \frac{\partial W_3}{\partial X_j} \\ \frac{\partial W_4}{\partial X_j} \\ \frac{\partial W_5}{\partial X_j} \\ \frac{\partial W_6}{\partial X_j} \end{Bmatrix}$$

$$\frac{\partial B_U(3,13)}{\partial X_j} = \begin{bmatrix} \kappa_{1,5}\kappa_{2,1} & \kappa_{1,5}\kappa_{2,2} & \kappa_{1,5}\kappa_{2,3} & \kappa_{1,5}\kappa_{2,4} & \kappa_{1,5}\kappa_{2,5} & \kappa_{1,5}\kappa_{2,6} \end{bmatrix} \begin{Bmatrix} \frac{\partial U_1}{\partial X_j} \\ \frac{\partial U_2}{\partial X_j} \\ \frac{\partial U_3}{\partial X_j} \\ \frac{\partial U_4}{\partial X_j} \\ \frac{\partial U_5}{\partial X_j} \\ \frac{\partial U_6}{\partial X_j} \end{Bmatrix}$$

$$\frac{\partial B_U(3,14)}{\partial X_j} = \begin{bmatrix} \kappa_{1,5}\kappa_{2,1} & \kappa_{1,5}\kappa_{2,2} & \kappa_{1,5}\kappa_{2,3} & \kappa_{1,5}\kappa_{2,4} & \kappa_{1,5}\kappa_{2,5} & \kappa_{1,5}\kappa_{2,6} \end{bmatrix} \begin{Bmatrix} \frac{\partial V_1}{\partial X_j} \\ \frac{\partial V_2}{\partial X_j} \\ \frac{\partial V_3}{\partial X_j} \\ \frac{\partial V_4}{\partial X_j} \\ \frac{\partial V_5}{\partial X_j} \\ \frac{\partial V_6}{\partial X_j} \end{Bmatrix}$$

$$\frac{\partial B_U(3,16)}{\partial X_j} = \begin{bmatrix} \kappa_{1,6}\kappa_{2,1} & \kappa_{1,6}\kappa_{2,2} & \kappa_{1,6}\kappa_{2,3} & \kappa_{1,6}\kappa_{2,4} & \kappa_{1,6}\kappa_{2,5} & \kappa_{1,6}\kappa_{2,6} \end{bmatrix} \begin{Bmatrix} \frac{\partial U_1}{\partial X_j} \\ \frac{\partial U_2}{\partial X_j} \\ \frac{\partial U_3}{\partial X_j} \\ \frac{\partial U_4}{\partial X_j} \\ \frac{\partial U_5}{\partial X_j} \\ \frac{\partial U_6}{\partial X_j} \end{Bmatrix}$$

$$\frac{\partial B_U(3,17)}{\partial X_j} = \begin{bmatrix} \kappa_{1,6}\kappa_{2,1} & \kappa_{1,6}\kappa_{2,2} & \kappa_{1,6}\kappa_{2,3} & \kappa_{1,6}\kappa_{2,4} & \kappa_{1,6}\kappa_{2,5} & \kappa_{1,6}\kappa_{2,6} \end{bmatrix} \begin{Bmatrix} \frac{\partial V_1}{\partial X_j} \\ \frac{\partial V_2}{\partial X_j} \\ \frac{\partial V_3}{\partial X_j} \\ \frac{\partial V_4}{\partial X_j} \\ \frac{\partial V_5}{\partial X_j} \\ \frac{\partial V_6}{\partial X_j} \end{Bmatrix}$$

$$\frac{\partial B_U(3,18)}{\partial X_j} = \begin{bmatrix} \kappa_{1,6}\kappa_{2,1} & \kappa_{1,6}\kappa_{2,2} & \kappa_{1,6}\kappa_{2,3} & \kappa_{1,6}\kappa_{2,4} & \kappa_{1,6}\kappa_{2,5} & \kappa_{1,6}\kappa_{2,6} \end{bmatrix} \begin{Bmatrix} \frac{\partial W_1}{\partial X_j} \\ \frac{\partial W_2}{\partial X_j} \\ \frac{\partial W_3}{\partial X_j} \\ \frac{\partial W_4}{\partial X_j} \\ \frac{\partial W_5}{\partial X_j} \\ \frac{\partial W_6}{\partial X_j} \end{Bmatrix}$$

$$\begin{Bmatrix} \frac{\partial B_c(1,3)}{\partial X_j} \\ \frac{\partial B_c(1,6)}{\partial X_j} \\ \frac{\partial B_c(1,9)}{\partial X_j} \\ \frac{\partial B_c(1,12)}{\partial X_j} \\ \frac{\partial B_c(1,15)}{\partial X_j} \end{Bmatrix} = \begin{bmatrix} \xi_1(2\xi_1 - 1) & \xi_2(2\xi_2 - 1) & \xi_3(2\xi_3 - 1) & 4\xi_1\xi_2 & 4\xi_2\xi_3 & 4\xi_1\xi_3 \end{bmatrix} \{\frac{\partial K_X}{\partial X_j}\}$$

$$= \begin{bmatrix} -2\xi_1(2\xi_1 - 1) & -2\xi_2(2\xi_2 - 1) & -2\xi_3(2\xi_3 - 1) & -8\xi_1\xi_2 & -8\xi_2\xi_3 & -8\xi_1\xi_3 \end{bmatrix} \{\frac{\partial a_4}{\partial X_j}\}$$

$$\begin{Bmatrix} \frac{\partial B_c(2,3)}{\partial X_j} \\ \frac{\partial B_c(2,6)}{\partial X_j} \\ \frac{\partial B_c(2,9)}{\partial X_j} \\ \frac{\partial B_c(2,12)}{\partial X_j} \\ \frac{\partial B_c(2,15)}{\partial X_j} \end{Bmatrix} = \begin{bmatrix} \xi_1(2\xi_1-1) & \xi_2(2\xi_2-1) & \xi_3(2\xi_3-1) & 4\xi_1\xi_2 & 4\xi_2\xi_3 & 4\xi_1\xi_3 \end{bmatrix} \{\frac{\partial K_Y}{\partial X_j}\}$$

$$= \begin{bmatrix} -2\xi_1(2\xi_1-1) & -2\xi_2(2\xi_2-1) & -2\xi_3(2\xi_3-1) & -8\xi_1\xi_2 & -8\xi_2\xi_3 & -8\xi_1\xi_3 \end{bmatrix} \{\frac{\partial a_6}{\partial X_j}\}$$

$$\begin{Bmatrix} \frac{\partial B_c(3,3)}{\partial X_j} \\ \frac{\partial B_c(3,6)}{\partial X_j} \\ \frac{\partial B_c(3,9)}{\partial X_j} \\ \frac{\partial B_c(3,12)}{\partial X_j} \\ \frac{\partial B_c(3,15)}{\partial X_j} \end{Bmatrix} = \begin{bmatrix} \xi_1(2\xi_1-1) & \xi_2(2\xi_2-1) & \xi_3(2\xi_3-1) & 4\xi_1\xi_2 & 4\xi_2\xi_3 & 4\xi_1\xi_3 \end{bmatrix} \{\frac{\partial 2K_{XY}}{\partial X_j}\}$$

$$= \begin{bmatrix} -2\xi_1(2\xi_1-1) & -2\xi_2(2\xi_2-1) & -2\xi_3(2\xi_3-1) & -8\xi_1\xi_2 & -8\xi_2\xi_3 & -8\xi_1\xi_3 \end{bmatrix} \{\frac{\partial a_5}{\partial X_j}\}$$

In which, $\frac{\partial a_4}{\partial X_j}, \frac{\partial a_5}{\partial X_j}$ and $\frac{\partial a_6}{\partial X_j}$ can be computed using Eqn.5.150 .

C.3 Fortran 95 reliability program descriptor

C.3.1 The Main structure of the Fortran Code

The main solution procedures for the reliability forumation include the FORM and sensitivity calculation using LST. The fortran code "Reliability.exe" is written using the structure illustrated in fig. C.2, and the code structure detailed in fig. C.3.

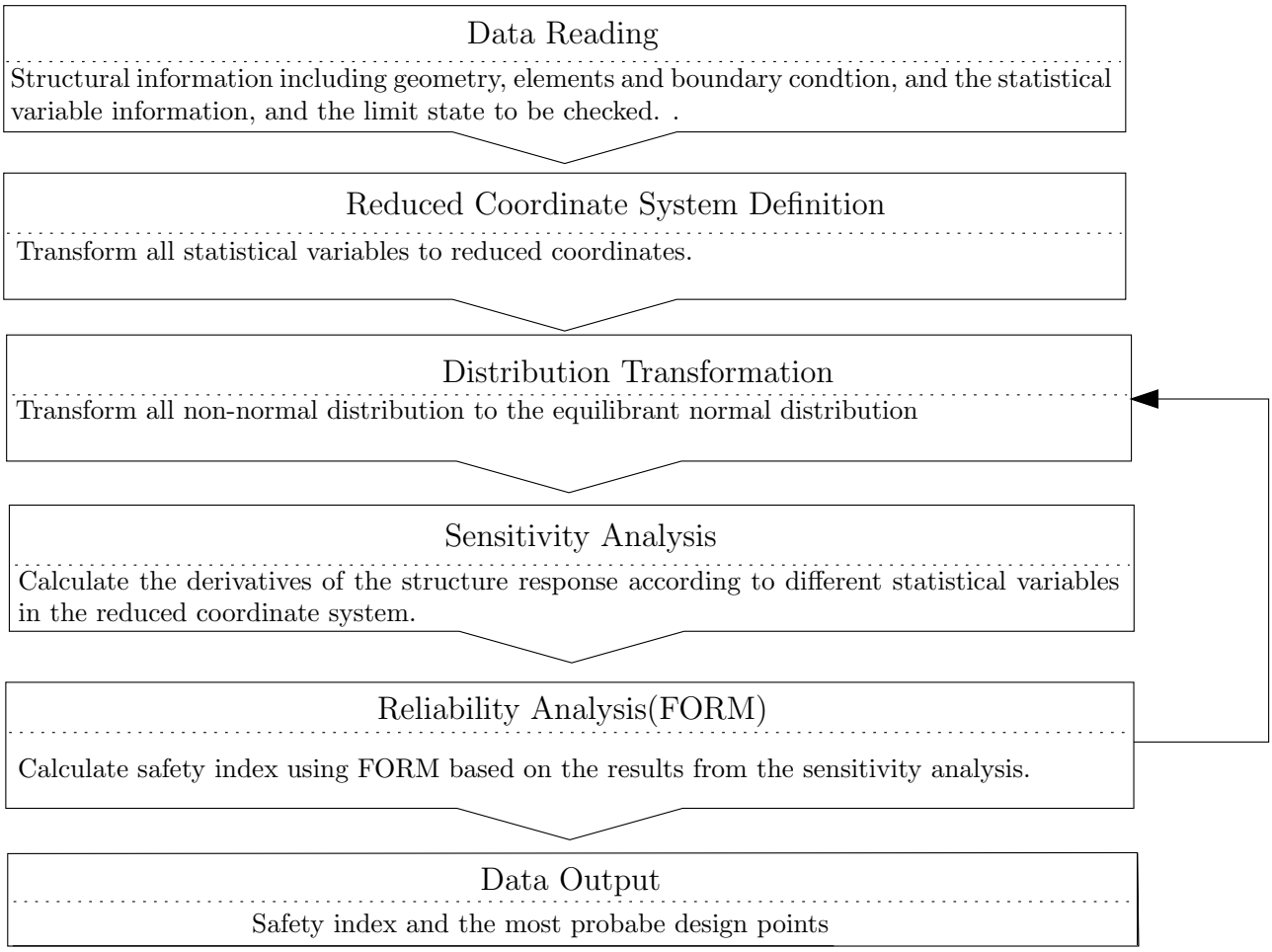

Figure C.2: The flow chart for Reliability.exe

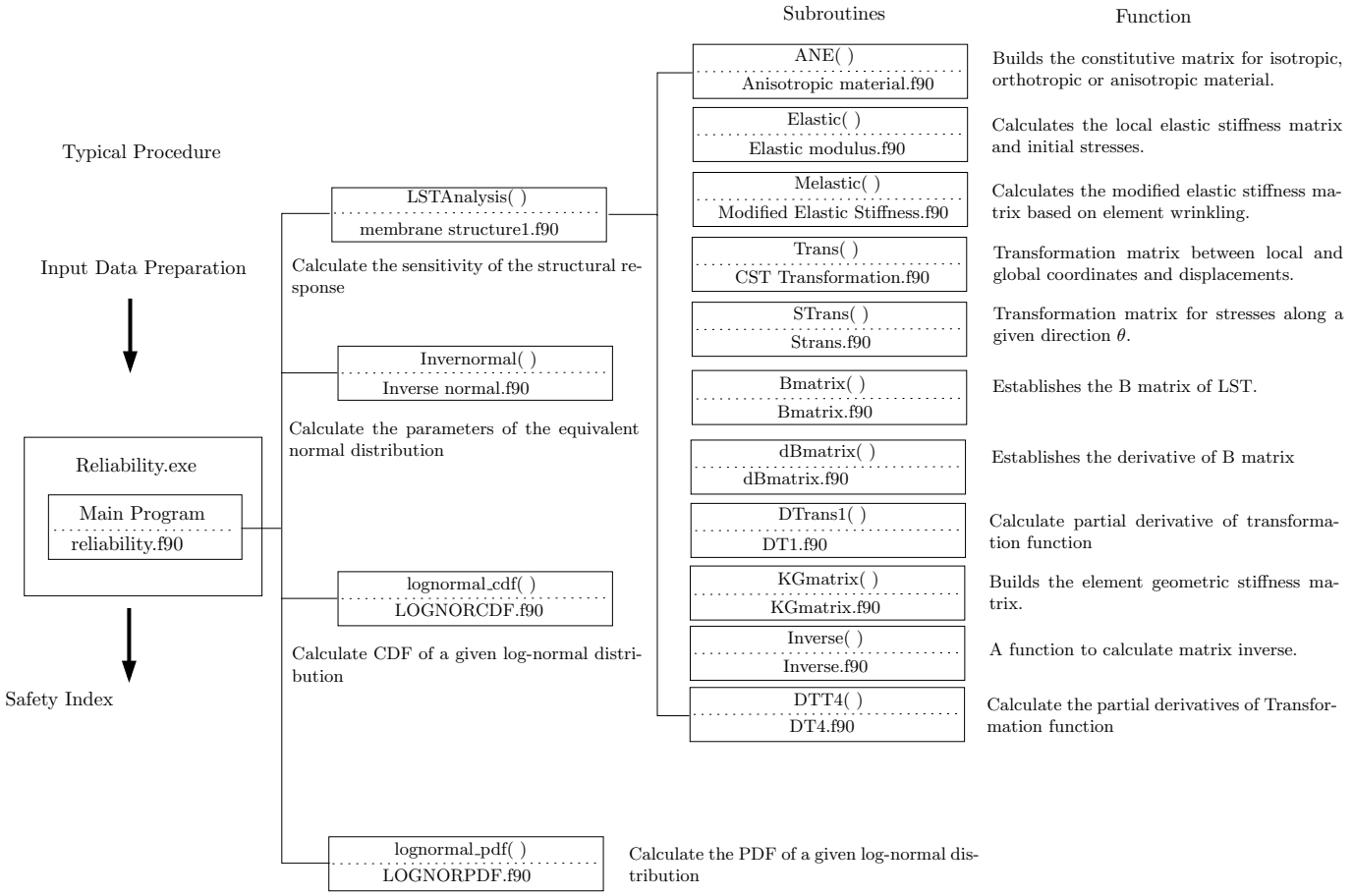

Figure C.3: The code structure and subroutines of Realiability.exe

C.4 Data Preparation, Pre- and Post- processing

The variables included in the input file for the reliability program are listed below:

Wswitch	Wrinkling procedure: 0 – disable, 1 – enable.
NN	Total number of the nodes.
co	Nodal coordinates in global coordinate system.
NE	Total number of the membrane elements.
NE1	Total number of the boundary cables (if the structure to be analyzed includes boundary cables).
enn	Node number included in each membrane element.
enn1	Node number included in each cable element.
F	Equivalent nodal force applied to the membrane .
α,β	The angles for anisotropic material defined in fig. C.4.

E_x	Young's modulus, fill.
E_y	Young's modulus, warp.
G_{xy}	Shear modulus.
v_{yx}	Poisson's ratio.
A_{ca}	Cross sectional area of the boundary cables
E_{ca}	Elastic modulus of the boundary cables
BN	Total number of fixed degree of freedoms
Bdy	Fixed D.O.F number
σ_{xi}	Initial stress along the fill direction
σ_{yi}	Initial stress along the warp direction
PType	The type number of different cable forces
P_N	Initial boundary cable forces
θ	Assumed fill direction in global xy plane.
InitD	Switch for the input of initial nodal displacements. 0 – no initial displacement, 1 – any initial displacement
ID	Initial nodal displacements.
Scontour	Choice of stress contour in Gid files. 1 – element stress , 2 – principal stresses
Error1	Allowable error top-limit
Error2	Allowable error bottom-limit (the residual error is between Error1 and Error2)
Dtype()	Distribution type: 1 – normal, 2 – log-normal, 3 – laplace, 4 – Gumbel, 5 – Frechet, 6 – Weibull
Dtype(EX)	Distribution type of Young'modulus in fill
PARA-EX	Distribution parameters of Young's modulus in fill
IniV(EX)	Initial value of Young's modulus in fill
Dtype(EY)	Distribution type of Young'modulus in warp
IniV(EY)	Initial value of Young'modulus in warp

PARA-EY	Distribution parameters of Young's modulus in warp
Dtype(GXY)	Distribution type of shear modulus
IniV(GXY)	Initial value of shear modulus
PARA-GXY	Distribution parameters of shear modulus
Dtype(vXY)	Distribution type of Possion's ratio
IniV(vXY)	Initial value of Possion's ratio
PARA-vXY	Distribution parameters of Possion's ratio
Dtype(Load)	Distribution type of load coefficient t_{load}
IniV(Load)	Initial value of load coefficient t_{load}
PARA-Load	Distribution parameter of load coefficient t_{load}
Dtype(STR)	Distribution type of material strength
IniV(STR)	Initial value of material strength
PARA-STR	Distribution parameter of material strength
Allow-SX	Allowable fill stress (kN/m)
Allow-SY	Allowable warp stress (kN/m)
Allow-SM	Allowable minimal stress (kN/m)
Allow-DIS	Allowable nodal displacement /deflection (m)
LMT	Choice of limit state, 1 – fill strength, 2 – warp strength, 3 – wrinkling, 4 – deflection.

The input file should be a txt document with the name "**input.txt**" and located in the same directory as the program executable file. The sequence and formats of the input variables in "**input.txt**" are :

1. Wswitch (I1)
2. NN (I5)
3. co (E20.10,1x,E20.10,E20.10)
4. NE (I5)
5. enn ((I5,I5,I5) for CST,(I5,I5,I5,I5,I5,I5) for LST
6. NE1 (I5)
7. enn1 (I5,I5)
8. F in x,y,z (E20.10,1x,E20.10,E20.10)

9. α,β,v_{yx} (F4.2,F4.2,F4.3)
10. A_{ca},E_{ca} (E20.10,1x,E20.10)
11. E_x,E_y,G_{xy} (E20.10,1x,E20.10,1x,E20.10)
12. BN (I5)
13. Bdy (I5)
14. σ_{xi},σ_{yi} (F6.3,F6.3)
15 $PType$ 16. P_N (F6.3)
17. θ (F6.3)
18. InitD (I5) (if InitD=0, then go 20)
19. ID (E20.10,1x,E20.10,1x,E20.10)
20. Scontour (I5)
21. Error1 (F6.3)
22. Error2 (F6.3)
23. DtypeEX (I5)
24. IniV(EX) (E20.10)
25. PARA-EX ((E20.10,1x,E20.10,1x,E20.10)
26. DtypeEY (I5)
27. IniV(EY) (E20.10)
28. PARA-EY ((E20.10,1x,E20.10,1x,E20.10)
29. DtypeGXY (I5)
30. IniV(GXY) (E20.10)
31. PARA-GXY ((E20.10,1x,E20.10,1x,E20.10)
32. DtypevXY (I5)
33. IniV(vXY) (E20.10)
34. PARA-vXY ((E20.10,1x,E20.10,1x,E20.10)
35. DtypeLoad (I5)
36. IniV(Load) (E20.10)
37. PARA-Load ((E20.10,1x,E20.10,1x,E20.10)
38. DtypeSTR (I5)
39. IniV(STR) (E20.10)
40. PARA-STR ((E20.10,1x,E20.10,1x,E20.10)
41. Allow-SX (E5.3) 42. Allow-SY (E5.3) 43. Allow-SM (E5.3) 44. Allow-DIS (E5.3) 45. LMT (I5)

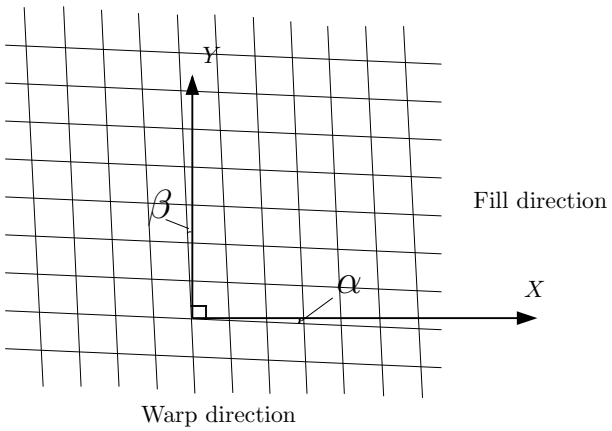

Figure C.4: Definition of α and β for an anisotropic material

in which, "I" and "F" imply integer and real formats respectively, and "E" also represents the real format but in an exponential form. The first integer following "I" ,"E" or "F" represents the total space used to accommodate the input number, and the number after decimal point indicates the decimal number of the variable. For example, "6" ,"6.0" and "6.00E+00" represent the same value but in the formats "I1", "F3.1", and "E8.2", respectively.

The numerical problem introduced in section 5.3.4 as fig. C.5 are provided as examples to demonstrate the operation of the reliability program.

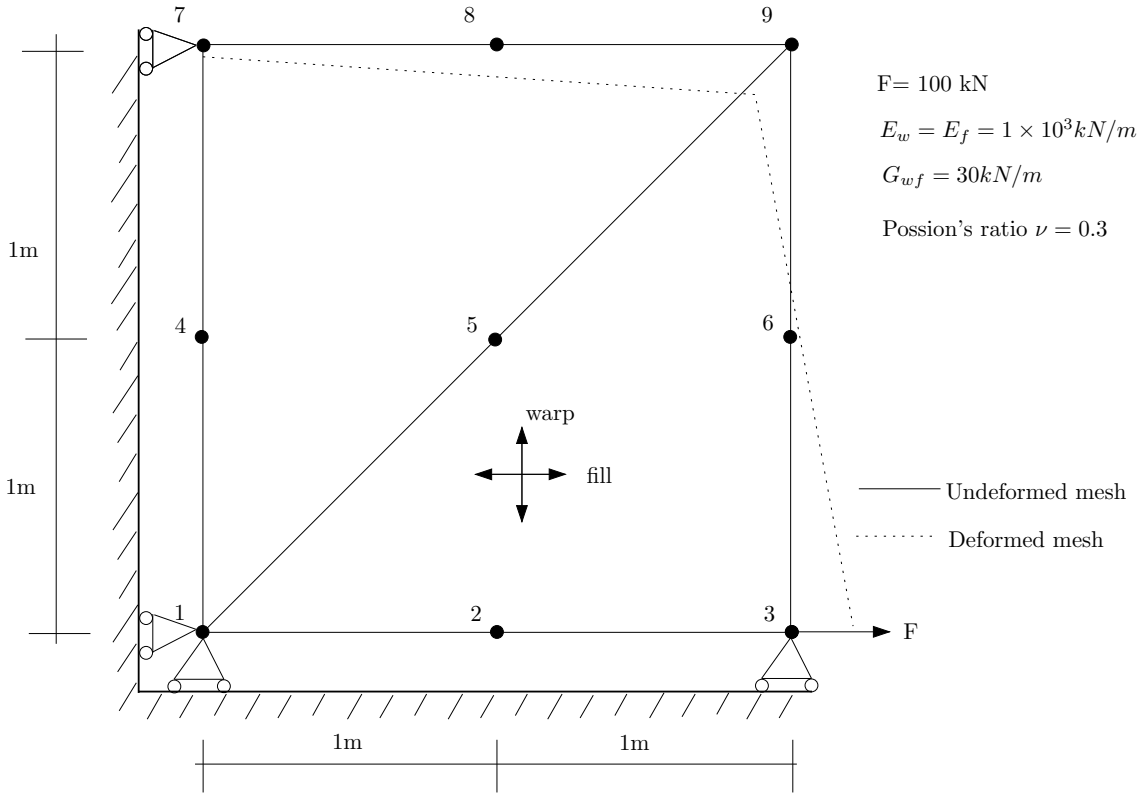

Figure C.5: Reliability analysis of Patch test using LST meshes

"**input.txt**" files as figure C.6are created by the user for the finite element reliability programs using the format previously described.

```
                                                    input.txt
0
9
    0.0000000000E+00     0.0000000000E+00     0.0000000000E+00
    0.1000000000E+01     0.0000000000E+00     0.0000000000E+00
    0.2000000000E+01     0.0000000000E+00     0.0000000000E+00
    0.0000000000E+00     1.0000000000E+00     0.0000000000E+00
    0.1000000000E+01     1.0000000000E+00     0.0000000000E+00
    0.2000000000E+01     1.0000000000E+00     0.0000000000E+00
    0.0000000000E+00     2.0000000000E+00     0.0000000000E+00
    0.1000000000E+01     2.0000000000E+00     0.0000000000E+00
    0.2000000000E+01     2.0000000000E+00     0.0000000000E+00
2
    1    3    9    2    6    5
    7    1    9    4    5    8
0
    0.0000000000E+00     0.0000000000E+00     0.0000000000E+00
    0.0000000000E+00     0.0000000000E+00     0.0000000000E+00
    0.1000000000E+00     0.0000000000E+00     0.0000000000E+00
    0.0000000000E+00     0.0000000000E+00     0.0000000000E+00
    0.0000000000E+00     0.0000000000E+00     0.0000000000E+00
    0.0000000000E+00     0.0000000000E+00     0.0000000000E+00
    0.0000000000E+00     0.0000000000E+02     0.0000000000E+00
    0.0000000000E+00     0.0000000000E+00     0.0000000000E+00
    0.0000000000E+00     0.0000000000E+00     0.0000000000E+00
0.00 0.00 0.3
    1.0000000000E+03     1.0000000000E+03     0.3000000000E+02
13
    1
    2
    3
    6
    9
   10
   12
   15
   18
   19
   21
   24
   27
0.000 0.000 0.000
0
0
1
0.002
0.001
1
    1.0000000000E+03
    1.0000000000E+03     1.0000000000E+02     0.0000000000E+00
1
    1.0000000000E+03
    1.0000000000E+03     1.0000000000E+02     0.0000000000E+00
1
    0.3000000000E+02
    0.3000000000E+02     3.0000000000E+00     0.0000000000E+00
1
    0.1000000000E+00
    0.1000000000E+00     0.0000000000E+00     0.0000000000E+00
1
    1.0000000000E+00
    1.0000000000E+00     0.1000000000E+00     0.0000000000E+00
1
    0.8000000000E+01
    0.8000000000E+01     2.0000000000E+00     0.0000000000E+00
0.350
0.500
0.200
0.005
1
```

Figure C.6: "input.txt" for reliability program.

The safety index estimated will be shown in the program as figure. C.7,

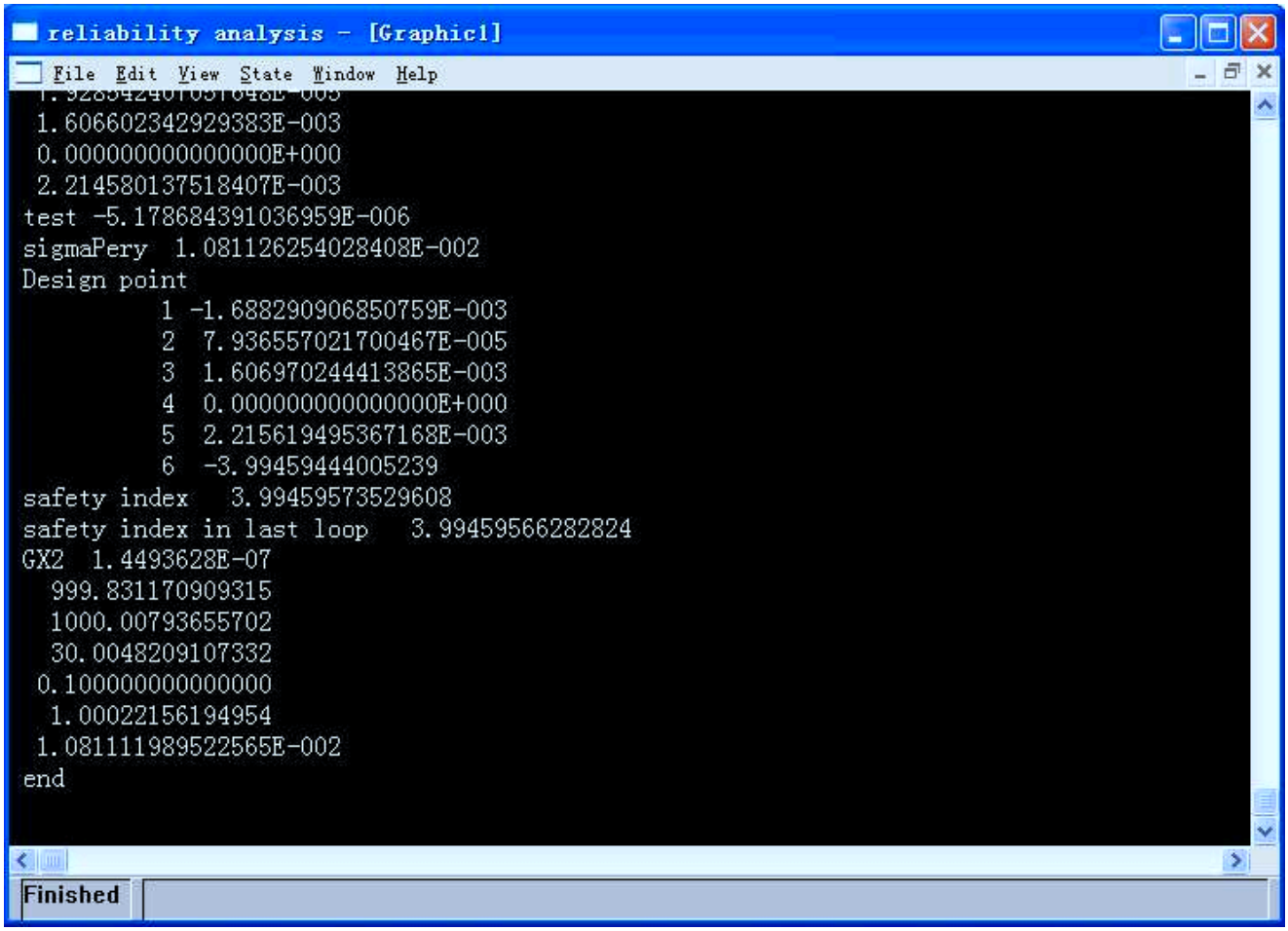

Figure C.7: Safety index calculated by the reliability program.

The program will compute safety index following FORM iterations, and if the difference between one and following iterations is less than 0.001, safety index will be idendified and program will end. The safety index will be displayed in the program window. As shown in figure.C.7, the safety index is converged to 3.9945.

Program input of Doncaster Canopy Example

The "**input.txt**" of the Doncaster Canopy in Chapter 5 is given as following:

0

377

-0.9030000000E+01	-0.6662000000E+01	0.1486900000E+02
0.9630904160E-01	-0.4405387143E+01	0.1915207955E+02
0.9082000000E+01	-0.7004000000E+01	0.1490100000E+02
0.1059600000E+02	-0.3327000000E+01	0.1426700000E+02
0.8983000000E+01	0.6466000000E+01	0.1413100000E+02
-0.1147000000E+01	0.1101800000E+02	0.1414900000E+02
-0.8906000000E+01	0.6627000000E+01	0.1424500000E+02
-0.1037300000E+02	-0.4113000000E+01	0.1440300000E+02
-0.2570000000E+00	0.7900000000E+00	0.2180700000E+02
0.7400000000E+00	0.3440000000E+00	0.2180700000E+02
0.1726000000E+01	0.6810000000E+00	0.2168900000E+02
0.2177000000E+01	0.1380000000E+01	0.2155000000E+02
0.1941000000E+01	0.2626000000E+01	0.2137600000E+02
0.6050000000E+00	0.3203000000E+01	0.2138100000E+02
-0.3760000000E+00	0.2651000000E+01	0.2153300000E+02
-0.5490000000E+00	0.1231000000E+01	0.2176000000E+02
0.1984941825E+00	0.4708647597E+00	0.2182403941E+02
0.1265630427E+01	0.4205997875E+00	0.2175820868E+02
0.2004177703E+01	0.9966198559E+00	0.2162002910E+02
0.2204917476E+01	0.2028779868E+01	0.2144970128E+02
0.1349478572E+01	0.3091850936E+01	0.2134738468E+02
0.5671788680E-01	0.3026726126E+01	0.2144624250E+02
-0.6542931284E+00	0.1965891595E+01	0.2165604109E+02
-0.3101341541E+01	-0.3991415425E+01	0.1820687893E+02
0.3124998781E+01	-0.3966250776E+01	0.1819527550E+02

0.9590268121E+01	-0.5047621399E+01	0.1472202446E+02
0.8914360229E+01	0.1454532153E+01	0.1482540679E+02
0.3505497763E+01	0.7882561811E+01	0.1495357119E+02
-0.4651021900E+01	0.8137440525E+01	0.1474083035E+02
-0.8495060757E+01	0.1087290286E+01	0.1501255632E+02
-0.4489127554E+01	-0.2944710984E+01	0.1778966830E+02
0.3076555353E+00	-0.2582284672E+01	0.1979580716E+02
0.4632190019E+01	-0.2877089527E+01	0.1770704813E+02
0.6335998222E+01	-0.1130219632E+01	0.1704682391E+02
0.6075074287E+01	0.4798900003E+01	0.1634208667E+02
-0.4957295622E+00	0.7809420369E+01	0.1637835155E+02
-0.5205086675E+01	0.4822571462E+01	0.1661168538E+02
-0.5222854044E+01	-0.1741722777E+01	0.1730415770E+02
-0.1698766375E+01	-0.5364632673E+00	0.2012757520E+02
0.5177231857E+00	-0.9936193068E+00	0.2068862757E+02
0.2619563345E+01	-0.3498052055E+00	0.1991690887E+02
0.3618093076E+01	0.4174586460E+00	0.1952920007E+02
0.3654288610E+01	0.3480275439E+01	0.1887673300E+02
0.1001699726E+00	0.5158542746E+01	0.1886235158E+02
-0.2310101367E+01	0.3480438937E+01	0.1917470778E+02
-0.2008138942E+01	0.7377082558E+00	0.1986389139E+02
-0.1912181706E+01	-0.2361658796E+01	0.1918184738E+02
0.2025905797E+01	-0.2004136441E+01	0.1940564664E+02
0.5515043217E+01	-0.2086140439E+01	0.1737742527E+02
0.6093820239E+01	0.1706182900E+01	0.1697086179E+02
0.2041910851E+01	0.4766560708E+01	0.1843841576E+02
-0.2903960276E+01	0.6222669436E+01	0.1668341168E+02

-0.5110516204E+01	0.1377174984E+01	0.1722430410E+02
-0.4366109979E+00	-0.8733283452E+00	0.2047000004E+02
0.1574693090E+01	-0.6761412562E+00	0.2040241950E+02
0.3040763677E+01	-0.4216466366E-01	0.1977039091E+02
0.3589989019E+01	0.2059068603E+01	0.1933092837E+02
0.1463928674E+01	0.3331302392E+01	0.2064653763E+02
-0.1010058885E+01	0.4349525569E+01	0.1911452723E+02
-0.2027303574E+01	0.1988219745E+01	0.1974442657E+02
-0.1638766285E+01	-0.4308066410E+01	0.1870386401E+02
0.1631639183E+01	-0.4262598611E+01	0.1873064643E+02
-0.6020980000E+01	-0.1237100000E+02	0.1552000000E+02
-0.1119000000E+01	-0.1321800000E+02	0.1580900000E+02
0.6224000000E+01	-0.1225900000E+02	0.1551800000E+02
-0.1161000000E+01	-0.1003900000E+02	0.1854800000E+02
-0.6020000000E+00	-0.1047100000E+02	0.1842500000E+02
0.2770000000E+00	-0.1003700000E+02	0.1862700000E+02
0.2980000000E+00	-0.9555000000E+01	0.1879900000E+02
-0.3940000000E+00	-0.9021000000E+01	0.1895100000E+02
-0.1177000000E+01	-0.9481000000E+01	0.1874600000E+02
-0.9359525220E+00	-0.1031824592E+02	0.1846116088E+02
-0.7618351139E-01	-0.1040594438E+02	0.1847684987E+02
0.3306093342E+00	-0.9798439516E+01	0.1871457288E+02
0.3825288811E-01	-0.9187718446E+01	0.1891537279E+02
-0.8684093974E+00	-0.9127240735E+01	0.1888747135E+02
-0.1227241822E+01	-0.9760348539E+01	0.1864327417E+02
-0.3492641551E+01	-0.1240366303E+02	0.1588034250E+02
0.2507866222E+01	-0.1202551651E+02	0.1608546147E+02

0.7107829316E+01	-0.9325471289E+01	0.1545797681E+02
-0.6888672640E+01	-0.9183442276E+01	0.1552623365E+02
-0.4333841359E+01	-0.1146576722E+02	0.1616684615E+02
-0.8736478313E+00	-0.1181249124E+02	0.1681688109E+02
0.3945345326E+01	-0.1127786982E+02	0.1622223645E+02
0.3232863856E+01	-0.8612588518E+01	0.1719502125E+02
-0.1093526482E+00	-0.6314134563E+01	0.1881622019E+02
-0.3555939155E+01	-0.8536148036E+01	0.1725185954E+02
-0.2410695983E+01	-0.1053679218E+02	0.1734081954E+02
-0.7176280021E+00	-0.1098832922E+02	0.1764763521E+02
0.1687984108E+01	-0.1042303967E+02	0.1740652863E+02
0.1378604351E+01	-0.9163106959E+01	0.1805027965E+02
-0.2826114197E+00	-0.7956469788E+01	0.1880182411E+02
-0.2063526149E+01	-0.9087552099E+01	0.1805095291E+02
-0.1908054047E+01	-0.1127835199E+02	0.1698627399E+02
0.8373163224E+00	-0.1125447422E+02	0.1702983749E+02
0.2470725645E+01	-0.9950136469E+01	0.1717956017E+02
0.1499494938E+01	-0.6733220774E+01	0.1825792077E+02
-0.1934289726E+01	-0.6778142427E+01	0.1821374129E+02
-0.3107463762E+01	-0.9894667352E+01	0.1716194008E+02
-0.1434908166E+01	-0.1066814164E+02	0.1768656214E+02
0.2493974452E+00	-0.1064597302E+02	0.1783887189E+02
0.1478111019E+01	-0.9783029841E+01	0.1778389356E+02
0.6367341752E+00	-0.8339321635E+01	0.1847657447E+02
-0.1277465248E+01	-0.8270392606E+01	0.1846758870E+02
-0.2123160512E+01	-0.9783486082E+01	0.1780896956E+02
-0.6061720280E+01	-0.5320839071E+01	0.1651668502E+02

-0.3799474486E+01	-0.3462830032E+01	0.1800698087E+02
-0.6719775848E+01	-0.4793289878E+01	0.1626765519E+02
-0.2507141029E+01	-0.3158724505E+01	0.1867269903E+02
-0.3203992629E+01	-0.2648090775E+01	0.1850404912E+02
-0.1771764600E+01	-0.3314424768E+01	0.1891873625E+02
-0.6431465613E+00	-0.3420406328E+01	0.1924933269E+02
-0.8279170836E+00	-0.2479193490E+01	0.1953577046E+02
-0.7800726942E+00	-0.4355434904E+01	0.1895615111E+02
0.2005322064E+00	-0.3481002771E+01	0.1942471796E+02
0.8692748038E+00	-0.4340594713E+01	0.1896192046E+02
0.9511362559E+00	-0.3404137767E+01	0.1924305714E+02
0.1808777642E+01	-0.3123168925E+01	0.1903510145E+02
0.1171085389E+01	-0.2305474246E+01	0.1963632969E+02
0.2549040913E+01	-0.2975355870E+01	0.1876332157E+02
0.3888624254E+01	-0.3422231384E+01	0.1796376910E+02
0.3325718815E+01	-0.2444714651E+01	0.1855278154E+02
0.6056949823E+01	-0.5469114593E+01	0.1645517235E+02
0.6800439720E+01	-0.4936003864E+01	0.1616775747E+02
0.9248569382E+01	-0.5996522476E+01	0.1485701178E+02
0.7067892970E+01	-0.3944963621E+01	0.1616093938E+02
0.7508012017E+01	-0.3555686254E+01	0.1596604810E+02
0.5084528625E+01	-0.2484040028E+01	0.1754461416E+02
0.7912896292E+01	-0.3075748592E+01	0.1578646507E+02
0.5938059924E+01	-0.1607483381E+01	0.1721367987E+02
0.1001740121E+02	-0.4131358757E+01	0.1453993031E+02
0.8412426950E+01	-0.2230625152E+01	0.1556490464E+02
0.9475611624E+01	-0.1058102129E+01	0.1474861865E+02

0.7632455818E+01	0.1545423055E+00	0.1594318589E+02
0.7492465185E+01	0.1560415270E+01	0.1587856770E+02
0.6231355269E+01	0.2852600654E+00	0.1703069075E+02
0.7511775892E+01	0.3139457342E+01	0.1562192093E+02
0.6097103368E+01	0.3249141539E+01	0.1668653508E+02
0.8649493732E+01	0.3981922640E+01	0.1467819501E+02
0.7485378372E+01	0.5596601101E+01	0.1515367880E+02
0.6202766195E+01	0.6838134731E+01	0.1479834893E+02
0.4831293515E+01	0.6370159398E+01	0.1568638447E+02
0.2778047077E+01	0.6262160117E+01	0.1663544990E+02
0.4062296763E+01	0.4761330901E+01	0.1738107174E+02
0.1524459571E+01	0.7883973840E+01	0.1569225066E+02
0.7822739052E+00	0.6271585332E+01	0.1740256220E+02
0.9819806509E+00	0.9191453373E+01	0.1481273858E+02
-0.8210617469E+00	0.9367781286E+01	0.1518720527E+02
-0.2709338358E+01	0.9389291314E+01	0.1462388582E+02
-0.2559962758E+01	0.7995446870E+01	0.1557845905E+02
-0.3760359184E+01	0.7176419480E+01	0.1569284327E+02
-0.1703397072E+01	0.7034714013E+01	0.1655356671E+02
-0.4935744039E+01	0.6473787188E+01	0.1569425185E+02
-0.4062196081E+01	0.5534421617E+01	0.1666666363E+02
-0.6694468524E+01	0.7128045911E+01	0.1466321400E+02
-0.7015584308E+01	0.5692608589E+01	0.1532321322E+02
-0.8306833015E+01	0.3923052151E+01	0.1484972219E+02
-0.6869877559E+01	0.2984746958E+01	0.1584051275E+02
-0.6785411970E+01	0.1254849479E+01	0.1608956239E+02
-0.5171839468E+01	0.3110093165E+01	0.1694975849E+02

-0.6863011079E+01	-0.3263491659E+00	0.1616541864E+02
-0.5183132336E+01	-0.1685403430E+00	0.1728944199E+02
-0.9065047661E+01	-0.1650623291E+01	0.1492333613E+02
-0.7763172307E+01	-0.2959971577E+01	0.1570689409E+02
-0.9453937057E+01	-0.5233182893E+01	0.1476931807E+02
-0.7103709065E+01	-0.4181360640E+01	0.1607013425E+02
-0.4863907061E+01	-0.2340145814E+01	0.1754755168E+02
-0.1785010716E+01	-0.1412725967E+01	0.1963265603E+02
-0.3035350130E+01	-0.1716302837E+01	0.1888590224E+02
-0.1175164771E+01	-0.1585397186E+01	0.1980651526E+02
-0.1071811788E+01	-0.6954957053E+00	0.2032387085E+02
-0.6957404718E+00	-0.1664448999E+01	0.1994231819E+02
0.3017962456E-01	-0.9274870179E+00	0.2059381591E+02
0.4102170523E+00	-0.1766688575E+01	0.2019554074E+02
0.1254539876E+01	-0.1485874617E+01	0.2004038188E+02
0.1757014630E+01	-0.1322065976E+01	0.1989094373E+02
0.1041766573E+01	-0.8363363324E+00	0.2057275852E+02
0.2322613480E+01	-0.1160528697E+01	0.1966422033E+02
0.2083412311E+01	-0.5186090284E+00	0.2019063903E+02
0.3605858356E+01	-0.1588942831E+01	0.1869609457E+02
0.4017632531E+01	-0.1187837194E+01	0.1857693206E+02
0.4207420379E+01	-0.1033163892E+01	0.1850167429E+02
0.2820638169E+01	-0.1921525869E+00	0.1985746779E+02
0.4504030337E+01	-0.8018977929E+00	0.1836777307E+02
0.3318785885E+01	0.1958166146E+00	0.1966895715E+02
0.4911698187E+01	-0.3473175440E+00	0.1819990722E+02
0.4796370379E+01	0.1049255776E+01	0.1822234124E+02

0.4772631077E+01	0.1844046645E+01	0.1813039117E+02
0.3604671347E+01	0.1235959510E+01	0.1946353734E+02
0.4840018475E+01	0.2588377257E+01	0.1791916797E+02
0.3611798487E+01	0.2750441365E+01	0.1913483306E+02
0.4815061408E+01	0.4099966209E+01	0.1753359995E+02
0.2876652742E+01	0.4120816921E+01	0.1868228053E+02
0.1725310068E+01	0.3986650459E+01	0.1952290930E+02
0.2524810272E+01	0.3386542046E+01	0.1975637124E+02
0.1078345450E+01	0.4969278273E+01	0.1867375875E+02
0.7578813212E+00	0.4213419891E+01	0.1974601493E+02
-0.1968488791E+00	0.6432681445E+01	0.1754950466E+02
-0.1375758603E+01	0.5662460293E+01	0.1775573886E+02
-0.1918369687E+01	0.5240711937E+01	0.1786408654E+02
-0.4526791059E+00	0.4754099800E+01	0.1900380792E+02
-0.2575079208E+01	0.4799932582E+01	0.1789966493E+02
-0.1655302236E+01	0.3919514273E+01	0.1916624043E+02
-0.3710695572E+01	0.4116083887E+01	0.1780579794E+02
-0.3669632865E+01	0.2438688881E+01	0.1818941381E+02
-0.3487961332E+01	0.1699582068E+01	0.1844446144E+02
-0.2155572576E+01	0.2741535223E+01	0.1948269024E+02
-0.3492654297E+01	0.1050461203E+01	0.1850548975E+02
-0.2006980878E+01	0.1369362872E+01	0.1983442904E+02
-0.3562272991E+01	-0.5168335777E+00	0.1850978312E+02
-0.3399592995E+01	-0.1127495096E+01	0.1863005008E+02
-0.1848160431E+01	0.9500601381E-01	0.2001643684E+02
-0.1030732895E+01	0.3716784177E+00	0.2086559373E+02
-0.9430510985E+00	0.1470089128E+00	0.2092327121E+02

-0.4030000000E+00	0.1010500000E+01	0.2178350000E+02
-0.3359137920E+00	-0.5032044271E-02	0.2110433343E+02
-0.1005250233E+00	-0.1450082523E+00	0.2109594556E+02
-0.2925290875E-01	0.6304323799E+00	0.2181551970E+02
0.1591491329E+00	-0.2366795807E+00	0.2111706535E+02
0.4692470912E+00	0.4074323799E+00	0.2181551970E+02
0.6254442655E+00	-0.2954314048E+00	0.2120369925E+02
0.1123398655E+01	-0.1606199735E+00	0.2109746538E+02
0.1365590445E+01	-0.6730903752E-01	0.2104645686E+02
0.1002815213E+01	0.3822998937E+00	0.2178260434E+02
0.1590808945E+01	0.6616007894E-01	0.2101893086E+02
0.1495815214E+01	0.5507998938E+00	0.2172360434E+02
0.2113788601E+01	0.2322925126E+00	0.2071829534E+02
0.2291801601E+01	0.3823372674E+00	0.2067090642E+02
0.2434328896E+01	0.5286398793E+00	0.2063948231E+02
0.1865088851E+01	0.8388099280E+00	0.2165451455E+02
0.2554711750E+01	0.6999823845E+00	0.2063436502E+02
0.2090588851E+01	0.1188309928E+01	0.2158501455E+02
0.2834422020E+01	0.9121005049E+00	0.2047845686E+02
0.2803670369E+01	0.1693488404E+01	0.2042374235E+02
0.2795498127E+01	0.2008896580E+01	0.2035813183E+02
0.2190958738E+01	0.1704389934E+01	0.2149985064E+02
0.2726510863E+01	0.2328251062E+01	0.2035039674E+02
0.2072958738E+01	0.2327389934E+01	0.2141285064E+02
0.2746958472E+01	0.3011235541E+01	0.2006008194E+02
0.1709678137E+01	0.2983878735E+01	0.2102815366E+02
0.1380827597E+01	0.3183433555E+01	0.2100182803E+02

0.1645239286E+01	0.2858925468E+01	0.2136169234E+02
0.1009388890E+01	0.3291248500E+01	0.2102582917E+02
0.9772392860E+00	0.3147425468E+01	0.2136419234E+02
0.3532717670E+00	0.4120338876E+01	0.2006161349E+02
-0.1741034302E+00	0.3744280081E+01	0.2022879162E+02
-0.4292112915E+00	0.3613094928E+01	0.2023272533E+02
0.3308589434E+00	0.3114863063E+01	0.2141362125E+02
-0.6494538617E+00	0.3442114357E+01	0.2028927196E+02
-0.1596410566E+00	0.2838863063E+01	0.2148962125E+02
-0.1292418042E+01	0.3028055734E+01	0.2029330837E+02
-0.1185421085E+01	0.2349227162E+01	0.2061543835E+02
-0.1228851738E+01	0.1977063833E+01	0.2065091459E+02
-0.5151465642E+00	0.2308445798E+01	0.2159452055E+02
-0.1203421785E+01	0.1616047167E+01	0.2073214845E+02
-0.6016465642E+00	0.1598445798E+01	0.2170802055E+02
-0.1188777772E+01	0.9761662446E+00	0.2075415976E+02
-0.4763914424E+01	-0.1224182766E+02	0.1575435898E+02
-0.3917191963E+01	-0.1193413615E+02	0.1604478898E+02
-0.5159913781E+01	-0.1190123615E+02	0.1580290076E+02
-0.2710155263E+01	-0.1181191382E+02	0.1639231019E+02
-0.3124144776E+01	-0.1134738895E+02	0.1655267956E+02
-0.2176222095E+01	-0.1210625281E+02	0.1632824464E+02
-0.1411814385E+01	-0.1155201930E+02	0.1691278793E+02
-0.2268114259E+01	-0.1269231965E+02	0.1592894894E+02
-0.9971064210E+00	-0.1249487945E+02	0.1627549378E+02
0.6052260939E+00	-0.1241433623E+02	0.1612363502E+02
0.8045096013E+00	-0.1194369842E+02	0.1646284083E+02

0.1649247087E+01	-0.1162517320E+02	0.1653130371E+02
-0.9141066021E-02	-0.1155291549E+02	0.1694598901E+02
0.3236303418E+01	-0.1166880343E+02	0.1617645184E+02
0.2400417244E+01	-0.1124396233E+02	0.1660007613E+02
0.4378519522E+01	-0.1188209121E+02	0.1589424313E+02
0.5086189061E+01	-0.1175940179E+02	0.1581254103E+02
0.6461542486E+01	-0.1073654003E+02	0.1556086639E+02
0.5566384078E+01	-0.1030557433E+02	0.1590947037E+02
0.4780596474E+01	-0.9655905935E+01	0.1631313894E+02
0.3211039793E+01	-0.1061360073E+02	0.1665541019E+02
0.5160155792E+01	-0.8970869621E+01	0.1629000077E+02
0.2854313449E+01	-0.9289135498E+01	0.1720183300E+02
0.7936278537E+01	-0.8024856729E+01	0.1526748526E+02
0.6161072556E+01	-0.7808380381E+01	0.1605298187E+02
0.3166100312E+01	-0.6270412564E+01	0.1765797907E+02
0.2302198615E+01	-0.5353684807E+01	0.1820541491E+02
0.2372681706E+01	-0.7684319640E+01	0.1774823408E+02
0.1551200294E+01	-0.5500379819E+01	0.1845540826E+02
0.7442585680E+00	-0.5296259273E+01	0.1875618857E+02
0.7062425202E+00	-0.6536501427E+01	0.1856065832E+02
-0.6435584643E-02	-0.5345288356E+01	0.1893561445E+02
-0.8599689581E+00	-0.5312090887E+01	0.1874213946E+02
-0.1766775782E+01	-0.5530146955E+01	0.1842523234E+02
-0.1030592827E+01	-0.6554718976E+01	0.1855251085E+02
-0.2502250916E+01	-0.5380022612E+01	0.1817544304E+02
-0.3320139516E+01	-0.6250262544E+01	0.1768922422E+02
-0.2739714273E+01	-0.7657964375E+01	0.1777177896E+02

-0.6283012012E+01	-0.7596978410E+01	0.1605404219E+02
-0.7784628689E+01	-0.7746926780E+01	0.1530865828E+02
-0.5216938411E+01	-0.8854842264E+01	0.1636274581E+02
-0.5000615136E+01	-0.9538646103E+01	0.1633495634E+02
-0.3335306457E+01	-0.9215003537E+01	0.1722149189E+02
-0.5643851009E+01	-0.1032270063E+02	0.1591029570E+02
-0.3703168226E+01	-0.1067437489E+02	0.1663425142E+02
-0.6223323949E+01	-0.1071028483E+02	0.1562228816E+02
-0.2177465338E+01	-0.1089681788E+02	0.1717631513E+02
-0.3344995283E+01	-0.1097014628E+02	0.1668845673E+02
-0.1679232979E+01	-0.1095146494E+02	0.1732699660E+02
-0.1913933743E+01	-0.1059658948E+02	0.1751758531E+02
-0.1313702941E+01	-0.1112359989E+02	0.1730934325E+02
-0.1079369385E+01	-0.1083409788E+02	0.1768158859E+02
-0.7962649717E+00	-0.1138705561E+02	0.1720407062E+02
0.4946493055E-01	-0.1113461540E+02	0.1734914466E+02
0.5322897544E+00	-0.1092911370E+02	0.1742194266E+02
-0.2174699860E+00	-0.1083316363E+02	0.1776164305E+02
0.1262479458E+01	-0.1083626993E+02	0.1724702037E+02
0.9657647748E+00	-0.1053139591E+02	0.1762596057E+02
0.2808814909E+01	-0.1082083789E+02	0.1672874565E+02
0.2059637450E+01	-0.1019165090E+02	0.1730255033E+02
0.1960040152E+01	-0.9876743465E+01	0.1747198351E+02
0.1576859284E+01	-0.1010395828E+02	0.1759943644E+02
0.1910311608E+01	-0.9558167289E+01	0.1760898706E+02
0.1427738775E+01	-0.9480758989E+01	0.1792261204E+02
0.2290933034E+01	-0.8879238561E+01	0.1759383075E+02

0.1433264334E+01	-0.7961824315E+01	0.1813882202E+02
0.1057008809E+01	-0.7547220949E+01	0.1833485962E+02
0.1010947977E+01	-0.8748290525E+01	0.1828616598E+02
0.2543023145E+00	-0.7313406449E+01	0.1863316956E+02
0.1690412537E+00	-0.8141199941E+01	0.1866095600E+02
-0.1973945221E+00	-0.7146473814E+01	0.1876559981E+02
-0.7770646772E+00	-0.8113498066E+01	0.1865775778E+02
-0.6847797150E+00	-0.7277737519E+01	0.1863710357E+02
-0.1588023829E+01	-0.7531712257E+01	0.1831291233E+02
-0.1986412564E+01	-0.7941738995E+01	0.1812357498E+02
-0.1674865007E+01	-0.8677116477E+01	0.1828595657E+02
-0.2793174927E+01	-0.8807233894E+01	0.1762800488E+02
-0.2574627592E+01	-0.9486130733E+01	0.1760081112E+02
-0.2608408775E+01	-0.9834551717E+01	0.1747394603E+02
-0.2099424964E+01	-0.9440438592E+01	0.1793514016E+02
-0.2265931037E+01	-0.1015890046E+02	0.1757546650E+02
-0.2747782753E+01	-0.1022143612E+02	0.1726154358E+02
-0.1281620384E+01	-0.1033026847E+02	0.1812600898E+02
-0.1767648882E+01	-0.1025946218E+02	0.1787360177E+02
-0.1167866102E+01	-0.1046020920E+02	0.1805817526E+02
-0.1048476261E+01	-0.1017862296E+02	0.1850458044E+02
-0.1007090911E+01	-0.1054601582E+02	0.1805146215E+02
-0.7689762610E+00	-0.1039462296E+02	0.1844308044E+02
-0.6577021515E+00	-0.1070634738E+02	0.1801524903E+02
-0.1741356996E+00	-0.1057669935E+02	0.1812288539E+02
0.7103827057E-01	-0.1049473929E+02	0.1814710548E+02
-0.3390917557E+00	-0.1043847219E+02	0.1845092493E+02

0.2692895369E+00	-0.1032336197E+02	0.1824997123E+02
0.1004082443E+00	-0.1022147219E+02	0.1855192493E+02
0.9619335755E+00	-0.1019048364E+02	0.1794061465E+02
0.8350815631E+00	-0.9898672099E+01	0.1818112054E+02
0.8670016860E+00	-0.9779913914E+01	0.1820686754E+02
0.3038046671E+00	-0.9917719758E+01	0.1867078644E+02
0.8556860673E+00	-0.9664598976E+01	0.1825909521E+02
0.3143046671E+00	-0.9676719758E+01	0.1875678644E+02
0.8124686822E+00	-0.9353602640E+01	0.1838645200E+02
0.4478641434E+00	-0.8955423484E+01	0.1860548285E+02
0.3157190862E+00	-0.8771930144E+01	0.1865538362E+02
0.1681264441E+00	-0.9371359223E+01	0.1885718639E+02
-0.1135774155E+00	-0.8607677149E+01	0.1880264594E+02
-0.1778735559E+00	-0.9104359223E+01	0.1893318639E+02
-0.3378969240E+00	-0.8489031274E+01	0.1885352199E+02
-0.6312046987E+00	-0.9074120368E+01	0.1891923567E+02
-0.5841527992E+00	-0.8570137586E+01	0.1879563870E+02
-0.1053055196E+01	-0.8712858303E+01	0.1863999669E+02
-0.1213752190E+01	-0.8887843127E+01	0.1858296146E+02
-0.1022704699E+01	-0.9304120368E+01	0.1881673567E+02
-0.1598077662E+01	-0.9281725173E+01	0.1836728467E+02
-0.1628321229E+01	-0.9626428683E+01	0.1825510352E+02
-0.1647368387E+01	-0.9760772005E+01	0.1819301785E+02
-0.1202120911E+01	-0.9620674270E+01	0.1869463709E+02
-0.1614745771E+01	-0.9903236469E+01	0.1816480173E+02
-0.1194120911E+01	-0.9899674270E+01	0.1859563708E+02
0.2375854746E+01	-0.4120318698E+01	0.1848083067E+02

-0.2382054047E+01 -0.4142333415E+01 0.1846921648E+02

166

1 24 31 106 107 108

24 47 31 109 110 107

47 61 32 111 112 113

61 2 32 114 115 112

2 62 32 116 117 115

62 48 32 118 119 117

48 25 33 120 121 122

25 3 33 123 124 121

3 26 33 125 126 124

26 49 33 127 128 126

49 26 34 127 129 130

26 4 34 131 132 129

4 27 34 133 134 132

27 50 34 135 136 134

50 27 35 135 137 138

27 5 35 139 140 137

5 28 35 141 142 140

28 51 35 143 144 142

51 28 36 143 145 146

28 6 36 147 148 145

6 29 36 149 150 148

29 52 36 151 152 150

52 29 37 151 153 154

29 7 37 155 156 153

7 30 37 157 158 156

30 53 37 159 160 158

53 30 38 159 161 162

30 8 38 163 164 161

8 1 38 165 166 164

1 31 38 108 167 166

31 47 39 110 168 169

47 54 39 170 171 168

54 47 40 170 172 173

47 32 40 113 174 172

32 48 40 119 175 174

48 55 40 176 177 175

55 48 41 176 178 179

48 33 41 122 180 178

33 49 41 128 181 180

49 56 41 182 183 181

56 49 42 182 184 185

49 34 42 130 186 184

34 50 42 136 187 186

50 57 42 188 189 187

57 50 43 188 190 191

50 35 43 138 192 190

35 51 43 144 193 192

51 58 43 194 195 193

58 51 44 194 196 197

51 36 44 146 198 196

36 52 44 152 199 198

52 59 44 200 201 199

59 52 45 200 202 203

52 37 45 154 204 202

37 53 45 160 205 204

53 60 45 206 207 205

60 53 46 206 208 209

53 38 46 162 210 208

38 39 46 211 212 210

38 31 39 167 169 211

16 39 9 213 214 215

39 54 9 171 216 214

54 17 9 217 218 216

17 54 10 217 219 220

54 40 10 173 221 219

40 55 10 177 222 221

55 18 10 223 224 222

18 55 11 223 225 226

55 41 11 179 227 225

41 56 11 183 228 227

56 19 11 229 230 228

19 56 12 229 231 232

56 42 12 185 233 231

42 57 12 189 234 233

57 20 12 235 236 234

20 57 13 235 237 238

57 43 13 191 239 237

43 58 13 195 240 239

58 21 13 241 242 240

21 58 14 241 243 244

58 44 14 197 245 243

44 59 14 201 246 245

59 22 14 247 248 246

22 59 15 247 249 250

59 45 15 203 251 249

45 60 15 207 252 251

60 23 15 253 254 252

23 60 16 253 255 256

60 46 16 209 257 255

46 39 16 212 213 257

63 78 82 258 259 260

78 94 82 261 262 259

94 78 83 261 263 264

83 78 64 263 265 266

64 79 83 267 268 266

79 95 83 269 270 268

95 79 84 269 271 272

79 65 84 273 274 271

65 80 84 275 276 274

80 96 84 277 278 276

96 80 85 277 279 280

80 3 85 281 282 279

3 25 85 123 283 282

25 97 85 284 285 283

97 62 86 286 287 288

62 2 86 116 289 287

2 61 86 114 290 289

61 98 86 291 292 290

98 24 87 293 294 295

24 1 87 106 296 294

1 81 87 297 298 296

87 81 99 298 299 300

99 81 82 299 301 302

81 63 82 303 260 301

82 94 88 262 304 305

94 100 88 306 307 304

100 94 89 306 308 309

94 83 89 264 310 308

83 95 89 270 311 310

95 101 89 312 313 311

101 95 90 312 314 315

95 84 90 272 316 314

84 96 90 278 317 316

96 102 90 318 319 317

102 96 91 318 320 321

96 85 91 280 322 320

85 97 91 285 323 322

97 103 91 324 325 323

103 97 86 324 288 326

92 103 86 327 326 328

104 92 86 329 328 330

98 104 86 331 330 292

104 98 93 331 332 333

98 87 93 295 334 332

87 99 93 300 335 334

99 105 93 336 337 335

88 105 99 338 336 339

99 82 88 302 305 339

88 100 66 307 340 341

100 72 66 342 343 340

72 100 67 342 344 345

100 89 67 309 346 344

89 101 67 313 347 346

101 73 67 348 349 347

73 101 68 348 350 351

101 90 68 315 352 350

90 102 68 319 353 352

102 74 68 354 355 353

74 102 69 354 356 357

102 91 69 321 358 356

91 103 69 325 359 358

103 75 69 360 361 359

75 103 92 360 327 362

70 75 92 363 362 364

76 70 92 365 364 366

104 76 92 367 366 329

76 104 71 367 368 369

104 93 71 333 370 368

93 105 71 337 371 370

105 77 71 372 373 371

77 105 66 372 374 375

105 88 66 338 341 374

62 25 48 376 120 118

24 61 47 377 111 109

62 97 25 286 284 376

61 24 98 377 293 291

110

31 108 1

108 1 1

39 169 1

169 31 1

39 214 1

214 9 1

7 156 2

156 37 2

37 204 2

204 45 2

45 251 2

251 15 2

6 148 3

148 36 3

36 198 3

198 44 3

44 245 3

245 14 3

5 140 4

140 35 4

35 192 4

192 43 4

43 239 4

239 13 4

4 132 5

132 34 5

34 186 5

186 42 5

42 233 5

233 12 5

3 282 6

282 85 6

85 322 6

322 91 6

91 358 6

358 69 6

65 274 7

274 84 7

84 316 7

316 90 7

90 352 7

352 68 7

64 266 8

266 83 8

83 310 8

310 89 8

89 346 8

346 67 8

82 260 9

260 63 9

88 305 9

305 82 9

66 341 9

341 88 9

1 296 10

296 87 10

87 334 10

334 93 10

93 370 10

370 71 10

92 364 11

364 70 11

86 328 11

328 92 11

2 289 11

289 86 11

2 115 11

115 32 11

32 174 11

174 40 11

40 221 11

221 10 11

30 163 12

163 8 12

7 157 12

157 30 12

29 155 13

155 7 13

6 149 13

149 29 13

28 147 14

147 6 14

5 141 14

141 28 14

27 139 15

139 5 15

4 133 15

133 27 15

26 131 16

131 4 16

3 125 16

125 26 16

80 281 17

281 3 17

65 275 17

275 80 17

79 273 18

273 65 18

64 267 18

267 79 18

78 265 19

265 64 19

63 258 19

258 78 19

81 303 20

303 63 20

1 297 20

297 81 20

8 165 21

165 1 21

0.4415363561-304 0.0000000000E+00 0.0000000000E+00

0.0000000000E+00 0.0000000000E+00 0.0000000000E+00

0.0000000000E+00 0.0000000000E+00 0.0000000000E+00

0.0000000000E+00 0.0000000000E+00 0.0000000000E+00

0.0000000000E+00 0.0000000000E+00 0.0000000000E+00

0.0000000000E+00 0.0000000000E+00 0.0000000000E+00

0.0000000000E+00 0.0000000000E+00 0.0000000000E+00

0.0000000000E+00 0.0000000000E+00 0.0000000000E+00

0.0000000000E+00 0.0000000000E+00 0.0000000000E+00

0.0000000000E+00 0.0000000000E+00 0.0000000000E+00

0.0000000000E+00 0.0000000000E+00 0.0000000000E+00

0.0000000000E+00 0.0000000000E+00 0.0000000000E+00

0.0000000000E+00 0.0000000000E+00 0.0000000000E+00

0.0000000000E+00 0.0000000000E+00 0.0000000000E+00

0.0000000000E+00 0.0000000000E+00 0.0000000000E+00

0.0000000000E+00 0.0000000000E+00 0.0000000000E+00

0.0000000000E+00 0.0000000000E+00 0.0000000000E+00

0.0000000000E+00 0.0000000000E+00 0.0000000000E+00

0.0000000000E+00 0.0000000000E+00 0.0000000000E+00

0.0000000000E+00 0.0000000000E+00 0.0000000000E+00

0.0000000000E+00 0.0000000000E+00 0.0000000000E+00

0.0000000000E+00	0.0000000000E+00	0.0000000000E+00
0.0000000000E+00	0.0000000000E+00	0.0000000000E+00
0.0000000000E+00	0.0000000000E+00	0.0000000000E+00
0.0000000000E+00	0.0000000000E+00	0.0000000000E+00
0.0000000000E+00	0.0000000000E+00	0.0000000000E+00
0.0000000000E+00	0.0000000000E+00	0.0000000000E+00
0.0000000000E+00	0.0000000000E+00	-0.6837300478E+01
0.0000000000E+00	0.0000000000E+00	-0.2574059068E+01
0.0000000000E+00	0.0000000000E+00	-0.3472536783E+01
0.0000000000E+00	0.0000000000E+00	-0.1202150955E+01
0.0000000000E+00	0.0000000000E+00	-0.1551058844E+01
0.0000000000E+00	0.0000000000E+00	-0.1346780485E+01
0.0000000000E+00	0.0000000000E+00	-0.1428040732E+01
0.0000000000E+00	0.0000000000E+00	-0.1502690063E+01
0.0000000000E+00	0.0000000000E+00	-0.1249913911E+01
0.0000000000E+00	0.0000000000E+00	-0.1141921455E+01
0.0000000000E+00	0.0000000000E+00	-0.1087709893E+01
0.0000000000E+00	0.0000000000E+00	-0.1231866380E+01
0.0000000000E+00	0.0000000000E+00	-0.1325283417E+01
0.0000000000E+00	0.0000000000E+00	-0.1201055668E+01
0.0000000000E+00	0.0000000000E+00	-0.1421528570E+01
0.0000000000E+00	0.0000000000E+00	-0.2919890356E+01
0.0000000000E+00	0.0000000000E+00	-0.1723481235E+01
0.0000000000E+00	0.0000000000E+00	-0.7369695015E+01
0.0000000000E+00	0.0000000000E+00	-0.4195336291E+01
0.0000000000E+00	0.0000000000E+00	-0.2072392776E+01
0.0000000000E+00	0.0000000000E+00	-0.3192286686E+01

0.0000000000E+00	0.0000000000E+00	-0.2333591737E+01
0.0000000000E+00	0.0000000000E+00	-0.1853293131E+01
0.0000000000E+00	0.0000000000E+00	-0.3043638632E+01
0.0000000000E+00	0.0000000000E+00	-0.1955838899E+01
0.0000000000E+00	0.0000000000E+00	-0.1829940805E+01
0.0000000000E+00	0.0000000000E+00	-0.5028788924E+01
0.0000000000E+00	0.0000000000E+00	-0.3198848119E+01
0.0000000000E+00	0.0000000000E+00	-0.4721859472E+01
0.0000000000E+00	0.0000000000E+00	-0.3195493932E+01
0.0000000000E+00	0.0000000000E+00	-0.2929966787E+01
0.0000000000E+00	0.0000000000E+00	-0.4446113816E+01
0.0000000000E+00	0.0000000000E+00	-0.3113443293E+01
0.0000000000E+00	0.0000000000E+00	-0.2773631237E+01
0.0000000000E+00	0.0000000000E+00	-0.5315576462E+01
0.0000000000E+00	0.0000000000E+00	-0.2541945225E+01
0.0000000000E+00	0.0000000000E+00	-0.4943700543E+01
0.0000000000E+00	0.0000000000E+00	-0.4772964929E+01
0.0000000000E+00	0.0000000000E+00	-0.3406950834E+01
0.0000000000E+00	0.0000000000E+00	-0.4843153102E+01
0.0000000000E+00	0.0000000000E+00	-0.3313827877E+01
0.0000000000E+00	0.0000000000E+00	-0.2471943491E+01
0.0000000000E+00	0.0000000000E+00	-0.4988596651E+01
0.0000000000E+00	0.0000000000E+00	-0.2516653160E+01
0.0000000000E+00	0.0000000000E+00	-0.3933028144E+01
0.0000000000E+00	0.0000000000E+00	-0.2730852999E+01
0.0000000000E+00	0.0000000000E+00	-0.2822411464E+01
0.0000000000E+00	0.0000000000E+00	-0.3859686881E+01

0.0000000000E+00	0.0000000000E+00	-0.2684490228E+01
0.0000000000E+00	0.0000000000E+00	-0.2545208866E+01
0.0000000000E+00	0.0000000000E+00	-0.6335926654E+01
0.0000000000E+00	0.0000000000E+00	-0.3790717787E+01
0.0000000000E+00	0.0000000000E+00	-0.6032964086E+01
0.0000000000E+00	0.0000000000E+00	-0.4261001199E+01
0.0000000000E+00	0.0000000000E+00	-0.4131314704E+01
0.0000000000E+00	0.0000000000E+00	-0.6302228148E+01
0.0000000000E+00	0.0000000000E+00	-0.3888714352E+01
0.0000000000E+00	0.0000000000E+00	-0.4283473248E+01
0.0000000000E+00	0.0000000000E+00	-0.7412725215E+01
0.0000000000E+00	0.0000000000E+00	-0.3129251967E+01
0.0000000000E+00	0.0000000000E+00	-0.4700384122E+01
0.0000000000E+00	0.0000000000E+00	-0.2554041407E+01
0.0000000000E+00	0.0000000000E+00	-0.1334118400E+01
0.0000000000E+00	0.0000000000E+00	-0.1861313657E+01
0.0000000000E+00	0.0000000000E+00	-0.7622372747E+00
0.0000000000E+00	0.0000000000E+00	-0.8700516447E+00
0.0000000000E+00	0.0000000000E+00	-0.9919293726E+00
0.0000000000E+00	0.0000000000E+00	-0.5565346212E+00
0.0000000000E+00	0.0000000000E+00	-0.1185760073E+01
0.0000000000E+00	0.0000000000E+00	-0.7971011693E+00
0.0000000000E+00	0.0000000000E+00	-0.5911786753E+00
0.0000000000E+00	0.0000000000E+00	-0.5544283389E+00
0.0000000000E+00	0.0000000000E+00	-0.1220965880E+01
0.0000000000E+00	0.0000000000E+00	-0.5569860252E+00
0.0000000000E+00	0.0000000000E+00	-0.1659933615E+01

0.0000000000E+00 0.0000000000E+00 -0.1044574368E+01

0.0000000000E+00 0.0000000000E+00 -0.7557074335E+00

0.0000000000E+00 0.0000000000E+00 -0.4471987551E+00

0.0000000000E+00 0.0000000000E+00 -0.1186673359E+01

0.0000000000E+00 0.0000000000E+00 -0.6781974470E+00

0.0000000000E+00 0.0000000000E+00 -0.2149096507E+01

0.0000000000E+00 0.0000000000E+00 -0.2193548210E+01

0.0000000000E+00 0.0000000000E+00 -0.1473577187E+01

0.0000000000E+00 0.0000000000E+00 -0.1235225992E+01

0.0000000000E+00 0.0000000000E+00 -0.2127945126E+01

0.0000000000E+00 0.0000000000E+00 -0.1143549265E+01

0.0000000000E+00 0.0000000000E+00 -0.2446156230E+01

0.0000000000E+00 0.0000000000E+00 -0.1591750593E+01

0.0000000000E+00 0.0000000000E+00 -0.1164636841E+01

0.0000000000E+00 0.0000000000E+00 -0.8965456328E+00

0.0000000000E+00 0.0000000000E+00 -0.1520700031E+01

0.0000000000E+00 0.0000000000E+00 -0.9127240109E+00

0.0000000000E+00 0.0000000000E+00 -0.2348654746E+01

0.0000000000E+00 0.0000000000E+00 -0.2098903400E+01

0.0000000000E+00 0.0000000000E+00 -0.1475763880E+01

0.0000000000E+00 0.0000000000E+00 -0.1187704102E+01

0.0000000000E+00 0.0000000000E+00 -0.2152909173E+01

0.0000000000E+00 0.0000000000E+00 -0.1312204932E+01

0.0000000000E+00 0.0000000000E+00 -0.3259080619E+01

0.0000000000E+00 0.0000000000E+00 -0.2804809985E+01

0.0000000000E+00 0.0000000000E+00 -0.1657619256E+01

0.0000000000E+00 0.0000000000E+00 -0.1424395274E+01

0.0000000000E+00	0.0000000000E+00	-0.2611837128E+01
0.0000000000E+00	0.0000000000E+00	-0.1093723752E+01
0.0000000000E+00	0.0000000000E+00	-0.2802876869E+01
0.0000000000E+00	0.0000000000E+00	-0.1915826670E+01
0.0000000000E+00	0.0000000000E+00	-0.1318848527E+01
0.0000000000E+00	0.0000000000E+00	-0.5822046645E+00
0.0000000000E+00	0.0000000000E+00	-0.6106112038E+00
0.0000000000E+00	0.0000000000E+00	-0.1962735547E+00
0.0000000000E+00	0.0000000000E+00	-0.5706734870E+00
0.0000000000E+00	0.0000000000E+00	-0.3114255781E+00
0.0000000000E+00	0.0000000000E+00	-0.1563358380E+00
0.0000000000E+00	0.0000000000E+00	-0.4051010823E+00
0.0000000000E+00	0.0000000000E+00	-0.1550897402E+00
0.0000000000E+00	0.0000000000E+00	-0.5076924917E+00
0.0000000000E+00	0.0000000000E+00	-0.3728108065E+00
0.0000000000E+00	0.0000000000E+00	-0.2274262409E+00
0.0000000000E+00	0.0000000000E+00	-0.1151296569E+00
0.0000000000E+00	0.0000000000E+00	-0.3748511232E+00
0.0000000000E+00	0.0000000000E+00	-0.1122965839E+00
0.0000000000E+00	0.0000000000E+00	-0.3985781474E+00
0.0000000000E+00	0.0000000000E+00	-0.2542186102E+00
0.0000000000E+00	0.0000000000E+00	-0.2288697153E+00
0.0000000000E+00	0.0000000000E+00	-0.1181950020E+00
0.0000000000E+00	0.0000000000E+00	-0.3443398737E+00
0.0000000000E+00	0.0000000000E+00	-0.1106747132E+00
0.0000000000E+00	0.0000000000E+00	-0.6822983772E+00
0.0000000000E+00	0.0000000000E+00	-0.6208536919E+00

0.0000000000E+00	0.0000000000E+00	-0.3324370540E+00
0.0000000000E+00	0.0000000000E+00	-0.1722204752E+00
0.0000000000E+00	0.0000000000E+00	-0.6167814321E+00
0.0000000000E+00	0.0000000000E+00	-0.1602165788E+00
0.0000000000E+00	0.0000000000E+00	-0.7665554097E+00
0.0000000000E+00	0.0000000000E+00	-0.3473898756E+00
0.0000000000E+00	0.0000000000E+00	-0.7403708784E-01
0.0000000000E+00	0.0000000000E+00	-0.3739931914E-01
0.0000000000E+00	0.0000000000E+00	-0.3712800147E+00
0.0000000000E+00	0.0000000000E+00	-0.3663776870E-01
0.0000000000E+00	0.0000000000E+00	-0.8294794279E+00
0.0000000000E+00	0.0000000000E+00	-0.6700408957E+00
0.0000000000E+00	0.0000000000E+00	-0.3618987689E+00
0.0000000000E+00	0.0000000000E+00	-0.1752037138E+00
0.0000000000E+00	0.0000000000E+00	-0.7160030267E+00
0.0000000000E+00	0.0000000000E+00	-0.1866950551E+00
0.0000000000E+00	0.0000000000E+00	-0.1037961667E+01
0.0000000000E+00	0.0000000000E+00	-0.6902958378E+00
0.0000000000E+00	0.0000000000E+00	-0.3747536301E+00
0.0000000000E+00	0.0000000000E+00	-0.1816421428E+00
0.0000000000E+00	0.0000000000E+00	-0.5449575631E+00
0.0000000000E+00	0.0000000000E+00	-0.1931114873E+00
0.0000000000E+00	0.0000000000E+00	-0.7377771856E+00
0.0000000000E+00	0.0000000000E+00	-0.4496270051E+00
0.0000000000E+00	0.0000000000E+00	-0.9163171071E+00
0.0000000000E+00	0.0000000000E+00	-0.1631956386E+01
0.0000000000E+00	0.0000000000E+00	-0.8523555024E+00

0.0000000000E+00	0.0000000000E+00	-0.8298438639E+00
0.0000000000E+00	0.0000000000E+00	-0.1063982952E+01
0.0000000000E+00	0.0000000000E+00	-0.5651935136E+00
0.0000000000E+00	0.0000000000E+00	-0.6783175514E+00
0.0000000000E+00	0.0000000000E+00	-0.1600079372E+01
0.0000000000E+00	0.0000000000E+00	-0.9217618209E+00
0.0000000000E+00	0.0000000000E+00	-0.1353659415E+01
0.0000000000E+00	0.0000000000E+00	-0.8841136550E+00
0.0000000000E+00	0.0000000000E+00	-0.6857026770E+00
0.0000000000E+00	0.0000000000E+00	-0.1049581753E+01
0.0000000000E+00	0.0000000000E+00	-0.9517547758E+00
0.0000000000E+00	0.0000000000E+00	-0.5973656922E+00
0.0000000000E+00	0.0000000000E+00	-0.2046023984E+01
0.0000000000E+00	0.0000000000E+00	-0.1448658292E+01
0.0000000000E+00	0.0000000000E+00	-0.2806450936E+01
0.0000000000E+00	0.0000000000E+00	-0.2456281589E+01
0.0000000000E+00	0.0000000000E+00	-0.1690935093E+01
0.0000000000E+00	0.0000000000E+00	-0.3094125996E+01
0.0000000000E+00	0.0000000000E+00	-0.1493778768E+01
0.0000000000E+00	0.0000000000E+00	-0.1995637050E+01
0.0000000000E+00	0.0000000000E+00	-0.7242388550E+01
0.0000000000E+00	0.0000000000E+00	-0.6752854045E+01
0.0000000000E+00	0.0000000000E+00	-0.2206364550E+01
0.0000000000E+00	0.0000000000E+00	-0.2357667413E+01
0.0000000000E+00	0.0000000000E+00	-0.1473395291E+01
0.0000000000E+00	0.0000000000E+00	-0.1329678487E+01
0.0000000000E+00	0.0000000000E+00	-0.1338186548E+01

0.0000000000E+00 0.0000000000E+00 -0.1195702349E+01

0.0000000000E+00 0.0000000000E+00 -0.1477585470E+01

0.0000000000E+00 0.0000000000E+00 -0.1549410585E+01

0.0000000000E+00 0.0000000000E+00 -0.1419306255E+01

0.0000000000E+00 0.0000000000E+00 -0.1971476488E+01

0.0000000000E+00 0.0000000000E+00 -0.6196390075E+01

0.0000000000E+00 0.0000000000E+00 -0.1935335984E+01

0.0000000000E+00 0.0000000000E+00 -0.6813822171E+01

0.0000000000E+00 0.0000000000E+00 -0.1877926322E+01

0.0000000000E+00 0.0000000000E+00 -0.2802155986E+01

0.0000000000E+00 0.0000000000E+00 -0.2231168538E+01

0.0000000000E+00 0.0000000000E+00 -0.1265727670E+01

0.0000000000E+00 0.0000000000E+00 -0.2489268256E+01

0.0000000000E+00 0.0000000000E+00 -0.1668003598E+01

0.0000000000E+00 0.0000000000E+00 -0.1182329381E+01

0.0000000000E+00 0.0000000000E+00 -0.4893001547E+00

0.0000000000E+00 0.0000000000E+00 -0.7242184850E+00

0.0000000000E+00 0.0000000000E+00 -0.2391721401E+00

0.0000000000E+00 0.0000000000E+00 -0.2508162743E+00

0.0000000000E+00 0.0000000000E+00 -0.2925538607E+00

0.0000000000E+00 0.0000000000E+00 -0.1913115183E+00

0.0000000000E+00 0.0000000000E+00 -0.4333331960E+00

0.0000000000E+00 0.0000000000E+00 -0.4052985167E+00

0.0000000000E+00 0.0000000000E+00 -0.3445637923E+00

0.0000000000E+00 0.0000000000E+00 -0.2398680882E+00

0.0000000000E+00 0.0000000000E+00 -0.6926090733E+00

0.0000000000E+00 0.0000000000E+00 -0.3599475051E+00

0.0000000000E+00	0.0000000000E+00	-0.8326811647E+00
0.0000000000E+00	0.0000000000E+00	-0.4482831053E+00
0.0000000000E+00	0.0000000000E+00	-0.2299943985E+00
0.0000000000E+00	0.0000000000E+00	-0.2728323288E+00
0.0000000000E+00	0.0000000000E+00	-0.5101435646E+00
0.0000000000E+00	0.0000000000E+00	-0.2508419631E+00
0.0000000000E+00	0.0000000000E+00	-0.1246854689E+01
0.0000000000E+00	0.0000000000E+00	-0.1216479438E+01
0.0000000000E+00	0.0000000000E+00	-0.9299678330E+00
0.0000000000E+00	0.0000000000E+00	-0.5914543462E+00
0.0000000000E+00	0.0000000000E+00	-0.8674221309E+00
0.0000000000E+00	0.0000000000E+00	-0.4959477971E+00
0.0000000000E+00	0.0000000000E+00	-0.6053683923E+00
0.0000000000E+00	0.0000000000E+00	-0.4911593645E+00
0.0000000000E+00	0.0000000000E+00	-0.8838774562E+00
0.0000000000E+00	0.0000000000E+00	-0.9088611147E+00
0.0000000000E+00	0.0000000000E+00	-0.1002824940E+01
0.0000000000E+00	0.0000000000E+00	-0.5262826928E+00
0.0000000000E+00	0.0000000000E+00	-0.1016339764E+01
0.0000000000E+00	0.0000000000E+00	-0.4716338750E+00
0.0000000000E+00	0.0000000000E+00	-0.2662441287E+00
0.0000000000E+00	0.0000000000E+00	-0.2529910557E+00
0.0000000000E+00	0.0000000000E+00	-0.2892431880E+00
0.0000000000E+00	0.0000000000E+00	-0.4971729826E+00
0.0000000000E+00	0.0000000000E+00	-0.1665038354E+00
0.0000000000E+00	0.0000000000E+00	-0.2778048100E+00
0.0000000000E+00	0.0000000000E+00	-0.7887046135E-01

0.0000000000E+00	0.0000000000E+00	-0.4183395388E-01
0.0000000000E+00	0.0000000000E+00	-0.1153222785E+00
0.0000000000E+00	0.0000000000E+00	-0.3703650747E-01
0.0000000000E+00	0.0000000000E+00	-0.1666604252E+00
0.0000000000E+00	0.0000000000E+00	-0.1166493313E+00
0.0000000000E+00	0.0000000000E+00	-0.6758044891E-01
0.0000000000E+00	0.0000000000E+00	-0.2827467711E-01
0.0000000000E+00	0.0000000000E+00	-0.2061829187E+00
0.0000000000E+00	0.0000000000E+00	-0.3930577180E-01
0.0000000000E+00	0.0000000000E+00	-0.3245688199E+00
0.0000000000E+00	0.0000000000E+00	-0.2100472973E+00
0.0000000000E+00	0.0000000000E+00	-0.1060401354E+00
0.0000000000E+00	0.0000000000E+00	-0.5235562426E-01
0.0000000000E+00	0.0000000000E+00	-0.1896727314E+00
0.0000000000E+00	0.0000000000E+00	-0.5368451114E-01
0.0000000000E+00	0.0000000000E+00	-0.3625279951E+00
0.0000000000E+00	0.0000000000E+00	-0.3109809252E+00
0.0000000000E+00	0.0000000000E+00	-0.2780200782E+00
0.0000000000E+00	0.0000000000E+00	-0.8444115035E-01
0.0000000000E+00	0.0000000000E+00	-0.2854127653E+00
0.0000000000E+00	0.0000000000E+00	-0.9183383748E-01
0.0000000000E+00	0.0000000000E+00	-0.1864439526E+00
0.0000000000E+00	0.0000000000E+00	-0.9461011511E-01
0.0000000000E+00	0.0000000000E+00	-0.2827699565E+00
0.0000000000E+00	0.0000000000E+00	-0.2666431892E+00
0.0000000000E+00	0.0000000000E+00	-0.2767828591E+00
0.0000000000E+00	0.0000000000E+00	-0.7848334779E-01

0.0000000000E+00 0.0000000000E+00 -0.3211546978E+00

0.0000000000E+00 0.0000000000E+00 -0.1706430001E+00

0.0000000000E+00 0.0000000000E+00 -0.9597284117E-01

0.0000000000E+00 0.0000000000E+00 -0.4778781360E-01

0.0000000000E+00 0.0000000000E+00 -0.2013199560E+00

0.0000000000E+00 0.0000000000E+00 -0.4818502756E-01

0.0000000000E+00 0.0000000000E+00 -0.1324843733E+01

0.0000000000E+00 0.0000000000E+00 -0.1240478779E+01

0.00 0.00 0.1

1.5680000000E+08 2.1660000000E-04

1.0000000000E+03 1.0000000000E+03 0.3000000000E+02

192

1

2

3

7

8

9

10

11

12

13

14

15

16

17

18

46

47

48

49

50

51

52

53

54

55

56

57

58

59

60

61

62

63

64

65

66

67

68

69

187

188

189

190

191

192

193

194

195

196

197

198

199

200

201

202

203

204

205

206

207

208

209

210

211

212

213

214

215

216

217

218

219

220

221

222

223

224

225

226

227

228

229

230

231

643

644

645

652

653

654

658

659

660

670

671

672

676

677

678

688

689

690

694

695

696

706

707

708

712

713

714

724

725

726

730

731

732

742

743

744

748

749

750

760

761

762

766

767

768

1027

1028

1029

1033

1034

1035

1045

1046

1047

1051

1052

1053

1063

1064

1065

1069

1070

1071

1081

1082

1083

1087

1088

1089

1093

1094

1095

1105

1106

1107

1117

1118

1119

1123

1124

1125

1.500 1.500 0.000

21

15.0

15.0

17.0

14.8

8.8

1.8

3.0

2.0

3.0

1.8

7.0

17.3

16.3

19.3

17.8

10.0

10.5

12.8

10.5

10.5

6.80

0

0

1

0.020

0.015

1

0.6380000000E+03

0.6380000000E+03 0.4100000000E+02 0.0000000000E+00

1

0.6120000000E+03

0.6120000000E+03 0.2000000000E+02 0.0000000000E+00

1

0.3000000000E+02

0.3000000000E+02 0.3000000000E+01 0.0000000000E+00

1

0.3000000000E+00

0.3000000000E+00 0.5000000000E-01 0.0000000000E+00

1

0.7300000000E+00

0.7300000000E+00 0.0000000000E+00 0.0000000000E+00

1

2.5000000000E+01

2.5000000000E+01 0.8000000000E+00 0.0000000000E+00

27.50

27.50

-1.000

-0.045

1